

Volume 65 Issue 1

- 1 **"*Bactricia nematodes* Kby., 1894" (Phasmida, Diapheromeridae, Diapheromerinae) is a *nomen nudum***
Martin H. Villet

- 9 **A new species of the genus *Ropalidia* Guérin-Méneville from central Africa (Insecta, Hymenoptera, Vespidae)**
Ozren Polašek

- 15 **Uncovering the hidden diversity of non-biting midges (Diptera, Chironomidae) from central Namibia, using morphology and DNA barcodes**
Viktor Baranov, Xiaolong Lin, Jeremy Hübner, Caroline Chimeno

“*Bactricia nematodes* Kby., 1894” (Phasmida, Diapheromeridae, Diapheromerinae) is a *nomen nudum*

Martin H. Villet¹ 

¹ Department of Zoology & Entomology, Rhodes University, African Street, Makhanda, 6140, South Africa
Corresponding author: Martin H. Villet (martin.villet@gmail.com)

Abstract

A review of published evidence indicates that *Bactricia nematodes* Kirby, 1894 is a ***nomen nudum*** because it is an unavailable name. The specimen collected during the Lund University Swedish South African Expedition and reported by this name is a male of *Bactricia bituberculata* (Schaum, 1857).

Key words: Lund University Swedish South African Expedition, nomen dubium, Phasmida, species inquirenda, stick insect

Introduction

The Lund University Swedish South Africa Expedition (LUSSAE) of 1950–1951 resulted in a series of volumes entitled “South African Animal Life”. In Volume 3, Klaus Günther reviewed the 20 specimens of stick insects that were collected on the expedition and assigned them to 10 species (Günther 1957). One male specimen (Fig. 1b) was assigned to “*Bactricia nematodes* K[ir]by., 1894” (Phasmidae, Heteronemiinae) (Günther 1957, 93). This record was apparently the source for a second, less detailed mention of *Bactricia nematodes* (Phasmatidae, Heteronemiinae) by Schoeman (1985). No other published references to *B. nematodes* are known.

Notes under the entry for *Bactricia* Kirby, 1896 on the comprehensive Phasmid Species File Online (PSFO) database (Brock et al. 2023) suggests that there is “no such species?” as *B. nematodes*, and that Schoeman (1985) makes “[r]eference to a *Bactricia* ‘nematodes’ in South Africa, clearly in error”. *Bactricia nematodes* is therefore currently a *nomen dubium* and consequently a *species inquirenda*.

This study is an account of the taxonomic nomenclature, intended identification and actual identity of Günther (1957) and Schoeman’s (1985) “*Bactricia nematodes*”.

Nomenclature

Günther’s (1957) mention of the name *Bactricia nematodes* is not associated with any description, diagnosis or illustration of the relevant specimen, so it is clearly not an attempt at an original description, for which Günther had ample



Academic editor: John Midgley
Received: 9 November 2023
Accepted: 7 December 2023
Published: 23 February 2024

ZooBank: <https://zoobank.org/86878B3B-6394-4ABA-8616-3AA45B9F1B80>

Citation: Villet MH (2024) “*Bactricia nematodes* Kby., 1894” (Phasmida, Diapheromeridae, Diapheromerinae) is a *nomen nudum*. African Invertebrates 65(1): 1–7. <https://doi.org/10.3897/AfrInvertebr.65.115507>

Copyright: © Martin H. Villet.
This is an open access article distributed under terms of the Creative Commons Attribution License (Attribution 4.0 International – CC BY 4.0).

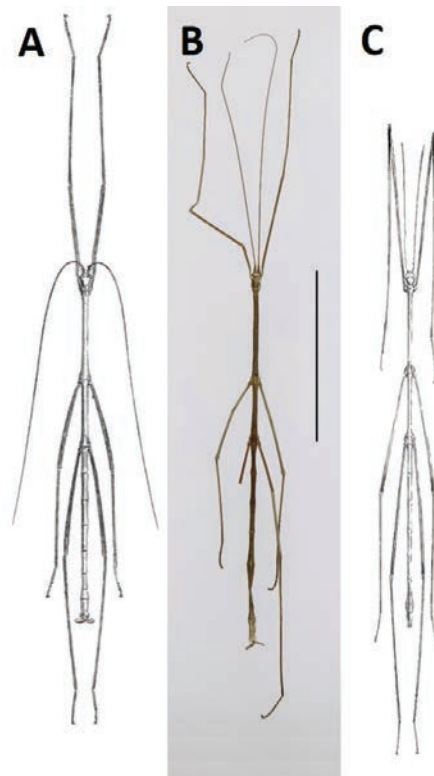


Figure 1. **A** Westwood's (1859: Plate V, fig. 5) illustration of *Bacteria trophinus* [sic] W. ♂ (No longer under copyright) **B** habitus of the LUSAE specimen identified as *Bactricia nematodes*. (CC BY-NC 2.0 Deed, Lund University Biological Museum: Entomology, downloaded 12 Nov 2023, original photographs and copyright licence available at http://www.flickr.com/search/?user_id=127240649%40N08&text=Bactricia%20spp) **C** Westwood's (1859: Plate V, fig. 7) illustration of *Lonchodes nematodes* [sic] de H. ♂ (No longer under copyright; also reproduced by Delfosse (2005: 37)). Scale bar: 50 mm.

experience in publishing before 1957 (Bragg and Zompro 2007). By citing Kirby as the taxonomic author of the name, Günther implied that *B. nematodes* was not intended as a new name (unless it was by reference). He was also explicit in his introduction to his chapter that he was certain of only one new species in the LUSAE sample, alluding to his original description of *Ramulus rubrotaeniatus* Günther, 1957 in this same publication. He illustrated this description of *R. rubrotaeniatus* and, since Günther usually illustrated his new species (Bragg and Zompro 2007), the lack of a figure of *B. nematodes* also suggests that no original description was intended in this context.

The species is also not validated by citation of the prior publication of "K[ir]by., 1894" (International Commission on Zoological Nomenclature (ICZN) 1999, Article 13.1.2) because Günther (1957) did not reference the work, none of Kirby's publications (listed on the comprehensive PSFO database) was published in 1894 and the lack of a reference for the citation disallows the detection of a misprint. The genus *Bactricia* was described two years after Günther's cited date (Kirby 1896), yet Günther (1957) did not use parentheses around the authorship of *B. nematodes* to indicate that the specific epithet had been described in another genus in 1894 and then recombined with *Bactricia* in or after 1896. A search of the PSFO database for another source of the specific epithet *nematodes* returned only *Phasma (Bacteria) nematodes* de Haan, 1842. De Haan's specific epithet has not been used elsewhere in combination with *Bactricia* Kirby, 1896 (Delfosse 2005; Brock et al. 2023) and so does not provide

an alternative source that may be validated by bibliographic reference. Kirby (1904) mentioned the epithet *nematodes* in two connections: *Phasma (Bacteria) nematodes* ♀ Haan, 1842 (and the combination *Lonchodes nematodes* ♀ Westwood) as a synonym of *Phasgania crawangensis* Haan, 1842 (Kirby 1904: 324) and *Phasma (Bacteria) nematodes* ♂ (and the combination *Lonchodes nematodes* ♂ *auct.*) as a synonym of *Baculum nematodes* ♂ Haan, 1842 (Kirby 1904: 328). Had he coined the epithet *nematodes* in 1894 or 1896, he would have mentioned that here. Nomenclaturally, "*Bactricia nematodes* Kby, 1894" is not an available name and, as such, is a *nomen nudum* (International Commission on Zoological Nomenclature (ICZN) 1999, Glossary).

Since there was no intent to describe a taxon, it seems that *Bactricia nematodes* is also a *nomen tantum* arising from misremembering the author of the genus *Bactricia* as the author of a constituent species, misremembering the publication date of Kirby's work and confusing *Ramulus nematodes* (de Haan) with another name. Bragg and Zompro (2007) discuss other *lapsus memoriae* in Günther's publications that support this inference.

Identity

This leads to the question of Günther's intended identification of the specimen. Günther (1957: 88) wrote, "... [die] einzige Art [von *Bactricia* Kby.] ... auch in der vorliegenden Ausbeute aus Transvaal enthalten ist" [... the only species [of *Bactricia* Kirby] ... is also included in the present sample from the Transvaal]. Since *Bactricia bituberculata* (Schaum, 1857) (a senior synonym of *Bacteria Trophimus* [sic] Westwood, 1859, the designated type species of *Bactricia* (see Brock (2004))) was the only valid species of *Bactricia* recognised at the time, it must be the species that he had in mind.

Phasma (Bacteria) nematodes is a large-bodied, wingless Asian species with a small head ornament (Delfosse 2005) and is, therefore, superficially physically similar to *B. bituberculata*; the two species are distinct in morphological detail and biogeography (Westwood 1859: Plate V, figs. 5, 7). Since Günther was very likely to have seen Westwood's plate (Westwood 1859: Plate V, figs. 5, 7) that meticulously illustrates the males of both *B. trophinus* (= *B. bituberculata* (see Brock (2004))) (Fig. 1A) and *R. nematodes* (Fig. 1c), it seems very unlikely that Günther intentionally referred the African specimen to de Haan's Asian species and his identification is more consistent with a nomenclatural *lapsus memoriae* involving these two species' names. Günther's (1953) *Poecilobactron* is a similar *nomen tantum*, a genus-level nomenclatural chimaera arising from misremembering *Thaumatobactron poecilosoma* Günther, 1929 (Bragg and Zompro 2007).

Finally, there is the question of the actual identity of the specimen. The LUS-SAE's specimens are now housed in the Biological Museum, Lund University and the curator of the phasmids very kindly made excellent photographs of the specimen available (Figs 1B, 2). The specimen has four labels (Fig. 2a) confirming its provenance on the LUS-SAE and its determination as *B. nematodes* by Klaus Günther. Morphologically, its shape, proportions and ornamentation (Fig. 1B) are practically identical to those of the males illustrated by Westwood (1859: Plate V, fig. 5), Kirby (1896: Plate XXXIX, fig. 3; redrawn in Brock (2004)) and Brunner von Wattenwyl (1907: Tab. XV, fig. 1) and consistent with the as-

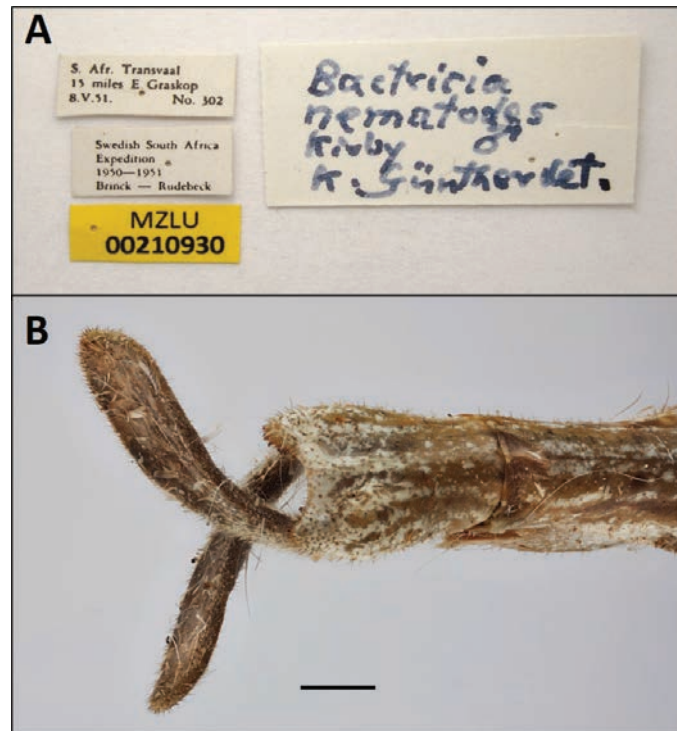


Figure 2. Specimen identified as *Bactricia nematodes* **A** labels **B** abdominal terga 9 and 10, and cerci, dorsal view. Scale bar: 1 mm. (CC BY-NC 2.0 Deed, Lund University Biological Museum: Entomology, downloaded 12 Nov 2023, original photographs and copyright licence available at http://www.flickr.com/search/?user_id=127240649%40N08&text=Bactricia%20spp).

sociated descriptions. What little variation there is lies well within the current concept of this species and its four synonyms (Brock 2004). The large, flat, wide, curved cerci (Figs 1B, 2B) are especially diagnostic in Africa.

This identification is affirmed by the locality data associated with the specimen: “15 miles E Graskop, 8.5. 1951 (loc. nr. 302)” (Günther 1957). In Volume 1 of the series, Brinck and Rudebeck (1955: 95) characterise Locality 302 as, “Fairly fast-running stream, at places forming pools with sandy and stony bottom. Shores overgrown by dense bush and tree vegetation”. The associated map (Brinck and Rudebeck 1955: Map IV) lacks geocoordinates, but overlaying it on a Google Earth Pro (<http://earth.google.com>) satellite image (using Pretoria, Delagoa Bay [= Maputo] and Beitbridge as landmarks) and seeking a likely stream that intercepts a tarred road suggests that the site is near 25°S, 31°E. These details place the specimen within the distribution and typical habitat of *B. bituberculata* (Fig. 3).

Finally, the obverse of the title page of the book containing Günther’s chapter bears its dates of copyright and printing, both 1956, but not an explicit date of publication. ICZN Article 21.3 provides that in such a case the publication date “is the earliest day on which the work is demonstrated to be in existence as a published work”. Evenhuis (2011) established that the book was received in the Lund University Library on 19 March 1957 and it is reasonable to assume that this library would have been amongst the first to obtain a copy because Lund University employed the publication’s editors and housed the specimens that Günther documented. Thus, the earliest known date when this chapter and, in particular, the description of *R. rubrotaeniatus*, was “obtainable” (sensu ICZN Article 8.1.2) is 19 March 1957.



Figure 3. Location of Locality 302, the collecting site of the LUSAE specimen attributed to *Bactricia nematodes* and neighbouring occurrences of *Bactricia bituberculata* in eSwatini and Mpumalanga and Limpopo provinces of South Africa. The dark areas are forest vegetation. ★ (white star) Type locality of *Hyrtacus carinatus* Kirby, 1902 (= *B. bituberculatus* (see Brock (2004))). Scale bar: 50 km.

Conclusion

Bactricia nematodes Kirby, 1894 is a *nomen nudum* and a *nomen tantum*. The specimen associated with this name (Fig. 1B) is a male of *Bactricia bituberculata* (Schaum, 1857).

Acknowledgements

I warmly thank Rune Bygebjerg (Biological Museum, Lund University, Sweden) for photographing the Lund University Expedition specimen; Janaïs Delpont for graphics; and Paul Brock, Denis Brothers, John Midgley and Riaan Stals for valuable advice and comments. Rhodes University facilitated this research logistically.

Additional information

Conflict of interest

The author has declared that no competing interests exist.

Ethical statement

No ethical statement was reported.

Funding

Rhodes University facilitated this research.

Author contributions

The author solely contributed to this work.

Author ORCIDs

Martin H. Villet  <https://orcid.org/0000-0002-4335-5667>

Data availability

All of the data that support the findings of this study are available in the main text. Google Inc. made resources publicly available through Google Search (<https://www.google.com/>) and Google Earth (<https://earth.google.com/>). Photographs of the Lund University Swedish South African Expedition specimen and its labels are available on-line at Flickr http://www.flickr.com/search/?user_id=127240649%40N08&text=Bactricia%20spp.

References

- Bragg PE, Zompro O (2007) Biographies of phasmatologists - 6. Klaus Günther. Phasmid Studies 16: 25–33. <https://www.biodiversitylibrary.org/item/207195>
- Brinck P, Rudebeck G (1955) List of localities investigated by the Swedish Expedition to Southern Africa in 1950–1951. In: Hanström B, Brinck P, Rudebeck G (Eds) South African animal life. Results of the Lund University Expedition in 1950–1951. Vol. 1. Almqvist and Wiksells Boktryckari AB, Goteborg, Uppsala, 62–100.
- Brock PD (2004) Taxonomic notes on giant southern African stick insects (Phasmida), including the description of a new *Bactrododema* species. Annals of the Transvaal Museum 41: 61–77. <https://journals.co.za/doi/epdf/10.10520/EJC83623>
- Brock PD, Büscher TH, Baker E (2023) Phasmida Species File Online. Version 5.0/5.0. <http://Phasmida.SpeciesFile.org> [Accessed December 2, 2023]
- Brunner von Wattenwyl K (1907) Die Insektenfamilie der Phasmiden. II. Phasmidae Anareolatae (Clitumnini, Lonchodini, Bacunculini). Wilhelm Engelmann, Leipzig, 181–340 [pls. VII–XV]. <https://archive.org/details/DieInsektenfamilieDerPhasmiden.Vol.II.PhasmidaeAnareolataeclitumnini>
- Delfosse E (2005) Taxinomie, répartition et élevage du Phasme bâton asiatique *Ramulus nematodes* (de Haan, 1842) (Insecta : Phasmatodea : Phasmatidae) [Taxonomy, distribution and rearing of the asiatic stick insect *Ramulus nematodes* (de Haan, 1842) (Insecta: Phasmatodea: Phasmatidae)]. Le bulletin d'Arthropoda 23: 29–41.
- Evenhuis NL (2011) [Dating of] South African Animal Life (1955–1974). <http://hbs.bishopmuseum.org/dating/safranimlife.html> [Accessed February 12, 2023]
- Günther K (1953) Über die taxonomische Gliederung und die geographische Verbreitung der Insektenordnung der Phasmatodea. Beiträge zur Entomologie 3: 541–563 [figs 1–4]. <https://doi.org/10.21248/contrib.entomol.3.5.541-563>
- Günther K (1957) Phasmatoptera. In: Hanström B, Brinck P, Rudebeck G (Eds) South African Animal life, results of the Lund University expedition in 1950–51. Vol. 3. Almqvist and Wiksells Boktryckari AB, Goteborg, Uppsala, 87–93.
- International Commission on Zoological Nomenclature (ICZN) [Eds] (1999) International code of zoological nomenclature. 4th ed. International Trust for Zoological Nomenclature, London, 306 pp. <https://www.iczn.org/the-code/the-code-online/>
- Kirby WF (1896) VI. On some new or rare Phasmidae in the Collection of the British Museum. Transactions of the Linnean Society of London. 2nd Series: Zoology 6: 447–475 [Plates XXXIX, XL]. <https://doi.org/10.1111/j.1096-3642.1896.tb00546.x>

- Kirby WF (1904) A synonymic catalogue of Orthoptera. Vol. I. Orthoptera Euplexoptera, Cursoria, et Gressoria. (Forficulidae, Hemimeridae, Blattidae, Mantidae, Phasmidae). Trustees of the British Museum (Natural History), London.
- Schoeman AS (1985) Order Phasmatodea (stick insects, walking sticks, leaf insects). In: Scholtz CH, Holm E (Eds) Insects of Southern Africa. Butterworths, Durban, 96–98.
- Westwood JO (1859) Catalogue of orthopterous insects in the collection of the British Museum. Part I. Phasmidæ. Trustees of the British Museum (Natural History), London, 1–195[, Plates I–XL, 1–8]. <https://doi.org/10.5962/bhl.title.65981>

A new species of the genus *Ropalidia* Guérin-Méneville from central Africa (Insecta, Hymenoptera, Vespidae)

Ozren Polašek^{1,2}

¹ University of Split, School of Medicine, Split, Croatia

² Algebra University College, Zagreb, Croatia

Corresponding author: Ozren Polašek (ozren.polasek@mefst.hr)

Abstract

Ropalidia chromis **sp. nov.** is described from the Democratic Republic of the Congo. It is characterized by a mixture of morphological features present in two large species groups of that genus, suggesting a separate phylogenetic lineage.

Key words: Social wasp, systematics, taxonomy

Introduction

Ropalidia Guérin-Méneville is a social-wasp genus distributed in the Ethiopian, Oriental and Australian regions, with 49 known African mainland species (Carpenter 1999; Kojima 1999; Polašek et al. 2022; Polašek et al. in press). The hallmark of the genus is the merged second tergum and sternum, with the exception of three species endemic to the New Guinea mainland that have overlapping sclerites (Kojima 2001).

Most of the African mainland species are divided into the *capensis*-group and the non-*capensis*-group of species, based on their morphology and genetic analysis, with only a few less common species with separate lineages (Polašek et al. in press).

A recent revision (Polašek et al. in press) identified an interesting pattern of increasing yellow or reddish colour and weaker punctation in eastern parts of Africa, as opposed to the primarily black body colour and much coarser punctation in western and central Africa. This pattern was seen across species but also in the intra-specific clusters of *R. guttatipennis* (de Saussure) and *R. aethiopica* (du Buysson), which both become darker or even black in Cameroon, Gabon and the Democratic Republic of the Congo.

This paper reports on a new species from the Democratic Republic of the Congo, characterized by a mixture of morphological features of two species groups of *Ropalidia*.



Academic editor: Denis Brothers

Received: 15 March 2023

Accepted: 15 December 2023

Published: 28 February 2024

ZooBank: <https://zoobank.org/E6D6D40F-815B-4EEF-BB9E-B75583FCF4AF>

Citation: Polašek O (2024) A new species of the genus *Ropalidia* Guérin-Méneville from central Africa (Insecta, Hymenoptera, Vespidae). African Invertebrates 65(1): 9–14. <https://doi.org/10.3897/AfrInvertebr.65.103539>

Copyright: © Ozren Polašek.

This is an open access article distributed under terms of the Creative Commons Attribution License (Attribution 4.0 International – CC BY 4.0).

Material and methods

A single dried specimen from the California Academy of Sciences in San Francisco, USA (CAS) collection was studied and photographed using Leica S9i stereoscopic microscope with an integrated camera. Photographs were stacked using Helicon 6.8.0 (Kharkiv, Ukraine). Metasomal terga, metasomal sterna and flagellomeres are abbreviated as T, S and AF, respectively.

Results

Ropalidia chromis Polašek, sp. nov.

<https://zoobank.org/40D46CC1-0288-4394-92D1-8BAD73076D05>

Figs 1–6

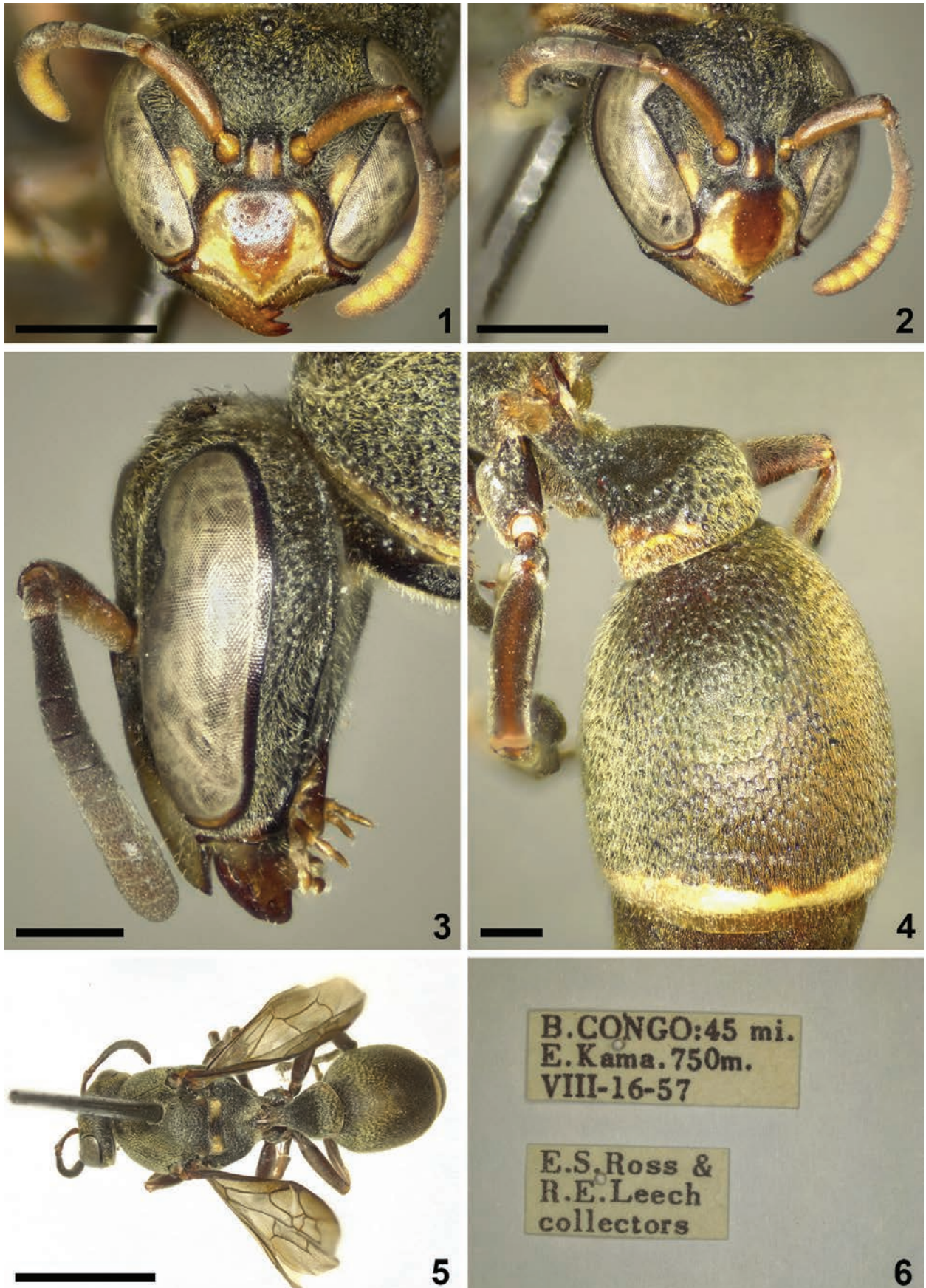
Material examined. Holotype: [Belgian] Congo: 45 mi. E Kama [Province of Maniema, DR Congo], 750 m, VIII-16-57/E.S. Ross & R.E. Leech collectors (California Academy of Sciences; Fig. 6); 1♀.

Diagnosis. This species is characterized by the basal cuticular sculpture and larger sparse punctures of the female clypeus, the substantially depressed area above the antennal sockets, elongated scape, thin gena, silvery-yellowish pubescence and setae of the head, mesosoma and metasoma, with angulate and coarsely punctate T1.

Description. Female. Wing length: 8.9 mm.

Head. Head in frontal view barely wider than high (Fig. 1). Clypeus about as wide as long (Fig. 1). Juxtamandibular lobes weakly developed, with shallow excavation (Fig. 1). Clypeal apex projecting well above juxtamandibular lobes, with acute tip (Fig. 1). Clypeus surface with basal sculpture and evenly spaced and well-defined smaller punctures (biphasic punctation pattern), thus resembling numerous *Polistes* Latreille species, but not *Ropalidia* (Fig. 1). Lower half of inner orbit impunctate, upper half with large and coarse punctures (Figs 1, 2). Entire area above antennal sockets markedly depressed; clypeal surface very flattened in lateral view (Fig. 2). Interantennal area elevated and flattened, covered by a punctation same as on clypeus (Fig. 1). Frons coarsely punctate, with weakly bent silvery-yellowish setae that are somewhat shorter than ocellar diameter (Fig. 3). Gena coarsely punctate, punctures diminished close to the occipital carina (Fig. 3). Gena at most half width of the compound eye (Fig. 3). Occipital carina sinuate and complete, reaching mandible (Fig. 3). Interocellar area raised posteriorly, with punctuation similar to that on frons; distance between posterior ocelli about 1.7× as long as distance between anterior and posterior ocellus. Distance between posterior ocellus and occipital carina as long as 0.6× of distance between posterior ocellus and inner eye margin. Eyes aetose (Fig. 2). Scape conspicuously elongate, about twice as long as AF1. AF2 as long as wide (Fig. 1), remaining flagellomeres wider than long; AF8 about twice as wide as long (Fig. 2).

Mesosoma. Mesosoma about 1.4× as long as wide. Pronotal carina complete and sharp, about equally wide laterally and dorsally, broadly rounded on humerus. Pronotum largely and coarsely punctate, punctures merge and create a punctation network close to inferior pronotal angle. Mesonotum 1.15 × as long as wide between tegulae in dorsal view, distinctly convex in



Figures 1–6. *Ropalidia chromis* sp. nov., female 1 head, frontal view 2 head, oblique view 3 head, lateral view 4 T1 and T2, lateral view 5 habitus, dorsal view 6 holotype labels.

Table 1. Comparative analysis of morphology and colouration pattern.

| Feature | <i>capensis</i> -group | <i>R. chromis</i> sp. nov. | non- <i>capensis</i> -group |
|--|--|----------------------------|---|
| Size (wing length) | 6.2–8.5 mm | 8.9 mm | 8.5–12.1 mm |
| Clavate female antenna (AF8 width to length) | Yes (2.0×) | Yes (2.0×) | No (up to 1.5×) |
| Scape to AF1 ratio | Commonly 1.5× | 2× | Commonly of equal length |
| AF2 | Commonly about as wide as long | About as wide as long | Commonly longer than wide |
| T1 punctation and shape | Weak, commonly globular | Strong, angular | Weak, rounded |
| The lower part of the inner orbit | Impunctate | Impunctate | Frequently punctate |
| Supraantennal area | Flattened | Depressed | Flattened |
| Interantennal area | Ridged | Flattened | Ridged |
| Clypeus punctation | Monophasic | Biphasic | Monophasic |
| Gena thickness | Commonly less than eye width (as low as 0.5× in <i>R. crassipunctata</i> Giordani Soika) | 0.5× eye width | Commonly equal, sometimes even broader than the eye width |
| Inferior propodeal carina | Not developed | Not developed | Commonly developed |
| Elongated second submarginal cell | No | Yes | Yes |
| Predominant clypeus colour pattern | Centrally attached spot | Centrally attached spot | Transversal apical yellow line |

lateral view, so that anterior third is below level of posterior margin. Median mesonotal suture thin and elongate, reaching more than half of mesonotum length. Mesonotum sparsely and shallowly punctate, punctures more than one diameter apart, shrinking in size towards scutellum. Scutellum flattened, without median carina, coarsely punctate, punctures about twice as large as those on mesonotum. Metanotum flattened and as wide as scutellum, anterior two thirds coarsely punctate, posterior third inflexed downwards and shiny; lateral metanotal angles rounded, but well-developed. Mesopleuron markedly convex, very coarsely punctate, punctures become reticulate dorsally; epicnemial carina very well developed and dull. Metapleuron with very large and shallow punctures close to anterior margin; punctures become smaller laterally, only to increase in size on lateral side of propodeum. Dorsal propodeal carina weakly developed and barely visible underneath pubescence, without inferior carina. Propodeal excavation shallow, shallowly punctate dorsally, impunctate and weakly striated ventrally. Entire mesosoma covered by short silvery-yellow pubescence (about half length of anterior ocellus diameter), with somewhat longer whitish setae on propodeal excavation. Second submarginal cell wide, with elongate median angle.

Metasoma. T1 about half width of T2 in dorsal view, strongly angulate in lateral view, enclosing angle of about 110° (Fig. 4). Anterior half dorsally inconspicuously, minutely punctate, laterally deeply and coarsely punctate. T2 1.2× as long as wide, with parallel sides. T2 and S2 shallowly punctate, with punctures gradually increasing and becoming large and coarse in centre of S2. T2 lamella yellow and translucent (Fig. 4). T2 covered by golden pubescence and yellowish protruding setae that extend over the lamella (Fig. 4).

Colour. Basal colour black (Fig. 1). Clypeus tricolourous, with black border, brown basally attached median spot nearly reaching apex, yellowish-white laterally (Fig. 2). Smaller yellowish spot adjacent to inner orbit, reddish-yellow interantennal area, mandible whitish with brown tip and blackish basal area (Figs 2, 3). Scape

dark brown dorsally, ferruginous ventrally (Fig. 2). Flagellum dorsally blackish, ventrally reddish, with several distal segments orange ventrally (Fig. 3). Pronotum with thin yellow line underneath carina (Fig. 4), scutellum faint reddish postero-laterally, metanotum with two large yellow spots occupying two thirds of total surface, propodeum entirely black (Fig. 1). Legs black, femora with thin reddish line on inner side; tarsi somewhat darker. Wings infuscated, with moderate darkening in tip of basal cell and majority of marginal cell (Fig. 5). T1 with reddish-yellow triangular mark laterally (Fig. 5). T2 with complete posterior yellow band, S2 with partial posterior band (interrupted medially); remaining terga and sterna black.

Male is unknown.

Etymology. The name is a Latinized form of “chrome”, a noun in apposition, with reference to the silvery-yellowish setae and pubescence of the head, mesosoma and metasoma.

Distribution. Democratic Republic of the Congo.

Comparative analysis. This species exhibits features seen in both *capensis*- and non-*capensis*-groups (Table 1). In addition, several features do not resemble either and present apparently autapomorphic features sufficient for species determination, including the depressed area above the antennal socket and a biphasic clypeus punctation (Table 1).

Discussion

The newly described species presents an interesting dilemma, since it does not seem to belong to either of the two large species groups within *Ropalidia*. In addition, it has several unique features, suggesting a separate lineage. Interestingly, it exhibits a homoplastic feature of clypeal punctation with *Polistes* Latreille, while the general appearance substantially resembles Eumeninae, with thin gena and depressed supraantennal area.

Interestingly, both colour and morphology of this species follow the east-west pattern previously described in other African *Ropalidia*, namely a darker basal body colour and stronger punctation in western and central Africa (Polašek et al. in press). In addition, several morphological features present in *R. chromis* sp. nov. are found in other species that are exclusively present in this part of Africa. These include angulate and strongly punctate T1 (present in *R. salebrosa*, a newly described species in Polašek et al., in press), coarser T2 punctation (similar to *R. crassipunctata* Giordani Soika), thin gena (also in *R. crassipunctata*) and a very strongly punctate mesopleuron (also present in *R. brazzai* du Buysson). This suggests converging evolutionary processes that seem to favour such features.

Acknowledgements

Brian L. Fisher, Robert L. Zuparko and Christopher Grinter are acknowledged for the loan of *Ropalidia* specimens from the California Academy of Sciences collection.

Additional information

Conflict of interest

The author has declared that no competing interests exist.

Ethical statement

No ethical statement was reported.

Funding

No funding was reported.

Author contributions

The author solely contributed to this work.

Data availability

All of the data that support the findings of this study are available in the main text.

References

- Carpenter JM (1999) Taxonomic Notes on Paper Wasps (Hymenoptera: Vespidae; Polistinae). *American Museum Novitates* 3259: 1–44.
- Kojima J (1999) Male genitalia and antennae in an Old World paper wasp genus *Ropalidia* Guérin-Méneville, 1831 (Insecta: Hymenoptera; Vespidae, Polistinae). *Natural History Bulletin of Ibaraki University* 3: 51–68.
- Kojima J (2001) *Ropalidia* wasps (Insecta: Hymenoptera; Vespidae, Polistinae) in New Guinea and its adjacent islands (first part). *Natural History Bulletin of Ibaraki University* 5: 31–60.
- Polašek O, Bellingan T, van Noort S (2022) A new species of paper wasp from the genus *Ropalidia* Guérin-Méneville from South Africa (Hymenoptera, Vespidae). *Journal of Hymenoptera Research* 90: 213–222. <https://doi.org/10.3897/jhr.90.81581>
- Polašek O, Onah I, Kehinde T, Rojo V, van Noort S, Carpenter JM (in press) Revision of the mainland African species of the Old World social wasp genus *Ropalidia* Guérin-Méneville 1831 (Hymenoptera; Vespidae). *Zootaxa*.

Uncovering the hidden diversity of non-biting midges (Diptera, Chironomidae) from central Namibia, using morphology and DNA barcodes

Viktor Baranov¹, Xiaolong Lin², Jeremy Hübner³, Caroline Chimeno³

¹ Estación Biológica de Doñana-CSIC/Doñana Biological Station-CSIC, Seville, Spain

² Engineering Research Center of Environmental DNA and Ecological Water Health Assessment, Shanghai Ocean University, Shanghai 201306, China

³ Bavarian State Collection of Zoology (SNSB-ZSM), Munich, Germany

Corresponding author: Viktor Baranov (viktor.baranov@ebd.csic.es)

Abstract

The first study results on the Chironomidae fauna of central Namibia (Khomas, Otjozondjupa and Hardap regions) are presented, based on morphology and DNA-barcoding. The preliminary investigation led to the discovery of a new species *Paraphaenocladus namibiae* sp. nov. (Chironomidae, Orthoclaadiinae) and 17 new country records for Namibia.

Key words: Biodiversity, DNA barcoding, first records, integrative taxonomy, new species



Academic editor: Burgert Muller

Received: 30 August 2023

Accepted: 3 April 2024

Published: 29 April 2024

ZooBank: <https://zoobank.org/CD3A2816-4574-42F6-AF5D-442E232B4239>

Citation: Baranov V, Lin X, Hübner J, Chimeno C (2024) Uncovering the hidden diversity of non-biting midges (Diptera, Chironomidae) from central Namibia, using morphology and DNA barcodes. African Invertebrates 65(1): 13–36. <https://doi.org/10.3897/AfrInvertebr.65.111920>

Copyright: © Viktor Baranov et al.
This is an open access article distributed under terms of the Creative Commons Attribution License (Attribution 4.0 International – CC BY 4.0).

Introduction

Non-biting midges (Chironomidae) are an integral part of aquatic and terrestrial ecosystems across the world. They perform vital ecosystem functions, including the connection of wetlands with their surrounding areas via the transfer of matter and energy (Gratton et al. 2008). This function is especially important in arid landscapes, where there are few other sources of organic matter (Zinchenko et al. 2014). Namibia is a very arid country and this poses a major challenge to the country's economy (Reid et al. 2007). Therefore, studying the wetlands' contribution to the productivity and functioning of ecosystems in Namibia is of utmost importance for the management of all other ecosystems in the region. In 2018, on the initiative of the NCRST (National Commission on Research, Science, and Technology of Namibia) a collective collection permit was issued to the Participants of the 9th International Congress of Dipterology, held in Windhoek. The aim of this permit and research project was to support and improve the knowledge of the Namibian dipteran fauna for the benefit of basic- and applied research, and for Namibia itself.

We present the first results of our investigation on the Chironomidae fauna of central Namibia (Khomas, Otjozondjupa and Hardap regions). These are based on morphological and molecular (using DNA barcoding) assessments of the material collected in 2018. This preliminary investigation has led to the discovery of a previously unknown *Paraphaenocladus* (Chironomidae, Orthoclaadiinae), *P. namibiae* sp. nov., and 17 new country records for Namibia.

Materials and methods

Collection sites

Specimens were collected from the Khomas, Otjozondjupa and Hardap regions of central Namibia between 27 November – 8 December 2018, under the collective research permit issued by NCRST (authorization number AN20181007).

Specimens were collected by either sweep netting the vegetation, collecting exuviae and larvae with aquatic hand nets, Malaise traps, or light traps (see Suppl. material 1 for the details) (Figs 1A–D, 2A–D). All insect material was then exported to Germany for processing under an export permit issued by the Ministry of Environment and Tourism of Namibia (Number 119666). The material is now deposited in the natural history collection of the National Museum of Namibia in Windhoek (NMNW) and the College of Fisheries and Life Science, Shanghai Ocean University, Shanghai, China (SHOU). BOLD TaxonID Tree is available as Suppl. material 2.

Morphological identification and material handling

We are following the morphological terminology of Sæther (1980). Specimens were mounted in Hydromatrix (Micro Tech Lab GmbH) and Euparal, as per standard procedures for mounting small Diptera (Kirk-Spriggs 2017). Specimens were then identified using the following keys: Freeman 1953, 1954a, b, c, 1955a, b, 1956, 1957, 1958; Lehmann 1979, 1981; Ekrem 2001; Ekrem et al. 2017; Gilka 2009; Andersen and Mendes 2010; Ferrington and Sæther 2011).

All slides were imaged using a Keyence VHX-6000 digital microscope, either using ring light- or cross-polarized coaxial illumination (Haug et al. 2008). The resulting images consist of vertical stacks and horizontal composites done with inbuilt microscope software (in case of VHX-6000) or PHOTOSHOP ELEMENTS CS 11 panorama functionality and PICOLAY open software (<http://www.picolay.de>).

DNA barcoding

Part of the sample was barcoded, with vouchers recovered afterwards. In the laboratory, we transferred the specimens to 96-well plates for processing via DNA barcoding. Lysis was performed at 56 °C for two hours only to ensure that all specimens remain undamaged. Then, we extracted the DNA using the NucleoSpin 96 Tissue Core Kit following the manufacturer's guidelines. We amplified the COI barcode region using the standard barcoding primers LepF1 and LepR1 (Ivanova and Grainger 2007).

The cleaned-up PCR products were sent to the LMU Sequencing Service at Biozentrum (Martinsried, Germany) for Sanger sequencing. Every specimen's COI barcode was sequenced as a forward and reverse strand. The traces were edited in BIOEDIT (Hall 1999), and a consensus sequence of the forward and reverse strands was obtained to be uploaded as a barcode to Barcode of Life Data System (BOLD, <http://www.boldsystems.org/>) (Ratnasingham and Hebert 2007). The original traces were uploaded as well. In addition, genomic DNA of a few specimens was extracted from the thorax or skin of larvae using Qiagen DNA Blood and Tissue Kit at the Shanghai Ocean University, Shanghai, China.

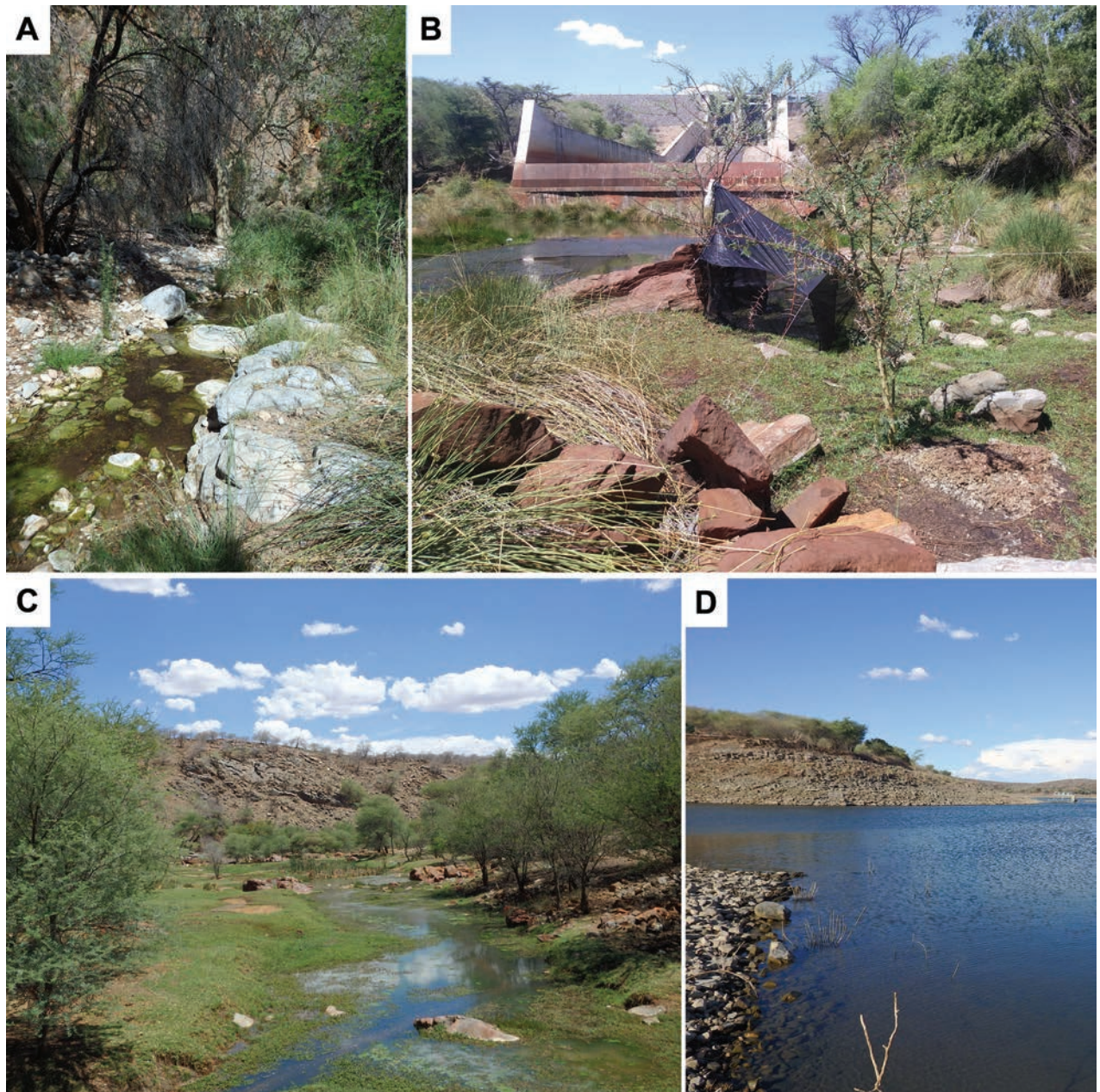


Figure 1. **A–D** photographs of the collection sites involved in this study **A** Naukluft Mountain Zebra Park, Tufa waterfalls; 24°15'47.88"S, 16°13'44.76"E; 1 Dec. 2018 **B** Malaise trap deployed at Von Bach Dam Nature Reserve, Swakop river outflow; 22°0'53.28"S, 16°57'12.24"E; 2 Dec. 2018; facing towards the dam **C** Von Bach Dam Nature Reserve, Swakop river outflow, river valley; 22°0'53.28"S, 16°57'12.24"E; 2 Dec. 2018; facing away the dam **D** Von Bach Dam Nature Reserve, immediately above the dam; 2 Dec. 2018; 22°0'53.28"S, 16°57'12.24"E.

PCR amplifications of DNA barcodes, with the universal primers LC01490 and HCO2198 (Folmer et al. 1994), were performed following the protocol from Lin et al. (2018). Sanger sequencing of the purified PCR products was conducted on the ABI 3730 at the BGI Genomic group (Beijing, China). Besides this, we also sent tissue samples of several specimens to the Canadian Centre for DNA Barcoding (CCDB, University of Guelph, Canada) using standard high throughput protocols (Hebert et al. 2018) to generate COI barcodes. In total, the 116 specimens successfully sequenced were added to the project on the Chironomidae of Namibia (<http://dx.doi.org/10.5883/DS-NAMCHIR>).



Figure 2. A–D photographs of the collection sites involved in this study **A** Windhoek, Arebbusch river 22°34'28.92"S, 17°3'15.84"E; 3 Dec. 2018 **B** Windhoek, Arebbusch river, Goreangab Reservoir; 22°31'44.4"S, 17°0'3.6"E; 3 Dec. 2018 **C** Windhoek, Arebbusch river; 22°34'28.92"S, 17°3'15.84"E; 3 Dec. 2018 **D** Windhoek, Arebbusch river; 22°34'28.92"S, 17°3'15.84"E.

Results

Examination of the material has yielded 23 species and morphotypes of Chironomidae, with one of them being undescribed, and 17 new country-level records for Namibia.

Tanypodinae Thienemann & Zavřel, 1916

Tanypus guttatipennis Goetghebuer, 1935

Fig. 3A, B

Material examined. NAMIBIA • 1♂; HARDAP; Naukluft Mountain Zebra Park, Tufa waterfalls; 24°15'47.88"S, 16°13'44.76"E; 1 Dec. 2018; G. M. Kwifte leg.; sweep net; NMNW (Fig. 1A).

Distribution. This is the first record of this species from Namibia, the species is otherwise widely distributed in the Afrotropical Region with records from Uganda, Democratic Republic of the Congo and South Africa (Freeman 1961; Freeman and Cranston 1980; Curtis 1991; Harrison 2004; Ashe and O'Connor 2009). No specimens of this species were successfully barcoded as a part of this project.



Figure 3. *Tanypus guttatipennis*, male A wing B hypopygium.

Orthoclaadiinae Lenz, 1921

Bryophaenocladus cristatus Wang, Sæther & Andersen, 2002

Fig. 4A–C

Material examined. NAMIBIA • 1♂; OTJOZONDJUPA; Von Bach Dam Nature Reserve, Swakop river outflow; 22°0'53.28"S, 16°57'12.24"E; 2–10 Dec. 2018; V. Baranov leg.; Malaise trap; NMNW (Fig. 1B–D). No specimens of this species were successfully barcoded as a part of this project.

Distribution. This is the first record of this species from Namibia, and outside of the species' type location in Ghana (Wang et al. 2002; Harrison 2004; Ashe and O'Connor 2012).

Corynoneura dewulfi Goetghebuer, 1935

Material examined. NAMIBIA • 5♂1♀; HARDAP; Naukluft Mountain Zebra Park, Tufa waterfalls; 24°15'47.88"S, 16°13'44.76"E; 1 Dec. 2018; G.M. Kwife leg.; sweep net; NMNW.

No specimens of this species were successfully barcoded as a part of this project.

Distribution. This is the first record of the species from Namibia (Freeman 1956; Freeman and Cranston 1980; Curtis 1991; Harrison 2004; Ashe and O'Connor 2012). The species is otherwise known from D.R. Congo, Ethiopia, South Africa, Tanzania, Uganda and Zimbabwe (Ashe and O'Connor 2012).

Cricotopus flavozonatus Freeman, 1953a

Fig. 4D, E

Material examined. NAMIBIA • several hundred ♂♀; HARDAP; Naukluft Mountain Zebra Park, Tufa waterfalls; 24°15'47.88"S, 16°13'44.76"E; 1–5 Dec. 2018; G. M. Kwife/V. Baranov/X. Lin leg.; sweep net; NMNW; SHOU; BOLD specimen code: NAM14, NAM04, NAM13, NAM12; BOLD sequence ID: NAMCH024-20, NAMCH023-20, NAMCH017-20, NAMCH006-19; BOLD BIN: BOLD:ACG906 •1♂ 2♀; KHOMAS; Windhoek; 22°36'43.2"S, 17°5'27.6"E; 1 Dec. 2018; G. M. Kwife/V.

Baranov/X. Lin leg.; NMNW; BOLD specimen code: NAM-Chiro31, NAM-Chiro32; BOLD sequence ID: NAMOE031-22, NAMOE032-22; BOLD BIN: BOLD:ACG9062.

Distribution. This is the first record of the species from Namibia. *Cricotopus flavozonatus* was previously recorded from Ethiopia, Uganda, South Africa, and Zimbabwe (Freeman 1956; Freeman and Cranston 1980; Curtis 1991; Harrison 2004; Ashe and O'Connor 2012).

***Cricotopus obscurus* Freeman, 1953**

Material examined. NAMIBIA • 3♂; KHOMAS; Windhoek, Arebbusch river; 22°34'28.92"S, 17°3'15.84"E; 7 Dec. 2018; G.M. Kvitte leg.; sweep net; NMNW; 119♂♀; OTJOZONDJUPA; Von Bach Dam Nature Reserve, Swakop river outflow; 22°0'53.28"S, 16°57'12.24"E; 2 Dec. 2018; V. Baranov leg.; sweep net; NMNW • 115♂♀; OTJOZONDJUPA; Von Bach Dam Nature Reserve, Swakop river outflow; 22°0'53.28"S, 16°57'12.24"E; 2–10 Dec. 2018; V. Baranov leg.; Malaise trap; NMNW • 1♂; OTJOZONDJUPA; Gross Barmen; 22°6'38.16"S, 16°44'42"E; 4 Dec. 2018; X. Lin leg.; sweep net; SHOU; No specimens of this species were successfully barcoded as a part of this project.

Distribution. Species is present in Namibia (Harrison 2004). Lesotho, South Africa, Zimbabwe, Senegal (uncertain) (Ashe and O'Connor 2012).

***Cricotopus scottae* Freeman, 1956**

Fig. 4F

Material examined. NAMIBIA • 1♂14♀; KHOMAS; Windhoek, Arebbusch river, Goreangab Reservoir; 22°31'44.4"S, 17°0'3.6"E; 3 Dec. 2018; X. Lin leg.; sweep net; SHOU; BOLD specimen code: NAM-Chiro7; BOLD sequence ID NAMOE007-22; BOLD BIN: BOLD:ADM9835 • 1♂1♀; OTJOZONDJUPA; Düsternbrook; 22°15'11.52"S, 16°54'1.44"E; 4 Dec. 2018; G.M. Kvitte leg.; sweep net; SHOU • 8♂1♀, 1 larva; OTJOZONDJUPA; Von Bach Dam Nature Reserve, Swakop river outflow; 22°0'53.28"S, 16°57'12.24"E; 2–10 Dec. 2018; V. Baranov leg.; Malaise trap; NMNW; BOLD specimen code: NAM-Chiro13, NAM-Chiro12; BOLD sequence ID: NAMOE013-22, NAMOE012-22; BOLD BIN: BOLD:ADM9835, BOLD:ACL1477; both, males and females, were barcoded (Fig. 6F).

Distribution. Species is present in Namibia (Harrison 2004). Species is otherwise known from Chad, D.R. Congo, Ethiopia, Niger, Nigeria, South Africa, Zimbabwe (Ashe and O'Connor 2012).

***Limnophyes* sp.**

Material examined. NAMIBIA • 1♂; KHOMAS; Windhoek, Arebbusch river, Goreangab Reservoir; 22°31'44.4"S, 17°0'3.6"E; 3 Dec. 2018; X. Lin leg.; sweep net; SHOU; BOLD specimen code: NAM85; BOLD: sequence ID: NAMCH069-19; BOLD BIN: BOLD:ACK4381.

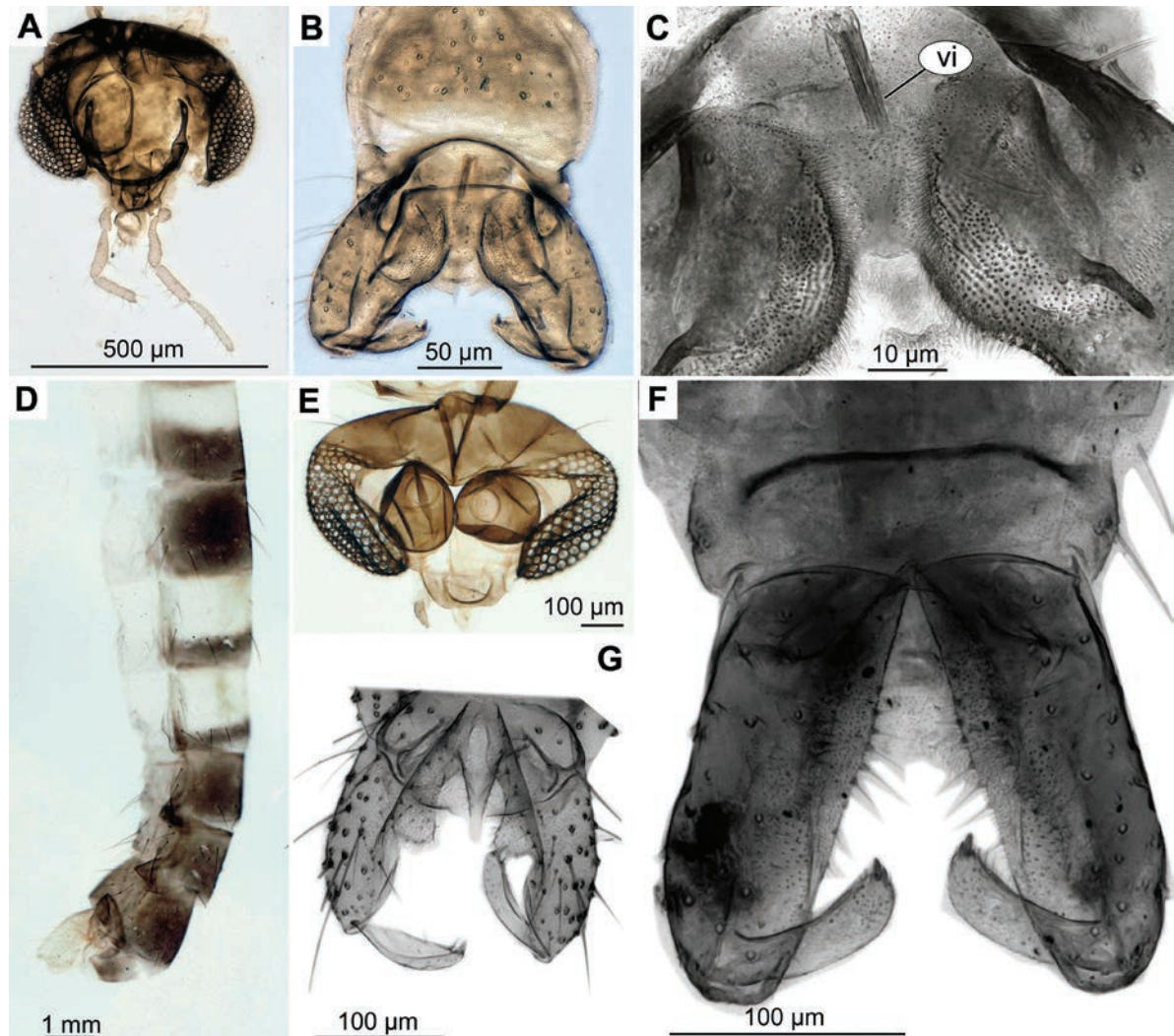


Figure 4. Orthoclaadiinae **A–C** *Bryophaenocladius cristatus* **D, E** *Cricotopus flavozonatus* **F** *Cricotopus scottae* **G** *Parametriocnemus scotti* **A, E** head, adult male **B, D, F, G** hypopygium **C** virga.

This is the first record of genus *Limnophyes* from Namibia (Freeman 1956; Freeman and Cranston 1980; Curtis 1991; Harrison 2004; Ashe and O'Connor 2012).

***Parametriocnemus scotti* (Freeman, 1956)**

Fig. 4G

Material examined. NAMIBIA • 8♂2♀, 1 larva; HARDAP; Naukluft Mountain Zebra Park, Tufa waterfalls; 24°15'47.88"S, 16°13'44.76"E; 1 Dec. 2018; G. M. Kvitte/V. Baranov, X. Lin leg.; Malaise trap; NMNW; BOLD specimen code: NAM37; NAM19; NAM-Chiro30; NAM-Chiro29; BOLD sequence ID NAMCH046-20; NAMOE030-22; NAMOE029-22; NAMCH007-19 BOLD:ADY1682.

Distribution. This is the first record of this species from Namibia (Freeman 1956; Freeman and Cranston 1980; Curtis 1991; Harrison 2004; Ashe and O'Connor 2012). The species is otherwise known from Ethiopia, Kenya, Madagascar, South Africa, Uganda, Zambia and Zimbabwe (Ashe and O'Connor 2012).

***Pseudosmittia unniae* Ferrington & Sæther, 2011**

Figs 5A–D, 6A–E

Material examined. NAMIBIA • 1♂1♀; KHOMAS; Windhoek, Arebbusch river, Goreangab Reservoir; 22°31'44.4"S, 17°0'3.6"E; 3 Dec. 2018; X. Lin leg.; sweep net; SHOU; BOLD specimen code NAM86 BOLD sequence ID NAMCH072-20; NAMCH070-20 BOLD BIN BOLD:ADW9545; BOLD:ACK7891 • 2♂; OTJOZONDJUPA; Von Bach Dam Nature Reserve, Swakop river outflow; 22°31'44.4"S, 17°0'3.6"E; 2–10 Dec. 2018; Malaise trap; V. Baranov leg.; NMNW; BOLD specimen code: NAM81, NAM89, BOLD sequence ID NAMCH065-20, NAMCH072-20, BOLD BIN: BOLD:ADW9545 • 9♂1♀, OTJOZONDJUPA; Gross Barmen; 22°6'38.16"S, 16°44'42"E; 4 Dec. 2018; X. Lin leg.; sweep net; SHOU; BOLD specimen code NAM61, NAM60, NAM59, NAM-Chiro51, NAM-Chiro50, NAM-Chiro49, NAM-Chiro48, NAM-Chiro45; BOLD sequence ID: NAMCH051-20, NAMCH050-20, NAMCH0549-20, NAMOE051-22, NAMOE050-22; NAMOE049-22, NAMOE048-22, NAMOE045-22, NAMOE044-22; BOLD BIN BOLD:AEG0717; BOLD:ADW9545.

Distribution. This is the first record of this species from Namibia (Ferrington and Sæther 2011; Ashe and O'Connor 2012). Comparison of current sequences with existing BINs on the BOLD system has shown the presence of this species also in South Africa.

***Psectrocladius* cf. *schlienzi* Wülker, 1956**

Material examined. NAMIBIA • 1♂; OTJOZONDJUPA; Gross Barmen; 22°6'38.16"S, 16°44'42"E; 4 Dec. 2018; X. Lin leg.; sweep net; SHOU; BOLD specimen code: NAM65; BOLD sequence ID: NAMCH055-20; BOLD BIN: BOLD:ACK4896.

Distribution. This is the first record of the species from Namibia, but numerous representatives of the same BIN were previously recorded from South Africa (BOLD: ACK4896, Freeman 1956; Freeman and Cranston 1980; Curtis 1991; Harrison 2004; Ashe and O'Connor 2012). It is worth noting that this species is otherwise distributed in the Palaearctic (Austria, Denmark, Finland, Germany, United Kingdom, Italy, Moldova, Mongolia, Netherlands, Norway, Portugal, Slovakia, Spain, Sweden, Switzerland) (Ashe and O'Connor 2012). It is, therefore, worth considering that the specimen that we have found belongs to a yet undescribed species of *Psectrocladius* related to *P. schlienzi*. More material is needed before we can test this hypothesis.

***Paraphaenocladus* Thienemann, 1924**

***Paraphaenocladus impensus* (Walker, 1856)**

Material examined. NAMIBIA • 1♂; KHOMAS; Windhoek, Arebbusch river, Goreangab Reservoir; 22°31'44.4"S, 17°0'3.6"E; 3 Dec. 2018; X. Lin leg.; sweep net; SHOU; BOLD specimen code: NAM83; BOLD sequence ID: NAMCH067-20; BOLD BIN: BOLD:ACK2655; .

Distribution. This is the first record of the species from Namibia, but numerous representatives of the same BIN were previously recorded from South

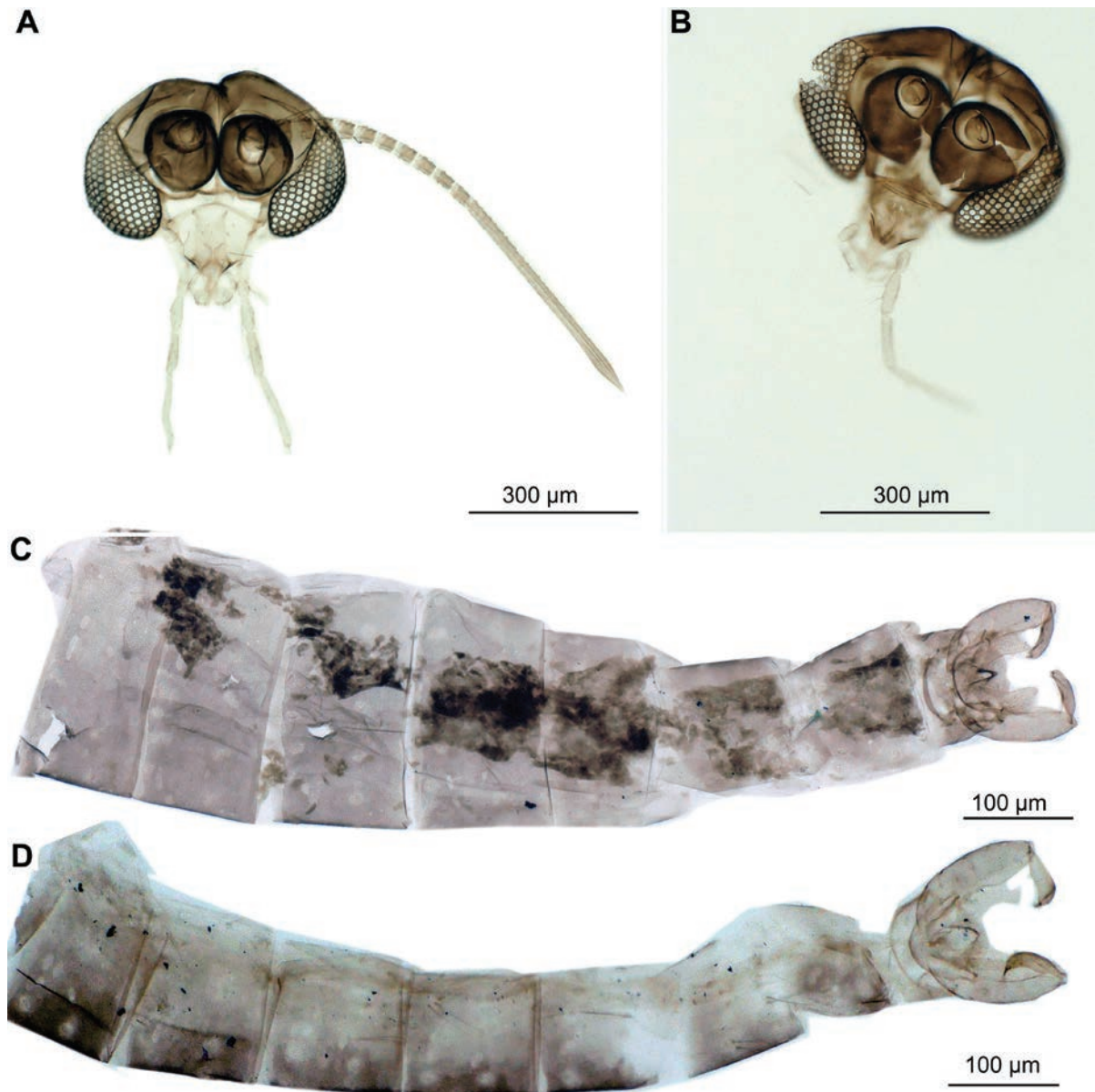


Figure 5. *Pseudosmittia unniae* adult male **A, B** heads **C, D** abdomens with hypopygium.

Africa (BOLD:ACK2655, Freeman 1956; Freeman and Cranston 1980; Curtis 1991; Harrison 2004; Ashe and O'Connor 2012). The species is otherwise known from the multiple countries in the Palearctic, Nearctic and Oriental regions. This is the first Afrotropical record (although the species is recorded from Palearctic parts of the African continent, i.e. Algeria) (Ashe and O'Connor 2012).

***Paraphaenocladus namibiae* Baranov, sp. nov.**

<https://zoobank.org/C91D58C6-2C92-4590-815E-AF68B47010E5>

Figs 7A–C, 8A, B

Material examined. Holotype. Namibia • 1♂; HARDAP; Naukluft Mountain Zebra Park, Tufa waterfalls; 24°15'47.88"S, 16°13'44.76"E; 1 Dec. 2018; V. Baranov leg.; sweep net; Holotype is deposited at NMNW.

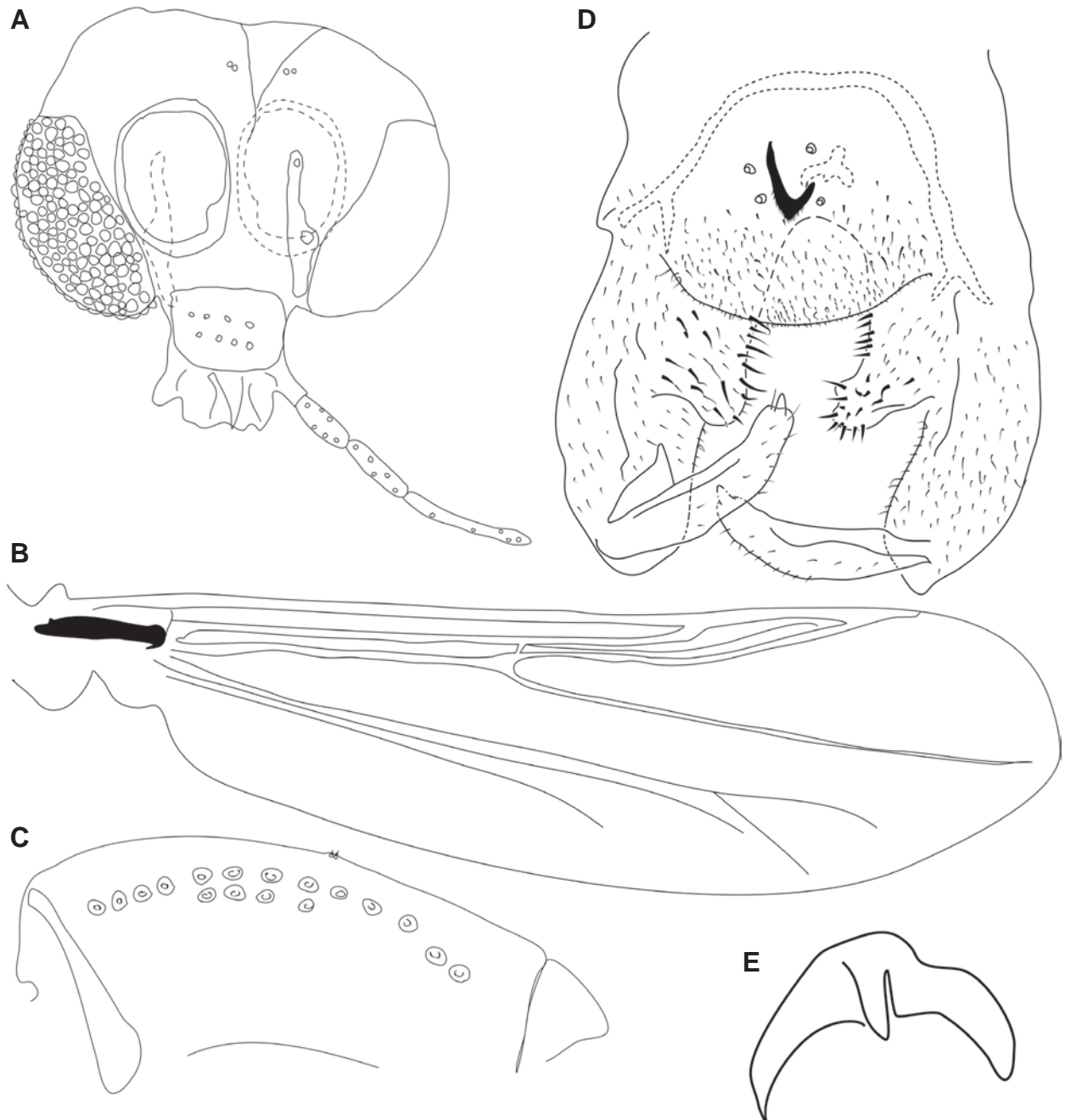


Figure 6. *Pseudosmittia unniae* adult male A Head B wing C scutum D hypopygium E virga.

Paratypes. NAMIBIA • 2♀; HARDAP; Naukluft Mountain Zebra Park, Tufa waterfalls; 24°15'47.88"S, 16°13'44.76"E; 1 Dec. 2018; V. Baranov leg.; sweep net; NMNW; BOLD specimen codes: NAM-Chiro27; NAM-Chiro28; BOLD sequence ID: NAMOE027-22, NAMOE028-22. (poorly preserved, used in barcoding, vouchers non-recovered).

Both sequences were of lower quality, providing rather inconclusive barcode-based identification (See Suppl. material 1). The closest match in BOLD v.4 database was *Corynoneura* sp. (private record), with match of the barcode of 87.99% (Suppl. material 3).

Diagnosis. Differs from all other known species of *Paraphaenocladus* based on the combination of the cell proximal to crossvein *r-m* with no setae, anal point

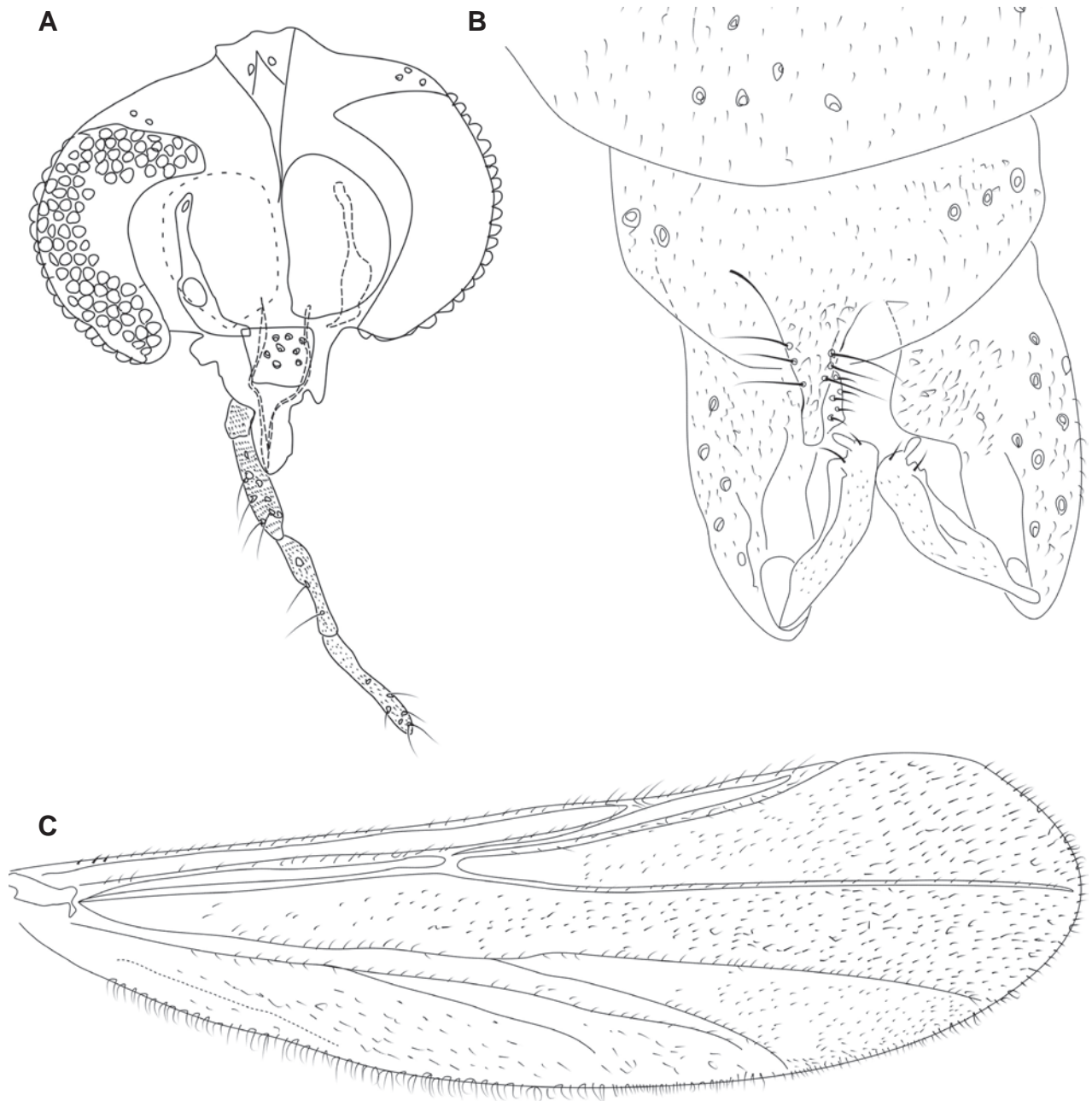


Figure 7. *Paraphaenocladus namibiae* sp. nov. holotype, adult male **A** head **B** hypopygium **C** wing.

of abdominal tergite X with parallel-sided tip, free of visible setae (except for a few microtrichia, virga absent, gonostylus with low, elongated crista dorsalis.

Description. Adult male (holotype, male; n=1).

Total length 1.9 mm, wing length 1.4 mm. Overall greenish colour, with yellow stripes on the scutum, small chironomid.

Antennae: holotype was missing antennae upon sorting out from the samples.

Head: Eyes with short, wedge-shaped extension. Temporal setae (n=1) 9, with 4 inner and 5 outer verticals, 3 orbital setae, clypeus with 8 setae. Tentorium 120 μ m. Palpomeres' length in μ m (n=1): 2nd -33, 3rd - 88, 4th -95, 5th -95 (Figs 7A, 8B).

Thorax: Anterpronotal setae -3, Dorsocentral setae -15, Acrostichals -5, scutellars - 8.

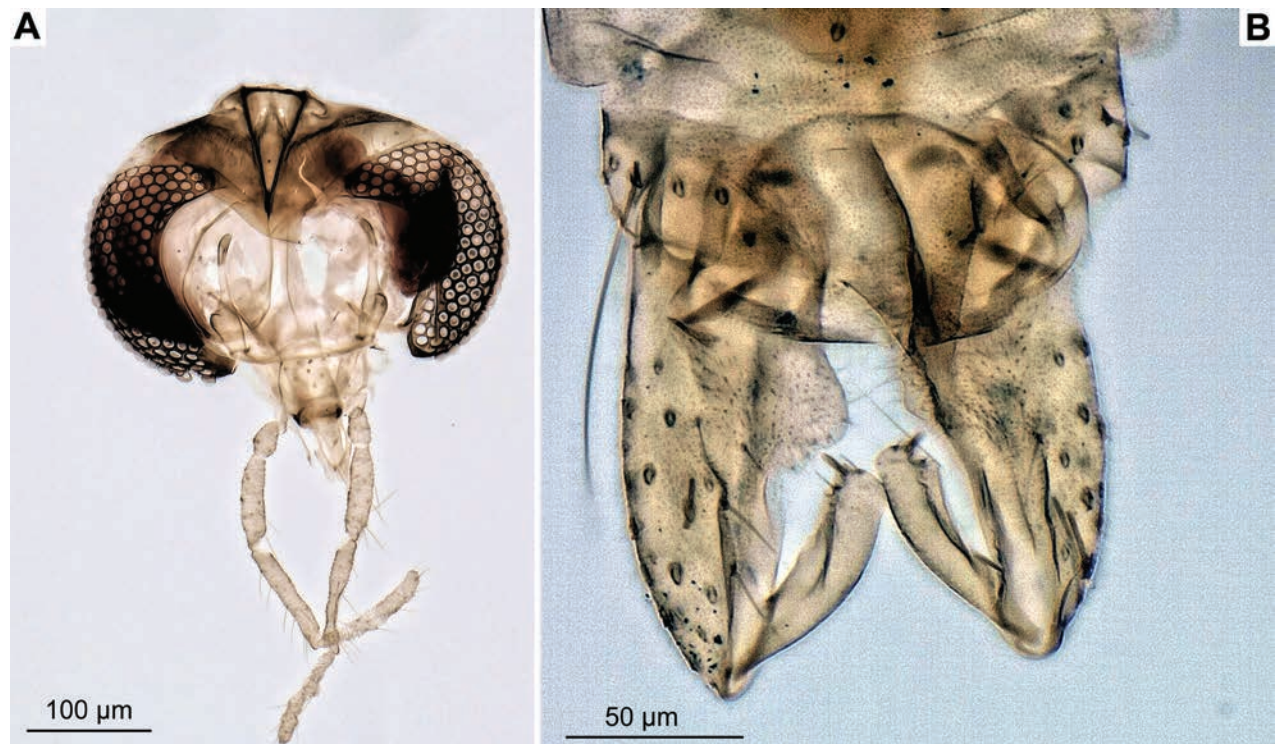


Figure 8. *Paraphaenocladius namibiae* sp. nov. holotype, adult male **A** head **B** hypopygium

Legs: all legs are missing tarsomeres. Fore and mid tibiae with one tibial spur, hind tibia with two spurs. Leg elements lengths as listed in Table 1.

Wing 1.4 mm long. Anal lobe strongly reduced. Costal extension 70 µm long, with 6 non-marginal setae. Cu_1 slightly sinuate. R with 28 setae. R_1 with 11 setae, R_{4+5} with 30 setae. $r-m$ bare, M bare, M_{1+2} with 61 setae, M_{3+4} with 48 setae. Cu with 29 setae, Cu_1 with 33 setae. CuP with 27 setae (Fig. 7C).

Hypopygium. Anal point with mostly bare apex (bearing some microtrichia), 12 µm long, 5 µm wide, tip parallel-sided. Anal point with three pairs of strong lateral setae at the base. Sternapodeme 65 µm long, phalapodeme 36 µm long. Virga absent. Gonocoxite 100 µm long, with large, rounded inferior volsella. Gonostylus 55 µm long. Megasetae 7 µm long. Gonostylus with a strong, apically rounded megasetae (Figs 7B, 8B).

Etymology. Named for Namibia, the species' country of origin.

Comments. Species was attributed to genus *Paraphaenocladius*, based on the combination of bare eyes with hairy wings, with Costal extension ending proximally to the tip of M_{3+4} and Cu_1 curved.

Based on the combination of the cell m proximal to crossvein $r-m$ with zero setae, triangular anal point, with basal setae and bare apex, longer than wide and absent virga, the new species appears to belong to the *P. dewulfi*-species group sensu Sæther & Wang, 1995. This group consists of three previously described species of *Paraphaenocladius*, inhabiting the Afrotropics: *P. dewulfi* (Goetghebuer, 1936), *P. cuneipennis* (Freeman, 1961) and *P. crassicaudatus* Sæther & Wang, 1995.

Among the three, *P. namibiae* sp. nov. is most like *P. crassicaudatus*, due to the general similarity of the hypopygium morphology, most evident in the relatively broad anal point, strong crista dorsalis and broad inferior volsella.

Distribution. Species is only known from its type locality so far (Fig. 1A).

Table 1. Length (in μm) of leg segments of *Paraphaenocladus namibiae* sp. nov., male (n = 1).

| Leg | Femora | Tibia | Ta1 | Ta2 | Ta3 | Ta4 | Ta5 |
|---------|--------|-------|-----|-----|-----|-----|-----|
| Foreleg | 300 | 250 | – | – | – | – | – |
| Midleg | 300 | 260 | – | – | – | – | – |
| Hindleg | 340 | 300 | – | – | – | – | – |

Chironominae Macquart, 1838**Tanytarsini Zavřel, 1916 [in Thienemann and Zavřel 1916]*****Cladotanytarsus pseudomancus* (Goetghebuer, 1934)**

Fig. 9A, B

Material examined. NAMIBIA • 500♂♀; OTJOZONDJUPA; Von Bach Dam Nature Reserve, Swakop river outflow; 22°0'53.28"S, 16°57'12.24"E; 2–10 Dec. 2018; Malaise trap; V. Baranov leg.; NMNW; BOLD specimen code: NAM-Chiro39; NAM-Chiro38; NAM-Chiro37; NAM-Chiro36; NAM-Chiro35: NAM50; NAM49; NAM51; NAM-Chiro41; NAM-Chiro40; BOLD sequence ID: NAMOE039-22; NAMOE038-22; NAMOE037-22; NAMOE036-22; NAMOE035-22; NAMCH013-19; NAMCH012-19; NAMCH048-20; NAMOE041-22; NAMOE040-22; BOLD BIN: BOLD:ACK2243 • 1♂; KHOMAS; Windhoek; 22°36'43.2"S, 17°5'27.6"E; 1 Dec. 2018; G. M. Kvifte, V. Baranov, X. Lin leg.; NMNW; BOLD specimen code: NAM-Chiro5; BOLD sequence ID: NAMOE005-22; BOLD BIN: BOLD:ACK2243 • 1♂; KHOMAS; Windhoek, Arebbuschrivier, Goreangab Reservoir; 22°31'44.4"S, 17°0'3.6"E; 3 Dec. 2018; X. Lin leg.; sweep net; SHOU; BOLD specimen code: NAM97; NAM93; BOLD sequence ID: NAMCH080-20; NAMCH076-20; BOLD BIN: BOLD:ACK2243 • 1 larva, 1 pupa; OTJOZONDJUPA; Gross Barmen; 22°6'38.16"S, 16°44'42"E; 4 Dec. 2018; X. Lin leg.; sweep net; SHOU.

Distribution. This is the first record of the species from Namibia (Freeman 1956; Freeman and Cranston 1980; Curtis 1991; Harrison 2004). *Cladotanytarsus pseudomancus* is a widespread species, thus far recorded from the Afrotropical Region, including Madagascar, from the Oriental Region: India (West Bengal), China (Hainan) and the Palearctic Region: Russian far east, France, Egypt, Saudi Arabia and Oman (Gilka 2009).

***Tanytarsus pallidulus* Freeman, 1954**

Fig. 9C

Material examined. NAMIBIA • 430♂♀; OTJOZONDJUPA; Von Bach Dam Nature Reserve, Swakop river outflow; 22°0'53.28"S, 16°57'12.24"E; 2–10 Dec. 2018; Malaise trap; V. Baranov leg.; NMNW • 1♂; KHOMAS, Windhoek, 22°36'43.2"S, 17°5'27.6"E; 8 Dec. 2018; G. M. Kvifte, V. Baranov, X. Lin leg.; NMNW; BOLD specimen code: NAM-Chiro6; BOLD sequence ID: NAMOE006-22; BOLD BIN: BOLD:AAH9824.

Distribution. This is the first record of the species from Namibia (Freeman 1956; Freeman and Cranston 1980; Curtis 1991; Harrison 2004). Otherwise, this species is occurring in South Africa, Mozambique, Nigeria, Zimbabwe, Democratic Republic of Congo and Saudi Arabia (Freeman 1956; Freeman and Cranston 1980; Cranston and Judd 1989; Ekrem 2001; Harrison 2004).

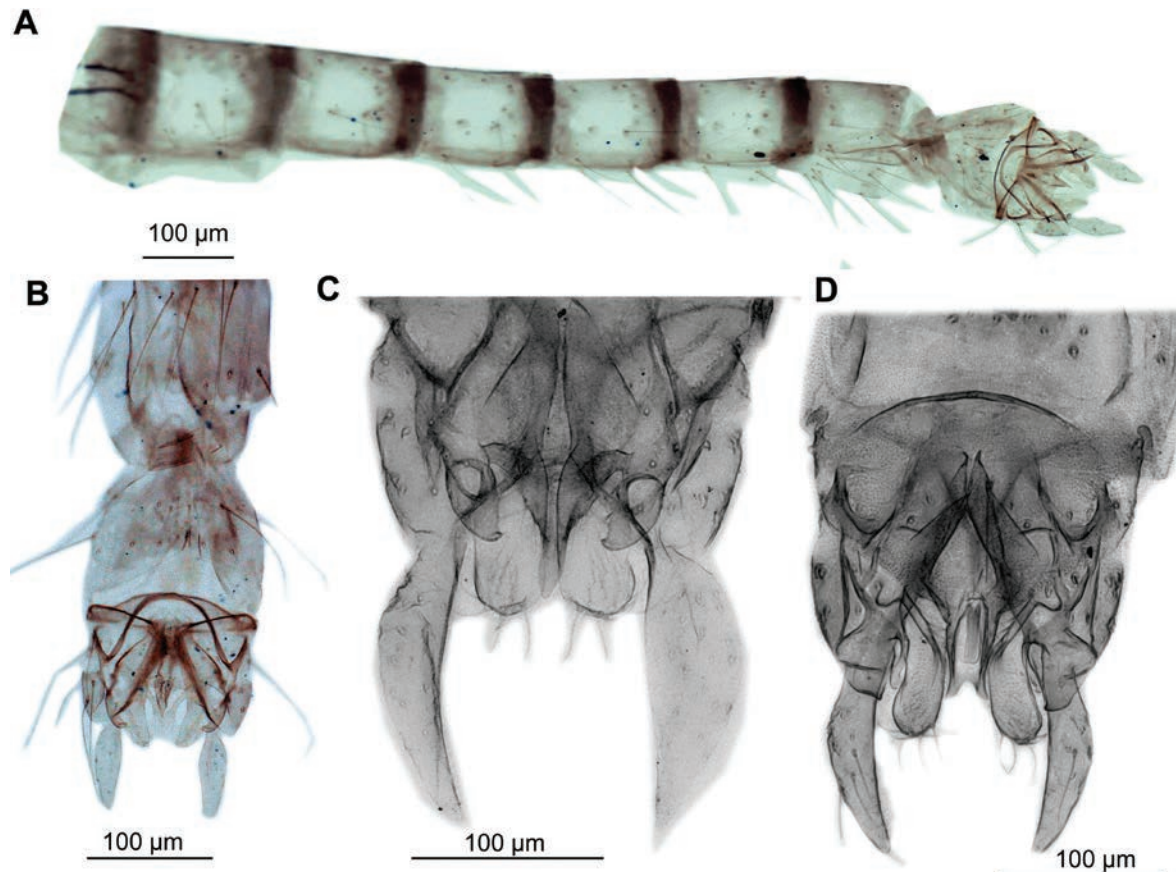


Figure 9. Tanytarsini, adult males, hypopygia **A, B** *Cladotanytarsus pseudomancus* **C** *Tanytarsus pallidulus* **D** *Tanytarsus bifurcus*.

Tanytarsus bifurcus Freeman, 1958

Fig. 9D

Material examined. NAMIBIA • 6♂; OTJOZONDJUPA; Von Bach Dam Nature Reserve, Swakop river outflow, 22°0'53.28"S, 16°57'12.24"E; 2–10 Dec. 2018; Malaise trap; V. Baranov leg.; NMNW • 1♂; HARDAP; Naukluft Mountain Zebra Park, Tufa waterfalls; 24°15'47.88"S, 16°13'44.76"E; 1–5 Dec. 2018; sweep net; G. M. Kvifte, V. Baranov, X. Lin leg.; SHOU; BOLD specimen code: NAM-Chiro19; BOLD sequence ID: NAMOE019-22; BOLD BIN: BOLD:ADU6503.

Distribution. This is the first record of the species from Namibia (Freeman and Cranston 1980; Curtis 1991; Harrison 2004). Otherwise this species is occurring in Burkina Faso, Chad, Mali, Nigeria and Ghana (Freeman 1958; Dejoux 1968a, 1968c, 1974; Freeman and Cranston 1980; Ekrem 2001).

Chironomini Macquart, 1838

Chironomus transvaalensis Kieffer, 1923

Fig. 10A, B

Material examined. NAMIBIA • 30♂24♀; KHOMAS; Windhoek, Arebbusch river; 22°34'28.92"S, 17°3'15.84"E; 3 Dec. 2018; X. Lin leg.; sweep net; SHOU; BOLD specimen code: NAM-Chiro3; BOLD sequence ID: NAMOE003-22 • 3♀;

KHOMAS; Windhoek, Arebbusch river, Goreangab Reservoir; 22°31'44.4"S; 17°0'3.6"E; 3 Dec. 2018; X. Lin leg.; sweep net; SHOU; BOLD specimen code: NAM-Chiro23; NAM-Chiro54; NAM-Chiro3; BOLD sequence ID: NAMOE023-22; NAMOE054-22; NAMOE003-22; BOLD BIN: BOLD:AAW3995 • 1♀; OTJOZOND-JUPA; Von Bach Dam Nature Reserve, Swakop river outflow; 22°0'53.28"S, 16°57'12.24"E; 2–10 Dec. 2018; V. Baranov leg.; Malaise trap; NMNW; BOLD specimen code: NAM-Chiro34; BOLD sequence ID: NAMOE034-22; BOLD BIN: BOLD:AAW3995 • 1♂14♀; OTJOZONDJUPA; Düstenbrook; 22°15'11.52"S, 16°54'1.44"E; 4 Dec. 2018; G. M. Kwifte leg.; NMNW.

Distribution. The species is widely distributed in Namibia and the rest of the Afrotropics, as well as southern Palaeartic (Lindner 1976; Curtis 1991; Harrison 2004).

***Chironomus calipterus* Kieffer, 1908**

Fig. 10C

Material examined. NAMIBIA • 67♂; OTJOZONDJUPA; Von Bach Dam Nature Reserve, Swakop river outflow; 22°0'53.28"S, 16°57'12.24"E; 2–10 Dec. 2018; V. Baranov leg.; Malaise trap; NMNW.

Distribution: The species is widely distributed in Namibia and rest of the Afrotropics as well as the southern Palaeartic (Freeman 1957; Lindner 1976; Curtis 1991; Harrison 2004; Andersen and Mendes 2010).

***Dicrotendipes fusconotatus* (Kieffer, 1922)**

Material examined. NAMIBIA • 3♂; KHOMAS; Windhoek, Arebbusch river, Goreangab Reservoir; 22°31'44.4"S; 17°0'3.6"E; 3 Dec. 2018; G.M. Kwifte leg.; sweep net; NMNW; BOLD specimen code: NAM-Chiro1; BOLD sequence ID: NAMOE001-22. • 1♂; HARDAP; Naukluft Mountain Zebra Park, Tufa waterfalls; 24°15'47.88"S; 16°13'44.76"E; 1 Dec. 2018; sweep net; V. Baranov leg.; NMNW.

No specimens of this species were successfully barcoded as a part of this project.

Distribution. This is the first record of the species from Namibia; otherwise it occurs in Chad, Democratic Republic of the Congo, Egypt, Israel, Niger, Nigeria, Uganda, South Africa and Zimbabwe (Freeman 1956; Freeman and Cranston 1980; Curtis 1991; Harrison 2004).

***Dicrotendipes septemmaculatus* (Becker, 1908)**

Fig. 10D

Material examined. NAMIBIA • 5♂, 2 larvae; 2 pupae; KHOMAS; Windhoek, Arebbusch river, Goreangab Reservoir; S22°52'90"S; 17°0'3.6"E; 3 Dec. 2018; G.M. Kwifte leg.; sweep net; NMNW; BOLD specimen code: NAM-Chiro4; NAM88; NAM95; NAM94; NAM91; NAM90; BOLD sequence ID: NAMOE004-22; NAMCH016-19; NAMCH078-20; NAMCH077-20;

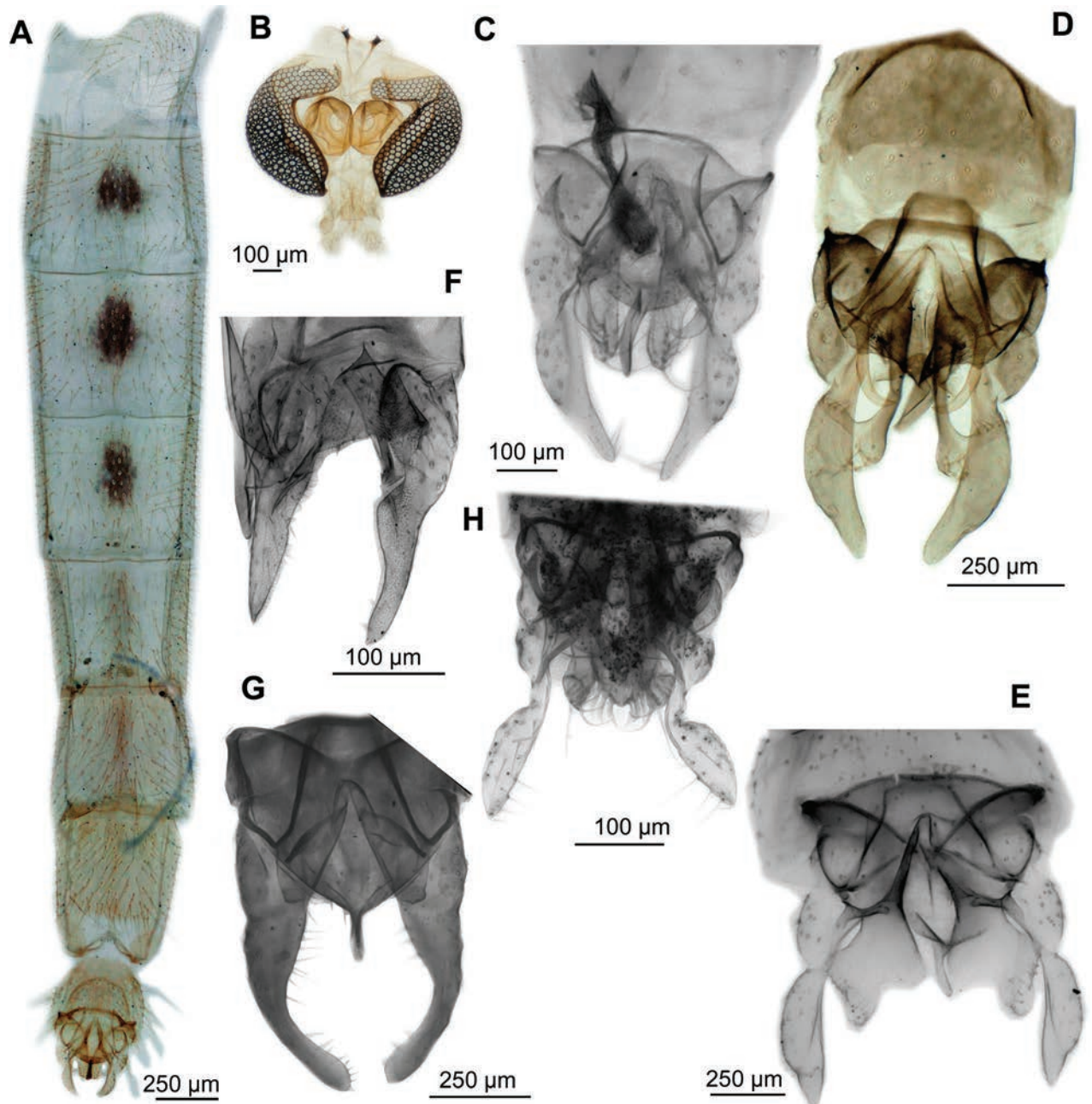


Figure 10. Chironomini, adult males **A, B** *Chironomus transvaalensis* **C** *Chironomus calipterus* **D** *Dicotendipes septemmaculatus* **E** *Kiefferulus brevipalpis* **F** *Parachironomus acutus* **G** *Paracladopelma rhodesianus* **H** *Polypedilum abyssiniae* **A, C–H** hypopygia **B** head.

NAMCH074-20; NAMCH073-20; BOLD BIN: BOLD:ACK4391 • 1♂; KHOMAS; Windhoek; 22°36'43.2"S, 17°5'27.6"E; 3 Dec. 2018; X. Lin leg.; light trap; SHOU; BOLD specimen code: NAM76; BOLD sequence ID: NAMCH015-19; BOLD BIN: BOLD:ADY3994 • 1♀; HARDAP; Naukluft Mountain Zebra Park, Tufa waterfalls; 24°15'47.88"S, 16°13'44.76"E; 1 Dec. 2018; V. Baranov leg.; sweep net; NMNW; BOLD specimen code: NAM-Chiro25; BOLD sequence ID: NAMOE025-22; BOLD BIN: BOLD:ACK4391 • 1♀; OTJOZONDJUPA; Gross Barmen; 22°6'38.16"S, 16°44'42"E; 4 Dec. 2018; X. Lin leg.; sweep net; SHOU; BOLD specimen code: NAM66; BOLD sequence ID: NAMCH056-20; BOLD BIN: BOLD:ACK4391.

Distribution. This is the first record of the species from Namibia, otherwise recorded from numerous countries: Algeria, Australia, Democratic Republic of the Congo, China, Egypt, Bangladesh, India, Indonesia, Japan, Lebanon, Myanmar, Namibia, Nigeria, South Africa, Spain, Sudan, Uganda and Zimbabwe (Freeman 1956; Freeman and Cranston 1980; Curtis 1991; Harrison 2004; Qi et al. 2012).

***Kiefferulus brevipalpis* (Kieffer, 1918)**

Fig. 10E

Material examined. NAMIBIA • 3♂2♀; OTJOZONDJUPA; Gross Barmen; 22°6'38.16"S, 16°44'42"E; 4 Dec. 2018; X. Lin leg.; sweep net; SHOU; BOLD specimen code: NAM-Chiro46; NAM67; NAM64; NAM63; NAM62; BOLD sequence ID: NAMOE046-22; NAMCH057-20; NAMCH054-20; NAMCH053-20; NAMCH052-20; BOLD BIN: BOLD:AFG1076; BOLD:ACK6259 • 7♂; KHOMAS; Windhoek; 22°36'43.2"S, 17°5'27.6"E; 3 Dec. 2018; X. Lin leg.; light trap; SHOU; BOLD specimen code: NAM-Chiro22; BOLD sequence ID: NAMOE022-22; BOLD BIN: BOLD:AFG1076.

Distribution. This is the first record of the species from Namibia, otherwise being recorded from Democratic Republic of the Congo, Ethiopia and Uganda, (as. *Nilodorum brevipalpis* (Kieffer, 1918)) (Freeman 1956; Freeman and Cranston 1980; Curtis 1991; Martin 1999).

***Parachironomus acutus* (Goetghebuer, 1936)**

Fig. 10F

Material examined. NAMIBIA • 1♂; OTJOZONDJUPA; Von Bach Dam Nature Reserve, Swakop river outflow; 22°0'53.28"S, 16°57'12.24"E; 2–10 Dec. 2018; V. Baranov leg.; Malaise trap; NMNW.

Distribution. This is the first record of the species from Namibia, otherwise species is recorded from Cameroon, Chad, Democratic Republic of the Congo, Madagascar, Nigeria and South Africa (Freeman 1956; Freeman and Cranston 1980; Curtis 1991; Harrison 2004). No specimens of this species were successfully barcoded as a part of this project. This species is often treated as "unplaced" within Chironomini (Freeman and Cranston 1980), we are following Ekrem et al. (2017) in placing this species in *Parachironomus*.

***Paracladopelma rhodesianus* (Kieffer, 1923)**

Fig. 10G

Material examined. NAMIBIA • 1♂; KHOMAS; Windhoek, Arebbusch river; 22°34'28.92"S, 17°3'15.84"E; 3 Dec. 2018; X. Lin leg.; sweep net; SHOU.

Distribution. This is the first record of the species from Namibia; the species was otherwise recorded from Botswana, South Africa and Zimbabwe (Freeman 1956; Freeman and Cranston 1980; Curtis 1991; Harrison 2004). No specimens of this species were successfully barcoded as a part of this project.

***Polypedilum abyssiniae* Kieffer, 1918**

Fig. 10H

Material examined. NAMIBIA: • 1♂; OTJOZONDJUPA; Von Bach Dam Nature Reserve, Swakop river outflow; 22°0'53.28"S, 16°57'12.24"E; 2–10 Dec. 2018; V. Baranov leg.; Malaise trap; NMNW.

Distribution. The species was previously recorded from Namibia (Kunene river) (Harrison 2004), otherwise it was recorded from Chad, Democratic Republic of the Congo, Ethiopia, Mali, South Africa, Sudan and Tanzania (Freeman 1956; Freeman and Cranston 1980; Curtis 1991; Harrison 2004). No specimens of this species were successfully barcoded as a part of this project.

Key to the *P. dewulfi* - species group sensu Sæther and Wang (1995) from the Afrotropical Region

- 1 Anal point with bare, spatulate tip, cell *m* proximal to *r-m* with 4–77 setae (widely distributed in Nearctic and Palaearctic, first Afrotropical record listed here, see below) ***P. impensus* (Walker)**
- Anal point with bare tip which might be parallel-sided (narrow or wider), or pointed, cell *m* proximal to *r-m* with 0–70 setae..... **2**
- 2 Bare apical part of the anal point long and narrow, cell *m* proximal to *r-m* with 0–7 setae (South Africa, D.R. Congo, Saudi Arabia, South Africa, Tanzania, Zimbabwe) ***P. dewulfi* (Goethgebuer)**
- Bare apical part of the anal point otherwise, cell *m* proximal to *r-m* with 10–70 setae..... **3**
- 3 Anal point with a narrow (2–5 µm) wide apex, completely devoid of setae; wing cuneiform..... ***P. cuneipennis* (Freeman)**
- Anal point with a wider apex, bearing a few setae; wing not cuneiform.... **4**
- 4 Apex of anal point very wide (16 µm), crista dorsalis of gonostylus is of similar height during its entire length.....
..... ***P. crassicaudatus* Sæther & Wang**
- Apex of anal point 5 µm, crista dorsalis forms a prominent triangular protrusion at the distal end of the gonostylus ***P. namibiae* sp. nov.**

Acknowledgments

We are grateful to Peter T. Cranston for his help with planning the fieldwork, based on his immense experience. The authors are grateful to Eugene Marais, for his help with the permit application process. We are grateful to Matthew R. McCurry for his help with improving the readability of the paper. We are also grateful to the National Commission on Research Science and Technology (NCRST) and the Ministry of Environment and Tourism of Namibia for their help with obtaining all the relevant permits and overall support of our fieldwork. We are grateful to the Canadian Centre for DNA Barcoding (CCDB, Guelph, Canada) for DNA sequencing. We would also like to acknowledge Gunnar M. Kvifte's support in collecting material. We are thankful to the editor Burgert Muller and an anonymous editor for their efforts in improving the manuscript.

Additional information

Conflict of interest

The authors have declared that no competing interests exist.

Ethical statement

Specimens were collected from the Khomas, Otjozondjupa and Hardap regions of central Namibia between 27 Nov. – 8 Dec. 2018, under the collective research permit issued by NCRST (authorization number AN20181007). All insect material was then exported to Germany for processing under an export permit issued by the Ministry of Environment and Tourism of Namibia (Number 119666).

Funding

Viktor Baranov's fieldwork was supported by LinnéSys: Systematics Research Fund (2018). V. Baranov's work is also funded by the State Agency of Innovation, within the Ramon y Cajal Program, grant number RYC2021-032144-I. The funders had no role in study design, data collection and analysis, decision to publish, or preparation of the manuscript. Viktor Baranov received funds supporting the payment of this publication fees through the CSIC Open Access Publication Support Initiative from the CSIC Unit of Information Resources for Research (URICI).

Author contributions

VB have conceptualised the study, obtained funding, have conducted morphological morphological identification of the specimens, have conducted the imaging and data analysis, and written a first draft.; VB and XL have conducted sampling; XL, CC and JH have conducted DNA barcoding lab work; All authors have worked on the 1st and 2nd drafts.

Author ORCIDs

Viktor Baranov  <https://orcid.org/0000-0003-1893-3215>

Xiaolong Lin  <https://orcid.org/0000-0001-6544-6204>

Jeremy Hübner  <https://orcid.org/0009-0007-5624-8573>

Caroline Chimeno  <https://orcid.org/0000-0001-9933-6492>

Data availability

All of the data that support the findings of this study are available in the main text or Supplementary Information.

References

- Andersen T, Mendes H (2010) Order Diptera, family Chironomidae (with the exception of the tribe Tanytarsini). *Arthropod fauna of the UAE* 3: 564–598.
- Ashe P, O'Connor JP (2009) *A World Catalogue of Chironomidae (Diptera)*. Part 1. Buchonomyiinae, Chilenomyiinae, Podonominae, Aphroteniinae, Tanyponidae, Usambaromyiinae, Diamesinae, Prodiamesinae and Telmatogetoninae. Irish Biogeographical Society/The National Museum of Ireland, Dublin, 445 pp.
- Ashe P, O'Connor JP (2012) *A world catalogue of Chironomidae (Diptera)*. Part 2. Orthocladiinae. Two volumes (Sections A, B). Irish Biogeographical Society, Dublin, [14] + [xvi +]468 pp., [6] + 500 pp.

- Curtis B (1991) Freshwater macro-invertebrates of Namibia. *Madoqua* 1991: 163–187.
- Cranston PS, Judd DD (1989) Diptera: Family Chironomidae of the Arabian Peninsula. *Fauna Saudi Arabia* 10: 236–289.
- Dejoux C (1968a) Contribution à l'étude des premiers états des Chironomides du Tchad. *Hydrobiologia* 31: 449–464. <https://doi.org/10.1007/BF00134446>
- Dejoux C (1968b) Le Lac Tchad et les Chironomides de sa partie Est. *Annales Zoologici Fennici* 5: 27–32.
- Dejoux C (1974) Contribution à la connaissance des Chironomides de l'Afrique de l'Ouest. *Entomologisk tidskrift* 95: 72–83.
- Ekrem T (2001) A review of Afrotropical *Tanytarsus* van der Wulp (Diptera: Chironomidae). *Tijdschrift voor Entomologie* 144(1): 5–40. <https://doi.org/10.1163/22119434-99900054>
- Ekrem T, Ashe P, Andersen T, Stur E (2017) Chapter 35. Chironomidae (non-biting midges). In: Kirk-Spriggs AH, Sinclair BJ (Eds) *Manual of Afrotropical Diptera*. Vol. 2. Nematoceros Diptera and lower Brachycera. Suricata 5. SANBI Graphics and Editing, Pretoria, 813–863.
- Ferrington Jr LC, Sæther OA (2011) A revision of the genera *Pseudosmittia* Edwards, 1932, *Allocladius* Kieffer, 1913, and *Hydrosmittia* gen. n. (Diptera: Chironomidae, Orthocladiinae). *Zootaxa* 2849(1): 1–314. <https://doi.org/10.11646/zootaxa.2849.1.1>
- Folmer O, Black M, Hoeh W, Lutz R, Vrijenhoek R (1994) DNA primers for amplification of mitochondrial cytochrome c oxidase subunit I from diverse metazoan invertebrates. *Molecular Marine Biology and Biotechnology* 3: 294–299.
- Freeman P (1953) Chironomidae (Diptera) from Western Cape province-I. *Proceedings of the Royal Entomological Society of London. Series B, Taxonomy* 22(7-8): 127–135. <https://doi.org/10.1111/j.1365-3113.1953.tb00071.x>
- Freeman P (1955a) A study of the Chironomidae (Diptera) of Africa south of the Sahara. Part I. *Bulletin of the British Museum (Natural History). Historical Series* 4: 1–67. [Natural History]
- Freeman P (1955b) A study of the Chironomidae (Diptera) of Africa south of the Sahara. Part IV. *Bull. Br. Mus.(Nat. Hist.). Entomol.* 6: 263–363. <https://doi.org/10.5962/bhl.part.17110>
- Freeman P (1956) A study of the Chironomidae (Diptera) of Africa south of the Sahara. Part II. *Bulletin of the British Museum (Natural History). Entomology* 4: 285–368.
- Freeman P (1957) A study of the Chironomidae (Diptera) of Africa South of the Sahara. Part III. *Bulletin of the British Museum (Natural History). Entomology* 5: 321–428. <https://doi.org/10.5962/bhl.part.1515>
- Freeman P (1958) A study of the Chironomidae (Diptera) of Africa South of the Sahara. Part IV. *Bulletin of the British Museum (Natural History). Entomology* 6(11): 26–364. <https://doi.org/10.5962/bhl.part.17110>
- Freeman P (1961) A collection of Chironomidae and Culicidae subfamily Dixinae (Diptera, Nematocera) from Madagascar. *Memoires de l'Institut Scientifique de Madagascar. Serie E, Entomologie* 12: 238–255.
- Freeman P, Cranston P (1980) Family Chironomidae. *Catalogue of the Diptera of the Afrotropical Region. British Museum (Natural History), London*: 175–202.
- Ghonaim, M., Ali, A., & Amer, M. (2005). *Cladotanytarsus* (Diptera: Chironomidae) from Egypt with description of a new species. *Oriental Insects* 39(1): 323–329. <https://doi.org/10.1080/00305316.2005.10417443>
- Gilka W (2009) Order Diptera, family Chironomidae, Tribe Tanytarsini. In: van Harten A (Ed.) *Arthropod Fauna of the United Arab Emirates*. Dar Al Ummah Print, Abu Dhabi, 667–682.

- Gratton C, Donaldson J, Zanden MJV (2008) Ecosystem Linkages Between Lakes and the Surrounding Terrestrial Landscape in Northeast Iceland. *Ecosystems* (New York, N.Y.) 11(5): 764–774. <https://doi.org/10.1007/s10021-008-9158-8>
- Hall TA (1999) BioEdit: a user-friendly biological sequence alignment editor and analysis program for Windows 95/98/NT. Oxford, 95–98.
- Harrison A (2004) The non-biting midges (Diptera: Chironomidae) of South Africa. University of Waterloo, Canada. <http://www.ru.ac.za/academic/departments/zooento/Martin/chironomidae>
- Haug JT, Haug C, Ehrlich M (2008) First fossil stomatopod larva (Arthropoda: Crustacea) and a new way of documenting Solnhofen fossils (Upper Jurassic, Southern Germany). *Palaeodiversity* 1: 103–109.
- Hebert PD, Braukmann TW, Prosser SW, Ratnasingham S, DeWaard JR, Ivanova NV, Janzen DH, Hallwachs W, Naik S, Sones JE, Zakharov EV (2018) A Sequel to Sanger: Amplicon sequencing that scales. *BMC Genomics* 19(1): 1–14. <https://doi.org/10.1186/s12864-018-4611-3>
- Ivanova NV, Grainger C (2007) Primer Sets for DNA Barcoding.
- Kirk-Spriggs AH (2017) Chapter 2. Collection and preservation of Diptera. In: Kirk-Spriggs AH, Sinclair BJ (Eds) Volume 1: Introductory chapters and keys to Diptera. Suricata 4. South African National Biodiversity Institute, Pretoria, 69–87.
- Lin X-L, Stur E, Ekrem T (2018) DNA barcodes and morphology reveal unrecognized species in Chironomidae (Diptera). *Insect Systematics & Evolution* 49(4): 329–398. <https://doi.org/10.1163/1876312X-00002172>
- Lindner E (1976) Zur Kenntnis der Dipterenfauna Sudwestafrikas. VI VIII. *Journal of South West African Scientific Society* 30: 75–86.
- Martin J (1999) Listing of names which have been applied in the genus *Kiefferulus* Goetghebuer. <https://www.chironomidae.net/Martin/Chironfiles/Kiefffile/Kieff.htm> [Accessed: 15/12/2023]
- Qi X, Lin XL, Wang XH (2012) Review of *Dicrotendipes* kieffer from China (Diptera, chironomidae). *ZooKeys* 183: 23–26. <https://doi.org/10.3897/zookeys.183.2834>
- Ratnasingham S, Hebert PD (2007) BOLD: The Barcode of Life Data System (<http://www.barcodinglife.org>). *Molecular Ecology Notes* 7(3): 355–364. <https://doi.org/10.1111/j.1471-8286.2007.01678.x>
- Reid H, Sahlén L, Stage J, MacGregor J (2007) The economic impact of climate change in Namibia. IIED, London, 46 pp.
- Sæther OA (1980) Glossary of chironomid morphology terminology (Diptera: Chironomidae). *Entomologica Scandinavica* (Supplement 14): 1–51.
- Sæther OA, Wang X (1995) Revision of the genus *Paraphaenocladus* Thienemann, 1924 of the world (Diptera: Chironomidae, Orthoclaadiinae). *Entomologica scandinavica supplement* 48: 1–69.
- Thienemann, A. and Zavřel, J. 1916. Die Metamorphose der Tanypinen. *Archiv für Hydrobiologie - Supplements* 2(3): 566–654.
- Wang XH, Sæther OA, Andersen T (2002) Afrotropical *Bryophaenocladus* Thienemann, 1934 (Diptera: Chironomidae). *Studia Dipterologica* 8: 447–462.
- Zinchenko TD, Gladyshev MI, Makhutova ON, Sushchik NN, Kalachova GS, Golovatyuk LV (2014) Saline rivers provide arid landscapes with a considerable amount of biochemically valuable production of chironomid (Diptera) larvae. *Hydrobiologia* 722(1): 115–128. <https://doi.org/10.1007/s10750-013-1684-5>

Supplementary material 1

Specimens/Taxa group A (core/source species)

Authors: Viktor Baranov, Xiaolong Lin, Jeremy Hübner, Caroline Chimeno

Data type: xlsx

Copyright notice: This dataset is made available under the Open Database License (<http://opendatacommons.org/licenses/odbl/1.0/>). The Open Database License (ODbL) is a license agreement intended to allow users to freely share, modify, and use this Dataset while maintaining this same freedom for others, provided that the original source and author(s) are credited.

Link: <https://doi.org/10.3897/AfrInvertebr.65.111920.suppl1>

Supplementary material 2

Tree Result - DS-NAMCHIR (116 records selected)

Authors: Viktor Baranov, Xiaolong Lin, Jeremy Hübner, Caroline Chimeno

Data type: pdf

Copyright notice: This dataset is made available under the Open Database License (<http://opendatacommons.org/licenses/odbl/1.0/>). The Open Database License (ODbL) is a license agreement intended to allow users to freely share, modify, and use this Dataset while maintaining this same freedom for others, provided that the original source and author(s) are credited.

Link: <https://doi.org/10.3897/AfrInvertebr.65.111920.suppl2>

Supplementary material 3

COI FULL DATABASE includes records without species designati...

Authors: Viktor Baranov, Xiaolong Lin, Jeremy Hübner, Caroline Chimeno

Data type: pdf

Copyright notice: This dataset is made available under the Open Database License (<http://opendatacommons.org/licenses/odbl/1.0/>). The Open Database License (ODbL) is a license agreement intended to allow users to freely share, modify, and use this Dataset while maintaining this same freedom for others, provided that the original source and author(s) are credited.

Link: <https://doi.org/10.3897/AfrInvertebr.65.111920.suppl3>

Volume 65 Issue 2

- 37 ***Selenogyrus foordi*, a new species and the first record of the subfamily Selenogyrinae Smith, 1990 from Guinea (Araneae, Theraphosidae)**
Danniella Sherwood, Arnaud Henrard, Didier Van Den Spiegel
- 49 **The first record of *Atherigona* from Lesotho (Diptera, Muscidae), with description of a new species**
Mokome M. J. Magoai, Burgert S. Muller
- 61 **Three new species of plexippine jumping spiders (Salticidae, Salticinae, Plexippini) from dry forest in Boeny region, north-western Madagascar**
Katie I. Murray, Jaime Escobar-Toledo, Brogan L. Pett
- 75 ***Foordus* gen. nov., a new genus of euophryine jumping spider from South Africa (Salticidae, Araneae)**
Galina N. Azarkina
- 85 **Soutpansberg Mountain: a spider hotspot in the Limpopo Province of South Africa (Arachnida, Araneae)**
Ansie S. Dippenaar-Schoeman, T. Caswell Munyai, Colin S. Schoeman, Norbert Hahn, Stefan H. Foord
- 115 ***Afrogarypus foordi* sp. nov. – a new pseudoscorpion species (Pseudoscorpiones, Geogarypidae) from South Africa**
Jan Andries Neethling, Danilo Harms
- 127 **On some new and poorly-known Chrysillini from arid western South Africa (Araneae, Salticidae)**
Charles Richard Haddad, Wanda Wesółowska
- 161 **A revision of Afrotropical *Asceua* (Araneae, Zodariidae), ant-eating spiders with puzzling distributions**
Rudy Jocqué, Arnaud Henrard
- 199 ***Metalacurbs foordi* sp. nov., a new Lacurbsinae (Opiliones, Laniatores, Biantidae) from Ankasa National Park, Ghana**
Abel Pérez-González, Vanesa Mamani
- 213 **The rare siphonophore *Rhizophysa eysenhardtii* Gegenbaur, 1859 (Hydrozoa, Siphonophora, Cystonectae) from False Bay, South Africa**
Gillian M. Mapstone, Jannes Landschoff

- 223** **Completing the web: identifying sampling bias and knowledge gaps within South African spider surveys (Arachnida, Araneae)**
Aileen C. van der Mescht, Charles R. Haddad, Stefan H. Foord, Ansie S. Dippenaar-Schoeman
- 247** **Revision of Afrotropical *Suragina* Walker, 1859 (Diptera, Athericidae)**
Burgert S. Muller, Vaughn R. Swart, Louwrens P. Snyman
- 329** **A new species and new records of *Chumma* (Araneae, Macrobonidae) from South Africa**
Yuri M. Marusik, Charles R. Haddad
- 339** **Small-scale variations in spider and springtail assemblages between termite mounds and the surrounding grassland matrix**
Hannelene Badenhorst, Charles Richard Haddad, Charlene Janion-Scheepers

Selenogyrus foordi, a new species and the first record of the subfamily Selenogyrinae Smith, 1990 from Guinea (Araneae, Theraphosidae)

Danniella Sherwood^{1,2}, Arnaud Henrard³, Didier Van Den Spiegel³

1 Arachnology Research Association, London, UK

2 Fundación Ariguanabo, San Antonio de los Baños, Cuba

3 Royal Museum for Central Africa, Tervuren, Belgium

Corresponding author: Danniella Sherwood (danni.sherwood@hotmail.com)



This article is part of:

Gedenkschrift for Prof. Stefan H. Foord

Edited by Galina Azarkina, Ansie

Dippenaar-Schoeman, Charles Haddad,

Robin Lyle, John Mldgley, Caswell Munyai

Academic editor: Ansie Dippenaar

Received: 24 May 2024

Accepted: 1 August 2024

Published: 16 August 2024

ZooBank: <https://zoobank.org/6D1528B6-39B6-46C1-B46E-3E1C2EF65C42>

Citation: Sherwood D, Henrard A, Van Den Spiegel D (2024) *Selenogyrus foordi*, a new species and the first record of the subfamily Selenogyrinae Smith, 1990 from Guinea (Araneae, Theraphosidae). African Invertebrates 65(2): 37–48. <https://doi.org/10.3897/AfrInvertebr.65.128284>

Copyright: © Danniella Sherwood et al.
This is an open access article distributed under terms of the Creative Commons Attribution License (Attribution 4.0 International – CC BY 4.0).

Abstract

A new spider species, *Selenogyrus foordi* **sp. nov.** (♂♀), is described from Mount Nimba, Guinea. Consequently, we provide the first *in vivo* photographs of a selenogyrine in the scientific literature and the first record of Selenogyrinae Smith, 1990 from Guinea. We also record *S. aureus* Pocock, 1897, described from Sierra Leone, from Massif du Ziam Biosphere Reserve, Guinea, representing the second known species for this country.

Key words: distribution, morphology, spider, tarantula, taxonomy

Introduction

Pocock (1897) described the genus *Selenogyrus* Pocock, 1897 to house two new species from Sierra Leone: *S. caeruleus* Pocock, 1897 (the type species) based on the female and *S. aureus* Pocock, 1897 based on the male. In the same work, he also transferred *Hapalopus africanus* Simon, 1887, which was described from the Ivory Coast based on the female by Simon (1887), newly combining this taxon as *Selenogyrus africanus*. For the next nine decades, the genus received no revisionary attention. However, it was overlooked by Pocock (1897) that Simon (1892: 139, 141) had indirectly transferred *H. africanus* to the genus *Cyclosternum* Ausserer, 1871, another genus to which it clearly did not belong (both *Cyclosternum* and *Hapalopus* Ausserer, 1875 are New World genera with urticating setae, and *Hapalopus* also possesses an abdomen pattern), which is where it was technically combined. Hirst (1908) illustrated the prolateral face of the chelicera of *S. aureus* as part of a broader work, but only for comparison purposes.

Smith (1986, 1987) presented drawings of the palpal bulb (in retrolateral view) and the tibial apophysis (in ventral view) of *S. aureus*, also providing a minimalistic redescription. He also gave a short redescription of *S. caeruleus* (as *S. "coeruleus"*, a *lapsus calami* and incorrect subsequent spelling) but without illustrations. *Selenogyrus africanus* and *S. brunneus* Strand, 1907 (an enigmatic species described from 'Western Africa' based on a supposed female,

later relegated as a *nomen dubium* by Nentwig et al. 2020) are simply listed, with neither descriptions nor illustrations.

Smith (1990) later provided more expansive redescrptions of *S. aureus* and *S. caeruleus*, also describing a new species based on a single female from Sierra Leone – *Selenogyrus austinius* Smith, 1990 (note: the World Spider Catalog (2024) considers this epithet a *lapsus calami* and corrected the spelling to *austini*, which we also follow here). He also established a new subfamily, Selenogyrinae Smith, 1990, to house *Selenogyrus*, predominately based on the remarkable intercheliceral stridulatory apparatus. All three species were illustrated and redescrbed in relative detail. Conversely, *S. africanus* was not redescrbed as Smith (1990) was unable to access the type specimen, and *S. brunneus* is provided with a brief textual redescrption but lacking illustrations. Nonetheless, Smith (1990) made the most significant advance in the taxonomy of the genus since its description by Pocock (1897). As mentioned above, the only other taxonomic act was that by Nentwig et al. (2020) who treated *S. brunneus* as a *nomen dubium*, primarily as the type material was destroyed during the Second World War.

Hitherto, the only taxonomic illustrations in the literature after Smith (1990) was by Schmidt (1993, 2003) who reproduced drawings from the earlier literature of *S. aureus* and *S. austini* respectively, making no novel taxonomic contributions to the genus *Selenogyrus* nor textual redescrptions. The World Spider Catalog (2024) currently recognises four species, three from Sierra Leone (*S. aureus*, *S. caeruleus* and *S. austini*) and one from the Ivory Coast (*S. africanus*), all known from a single sex. The species known from females are in urgent need of review and more material from Sierra Leone is needed to confirm whether they are valid. This work is outside the scope of the present one and is being undertaken by a colleague (R. Gallon pers. comm.).

In this work, we describe a new species of *Selenogyrus* based on type material of both sexes from Mount Nimba, Guinea, which is a notable African biodiversity hotspot where a number of new spiders have been described during the present century (e.g. Rollard and Wesolowska 2002; Zonstein 2018). Simultaneously, we provide the first record of the subfamily Selenogyrinae from Guinea and provide, to our knowledge, the first published photographs of a selenogyriine *in vivo*. *Selenogyrus aureus* is also newly recorded for Guinea.

Materials and methods

Specimens were examined under binocular microscopes. Photographs of the palpal bulb, tibial apophysis, spermathecae, and habitus were made by DS using a Leica DMC500 digital camera mounted on a Leica MZ16A and stacked using the Leica Application Suite (**LAS**) v. 4.13. Abbreviations, Repositories: **NHMUK** = Natural History Museum, London, United Kingdom; **RMCA** = Royal Museum for Central Africa, Tervuren, Belgium. Structures: A = apical keel (of embolus); ALE = anterior lateral eyes, AME = anterior median eyes, PLE = posterior lateral eyes, PME = posterior median eyes; PB = prolateral branch (of tibial apophysis), PS = prolateral superior keel (of embolus); RB = retrolateral branch (of tibial apophysis), RS = retrolateral superior keel (of embolus). Other: coll. = collector; colln. = collection; det. = determined by. Leg spine terminology follows Petrunkevitch (1925) with modifications: = dorsal, v = ventral, r = retro-

lateral, p = prolateral. Leg formulae start with the longest leg to the shortest in order of decreasing size, e.g. 4,1,2,3. All measurements are in mm. Maps were made using SimpleMappr (Shorthouse 2010). Type material of the new species is deposited in RMCA. Micro-computed tomography analyses were performed by AH, the structures were dehydrated in graded ethanol (70–95%) and stained with a 1% Lugol's iodine solution for 24 hours. After washing in pure acetone, the samples were air-dried for 24 hours, and then gently fixed with a piece of tape on a carbon stick. The pieces were scanned with an XREUniTOM (Tescan XRE, Ghent, Belgium) piloted with Aquila software, at 70 keV and 2 W (additional settings: exposure time: 500–700 ms, voxel size: 0.97–1.52 μm , total of 2000 projections). The obtained model was first processed with the Aquila reconstruction software windows version 1.1, followed by segmentation and mesh generation in the 3D analysis Windows-based software Dragonfly 2019 (Object Research Systems (ORS), Canada, <https://www.theobjects.com/dragonfly/index.html>). The model was further processed in GOM Inspect (<https://www.gom.com>). In accordance with the International Code of Zoological Nomenclature, this article was registered in ZooBank prior to publication: <https://zoobank.org/6D1528B6-39B6-46C1-B46E-3E1C2EF65C42>.

Other type material examined not listed in main paper

Holotype ♀ *Selenogyrus austini* (NHMUK 1899.11.15.5–6), Sierra Leone, 1898, leg. E. E. Austin; holotype ♀ *Selenogyrus caeruleus* (NHMUK 1896.12.20.21–25), Sierra Leone [sic!], leg. Surg. Capt. Clements.

Taxonomy

Theraphosidae Thorell, 1869

Selenogyrinae Smith, 1990

Selenogyrus Pocock, 1897

Selenogyrus foordi sp. nov.

<https://zoobank.org/F659090C-B69A-4DB2-8D0F-810C4413E5C6>

Material examined. Holotype: GUINEA • 1 ♂; Keoulanta, Mount Nimba, Guinea, (7°42'23"N, 8°20'48"W; 515 m a.s.l.; 20/11/2017; C. Allard, P. Bumou, A. Henrard, D. Van den Spiegel, A. Samoura, and M. Bamba leg.; NIMBA-2017-088; BE_RMCA_ARA.Ara.246088.

Paratype: GUINEA • 1 ♀; Seringbara, Mount Nimba, Guinea, 7°40'N, 8°26'W; 599 m a.s.l.; gallery forest; 09/10/2008; D. Van den Spiegel leg.; BE_RMCA_ARA.Ara.222490.

Diagnosis. Males of *Selenogyrus foordi* sp. nov. can be distinguished from *S. aureus* by the thinner apical taper of the embolus (embolus wider at apex in *S. aureus*) and the presence of darkened femora and white markings on the distal third tibiae *in vivo* (femora with golden tinge and lacking white markings on the distal third of the tibiae in *S. aureus*). Females of *S. foordi* sp. nov. can be distinguished from *S. africanus*, *S. austini*, and *S. caeruleus* by the medially flared receptacles of the spermathecae (not medially flared in *S. africanus*, *S. austini*, and *S. caeruleus*).

Etymology. The specific epithet is an eponym honouring our colleague the late Stefan Foord (1971–2023), in recognition of his significant contributions to African arachnology, and in remembrance of his kind and collaborative spirit.

Description of holotype male (BE_RMCA_Ara.246088). Total length including chelicerae: 26.7. Carapace: (damaged) length 12.0, width 10.5. Caput: slightly raised. Ocular tubercle: (damaged during capture, not measurable). Eyes (interpreted in life): AME > ALE, ALE > PLE, PLE > PME, anterior eye row procurved, posterior row slightly recurved. Clypeus: narrow; clypeal fringe: long. Fovea: deep, procurved. Chelicera: length 4.3, width 1.8. Abdomen: length 10.4, width 6.4. Maxilla with 100–150 cuspules covering approximately 32% of the proximal edge. Labium: length 1.2, width 1.5, with 200–220 cuspules most separated by 0.5–1.0 × the width of a single cuspule. Labio-sternal mounds: separate, raised. Sternum: length 4.9, width 3.6, with three pairs of sigilla. Tarsi I–II and IV fully scopulate, tarsus III missing (but confirmed undivided in paratypes examined). Metatarsal scopulae: I 85%; II 78%; III 43%; IV 17%. Lengths of legs and palpal segments: see Table 1, legs 4,1,2,3. Spination: femur I d 0–0–1, II d 0–0–1, palp d 0–0–1, patella III p 0–0–1, tibia II d 0–2–1, v 2–1–3, III d 2–2–2, v 3–1–3, IV d 1–1–2, v 2–1–3, palp p 0–1–2, metatarsus I v 0–0–1 (apical), II v 2–0–3 (apical), III d 2–2–3, v 3–2–3 (apical), IV d 4–6–3, v 4–6–6 (3 apical). Tibia I with paired tibial apophysis, RB longer than PB, PB with 2 prolateral megaspines situated medially, almost as long as branch; RB with one prolatero-apical megaspine, much shorter than branch (Figs 4A–F, 5A–F). Femur III: slightly incrassate. Palpal tibia: unmodified. Palpal cymbium: unmodified. Metatarsus I: straight, unmodified. Posterior lateral spinnerets with three segments, basal 1.1, median 0.5, digitiform apical (missing). Posterior median spinnerets with one segment. Palpal bulb with TH weakly developed; embolus filiform, tapering strongly in apical third; PS, RS, and A weakly developed, PS and RS apically fused (Figs 2A–I, 3A–D). Stridulation organ: prolateral face of chelicera furnished with clavate stridulatory lyra. Colour in alcohol: brown (Figs 1A–B).

Description of paratype female (BE_RMCA_Ara.222490). Total length including chelicerae: 52.3. Carapace: length 20.0, width 18.0. Caput: raised. Ocular tubercle: slightly raised, length 3.3, width 1.5. Eyes: ALE > AME, AME > PLE, PLE > PME, anterior row procurved, posterior row recurved. Clypeus: narrow; clypeal fringe: short. Fovea: deep, procurved. Chelicera: length 12.3, width 8.3. Abdomen: length 24.0, width 15.5. Maxilla with 160–180 cuspules, covering approximately 40% of proximal edge. Labium: length 2.7, width 3.4,

Table 1. *Selenogyrus foordi* sp. nov. holotype male (BE_RMCA_Ara.246088), podomere lengths, * = missing segment, ≥ = total length calculated based solely on measurements of known segments in each case and thus will differ from true total length.

| | I | II | III | IV | Palp |
|------------|------|------|-------|------|------|
| Femur | 12.6 | 11.4 | 10.0 | 13.6 | 7.2 |
| Patella | 6.0 | 5.7 | 4.6 | 5.3 | 3.5 |
| Tibia | 10.4 | 9.5 | 7.2 | 11.0 | 6.9 |
| Metatarsus | 11.1 | 10.1 | 11.6 | 16.5 | – |
| Tarsus | 7.4 | 5.5 | * | 7.0 | 2.3 |
| Total | 47.5 | 42.2 | ≥33.4 | 53.4 | 19.9 |

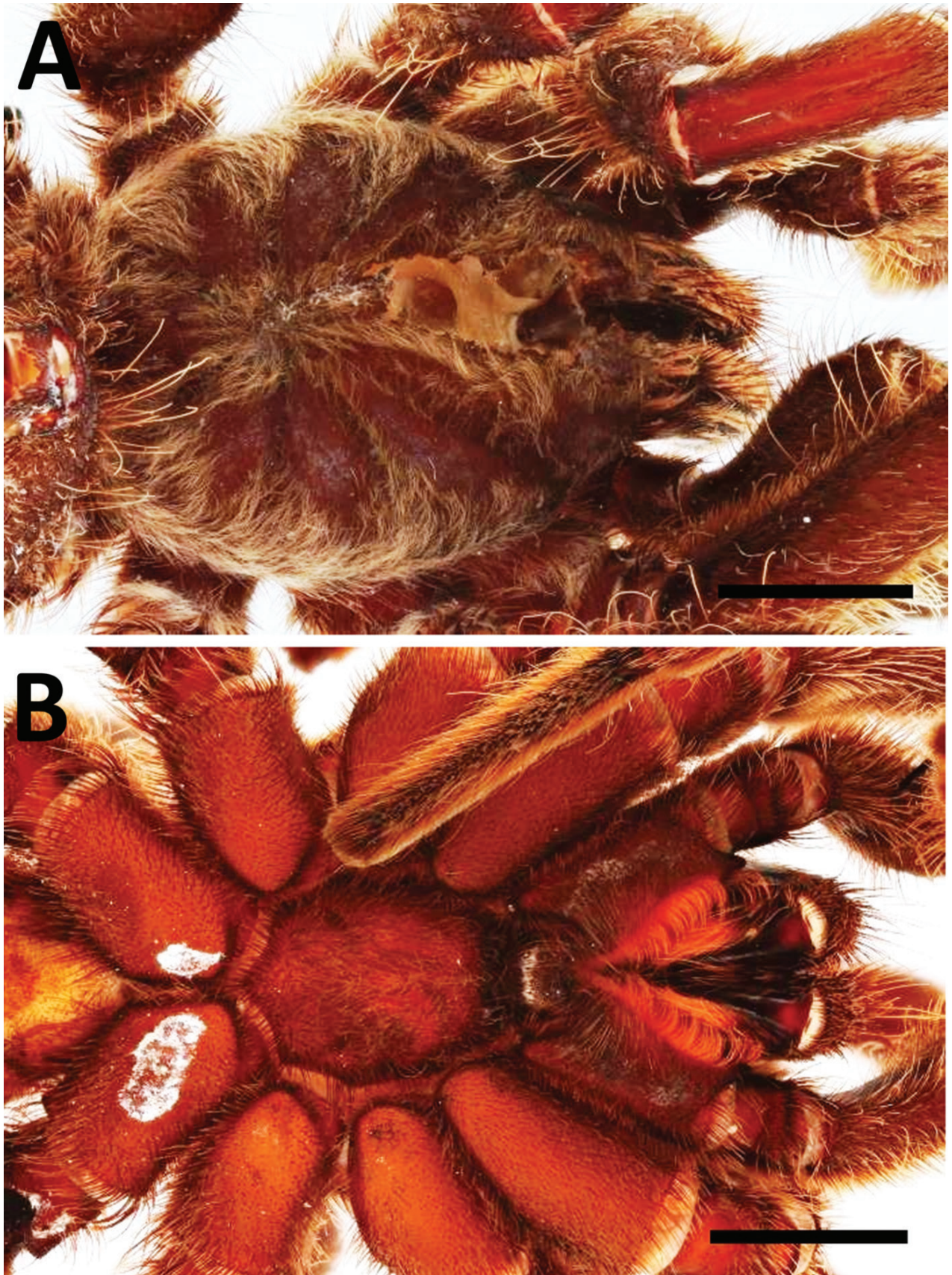


Figure 1. *Selenogyrus foordi* sp. nov. holotype male (BE_RMCA_ARA.Ara.246088) **A** close-up of carapace (damaged), dorsal view **B** close-up of maxilla, labium, and sternum, ventral view. Scale bars: 5 mm.

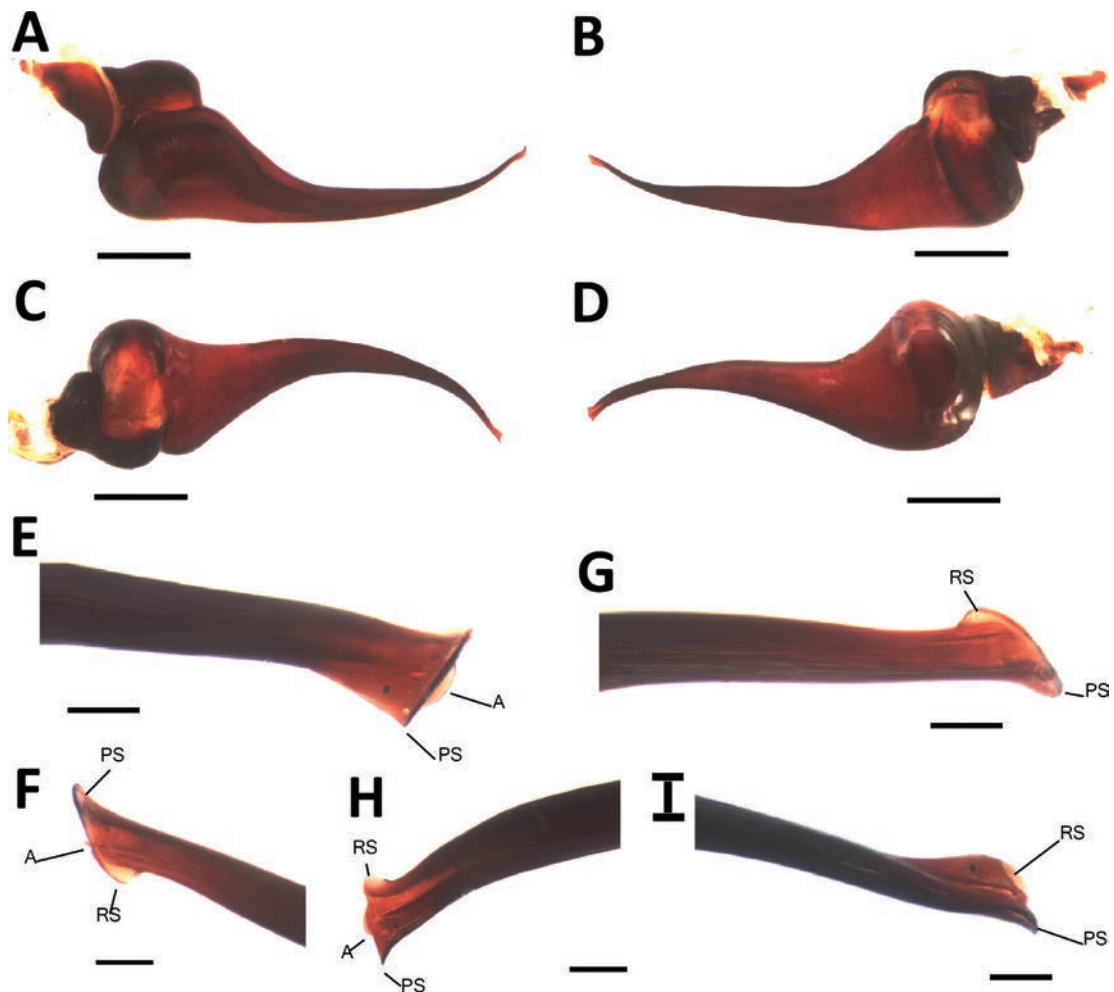


Figure 2. *Selenogyrus foordi* sp. nov. holotype male (BE_RMCA_ARA.Ara.246088), palpal bulb (left-hand side) **A** prolateral view **B** retrolateral view **C** dorsal view **D** ventral view **E** close-up of embolus, prolatero-dorsal view **F** close-up of embolus, retrolateral view **G** close-up of embolus, dorsal view **H** close-up of embolus, ventral view **I** close-up of embolus, ventro-retrolateral view. Scale bars: 1 mm (**A–D**); 0.1 mm (**E–I**).

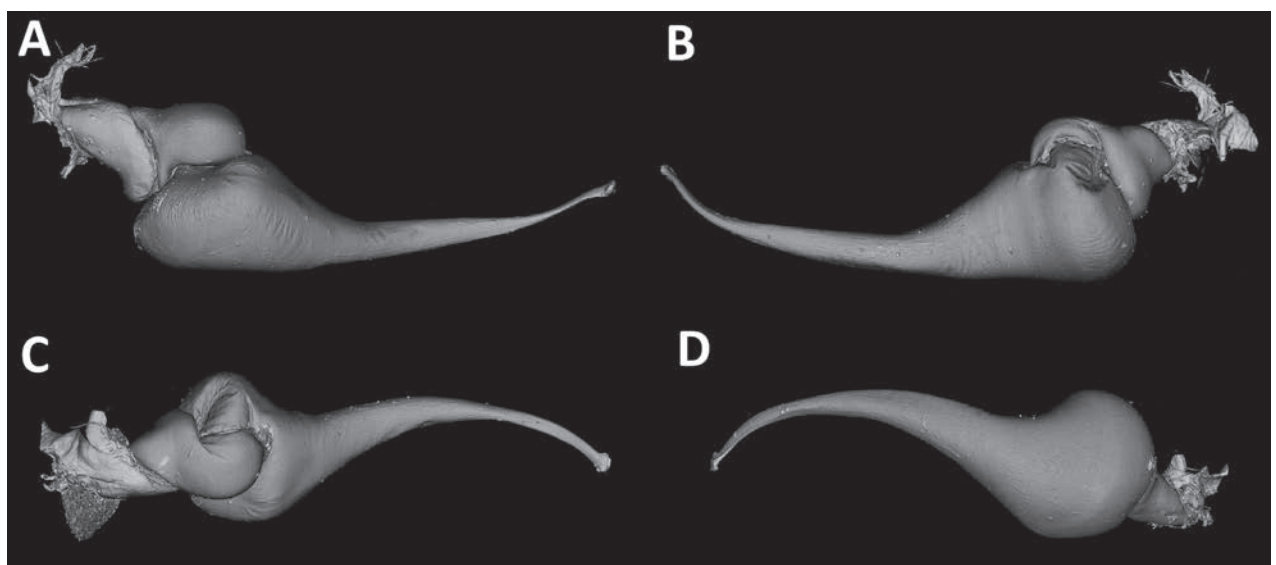


Figure 3. *Selenogyrus foordi* sp. nov. holotype male (BE_RMCA_ARA.Ara.246088), micro-computed tomography of palpal bulb (left-hand side) **A** prolateral view **B** retrolateral view **C** dorsal view **D** ventral view.

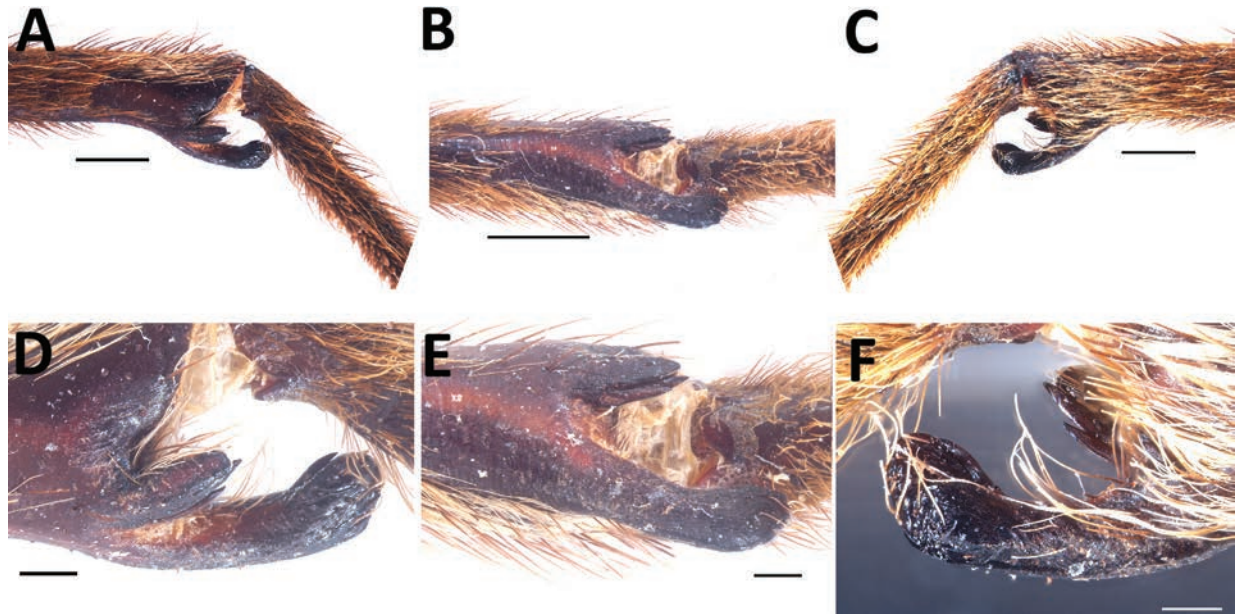


Figure 4. *Selenogyrus foordi* sp. nov. holotype male (BE_RMCA_ARA.Ara.246088), tibial apophysis (left-hand side) **A** prolateral view **B** ventral view **C** retrolateral view **D** close-up, prolateral view **E** close-up, ventral view **F** close-up, retrolateral view. Scale bars: 2 mm (**A–C**); 0.5 mm (**D–F**).

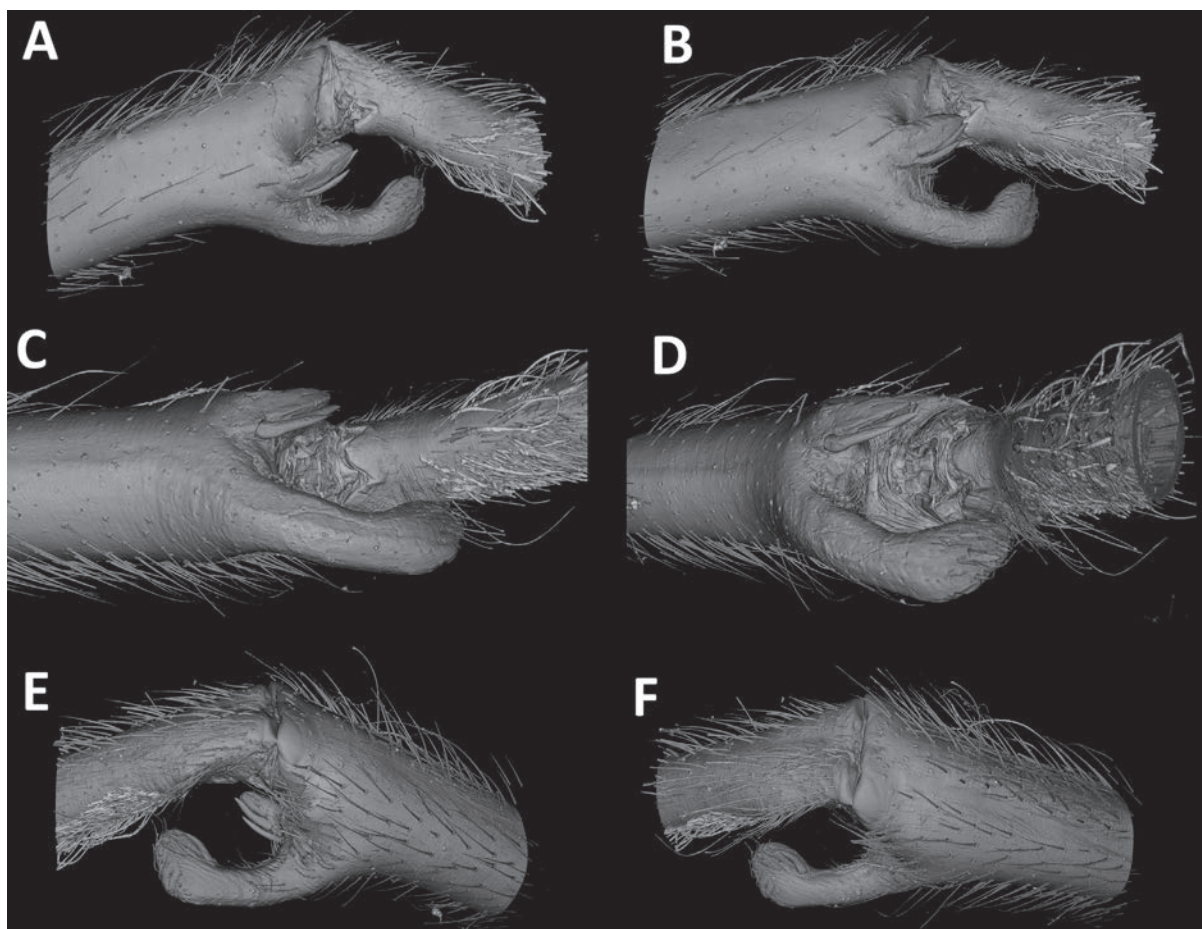


Figure 5. *Selenogyrus foordi* sp. nov. holotype male (BE_RMCA_ARA.Ara.246088), micro-computed tomography of tibial apophysis (left-hand side) **A** prolateral view **B** prolatero-ventral view **C** ventral view **D** ventro-apical view **E** retrolateral view **F** dorso-retrolateral view.

Table 2. *Selenogyrus foordi* sp. nov. paratype female (BE_RMCA_ARA.Ara.222490), podomere lengths.

| | I | II | III | IV | Palp |
|------------|------|------|------|------|------|
| Femur | 16.4 | 14.4 | 12.5 | 16.8 | 5.8 |
| Patella | 9.4 | 6.5 | 7.1 | 8.1 | 3.0 |
| Tibia | 12.5 | 10.2 | 8.2 | 12.1 | 3.8 |
| Metatarsus | 11.2 | 10.1 | 11.1 | 17.1 | – |
| Tarsus | 7.3 | 7.1 | 5.7 | 7.7 | 4.0 |
| Total | 56.8 | 48.3 | 44.6 | 61.8 | 16.6 |

with 130–160 labial cuspules most separated by 0.5–1.0 × the width of a single cuspule. Labio-sternal mounds: separate, raised. Sternum: length 8.7, width 7.8, with three pairs of sigilla. Tarsi I–IV fully scopulate. Metatarsal scopulae: I 83%; II 65%; III 49%; IV 23%. Lengths of leg and palpal segments: see Table 2, legs 4,1,2,3. Spination: femur palp d 0–0–1, tibia I v 0–0–3, II v 0–0–3, III v 2–1–2, p 0–1–0, r 0–1–0, IV v 1–1–3, p 0–1–0, r 0–1–1, palp p 0–2–2, r 0–0–2, metatarsus I r 0–0–3, II r 0–0–3, III d 0–0–2, v 2–2–4 (3 apical), p 1–1–2, r 1–1–0, IV v 3–4–5 (3 apical), r 1–1–0. Posterior lateral spinnerets with three segments: basal 2.2, medial 2.0, digitiform apical 3.3. Posterior median spinnerets with one segment. Spermathecae with two distinct and separate receptacles, basally wider than apex, medially with prolateral and retrolateral flaring, tapering gently thereafter to apex, each receptacle with a single indistinct lobe without neck constriction (Fig. 2D). Stridulation organ: prolateral face of chelicera furnished with clavate stridulatory lyra (Fig. 2C). Colour in alcohol: brown (Figs 2A–B).

Colour *in vivo*. Male with carapace with turquoise pubescence, with alternating radial bands of fawn and dark green, lateral margins with bands of sepia-coloured bristles, anterior margin fawn. Chelicerae with tawny-brown bristles, endites with long red-brown bristles apically. Palp dark brown, apically with a white blotch. Legs: femora dark brown, with long brown bristles ventrally; patellae dark brown with some lighter bristles; tibiae brown in proximal half and white in distal half; metatarsi light brown with distal part paler; tarsi light brown; all legs with numerous long light bristles, more densely distributed on legs 3 and 4. Abdomen dark brown, with a slightly coppery sheen and light, long, brown bristles; spinnerets brown (Figs 6A–C). Female overall black, with orange-red hairs densely distributed on legs (Fig. 7E).

Distribution. Known only from Mount Nimba, Guinea.

New distribution record

Selenogyrus aureus Pocock, 1897

Selenogyrus aureus Pocock, 1897: 768, pl. 41, fig. 2.

Selenogyrus aureus: Hirst, 1908: 402, fig. 1.

Selenogyrus aureus: Smith, 1987: 98, fig. 100h.

Selenogyrus aureus: Smith, 1990: 138, figs 892–911.

Selenogyrus aureus: Schmidt, 1993: 58, figs 35.

Selenogyrus aureus: Schmidt, 2003: 116, fig. 63.



Figure 6. *Selenogyrus foordi* sp. nov. holotype male (BE_RMCA_ARA.Ara.246088), habitus *in situ* at type locality **A** general view **B** same, on different background **C** frontal view, specimen in defensive posture.

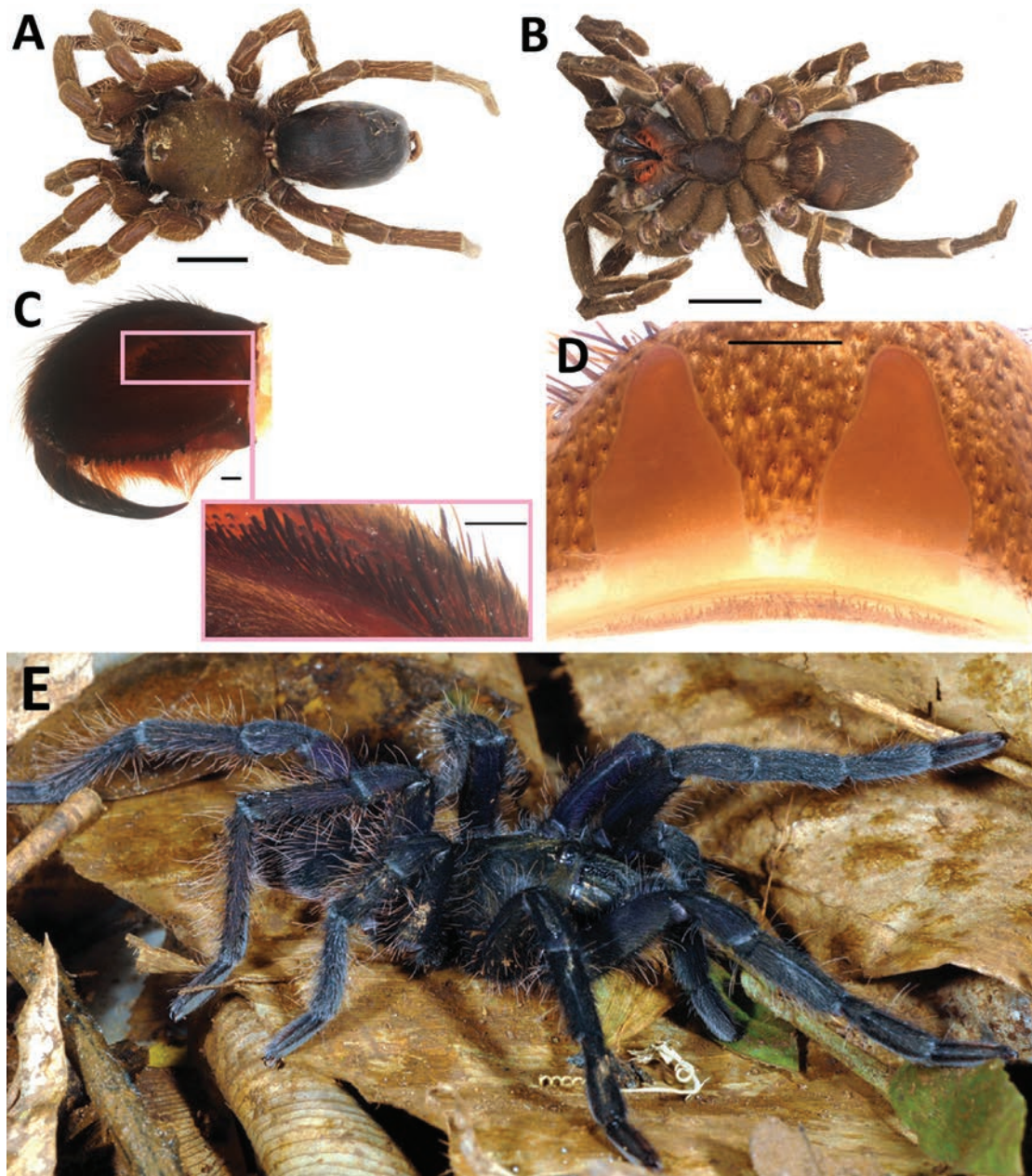


Figure 7. *Selenogyrus foordi* sp. nov. paratype female (BE_RMCA_ARA.Ara.222490) **A** habitus, dorsal view **B** habitus, ventral view **C** chelicera, prolateral view (inset: close-up of stridulatory lyra) **D** spermathecae, dorsal view **E** habitus *in vivo*. Scale bars: 10 mm (**A–B**); 0.5 mm (**D**); 0.1 mm (**C**).

Material examined. Holotype: SIERRA LEONE • 1♂; Sierre Leone [*sic!*]; no collector or date given; NHMUK 1865.83.

Non-type: GUINEA • 1♂; Massif du Zياما Biosphere Reserve, Guinea, 8°24'N, 9°17'W; pitfall traps in rainforest; 10/07/1998; leg. D. Flomo; BE_RMCA_ARA.Ara.216682 • 1♂; same data except 23/07/1998; BE_RMCA_ARA.Ara.216680 • 1♂; same data except 13/04/1998; BE_RMCA_ARA.Ara.216681 • 1♂; same data except no date; BE_RMCA_ARA.Ara.216683.

Diagnosis. See diagnosis for *S. foordi* sp. nov.

Distribution. Guinea (new record) and Sierra Leone (World Spider Catalog 2024).

Remarks. We provide photomicrographs of the palpal bulb of the holotype male (Figs 8A–D) to assist in identification of this species, but do not give a full

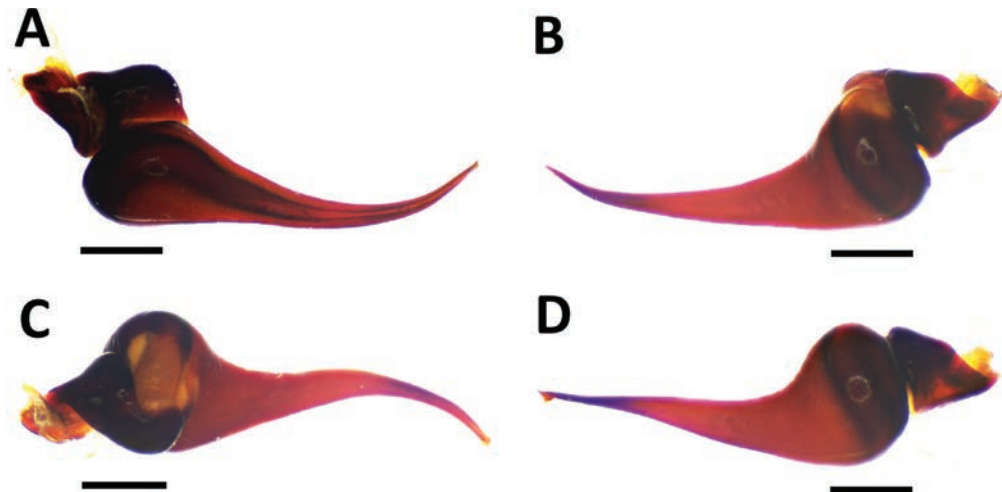


Figure 8. *Selenogyrus aureus* Pocock, 1897 holotype male (NHMUK 1865.83), palpal bulb (left-hand side) **A** prolateral view **B** retrolateral view **C** dorsal view **D** ventral view. Scale bars: 1 mm.

description of the specimen since this will be forthcoming in a separate work by another colleague (R. Gallon pers. comm.).

Acknowledgements

First and foremost, we warmly thank Galina Azarkina (Institute of Systematics and Ecology of Animals, Novosibirsk) and John Midgeley (KwaZulu-Natal Museum, Durban) for invitation to submit this work to the special issue commemorating Stefan Foord. We also thank Richard Gallon (British Arachnological Society) for his helpful comments and for allowing us to publish the new species description ahead of his revision of the African theraphosid subfamilies. Pedro Peñaherrera-R. (Universidad San Francisco de Quito, Ecuador) is thanked for discussion on embolar keel homology. We also thank Sergei Zonstein (Steinhart Museum of Natural History) and Ansie Dippenaar-Schoeman (South African National Survey of Arachnida) for their comments which improved the final manuscript.

Additional information

Conflict of interest

The authors have declared that no competing interests exist.

Ethical statement

No ethical statement was reported.

Funding

No funding was reported.

Author contributions

DS identified all specimens, produced photomicrographs and plates, made the diagnosis and descriptions, wrote the first draft of the manuscript and edited the revised manuscript. AH collected specimens, produced photomicrographs and plates, took additional measurements for descriptions, and edited the revised manuscript. DVDS collected specimens, provided locality and ecological data, and edited the revised manuscript.

Author ORCIDs

Danniella Sherwood  <https://orcid.org/0000-0001-8170-9529>

Arnaud Henrard  <https://orcid.org/0000-0003-3270-7193>

Didier Van Den Spiegel  <https://orcid.org/0000-0002-8696-9810>

Data availability

All of the data that support the findings of this study are available in the main text.

References

- Hirst AS (1908) On a new type of stridulating-organ in mygalomorph spiders, with the description of a new genus and species belonging to the suborder. *Annals and Magazine of Natural History* [8] 2(11): 401–405. <https://doi.org/10.1080/00222930808692503>
- Nentwig W, Blick T, Gloor D, Jäger P, Kropf C (2020) How to deal with destroyed type material? The case of Embrik Strand (Arachnida: Araneae). *Arachnologische Mitteilungen* 59(1): 22–29. <https://doi.org/10.30963/aramit5904>
- Petrunkévitch A (1925) Arachnida from Panama. *Transactions of the Connecticut Academy of Arts and Sciences* 27: 51–248.
- Pocock RI (1897) On the spiders of the suborder Mygalomorphae from the Ethiopian Region, contained in the collection of the British Museum. *Proceedings of the Zoological Society of London* 65(3): 724–774. [pl. 46–48] <https://doi.org/10.1111/j.1096-3642.1897.tb03116.x>
- Rollard C, Wesółowska W (2002) Jumping spiders (Arachnida, Araneae, Salticidae) from the Nimba Mountains in Guinea. *Zoosystema* 24: 283–307.
- Schmidt G (1993) *Vogelspinnen: Vorkommen, Lebensweise, Haltung und Zucht, mit Bestimmungsschlüsseln für alle Gattungen, Vierte Auflage*. Landbuch, Hannover, 151 pp.
- Schmidt G (2003) *Die Vogelspinnen: Eine weltweite Übersicht*. Neue Brehm-Bücherei, Hohenwarsleben, 383 pp.
- Shorthouse DP (2010) SimpleMappr, an online tool to produce publication-quality point maps. <https://www.simplemappr.net>
- Simon E (1887) *Études arachnologiques. 19e Mémoire. XXVII. Arachnides recueillis à Assinie (Afrique occidentale) par MM. Chaper et Alluaud*. *Annales de la Société Entomologique de France* 7(6): 261–276.
- Simon E (1892) *Histoire naturelle des araignées. Deuxième édition, tome premier*. Roret, Paris, 256 pp. <https://doi.org/10.5962/bhl.title.51973>
- Smith AM (1986) *The tarantula: classification and identification guide*. Fitzgerald Publishing London, 179 pp.
- Smith AM (1987) *The tarantula: classification and identification guide (2nd edn.)*. Fitzgerald Publishing, London, 179 pp.
- Smith AM (1990) *Baboon spiders: Tarantulas of Africa and the Middle East*. Fitzgerald Publishing, London, 142 pp.
- World Spider Catalog (2024) *World Spider Catalog, version 25.0*. Natural History Museum, Bern. <https://www.wsc.nmbe.ch> [accessed on 2nd August 2024]
- Zonstein SL (2018) Notes on the spider genus *Acontius*, with a description of two new species from Guinea and Burundi (Aranei: Cyrtaucheniidae). *Arthropoda Selecta* 27(3): 219–226. <https://doi.org/10.15298/arthscl.27.3.04>

The first record of *Atherigona* from Lesotho (Diptera, Muscidae), with description of a new species

Mokome M. J. Magoai¹ , Burgert S. Muller¹ 

¹ Department of Terrestrial Invertebrates, National Museum, Bloemfontein, South Africa
Corresponding author: Mokome M. J. Magoai (jarmaine.mmj@gmail.com)

Abstract

Eight species of *Atherigona* Rondani, 1856 are recorded from Lesotho for the first time: *Atherigona angulata* Deeming, 1971, *Atherigona chrysohypene* Muller, 2015, *Atherigona kirkspriggsi* Muller, 2015, *Atherigona laevigata* (Loew, 1852), *Atherigona lineata ugandae* van Emden, 1940, *Atherigona londti* Muller, 2015, *Atherigona rubricornis* Stein, 1913 and a new species *Atherigona jordaensi* **sp. nov.** The new species is described and diagnoses for all known species from Lesotho are provided with a brief discussion on their distribution in the country.

Key words: Afrotropical Region, new records, shoot flies, Southern Africa, taxonomy

This article is part of:

The Diptera of Lesotho

Edited by John Midgley, Burgert Muller,
Genevieve Theron, Kurt Jordaens



Academic editor: Genevieve Theron

Received: 10 July 2024

Accepted: 19 August 2024

Published: 3 September 2024

ZooBank: <https://zoobank.org/C06A15ED-2AF6-4F52-A6D5-BB4567DA3480>

Citation: Magoai MMJ, Muller BS (2024) The first record of *Atherigona* from Lesotho (Diptera, Muscidae), with description of a new species. African Invertebrates 65(2): 49–60. <https://doi.org/10.3897/AfrInvertebr.65.131744>

Copyright:

© Mokome M. J. Magoai & Burgert S. Muller.
This is an open access article distributed under
terms of the Creative Commons Attribution
License (Attribution 4.0 International – CC BY 4.0).

Introduction

Atherigona Rondani, 1856 is one of the most speciose genera of Muscidae, with some 260 species described, of which ca 168 species are known to occur in the Afrotropical region (Dike 2003; Couri et al. 2006; Muller 2015; Muller and Mostovski 2018; Deeming 2019; Deeming 2022). The identification key to Afrotropical Muscidae by Couri (2007) can be used to reliably identify the genus within the Region. It consists of two subgenera, *Atherigona sensu stricto* and *Atherigona (Acritochaeta)* Grimshaw, 1901 (Suh and Kwon 2018). *Atherigona s. str.* attacks cultivated crops; the larvae feeding mostly on Poaceae which includes several cereal crops (Suh and Kwon 2018). *Atherigona tritici* Pont & Deeming, 2001, *Atherigona naqvii* Steyskal, 1966 and *Atherigona lineata* (Adams, 1905) have been reported to cause harm to cereal crops, with *A. tritici* resulting in about 10% wheat yield loss (Pont and Deeming 2001; Muller and Mostovski 2018). *Atherigona soccata* Rondani, 1871, better known as the sorghum shoot fly is one of the most notorious pest species known to occur in Africa. It causes dead heart symptoms, especially in sorghum, but also millet and maize (Van den Berg et al. 2005). It is widespread and infestations have resulted in up to 90% yield loss across Africa, Asia and, Latin America (Young and Teetes 1977; Sherwill et al. 1999; Muller and Mostovski 2018).

The larvae of *Atherigona (Acritochaeta)* species, in contrast, are typically considered saprophages or facultative predators in decaying organic matter (Skidmore 1985; Grzywacz et al. 2013); additionally Kovac et al. (2023)

described *Atherigona (Acritochaeta) culicivora* Kovac, Pont & Deeming, 2023 from Thailand that is subaquatic and preys on mosquito larvae. In contrast, *Atherigona (Acritochaeta) orientalis* Schiner, 1868, is a pest of agricultural crops such as peppers, tomatoes, and sorghum (Savage 2016; Roditakis et al. 2023).

The Diptera of Lesotho are generally poorly studied and Midgley et al. (2023) provided a summary of the history of collecting in Lesotho, as well as detailed information on recent collecting trips. This collecting paucity is further emphasized by papers such as Muller and Midgley (2022) where they report on the first record of a similarly speciose genus *Coenosia* Meigen, 1826 from Lesotho. *Coenosia* is quite well known from the surrounding South Africa, yet conversely the genus was unrecorded for Lesotho. This holds true for *Atherigona* and most other muscid genera.

Although Lesotho shares much of its vegetation (Mucina and Rutherford 2006) and geology with South Africa, it is on average 900 metres higher above sea level than South Africa (Midgley et al. 2023), and this difference in elevation compared to South Africa may result in differences in insect diversity. As insect pests, *Atherigona* species may potentially contribute to agricultural challenges in Lesotho. However, more information on the diversity and distribution of the genus is needed before potential management practices may be implemented. This could allow local subsistence farmers and land managers to better manage pest species if present. To this end, a species checklist of newly recorded *Atherigona* is provided, with a description of *A. jordaensi* sp. nov., from southeastern Lesotho. This should be seen as a springboard to the future study of the group in Lesotho.

Material and methods

Collection abbreviations (Curators in parentheses)

AMGS Albany Museum, Makhanda, South Africa (Terence Bellingan);

BMSA National Museum, Bloemfontein, South Africa (Gimo Daniel);

NMSA KwaZulu-Natal Museum, Pietermaritzburg, South Africa (Kirstin Williams).

Locality and collecting methods

Specimens were collected either by hand using a sweep net or through Malaise trapping. Specimens were examined from 8 sites: 5 Lesotho Highland Basalt Grassland sites and 1 Western Lesotho Basalt Shrubland site within the Drakensberg Grassland Bioregion, and 2 Basotho Montane Shrubland site within Mesic Highveld Grassland Bioregion (Figs 1, 2).

Specimen treatment

Male terminalia were macerated in 10% heated potassium hydroxide (KOH) for approximately 10 minutes and the trifoliate process (Figs 4–11) exposed. Specimens were identified using a combination of the keys provided by Dike (1989) and Muller (2015). All measurements of *A. jordaensi* sp. nov., were made using a Nikon SMZ745T stereomicroscope with attached Motic camera and Motic Images Plus 3 software. The habitus photo of *A. jordaensi* sp. nov. was taken using a Canon 850D camera, and illustrations of terminalia made using a combination of Adobe Illustrator and Photoshop CC 2024.



Figures 1, 2. Sampling localities and vegetation examples 1 roadside swamp, 30°13.690'S, 28°8.445'E, Lesotho Highland Basalt Grassland (*A. jordaensi* sp. nov. type locality) 2 near Molimo Nthuse Lodge, on God Help Me Pass, A3, 29°25.386'S, 27°54.330'E, Western Lesotho Basalt Shrubland. (Fig. 1: Midgley et al. 2023, p215, fig. 27).

Taxonomy

Genus *Atherigona* Rondani, 1856

Subgenus *Atherigona* Rondani, 1856

***Atherigona angulata* Deeming, 1971**

Fig. 4

Atherigona angulata Deeming, 1971: 157, figs 54, 55; Deeming 1981: 105; Muller 2015: 858, fig. 5.

Material examined. LESOTHO • 2♂; Mamathes [now Masupha], Basutoland; [29°8.000'S, 27°51.000'E]; 30 Apr. 1949; C. Jacot Guillarmod leg. (AMGS) • 1♂; Masupha, Basutoland; [29°8.000'S, 27°51.000'E]; 10 Jun. 1948; C. Jacot Guillarmod leg. (AMGS) • 1♂; Mamathes, Basutoland; [29°8.000'S, 27°51.000'E]; 8 Feb. 1948; C. Jacot Guillarmod leg. (AMGS).

Other material examined. SOUTH AFRICA • 1♂; Free State, Brandfort, Florisbad Research Station; 28°46.039'S, 26°04.234'E; 4–6 Apr. 2009; A.H. Kirk-Spriggs leg.; Malaise traps, Acacia, Savanna; BMSA(D)05575 • 1♂; Free State, Brandfort, Soetdoring Nature Reserve, train camp; 28°50.934'S, 26°01.996'E; 5–6 Apr. 2009; A.H. & M.K. Kirk-Spriggs leg.; Malaise traps, Acacia, Savanna thicket; BMSA(D)05494.

Diagnosis. This species has golden/yellow vibrissa, similar to that of *Atherigona pulla* (Wiedemann, 1830) and *Atherigona chrysohypene* Muller, 2015. It can be distinguished from *A. pulla* by the shape of the trifoliate process, with the median piece bent at a right-angle when viewed in profile (Fig. 4b) compared to a linear median piece in *A. pulla*. It can be distinguished from *A. chrysohypene* by the shape of the hypopygial prominence which is knoblike (Fig. 4) and with an apical emargination, compared to that of *A. chrysohypene* which is bilobate (Fig. 5).

Distribution. Botswana, Lesotho (new record), Namibia, Nigeria, South Africa, Saudi Arabia.

***Atherigona chrysohypene* Muller, 2015**

Fig. 5

Atherigona chrysohypene Muller, 2015: 863, fig. 46.

Material examined. LESOTHO • 4♂; Mamathes [Masupha], Basutoland; [29°8.000'S, 27°51.000'E]; 16 May 1948; C. Jacot Guillarmod leg. (AMGS) • 1♂; Masupha, Basutoland; [29°8.000'S, 27°51.000'E]; 24 May 1948; C. Jacot Guillarmod leg. (AMGS) • 1♂; Mamathes [Masupha], Basutoland; [29°8.000'S, 27°51.000'E]; 30 May 1948; C. Jacot Guillarmod leg. (AMGS) • 2♂; Mamathes [Masupha], Basutoland; [29°8.000'S, 27°51.000'E]; 10 Jun. 1948; C. Jacot Guillarmod leg. (AMGS).

Diagnosis. This species is similar to *A. pulla* and *A. angulata* due to its golden yellow vibrissa. However, it can be distinguished from both by its bilobate hypopygial prominence (Fig. 5), while *A. pulla* and *A. angulata* have the hypopygial prominence knoblike (e.g. Fig. 4).

Distribution. Lesotho (new record), South Africa.

***Atherigona jordaensi* sp. nov.**

<https://zoobank.org/C6F47D05-FC8D-4B09-B51C-CFDADBBCC098>

Figs 3, 6

Material examined. Type material examined: Holotype: LESOTHO • 1♂; Quting, Mphaki, Roadside swamp; 30°13.690'S, 28°8.445'E; 30 Nov. 2022; K. Jordaens, J. Midgley, B. Muller and G. Theron leg.; Hand collecting; Lesotho Highland Basalt Grassland; BMSA(D)134684. The holotype is in good condition. Paratypes: LESOTHO • 2♂; Same data as holotype; (BMSA(D)134681; NMSA DIP 223216) • 3♂; Quting, Mphaki, Roadside seep/stream; 30°12.882'S, 28°8.307'E; 2221 m; 28–30 Nov. 2022; K. Jordaens, J. Midgley, B. Muller and G. Theron leg.; Hand collecting; Lesotho Highland Basalt Grassland; (BMSA(D)134678, 134675; NMSA-DIP 223217) • 2♂; Maseru District, God Help Me Pass, A3, nr, Molimo Nthuse Lodge; 29°25.386'S, 27°54.330'E; 2025 m; 29 Jan. 2023; B.S. Muller And G. Theron leg.; Sweep net, Mixed Forest vegetation; (BMSA(D)132581; NMSA-DIP 223218) • 1♂; Quting, Letseng la Letsie at; 30°18.772'S, 28°10.062'E; 2410 m; 29 Nov. 2022; K. Jordaens, J. Midgley, B. Muller and G. Theron leg.; Hand collecting, Lesotho Highland Basalt Grassland; BMSA(D)134693.

Other material examined. SOUTH AFRICA • 2♂; Free State, Harrismith, Scotland farm at; 27°58.992'S, 29°37.151'E; 10–12 Nov. 2009; A.H. Kirk-Spriggs leg.; Malaise traps, dense *Leucosedea*-dominated scrub; (BMSA(D)12781, 12783).

Type condition. The following 7♂ paratypes were dissected: BMSA(D)134681, 134680, 134678, 134675, 134674, 132581, 134693.

Deposition information. Holotype and paratypes are deposited at National Museum, Bloemfontein, except for NMSA-DIP 223216, 223217, 223218 that are deposited at the KwaZulu-Natal Museum.

Diagnosis. This species is most similar to *Atherigona decempilosa* Dike, 1989. It will key out to couplet 30 in Muller (2015). It can be separated from *A. decempilosa* by having the median piece of the trifoliate process medially dilated in profile (Fig. 6) not “apically dilated and bifid” and the basal lateral area of the lateral plates curve upward and do not appear “angular”. Additionally, the



Figure 3. Photo of *Atherigona jordaensi* sp. nov. Holotype male. Scale bar: 1 mm.

hood of *A. jordaensi* is not as well-developed as in *A. decempilosa* (Muller 2015, fig. 25). Lastly, *A. decempilosa* has some degree of infuscation on all of its legs whereas *A. jordaensi* only has the foreleg somewhat infuscated.

Description. Measurements (Holotype): Body length: 3.84 mm wing: 3.66 mm, rm crossvein ratio: 0.375.

Male. Head: Ground colour dark; all head setae and setulae infuscated; upper occiput grey dusted posteriorly with narrow median part glossy, laterally also grey dusted, however, lower occiput golden-grey dusted; ocellar triangle grey dusted; with three pairs of strong proclinate frontal setae and two weaker and shorter setae on frontal angle, also with two pairs of orbital setae; parafacial silver-grey dusted, at narrowest as wide as arista base; scape and pedicel entirely infuscated; postpedicel infuscated; arista infuscated; palpus infuscated, apically dilated and truncated, with some short infuscated setulae and mostly longer hyaline setulae; four well-developed vibrissal setae surrounded by 3–4 setulae.

Thorax: Ground colour dark; postpronotal lobe grey dusted, lobe with three setae and 8–14 setulae; scutum golden-grey dusted, with faint 2–4 dorsocentral vittae, not extending to the scutellum; scutellum golden-grey dusted dorsally, margins more densely golden-grey dusted; one pair of basal setae, one pair of discal setae and 3–8 discal setulae, one pair of subbasal setae and one pair of apical setae, subbasal and apical pair subequal; pleura golden-grey dusted; proepisternum inconspicuous, with two setae, one stronger than the other, and one setula (some specimens with an additional much weaker setula); katepisternal setae 1:1:1.

Legs: All legs yellow except for apical half of fore femur, excluding apex, apical 2/3 of fore tibia and fore tarsi that are infuscated; leg chaetotaxy: fore tarsi without any specialised chaetotaxy.

Wings: Hyaline; veins light-brown; halteres with white knob and yellow stalk; calypters somewhat light-brown.

Abdomen: All tergites and sternites yellow and without any dorsal median vittae; tergite 1+2 immaculate; tergite 3 with two small spots (some specimens appearing to have a large mark underneath each spot), ca 2× the size of those on tergite 4; tergite 4 also with two small spots; tergite 5 immaculate.

Terminalia (Fig. 6): Hypopygial prominence knob-shaped with two anteriorly projecting tubercles. Trifoliate process infuscated except for brown stem; median piece of the trifoliate process medially dilated in profile; lateral plates wider than median piece in profile, inner lobes present. Surstylus not infuscated.

Female. Unknown

Etymology. Named after Dr Kurt Jordaens of the Royal Museum for Central Africa, Tervuren, for his contribution to the study of Diptera in Lesotho.

Distribution. Lesotho, South Africa.

***Atherigona kirkspriggsi* Muller, 2015**

Fig. 7

Atherigona kirkspriggsi Muller, 2015: 875, fig. 33.

Material examined. LESOTHO • 17♂; Leribe District, Motebong Lodge, Katse Dam area; 29°6.060'S, 28°30.084'E; 2063 m; 10–13 Dec. 2021; J.M. Midgley, B. Muller leg.; Malaise trap, Garden entertainment area; (BMSA(D)130773, 130775, 130776, 130777, 130778, 130779, 130783, 130809, 130810, 130826, 130844, 130848, (NMSA-DIP 213809, 213810, 213812, 213813, 213814)) • 1♂; Quting, Mphaki Farmers Training Centre; 30°11.598'S, 28°7.831'E; 2046 m; 01–27 Nov.– Dec. 2022; K. Jordaens, J. Midgley, B. Muller and G. Theron leg.; Malaise trap, Lesotho Highland Basalt Grassland, Garden; BMSA(D)134687.

Diagnosis. This species is similar to *Atherigona lineata torrida* Deeming, 1971. However, it differs from it by having a tridentate hypopygial prominence (Fig. 7) and infuscated mid and hind leg tarsi, compared to the bifurcated hypopygial prominence and brown tarsi in *Atherigona lineata lineata* (Adams, 1905).

Distribution. Lesotho (new record), South Africa.

***Atherigona laevigata* (Loew, 1852)**

Fig. 8

Coenosia laevigata Loew, 1852: 660.

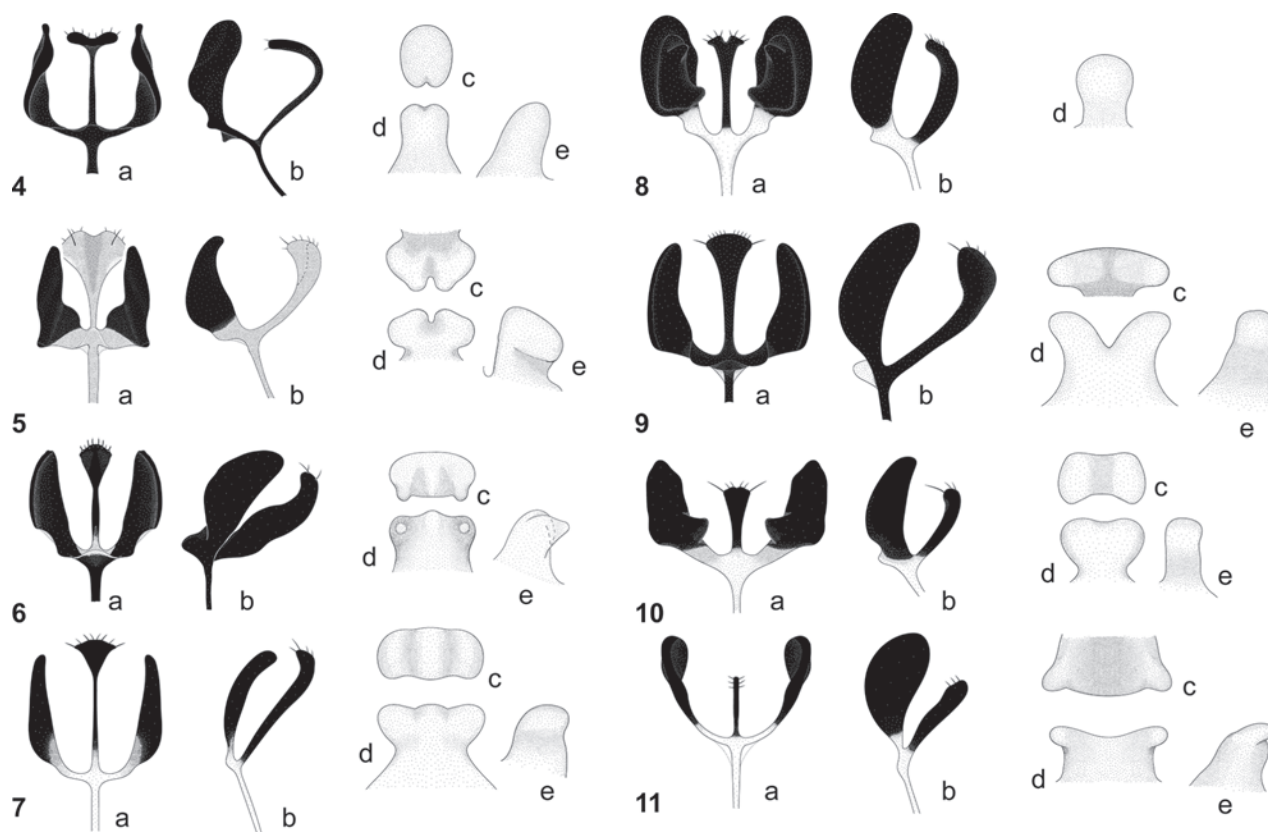
Atherigona laevigata: Van Emden 1940: 113, figs 6, 56; Deeming 1971: 148, figs 13–18; Pont 1991: 341; Muller 2015: 877, fig. 7, Muller and Mostovski 2018: 350, fig. 6, Deeming 2022: 127.

Atherigona scutellaris Stein in Becker 1903: 110.

Atherigona minuta Schnabl & Dziedzicki, 1911: 183.

Material examined. LESOTHO • 1♂; Mamathes [Masupha], Basutoland; [29°8.000'S, 27°51.000'E]; 16 May 1948; C. Jacot Guillarmod leg.

Other material examined. SOUTH AFRICA • 1♂; Free State, Brandfort, Florisbad Research Station; 28°46.039'S, 26°04.234'E; 4–6 Apr. 2009; A.H. Kirk-Spriggs leg.; Malaise traps, Acacia, Savanna; BMSA(D)05529 • 1♂; KwaZulu-Natal,



Figures 4–11. Trifoliolate process and hypopygial prominence of 4 *A. angulata* 5 *A. chrysohypene* 6 *A. jordaensi* sp. nov. 7 *A. kirkspriggsi* 8 *A. laevigata* 9 *A. lineata ugandae* 10 *A. londti* 11 *A. rubricornis*. Trifoliolate process: a posterior view b in profile. Hypopygial prominence c dorsal view d posterior view e in profile.

Ndumo Game Reserve, Shokwe area at: 26°52.125'S, 32°13.731'E; 30 Nov.–4 Dec. 2009; A.H. Kirk-Spriggs leg.; Malaise traps, Ficus forest; BMSA(D)15826.

Diagnosis. This species can be distinguished from other Afrotropical species by its glossy frontal plate and infuscated frontal vitta with apical third yellow in combination with a knoblike hypopygial prominence (Fig. 8).

Distribution. AFROTROPICAL – Angola, Comoros, Democratic Republic of Congo, Ethiopia, Kenya, Lesotho (new record), Madagascar, Mali, Mauritius, Mozambique, Namibia, Nigeria, Rwanda, Seychelles, South Africa, Tanzania, Uganda, Zambia, Zimbabwe. PALAEARCTIC – Cyprus, Egypt, Iraq, Israel, Jordan, Saudi Arabia, UAE, Yemen.

Atherigona lineata ugandae van Emden, 1940

Fig. 9

Atherigona lineata ugandae van Emden, 1940: 137, figs 18, 39. Deeming 1971: 177, figs 134–138; Deeming 2000: 285; Muller 2015: 882, fig. 53.

Material examined. LESOTHO • 3♂; Mamathes [Masupha], Basutoland; [29°8.000'S, 27°51.000'E]; 16 May 1948; C. Jacot Guillarmod leg.

Other material examined. SOUTH AFRICA • 2♂; Free State, Brandfort, Florisbad Research Station; 28°46.039'S, 26°04.234'E; 4–6 Apr. 2009; A.H. Kirk-Spriggs leg.; Malaise traps, Acacia, Savanna; (BMSA(D)05530, 05590).

Diagnosis. *Atherigona lineata* and its subspecies can be distinguished from other similar species by the combination of an infuscated frontal vitta and palpus, and a bifurcated hypopygial prominence. The subspecies *A. lineata lineata*, *A. lineata torrida*, and *A. lineata ugandae* can be distinguished from one another based on the following: *A. lineata lineata* and *A. lineata torrida* have the fore femur infuscated on at least the apical third (the fore femur of *A. lineata ugandae* is entirely yellow). Additionally, the shape of the lateral lobes of the trifoliate process and the depth of the bifurcation of the hypopygial prominence differs in these two subspecies. *A. lineata ugandae* has the hood area of the trifoliate process infuscated (hyaline for the other two) and has a much deeper, wider and pronounced bifurcation compared to others (Fig. 9).

Distribution. Angola, Botswana, Chad, Ethiopia, Kenya, Lesotho (new record), Malawi, Mali, Namibia, Nigeria, Rwanda, South Africa, Uganda.

***Atherigona londti* Muller, 2015**

Fig. 10a–e

Atherigona londti Muller, 2015: 882, fig. 48.

Material examined. LESOTHO • 2♂; Leribe, Motebong Lodge, Katse Dam area; 29°6.060'S, 28°30.084'E; 2063 m; 10–13 Dec. 2021; J.M. Midgley and B. Muller leg.; Malaise trap, Garden entertainment area; (BMSA(D)130774, NMSA-DIP 213800). 3♂; Maseru, Roma Trading Post Lodge; 29°26.592'S, 27°42.224'E; 1640 m; 24–27 Nov. 2022; K. Jordaens, J. Midgley, B. Muller and G. Theron leg.; Malaise trap, Basotho Montane Shrubland, Garden; (BMSA(D)134689,134691,134690).

Diagnosis. This species' scutellum is similar to *Atherigona flavifinis* Muller, 2015 (fig. 16 in Muller 2015) and *Atherigona latibasilaris* Muller, 2015 (fig. 40 in Muller 2015) in having the apex of the scutellum yellow. However, the trifoliate process and hypopygial prominence differ greatly. It keys close to *Atherigona hyalinipennis* van Emden, 1959 and *Atherigona secrecauda* Séguy, 1938 using the keys provided by Deeming (1971) and Dike (1989) but the trifoliate process (Fig. 10) of *A. londti* does not have the wing-like projections of the hood present as in *A. secrecauda*, nor does it have the cordiform median piece of *A. hyalinipennis*.

Distribution. Lesotho (new record), South Africa.

***Atherigona rubricornis* Stein, 1913**

Fig. 11a–e

Atherigona rubricornis Stein, 1913: 531; van Emden 1940: 101, figs. 15, 51; Deeming 1971: 157, figs 47, 48 (*A. tritici* Pont & Deeming figured); Deeming 1979: 39, figs 19 (female tergite 8); Pont and Deeming 2001: 298, figs 1–4; Muller 2015: 897, fig. 38.

Material examined. LESOTHO • 1♂; Mamathes [Masupha], Basutoland; [29°8.000'S, 27°51.000'E]; 30 Apr. 1949; C. Jacot Guillarmod leg. • 1♂; Mamathes [Masupha], Basutoland; [29°8.000'S, 27°51.000'E]; 10 Jun. 1948; C. Jacot Guillarmod leg.

Other material examined. SOUTH AFRICA • 1 ♂; Free State, Brandfort, Florisbad Research Station; 28°46.039'S, 26°04.234'E; 4–6 Apr. 2009; A.H. Kirk-Spriggs leg.; Malaise traps, Acacia, Savanna; BMSA(D)05581 • 1 ♂; KwaZulu-Natal, Royal Natal National Park, Thendele; 28°42.378'S, 28°56.083'E; 15–17.ii.2010; A.H. Kirk-Spriggs leg.; Malaise traps, *Leucosedeae*-dominated scrub; BMSA(D)19723.

Diagnosis. This species is similar to *A. tritici* (which was previously regarded as a form of *A. rubricornis*), but *A. tritici* differs from it by having a median piece with a dilated apical appearance in profile. *Atherigona rubricornis* can be distinguished from other species by its partially yellow frontal vitta and the trifoliate process with median piece linear in posterior view (Fig. 11).

Distribution. Botswana, Chad, Kenya, Lesotho (new record), Namibia, Nigeria, South Africa, Uganda, Zimbabwe.

Discussion

Atherigona is abundant throughout southern Africa and is especially well-recorded and known in South Africa (Muller 2015). Its marked abundance coupled with the lack of previous records from Lesotho highlight the need for more rigorous sampling in order to get a more complete picture of the diversity of the group within the country. Neither *A. soccata* nor *A. orientalis*, known pest species, have been recorded from Lesotho as yet, but the recent expeditions to Lesotho (e.g. Midgley et al. 2023) were more focussed on Alpine areas and less disturbed natural areas, with only 8 out of 30 collecting sites yielding *Atherigona*. To truly record the diversity of *Atherigona* in Lesotho, future surveys will have to be expanded to more *Atherigona*-focussed sampling sites and especially disturbed areas. One would also have to involve local authorities and collaborate with local commercial and subsistence farmers and their surroundings.

Acknowledgements

The Lesotho Ministry of Tourism, Environment and Culture, Department of Environment is thanked for issuing permits to undertake fieldwork. Authors are thankful to the curators for supplying additional study material. The National Museum, Bloemfontein is thanked for its continued support.

Additional information

Conflict of interest

The authors have declared that no competing interests exist.

Ethical statement

MMJM confirms ethical clearance, number NMB ECC 2024/04, forming part of project 567 of the National Museum, Bloemfontein, South Africa.

Funding

Field expeditions in 2021, 2022 and 2023 were funded through DIPoDIP (Diversity of Pollinating Diptera in South African biodiversity hotspots) which is financed by the Directorate-general Development Cooperation and Humanitarian Aid through the Framework agreement with KMMA.

Author contributions

M.M.J. Magoai conceptualised the project with inputs from B.S. Muller. Magoai identified, described and revised the species, and wrote the first draft of the manuscript. Muller illustrated and photographed specimens, and commented and made additions to the final draft.

Author ORCIDs

Mokome M. J. Magoai  <https://orcid.org/0009-0004-0266-9629>

Burgert S. Muller  <https://orcid.org/0000-0002-7304-4050>

Data availability

All of the data that support the findings of this study are available in the main text.

References

- Becker T (1903) Aegyptische Dipteren (Fortsetzung und Schluss). *Mitteilungen aus dem Zoologischen Museum in Berlin* 2: 67–195.
- Couri MS (2007) A key to Afrotropical genera of Muscidae (Diptera). *Revista Brasileira de Zoologia* 24(1): 175–184. <https://doi.org/10.1590/S0101-81752007000100022>
- Couri MS, Pont AC, Penny ND (2006) Muscidae (Diptera) from Madagascar: identification keys, descriptions of new species, and new records. *Proceedings of the California Academy of Sciences, Fourth Series* 57(29): 799–923.
- Deeming JC (1971) Some species of *Atherigona* Rondani (Diptera, Muscidae) from northern Nigeria, with special reference to those injurious to cereal crops. *Bulletin of Entomological Research* 61: 133–190. <https://doi.org/10.1017/S0007485300057527>
- Deeming JC (1979) New and little known species of *Atherigona* Rondani (Dipt, Muscidae) from Nigeria and Cameroon. *Entomologist's Monthly Magazine* 114: 31–52.
- Deeming JC (1981) New and little-known African species of *Atherigona* Rondani (Dipt, Muscidae). *Entomologist's Monthly Magazine* 117: 99–113.
- Deeming JC (2000) Muscidae: Atherigonini (Diptera: Muscoidea). *Cimbebasia Memoir* 9: 283–287.
- Deeming JC (2019) Biology, ecology, distribution and taxonomy of immature stages of *Atherigona* (ss) *hyalinipennis* van Emden (Diptera: Muscidae), a pest of the cereal crop tef (*Eragrostis tef*) and the fodder crop Rhodes grass (*Chloris gayana*). *Entomologist's Monthly Magazine* 155(2): 107–112. <https://doi.org/10.31184/M00138908.1552.3971>
- Deeming JC (2022) Some Afrotropical species of *Atherigona* Rondani (Diptera: Muscidae) revisited and a new species described. *European Journal of Taxonomy* 847: 121–144. <https://doi.org/10.5852/ejt.2022.847.1987>
- Dike MC (1989) A key for the identification of Afrotropical species of the shoot-fly subgenus *Atherigona* of *Atherigona* (Diptera: Muscidae), with a description of some new species from Africa. *Bulletin of Entomological Research* 79: 545–566. <https://doi.org/10.1017/S000748530001871X>
- Dike MC (2003) Distributional patterns of Afrotropical species of *Atherigona* Rondani (Diptera: Muscidae). *Cimbebasia* 19: 215–221.
- Grzywacz A, Pape T, Hudson WG, Gomez S (2013) Morphology of immature stages of *Atherigona reversura* (Diptera: Muscidae), with notes on the recent invasion of North

- America. *Journal of Natural History* 47: 1055–1067. <https://doi.org/10.1080/00222933.2012.742244>
- Kovac D, Pont AC, Deeming JC (2023) *Atherigona culicivora*, new species (Insecta: Diptera: Muscidae), a bamboo shoot-fly feeding on mosquito larvae. *The Raffles Bulletin of Zoology* 71: 583–595. <https://doi.org/10.26107/RBZ-2023-0044>
- Loew H (1852) Hr. Peters legte Diagnosen und Abbildungen der von ihm in Mossambique neu entdeckten Dipteren vor, welche von Hrn. Professor Loew bearbeitet worden sind. Bericht über die zur Bekanntmachung geeigneten Verhandlungen der Königlichen Preussischen Akademie der Wissenschaft zu Berlin 1852: 658–661.
- Midgley JM, Muller BS, Theron GL, Phoofo M, Bellingan TA, Jordaens K (2023) The Diptera of Lesotho: A history of collecting in the Mountain Kingdom, summary of recent collecting sites and introduction to the topical collection in African Invertebrates. *African Invertebrates* 64(3): 207–220. <https://doi.org/10.3897/AfrInvertebr.64.108525>
- Mucina L, Rutherford MC [Eds] (2006) The vegetation of South Africa, Lesotho and Swaziland. South African National Biodiversity Institute, Pretoria, 807 pp.
- Muller BS (2015) Illustrated key and systematics of male South African *Atherigona* s. str. (Diptera: Muscidae). *African Invertebrates* 56(3): 845–918. <https://doi.org/10.10520/EJC183859>
- Muller BS, Midgley JM (2022) How strange: *Coenosia curiosa* sp. nov. (Diptera: Muscidae), the first recorded Tiger fly from Lesotho, with revision of the *Coenosia globuliset*a-group. *Zootaxa* 5222(4): 367–377. <https://doi.org/10.11646/zootaxa.5222.4.5>
- Muller BS, Mostovski MB (2018) A key to males of *Atherigona* s. str. (Diptera: Muscidae) from Mali, with new records and a new species for the country. *Zootaxa* 4425(2): 342–356. <https://doi.org/10.11646/zootaxa.4425.2.9>
- Pont AC (1991) A review of the Fanniidae and Muscidae (Diptera) of the Arabian Peninsula. *Fauna of Saudi Arabia* 12: 312–365.
- Pont AC, Deeming JC (2001) A shoot-fly *Atherigona tritici* sp. n. (Diptera: Muscidae), attacking wheat *Triticum aestivum* in Egypt. *Bulletin of Entomological Research* 91(4): 297–300. <https://doi.org/10.1079/BER2001109>
- Roditakis E, Kremi K, Mylona K, Georgousis V, Avtzis DN, Simoglou KB (2023) First Report of the Pepper Fruit Fly *Atherigona orientalis* (Schiner 1968) (Diptera: Muscidae) Infesting Commercial Pepper Crops in Greece. *Insects* 14(4): 393. <https://doi.org/10.3390/insects14040393>
- Savage J (2016) First Canadian records of the Bermuda grass stem maggot, *Atherigona reversura* (Diptera: Muscidae). *Journal of the Entomological Society of Ontario* 147: 3–6.
- Schnabl J, Dziedzicki H (1911) Die Anthomyiden. *Nova Acta Academiae Caesarea Leopoldino-Carolinae Germanicum Naturae Curiosorum* 95(2): 53–358.
- Sherwill T, Byrne M, Van Den Berg J (1999) Shoot fly species on sorghum in the Mpumalanga subtropics of South Africa: Relative abundance and infestation levels. *African Plant Protection* 5(1): 31–35.
- Skidmore P (1985) The biology of the Muscidae of the world. Series Entomologica 29. Dr W. Junk Publishers, Dordrecht, xiv + 550 pp.
- Stein P (1913) Neue afrikanische Anthomyiden. *Annales Historico-Naturales Musei Nationalis Hungarici* 11: 457–583.
- Suh SJ, Kwon YJ (2018) Taxonomy of the genus *Atherigona* Rondani (Diptera: Muscidae) from Korea. *Entomological Research* 48(3): 187–197. <https://doi.org/10.1111/1748-5967.12277>

- Van den Berg J, Bronkhorst L, Mgonja M, Obilana AB (2005) Resistance of sorghum varieties to the shoot fly, *Atherigona soccata* Rondani (Diptera: Muscidae) in Southern Africa. *International Journal of Pest Management* 51(1): 1–5. <https://doi.org/10.1080/09670870400016503>
- Van Emden FI (1940) Muscidae: B—Coenosiinae. *British Museum (Natural History) Ruwenzori Expedition 1934–35. Vol. 2. No 4. British Museum (Natural History), London*, 91–255.
- Wiedemann CRW (1830) *Aussereuropäische zweiflügelige Insekten Volume 2. Schulzischen Buchhandlung, Hamm*, xii + 684 pp.
- Young WR, Teetes GL (1977) Sorghum entomology. *Annual Review of Entomology* 22: 193–218. <https://doi.org/10.1146/annurev.en.22.010177.001205>

Three new species of plexippine jumping spiders (Salticidae, Salticinae, Plexippini) from dry forest in Boeny region, north-western Madagascar

Katie I. Murray^{1,2,3}, Jaime Escobar-Toledo^{1,3}, Brogan L. Pett^{1,2,3}

1 *SpiDiverse, Biodiversity Inventory for Conservation npo (BINCO), 3380 Walmersumstraat, Glabbeek, Belgium*

2 *Centre for Ecology and Conservation, College of Life and Environmental Sciences, University of Exeter, Penryn Campus, Penryn, Cornwall, TR10 9FE, UK*

3 *Operation Wallacea, Lincolnshire, UK*

Corresponding author: Brogan L. Pett (brogan.pett@outlook.com)

Abstract

Despite being the most diverse family of spiders, Salticidae (jumping spiders) are poorly studied in Madagascar with only 47 of the total 105 species recorded in the last 100 years. Here, we describe three new species of Plexippini Simon, 1901 from dry forests in North-western Madagascar as part of an ongoing biomonitoring programme. This paper increases the number of species in the genus *Evarcha* Simon, 1902 from 93 to 95 and *Thyene* Simon, 1885 from 55 to 56. Additionally, we publish specimen records of *Plexippus petersi* (Karsch, 1878) from Madagascar for the first time. All new species are diagnosed and illustrated through photographs and drawings.

Key words: Afrotropics, discovery, *Evarcha*, new record, new species, taxonomy, *Thyene*



Academic editor: Galina N. Azarkina

Received: 4 May 2024

Accepted: 20 September 2024

Published: 28 October 2024

ZooBank: <https://zoobank.org/2FE3F7D4-857D-4291-8885-289765927667>

Citation: Murray KI, Escobar-Toledo J, Pett BL (2024) Three new species of plexippine jumping spiders (Salticidae, Salticinae, Plexippini) from dry forest in Boeny region, north-western Madagascar. *African Invertebrates* 65(2): 61–74. <https://doi.org/10.3897/AfrInvertebr.65.126810>

Copyright: © Katie I. Murray et al.
This is an open access article distributed under terms of the Creative Commons Attribution License (Attribution 4.0 International – CC BY 4.0).

Introduction

Salticidae (Araneae) is the most diverse family of spiders in the world, with 6,654 species known from 681 genera (WSC 2024). More than 1,000 salticid species are known from the Afrotropical region; however, sampling remains geographically biased and not of equal coverage. The salticid fauna of many areas is still poorly studied and understood. Madagascar has 105 species of salticid recorded from 40 genera (WSC 2024). Yet, of the 105 species, only 47 have been documented in the past 100 years (WSC 2024). Madagascar has long been recognised as a global biodiversity hotspot (Mittermeier et al. 1998, Myers et al. 2000) where habitat diversity and endemism, proportionate to land area, are especially pronounced in a global sense (Mittermeier et al. 2011). The limited research on spiders on Madagascar to date highlights the high numbers of undescribed species (Wood 2008; Jäger 2020; Griswold et al. 2022).

The Plexippini of Madagascar include several genera whose boundaries are unclear. Species of *Evarcha* Simon, 1902 are generally separated from their closest morphologically resembling relative in *Hyllus* C. L. Koch, 1846 by a narrower carapace not clearly wider than eye field (vs. much

more rounded, clearly wider than eye field), and with epigynal pockets (vs. absent). *Evarcha madagascariensis* Prószyński, 1992 is the sole representative of its genus on the island, known from a single holotype male. *Thyene* Simon, 1885 are flattened plexippines with a strong stout leg I, tufts of distinct dark bristles lateral to posterior of ALEs and relatively homogenous pedipalps, with a circular tegulum twice encircled by the embolus and a thin tibial apophysis (Wesołowska 2006). Three species of *Thyene* are known from Madagascar, with none recorded through positive specimen identification since 1908.

A biodiversity inventory focusing on an area of enigmatic dry forests in Mariarano, north-western Madagascar has been collecting spiders as part of a biomonitoring project in 2017, 2018 and 2023 by the Biodiversity Inventory for Conservation (BINCO; www.binco.eu), Operation Wallacea (www.opwall.com), and the Development and Biodiversity Conservation Action for Madagascar (DBCAM). Previous work in the area (Fig. 1) has discovered numerous putative endemics, e.g. a couple of new spider species to date (Jocque et al. 2017; Jocqué and Jocque 2021; Pett and Rabemananjara 2022), with many more in preparation. We begin the process of tackling the salticids of the area with this project on the Plexippini Simon, 1901 fauna. The aims and objectives of this study are to describe three new species and report the first specimen record of *Plexippus petersi* (Karsch, 1878) from Madagascar.

Materials and methods

Spiders were collected in June–August 2017, 2018, 2023 during an expedition in north-western Madagascar. All material is preserved in 70% ethanol. The left pedipalp of several males were dissected and illustrated. The illustrated female epigynes were first dissected using a custom-made fine hooked needle to excise the epigynal plate, digested in warm lactic acid solution for 3–5 minutes before being observed in methyl salicylate. The cleared epigyne was temporarily prepared on a slide and examined with a compound microscope. Examinations were carried out with an AmScope ZM-4T stereomicroscope or an Olympus BX61. Images were taken using either a Zeiss Discovery V12 with an AxioCam 208 colour camera. All images were z-stacked with between 10–30 images merged into a single photomontage using Helicon Focus 6.7 (www.helicon-soft.com). Images were adjusted in Adobe Photoshop version 21.0.1 for contrast and white balance. Drawings of genitalia were made by KM. Plates were also composed in Adobe Photoshop. All measurements are in millimetres (mm). Maps were made with simplemappr (Shorthouse 2010).

Abbreviations: **AER** = anterior eye row, **AL** = abdomen length, **AME** = anterior median eyes, **ALE** = anterior lateral eyes, **AW** = abdomen width, **CD** = copulatory ducts, **CH** = carapace height, **CL** = carapace length, **CW** = carapace width, **PME** = posterior median eyes, **PLE** = posterior lateral eyes, **PER** = posterior eye row, **SL** = sternum length, **ST I & ST II** = spermathecae I (posterior) and II (anterior), **SW** = sternum width, **TL** = total length, **ORW** = ocular row width.

Collection abbreviation: **RMCA**—Royal Museum for Central Africa, Tervuren, Belgium (A. Henrard & D. Van den Spiegel).



Figure 1. Type locality of all three new species.

Results

Taxonomy

Family Salticidae Blackwall, 1841

Subfamily Salticinae Blackwall, 1841

Clade Salticoida Maddison & Hedin, 2003

Tribe Plexippini Simon, 1901

Subtribe Plexippina Maddison, 2015

Genus *Evarcha* Simon, 1902

Type species. *Evarcha falcata* (Clerck, 1757), by subsequent designation.

Diagnosis. *Evarcha* are medium-sized plexippine salticids displaying a vast diversity in genital morphology: the embolus may be short, stout and compact or range to very long and filamentous; tegulum ranges from round, oval to conical and may bear distinctive outgrowths/ expansions; single RTA present; insemination ducts range from broad and membranous to thin and tube-shaped; Leg III longer than IV (Wang et al. 2024; Zamani et al. 2017; Žabka 1993). However, it has been suggested that *Evarcha*, as currently defined, acts as a 'dumping ground' genus and likely harbours many unrelated species, and cryptic generic diversity (Kanesharatnam and Benjamin 2020). Thus, a universal definition of the genus is difficult to propose (Wang et al. 2024).

***Evarcha tsipikafotsy* sp. nov.**

<https://zoobank.org/55A72979-FAFC-4D36-86D2-83E4BEA4B77D>

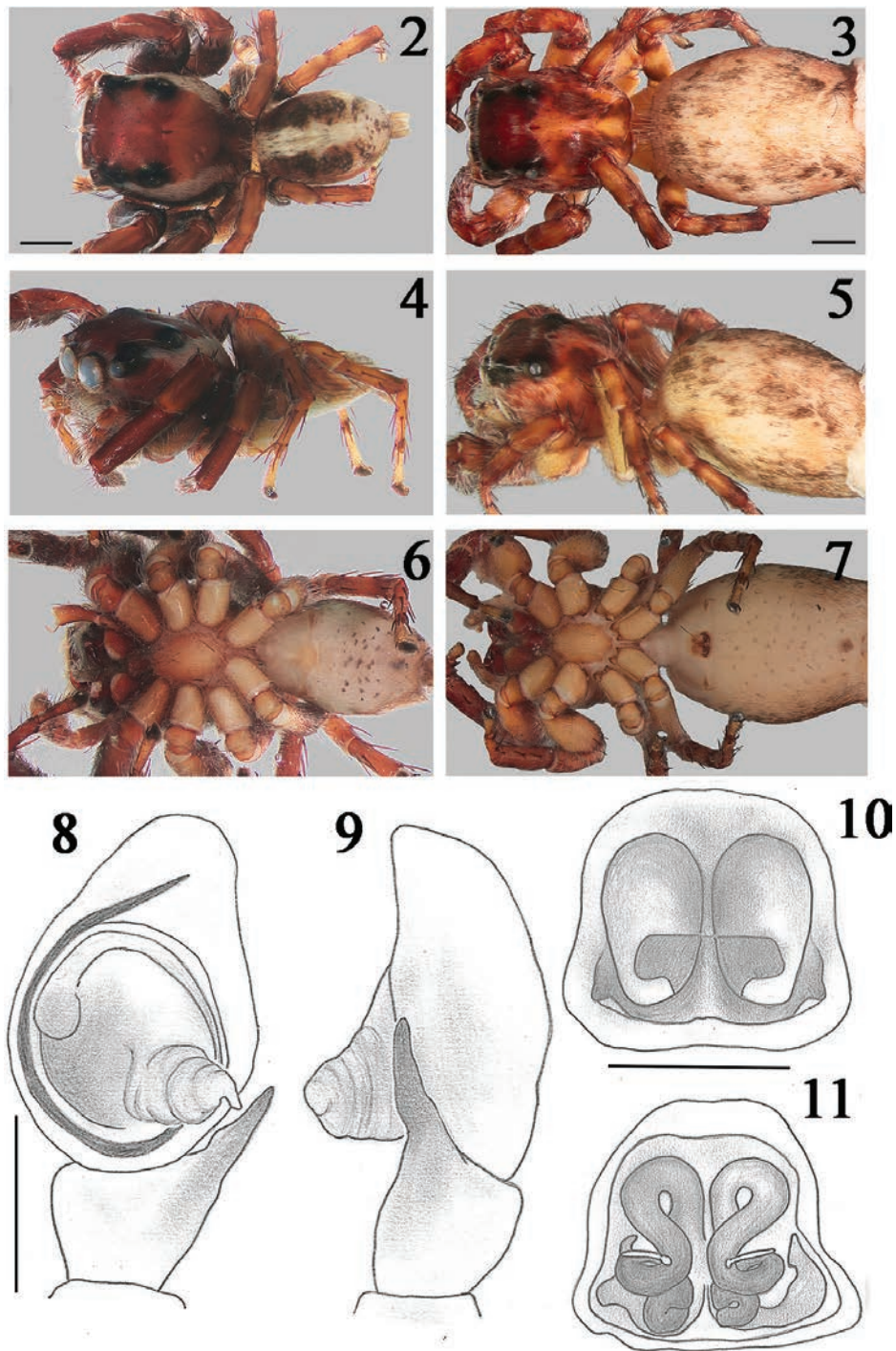
Figs 2–19

Material examined. Holotype • ♂: MADAGASCAR; Mahajanaga province, Mariarano classified forest, Antafiameva camp; 15.46°S, 46.74°E; 12 July 2017, 20:06; "Savannah next to dry forest", Jonas Merckx leg. (BE_RMCA_ARA.Ara.247698).

Paratypes • 1 ♀ MADAGASCAR; Mahajanaga province (all), Mariarano classified forest (all), Mariarano camp; 15.48°S, 46.69°E; 17 June 2018, 20:06; "Savannah next to dry forest", Jonas Merckx leg. (BE_RMCA_ARA.Ara.247699) Mariarano camp, • 1 ♂; 15.29°S, 46.41°E; 20 June 2023, 09:00; "Margin of tropical dry forest", Jaime Escobar-Toledo leg. (BE_RMCA_ARA.Ara.247700) Mariarano camp, • 1 ♀; 15.29°S, 46.41°E; 22 June 2023, 20:30; "Margin of tropical dry forest", Jaime Escobar-Toledo leg. (BE_RMCA_ARA.Ara.247701) Mariarano camp, • 1 ♀; 15.29°S, 46.41°E; 23 June 2023, 8:30; "Margin of tropical dry forest", Jaime Escobar-Toledo leg. (BE_RMCA_ARA.Ara.247702) Matsedroy camp, • 1 ♂; 15.29°S, 46.39°E; 3 July 2023, 10:00; "Open tropical dry forest", Jaime Escobar-Toledo leg. (BE_RMCA_ARA.Ara.247703) Matsedroy camp, • 1 ♂; 15.29°S, 46.39°E; 9 July 2023, 21:00; "Open tropical dry forest", Jaime Escobar-Toledo leg. (BE_RMCA_ARA.Ara.247704) Matsedroy camp, • 1 ♂, 1 ♀; 15.29°S, 46.38°E; 11 July 2023, 19:45; "Tropical dry forest", Jaime Escobar-Toledo leg. (BE_RMCA_ARA.Ara.247705) Mariarano camp, • 1 ♂; 15.29°S, 46.41°E; 16 July 2023, 08:00; "Margin of tropical dry forest", Jaime Escobar-Toledo leg. (BE_RMCA_ARA.Ara.247706).

Etymology. The specific epithet is a noun in apposition, amalgamating the Malagasy words for "stripes" (*tsipika*) and "white" (*fotsy*) (this is the correct conjugation of the words in Malagasy). Reference is made to the stripes of white setae on the lateral parts of the carapace.

Diagnosis. *Evarcha tsipikafotsy* sp. nov. is distinctive in palpal conformation from most *Evarcha*, with a similar body form and colour pattern. *Evarcha tsipikafotsy* is most similar in palpal conformation to *E. madagascariensis* Prószyński, 1992 (Madagascar) and *E. patagiata* (O. Pickard-Cambridge, 1872) (The Levant) in sharing a singular large RTA, an embolus running clockwise along edge of cymbium for over 1/3 cymbium length and a moderate posterior tegular expansion. *Evarcha tsipikafotsy* sp. nov. is clearly separated from those species by (i) posterior tegular expansion that is projected distinctly at 4 o'clock position with a separate finger-like protrusion (vs. projected at 5 o'clock position without finger-like protrusion or small projection at 6 o'clock position, respectively); (ii) embolus that is about 2/3 length of cymbium and follows margin (vs. just under 1/2 length of cymbium in both species, additionally embolus is projected a small distance away from tegulum in *E. patagiata*); (iii) RTA that is sinuous at apex (vs. not with sinuous apex); additionally, *Evarcha tsipikafotsy* sp. nov. is further separated from *E. madagascariensis* by having only a small RL cymbial expansion (vs. very large), and an RTA that does not make contact with RL cymbial expansion (vs. does make contact). Females are most similar in epigynum conformation to *E. arcuata* (Clerck, 1757) (Most of Europe, Northern Asia, Libya and Mexico) with coiled CD and moderately large epigynal atria (separated by a distinctive arch). *Evarcha tsipikafotsy* sp. nov. is clearly separated from *E. arcuata* by: (i) thick tightly coiled CD (vs. thin, less tightly coiled); (ii) FD approximately halfway up the epigynal region (vs. 3/4 vertically high),



Figures 2–11. *Evarcha tsipikafotsy* sp. nov. 2, 4, 6 male holotype habitus 3, 5, 7 female paratype habitus 8, 9 male pedipalp 10, 11 female epigyne 2, 3, 11 dorsal 4, 5 lateral 3, 6, 7, 8, 10 ventral 9 retrolateral. Scale bars: 1 mm (2–7); 0.5 mm (8–11).

(iii) epigynal arch long and thin (vs. short and broader), (iv) atria large and deep, about $\frac{3}{4}$ entire surface of epigynal region (vs. much smaller, about $\frac{1}{4}$ surface of epigynal region).

Taxonomic notes. *Carrhotus harringtoni* Prószyński, 1992 external epigyne resembles *E. tsipikafotsy* sp. nov., but the internal ST and CD are markedly different from species of *Evarcha* s. s., with large oval ST and a simpler CD pattern that is closer to *Carrhotus* species than to that of *Evarcha*. However, we consider the generic identity of *C. harringtoni* to be unclear and require further investigation.



Figures 12, 13. *Evarcha tsipikafotsy* sp. nov. in vivo images, male. Photo credits: J.E.T.

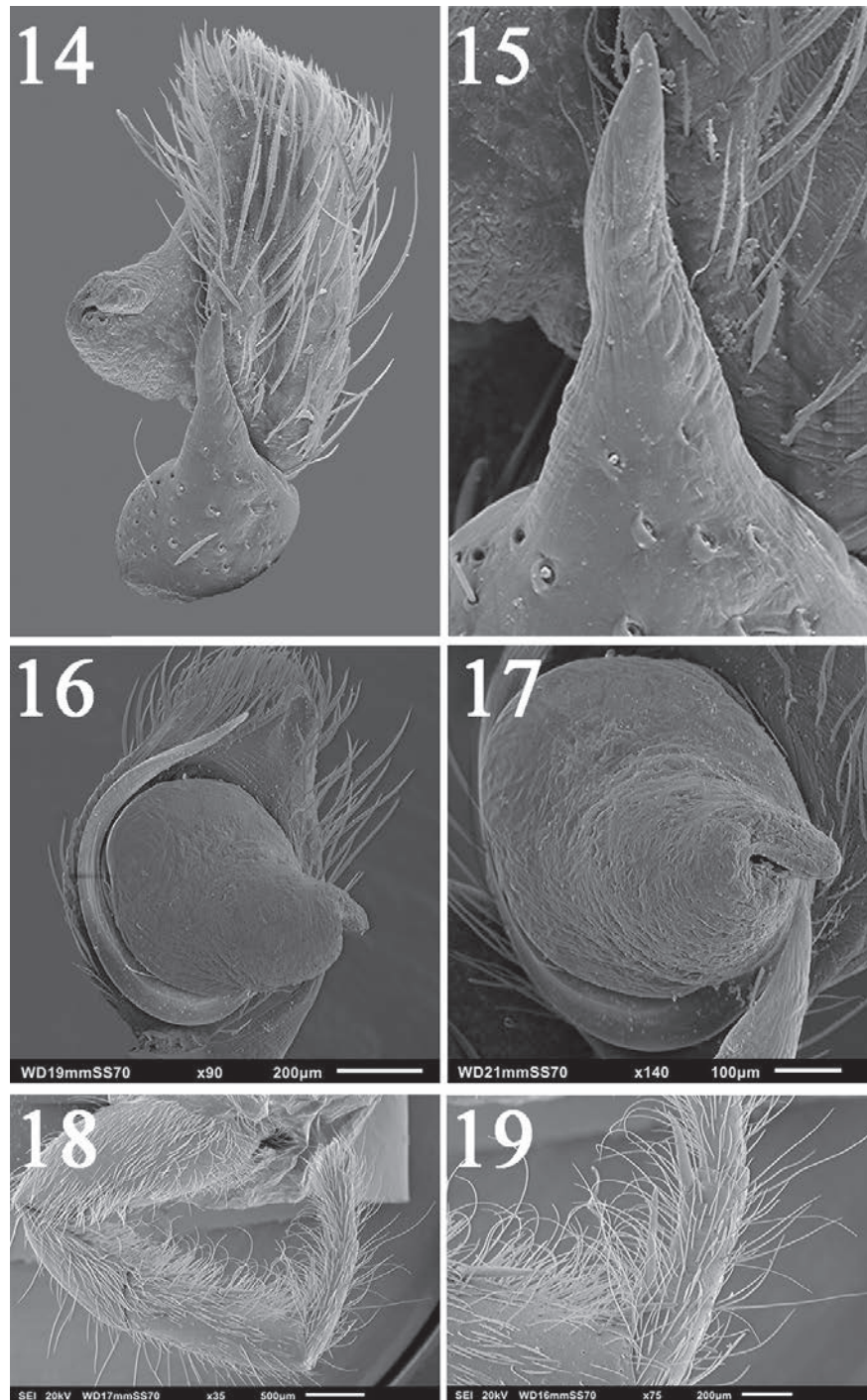
Description. Male (holotype). Measurements. TL 6.48, CL 3.48, CW 2.96, CH 2.2, SL 1.36, SW 0.92, AL 4, AW 2.04, chelicera length 1.2, chelicera width 0.64. Legs. I: 2.56, 1.88, 1.8, 1.16, 0.96. II: 2, 1.24, 1.36, (remaining segments missing). III: 2.84, 1, 1.28, 1.08, 0.92. IV: 2.36, 1.04, 1.4, 1.04, 0.56. Eyes: AME – 0.62, ALE – 0.32, PME – 0.1, PLE – 0.26, ORW – 0.236.

Colouration: Carapace generally orangish-brown, dark brown in vivo, with lateral fringes of white setae just ventral to PER, band of sparser black setae ventral; chelicerae brown; legs 1,2 brownish; legs 3,4 orangish; coxae pale beige both dorsally and ventrally; abdomen generally beige with a mostly contiguous white band down abdomen centre, venter beige with sparse brown spots (figs 12, 13).

Carapace: High, flat, declining sharply just posterior to fovea, foveal depression very shallow; several very long setae projected anteriorly just ventral of PME; fringe of white setae mid-length and appressed to carapace; sparse patches of white setae between eyes. **Sternum:** Oval shape, widest around midpoint. **Legs:** Legs 1,2 slightly broader; dense fringe of setae on patellae & tibiae I & II. **Chelicerae:** One tooth on retromargin, two teeth on promargin, retromarginal tooth larger than largest promarginal tooth, promarginal teeth close together with apical one three times the size of smallest one. **Abdomen:** Ovoid, widest halfway along length; several longish thick white setae protrude at a 45°–30° angle at anterior margin; venter dull. **Leg spination:** I: F 3d 2pl, P 1d 2pl 2rl, Ti 2pl v3-3, Mt v2-2. II: F 3d 1pl 2rl, P 1pl 1rl, Ti 3pl 3v, Mt v2-2. **Pedipalp:** Cymbium orange to brown; RTA thick, comparable length to the tibia, protrudes along edge of cymbium without another point of contact; tegulum circular with sperm duct dark red to brown, follows curve of tegulum clockwise from 9 o'clock to behind the tegular expansion at 5 o'clock; long embolus originating from 5 o'clock behind tegular expansion in ventral view and contours the edge of the tegulum before branching off at 10 o'clock and up towards apex of the cymbium (figs 14–19).

Female. Measurements. CL 4.12, CW 3.28, CH 2.42, AL 7.08, AW 4.20, SL 1.72, SW 0.86, Leg measurements: I: 2.24, 1.32, 1.72, 1.20, 0.68. II: 1.92, 1.20, 1.42, 1.00, 0.76. III: 2.80, 1.32, 1.50, 1.72, 0.88. IV: 2.56, 1.08, 1.72, 1.76, 0.84. Eyes: AME 0.64, ALE 0.38, PME 0.12, PLE 0.32.

Leg spination: I: F 4d 2pl, P 1d, Ti v3-3, Mt v2-2. II: F 3d 2pl, P 1d, Ti pl2 v3-3, Mt v2-2.



Figures 14–19. *Evarcha tsipikafotsy* sp. nov. S.E.M micrographs 14–17 male left pedipalp 18, 19 leg I 14, 15- retrolateral 16, 17- ventral to prolateral 18 prolateral dorsal 19 prolateral dorsal detail of tibia.

General colouration, pattern and somatic morphology the same as in male. Except; carapace slightly lighter and mottled, dark brown-black patches around eyes from ORW to fovea, much sparser fringe of white setae and no band of black setae on carapace, no vertical stripes on abdomen, instead beige with interspersed patches of beige, brown and black setae.

Epigyne: epigynal region longer than wide by about 1.5×; copulatory openings at anterior margin directed anteriorly, CD long and thin, directed straight posteriorly, suboval ST moderately large, separated by about half their width.

***Evarcha vavannyangisy* sp. nov.**

<https://zoobank.org/3A76F40D-4E6C-4E93-88D3-E2A065188704>

Figs 20–25

Material examined. Holotype • ♂: MADAGASCAR; Mahajanaga province, Mariarano classified forest, Matsedroy camp; 15.471°S, 46.744°E; 13 July 2017, 20:06; “Savannah next to dry forest”, Yi Wang leg. (BE_RMCA_ARA.Ara.247707).

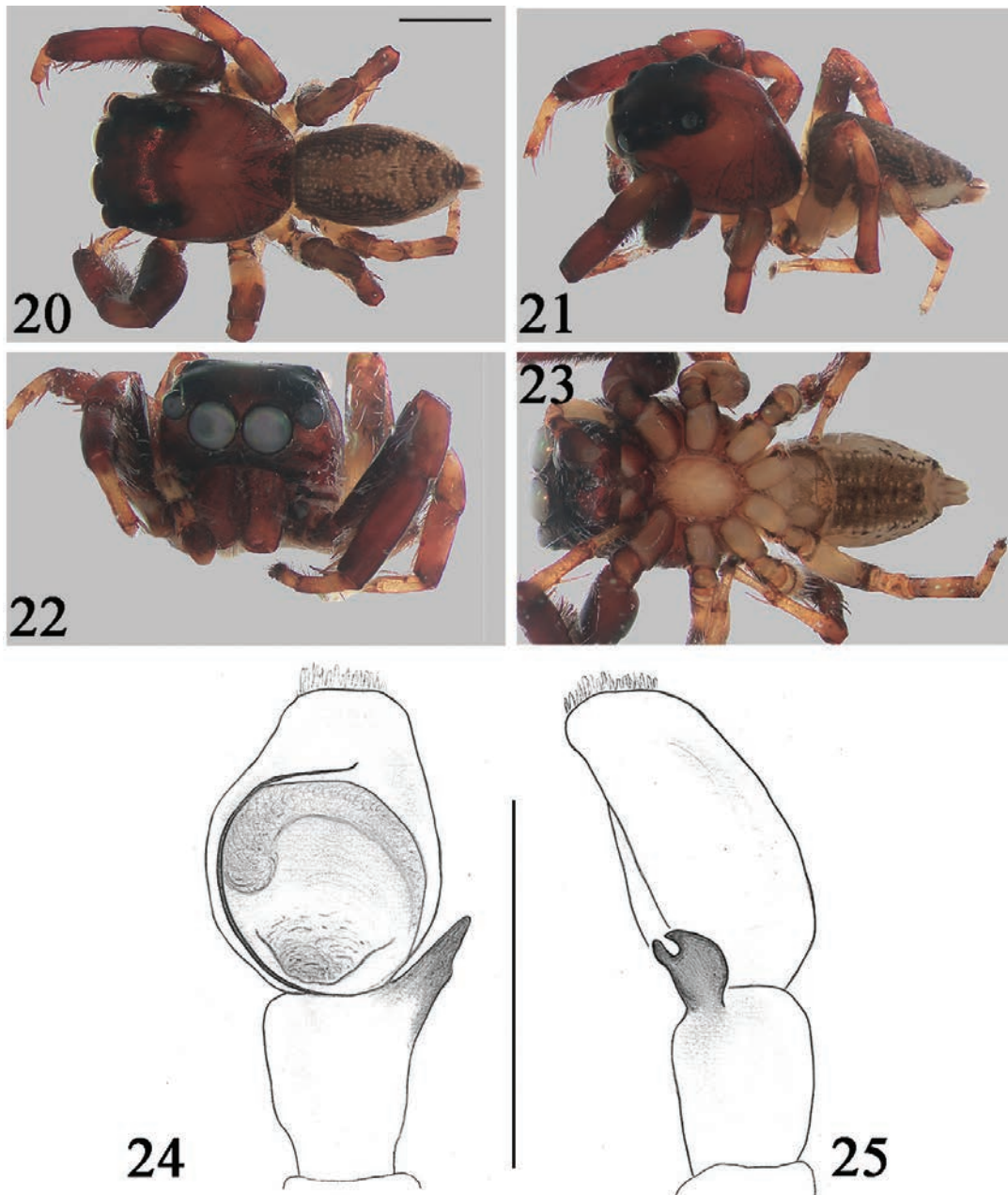
Etymology. The specific epithet is a noun in apposition, amalgamating the Malagasy words for “squid” and “beak”. Reference is made to the bifurcated RTA.

Diagnosis. *Evarcha vavannyangisy* sp. nov. is highly distinctive in the genus. However, some similarities in palpal conformation exist with *E. zayu* Wang, Mi & Li, 2024 (China) and *E. amanzi* Wesolowska & Haddad, 2018 (South Africa). *E. vavannyangisy* shares a bifurcated RTA, basomedian tegular expansion and embolus approximately half the perimeter of the bulb with *E. zayu*, but can be separated by: (i) deeply bifurcated RTA (vs. shallow); (ii) very small basomedian tegular bump (vs. very pronounced tegular expansion); and (iii) embolus slender for its entire length (vs. much broader). Additionally, *E. zayu* is from mainland China. *E. vavannyangisy* sp. nov. shares a deeply bifurcated RTA with only one congener, *E. amanzi* Wesolowska & Haddad, 2018 (South Africa), but can be readily separated by: (i) basomedian tegular expansion very small (vs. well projected posteriorly); and (ii) embolus runs approximately half the perimeter of the bulb (vs. arising 10 o'clock position and running until 12 o'clock position).

Description. Male (holotype). Measurements. CL 2.68, CW 2.36, AL 2.44, AW 1.56, SL 1.00, SW 0.76. Leg measurements: I: 1.80, 0.88, 1.64, 1.04, 0.56. II: 1.40, 0.76, 0.84, 0.68, 0.44. III: 2.04, 0.84, 1.20, 1.00, 0.60. IV: 1.32, 0.60, 0.84, 0.90, 0.56. PME 0.11, PLE 0.20, ALE 0.30, AME 0.56.

Colouration: Carapace generally brownish orange, black patches around eyes, white setae ventral to PLE, scant black mottling at posterior margin. Chelicerae, maxilla, labium, deep reddish brown. Sternum & coxae pale brownish. Leg I dark reddish brown, legs II – IV generally brownish, with pale basal half of femorae. Abdomen generally brownish, with considerable alternations between pale and black mottlings, venter cream with black mottling. **Carapace:** generally rounded, very slightly longer than wide, moderately high, highest at PLE. Long, sparse, fine white setae around clypeus directed medially. **Sternum:** suboval, about 1.5× long as wide. **Legs:** Leg I much broader, with field of long, erect setae ventrally on Ti I. Field of long white prolateral ventral setae on patellae I. **Abdomen:** oval, about twice as long as wide. **Pedipalp:** femur slightly longer than patella and tibia together; many long fine setae prolaterally on tibia, long setae thicker retrolaterally, RTA about 0.8× length of tibia, projected at 1 o'clock position, bifurcated with squid-beak-like appearance, rounded ventral element and sharp pointed dorsal element; cymbium almost as long as tibia, with truncated anterior margin, tegulum round, embolus slender, wrapping around tegulum for just over half a turn, arising at 5'30 position and terminating at around 0'15 position, very small basomedian tegular bump.

Leg spination: I: F d2 pl, P pld1, Ti pl2 v3-3, Mt v2-2. II: F pl2 d2 rl2, P pl1 d1, Ti pl2 v3-3, Mt v2-2.



Figures 20–25. *Evarcha vavanyangisy* sp. nov. 20–23 male holotype habitus 24, 25 male pedipalp 20 dorsal 21 lateral 22 frontal 23, 24 ventral 25 retrolateral. Scale bars: 1 mm (20–23); 0.5 mm (24, 25).

Genus *Thyene* Simon, 1885

Diagnosis. Medium-sized spiders, with flattened body. Cephalothorax wide, rounded, abdomen narrower. Leg I hairy, considerably stouter and longer than rest. Characteristic tufts of long black bristles near anterior lateral eyes forming ‘horns’. Structure of genital organs very similar in all members of the genus. Male palp with rounded tegulum twice surrounded by embolus and with single thin tibial apophysis. Species difficult to identify; easier to distinguish by the coloration, especially abdominal pattern, than genital organ structure. The genus includes more than 40 species, the majority distributed in Africa (Wesołowska 2006).

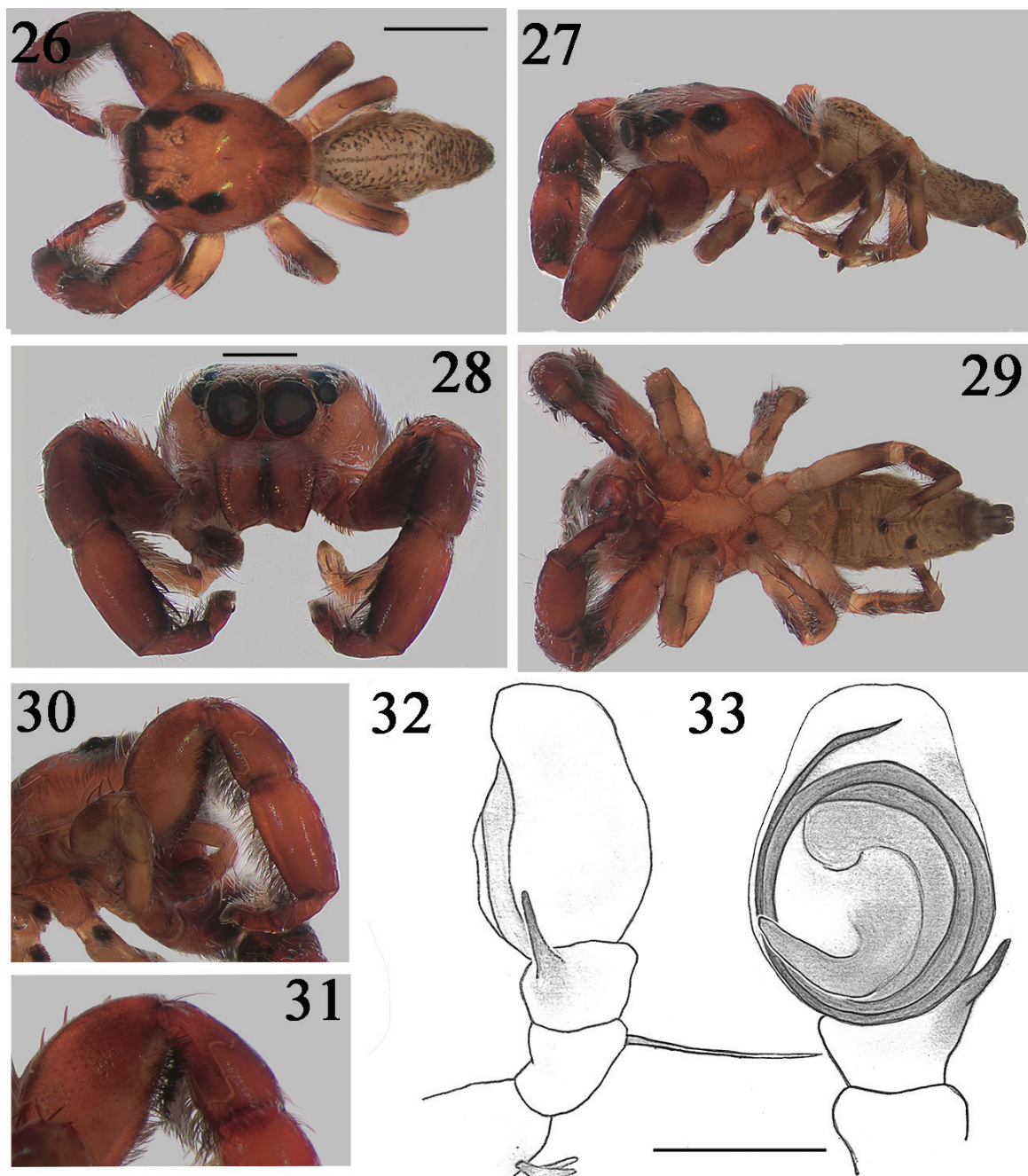
***Thyene volombavatanany* sp. nov.**

<https://zoobank.org/5FE25671-57FC-4440-87F6-B97242C834B2>

Figs 26–31

Material examined. Holotype • ♂ MADAGASCAR; Mahajanga province, Mariarano classified forest; 15.468°S, 46.741°E; 28 June 2017, 20:25; “long grass, net sweep”, Brogan L. Pett leg. (BE_RMCA_ARA.Ara.247708).

Etymology. The specific epithet is a noun in apposition, amalgamating the Malagasy words for “arm” (tanany) and “moustache” (volombava). Reference is made to the extensive hairs on the ventral part of the femur and tibiae.



Figures 26–33. *Thyene volombavatanany* sp. nov. 26–31 male holotype habitus 32, 33 pedipalp 26 frontal 27 lateral 28 dorsal 29 ventral 30– leg I 31 femur I detail 32 retrolateral 33 ventral. Scale bars: 1 mm (26–31); 0.5 mm (32, 33).

Diagnosis. *Thyene volombavatanany* sp. nov. resembles *T. aperta* (G. W. Peckham & E. G. Peckham, 1903) (Ivory Coast, Tanzania, Zimbabwe) by the elongated body, large legs I and in general palpal conformation. Both share a bulb rounded, twice surrounded by embolus running clockwise with narrow, long, flat tegular expansion prolaterally at base. *Thyene volombavatanany* sp. nov. is distinguished by: (i) an abdomen that is generally uniform in colouration with black mottling without white spot (vs. large black area divided into three parts with distinct white spot); (ii) RTA that is approximately the length of the tibia with an apex that is about 1/3 basal tibia width (vs. 1/2 length of tibia and apex under).

Description. Male (holotype). Measurements. CL 2.52, CW 1.94, CH 1.04, SL 1.02, SW 0.48, AL 2.82, AW 1.12. AME 0.44, ALE 0.20, PME 0.09, PLE 0.15. Leg I: 1.22, 0.80, 1.16, 0.76, 0.40. Leg II: 0.88, 0.64, 0.68, 0.42, 0.28. Leg III: 1.04, 0.66, 0.68, 0.76, 0.40. Leg IV: 1.28, 0.64, 0.78, 0.74, 0.40.

Colouration: carapace generally light orangish brown, eyes ringed with dark brown patches, pale streak from fovea to posterior margin; chelicerae orange; sternum, coxae generally pale orange; legs II – IV pale orange-beige with faint brown retro lateral and prolateral patches; labium, maxillae, legs I orangish brown with black ventral femoral setae; abdomen beige with some brown-black mottling; pedipalp orangish-brown. **Carapace:** low and flat, highest at PLE, shallow depression midway between lateral eyes; patches of short thick white setae around fovea, posterior to AME, ventral to PLE, ventral lateral part of carapace; ventral lateral sparse strip of long thin black setae. **Sternum:** broadly oval-shaped, widest between coxae II & III, margin darker orange than centre. **Legs:** Legs I much broader and darker; dense long black ventral setae interspersed with longer sparser white ventral setae on femur, patella, tibia. **Abdomen:** long and thin, more than twice as long as wide; beige with brown-black mottling; long brown lateral setae; brown and white tuft of setae at anterior face. **Pedipalp:** femur slightly longer than patella and tibia together, patella and tibia about the same length; RTA thumb-like, short and rounded; SD arises medially and loops around tegulum for half its length; embolus moderately short and straight, directed prolaterally tapering to a sharp point. **Leg spination:** I: F d3 pl2, P pl1, Ti v4-3, Mt v2-2; II: F d2 pl3, P pl1 (small), Ti pl2 v1-2, Mt v2-2.

New Record

Genus *Plexippus* C. L. Koch, 1846

Plexippus petersi (Karsch, 1878)

Figs 34–36

Euophrys petersii Karsch, 1878: 332, pl. 2, fig. 7.

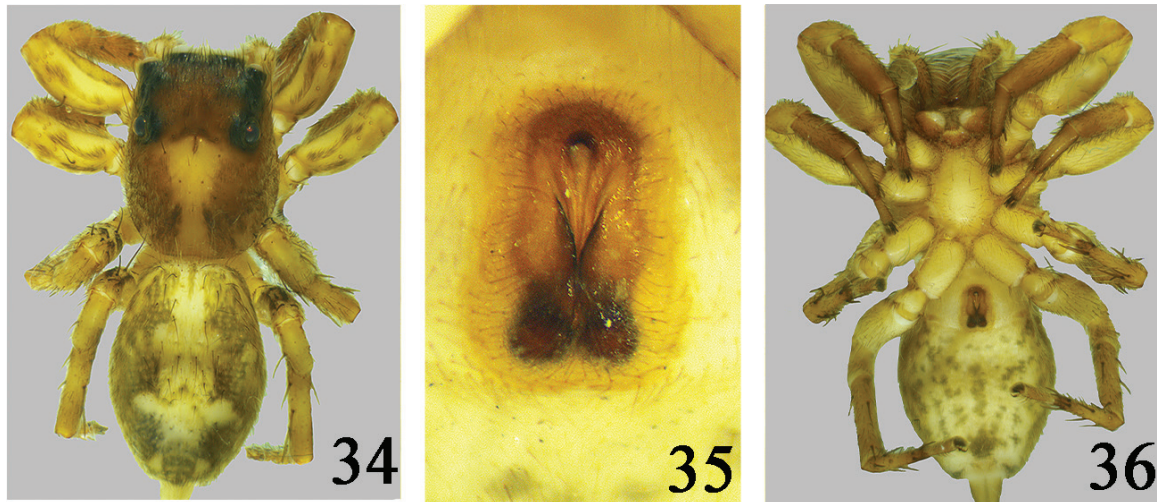
Plexippus petersi Simon 1903: 728.

Marpissa calcutaensis Tikader, 1974: 210, figs 9–10.

Plexippus calcutaensis Nenilin 1984: 6. *Plexippus petersi*: Žabka, 1985: 433, figs 464–470.

Description. See Žabka (1985); illustrated in this paper (figs 34–36).

Material examined. • 1 ♀ Madagascar; Mahajanga province, Mariarano classified forest; 15.470°S, 46.742°E; 21 June 2017, 16:20; Brogan L. Pett leg. (BINCO_MAD_17_0129_1).



Figures 34–36. *Plexippus petersi* (Karsch, 1878) female 34 habitus dorsal 35 epigyne ventral 36 habitus ventral.

Distribution. The species is recorded from many countries across south-eastern Asia (WSC 2024). The only published specimen records in Africa are from Mozambique (Simon 1903), with specimens putatively identified from south-western Kenya, northern Tanzania, and far eastern Madagascar (SMNS database). Thus, this is the first confirmed specimen record from Madagascar.

Acknowledgements

We would like to thank the people living around Mariarano for their collaboration and guidance on the numerous excursions in this region. Many thanks also to DBCAM for supporting the expedition of Operation Wallacea, and also to the enthusiastic volunteers who assisted with sample collection in the field. Joseph Faulks is thanked for allowing BLP to access the bioimaging facilities at the University of Exeter's Penryn campus. BLP thanks Dr. Merlijn Jocque of BINCO (Belgium) and Royal Belgian Institute of Natural Sciences (RBINS) for supporting the spider workgroup of BINCO (SpiDiverse).

Additional information

Conflict of interest

The authors have declared that no competing interests exist.

Ethical statement

No ethical statement was reported.

Funding

This work was supported by University of Exeter and Biodiversity Inventory for Conservation.

Author contributions

KM & BLP primarily identified and diagnosed specimens, KM made the drawings, BLP imaged specimens, both created plates. JET & BLP collected specimens. KM & BLP wrote the first drafts of the manuscript and edited the revised manuscript. JET revised the manuscript and provided in vivo images. All authors conceptualised the study.

Author ORCIDs

Katie I. Murray  <https://orcid.org/0009-0007-2042-2285>

Jaime Escobar-Toledo  <https://orcid.org/0009-0007-2495-780X>

Brogan L. Pett  <https://orcid.org/0000-0002-0461-3715>

Data availability

All of the data that support the findings of this study are available in the main text.

References

- Clerck C (1757) Svenska spindlar: uti sina hufvud-slågter indelte samt under några och sextio särskildte arter beskrefne: och med illuminerade figurer uplyste. Literis Laur, 154 pp. <https://doi.org/10.5962/bhl.title.119890>
- Griswold C, Ubick D, Ledford J, Polotow D (2022) A revision of the Malagasy crack-leg spiders of the genus *Uduba* Simon 1880 (Araneae, Udubidae), with description of 35 new species from Madagascar. *Proceedings of the California Academy of Sciences* 67(4, Supplement 2): 1–193.
- Jäger P (2020) *Thunberga* gen. nov., a new genus of huntsman spiders from Madagascar (Araneae: Sparassidae: Heteropodinae). *Zootaxa* 4790(2): 245–260. <https://doi.org/10.11646/zootaxa.4790.2.3>
- Jocqué R, Jocque M (2021) A new species of *Katableps* (Araneae: Lycosidae) from a remnant forest patch on Madagascar. *Arachnology* 18(9): 1013–1016. <https://doi.org/10.13156/arac.2021.18.9.1013>
- Jocque M, Wellens S, Andrianarivosoa JD, Rakotondraparany F, The Seing S, Jocqué R (2017) A new species of *Ocyale* (Araneae, Lycosidae) from Madagascar, with first observations on the biology of a representative in the genus. *European Journal of Taxonomy* 355(355): 1–13. <https://doi.org/10.5852/ejt.2017.355>
- Kanesharatnam N, Benjamin SP (2020) Phylogenetic relationships and systematics of the jumping spider genus *Colopsus* with the description of eight new species from Sri Lanka (Araneae: Salticidae). *Journal of Natural History* 54(43–44): 2763–2814. <https://doi.org/10.1080/00222933.2020.1869335>
- Karsch F (1878) Übersicht der von Peters in Mossambique gesammelten Arachniden. *Monatsberichte der Königlich Preussischen Akademie der Wissenschaften zu Berlin*, 332–338.
- Mittermeier RA, Myers N, Thomsen JB, Da Fonseca GA, Olivieri S (1998) Biodiversity hotspots and major tropical wilderness areas: Approaches to setting conservation priorities. *Conservation Biology* 12(3): 516–520. <https://doi.org/10.1046/j.1523-1739.1998.012003516.x>
- Mittermeier RA, Turner WR, Larsen FW, Brooks TM, Gascon C (2011) Global biodiversity conservation: the critical role of hotspots. *Biodiversity hotspots: distribution and protection of conservation priority areas*. Springer, Berlin/Heidelberg, 3–22. https://doi.org/10.1007/978-3-642-20992-5_1
- Myers N, Mittermeier RA, Mittermeier CG, Da Fonseca GA, Kent J (2000) Biodiversity hotspots for conservation priorities. *Nature* 403(6772): 853–858. <https://doi.org/10.1038/35002501>
- Peckham GW, Peckham EG (1903) New species of the family Attidae from South Africa, with notes on the distribution of the genera found in the Ethiopian region. *Transactions of the Wisconsin Academy of Sciences, Arts and Letters* 14(1): 173–278.

- Pett BL, Rabemananjara PB (2022) A new species of *Copa* (Araneae: Corinnidae: Castianeirinae) from dry forests in the north west of Madagascar. *Zootaxa* 5115(2): 281–287. <https://doi.org/10.11646/zootaxa.5115.2.7>
- Pickard-Cambridge O (1872) General list of the spiders of Palestine and Syria, with descriptions of numerous new species, and characters of two new genera. *Proceedings of the Zoological Society of London* 40(1): 212–354.
- Shorthouse DP (2010) SimpleMapppr, an online tool to produce publication-quality point maps. <https://www.simplemapppr.net> [accessed April 06, 2024]
- Simon E (1903) *Histoire naturelle des araignées*. Deuxième édition, tome second. Roret, Paris, 669–1080. <https://doi.org/10.5962/bhl.title.51973>
- Wang C, Mi X, Li S (2024) Eleven species of jumping spiders from Sichuan, Xizang, and Yunnan, China (Araneae, Salticidae). *ZooKeys* 1192: 141–178. <https://doi.org/10.3897/zookeys.1192.114589>
- Wesołowska W (2006) Jumping spiders from the Brandberg massif in Namibia (Araneae: Salticidae). *African Entomology* 14(2): 225–256.
- Wood H (2008) A revision of the assassin spiders of the *Eriauchenius gracilicollis* group, a clade of spiders endemic to Madagascar (Araneae: Archaeidae). *Zoological Journal of the Linnean Society* 152(2): 255–296. <https://doi.org/10.1111/j.1096-3642.2007.00359.x>
- World Spider Catalog (2024) World Spider Catalog. Version 25.0. Natural History Museum Bern, <http://wsc.nmbe.ch>. <https://doi.org/10.24436/2> [accessed on 04.05.2024]
- Żabka M (1985) Systematic and zoogeographic study on the family Salticidae (Araneae) from Viet-Nam. *Annales Zoologici, Warszawa* 39: 197–485.
- Żabka M (1993) Salticidae (Arachnida: Araneae) of the Oriental, Australian and Pacific regions. X.* Genera *Afraflacilla* Berland & Millot 1941 and *Evarcha* Simon 1902. *Invertebrate Systematics* 7(2): 279–295. <https://doi.org/10.1071/IT9930279>
- Zamani A, Hosseinpour A, Azizi K, Soltani A (2017) A new species of the jumping spider genus *Evarcha* (s. lat.) from southwestern Iran (Araneae: Salticidae). *Peckhamia* 150(1): 1–5.

Foordus gen. nov., a new genus of euophryine jumping spider from South Africa (Salticidae, Araneae)

Galina N. Azarkina^{1,2} 

¹ Laboratory of Systematics of Invertebrate Animals, Institute of Systematics and Ecology of Animals, Siberian Branch of the Russian Academy of Sciences, Frunze Street 11, Novosibirsk 630091, Russia

² Department of Zoology and Centre for Invasion Biology, University of Venda, Thohoyandou, 0950, South Africa

Corresponding author: Galina N. Azarkina (urmakuz@gmail.com)

Abstract

A new monotypic genus *Foordus* **gen. nov.** with *Foordus stefani* **sp. nov.** as the type species is described. A short discussion on other Salticidae with disjunctive distributions is provided.

Key words: Afrotropics, description, KwaZulu-Natal, new species



This article is part of:

Gedenkschrift for Prof. Stefan H. Foord

Edited by Galina Azarkina, Ansie Dippenaar-Schoeman, Charles Haddad, Robin Lyle, John Mldgley, Caswell Munyai

Academic editor: Ansie Dippenaar

Received: 24 September 2024

Accepted: 19 October 2024

Published: 8 November 2024

ZooBank: <https://zoobank.org/C0E6B6AA-E2E4-49B0-999A-B9AC6FD813E5>

Citation: Azarkina GN (2024) *Foordus* gen. nov., a new genus of euophryine jumping spider from South Africa (Salticidae, Araneae). African Invertebrates 65(2): 75–83. <https://doi.org/10.3897/AfrInvertebr.65.137760>

Copyright: © Galina N. Azarkina.
This is an open access article distributed under terms of the Creative Commons Attribution License (Attribution 4.0 International – CC BY 4.0).

Introduction

Euophryines is one of the largest groups among jumping spiders (Salticidae), reported from all continents other than Antarctica (Zhang and Maddison 2015). Currently, 6 genera and 50 species are known from South Africa (Dippenaar-Schoeman et al. 2023). Four genera among these are confined to Southern Africa (*sensu* Dippenaar-Schoeman and Jocqué 1997), with most species recorded from South Africa.

The tribe Euophryini of the Afrotropical Region was revised ten years ago, with two new genera and thirty three new species described (Wesołowska et al. 2014). The largest genus is *Thyenula* Simon, 1902 with 20 species followed by *Euophrys* C.L. Koch, 1834 (16 species). Two genera, *Rumburak* Wesołowska, Azarkina & Russell-Smith, 2014 (7 species) and the monotypic *Yimbulunga* Wesołowska, Azarkina & Russell-Smith, 2014, are found only in South Africa. *Chinophrys* Zhang & Maddison, 2012 is the only other genus with only one species known from South Africa, most species of which are distributed in China (WSC 2024). Yet, it is most likely that many species or even genera still remain undescribed.

In this paper I report another monotypic new genus of tiny euophryine, *Foordus* gen. nov. from South Africa.

Material and methods

The specimens used in this study are shared between the following collections (curator names are in parentheses):

| | |
|-------------|---|
| ISEA | Institute of Systematics and Ecology of Animals SB RAS, Novosibirsk, Russia (G.N. Azarkina) |
| MMUM | Manchester Museum, University of Manchester, United Kingdom (D. Arzuza Buelvas) |
| NCA | National Collection of Arachnida, Pretoria, South Africa (A.S. Dippenaar-Schoeman, P. Marais) |
| SMF | Senckenberg Natural History Museum, Frankfurt am Main, Germany (P. Jäger) |
| TMSA | Ditsong National Museum of Natural History, Pretoria, South Africa (T. Bird) |
| ZISP | Zoological Institute RAS, St Petersburg, Russia (D.V. Logunov) |

Specimens were studied in 70% ethanol and a description of their colouration refers to that of preserved specimens. The epigyne was detached and macerated in 10% KOH overnight. After photos were taken and drawings were made, dissected parts were stored in microvials with the specimens. All drawings were made with the aid of a reticular eyepiece attached to a MBS–10 stereomicroscope. Photographs of preserved specimens were taken with a Canon EOS 550D camera attached to a Zeiss Stemi–2000 stereomicroscope. Stacked images were combined using Helicon Focus. The drawings were edited in Adobe Photoshop and Corel Draw.

The abbreviations used in the text are as follows:

| | |
|------------|-----------------------|
| AME | anterior median eyes; |
| Ap | apical; |
| BH | basal haematodocha; |
| C | cymbium; |
| D | dorsal; |
| DH | distal haematodocha; |
| E | embolus; |
| Fm | femur; |
| Mt | metatarsus; |
| Pr | prolateral; |
| Rt | retrolateral; |
| SR | salticid radix; |
| Tg | tegulum; |
| Ti | tibia; |
| V | ventral. |

The sequence of leg segments in measurement data is as follows: femur + patella + tibia + metatarsus + tarsus (total). All measurements are in millimeters (mm). Leg setation follows Ono (1988). Terminology follows

Zhang and Maddison (2015) and Azarkina and Haddad (2020). The distribution map was produced using the online mapping software SimpleMapp (Shorthouse 2010).

Results

Family Salticidae Blackwall, 1841

Subfamily Salticinae Blackwall, 1841

Tribe Euophryini Simon, 1901

Foordus gen. nov.

<https://zoobank.org/5BD45DF7-9EB3-4C21-9245-AE51BBF03366>

Type species. *Foordus stefani* sp. nov., designated here.

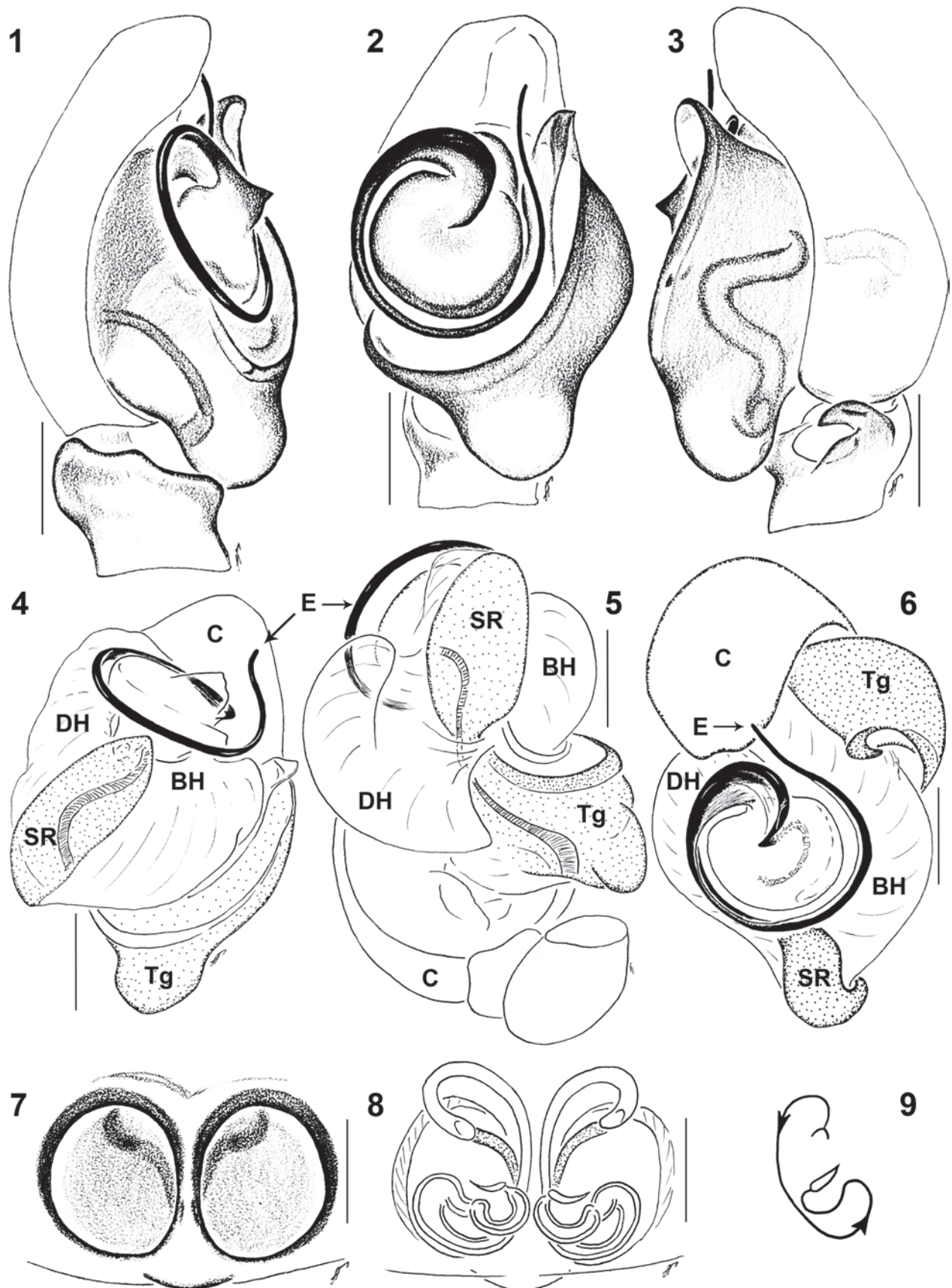
Diagnosis. The genus *Foordus* gen. nov. is most similar to the South-Asian genus *Cytaea* Keyserling, 1882 in having a retrolateral outgrowth of the tegulum near the embolic coil apically (cf. Figs 1–3 and Trębicki et al. 2021: figs 5E, 8E) but differs from *Cytaea* in an embolic division that has an outgrowth at the base which is absent in *Cytaea alburna* Keyserling, 1882 (cf Figs 1, 3 and Trębicki et al. 2021: figs 5D–G). Females differ in having a wider epigynal septum (Fig. 7) while *Cytaea* has a thin median guide (Fig. 7 and Trębicki et al. 2021: figs 5A–B). Moreover, all members of the genus *Cytaea* are larger in size and have fissentate chelicerae while *Foordus* gen. nov. has unidentate chelicerae.

Etymology. The new genus is a patronym in honour of the late Prof. Stefan Hendrik Foord. Gender masculine.

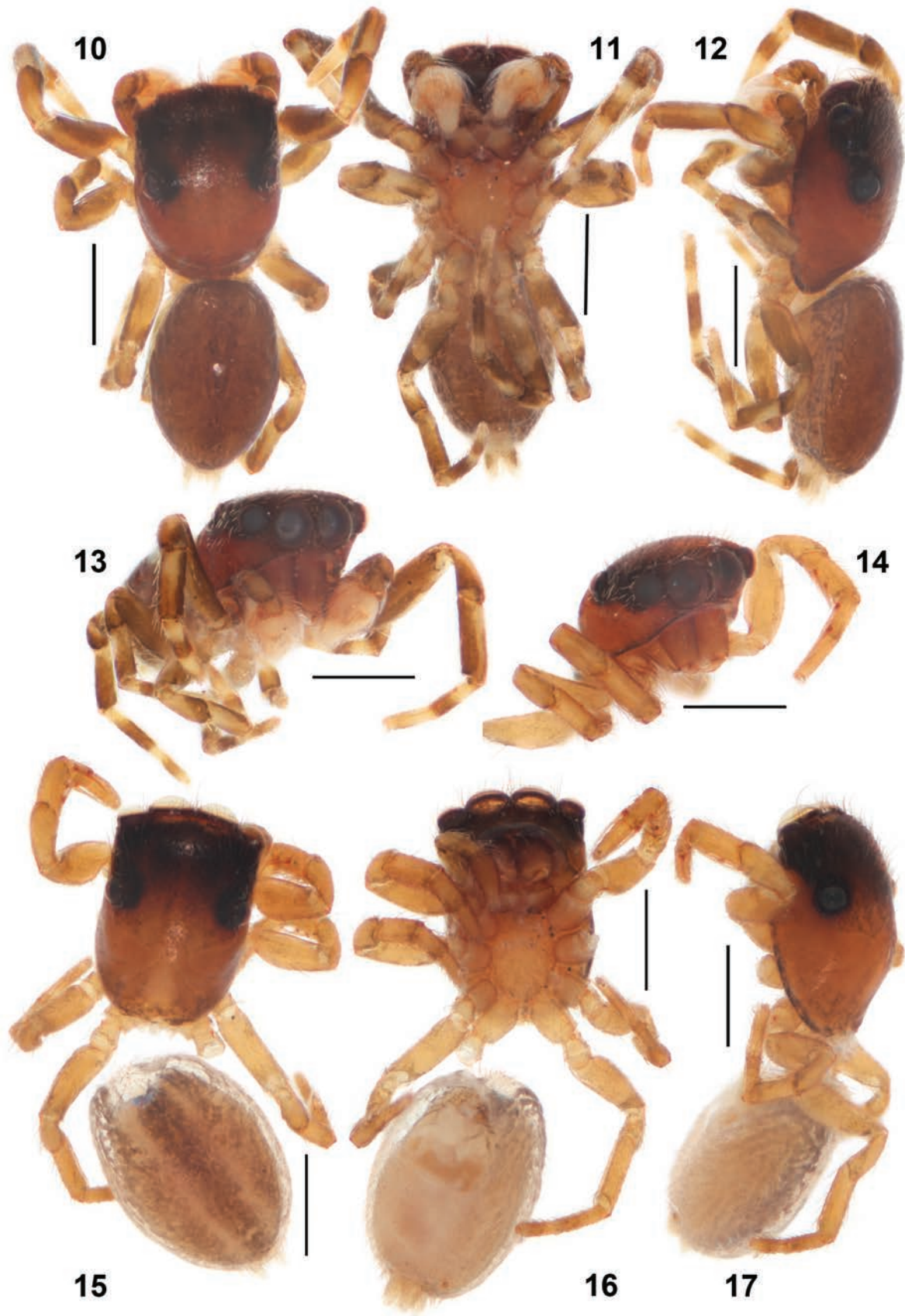
Definition. Tiny spiders with body length from 2.05 mm in male to 2.40 mm in female. Sexes similar in general body shape, males have a shiny scutum that covers the dorsal side of the abdomen (Figs 10, 12). Carapace rather low, with very low clypeus. Chelicerae unidentate, with two teeth promarginally and one tooth retromarginally. Legs subequal in size and length. Leg formula: I–IV/III/II in males and IV/I/III/II in female. Female palp of general form, without either macrosetae or an apical claw. Male palp: cymbium more or less round, of usual euophryine form. Tibia short, with a small ventral bump, retrolateral tibial apophysis bent ventrally at almost 90° (Fig. 3). Embolic division forms a round coil prolatero-ventrally, with salticid radix placed prolaterally (Figs 1, 2). Embolic coil has triangular outgrowth at the base, forming a single circle (Figs 1, 3, 4). Tegulum and salticid radix separated from each other by the basal haematodocha, embolic coil separated from salticid radix by the distal haematodocha (Figs 4–6). Female copulatory organs: Median septum narrow, with two round windows with wings on outer rim and openings to copulatory ducts close to its anterior end, supported by stiffeners. Vulva with long copulatory ducts and tube-shaped spermathecae, fertilization ducts located in the middle part near septum.

Composition. Monotypic genus, *Foordus stefani* gen. and sp. nov.

Distribution. Known only from the type location (KwaZulu-Natal Province, South Africa).



Figures 1–9. *Foordus stefani* gen. and sp. nov.: Male holotype (1–6) and female paratype (7–9) 1 male palp, prolateral 2 same, ventral 3 same, retrolateral 4 expanded male palp, ventral 5 same, ventro-basal 6 same, apical 7 epigyne, ventral 8 epigyne, dorsal 9 Diagrammatic course of the insemination ducts. Scale bars: 0.1 mm.



Figures 10–17. *Foordus stefani* gen. and sp. nov.: Male holotype (10–13) and female paratype (14–17) 10 male habitus, dorsal 11 same, ventral 12 same, same, lateral 13 same, frontal 14 female habitus, frontal 15 same, dorsal 16 same, ventral 17 same, lateral. Scale bars: 0.5 mm.

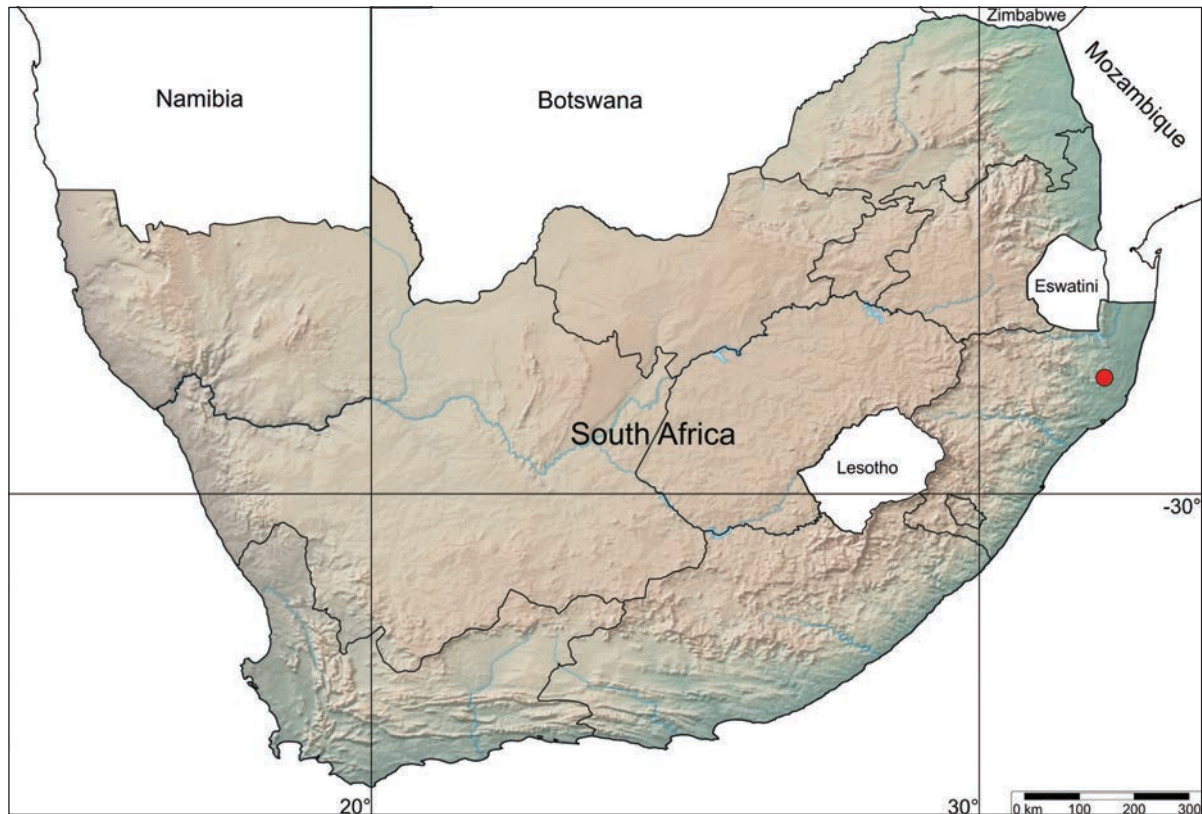


Figure 18. Distribution of the genus *Foordus* gen. nov.

***Foordus stefani* sp. nov.**

<https://zoobank.org/9AD094F4-36D4-4A56-B6DF-403C782AAD80>

Figs 1–18

Type material. Holotype. SOUTH AFRICA • ♂; KwaZulu-Natal Province; Hluhluwe Imfolozi Game Reserve; 28.0833°S, 32.0667°E; 18 Nov. 1992; S. Endrödy-Younga leg.; TMSA 25041.

Paratypes. SOUTH AFRICA • 2♂; same with Holotype; TMSA 22228 • 1♂; same; TMSA 22218 • 1♂1♀; same; TMSA 22209 • 2♂; same but 18 Nov. 1992; TMSA 22240 • 1♂; same; ISEA 001.9106 • 1♂; same; NCA 2024/18 • 1♂; same; MMUE G7709.1 • 1♂; same; SMF • 1♂; same; ZISP ARA_ARA_0000822.

Diagnosis. Same with generic.

Description. Male. Total length 2.05. Carapace 1.05 long, 0.78 wide. Abdomen 1.00 long, 0.65 wide. Ocular area 0.45 long, 0.70 wide anteriorly, 0.70 wide posteriorly. Cheliceral length 0.35. Clypeal height 0.05. Height at PLE 0.45. Diameter of AME 0.25. Length of leg segments: I 0.55 + 0.35 + 0.40 + 0.30 + 0.25 (1.85). II 0.45 + 0.30 + 0.28 + 0.20 + 0.25 (1.48). III 0.45 + 0.25 + 0.30 + 0.30 + 0.25 (1.55). IV 0.55 + 0.30 + 0.35 + 0.35 + 0.30 (1.85). Leg setation: I: Fm d 0-1-1, Ti v-pr 0-1-1 ap, v-rt 1-1-1 ap, Mt v 2-2 ap. II: Fm d 0-1-1, Ti v-pr 1-1-0, Mt v 2-2 ap. III: Fm d 0-1-1, pr & rt 0-1-0, v-pr 0-1-1 ap, Mt pr & rt 0-1 ap, v 0-2 ap. IV: Fm d 0-1-1, Ti v-pr 0-0-1 ap, Mt pr 0-0-1, v 0-2 ap. Colouration (in alcohol, Figs 10–13). Carapace brown, with dark brown eye field and dark brown rings around eyes. Clypeus brown. Chelicerae light-brown, pale apically. Sternum yellow-brown. Abdomen with dark brown shiny scutum that covers the entire abdomen dorsally. Venter brown. Book lung covers yellow-brown. Spinnerets brown posteriorly, yellow anteriorly.

low anteriorly. All legs yellow. Femora of all legs dark brown pro- and retrolaterally, remaining dark brown distally. Palps dark brown, cymbium yellow, covered with short white setae. Male palps as in Figs 1–6: similar to generic description.

Female. Total length 2.10. Carapace 1.10 long, 0.75 wide. Abdomen 1.30 long, 0.85 wide. Ocular area 0.45 long, 0.75 wide anteriorly, 0.73 wide posteriorly. Cheliceral length 0.30. Clypeal height 0.05. Height at PLE 0.40. Diameter of AME 0.25. Length of leg segments: I 0.55 + 0.30 + 0.35 + 0.25 + 0.25 (1.70). II 0.45 + 0.25 + 0.25 + 0.20 + 0.25 (1.40). III 0.45 + 0.25 + 0.25 + 0.30 + 0.25 (1.50). IV 0.55 + 0.25 + 0.40 + 0.35 + 0.30 (1.85). Leg setation: I: Ti v-pr 0-1-1 ap, v-rt 1-1-1 ap, Mt v 2-2 ap. II: Ti v-pr 1-1-0, Mt v 2-2 ap. III: Ti pr & rt 0-1-0, v-pr 0-0-1 ap, Mt pr & rt 0-1 ap, v 0-2 ap. IV: Ti rt 0-1-0, v-pr 0-0-1 ap, Mt rl 0-0-1, v-pr 0-1 ap. Colouration (in alcohol, Figs 14–17). Carapace brown, with dark brown eye field and black rings around eyes. Thoracic part with yellow-brown longitudinal band medially. Clypeus brown. Chelicerae yellow-brown. Sternum brownish-yellow. Labium and endites brownish-yellow, pale apically. Abdomen grey-brown dorsally, with two thin yellow longitudinal bands medially. Venter pale-yellow. Spinnerets and book-lung covers pale yellow. All legs and palps dark yellow, tinged with brown. Epigyne and vulva as in Figs 7–9, similar to generic description.

Etymology. The new species is named after the South African arachnologist, the late Prof. Stefan Hendrik Foord, for his contribution to African arachnology.

Discussion and conclusion

The new genus *Foordus* gen. nov. is similar to *Cytaea*, distributed from India to Australia and Samoa to the East and South (WSC 2024). A few genera are known with a distribution in the Afrotropics and South-East Asia. They include *Chinophrys* with one species in South Africa and the rest of the species in SE Asia and *Orsima* Simon, 1901 with one species in West Africa and two species in SE Asia. Previously some species that have a similar distribution (Afrotropics and SE Asia) were carefully reexamined and found to belong to different genera. For example, two species of *Afromarengo* Benjamin, 2004 were first described in *Marengo* Wanless, 1978 and later moved to *Afromarengo* that occurs only in the Afrotropics (Wanless 1978; Benjamin 2004). Likewise, *Ballagascar insularis* G.W. Peckham & E.G. Peckham, 1885 and *Wandawe benjamini* (Wesołowska and Haddad 2013) were originally placed in *Colaxes* Simon, 1900 (Wesołowska 2019 and Wesołowska and Haddad 2013) and later moved to other genera (Azarkina and Haddad 2020).

With *Foordus stefani* gen. and sp. nov. the number of euophryines from South Africa is raised to 7 genera and 51 species in total. Two of the genera are monotypic, *Foordus* gen. nov. (with *F. stefani* sp. nov.) and *Yimbulunga* (with *Y. foordi* Wesołowska, Azarkina & Russell-Smith, 2014). Thus, among these seven genera, five genera are only found in the Afrotropics, while two genera, *Chinophrys* and *Euophrys*, are found outside of Afrotropics. The genus *Euophrys* is most likely polyphyletic and some of the African members will in future be moved to other, undescribed genera.

Despite a considerable similarity with *Cytaea*, I decided to describe a new genus of euophryine jumping spider, *Foordus* gen. nov. until further material is found and a full detailed diagnosis for the genus *Cytaea* is provided (it seems that the genus *Cytaea* is polyphyletic). Molecular methods may help to resolve this issue in the future.

Acknowledgements

The curators of the Ditsong Museum (Audrey Ndaba and Tharina Bird) are thanked for loaning the material at their disposal for this study. Robyn Lyle (Pretoria, South Africa) is thanked for assistance in obtaining material from the Ditsong Museum. I wish to thank Ansie Dippenaar-Schoeman, Robin Lyle and Petro Marais for providing facilities during my stay in Pretoria. Dmitri Logunov is thanked for short discussion on the generic status. Special thanks go to Anthony Russell-Smith (United Kingdom) for editing the English of the final draft. This paper would not have been possible without Charles Haddad's help and a grant from the National Research Foundation of South Africa in the Competitive Program for Rated Researchers (#95569). Ansie Dippenaar-Schoeman, G.B. Edwards (USA) and anonymous referee are thanked for their critical comments that improved the paper.

Additional information

Conflict of interest

The author has declared that no competing interests exist.

Ethical statement

No ethical statement was reported.

Funding

This work was partly supported by Federal Fundamental Scientific Research Program, project 1021051703269-9-1.6.12 and a grant from the University of Venda RPC committee (Grant no. P109) and funding through the NRF Chair in Biodiversity Value and Change. The KwaZulu-Natal Museum funded the production of this publication.

Author contributions

The author solely contributed to this work.

Author ORCIDs

Galina N. Azarkina  <https://orcid.org/0000-0002-9328-3913>

Data availability

All of the data that support the findings of this study are available in the main text.

References

- Azarkina GN, Haddad CR (2020) Partial revision of the Afrotropical Ballini, with the description of seven new genera (Araneae: Salticidae). *Zootaxa* 4899(1): 15–92. <https://doi.org/10.11646/zootaxa.4899.1.4>
- Benjamin SP (2004) Taxonomic revision and phylogenetic hypothesis for the jumping spider subfamily Ballinae (Araneae, Salticidae). *Zoological Journal of the Linnean Society* 142(1): 1–82. <https://doi.org/10.1111/j.1096-3642.2004.00123.x>
- Dippenaar-Schoeman AS, Jocqué R (1997) African Spiders: An Identification Manual. Plant Protection Research Institute Handbook 9. Plant Protection Research Institute, Pretoria, 392 pp.

- Dippenaar-Schoeman AS, Haddad CR, Lotz LN, Booysen R, Steenkamp RC, Foord SH (2023) Checklist of the spiders (Araneae) of South Africa. *African Invertebrates* 64(3): 221–281. <https://doi.org/10.3897/AfrInvertebr.64.111047>
- Ono H (1988) A revisional study of the spider family Thomisidae (Arachnida, Araneae) of Japan. National Science Museum, Tokyo, 252 pp.
- Shorthouse DP (2010) SimpleMappr, an online tool to produce publication-quality point maps. <http://www.simplemappr.net> [accessed on 15.09.2024]
- Trębicki Ł, Patoleta BM, Dabert M, Żabka M (2021) Redescription of type species of the genus *Cytaea* Keyserling, 1882 (Araneae: Salticidae) – an integrative approach. *The European Zoological Journal* 88(1): 933–947. <https://doi.org/10.1080/24750263.2021.1961029>
- Wanless FR (1978) A revision of the spider genus *Marengo* (Araneae: Salticidae). *Bulletin of the British Museum, Natural History. Zoology* 33: 259–278. <https://doi.org/10.5962/p.28739>
- Wesołowska W (2019) *Colaxes insularis* (Peckham & Peckham, 1885) is a valid species of jumping spiders (Araneae: Salticidae: Ballinae). *Israel Journal of Entomology* 49: 57–61.
- Wesołowska W, Haddad CR (2013) New data on the jumping spiders of South Africa (Araneae: Salticidae). *African Invertebrates* 54: 177–240.
- Wesołowska W, Azarkina GN, Russell-Smith A (2014) Euophryine jumping spiders of the Afrotropical Region—new taxa and a checklist (Araneae: Salticidae: Euophryinae). *Zootaxa* 3789(1): 1–72. <https://doi.org/10.11646/zootaxa.3789.1.1>
- WSC (2024) World Spider Catalog. Version 25.5. Natural History Museum Bern. <http://wsc.nmbe.ch> [accessed on 15.09.2024]
- Zhang JX, Maddison WP (2015) Genera of euophryine jumping spiders (Araneae: Salticidae), with a combined molecular morphological phylogeny. *Zootaxa* 3938(1): 1–147. <https://doi.org/10.11646/zootaxa.3938.1.1>

Soutpansberg Mountain: a spider hotspot in the Limpopo Province of South Africa (Arachnida, Araneae)

Ansie S. Dippenaar-Schoeman¹, T. Caswell Munyai², Colin S. Schoeman¹, Norbert Hahn³,
Stefan H. Foord^{1,†}

¹ SARChI-Chair on Biodiversity Value and Change, Department of Zoology and Centre for Invasion Biology, School of Mathematical and Natural Science, University of Venda, Private Bag X5050, Thohoyandou 0950, South Africa

² School of Life Sciences, College of Agriculture, Engineering and Science, University of KwaZulu-Natal, Private Bag X01, Scottsville 3209, South Africa

³ Visiting Professor, Department of Biological Sciences, Faculty of Science, Engineering and Agriculture, University of Venda, Thohoyandou, South Africa

Corresponding authors: Ansie S. Dippenaar-Schoeman (dippenaaransie@gmail.com); Norbert Hahn (norbert.hahn@gmail.com)



This article is part of:

Gedenkschrift for Prof. Stefan H. Foord

Edited by Galina Azarkina, Ansie Dippenaar-Schoeman, Charles Haddad, Robin Lyle, John Mldgley, Caswell Munyai

Academic editor: Charles Haddad

Received: 20 August 2024

Accepted: 21 October 2024

Published: 12 November 2024

ZooBank: <https://zoobank.org/933643D5-6D41-451A-8A87-30D0BA362542>

Citation: Dippenaar-Schoeman AS, Munyai TC, Schoeman CS, Hahn N, Foord SH (2024) Soutpansberg Mountain: a spider hotspot in the Limpopo Province of South Africa (Arachnida, Araneae). *African Invertebrates* 65(2): 85–114. <https://doi.org/10.3897/AfrInvertebr.65.135136>

Copyright: ©

Ansie S. Dippenaar-Schoeman et al.

This is an open access article distributed under terms of the Creative Commons Attribution License (Attribution 4.0 International – CC BY 4.0).

Abstract

The Soutpansberg Mountain (SM) range in the northern part of the Limpopo Province within the Vhembe Biosphere Reserve, is a refuge for high diversity of organisms due to its geological history and location. As part of the South African National Survey of Arachnida (SANSA), the spider diversity of the Soutpansberg Mountain was determined over 27 years: 58 families, 293 genera, and 585 species were recorded. The Salticidae with 85 species, followed by Thomisidae (81 species), Araneidae, and Gnaphosidae, with 45 species each, are the most species-rich, while 11 families are represented by single species. Global distributions, endemism, and conservation assessment are provided for each species using IUCN criteria. Most species (516, 88.1%) are widely distributed with no known threats and are of Least Concern, whereas eight species (1.4%) are of special concern. Of these, five species are Rare and one each is Critically Rare, Vulnerable, and Near Threatened. Twenty-five new species have been described from the SM since 1997, but 17 species (2.9%) are still Data Deficient, and 44 species were not evaluated due to unresolved taxonomy. The SM represents a spider biodiversity hotspot in the Limpopo Province, representing 25.4% of the total spider fauna of South Africa and 64.3% of the known spider fauna of the Limpopo Province.

Key words: Conservation biogeography, endemism, faunistic surveys, global distribution, SANSA, Savanna biome, South African National Survey of Arachnida

Introduction

The emerging field of conservation biogeography concerns species' distribution dynamics and how they relate to biodiversity conservation (Robertson et al. 2010), and its main currency is valid species-level determinations and distribution data. Biodiversity is one of the most important concepts in contemporary biology and has many applications. In November 1995, South Africa ratified the Convention on Biological Diversity (CBD) and pledged to develop a strategic plan for biodiversity conservation and sustainable use. To meet the

requirements of the CBD, the SANSA was initiated in 1997 with the main aim of discovering, describing and making an inventory of the South African arachnid fauna (Dippenaar-Schoeman et al. 2015). The species distribution data collected since 1997 provided the essential foundational information necessary for the conservation assessments to compile a Red Data List of the Araneae of South Africa (Foord et al. 2020) and a published national checklist of 2265 species (Dippenaar-Schoeman et al. 2023).

The Limpopo Province covers 10.6% of South Africa, and more than 95% of the Limpopo Province falls within the Savanna Biome (Foord et al. 2011; Dippenaar-Schoeman et al. 2013a). The province is one of the more extensively sampled regions, and from the 286 sites sampled, 905 known spider species were documented (Dippenaar-Schoeman et al. 2023). The published records of some of the major surveys undertaken in the province are: Atherstone Game Reserve; Blouberg Nature Reserve (Muelelwa et al. 2010; Foord et al. 2019); Farm Amsterdam, Dendron District (Dippenaar-Schoeman et al. 1978); Farm Zandrivier, Lephalale; Ka-Ndengeza and Vyeboom Villages (Joseph et al. 2017; Foord et al. 2018); Lekgalameetse Nature Reserve (Foord et al. 2016); Little Leigh (Foord et al. 2013); Luvhondo Nature Reserve (Foord et al. 2002, 2008); Makelali Nature Reserve (Whitmore et al. 2001, 2002); Marakele National Park (Dippenaar-Schoeman et al. 2021); Nylsvley Nature Reserve (Dippenaar-Schoeman et al. 2009); Pietersburg Nature Reserve (Dippenaar et al. 2008); Rust de Winter cotton surveys (Dippenaar-Schoeman et al. 1999, 2013b); Sovenga Hill (Modiba et al. 2005); Syferkuil; Venetia Limpopo Nature Reserve; Vhembe Biosphere Reserve (Schoeman and Foord 2021); Western Soutpansberg Transect (WST) (Munyai and Foord 2012a; Foord et al. 2013, 2022) and Waterberg Biosphere (Foord 2023). The province is characterized by a complex mosaic of habitats, and the 55 endemic spider species so far recorded indicate a high degree of endemism (Dippenaar-Schoeman et al. 2023).

The Soutpansberg is the northernmost mountain range in South Africa, situated in the northern part of the Limpopo Province and within the Vhembe Biosphere Reserve and Savanna Biome. It is one of the oldest mountain ranges in southern Africa, and it is assumed that this geomorphological feature was created by faulting that occurred about 150 Ma ago (Haddon and McCarthy 2005), and that during the last \pm 60 Ma, erosion formed the landscape as we see it today. Due to its age the Soutpansberg harbours spider species that belong to ancient evolutionary lineages (Jocqué 2008; Haddad 2009; Jocqué et al. 2013; Jocqué and Henrard 2015). This ancient mountain range is influenced by diverse biogeographical elements and contemporary drivers of change (Hahn 2011). Its geological history and location constitute a refuge for a high diversity of organisms. It is a major centre of plant endemism and biodiversity and has the highest plant generic and family-level diversity among the 18 Centres of Plant Endemism in southern Africa (Van Wyk and Smith 2001).

The research findings on spiders in the SM is presented herein, providing a measure of what has been achieved and identifies directions for future research. The annotated checklist consolidates all the data on spider species sampled and described from the SM. It provides information on the global distribution, endemism, and conservation status for all 585 species and highlights species of special concern and those that are data deficient. Lastly, we comment on the significance of the SM as a biodiversity hotspot in the Limpopo Province within a national context.

Material and methods

Study area

The SM range stretches about 210 km eastward and forms a geographic unit with the Makgabeng Plateau, Blouberg Mountain to the west and the Waterberg to the south. The Western Soutpansberg (WSM), stretching from Wyllie's Poort to the town of Vivo about 70 km west, is the most intensive sampled region of the mountain (Fig. 1). The SM incorporates the mountain massif proper and includes a 25 km boundary stretching into the surrounding flat lands (Foord et al. 2002) (Fig. 2). The Soutpansberg's upper southern slopes are characterised by a more temperate climate, being strongly influenced by orographic cloud precipitation, whereas the northern slopes are much drier and hotter (Hahn 2006; Mostert et al. 2008). The highest peak of the SM is Lajuma (23°02'S, 29°26'E) at 1747 m a.s.l. Spider data was sampled from sixteen survey sites, and one transect on the SM (Fig. 1, Table 1).

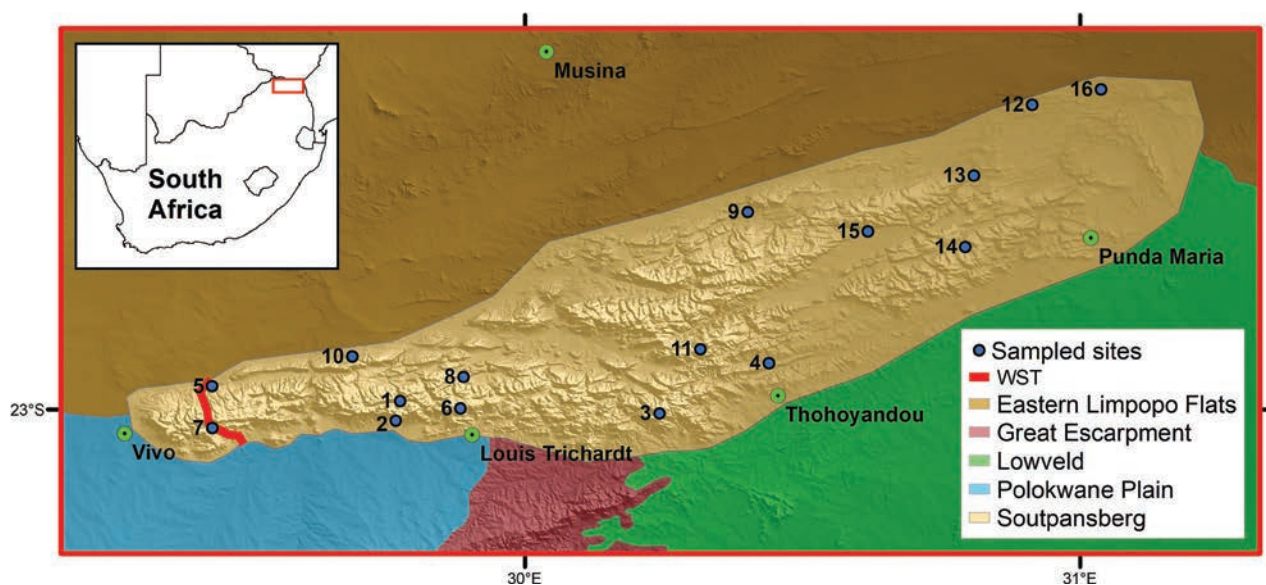


Figure 1. Map of Soutpansberg Mountain (SM), showing the 16 sites (1–16) and Western Soutpansberg Transect (WST, red band) sampled under the supervision of Prof S. Foord, students and collaborators.



Figure 2. University of Venda students sampling spiders on the middle plateau of the Soutpansberg Mountain (SM).

Table 1. Sites sampled on the Soutpansberg Mountain (SM) with the number of spider specimens collected. * Denotes sites sampled during the Vhembe Biosphere Survey (see Fig. 1).

| Sites on soutpansberg | Coordinates | No spider specimens sampled |
|---|-----------------|-----------------------------|
| 1. Bluegumspoort (farm) * | -22.965, 29.894 | 31 |
| 2. Buzzard Mountain * | -23.003, 29.770 | 52 |
| 3. Entabeni State Forest * | -23.018, 30.243 | 266 |
| 4. Gondeni (Communal land) * | -22.913, 30.064 | 72 |
| 5. Goro Game Reserve * | -22.939, 29.428 | 662 |
| 6. Hanglip State Forest * | -22.998, 29.886 | 62 |
| 7. Lajuma (part of Lhuvhondo Nat. Res.) * | -23.038, 29.441 | 1759 |
| 8. Little Leigh (farm, now Morningsun) | -22.934, 29.894 | 1072 |
| 9. Nwanedi Game Reserve * | -22.644, 30.370 | 64 |
| 10. Rochdale (farm). Waterpoort | -22.533, 29.417 | 72 |
| 11. Thathe Vondo State Forest * | -22.876, 30.323 | 11 |
| 12. Tshikondeni area | -22.451, 30.913 | 227 |
| 13. Tshulu River Research Camp | -22.579, 30.809 | 170 |
| 14. Vhurivhuri | -22.707, 30.793 | 310 |
| 15. Vhuvha (Communal land) | -22.679, 30.617 | 14 |
| 16. Wallers Camp | -22.424, 31.037 | 142 |
| Red band-Western Soutpansberg Transect (WST) (11 sites) | | 10541 |
| | | 15527 |

Collecting methods

The SM spiders were sampled over 27 years from 27 sites using different collecting methods. For the SANSA surveys, a standardised rapid sampling protocol was followed, sampling ground-dwelling spiders with pitfall traps, leaf litter sifting, and active searching at the base of grass tussocks and under rocks. Plant-dwelling species were collected by beating, sweeping, actively searching on vegetation and flowers, and tree fogging (Haddad and Dippenaar-Schoeman 2015).

During the 6-year long-term surveys in the WS, spiders were sampled twice a year during the hot-dry and hot-wet seasons in 11 elevational zones spaced at 200 m altitudinal distances. Sampling within a zone consisted of four replicates at least 300 m apart. Replicates contained ten pitfall traps in a 10 × 50 grid. Traps were left open for five days (Foord et al. 2022). Voucher specimens sampled from the SM are housed at the National Collection of Arachnida (NCA) at the Agricultural Research Council (ARC) in Pretoria, South Africa.

Source of information

Information on spider diversity for the SM was obtained from different datasets. Data was extracted from taxonomic (66) and faunistic (8) published papers and primary specimens' data housed in natural history museums gathered by visiting scientists.

The following national and international projects were involved.

1. The SANSA project (1997 to 2023) involved the ARC and the South African National Biodiversity Institute (SANBI), Threatened Species Programme phase 2, which received funding in 2006 through the Royal Norwegian Ministry for surveys to obtain data to produce a Red List of South African spiders.

2. In 2008, Dr Rudy Jocqué of the African Museum in Belgium and twelve researchers from Africa, Belgium, Germany, South America, Switzerland and the United States of America were funded through the international PBI-Oonopidae project to visit the SM over ten days. The group conducted tree fogging in Afro-montane high forests and closed woodlands, using it as a collecting method for the family Oonopidae.
3. Prof S. Foord received funding and logistic support from the Department of Science & Technology (DST) – National Research Foundation (NRF) and through the Centre of Excellence for Invasion Biology for long-term surveys (2009–2015).
4. Prof S. Foord received further funding from the South African Research Chairs Initiative (SARChI) on Biodiversity Value and Change in the Vhembe Biosphere Reserve, which was hosted and supported by the University of Venda to further support the various additional surveys from 2016 onwards.

Soutpansberg Mountain surveys

Surveys by the universities of Ghent, Pretoria and Venda were undertaken to address research projects by students and collaborators. During the first surveys (1996–2002) hand collection, sweeping, beating, and pitfall traps were used to produce the first checklist of the SM, listing 46 families and 127 species (Foord et al. 2002). This was followed in 2004–2005 by a study on fine-scale variation in spider assemblages in five representative vegetation types. The vegetation types were assessed in terms of spider family and species present, as well as levels of endemism and differences related to vegetation structure. The results suggest that endemic spider taxa are more associated with tall forest and to a lesser extent, woodland (Foord et al. 2008).

In November–December (2005) and late summer March (2006), surveys were conducted on the Blouberg Nature Reserve and Little Leigh in the SM to try to develop standardised and optimised methods for rapid biodiversity assessments (Muelelwa et al. 2010). Results showed that collector experience did not affect the inventory results, whereas the time of day when sampling took place had a very small yet significant effect. Seasonality only affected abundance and richness but not assemblage composition.

Several factors affect the inclusion of spiders in conservation planning initiatives, and surrogates could help their incorporation. Including spiders in biodiversity inventories is desirable, but the demand for time and resources is immense. Foord et al. (2013) tested the performance of several surrogate measures, such as using higher taxa (genus, family), cross-taxon surrogates that are subsets of the spider assemblages (only certain spider families) or non-overlapping groups (woody vegetation and birds) and the use of morphospecies. The results show that using morphospecies as estimators cautiously supported species richness estimates.

A very important contribution to our knowledge of spiders of the SM were the long-term transect surveys, funded by the DST-NRF Centre for Invasion Biology at the University of Stellenbosch, to investigate the possible effect of climate change on spiders. The first transect survey was undertaken in the Cederberg Mountains in the Western Cape (Foord and Dippenaar-Schoeman 2016). The second transect survey in the WSM began in 2006. The initial transect was laid

out by Prof N. Hahn in an approximate north-south orientation (Fig. 1) across one of the narrowest sections of the WSM just below its highest point, Lajuma. The transect comprised nine sampling sites spaced at every 200 m contour interval over a distance of 17.4 km. The transect was subsequently expanded to incorporate four replicates at each site as part of Dr C. Munyai's MSc and PhD studies (2009–2015). Two additional sampling sites were added, and pitfall traps were used to sample twice a year during this period onwards. The altitudinal transect represents a gradient from open grassy habitats to woodland, shrubland, sedge-land, forest and thicket. These transect surveys provided the most cost-effective and succinct picture of the response of organisms and biotic assemblages to global climate change in the tropics and subtropics (Munya and Foord 2012a, b; Munyai and Foord 2015; Foord and Dippenaar-Schoeman 2016).

Between 2012–2013, Dr C. Schoeman studied the beta diversity and turnover of beetles and spiders using pitfall traps across five longitudinal transects in the Vhembe Biosphere Reserve, representing the different vegetation units in the region. Eleven Vhembe sites (indicated in Table 1 with an asterisk) sampled were from the SM (Table 1, Fig. 1) (Schoeman and Foord 2021).

Identification and voucher specimens

Assessing the SM's spider diversity was particularly challenging because of the large number of specimens sampled (>15 500) and the large number of species (585) identified. Only 44 species that were immature, new, or with unresolved taxonomy could not be determined to species level. One of the constraints for spider surveys is the lack of good taxonomic revisions for many of the larger spider families in Africa. No revisions or keys are available, making species-level identification time-consuming and difficult.

To address the taxonomic constraints, the 72 online photo identification guides for the South African spider families were used. The SANSA guides contain known information on all the genera and species listed in South Africa. Species-level information includes distribution maps for species, drawings and photographs of diagnostic morphological characteristics, notes on their behaviour, a conservation assessment and possible threats. Complete guides can be downloaded from the World Spider Catalog (<http://wsc.nmbe.ch>, doi: 10.24436/2) as well as from Zenodo (<https://zenodo.org/communities/sansa/>). The availability of a large number of specimens taken over different seasons resulted in most of the species being identified from both adult and immature specimens.

All the material sampled was sorted, identified and databased by the first author (Prof A. Dippenaar-Schoeman). The identification of Corinnidae, Salticidae and Trachelidae was done by Prof C.R. Haddad (Department of Entomology and Zoology, University of the Free State, South Africa). The voucher specimens are housed at the NCA in Pretoria.

Endemicity

The endemicity index (END) was provided for each species. It was calculated based on the global distribution of a species and included six endemicity categories, ranging from **6**: species known only from the type locality (SM); **5**: species known from several localities in the Limpopo Province; **4**: species sam-

pled from two adjacent provinces; **3**: species sampled from \geq three provinces in South Africa; **2**: species occur outside South Africa, but within southern Africa; **1**: species found throughout the Afrotropical Region; **0**: species occur beyond the Afrotropical Region and generally include widespread cosmopolitan species. The terms used are **SAE**: species endemic to South Africa; **STHE**: species endemic to southern Africa; **AE**: species endemic to the Afrotropical Region; and **C**: species that also occur beyond the Afrotropical Region.

Conservation assessment

As part of the Red Listing Spider project, the preliminary conservation status of all South African spider species was determined using the International Union for Conservation of Nature and Natural Resources (IUCN) criteria (Foord et al. 2020). The immature and possibly new species collected that could not be identified to species level using current taxonomic literature were not evaluated (**NE**). Preliminary conservation status of species as determined are listed with the following codes: **DD** (Data Deficient): species usually known from only one sex or based on old material without detailed locality data and where the species is difficult to identify; **LC** (Least Concern): species with a broad distribution (categories 0–2), without known threats; those of categories 3 and 4 are South African endemics (SAE) and many of them are also LC. Species of special concern (Rare, Critically Rare, Vulnerable and Threatened) usually belong to categories 5 or 6.

Results and discussion

Family diversity

In compiling the checklist, approximately 15 527 records from 27 sites were available from SM until the end of 2023 and 58 families, 293 genera and 585 species were recorded. The Salticidae (85 spp.), Thomisidae (81 spp.), Araneidae (45 spp.) and Gnaphosidae (45 spp.) were the most species-rich families, and 11 families are only represented by a single species (Table 2). Results from surveys in the Limpopo Province show that the same four spider families consistently dominate species richness (Foord et al. 2011; Haddad et al. 2013). Although South Africa has the richest described spider fauna on the African continent (Dippenaar-Schoeman et al. 2023), many families have never been subjected to revision and continue to present a considerable identification challenge to taxonomists. During this study, families with large proportions of undescribed species include the Ageleidae, Araneidae, Cyrtaucheniidae, Theridiidae and Trachelidae. Representatives of some of the ground and plant-hunting spider species of the Soutpansberg are provided in Figs 3–17 and some of the web-building spider species in Figs 18–32.

Salticidae

The Salticidae are free-living spiders that live on tree trunks, soil, rocks, and vegetation. They build small silk nests attached to various substrates to moult, oviposit, and sometimes to mate or occupy when inactive (Dippenaar-Schoeman 2023). The 85 salticid species from SM represent 14.5% of the total fauna (Table 2). The genus *Thyene* Simon, 1885 is one of the most species-rich genera in the SM, with

Table 2. Spider diversity of the Soutpansberg Mountain (SM) with families and their total number of genera (GEN) and species (SPP.) sampled.

| Family | GEN | SPP. | % | Family | GEN | SPP. | % |
|------------------|-----|------|-----|--------------------|------------|------------|------------|
| Agelenidae | 4 | 9 | 1.7 | Mimetidae | 3 | 3 | 0.5 |
| Anapidae | 1 | 1 | 0.2 | Nesticidae | 1 | 1 | 0.2 |
| Araneidae | 22 | 45 | 7.7 | Oecobiidae | 2 | 2 | 0.3 |
| Archaeidae | 1 | 2 | 0.3 | Oonopidae | 3 | 4 | 0.7 |
| Barychelidae | 2 | 2 | 0.4 | Orsolobidae | 2 | 2 | 0.3 |
| Bemmeridae | 1 | 1 | 0.2 | Oxyopidae | 3 | 21 | 3.6 |
| Caponiidae | 1 | 1 | 0.2 | Palpimanidae | 2 | 5 | 0.9 |
| Cheiracanthiidae | 2 | 14 | 2.4 | Penestomidae | 1 | 1 | 0.2 |
| Clubionidae | 1 | 8 | 1.5 | Philodromidae | 6 | 16 | 2.7 |
| Corinnidae | 11 | 14 | 2.4 | Pholcidae | 3 | 7 | 1.2 |
| Ctenidae | 2 | 4 | 0.7 | Phyxelididae | 3 | 3 | 0.5 |
| Cyatholipidae | 1 | 2 | 0.3 | Pisauridae | 9 | 11 | 1.9 |
| Cyrtachenidae | 1 | 5 | 0.9 | Prodidomidae | 4 | 7 | 1.2 |
| Deinopidae | 2 | 2 | 0.3 | Salticidae | 43 | 85 | 14.5 |
| Dictynidae | 3 | 3 | 0.5 | Scytodidae | 1 | 4 | 0.7 |
| Entypesidae | 1 | 2 | 0.3 | Segestriidae | 1 | 1 | 0.2 |
| Eresidae | 4 | 7 | 1.2 | Selenopidae | 2 | 9 | 1.5 |
| Euagridae | 1 | 1 | 0.2 | Sicariidae | 2 | 3 | 0.5 |
| Filistatidae | 1 | 1 | 0.2 | Sparassidae | 4 | 8 | 1.4 |
| Gallieniellidae | 2 | 2 | 0.3 | Stasimopidae | 1 | 1 | 0.2 |
| Gnaphosidae | 18 | 45 | 7.7 | Tetragnathidae | 5 | 14 | 2.4 |
| Hahniidae | 1 | 1 | 0.2 | Theraphosidae | 5 | 6 | 1.0 |
| Hersiliidae | 2 | 4 | 0.7 | Theridiidae | 20 | 28 | 4.8 |
| Idiopidae | 4 | 4 | 0.7 | Thomisidae | 22 | 81 | 13.8 |
| Linyphiidae | 6 | 7 | 1.2 | Trachelidae | 10 | 14 | 2.4 |
| Liocranidae | 1 | 2 | 0.3 | Trochanteriidae | 1 | 3 | 0.5 |
| Lycosidae | 13 | 20 | 3.4 | Uloboridae | 4 | 5 | 0.9 |
| Macrobonidae | 3 | 3 | 0.5 | Zodariidae | 15 | 25 | 4.3 |
| Migidae | 2 | 2 | 0.3 | Zoropsidae | 1 | 1 | 0.2 |
| | | | | 58 families | 293 | 585 | 100 |

11 species. Almost half of the species (49.4%) are African endemics, 28.2% are southern African endemics, and three species are known more widely than Africa (Table 6). Three species were recently described from SM: *Phintella lajuma* Haddad & Wesolowska, 2013 (Fig. 14), *Rumburak tuberatus* Wesolowska, Azarkina & Russell-Smith, 2014 (Fig. 15) and *Tomomingi szutsi* Wesolowska & Haddad, 2013. Two salticid species were undetermined, but the *Langelurillus* species was identified as new and is awaiting taxonomic description.

Thomisidae

The thomisids are free-living spiders commonly found on grass, shrubs, flowers and trees, with only a few species occurring on the soil surface (Dippenaar-Schoeman 2023). The 81 species recorded from the SM represent 13.8% of the total fauna (Table 2), and *Thomisus* Walckenaer, 1805 (9 spp.) is the most species-rich genus. Wind easily disperses juvenile thomisids, and most species have a wide distribution. Fifty-eight species (71.6%) are African endemics, 17.3% are southern African endemics, and five species are known more widely than Africa. Only four species are South African endemics (Table 6). Although



Figures 3–17. Representative hunting spiders of the Soutpansberg Mountain **3** *Afrarchaea entabeniensis* (Archaeidae) **4** *Cheiramiona lajuma* (Cheiracanthiidae) **5** *Hortipes contubernalis* (Corinnidae) **6** *Vendaphaea lajuma* (Corinnidae) **7** *Afropesa schoutedeni* (Entypesidae) **8** *Drassodella venda* (Gallieniellidae) **9** *Asemesthes ceresicola* (Gnaphosidae) **10** *Ibala arcus* (Gnaphosidae) **11** *Tyrotama soutpansbergensis* (Hersilliidae) **12** *Evippomma squamulatum* (Lycosidae) **13** *Nilus massajae* (Pisauridae) **14** *Phintella lajuma* (Salticidae) **15** *Rumburak tuberatus* (Salticidae) **16** *Heriaeus crassispinus* (Thomisidae) **17** *Cydrela schoemanae* (Zodariidae). Photo credits: **3** L. Lotz **6** C. Haddad **4, 5, 7–17** P. Webb.

no thomisids species have been newly described from SM, specimens were included in several generic revisions, e.g. *Heriaeus crassispinus* Lawrence, 1942 (Fig. 16), *Mystaria savannensis* Lewis & Dippenaar-Schoeman, 2014 and *Sylligma ndumi* Honiball & Dippenaar-Schoeman, 2011.

Araneidae

The Araneidae are web-dwellers and produce typical or modified orb-webs; 45 species are known from SM, which represents 7.7% of the total spider fauna (Table 2). The taxonomy of many genera in Africa is still unresolved, and six of the 45 species were not assessed for IUCN due to a lack of taxonomic resolution. The family is diverse, and 22 genera have been sampled. The species have a wide distribution, and 21 species (46.6%) are African endemics, 15.5% are southern African endemics, and eight species are known more widely than Africa. Only three species, *Nemoscolus elongatus* Lawrence, 1947, *Singa albodorsata* Kauri, 1950 and *Ursa turbinata* Simon, 1895 are South African endemics (Table 6).

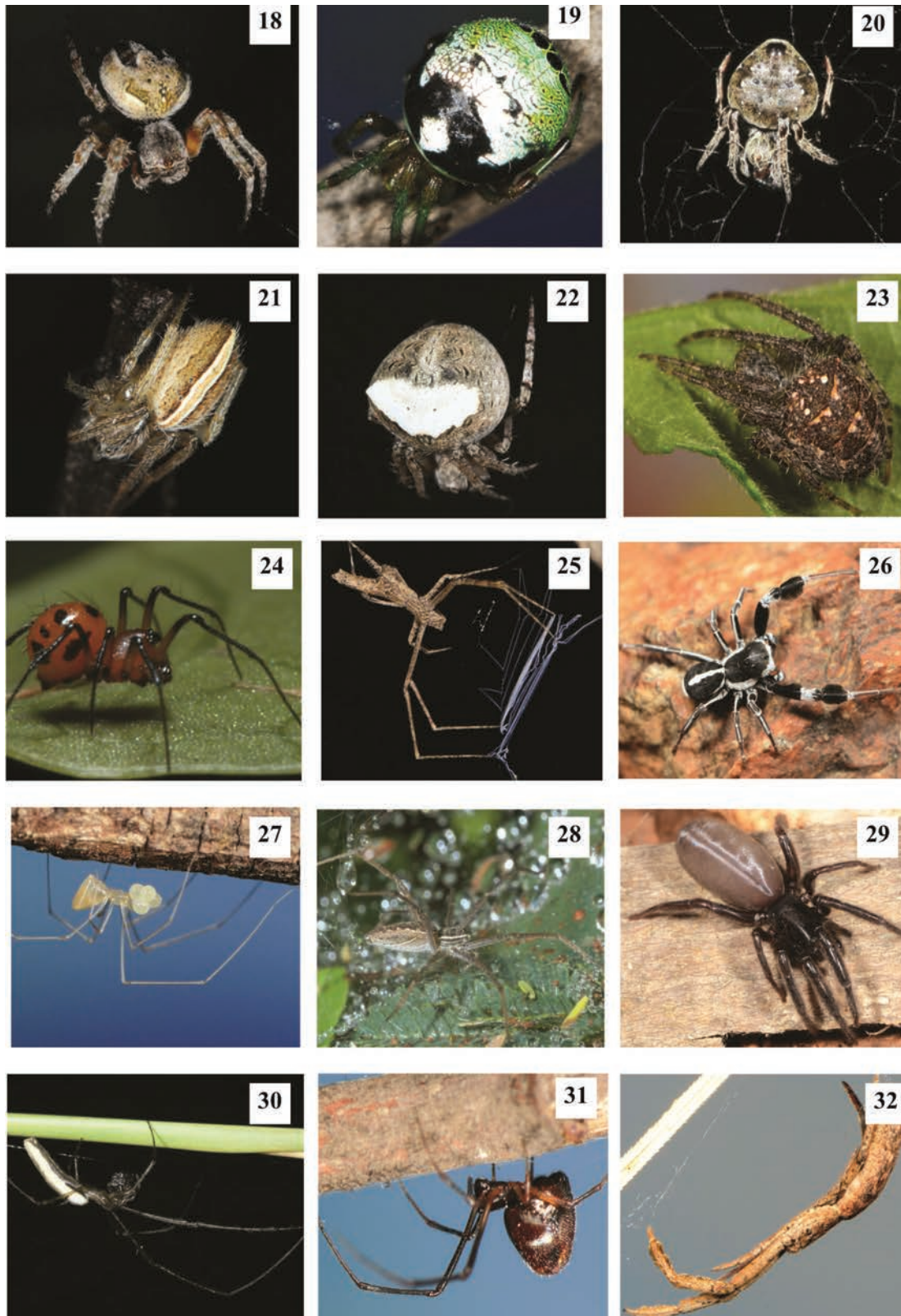
Gnaphosidae

The gnaphosids are free-living spiders and commonly found on the ground and low vegetation (Dippenaar-Schoeman 2023). The diversity of Gnaphosidae is generally higher in more arid savanna habitats in South Africa. The 18 genera and 45 species collected from the SM represent 7.7% of the SM spider fauna (Table 2). *Zelotes* Gistel, 1848 (Gnaphosidae, 14 spp.) and *Asemesthes* Simon, 1887 (Gnaphosidae, 10 spp.) are the most species-rich genera (Table 6). Eight species (17.8%) are African endemics, 23 species (51.1%) are southern African endemics, only one species, *Setaphis subtilis* (Simon, 1897), is known more widely than Africa, and 12 species (8.3%) are South African endemics. The species *Asemesthes ceresicola* Tucker, 1923 (Fig. 9) and *Ibala arcus* (Tucker, 1923) (Fig. 10) were the most abundant species and recorded from most of the localities.

Endemicity

Of the species identified at the species level, 231 (39.5%) have a wide distribution throughout Africa, 36 (6.2%) are also found in countries beyond Africa, 152 (26%) occur more widely in southern Africa, and 116 species (22.3%) are endemic to South Africa (Table 3). Of the 44 species not evaluated, 23 could not be determined to species level due to unresolved taxonomy. However, 20 spp. have already been identified as possibly new to science, which will increase the number of endemic species in the SM (Table 5). The new species represent several families poorly represented in the Limpopo Province, e.g., the Cyrtaucheniidae, Macrobnidae, Migidae, Penestomidae and Stasimopidae.

Since 1997, 66 articles containing information on species collected on the SM have been published. Of these, 50 were generic revisions for species belonging to 20 families. Taxonomic work resulted in recognising 25 species newly described from the SM since 1997 (indicated in Table 6 with an asterisk). The Limpopo Province now has 55 endemic species (Dippenaar-Schoeman et al. 2023) and 20 of these species have been recorded from the SM, with four species being endemic to the SM: *Afrarchaea entabeniensis* Lotz,



Figures 18–32. Representative web-building spiders of the Soutpansberg Mountain **18** *Araneus nigroquadratus* (Araneidae) **19** *Bijoaraneus legonensis* (Araneidae) **20** *Eriovixia excelsa* (Araneidae) **21** *Kilima decens* (Araneidae) **22** *Neoscona subfusca* (Araneidae) **23** *Pararaneus spectator* (Araneidae) **24** *Cyatholipus isolatus* (Cyatholipidae) **25** *Menneus camelus* (Deinopidae) **26** *Stegodyphus mimosarum* (Eresidae) **27** *Quamtana entabeni* (Pholcidae) **28** *Euprostenopsis vuattouxi* (Pisauridae) **29** *Ariadna bilineata* (Segestriidae) **30** *Tetragnatha bogotensis* (Tetragnathidae) **31** *Argyrodes zonatus* (Theridiidae) **32** *Miagrammopes brevicaudus* (Uloboridae). Photos credits: **24** J. Miller; rest P. Webb.

2003 (Archaeidae, Fig. 3), *Afropesa schoutedeni* (Benoit, 1965) (Fig. 7) and *A. schwendingeri* Zonstein & Ríos-Tamayo, 2021 (Entypesidae), and *Loxosceles haddadi* Lotz, 2017 (Sicariidae). However, more data is needed for these species, as two are listed as Data Deficient.

Table 3. Endemicity of the 585 spider species sampled at the Soutpansberg Mountain (SM).

| Endemicity | Spp. | % |
|---|------|------|
| 0 – Africa and wider (C) | 36 | 6.2 |
| 1 – African endemics (AE) | 231 | 39.5 |
| 2 – Southern African endemics (STHE) | 152 | 26 |
| 3 – SA endemics (SAE) | 92 | 15.7 |
| 4 – SA (SAE): 2 adjacent provinces | 10 | 1.7 |
| 5 – Limpopo Province endemics (LPE) | 16 | 2.7 |
| 6 – Known only from the type locality | 4 | 0.7 |
| Not evaluated: new (20 spp.); undetermined (22 spp.); immature (2 spp.) | 44 | 7.5 |

Table 4. Conservation status of the spider species sampled from the Soutpansberg Mountain (SM).

| Conservation status | Spp. | % |
|--------------------------------|------|---------|
| Data Deficient (DD) | 17 | 2.9 |
| Least Concern (LC) | 516 | 88.2 |
| Species special concern | | |
| Rare (RA) | 5 | 0.9 |
| Critical Rare (CR) | 1 | 0.2 |
| Vulnerable (VU) | 1 | 0.2 |
| Near Threatened (NT) | 1 | 0.2 |
| Not evaluated (NE) | 44 | 7.5 |
| | 585 | ~100.00 |

Table 5. Species of special concern from the Soutpansberg Mountain (SM). Conservation status (CON) and Endemicity (END): CR = Critical Rare; RA = Rare; VU = Vulnerable; NT = Near Threatened; LE = Limpopo endemic; SME = Soutpansberg endemic.

| Species | CON | END |
|--|-----|----------|
| Archaeidae | | |
| <i>Afrarchaea entabeniensis</i> Lotz, 2003 (Fig. 3) | CR | LE (SME) |
| Corinnidae | | |
| <i>Hortipes contubernalis</i> Bosselaers & Jocqué, 2000 (Fig. 5) | RA | LE |
| Cyatholipidae | | |
| <i>Cyatholipus isolatus</i> Griswold, 1987 (Fig. 24) | NT | Near LE |
| Hersiliidae | | |
| <i>Tyrotama soutpansbergensis</i> Foord & Dippenaar-Schoeman, 2005 (Fig. 11) | VU | LE |
| Pholcidae | | |
| <i>Quamtana entabeni</i> Huber, 2003 (Fig. 27) | RA | LE |
| <i>Smeringopus hanglip</i> Huber, 2012 | RA | LE |
| Tetragnathidae | | |
| <i>Diphya wesolowskiae</i> Omelko, Marusik & Lyle, 2020 | RA | LE |
| Zodariidae | | |
| <i>Australutica africana</i> Jocqué, 2008 | RA | LE |

Table 6. Checklist of the spider species from the Soutpansberg Mountain in Limpopo Province listing their endemity score (END), conservation status (CS) and global distribution score (DIS). * Species described from Soutpansberg Mountain.

| Family / Species | END | CS | DIS |
|---|-----|----|------|
| Family Agelenidae C.L. Koch, 1837 | | | |
| <i>Agelena australis</i> Simon, 1896 | 1 | LC | AE |
| <i>Agelena gaerdesi</i> Roewer, 1955 | 2 | LC | STHE |
| <i>Agelena</i> sp. 3 (undetermined) | – | NE | – |
| <i>Benoitia deserticola</i> (Simon, 1910) | 2 | LC | STHE |
| <i>Benoitia ocellata</i> (Pocock, 1900) | 1 | LC | AE |
| <i>Benoitia</i> sp. 3 (undetermined) | – | NE | – |
| <i>Benoitia</i> sp. 4 (undetermined) | – | NE | – |
| <i>Mistaria zuluana</i> (Roewer, 1955) | 2 | LC | STHE |
| <i>Olorunia punctata</i> Lehtinen, 1967 | 1 | LC | AE |
| Family Anapidae Simon, 1895 | | | |
| <i>Crozetulus rhodesiensis</i> Brignoli, 1981 | 2 | LC | STHE |
| Family Araneidae Clerck, 1757 | | | |
| <i>Acanthepeira</i> sp. 1 (undetermined) | – | NE | – |
| <i>Arachnura scorpionoides</i> Vinson, 1863 | 1 | LC | AE |
| <i>Araneus apricus</i> Karsch, 1884 | 1 | LC | AE |
| <i>Araneus nigroquadratus</i> Lawrence, 1937 (Fig. 18) | 2 | LC | STHE |
| <i>Araneus strupifer</i> (Simon, 1886) | 1 | LC | AE |
| <i>Araneus</i> sp. 4 (undetermined) | – | NE | – |
| <i>Araneus</i> sp. 5 (new) | – | NE | – |
| <i>Argiope australis</i> (Walckenaer, 1805) | 1 | LC | AE |
| <i>Argiope lobata</i> (Pallas, 1772) | 0 | LC | C |
| <i>Argiope levii</i> Bjørn, 1997 | 1 | LC | AE |
| <i>Bijoaraneus legonensis</i> (Grasshoff & Edmunds, 1979) (Fig. 19) | 1 | LC | AE |
| <i>Caerostris sexcuspidata</i> (Fabricius, 1793) | 1 | LC | AE |
| <i>Caerostris vicina</i> (Blackwall, 1866) | 1 | LC | AE |
| <i>Chorizopes</i> sp. 1 (undetermined) | – | NE | – |
| <i>Cyclosa insulana</i> (Costa, 1834) | 0 | LC | C |
| <i>Cyclosa oculata</i> (Walckenaer, 1802) | 0 | LC | C |
| <i>Cyphalonotus larvatus</i> (Simon, 1881) | 1 | LC | AE |
| <i>Cyrtophora citricola</i> (Forsskål, 1775) | 0 | LC | C |
| <i>Eriovixia excelsa</i> (Simon, 1889) (Fig. 20) | 0 | LC | C |
| <i>Gasteracantha milvoides</i> Butler, 1873 | 1 | LC | AE |
| <i>Gasteracantha sanguinolenta</i> C.L. Koch, 1844 | 1 | LC | AE |
| <i>Gea</i> sp. 1 (undetermined) | – | NE | – |
| <i>Hypsosinga holzapfelae</i> (Lessert, 1936) | 2 | LC | STHE |
| <i>Hypsosinga lithyphantoides</i> Caporiacco, 1947 | 1 | LC | AE |
| <i>Isoxya tabulata</i> (Thorell, 1859) | 1 | LC | AE |
| <i>Kilima decens</i> (Blackwall, 1866) (Fig. 21) | 1 | LC | AE |
| <i>Nemoscolus cotti</i> Lessert, 1933 | 2 | LC | STHE |
| <i>Nemoscolus elongatus</i> Lawrence, 1947 | 3 | LC | SAE |
| <i>Nemoscolus tubicola</i> (Simon, 1887) | 2 | LC | STHE |
| <i>Nemoscolus vigintipunctatus</i> Simon, 1897 | 2 | LC | STHE |
| <i>Neoscona blondeli</i> (Simon, 1886) | 1 | LC | AE |
| <i>Neoscona penicillipes</i> (Karsch, 1879) | 1 | LC | AE |
| <i>Neoscona quincasea</i> Roberts, 1983 | 1 | LC | AE |
| <i>Neoscona rapta</i> (Thorell, 1899) | 1 | LC | AE |
| <i>Neoscona subfusca</i> (C.L. Koch, 1837) (Fig. 22) | 0 | LC | C |
| <i>Neoscona triangula</i> (Keyserling, 1864) | 0 | LC | C |
| <i>Pararaneus spectator</i> (Karsch, 1885) (Fig. 23) | 0 | LC | C |

| Family / Species | END | CS | DIS |
|--|-----|----|------|
| <i>Pararaneus</i> sp. 2 (immature) | – | NE | – |
| <i>Prasonica albolimbata</i> Simon, 1895 | 1 | LC | AE |
| <i>Prasonica seriata</i> Simon, 1895 | 1 | LC | AE |
| <i>Singa albodorsata</i> Kauri, 1950 | 3 | LC | SAE |
| <i>Singa lawrencei</i> (Lessert, 1930) | 1 | LC | AE |
| <i>Ursa turbinata</i> Simon, 1895 | 3 | LC | SAE |
| <i>Trichonephila fenestrata</i> (Thorell, 1859) | 2 | LC | STHE |
| <i>Trichonephila senegalensis annulata</i> (Thorell, 1859) | 2 | LC | STHE |
| Family Archaeidae C.L. Koch & Berendt, 1854 | | | |
| <i>Afrarchaea bergae</i> Lotz, 1996 * | 4 | LC | SAE |
| <i>Afrarchaea entabeniensis</i> Lotz, 2003 * (Fig. 3) | 6 | CR | SAE |
| Family Barychelidae Simon, 1889 | | | |
| <i>Pisenor notius</i> Simon, 1889 | 1 | LC | AE |
| <i>Sipalolasma humicola</i> (Benoit, 1965) | 1 | LC | AE |
| Family Bemmeridae Simon, 1903 | | | |
| <i>Homostola pardalina</i> (Hewitt, 1913) | 3 | LC | SAE |
| Family Caponiidae Simon, 1890 | | | |
| <i>Caponia chelifera</i> Lessert, 1936 | 2 | LC | STHE |
| Family Cheiracanthiidae Wagner, 1887 | | | |
| <i>Cheiracanthium aculeatum</i> Simon, 1884 | 1 | LC | AE |
| <i>Cheiracanthium africanum</i> Lessert, 1921 | 1 | LC | AE |
| <i>Cheiracanthium angolensis</i> Lotz, 2007 | 2 | LC | STHE |
| <i>Cheiracanthium furculatum</i> Karsch, 1879 | 1 | LC | AE |
| <i>Cheiracanthium schenkeli</i> Caporiacco, 1949 | 1 | LC | AE |
| <i>Cheiracanthium vansoni</i> Lawrence, 1936 | 1 | LC | AE |
| <i>Cheiramiona clavigera</i> (Simon, 1897) | 3 | LC | SAE |
| <i>Cheiramiona filipes</i> (Simon, 1898) | 2 | LC | STHE |
| <i>Cheiramiona krugerensis</i> Lotz, 2003 | 3 | LC | SAE |
| <i>Cheiramiona lajuma</i> Lotz, 2003 * (Fig. 4) | 3 | LC | SAE |
| <i>Cheiramiona langi</i> Lotz, 2003 * | 2 | DD | STHE |
| <i>Cheiramiona mlawula</i> Lotz, 2003 | 2 | LC | STHE |
| <i>Cheiramiona paradisus</i> Lotz, 2003 | 2 | LC | STHE |
| <i>Cheiramiona simplicatarsis</i> (Simon, 1910) | 3 | LC | SAE |
| Family Clubionidae Wagner, 1887 | | | |
| <i>Clubiona abbajensis</i> Strand, 1906 | 1 | LC | AE |
| <i>Clubiona africana</i> Lessert, 1921 | 1 | LC | AE |
| <i>Clubiona bevisi</i> Lessert, 1923 | 3 | LC | SAE |
| <i>Clubiona durbana</i> Roewer, 1951 | 3 | LC | SAE |
| <i>Clubiona godfreyi</i> Lessert, 1921 | 1 | LC | AE |
| <i>Clubiona lawrencei</i> Roewer, 1951 | 2 | LC | STHE |
| <i>Clubiona pongolensis</i> Lawrence, 1952 | 3 | LC | SAE |
| <i>Clubiona pupillaris</i> Lawrence, 1938 | 3 | LC | SAE |
| Family Corinnidae Karsch, 1880 | | | |
| <i>Apochinomma formicaeforme</i> Pavesi, 1881 | 1 | LC | AE |
| <i>Cambalida dippenaarae</i> Haddad, 2012 | 1 | LC | AE |
| <i>Cambalida fulvipes</i> (Simon, 1896) | 1 | LC | AE |
| <i>Coenoptychus tropicalis</i> (Haddad, 2004) | 1 | LC | AE |
| <i>Copa flavoplumosa</i> Simon, 1885 | 1 | LC | AE |
| <i>Corinnomma lawrencei</i> Haddad, 2006 | 1 | LC | AE |
| <i>Corinnomma semiglabrum</i> (Simon, 1896) | 1 | LC | AE |
| <i>Graptartia granulosa</i> Simon, 1896 | 1 | LC | AE |
| <i>Hortipes contubernalis</i> Bosselaers & Jocqué, 2000 * (Fig. 5) | 5 | RA | SAE |
| <i>Merenius simoni</i> Lessert, 1921 | 1 | LC | AE |
| <i>Messapus natalis</i> (Pocock, 1898) | 2 | LC | STHE |

| Family / Species | END | CS | DIS |
|---|-----|----|------|
| <i>Pronophaea natalica</i> Simon, 1897 | 3 | LC | SAE |
| <i>Pronophaea</i> sp. 2 (new) | – | NE | – |
| <i>Vendaphaea lajuma</i> Haddad, 2009 * (Fig. 6) | 5 | DD | SAE |
| Family Ctenidae Keyserling, 1877 | | | |
| <i>Anahita</i> sp. 1 (undetermined) | – | NE | – |
| <i>Ctenus gulosus</i> Des Arts, 1912 | 2 | LC | STHE |
| <i>Ctenus pulchriiventris</i> (Simon, 1896) | 2 | LC | STHE |
| <i>Ctenus transvaalensis</i> Benoit, 1981 | 3 | LC | SAE |
| Family Cyatholipidae Simon, 1894 | | | |
| <i>Cyatholipus isolatus</i> Griswold, 1987 * (Fig. 24) | 4 | NT | SAE |
| <i>Cyatholipus</i> sp. 2 (new) | – | NE | – |
| Family Cyrtaucheniidae Simon, 1889 | | | |
| <i>Ancylotrypa brevipalpis</i> (Hewitt, 1916) | 3 | LC | SAE |
| <i>Ancylotrypa elongata</i> Purcell, 1908 | 2 | LC | STHE |
| <i>Ancylotrypa nuda</i> (Hewitt, 1916) | 3 | LC | SAE |
| <i>Ancylotrypa</i> sp. 4 (new) | – | NE | – |
| <i>Ancylotrypa</i> sp. 5 (new) | – | NE | – |
| Family Deinopidae C.L. Koch, 1850 | | | |
| <i>Asianopsis cornigera</i> (Gerstäcker, 1873) | 1 | LC | AE |
| <i>Menneus camelus</i> Pocock, 1902 (Fig. 25) | 3 | LC | SAE |
| Family Dictynidae O. Pickard-Cambridge, 1871 | | | |
| <i>Archaeodictyna conducta</i> (O.Pickard-Cambridge, 1876) | 0 | LC | C |
| <i>Dictyna</i> sp. 1 (undetermined) | – | NE | – |
| <i>Mashimo leleupi</i> Lehtinen, 1967 | 1 | LC | AE |
| Family Entypesidae Bond, Opatova & Hedin, 2020 | | | |
| <i>Afropesa schoutedeni</i> (Benoit, 1965) * (Fig. 7) | 6 | LC | SAE |
| <i>Afropesa schwendingeri</i> Zonstein & Ríos-Tamayo, 2021* | 6 | DD | SAE |
| Family Eresidae C.L. Koch, 1845 | | | |
| <i>Dresserus colsoni</i> Tucker, 1920 | 3 | LC | SAE |
| <i>Paradonea presleyi</i> Miller, Griswold, Scharff, Rezac, Szuts & Marhabaie, 2012 | 2 | LC | STHE |
| <i>Paradonea</i> sp. 2 (new) | – | NE | – |
| <i>Seothyra fasciata</i> Purcell, 1904 | 2 | LC | STHE |
| <i>Stegodyphus africanus</i> (Blackwall, 1866) | 1 | LC | AE |
| <i>Stegodyphus dumicola</i> Pocock, 1898 | 2 | LC | STHE |
| <i>Stegodyphus mimosarum</i> Pavesi, 1883 (Fig. 26) | 1 | LC | AE |
| Family Euagridae Raven, 1979 | | | |
| <i>Allothele malawi</i> Coyle, 1984 | 1 | LC | AE |
| Family Filistatidae Simon, 1864 | | | |
| <i>Andoharano ansieae</i> Zonstein & Marusik, 2015 | 2 | LC | STHE |
| Family Gallieniellidae Millot, 1947 | | | |
| <i>Austrachelas entabeni</i> Haddad & Mbo, 2017 * | 5 | DD | SAE |
| <i>Drassodella venda</i> Mbo & Haddad, 2019 * (Fig. 8) | 5 | LC | SAE |
| Family Gnaphosidae Banks, 1892 | | | |
| <i>Afrodrassex balrog</i> Haddad & Booysen, 2022 | 2 | LC | STHE |
| <i>Ammoxenus psammodromus</i> Simon, 1910 | 2 | LC | STHE |
| <i>Aneplasa interrogationis</i> Tucker, 1923 | 3 | LC | SAE |
| <i>Aphantaulax inornata</i> Tucker, 1923 | 2 | LC | STHE |
| <i>Asemesthes ceresicola</i> Tucker, 1923 (Fig. 9) | 3 | LC | SAE |
| <i>Asemesthes flavipes</i> Purcell, 1908 | 2 | LC | STHE |
| <i>Asemesthes fodina</i> Tucker, 1923 | 2 | LC | STHE |
| <i>Asemesthes lineatus</i> Purcell, 1908 | 1 | LC | AE |
| <i>Asemesthes numisma</i> Tucker, 1923 | 2 | LC | STHE |
| <i>Asemesthes pallidus</i> Purcell, 1908 | 3 | LC | SAE |

| Family / Species | END | CS | DIS |
|--|-----|----|------|
| <i>Asemesthes paynteri</i> Tucker, 1923 | 3 | LC | SAE |
| <i>Asemesthes purcelli</i> Tucker, 1923 | 2 | LC | STHE |
| <i>Asemesthes reflexus</i> Tucker, 1923 | 3 | LC | SAE |
| <i>Asemesthes</i> sp. 10 (new) | – | NE | – |
| <i>Camillina cordifera</i> (Tullgren, 1910) | 1 | LC | AE |
| <i>Drassodes helenae</i> Purcell, 1907 | 3 | LC | SAE |
| <i>Drassodes solitarius</i> Purcell, 1907 | 2 | LC | STHE |
| <i>Echemus erutus</i> Tucker, 1923 | 2 | LC | STHE |
| <i>Ibala arcus</i> (Tucker, 1923) (Fig. 10) | 2 | LC | STHE |
| <i>Ibala bilinearis</i> (Tucker, 1923) | 2 | LC | STHE |
| <i>Ibala bulawayensis</i> (Tucker, 1923) | 2 | LC | STHE |
| <i>Leptodrassex murphyi</i> Haddad & Booysen, 2022 | 2 | LC | STHE |
| <i>Megamyrmaekion transvaalense</i> Tucker, 1923 | 3 | LC | SAE |
| <i>Nomisia varia</i> (Tucker, 1923) | 2 | LC | STHE |
| <i>Pterotricha auris</i> (Tucker, 1923) | 3 | LC | SAE |
| <i>Rastellus kariba</i> Platnick & Griffin, 1990 | 2 | LC | STHE |
| <i>Scotophaeus marleyi</i> Tucker, 1923 | 3 | LC | SAE |
| <i>Setaphis subtilis</i> (Simon, 1897) | 0 | LC | C |
| <i>Xerophaeus appendiculatus</i> Purcell, 1907 | 3 | LC | SAE |
| <i>Xerophaeus aurariarum</i> Purcell, 1907 | 2 | LC | STHE |
| <i>Xerophaeus bicavus</i> Tucker, 1923 | 3 | LC | SAE |
| <i>Zelotes aestus</i> (Tucker, 1923) | 2 | LC | STHE |
| <i>Zelotes aridus</i> (Purcell, 1907) | 1 | LC | AE |
| <i>Zelotes caldarius</i> (Purcell, 1907) | 2 | LC | STHE |
| <i>Zelotes chinguli</i> Fitzpatrick, 2007 | 2 | LC | STHE |
| <i>Zelotes corrugatus</i> (Purcell, 1907) | 1 | LC | AE |
| <i>Zelotes fuliginus</i> (Purcell, 1907) | 1 | LC | AE |
| <i>Zelotes haplodrassoides</i> (Denis, 1955) | 1 | LC | AE |
| <i>Zelotes humilis</i> (Purcell, 1907) | 2 | LC | STHE |
| <i>Zelotes namaquus</i> FitzPatrick, 2007 | 3 | LC | SAE |
| <i>Zelotes natalensis</i> Tucker, 1923 | 2 | LC | STHE |
| <i>Zelotes otavi</i> Fitzpatrick, 2007 | 2 | LC | STHE |
| <i>Zelotes radiatus</i> Lawrence, 1928 | 2 | LC | STHE |
| <i>Zelotes scrutatus</i> (O.P.-Cambridge, 1872) | 1 | LC | AE |
| <i>Zelotes tuckeri</i> Roewer, 1951 | 1 | LC | AE |
| Family Hahniidae Bertkau, 1878 | | | |
| <i>Hahnia tabulicola</i> Simon, 1898 | 1 | LC | AE |
| Family Hersiliidae Thorell, 1869 | | | |
| <i>Hersilia sagitta</i> Foord & Dippenaar-Schoeman, 2006 | 1 | LC | AE |
| <i>Hersilia sericea</i> Pocock, 1899 | 2 | LC | AE |
| <i>Hersilia setifrons</i> Lawrence, 1928 | 2 | LC | STHE |
| <i>Tyrotama soutpansbergensis</i> Foord & Dippenaar-Schoeman, 2005 * (Fig. 11) | 5 | VU | SAE |
| Family Idiopidae Simon, 1889 | | | |
| <i>Ctenolophus fenoulheti</i> Hewitt, 1913 | 3 | LC | SAE |
| <i>Galeosoma vandami</i> Hewitt, 1913 | 5 | LC | SAE |
| <i>Idiops castaneus</i> Hewitt, 1913 | 4 | LC | SAE |
| <i>Segregara paucispinulosus</i> (Hewitt, 1915) | 5 | LC | SAE |
| Family Linyphiidae Blackwall, 1859 | | | |
| <i>Agyneta habra</i> (Locket, 1968) | 1 | LC | AE |
| <i>Agyneta natalensis</i> (Jocqué, 1984) | 3 | LC | SAE |
| <i>Agyneta prosectoides</i> (Locket & Russell-Smith, 1980) | 1 | LC | AE |
| <i>Mecynidis dentipalpis</i> Simon, 1894 | 2 | LC | STHE |
| <i>Metaleptyphantes perexiguus</i> (Simon & Fage, 1922) | 1 | LC | AE |

| Family / Species | END | CS | DIS |
|--|-----|----|------|
| <i>Microlinyphia sterilis</i> (Pavesi, 1883) | 1 | LC | AE |
| <i>Neriere natalensis</i> Van Helsdingen, 1969 | 3 | LC | SAE |
| Family Liocranidae Simon, 1897 | | | |
| <i>Rhaeboctesis exilis</i> Tucker, 1920 | 3 | LC | SAE |
| <i>Rhaeboctesis trinotatus</i> Tucker, 1920 | 2 | LC | STHE |
| Family Lycosidae Sundevall, 1833 | | | |
| <i>Allocosa exserta</i> Roewer, 1959 | 2 | LC | STHE |
| <i>Allocosa lawrencei</i> (Roewer, 1951) | 2 | LC | STHE |
| <i>Allocosa testacea</i> Roewer, 1959 | 3 | DD | SAE |
| <i>Evippomma squamulatum</i> (Simon, 1898) (Fig. 12) | 2 | LC | STHE |
| <i>Foveosa foveolata</i> (Purcell, 1903) | 1 | LC | AE |
| <i>Hippasa elienae</i> Alderweireldt & Jocqué, 2005 | 1 | LC | AE |
| <i>Hippasa funerea</i> Lessert, 1925 | 2 | LC | STHE |
| <i>Hippasosa guttata</i> (Karsch, 1878) | 1 | LC | AE |
| <i>Hogna spenceri</i> (Pocock, 1898) | 1 | LC | AE |
| <i>Minicosa neptuna</i> Alderweireldt & Jocqué, 2006 | 3 | LC | STHE |
| <i>Pardosa crassipalpis</i> Purcell, 1903 | 2 | LC | STHE |
| <i>Pardosa leipoldti</i> Purcell, 1903 | 2 | LC | STHE |
| <i>Pardosa umtalica</i> Purcell, 1903 | 1 | LC | AE |
| <i>Proevippa albiventris</i> (Simon, 1898) | 2 | LC | STHE |
| <i>Proevippa fascicularis</i> (Purcell, 1903) | 2 | LC | STHE |
| <i>Proevippa wanlessi</i> (Russell-Smith, 1981) | 3 | LC | SAE |
| <i>Trabea heterocolata</i> Strand, 1913 | 1 | LC | AE |
| <i>Trabea purcelli</i> Roewer, 1951 | 1 | LC | AE |
| <i>Zenonina albocaudata</i> Lawrence, 1952 | 3 | LC | SAE |
| Lycosidae sp. 1 (undetermined) | – | NE | – |
| Family Macrobnidae Bonnet, 1957 | | | |
| <i>Chresiona invalida</i> (Simon, 1898) | 3 | LC | SAE |
| <i>Pseudauximus annulatus</i> Purcell, 1908 | 4 | DD | SAE |
| New genus (new species) | – | NE | – |
| Family Migidae Simon, 1889 | | | |
| <i>Moggridgea pyimi</i> Hewitt, 1914 | 2 | LC | STHE |
| <i>Poecilomigas</i> sp. 1 (new) | – | NE | – |
| Family Mimetidae Simon, 1881 | | | |
| <i>Anansi natalensis</i> (Lawrence, 1938) | 3 | LC | SAE |
| <i>Ero lawrencei</i> Unzicker, 1966 | 2 | LC | STHE |
| <i>Mimetus cornutus</i> Lawrence, 1947 | 2 | LC | STHE |
| Family Nesticidae Simon, 1894 | | | |
| <i>Nesticella benoiti</i> (Hubert, 1970) | 2 | LC | STHE |
| Family Oecobiidae Blackwall, 1862 | | | |
| <i>Oecobius navus</i> Blackwall, 1859 | 0 | LC | C |
| <i>Uroecobius ecribellatus</i> Kullmann & Zimmermann, 1976 | 3 | LC | SAE |
| Family Oonopidae Simon, 1890 | | | |
| <i>Gamasomorpha australis</i> Hewitt, 1915 | 3 | LC | SAE |
| <i>Gamasomorpha humicola</i> Lawrence, 1947 | 3 | LC | SAE |
| <i>Opopaea speciosa</i> (Lawrence, 1952) | 1 | LC | AE |
| <i>Orchestina fannesi</i> Henrad & Jocqué 2012 | 2 | LC | STHE |
| Family Orsolobidae Cooke, 1965 | | | |
| <i>Afrilobus</i> sp. 1 (new) | – | NE | – |
| <i>Azanielobus lawrencei</i> Griswold & Platnick, 1987 | 2 | LC | STHE |
| Family Oxyopidae Thorell, 1869 | | | |
| <i>Hamataliwa fronticornis</i> (Lessert, 1927) | 1 | LC | AE |
| <i>Hamataliwa kulczynskii</i> (Lessert, 1915) | 1 | LC | AE |
| <i>Hamataliwa rostrifrons</i> (Lawrence, 1928) | 2 | LC | STHE |

| Family / Species | END | CS | DIS |
|---|-----|----|------|
| <i>Hamataliwa rufocaligata</i> Simon, 1898 | 1 | LC | AE |
| <i>Hamataliwa strandi</i> (Lessert, 1923) | 2 | LC | STHE |
| <i>Oxyopes angulitarsus</i> Lessert, 1915 | 1 | LC | AE |
| <i>Oxyopes bedoti</i> Lessert, 1915 | 1 | LC | AE |
| <i>Oxyopes bonneti</i> Lessert, 1933 | 2 | LC | STHE |
| <i>Oxyopes bothai</i> Lessert, 1915 (Fig. 12) | 1 | LC | AE |
| <i>Oxyopes dumonti</i> (Vinson, 1863) | 1 | LC | AE |
| <i>Oxyopes falconeri</i> Lessert, 1915 | 1 | LC | AE |
| <i>Oxyopes flavipalpis</i> (Lucas, 1858) | 1 | LC | AE |
| <i>Oxyopes hoggi</i> Lessert, 1915 | 1 | LC | AE |
| <i>Oxyopes jacksoni</i> Lessert, 1915 | 1 | LC | AE |
| <i>Oxyopes longispinosus</i> Lawrence, 1938 | 3 | LC | SAE |
| <i>Oxyopes pallidecoloratus</i> Strand, 1906 | 1 | LC | AE |
| <i>Oxyopes russoi</i> Caporiacco, 1940 | 1 | LC | AE |
| <i>Oxyopes schenkeli</i> Lessert, 1917 | 1 | LC | AE |
| <i>Oxyopes singularis</i> Lessert, 1927 | 1 | LC | AE |
| <i>Peucectia crucifera</i> Lawrence, 1927 | 2 | LC | STHE |
| <i>Peucectia viridis</i> (Blackwall, 1858) | 1 | LC | AE |
| Family Palpimanidae Thorell, 1870 | | | |
| <i>Diaphorocellus biplagiatus</i> Simon, 1893 | 2 | LC | STHE |
| <i>Palpimanus armatus</i> Pocock, 1898 | 2 | LC | STHE |
| <i>Palpimanus potteri</i> Lawrence, 1937 | 3 | LC | SAE |
| <i>Palpimanus pseudarmatus</i> Lawrence, 1952 | 3 | LC | SAE |
| <i>Palpimanus transvaalicus</i> Simon, 1893 | 3 | LC | SAE |
| Family Penestomidae Simon, 1903 | | | |
| <i>Penestomus</i> sp. 1 (new) | – | NE | – |
| Family Philodromidae Thorell, 1869 | | | |
| <i>Hirriusa arenacea</i> (Lawrence, 1927) | 2 | LC | STHE |
| <i>Hirriusa bidentata</i> (Lawrence, 1927) | 2 | LC | STHE |
| <i>Hirriusa variegata</i> (Simon, 1895) | 3 | LC | SAE |
| <i>Philodromus brachycephalus</i> Lawrence, 1952 | 1 | LC | AE |
| <i>Philodromus browningi</i> Lawrence, 1952 | 2 | LC | STHE |
| <i>Philodromus grosi</i> Lessert, 1943 | 1 | LC | AE |
| <i>Philodromus guineensis</i> Millot, 1941 | 1 | LC | AE |
| <i>Philodromus</i> sp. 5 (undetermined) | – | NE | – |
| <i>Suemus punctatus</i> Lawrence, 1938 | 2 | LC | STHE |
| <i>Thanatus dorsilineatus</i> Jézéquel, 1964 | 1 | LC | AE |
| <i>Thanatus vulgaris</i> Simon, 1870 | 0 | LC | C |
| <i>Tibellus australis</i> (Simon, 1910) | 2 | LC | STHE |
| <i>Tibellus bruneitarsis</i> Lawrence, 1952 | 2 | LC | STHE |
| <i>Tibellus minor</i> Lessert, 1919 | 1 | LC | AE |
| <i>Tibellus sunetae</i> Van den Berg & Dippenaar-Schoeman, 1994 | 2 | LC | STHE |
| New genus (new species) | – | NE | – |
| Family Pholcidae C. L. Koch, 1850 | | | |
| <i>Leptopholcus gracilis</i> Berland, 1920 | 1 | LC | AE |
| <i>Quamtana bonamanzi</i> Huber, 2003 | 3 | LC | SAE |
| <i>Quamtana entabeni</i> Huber, 2003 * (Fig. 27) | 5 | RA | SAE |
| <i>Quamtana hectori</i> Huber, 2003 | 3 | LC | SAE |
| <i>Quamtana lajuma</i> Huber, 2003 * | 5 | DD | SAE |
| <i>Smeringopus hanglip</i> Huber, 2012* | 5 | RA | SAE |
| <i>Smeringopus natalensis</i> Lawrence, 1947 | 2 | LC | STHE |
| Family Phyxelididae Lehtinen, 1967 | | | |
| <i>Phyxelida makapanensis</i> Simon, 1894 | 3 | LC | SAE |
| <i>Vidole sothoana</i> Griswold, 1990 | 2 | LC | STHE |

| Family / Species | END | CS | DIS |
|--|-----|----|------|
| <i>Xevioso kulufa</i> Griswold, 1990 * | 3 | LC | SAE |
| Family Pisauridae Simon, 1890 | | | |
| <i>Afropisaura rothiformis</i> (Strand, 1908) | 1 | LC | AE |
| <i>Charminus ambiguus</i> (Lessert, 1925) | 1 | LC | AE |
| <i>Chiasmopes lineatus</i> (Pocock, 1898) | 1 | LC | AE |
| <i>Cispius problematicus</i> Blandin, 1978 | 1 | LC | AE |
| <i>Euprostenops bayaonianus</i> Brito Capello 1867 | 1 | LC | AE |
| <i>Euprostenopsis pulchella</i> (Pocock, 1902) | 2 | LC | STHE |
| <i>Euprostenopsis vuattouxi</i> Blandin, 1977 (Fig. 28) | 1 | LC | AE |
| <i>Maypacijs roeweri</i> Blandin, 1975 | 1 | LC | AE |
| <i>Nilus margaritatus</i> (Pocock, 1898) | 1 | LC | AE |
| <i>Nilus massajae</i> (Pavesi, 1883) (Fig. 13) | 1 | LC | AE |
| <i>Rothus aethiopicus</i> (Pavesi, 1883) | 1 | LC | AE |
| Family Prodidomidae Simon, 1884 | | | |
| <i>Austrodomus scaber</i> (Purcell, 1904) | 2 | LC | STHE |
| <i>Eleleis limpopo</i> Rodrigues & Rheims, 2020 | 1 | LC | AE |
| <i>Prodidomus capensis</i> Purcell, 1904 | 3 | LC | SAE |
| <i>Theuma elucubata</i> Tucker, 1923 | 3 | LC | SAE |
| <i>Theuma fusca</i> Purcell, 1907 | 2 | LC | STHE |
| <i>Theuma purcelli</i> Tucker, 1923 | 3 | LC | SAE |
| <i>Theuma maculata</i> Purcell, 1907 | 2 | LC | STHE |
| Family Salticidae Blackwall, 1841 | | | |
| <i>Afraflacilla altera</i> (Wesołowska, 2000) | 2 | LC | STHE |
| <i>Afraflacilla elegans</i> (Wesołowska & Cumming, 2008) | 2 | LC | STHE |
| <i>Asemonea clara</i> Wesołowska & Haddad, 2013 | 3 | LC | SAE |
| <i>Baryphas ahenus</i> Simon, 1902 | 1 | LC | AE |
| <i>Belippo meridionalis</i> Wesołowska & Haddad, 2013 | 3 | LC | SAE |
| <i>Bianor albobimaculatus</i> (Lucas, 1846) | 0 | LC | C |
| <i>Cyrba lineata</i> Wanless, 1984 | 2 | LC | STHE |
| <i>Cyrba nigrimana</i> Simon, 1900 | 3 | LC | SAE |
| <i>Dendryphantes hararensis</i> Wesołowska & Cumming, 2008 | 2 | LC | STHE |
| <i>Evarcha flagellaris</i> Haddad & Wesołowska, 2011 | 1 | LC | AE |
| <i>Evarcha ignea</i> Wesołowska & Cumming, 2008 | 1 | LC | AE |
| <i>Evarcha prosimilis</i> Wesołowska & Cumming, 2008 | 1 | LC | AE |
| <i>Evarcha wernerii</i> (Simon, 1906) | 1 | LC | AE |
| <i>Festucula leroyae</i> Azarkina & Foord, 2014 | 2 | LC | STHE |
| <i>Goleba puella</i> (Simon, 1885) | 1 | LC | AE |
| <i>Habrocestum auricomum</i> Haddad & Wesołowska, 2013 | 5 | DD | SAE |
| <i>Habrocestum superbum</i> Wesołowska, 2000 | 2 | LC | STHE |
| <i>Helafricanus debilis</i> (Simon, 1901) | 1 | LC | AE |
| <i>Helafricanus pistaciae</i> (Wesołowska, 2003) | 2 | LC | STHE |
| <i>Helafricanus trepidus</i> Simon, 1910 | 2 | LC | STHE |
| <i>Holcolaetis zuluensis</i> Lawrence, 1937 | 1 | LC | AE |
| <i>Hyllus argyrotoxis</i> Simon, 1902 (Fig. 18) | 1 | LC | AE |
| <i>Hyllus brevitarsis</i> Simon, 1902 (Fig. 17) | 1 | LC | AE |
| <i>Hyllus dotatus</i> (Peckham & Peckham, 1903) | 1 | LC | AE |
| <i>Hyllus treleaveni</i> Peckham & Peckham, 1903 | 1 | LC | AE |
| <i>Iranattus principalis</i> Wesołowska, 2000 | 1 | LC | AE |
| <i>Icius insolidus</i> (Wesołowska, 1999) | 2 | LC | STHE |
| <i>Langelurillus minutus</i> Wesołowska & Cumming, 2011 | 2 | LC | STHE |
| <i>Langelurillus</i> sp. 1 (new) | – | NE | – |
| <i>Langona bethae</i> Wesołowska & Cumming, 2011 | 2 | LC | STHE |
| <i>Langona bisecta</i> Lawrence, 1927 | 2 | LC | STHE |
| <i>Langona tortuosa</i> Wesołowska, 2011 | 2 | LC | STHE |

| Family / Species | END | CS | DIS |
|--|-----|----|------|
| <i>Massagris</i> sp. 1 (undetermined) | – | NE | – |
| <i>Menemerus minshullae</i> Wesolowska, 1999 | 1 | LC | AE |
| <i>Menemerus natalis</i> Wesolowska, 1999 | 3 | LC | SAE |
| <i>Menemerus zimbabwensis</i> Wesolowska, 1999 | 2 | LC | STHE |
| <i>Mexcala quadrimaculata</i> (Lawrence, 1942) | 2 | LC | STHE |
| <i>Mogrus mathisi</i> (Berland & Millot, 1941) | 0 | LC | C |
| <i>Myrmarachne ichneumon</i> (Simon, 1886) | 1 | LC | AE |
| <i>Myrmarachne inflatipalpis</i> Wanless, 1978 | 1 | LC | AE |
| <i>Myrmarachne lulengana</i> Roewer, 1965 | 1 | LC | AE |
| <i>Myrmarachne marshalli</i> Peckham & Peckham, 1903 | 1 | LC | AE |
| <i>Natta horizontalis</i> Karsch, 1879 | 1 | LC | AE |
| <i>Nigorella hirsuta</i> Wesolowska, 2009 | 2 | LC | STHE |
| <i>Pachyballus transversus</i> Simon, 1900 | 1 | LC | AE |
| <i>Parajotus obscurifemoratus</i> Peckham & Peckham, 1903 | 3 | LC | SAE |
| <i>Parajotus refulgens</i> Wesolowska, 2000 | 1 | LC | AE |
| <i>Pellenes bulawayoensis</i> Wesolowska, 2000 | 2 | LC | STHE |
| <i>Pellenes modicus</i> Wesolowska & Russell-Smith, 2000 | 1 | LC | AE |
| <i>Pellenes pulcher</i> Logunov, 1995 | 0 | LC | C |
| <i>Pellenes tharinae</i> Wesolowska, 2006 | 2 | LC | STHE |
| <i>Phintella aequipes</i> (Peckham & Peckham, 1903) | 1 | LC | AE |
| <i>Phintella australis</i> (Simon, 1902) | 3 | LC | SAE |
| <i>Phintella lajuma</i> Haddad & Wesolowska, 2013 * (Fig. 14) | 3 | LC | SAE |
| <i>Phlegra simplex</i> Wesolowska & Russell-Smith, 2000 | 1 | LC | AE |
| <i>Phlegra varia</i> Wesolowska & Russell-Smith, 2000 | 1 | LC | AE |
| <i>Pignus simoni</i> (Peckham & Peckham, 1903) | 2 | LC | STHE |
| <i>Portia schultzi</i> Karsch, 1878 | 1 | LC | AE |
| <i>Pseudicius</i> sp. 1 (undetermined) | – | NE | – |
| <i>Rhene machadoi</i> Berland & Millot, 1941 | 1 | LC | AE |
| <i>Rumburak tuberatus</i> Wesolowska, Azarkina & Russell-Smith, 2014 * (Fig. 15) | 5 | DD | SAE |
| <i>Sonoita lightfooti</i> Peckham & Peckham, 1903 | 1 | LC | AE |
| <i>Stenaelurillus guttiger</i> (Simon, 1901) | 2 | LC | STHE |
| <i>Stenaelurillus termitophagus</i> (Wesolowska & Cumming, 1999) | 2 | LC | STHE |
| <i>Tanzania parvulus</i> Wesolowska, Azarkina & Russell-Smith, 2014 | 3 | LC | SAE |
| <i>Thyene bilineata</i> Lawrence, 1927 | 2 | LC | STHE |
| <i>Thyene bucculenta</i> (Gerstäcker, 1873) | 1 | LC | AE |
| <i>Thyene coccineovittata</i> (Simon, 1886) | 1 | LC | AE |
| <i>Thyene dakarensis</i> (Berland & Millot, 1941) | 1 | LC | AE |
| <i>Thyene inflata</i> (Gerstäcker, 1873) | 1 | LC | AE |
| <i>Thyene leighi</i> Peckham & Peckham, 1903 | 1 | LC | AE |
| <i>Thyene muticus</i> (Simon, 1902) | 1 | LC | AE |
| <i>Thyene natalii</i> Peckham & Peckham, 1903 | 1 | LC | AE |
| <i>Thyene ogdeni</i> Peckham & Peckham, 1903 | 1 | LC | AE |
| <i>Thyene semiargentea</i> (Simon, 1884) | 1 | LC | AE |
| <i>Thyene thyenioides</i> (Lessert, 1925) | 1 | LC | AE |
| <i>Thyenula aurantiaca</i> (Simon, 1902) | 2 | LC | STHE |
| <i>Thyenula oranjensis</i> Wesolowska, 2001 | 3 | LC | SAE |
| <i>Thyenula sempiterna</i> Wesolowska, 2000 | 2 | LC | STHE |
| <i>Thyenula wesolowskae</i> Zhang & Maddison, 2012 | 4 | LC | SAE |
| <i>Tomomingi szutsi</i> Wesolowska & Haddad, 2013 * | 4 | DD | SAE |
| <i>Trapezocephalus lesserti</i> (Wesolowska, 1986) | 1 | LC | AE |
| <i>Trapezocephalus orchestra</i> (Simon, 1885) | 1 | LC | AE |
| <i>Tusitala barbata</i> Peckham & Peckham, 1902 | 1 | LC | AE |
| <i>Tusitala hirsuta</i> Peckham & Peckham, 1902 | 1 | LC | AE |

| Family / Species | END | CS | DIS |
|--|-----|----|------|
| Family Scytodidae Blackwall, 1864 | | | |
| <i>Scytodes clavata</i> Benoit, 1965 | 1 | LC | AE |
| <i>Scytodes maritima</i> Lawrence, 1938 | 3 | LC | SAE |
| <i>Scytodes quinqu</i> Lawrence, 1927 | 2 | LC | STHE |
| <i>Scytodes thoracica</i> (Latreille, 1802) | 0 | LC | C |
| Family Segestriidae Simon, 1893 | | | |
| <i>Ariadna bilineata</i> Purcell, 1904 (Fig. 29) | 3 | LC | SAE |
| Family Selenopidae Simon, 1897 | | | |
| <i>Anyphops barbertonensis</i> (Lawrence, 1940) | 1 | LC | AE |
| <i>Anyphops leleupi</i> Benoit, 1972 | 4 | LC | SAE |
| <i>Anyphops ngome</i> Corronca, 2005 | 3 | LC | SAE |
| <i>Anyphops reservatus</i> (Lawrence, 1937) | 3 | LC | SAE |
| <i>Anyphops spenceri</i> (Pocock, 1896) | 3 | LC | SAE |
| <i>Selenops brachycephalus</i> Lawrence, 1940 | 2 | LC | STHE |
| <i>Selenops dilon</i> Corronca, 2002 | 4 | DD | SAE |
| <i>Selenops tenebrosus</i> Lawrence, 1940 | 2 | LC | STHE |
| <i>Selenops zuluanus</i> Lawrence, 1940 | 2 | LC | STHE |
| Family Sicariidae Keyserling, 1880 | | | |
| <i>Hexophthalma hahni</i> (Karsch, 1878) | 2 | LC | STHE |
| <i>Loxosceles haddadi</i> Lotz, 2017 * | 6 | DD | SAE |
| <i>Loxosceles simillima</i> Lawrence, 1927 | 1 | LC | AE |
| Family Sparassidae Bertkau, 1872 | | | |
| <i>Eusparassus borakalalo</i> Moradmand, 2013 | 4 | LC | SAE |
| <i>Olios correvoni nigrifrons</i> Lawrence, 1928 | 1 | LC | AE |
| <i>Olios sjostedti</i> Lessert, 1921 | 1 | LC | AE |
| <i>Olios</i> sp. 3 (undetermined) | – | NE | – |
| <i>Palystes leroyorum</i> Croeser, 1996 | 3 | LC | SAE |
| <i>Palystes superciliosus</i> L. Koch, 1875 | 2 | LC | STHE |
| <i>Pseudomicrommata longipes</i> (Bösenberg & Lenz, 1895) | 1 | LC | AE |
| <i>Pseudomicrommata vittigera</i> (Simon, 1897) | 2 | LC | STHE |
| Family Stasimopidae Bond, Opatova & Hedin, 2020 | | | |
| <i>Stasimopus</i> sp. 1 (new) | – | NE | – |
| Family Tetragnathidae Menge, 186 | | | |
| <i>Diphya foordi</i> Omelko, Marusik & Lyle, 2020 * | 3 | LC | SAE |
| <i>Diphya wesolowskiae</i> Omelko, Marusik & Lyle, 2020 * | 3 | RA | SAE |
| <i>Leucauge argyrescens</i> Benoit, 1978 | 1 | LC | AE |
| <i>Leucauge decorata</i> (Blackwall, 1864) | 0 | LC | C |
| <i>Leucauge festiva</i> (Blackwall, 1866) | 1 | LC | AE |
| <i>Leucauge levanderi</i> (Kulczynski, 1901) | 1 | LC | AE |
| <i>Leucauge medjensis</i> Lessert, 1930 | 1 | LC | AE |
| <i>Leucauge thomeensis</i> Kraus, 1960 | 1 | LC | AE |
| <i>Meta meruensis</i> Tullgren, 1910 | 1 | LC | AE |
| <i>Pachygnatha leleupi</i> Lawrence, 1952 | 1 | LC | AE |
| <i>Tetragnatha bogotensis</i> Keyserling, 1865 (Fig. 30) | 0 | LC | C |
| <i>Tetragnatha keyserlingi</i> Simon, 1890 | 0 | LC | C |
| <i>Tetragnatha nitens</i> (Audouin, 1826) | 0 | LC | C |
| <i>Tetragnatha subsquamata</i> Okuma, 1985 | 1 | LC | AE |
| Family Theraphosidae Thorell, 1869 | | | |
| <i>Augacephalus junodi</i> (Simon, 1904) | 2 | LC | STHE |
| <i>Ceratogyrus brachycephalus</i> Hewitt, 1919 | 4 | DD | SAE |
| <i>Ceratogyrus darlingi</i> Pocock, 1897 | 2 | LC | STHE |
| <i>Harpactirella overdijki</i> Gallon, 2010 | 3 | DD | SAE |
| <i>Idiothele nigrofulva</i> (Pocock, 1898) | 2 | LC | STHE |
| <i>Pterinochilus lugardi</i> Pocock, 1900 | 1 | LC | AE |

| Family / Species | END | CS | DIS |
|---|-----|----|------|
| Family Theridiidae Sundevall, 1833 | | | |
| <i>Anelosimus nelsoni</i> Agnarsson, 2006 | 3 | LC | SAE |
| <i>Argyrodes convivans</i> Lawrence, 1937 | 2 | LC | STHE |
| <i>Argyrodes zonatus</i> (Walckenaer, 1841) (Fig. 31) | 1 | LC | AE |
| <i>Chorizopella tragardhi</i> Lawrence, 1947 | 3 | LC | SAE |
| <i>Chryso</i> sp. 1 (undetermined) | – | NE | – |
| <i>Coleosoma cf blandum</i> O.P.-Cambridge, 1882 | – | NE | – |
| <i>Coscinida tibialis</i> Simon, 1895 | 0 | LC | C |
| <i>Dipoena</i> sp. 1 (undetermined) | – | NE | – |
| <i>Episinus bilineatus</i> Simon, 1894 | 2 | LC | STHE |
| <i>Episinus marignaci</i> (Lessert, 1933) | 2 | LC | STHE |
| <i>Euryopsis episinoides</i> (Walckenaer, 1847) | 0 | LC | C |
| <i>Euryopsis funebris</i> (Hentz, 1850) | 0 | LC | C |
| <i>Latrodectus geometricus</i> C.L. Koch, 1841 | 0 | LC | C |
| <i>Latrodectus renivulvatus</i> Dahl, 1902 | 1 | LC | AE |
| <i>Phoroncidia eburnea</i> (Simon, 1895) | 3 | LC | SAE |
| <i>Phycosoma martinae</i> (Roberts, 1983) | 0 | LC | C |
| <i>Platnickina adamsoni</i> (Berland, 1934) | 0 | LC | C |
| <i>Rhomphaea nasica</i> (Simon, 1873) | 0 | LC | C |
| <i>Rubroridion</i> sp. 1 (undetermined) | – | NE | – |
| <i>Steatoda capensis</i> Hann, 1990 | 0 | LC | C |
| <i>Steatoda grossa</i> (C.L. Koch, 1838) | 1 | LC | C |
| <i>Theridion pictum</i> (Walckenaer, 1802) | 0 | LC | C |
| <i>Theridion purcelli</i> O.P.-Cambridge, 1904 | 3 | LC | SAE |
| <i>Theridion</i> sp. 1 (undetermined) | – | NE | – |
| <i>Theridion</i> sp. 2 (undetermined) | – | NE | – |
| <i>Thymoites</i> sp. 1 (undetermined) | – | NE | – |
| <i>Thwaitesia</i> sp. 1 (undetermined) | – | NE | – |
| <i>Tidarren scenicum</i> (Thorell, 1899) | 1 | LC | AE |
| Family Thomisidae Sundevall, 1833 | | | |
| <i>Ansiae tuckeri</i> (Lessert, 1919) | 1 | LC | AE |
| <i>Borboropactus silvicola</i> (Lawrence, 1938) | 3 | LC | SAE |
| <i>Camaricus nigrotesselatus</i> Simon, 1895 | 1 | LC | AE |
| <i>Diaea puncta</i> Karsch, 1884 | 1 | LC | AE |
| <i>Geraesta congoensis</i> (Lessert, 1943) | 1 | LC | AE |
| <i>Heriaeus crassispinus</i> Lawrence, 1942 (Fig. 16) | 1 | LC | AE |
| <i>Heriaeus peterwebbi</i> Van Niekerk & Dippenaar-Schoeman, 2013 | 2 | LC | STHE |
| <i>Misumenops rubrodecoratus</i> Millot, 1942 | 1 | LC | AE |
| <i>Monaeses austrinus</i> Simon, 1910 | 1 | LC | AE |
| <i>Mystaria flavogutatta</i> (Lawrence, 1952) | 1 | LC | AE |
| <i>Mystaria lata</i> (Lawrence, 1927) | 2 | LC | STHE |
| <i>Mystaria rufolimbata</i> Simon, 1895 | 1 | LC | AE |
| <i>Mystaria savannensis</i> Lewis & Dippenaar-Schoeman, 2014 | 1 | LC | AE |
| <i>Oxytate argenteooculata</i> (Simon, 1886) | 1 | LC | AE |
| <i>Oxytate concolor</i> (Caporiacco, 1947) | 1 | LC | AE |
| <i>Oxytate ribes</i> (Jézéquel, 1964) | 1 | LC | AE |
| <i>Ozyptilla caenosa</i> Jézéquel, 1966 | 1 | LC | AE |
| <i>Pactactes compactus</i> Lawrence, 1947 | 3 | LC | SAE |
| <i>Parabomis martini</i> Lessert, 1919 | 1 | LC | AE |
| <i>Pherecydes ionae</i> Dippenaar-Schoeman, 1980 | 1 | LC | AE |
| <i>Pherecydes lucinae</i> Dippenaar-Schoeman, 1980 | 3 | LC | SAE |
| <i>Pherecydes nicolaasi</i> Dippenaar-Schoeman, 1980 | 3 | LC | SAE |
| <i>Pherecydes zebra</i> Lawrence, 1927 | 1 | LC | AE |
| <i>Runcinia aethiops</i> (Simon, 1901) | 1 | LC | AE |

| Family / Species | END | CS | DIS |
|--|-----|----|------|
| <i>Runcinia flavida</i> (Simon, 1881) | 0 | LC | C |
| <i>Simorcus cotti</i> Lessert, 1936 | 1 | LC | AE |
| <i>Sylligma ndumi</i> Honiball & Dippenaar-Schoeman 2011 | 2 | LC | STHE |
| <i>Synema decens</i> (Karsch, 1878) | 2 | LC | STHE |
| <i>Synema diana</i> (Audouin, 1826) | 1 | LC | AE |
| <i>Synema imitatrix</i> (Pavesi, 1883) | 1 | LC | AE |
| <i>Synema langheldi</i> Dahl, 1907 | 1 | LC | AE |
| <i>Synema nigrotibiale</i> Lessert, 1919 | 1 | LC | AE |
| <i>Synema vallotoni</i> Lessert, 1923 | 2 | LC | STHE |
| <i>Thomisops bullatus</i> Simon, 1895 | 2 | LC | STHE |
| <i>Thomisops pupa</i> Karsch, 1879 | 1 | LC | AE |
| <i>Thomisus australis</i> Comellini, 1957 | 1 | LC | AE |
| <i>Thomisus citrinellus</i> Simon, 1875 | 0 | LC | C |
| <i>Thomisus congoensis</i> Comellini, 1957 | 1 | LC | AE |
| <i>Thomisus dalmasi</i> Lessert, 1919 | 1 | LC | AE |
| <i>Thomisus daradioides</i> Simon, 1890 | 0 | LC | C |
| <i>Thomisus granulatus</i> Karsch, 1880 | 1 | LC | AE |
| <i>Thomisus kalaharinus</i> Lawrence, 1936 | 1 | LC | AE |
| <i>Thomisus scrupeus</i> (Simon, 1886) | 1 | LC | AE |
| <i>Thomisus spiculosus</i> Pocock, 1901 | 1 | LC | AE |
| <i>Tmarus africanus</i> Lessert, 1919 | 1 | LC | AE |
| <i>Tmarus cameliformis</i> Millot, 1942 | 1 | LC | AE |
| <i>Tmarus comellinii</i> Garcia-Neto, 1989 | 1 | LC | AE |
| <i>Tmarus foliatus</i> Lessert, 1928 | 1 | LC | AE |
| <i>Tmarus planetarius</i> Simon, 1903 | 1 | LC | AE |
| <i>Xysticus natalensis</i> Lawrence, 1938 | 2 | LC | STHE |
| <i>Synema decens</i> (Karsch, 1878) | 2 | LC | STHE |
| <i>Synema diana</i> (Audouin, 1826) | 1 | LC | AE |
| <i>Synema imitatrix</i> (Pavesi, 1883) | 1 | LC | AE |
| <i>Synema langheldi</i> Dahl, 1907 | 1 | LC | AE |
| <i>Synema nigrotibiale</i> Lessert, 1919 | 1 | LC | AE |
| <i>Synema vallotoni</i> Lessert, 1923 | 2 | LC | STHE |
| <i>Thomisops bullatus</i> Simon, 1895 | 2 | LC | STHE |
| <i>Thomisops pupa</i> Karsch, 1879 | 1 | LC | AE |
| <i>Thomisus australis</i> Comellini, 1957 | 1 | LC | AE |
| <i>Thomisus citrinellus</i> Simon, 1875 | 0 | LC | C |
| <i>Thomisus congoensis</i> Comellini, 1957 | 1 | LC | AE |
| <i>Thomisus dalmasi</i> Lessert, 1919 | 1 | LC | AE |
| <i>Thomisus daradioides</i> Simon, 1890 | 0 | LC | C |
| <i>Thomisus granulatus</i> Karsch, 1880 | 1 | LC | AE |
| <i>Thomisus kalaharinus</i> Lawrence, 1936 | 1 | LC | AE |
| <i>Thomisus scrupeus</i> (Simon, 1886) | 1 | LC | AE |
| <i>Thomisus spiculosus</i> Pocock, 1901 | 1 | LC | AE |
| <i>Tmarus africanus</i> Lessert, 1919 | 1 | LC | AE |
| <i>Tmarus cameliformis</i> Millot, 1942 | 1 | LC | AE |
| <i>Tmarus comellinii</i> Garcia-Neto, 1989 | 1 | LC | AE |
| <i>Tmarus foliatus</i> Lessert, 1928 | 1 | LC | AE |
| <i>Tmarus planetarius</i> Simon, 1903 | 1 | LC | AE |
| <i>Xysticus natalensis</i> Lawrence, 1938 | 2 | LC | STHE |
| <i>Xysticus urbensis</i> Lawrence, 1952 | 2 | LC | STHE |
| <i>Tmarus africanus</i> Lessert, 1919 | 1 | LC | AE |
| <i>Tmarus cameliformis</i> Millot, 1942 | 1 | LC | AE |
| <i>Tmarus comellinii</i> Garcia-Neto, 1989 | 1 | LC | AE |
| <i>Tmarus foliatus</i> Lessert, 1928 | 1 | LC | AE |
| <i>Tmarus planetarius</i> Simon, 1903 | 1 | LC | AE |

| Family / Species | END | CS | DIS |
|--|-----|----|------|
| <i>Xysticus natalensis</i> Lawrence, 1938 | 2 | LC | STHE |
| <i>Xysticus urbensis</i> Lawrence, 1952 | 2 | LC | STHE |
| Family Trachelidae Simon, 1897 | | | |
| <i>Afroseto martini</i> (Simon, 1897) | 2 | LC | STHE |
| <i>Coronarachne unigena</i> Haddad & Lyle, 2024 * | 3 | LC | SAE |
| <i>Falcaranea maputensis</i> Haddad & Lyle, 2024 | 2 | LC | STHE |
| <i>Fuchiba aquilonia</i> Haddad & Lyle, 2008 * | 2 | LC | STHE |
| <i>Fuchibotulus kigelia</i> Haddad & Lyle, 2008 | 2 | LC | STHE |
| <i>Jocquestus incurvus</i> Lyle & Haddad, 2018 * | 4 | LC | SAE |
| <i>Orthobula radiata</i> Simon, 1897 | 1 | LC | AE |
| <i>Patelloseto secutor</i> Lyle & Haddad, 2010 | 2 | LC | STHE |
| <i>Thysanina serica</i> Simon, 1910 | 2 | LC | STHE |
| <i>Thysanina transversa</i> Lyle & Haddad, 2006 * | 3 | LC | SAE |
| <i>Trachelas scopulifer</i> Simon, 1896 | 3 | DD | SAE |
| <i>Trachelas</i> sp. 1 (new) | – | NE | – |
| <i>Trachelas</i> sp. 2 (new) | – | NE | – |
| <i>Trachelas</i> sp. 3 (new) | – | NE | – |
| Family Trochanteriidae Karsch, 1879 | | | |
| <i>Platyoides alpha</i> Lawrence, 1928 | 2 | LC | STHE |
| <i>Platyoides pusillus</i> Pocock, 1898 | 1 | LC | AE |
| <i>Platyoides walteri</i> (Karsch, 1886) | 1 | LC | AE |
| Family Uloboridae Thorell, 1869 | | | |
| <i>Hyptiotes akermani</i> Wiehle, 1964 | 3 | LC | SAE |
| <i>Miagrammopes brevicaudus</i> O.P.-Cambridge, 1882 (Fig. 32) | 2 | LC | STHE |
| <i>Miagrammopes constrictus</i> Purcell, 1904 | 3 | LC | SAE |
| <i>Uloborus plumipes</i> Lucas, 1846 | 0 | LC | C |
| <i>Zosis geniculata</i> (Olivier, 1789) | 1 | LC | AE |
| Family Zodariidae Thorell, 1881 | | | |
| <i>Australutica africana</i> Jocqué, 2008 * | 5 | RA | SAE |
| <i>Ballomma neethlingi</i> Jocqué & Henrard, 2015 * | 5 | DD | SAE |
| <i>Caesetius bevisi</i> (Hewitt, 1916) | 2 | LC | STHE |
| <i>Caesetius globicoxis</i> (Lawrence, 1942) | 3 | LC | SAE |
| <i>Caesetius inflatus</i> Jocqué, 1991 | 1 | LC | AE |
| <i>Capheris crassimana</i> (Simon, 1887) | 2 | LC | STHE |
| <i>Capheris decorata</i> Simon, 1904 | 1 | LC | AE |
| <i>Chariobas cylindraceus</i> Simon, 1893 | 1 | LC | AE |
| <i>Cydrela schoemanae</i> Jocqué, 1991 (Fig. 17) | 3 | LC | SAE |
| <i>Cydrela spinifrons</i> Hewitt, 1915 | 3 | LC | SAE |
| <i>Cydrela spinimana</i> Pocock, 1898 | 3 | LC | SAE |
| <i>Cydrela</i> sp. 4 (new) | – | NE | – |
| <i>Cyriocetea marken</i> Platnick & Jocqué, 1992 | 5 | DD | SAE |
| <i>Diores auricula</i> Tucker, 1920 | 2 | LC | STHE |
| <i>Diores lesserti</i> Lawrence, 1952 | 3 | LC | STHE |
| <i>Diores magicus</i> Jocqué & Dippenaar-Schoeman, 1992 | 2 | LC | STHE |
| <i>Diores recurvatus</i> Jocqué, 1990 | 2 | LC | STHE |
| <i>Diores triarmatus</i> Lessert, 1929 | 1 | LC | AE |
| <i>Heradida bicincta</i> Simon, 1910 | 2 | LC | STHE |
| <i>Mastidiores</i> sp. 1 (undetermined) | – | NE | – |
| <i>Microdiores</i> sp. 1 (undetermined) | – | NE | – |
| <i>Psammorygma aculeatum</i> (Karsch, 1878) | 3 | LC | SAE |
| <i>Ranops robinae</i> Jocqué & Henrard, 2020 | 3 | LC | SAE |
| <i>Systemoplacis fagei</i> (Lawrence, 1936) | 3 | LC | SAE |
| <i>Thaumastochilus</i> sp. 1 (immature) | – | NE | – |
| Family Zoropsidae Bertkau, 1882 | | | |
| <i>Griswoldia leleupi</i> (Griswold, 1991) | 5 | LC | SAE |

Conservation status

Most species (516 spp., 88.2%) have a wide distribution without known threats and are listed as Least Concern (Table 4). Sufficient data is still lacking for 17 spp. (2.9%), which are listed as Data Deficient. Forty-four species (7.5%) were not evaluated because they were either new or current taxonomic support was lacking (Table 6).

Species of special concern

The spider fauna of the SM has eight species listed as being of special concern (Table 4), which include the following: Rare (5 spp.), Critically Rare (1 sp.), Vulnerable (1 sp.) or Near Threatened (1 sp.) (Table 5). IUCN uses the term “rare” as a designation for species found in isolated geographical locations. Rare species are generally considered threatened because a small population size is less likely to recover from ecological disasters. All these species require further collection and monitoring to improve our knowledge of their distribution. This can only be achieved through a concerted collecting effort in under-sampled areas and developing taxonomic expertise dedicated to revising and describing the fauna (Dippenaar-Schoeman et al. 2023).

Conclusion

The last decade has seen exponential growth in the knowledge of spiders in South Africa, but several more species are to be discovered, and distribution patterns determined. The first checklist (Foord et al. 2002) was published more than two decades ago and listed 127 species from the SM, but the number has since increased to 585 species with the publication of this checklist. Owen (2010) has stressed the importance of continued long-term monitoring when assessing the diversity, particularly for invertebrates whose populations show major inter-seasonal and inter-annual fluctuations. The SM represents an old and climatically stable geographic feature in Limpopo Province, which provides refuge for 585 spider species. The species collected represent 25.4% of the total spider fauna of South Africa and 64.3% of the Limpopo Province fauna. Conservation biologists must prioritise their efforts, limited funds, manpower, and time, and this necessitates the identification of hotspots for conservation (Myers et al. 2000). The spider data emphasises the significance of the SM as a biodiversity hotspot with high spider endemism in the Limpopo Province. Eight species are of special concern that need to be monitored in the future. The broad range of ecological studies in the SM that have included spiders as indicator taxa not only elucidates the impacts of various anthropogenic factors on their faunistic composition but has also provided invaluable material to better understand the distribution patterns of the fauna. However, there is still a considerable taxonomic deficit for many groups, and resolving this shortfall is essential to better conserve the unique taxa occurring in the SM. Mapping patterns of endemism, rarity and threats across the landscape is the starting point for such a process, while Red List assessments provide the framework for evaluating these criteria at the species level, linking them to extinction risk and guiding conservation initiatives. This will require investment in capacity building through postgraduate student

development, sourcing targeted funding from the government and the private sector, attracting international researchers to work on the South African spider fauna, promoting the importance of natural history collections to society, and by improving financial support to ensure their long-term use and development.

Acknowledgements

This paper is dedicated to the memory of our late colleague and co-author, Professor Stefan Foord, whose incredible contribution to the success of SANSA as an ecologist, data analyst and taxonomist will be sorely missed in the years to come. The authors would like to thank the Agricultural Research Council (ARC); the South African National Biodiversity Institute (SANBI), Threatened Species Programme for funding the South African National Survey of Arachnida (SANSA); support of the National Research Foundation (NRF) and the Department of Science & Technology (DST) through the Centre of Excellence for Invasion Biology and the South African Research Chairs Initiative (SARChI) Chair on Biodiversity Value and Change in the Vhembe Biosphere Reserve; the staff of the Arachnology section of the ARC–National Collection of Arachnida for their assistance with processing and databasing the material collected; all the people from the University of Venda for their survey efforts, particularly Jerry Molepo, Evans Mauda and Ratshibvumo Tshikambu for field and lab support; Leon Lotz, Charles Haddad, Jeremy Miller and the late Peter Webb for their photographs; and land owners for making their properties available for surveys: Dave Dewsnap, Steven and Marianne Fick, Stefan Otto, Jabu and Birthe Linden and Lajuma Research Station.

Additional information

Conflict of interest

The authors have declared that no competing interests exist.

Ethical statement

No ethical statement was reported.

Funding

This research was supported by a grant from the University of Venda RPC committee (Grant no. P109) and funding through the NRF Chair in Biodiversity Value and Change.

Author contributions

ASD conceptualised, identified material, managed the database and wrote the first draft; CM collected and curated data and comments on drafts of the manuscript; CS was involved in specimen sampling and commented on drafts of the manuscript; NH assisted with the planning and layout of the transect and specimen sampling, prepared the map, and commented on the manuscript drafts; SF was the manager of all the surveys.

Author ORCIDs

Ansie S. Dippenaar-Schoeman  <https://orcid.org/0000-0003-1532-1379>

T. Caswell Munyai  <https://orcid.org/0000-0002-1562-2385>

Colin S. Schoeman  <https://orcid.org/0000-0001-8585-5857>

Norbert Hahn  <https://orcid.org/0000-0002-1186-7713>

Stefan H. Foord  <https://orcid.org/0000-0002-9195-2562>

Data availability

All data supporting this study's findings are available in the SANSA database.

References

- Bosselaers J, Jocqué R (2000) *Hortipes*, a huge genus of tiny Afrotropical spiders (Araneae, Liocranidae). *Bulletin of the American Museum of Natural History* 256(1): 1–108. [https://doi.org/10.1206/0003-0090\(2000\)256<0004:HAHGOT>2.0.CO;2](https://doi.org/10.1206/0003-0090(2000)256<0004:HAHGOT>2.0.CO;2)
- Dippenaar SM, Dippenaar-Schoeman AS, Modiba MA, Khoza TT (2008) A checklist of spiders (Arachnida, Araneae) of the Polokwane Nature Reserve, Limpopo Province, South Africa. *Koedoe* 50(1): 10–17. <https://doi.org/10.4102/koedoe.v50i1.128>
- Dippenaar-Schoeman AS, Genis NdL, Van Ark H, Viljoen JH (1978) The effect of Diel-drin cover spraying on some South African spiders and scorpions. *Phytophylactica* 10: 115–122.
- Dippenaar-Schoeman AS (2023) *Field Guide of the Spiders of South Africa*. Struik Nature, 400 pp.
- Dippenaar-Schoeman AS, Van den Berg AM, Van den Berg A (1999) Spiders in South African cotton fields: species diversity and abundance (Arachnida: Araneae). *African Plant Protection* 5: 93–103.
- Dippenaar-Schoeman AS, Van den Berg A, Prendini L (2009) Spiders and Scorpions (Arachnida; Araneae, Scorpiones) of the Nylsvley Nature Reserve, South Africa. *Koedoe* 51(1): a161. <https://doi.org/10.4102/koedoe.v51i1.161>
- Dippenaar-Schoeman AS, Foord SH, Haddad CR (2013a) *Spiders of the Savanna Biome*. University of Venda & Agricultural Research Council, 134 pp.
- Dippenaar-Schoeman AS, Van den Berg AM, Haddad CR, Lyle R (2013b) Spiders in South African agroecosystems: A review (Arachnida, Araneae). *Transactions of the Royal Society of South Africa* 68: 57–74. <https://doi.org/10.1080/0035919X.2012.755136>
- Dippenaar-Schoeman AS, Haddad CR, Foord SH, Lyle R, Lotz LN, Marais P (2015) South African National Survey of Arachnida (SANSA): review of current knowledge, constraints and future needs for documenting spider diversity (Arachnida: Araneae). *Transactions of the Royal Society of South Africa* 70(3): 245–275. <https://doi.org/10.1080/0035919X.2015.1088486>
- Dippenaar-Schoeman AS, Foord SH, Haddad CR (2021) A list of spider species found in the Marakele National Park, Limpopo Province, South Africa (Arachnida: Araneae). *SANSA Newsletter* 37: 9–15. <https://doi.org/10.5281/zenodo.5948097>
- Dippenaar-Schoeman AS, Haddad CR, Lotz LN, Booysen R, Steenkamp RC, Foord SH (2023) Checklist of the spiders (Araneae) of South Africa. *African Invertebrates* 64(3): 221–289. <https://doi.org/10.3897/AfrInvertebr.64.111047>
- FitzPatrick MJ (2007) A taxonomic revision of the Afrotropical species of *Zelotes* (Arachnida: Araneae: Gnaphosidae). *Arachnology* 14(3): 97–172. <https://doi.org/10.13156/arac.2011.14.3.97>
- Foord SH (2023) Pitfall trapping in the Waterberg massif. *SANSA Newsletter* 45: 4. <https://doi.org/10.5281/zenodo.7827671>
- Foord SH, Dippenaar-Schoeman AS (2016) The effect of elevation and time on mountain spider diversity: A view of two aspects in the Cederberg mountains of South Africa. *Journal of Biogeography* 43(12): 2354–2365. <https://doi.org/10.1111/jbi.12817>

- Foord SH, Dippenaar-Schoeman AS, van der Merwe M (2002) A check list of the spider fauna of the Western Soutpansberg, South Africa (Arachnida: Araneae). *Koedoe* 45(2): 35–43. <https://doi.org/10.4102/koedoe.v45i2.25>
- Foord SH, Mafadza M, Dippenaar-Schoeman AS, Van Rensburg BJ (2008) Micro-scale heterogeneity of spiders (Arachnida: Araneae) in the Soutpansberg, South Africa: a comparative survey and inventory in representative habitats. *African Zoology* 43(2): 156–174. <https://doi.org/10.3377/1562-7020-43.2.156>
- Foord SH, Dippenaar-Schoeman AS, Haddad CR, Lotz LN, Lyle R (2011) The faunistic diversity of spiders (Arachnida: Araneae) of the Savanna Biome in South Africa. *Transactions of the Royal Society of South Africa* 66(3): 170–201. <https://doi.org/10.1080/0035919X.2011.639406>
- Foord SH, Dippenaar-Schoeman AS, Stam EM (2013) Surrogates of spider diversity, leveraging the conservation of a poorly known group in the Savanna Biome of South Africa. *Biological Conservation* 161: 203–212. <https://doi.org/10.1016/j.biocon.2013.02.011>
- Foord SH, Dippenaar-Schoeman AS, Jocqué R, Haddad CR, Lyle R, Webb P (2016) South African National Survey of Arachnida: A checklist of the spiders (Arachnida, Araneae) of the Lekgalameetse Nature Reserve, Limpopo province, South Africa. *Koedoe* 58(1): 8 pp. <https://doi.org/10.4102/koedoe.v58i1.1405>
- Foord SH, Swanepoel LH, Evans SW, Schoeman CS, Erasmus BFN, Schoeman MC, Keith M, Smith A, Mauda EV, Maree N, Nembudani N, Dippenaar-Schoeman AS, Munyai TC, Taylor PJ (2018) Animal taxa contrast in their scale-dependent responses to land use change in rural Africa. *PLoS One* 13(5): e0194336. <https://doi.org/10.1371/journal.pone.0194336>
- Foord SH, Dippenaar-Schoeman AS, Haddad CR, Lyle R, Lotz LN, Sethusa T, Raimondo D (2020) The South African National Red List of spiders: Patterns, threats, and conservation. *The Journal of Arachnology* 48(2): 110–118. <https://doi.org/10.1636/0161-8202-48.2.110>
- Foord SH, Dippenaar-Schoeman AS, Munyai CT (2022) Spiders across the Soutpansberg. *SANSA Newsletter* 41: 5. <https://doi.org/10.5281/zenodo.6482312>
- Griswold CE (1987) A review of the southern African spiders of the family Cyatholipidae Simon, 1894 (Araneae: Araneomorphae). *Annals of the Natal Museum* 28: 499–542.
- Haddad CR (2009) *Vendaphaea*, a new dark sac spider genus apparently endemic to the Soutpansberg Mountains, South Africa (Araneae: Corinnidae). *African Invertebrates* 50(2): 269–278. <https://doi.org/10.5733/afin.050.0204>
- Haddad CR, Dippenaar-Schoeman AS (2015) Diversity of non-acarine arachnids of the Ophathe Game Reserve, South Africa: Testing a rapid sampling protocol, *Koedoe* 57(1): Art. #1255, 15 pp. <https://doi.org/10.4102/koedoe.v57i1.1255>
- Haddad CR, Dippenaar-Schoeman AS, Foord SH, Lotz L, Lyle R (2013) The faunistic diversity of spiders (Arachnida, Araneae) of the Grassland Biome in South Africa. *Transactions of the Royal Society of South Africa* 68(2): 97–122. <https://doi.org/10.1080/0035919X.2013.773267>
- Hahn N (2006) Floristic diversity of the Soutpansberg, Limpopo Province, South Africa. Ph.D. thesis, University of Pretoria, Pretoria.
- Hahn N (2011) Refinement of the Soutpansberg Geomorphic Province, Limpopo, South Africa. *Transactions of the Royal Society of South Africa* 66(1): 32–40. <https://doi.org/10.1080/0035919X.2011.566422>
- Huber BA (2003) Southern African pholcid spiders: revision and cladistic analysis of *Quamtana* gen. nov. and *Spermaphora* Hentz (Araneae: Pholcidae), with notes on

- male-female covariation. *Zoological Journal of the Linnean Society* 139(4): 477–527. <https://doi.org/10.1046/j.0024-4082.2003.00082.x>
- Jocqué R (2008) A new candidate for a Gondwanaland distribution in Zodariidae (Araneae): *Australutica* in Africa. *ZooKeys* 1: 59–66. <https://doi.org/10.3897/zookeys.1.10>
- Jocqué R, Henrard A (2015) *Ballomma*, a new Afrotropical genus in the Cryptothelinae (Araneae, Zodariidae): Eyes on the run. *European Journal of Taxonomy* 163(163): 1–24. <https://doi.org/10.5852/ejt.2015.163>
- Jocqué R, Alderweireldt M, Dippenaar-Schoeman A (2013) Biodiversity, an African perspective. In: Penney D (Ed.) *Spider research in the 21st century*. Siri Scientific press, 18–57.
- Joseph GS, Mauda EV, Seymour CL, Munyai TC, Dippenaar-Schoeman A, Foord SH (2017) Landuse change in savannas disproportionately reduces functional diversity of invertebrate predators at the highest trophic levels: Spiders as an example. *Ecosystems* (New York, N.Y.) 21(5): 930–942. <https://doi.org/10.1007/s10021-017-0194-0>
- Lotz LN (1996) Afrotropical Archaeidae (Araneae): 1. New species of *Afrarchaea* with notes on *Afrarchaea godfreyi* (Hewitt, 1919). *Navorsing van die Nasionale Museum Bloemfontein* 12: 141–160.
- Lotz LN (2003) Afrotropical Archaeidae: 2. New species of the genera *Archaea* and *Afrarchaea* (Arachnida: Araneae). *Navorsing van die Nasionale Museum Bloemfontein* 19: 221–240.
- Modiba M, Dippenaar S, Dippenaar-Schoeman AS (2005) A checklist of spiders from Sovenga Hill, an inselberg in the Savanna Biome, Limpopo Province, South Africa (Arachnida: Araneae). *Koedoe* 48(2): 109–115. <https://doi.org/10.4102/koedoe.v48i2.95>
- Mostert THC, Bredenkamp GJ, Klopper HL, Verwey C, Mostert RE, Hahn N (2008) Major vegetation types of the Soutpansberg Conservancy and the Blouberg Nature Reserve, South Africa. *Koedoe* 50(1): 32–48. <https://doi.org/10.4102/koedoe.v50i1.125>
- Muelwa M, Foord SH, Dippenaar-Schoeman AS, Stam EM (2010) Towards a standardized and optimized protocol for rapid biodiversity assessments: Spider species richness and assemblage composition in two savanna vegetation types. *African Zoology* 45(2): 273–290. <https://doi.org/10.3377/004.045.0206>
- Munyai TC, Foord SH (2012a) Ants on a mountain: Spatial, environmental and habitat associations along an altitudinal transect in a centre of endemism. *Journal of Insect Conservation* 16(5): 677–695. <https://doi.org/10.1007/s10841-011-9449-9>
- Munyai TC, Foord SH (2012b) Temporal patterns of ant diversity across a mountain with climatically contrasting aspects in the tropics of Africa. *PLoS One* 10(3): e0122035. <https://doi.org/10.1371/journal.pone.0122035>
- Myers N, Mittermeier RA, Mittermeier CG, da Fonseca GAB, Kent J (2000) Biodiversity hotspots for conservation priorities. *Nature* 403(6772): 853–858. <https://doi.org/10.1038/35002501>
- Owen J (2010) *Wildlife of a garden: A Thirty-year study*. Royal Horticultural Society, London.
- Robertson MP, Cumming GS, Erasmus BFN (2010) Getting the most out of atlas data. *Diversity & Distributions* 16(3): 363–375. <https://doi.org/10.1111/j.1472-4642.2010.00639.x>
- Schoeman CS, Foord SH (2021) Buffer zones maximize invertebrate conservation in a Biosphere Reserve. *Journal of Insect Conservation* 25(4): 597–609. <https://doi.org/10.1007/s10841-021-00326-7>
- Van Wyk AE, Smith GF (2001) *Regions of Floristic Endemism in Southern Africa*. Umdaus Press, Pretoria.

- Whitmore C, Slotow R, Crouch TE, Dippenaar-Schoeman AS (2001) Checklist of spiders (Araneae) from a savanna ecosystem, Northern Province, South Africa: Including a new family record. *Durban Museum Novitates* 26: 10–19.
- Whitmore C, Slotow R, Crouch TE, Dippenaar-Schoeman AS (2002) Diversity of spiders (Araneae) in a Savanna reserve, Northern Province, South Africa. *The Journal of Arachnology* 30(2): 344–356. [https://doi.org/10.1636/0161-8202\(2002\)030\[0344:DOSAIA\]2.0.CO;2](https://doi.org/10.1636/0161-8202(2002)030[0344:DOSAIA]2.0.CO;2)

Afrogarypus foordi sp. nov. – a new pseudoscorpion species (Pseudoscorpiones, Geogarypidae) from South Africa

Jan Andries Neethling¹, Danilo Harms^{2,3,4}

¹ Terrestrial Invertebrates Department, National Museum, P.O. Box 266, Bloemfontein 9300, South Africa

² Museum of Nature Hamburg - Zoology, Leibniz Institute for Analysis of Biodiversity Change (LIB), Martin-Luther-King-Platz 3, D-0146 Hamburg, Germany

³ Harry Butler Institute, Murdoch University, Murdoch, Australia

⁴ Department of Zoology and Entomology, University of the Free State, Bloemfontein 9301, South Africa

Corresponding author: Jan Andries Neethling (ja.neethling@nasmus.co.za)

Abstract

A new species of pseudoscorpion, *Afrogarypus foordi* sp. nov. (Pseudoscorpiones, Geogarypidae), is described in honour of South African arachnologist Stefan Hendrik Foord. The species is described from both sexes and known from near Fauresmith, Free State, South Africa. It is amongst the smallest species of *Afrogarypus* (chela length ca. 0.6–0.8 mm) and differs from its congeners by lacking trichobothrium *isb* on the fixed chelal finger, monotarsate legs I and II, and details of the galea and dentation of the chelal fingers.

Key words: Afrotropical region, Arachnida, false scorpions, morphology, systematics taxonomy



This article is part of:

Gedenkschrift for Prof. Stefan H. Foord

Edited by Galina Azarkina, Ansie Dippenaar-Schoeman, Charles Haddad, Robin Lyle, John Midgley, Caswell Munyai

Academic editor: Galina N. Azarkina

Received: 23 September 2024

Accepted: 24 October 2024

Published: 19 November 2024

ZooBank: <https://zoobank.org/978DEAE3-8C96-4608-A52C-651F016F9DB5>

Citation: Neethling JA, Harms D (2024) *Afrogarypus foordi* sp. nov. – a new pseudoscorpion species (Pseudoscorpiones, Geogarypidae) from South Africa. African Invertebrates 65(2): 115–126. <https://doi.org/10.3897/AfrInvertebr.65.137694>

Copyright: ©

Jan Andries Neethling & Danilo Harms.

This is an open access article distributed under terms of the Creative Commons Attribution License (Attribution 4.0 International – CC BY 4.0).

Introduction

The pseudoscorpion family Geogarypidae is well represented in the Afrotropical region and comprises the African endemic genus *Afrogarypus* Beier, 1931 (26 recent species) and the cosmopolitan genus *Geogarypus* Chamberlin, 1930 that includes 52 recent species and three fossil species from Baltic amber of Eocene age (Henderickx 2005; WPC 2024). Both genera are common in warm temperate and (sub)tropical regions and the South African fauna is quite diverse with 12 valid species of *Afrogarypus* and nine species of *Geogarypus* (WPC 2024). These species have been recorded from all biomes of the country, including arid Karoo landscapes in the northwest, although they are most common along the mesic coastal sides of the country's mountains. The family has also seen recent taxonomic work and a detailed and illustrated revision of the South African fauna is available (Neethling and Haddad 2016). An updated identification key and descriptions of three new species have also been published recently (Neethling 2024).

Geogarypids are four-eyed and rather flat pseudoscorpions that vary in size between a few millimetres to almost a centimetre (Neethling 2024). They are usually collected from leaf litter habitats, although they can also be found under rocks and decaying tree bark (Nassirkhani 2014; Battirolo et al. 2017). In South Africa, these pseudoscorpions can be locally abundant in leaf litter hab-

itats of indigenous or undisturbed forests and are probably amongst the most common pseudoscorpions in South Africa.

The present paper documents and names an additional species of *Afrogarypus* that we name in honour of South African arachnologist Stefan Henrik Foord. This new species is amongst the smallest of the genus (body length ♀ 1.38–1.54 mm, ♂ 1.17–1.26 mm) and known from Bankfontein Farm near Fauresmith, Free State in the grassland biome of South Africa. It is described from both sexes and diagnosed against all other species of *Afrogarypus* in the country. The species represents an interesting case of trichobothria reduction since trichobothrium *isb* on the fixed chelal finger is absent. Such reductions might result from neoteny and the loss of *isb* occurs independently in several pseudoscorpion genera that belong to the families Garypidae (e.g. *Synsphyronus* Chamberlin, 1930), Garypinidae (e.g. *Solinellus* Muchmore, 1979), Geogarypidae (*Geogarypus*), Neobisiidae (*Microbisium* Chamberlin, 1930), Sternophoridae (*Afrosterphorus* Beier, 1967) and Syarninidae (*Microblothrus* Mahnert, 1985; also see Harvey 2023 for a review on this topic). *Afrogarypus foordi* sp. nov. also shows tarsal reduction in legs I and II that are monotarsate and not divided like in most other species. Tarsal reduction is less common in pseudoscorpions than the reduction of trichobothria but has been recorded in the families Garypidae (e.g. *Synsphyronus* in Australia; Cullen and Harvey 2021) and Geogarypidae (see below or Neethling and Haddad 2016). Both reductive features (trichobothria and leg tarsi) are recorded here for the second time in the South African geogarypid fauna.

Materials and methods

Specimen origin

The specimens were obtained from the Arachnology wet collection of the Terrestrial Invertebrates department of the National Museum in Bloemfontein, South Africa (NMBA). While working through, and updating, the pseudoscorpion collection, the first author noted a number of Geogarypidae specimens originally identified as *Afrogarypus subimpressus* (Beier, 1955) from three sites located in the interior of the country. Given that the type locality of the species is at Cape Point Nature Reserve in the Western Cape, the specimens were re-examined and found to belong to a novel *Afrogarypus* species. All specimens were deposited back in the Arachnology wet collection of the National Museum Bloemfontein, South Africa, after identifications and descriptions were made, with NMBAP being the accession sequence for pseudoscorpions.

Morphological analysis

The specimens were sorted, identified and sexed using a Novel NSZ-606 stereomicroscope. Lactic acid clearing followed the same method as in Neethling and Haddad (2016). Specimens were cleared in 90% lactic acid with the desired structures (the chelicerae, pedipalps, leg I and leg IV) dissected afterwards under a stereomicroscope, using fine pins (Hu and Zhang 2012). Dissected parts were kept in microvials and stored with the rest of the specimens. These were then individually mounted on standard microscope slides, with small pieces of nylon fishing line used to elevate a standard slip above the structures (Harvey

2010). The slides were examined with a Nikon Eclipse 50i Binocular microscope fitted with a Nikon Digital Sight DS-U3 system equipped with a Nikon DS-Fi1 5 Megapixel camera. High resolution digital photographs, as well as digital measurements, were made using NIS Elements Imaging Software 64-bit v.3.22.00 (Build 710) 2010. Adobe Photoshop CS5 Extended 64-bit v.12.0 2010 (Adobe Inc.) was used to create extended focal range images of the studied structures via stacking of the digital photographs. These images were then traced to produce line drawings. Distribution maps were generated using the software program Quantum GIS Hannover version 3.16 (QGIS Development Team 2020).

Terminology mostly follows Harvey (1992) except for the chelicerae, which follows Judson (2007). Ratios are given as Length / Width or Depth for legs I and IV. Chaetotaxy, obtained from cleared specimens, given as ♀(♂).

The following abbreviations are used in the figures and text:

| Chela trichobothria | | Chelicera setae | |
|---------------------|-----------------------|-----------------|----------------|
| b | basal | es | exterior seta |
| sb | sub-basal | bs | basal seta |
| st | sub-terminal | sbs | sub-basal seta |
| t | terminal | is | interior seta |
| ib | interior basal | ls | laminal seta |
| isb | interior sub-basal | gs | galeal seta |
| ist | interior sub-terminal | | |
| it | interior terminal | | |
| eb | exterior basal | | |
| esb | exterior sub-basal | | |
| est | exterior sub-terminal | | |
| et | exterior terminal | | |

Taxonomy

Family Geogarypidae Chamberlin, 1930

Genus *Afrogarypus* Beier, 1931

Afrogarypus: Beier 1931: 317 (original description); Harvey 1986: 758; Harvey 1991: 249; Neethling and Haddad 2016: 7–9.

Geogarypus (*Afrogarypus*): Beier 1932: 236; Beier 1955: 301; Heurtault 1970: 1365.

Type species. *Garypus senegalensis* Balzan, 1892, by original designation.

Afrogarypus foordi sp. nov.

<https://zoobank.org/5B894EA4-88E9-401C-9A0F-761BB6392F84>

Figs 1–4

Type materials. *Holotype* · 1 ♀, SOUTH AFRICA, Free State, Fauresmith, Bankfontein Farm, 30°04'S, 24°53'E, 1192 m a.s.l., Hillside Shrubs, Leaf litter sifting, leg. University of the Free State Entomology Students, 04.IV.2015 (NMBAP 00279).

Paratype • 1 ♂, Same data as holotype (NMBAP 00466).

Other material examined. SOUTH AFRICA: Free State • 1 ♂, Bethulie, Tussen die Riviere Nature Reserve, 30°30'S, 26°07'E, 1286 m a.s.l., Shrubs against Rocky Hill in Veld, Leaf litter sifting, leg. L. Lotz & C.R. Haddad, 16.X.2008 (NMBAP 00135) • 2 ♀, Fauresmith, Bankfontein Farm, 30°04'S, 24°53'E, 1187 m a.s.l., Tree Grove in Veld, Leaf litter sifting, leg. University of the Free State Entomology Students, 02.IV.2015 (NMBAP 00237); Western Cape • 1 ♀, 3 ♂, Beaufort West, Karoo National Park, Klipspringer Pass, 32°19'S, 22°27'E, 1126 m a.s.l., Karoo Shrubs, Leaf litter sifting, leg. J.A. Neethling, 14.XI.2012 (NMBAP 00175).

Etymology. The species is named in remembrance of Professor Stefan Hendrik Foord, our friend and colleague, for his contributions to Arachnology, and for his outstanding contributions to the biodiversity and ecology of South African spiders.

Diagnosis. Small species (chela length ♀ 0.71–0.79 mm, ♂ 0.58–0.63 mm), with a wide depression located dorsally, before the fixed finger, on the chelae of both females and males; cheliceral hand with five acuminate setae; female galea with seven rami, male galea simple and with no rami; rallum present as a simple single blade. Differs from *Afrogarypus carmenae* Neethling & Haddad, 2016, *A. excelsus* (Beier, 1964), *A. haddadi* Neethling, 2024, *A. impressus* (Tullgren, 1907b), *A. megamolaris* Neethling & Haddad, 2016, *A. minutus* (Tullgren, 1907a), *A. pseudotriangularis* Neethling, 2024, *A. purcelli* (Ellingsen, 1912), *A. robustus* (Beier, 1947), *A. subimpressus* (Beier, 1955) and *A. triangularis* (Ellingsen, 1912) by both lacking trichobothrium **isb** on the fixed chelal finger, as well as having monotarsate legs I and II. Differs from *Afrogarypus castigatus* Neethling & Haddad, 2016, by having seven rami, arranged in an arc across the tip, on the female galea, as opposed to nine arranged in two groups, one on each side of the galea; having a broad, well developed sulcus on the dorsal surface of the chela, as opposed a wide, shallow concave region; having a chelal movable finger the same length to longer than the chelal hand (chelal movable finger ♀ 1.00–1.13, ♂ 1.03–1.23 times longer than chelal hand without pedicel), as opposed to a chelal movable finger shorter than the chelal hand (chelal movable finger ♀ 0.68–0.78, ♂ 0.69–0.75 times longer than chelal hand without pedicel); having the granulated texture of the chelal hand terminate above trichobothrium **esb**, as opposed to having a pronounced granulated ridge terminating between **est** and **ist** and spanning approximately along half the total fixed finger length; having trichobothrium **it** directly above **et**, as opposed to **it** situated further back, between **et** and **t**, and trichobothrium **t** situated equidistant between **ist** and **et**, as opposed to **t** being close to **ist**.

Description. Carapace: Strongly sub-triangular, narrow furrow posterior to the eyes (Figs 1A, C, 3H). Heavily constricted anteriorly into a cucullus, constriction beginning at the medial furrow. Two pairs of corneate eyes situated on ocular tubercles, located about one-third away from the anterior edge. Uniformly granular in texture, dark brown from cucullus to furrow, with a slightly lighter posterior edge in both sexes. Four prominent acuminate setae located on anterior edge, row of acuminate setae (♀ 9–11 ♂ 8–9) seated within rims, located on the posterior margin. Numerous small acuminate setae present on carapace.

Abdomen: Wider than carapace and subovate. Tergites granular in texture in both sexes, retaining mostly the same coloration as the posterior edge of the carapace. Tergites I and II each with a faint darker median spot, as well as a faint

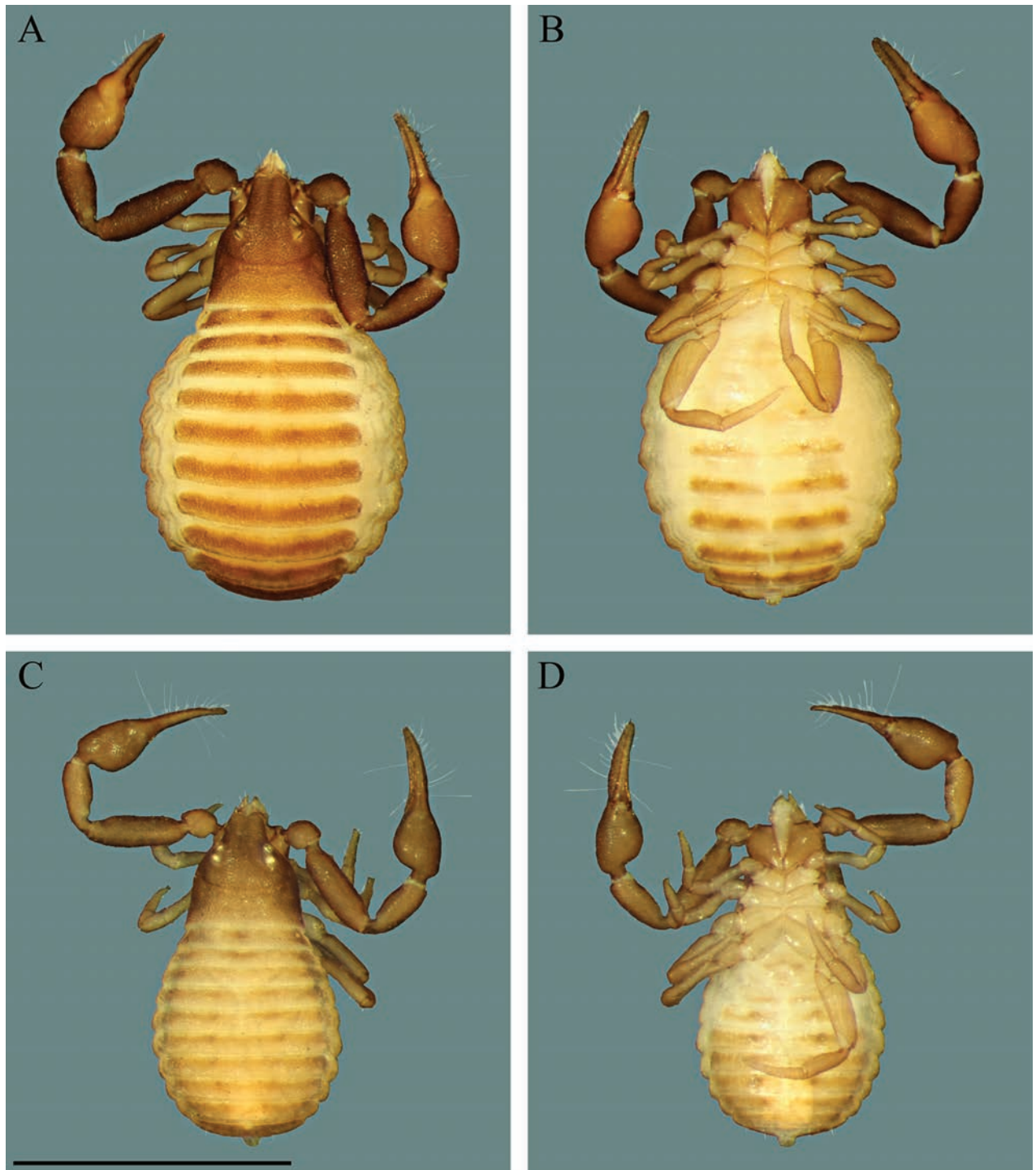


Figure 1. Digital microscope photographs of *Afrogarypus foordi* sp. nov., female holotype (**A, B**) and male paratype (**C, D**) **A, C** dorsal view **B, D** ventral view. Scale bar: 1.00 mm.

darker spot at each edge of the tergite. Tergite I–VIII uniform in colour, tergites IX–XI darker brown, tergite XII uniformly lighter in colour (Fig. 1A, C). Tergal setae acuminate and located on the posterior of each tergite. Sternite XII same colour as tergite XII in both sexes. In female, sternites range in colour from tan in sternites II–IV to light brown in sternites V–XI, becoming darker from sternite V to XI. Central tan-coloured region present on sternites V–X, giving these sternites a divided appearance. Sternites V–IX with paired faint darker spots. Male

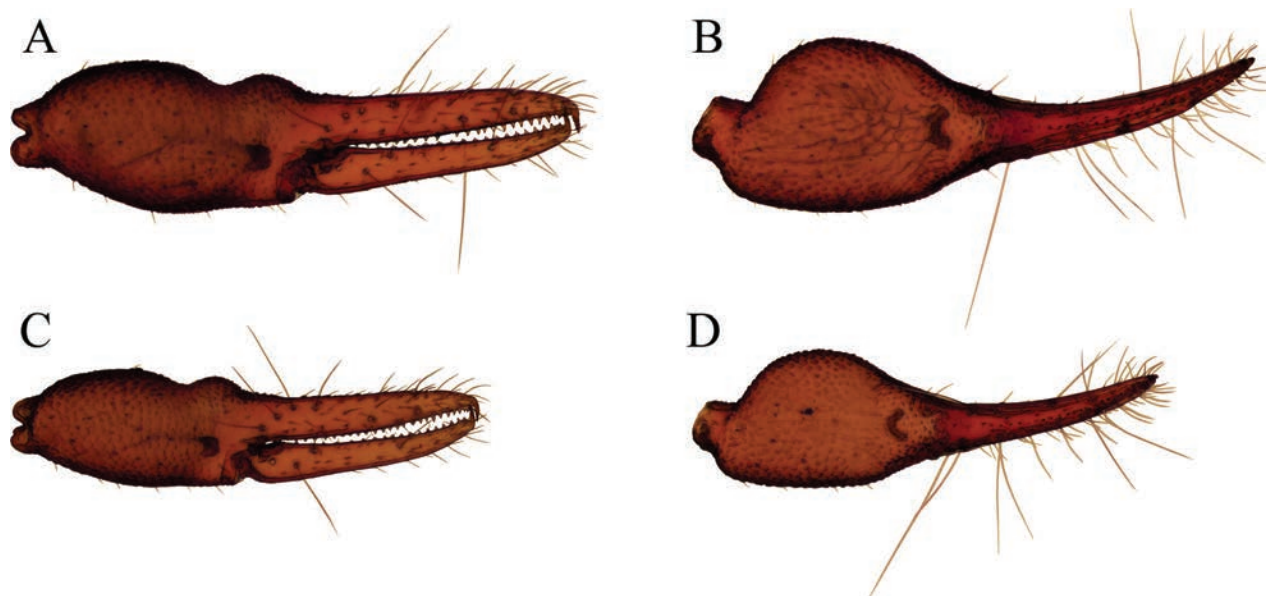


Figure 2. Digital microscope photographs of non-type (NMBAP 00175) *Afrogarypus foordi* sp. nov. right chela: female (A, B) and male (C, D) A, C retrolateral view B, D dorsal view. Scale bar: 1.00 mm.

sternites II–III tan colour, sternites IV–XI light brown, becoming darker from sternite IV to XI. Central tan-coloured region present on sternites IV–IX, giving these sternites a divided appearance. Sternites V–IX with paired faint darker spots (Fig. 1B, D). Female operculum with 11 acuminate setae on the anterior genital plate, separated into five setae distributed along the posterior margin of the genital plate, and two groups of three setae each situated just anterior of the posterior row, separated by two prominent lyriform fissures, near the centre. Male operculum with ten acuminate setae on the anterior genital plate, separated into seven setae distributed along the posterior margin of the genital plate, and three setae anterior to these. Two prominent lyriform fissures present centrally, just anterior to the posterior setae row. Male sternite III with 15 acuminate setae, separated into four setae located along the anterior margin of the sternite, at the edge of the genital opening, three setae located centrally behind these and eight setae distributed along the posterior margin of the sternite. Pleural membrane wrinkled-plicate, cream in both sexes. Lateral sclerites absent in both sexes.

Tergal chaetotaxy: 8(8): 12(9): 10(10): 10(9): 12(10): 9(9): 8(10): 8(9): 7(8): 6(7): 6(8): 2(2).

Sternal chaetotaxy: ?(?): 11(9): 8(15): 11(11): 16(13): 13(14): 14(12): 11(10): 7(7): 6(6): 4(4): 2(2).

Pedipalp: In both sexes all segments granular in texture with small acuminate setae scattered over the surface, except the pedicels. Trochanter, femur and patella dark brown in colour, female chela somewhat lighter, male chela same colour as preceding palp segments. Trochanter rounded in shape, distinct apophysis present ventrally. Femur ratios overlap considerably in females and males, 3.07–3.43 (♀) to 2.92–3.33 (♂) times longer than wide. Femur constricted at pedicel, widening quickly to form base, then widening slightly before constricting again at end. Patella constricted and distinctly angled at pedicel, widening markedly into a cone, 2.43–2.77 (♀) to 2.33–2.73 (♂) times longer than wide. Several small lyriform fissures present on a bulge on the dorsal surface, just distal of base. Disto-prolateral excavation present (Fig. 3B).

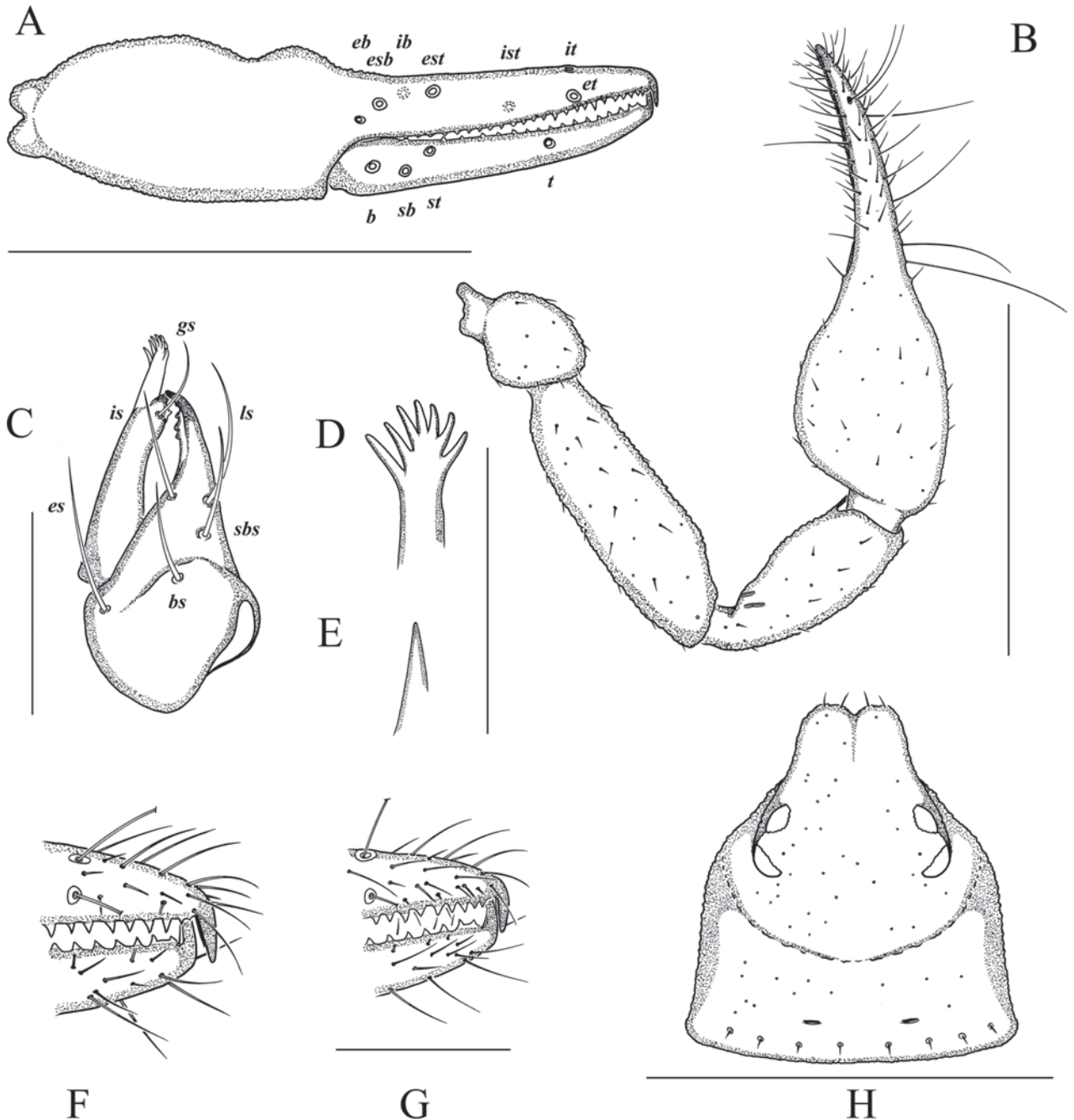


Figure 3. *Afrogarypus foordi* sp. nov. (NMBAP 00175) **A** female right chela, retrolateral view **B** female right pedipalp, dorsal view **C** female left chelicera, dorsal view **D** female galea **E** male galea **F** female chelal fingers, anterior retrolateral view **G** male chelal fingers, anterior retrolateral view **H** female carapace, dorsal view. Scale bars: 0.50 mm (**A**, **B**, **H**); 0.10 mm (**C**, **F**, **G**); 0.05 mm (**D**, **E**).

Chela: Uniformly brown in both sexes. Hand granular in texture up to base of movable finger, granular texture terminating above trichobothrium **esb** in both sexes. Broad, well-developed sulcus present on dorsal surface, located just proximal to the base of the fixed finger. Dorsal bulge located just anterior of sulcus. Female sulcus marginally deeper, male sulcus shallower (Fig. 2A, C). Hand of both sexes strongly convex on the prolateral edge, much less so on the retrolateral edge (Fig. 2B, D). Male chelae smaller. Both sexes with a short pedicel (pedicel 0.13–0.14 ♀ 0.14–0.16 ♂ times longer than chelal hand) and

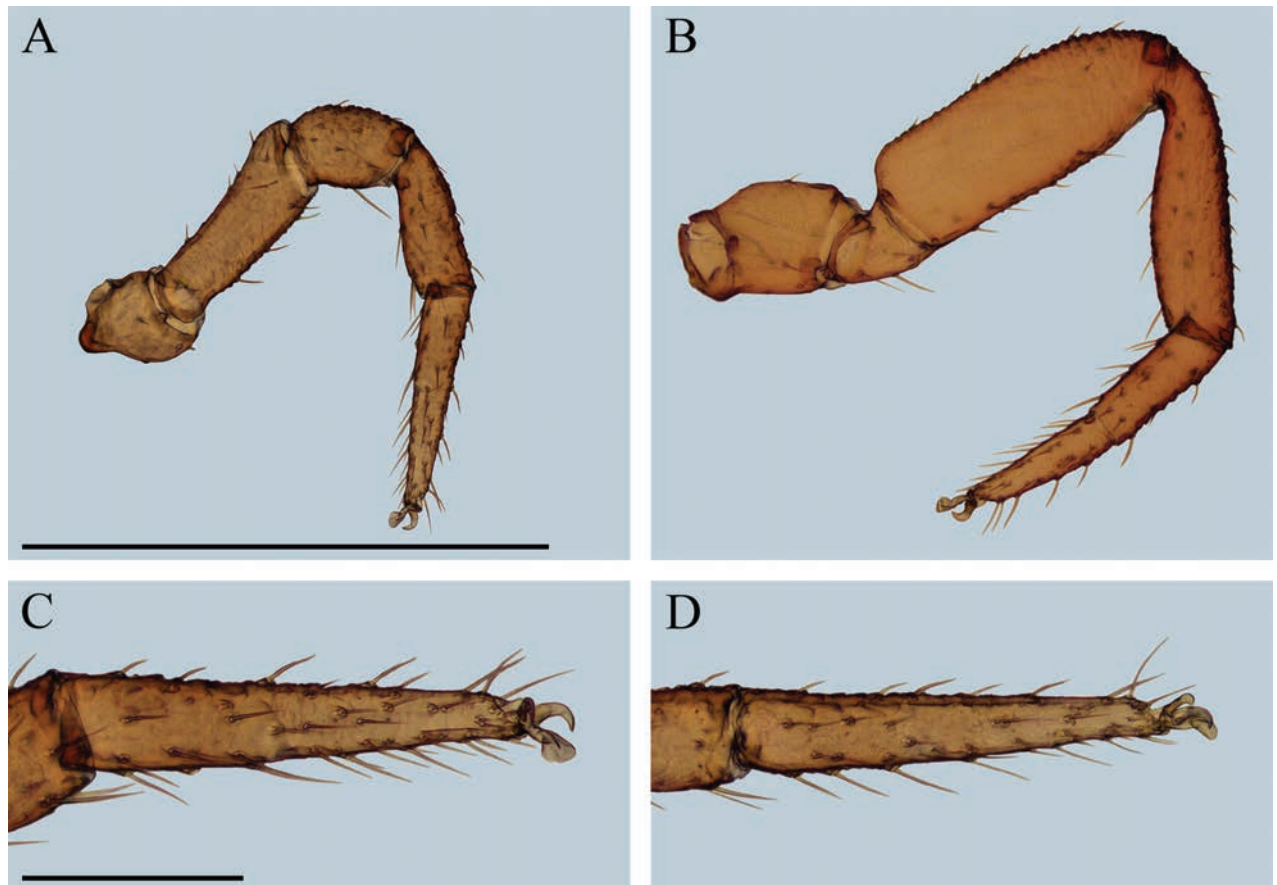


Figure 4. Digital microscope photographs of non-type (NMBAP 00175) *Afrogarypus foordi* sp. nov. leg morphology: female (**A**, **B**, **C**) and male (**D**) **A** monotsarate leg I, lateral view **B** diplotarsate leg IV, lateral view **C** female fused tarsal segments of leg I **D** male fused tarsal segments of leg I. Scale bars: 0.50 mm (**A**, **B**); 0.10 mm (**C**, **D**).

a prolaterally slanted posterior hand edge. Fingers narrow and curved slightly prolaterally, as long to slightly longer than chelal hand in both sexes. Venom apparatus present on both fingers. Fixed and movable chelal fingers with seven and four trichobothria respectively as in fig. 3A. Trichobothrium *isb* absent in both sexes.

Chelal teeth strongly sclerotized, acute and retrorse in both sexes. Female fixed finger with 23–25 teeth. First two teeth behind venom apparatus distinctly smaller than the proceeding teeth (Fig. 3F), rest of the teeth spaced equidistant from each other along the fixed chelal finger, reducing in size proximally, still acute. Female movable finger with 17–19 teeth. First two teeth behind venom apparatus distinctly smaller and situated on a raised ridge. Rest of the teeth larger, both reducing in size proximally, as well as becoming spaced further apart. Male fixed finger with 24–25 teeth. First two teeth just behind venom apparatus distinctly smaller and spaced closer together than the proceeding teeth (Fig. 3G). Rest of the teeth spaced equidistant from each other along the fixed chelal finger, reducing in size proximally, still acute. Male movable finger with 18–19 teeth. First two teeth behind venom apparatus distinctly smaller and situated on a raised ridge. Rest of the teeth larger, both reducing in size proximally, as well as becoming spaced further apart.

Chelicera: Hand with five long and acuminate setae (Fig. 3C). Fixed finger of both sexes with four to five teeth. Female movable finger with one to two very

small teeth, male movable finger without any discernible teeth. Galea complex, with seven rami (♀) (Fig. 3D), simple with no rami (♂) (Fig. 3E). Rallum with a single blade in both sexes. Serrula exterior with 16–17 lamellae (♀), 15–16 lamellae (♂). Lamina exterior present in both sexes.

Coxae and legs: Pedipalpal coxae same colour to slightly lighter than rest of pedipalps. Coxae I–IV tan to light brown. Legs I–IV light brown in colour. Legs I and II monotarsate (Figs. 4A, C, D), legs III and IV diplotarsate (Fig. 4B). All legs with simple claws; arolium longer than claws.

Measurements (mm): Body length ♀ 1.38–1.54 ♂ 1.17–1.26; Carapace ♀ 0.48–0.52 × 0.46–0.49 (0.98–1.13) ♂ 0.46–0.49 × 0.41–0.43 (1.07–1.20); Chelicera ♀ 0.16–0.18 × 0.09–0.11 (1.45–2.00) ♂ 0.13–0.14 × 0.07–0.08 (1.63–2.00), movable finger length ♀ 0.10–0.11 ♂ 0.07–0.08; Pedipalps: femur ♀ 0.46–0.48 × 0.14–0.15 (3.07–3.43) ♂ 0.38–0.40 × 0.12–0.13 (2.92–3.33), patella ♀ 0.34–0.36 × 0.13–0.14 (2.43–2.77) ♂ 0.28–0.30 × 0.11–0.12 (2.33–2.73), chela ♀ 0.71–0.79 × 0.22–0.25 (2.84–3.59) ♂ 0.58–0.63 × 0.17–0.19 (3.05–3.71), hand ♀ 0.32–0.34 × 0.22–0.25 (1.28–1.55) ♂ 0.26–0.29 × 0.17–0.19 (1.37–1.71), movable finger length ♀ 0.34–0.36 ♂ 0.30–0.32; Leg I: femur ♀ 0.21–0.22 × 0.08–0.09 (2.33–2.75) ♂ 0.17–0.18 × 0.07 (2.43–2.57), patella ♀ 0.11–0.12 × 0.08–0.09 (1.22–1.50) ♂ 0.10–0.11 × 0.06 (1.67–1.83), tibia ♀ 0.15–0.17 × 0.06–0.07 (2.14–2.83) ♂ 0.13–0.15 × 0.05–0.06 (2.17–3.00), metatarsus–tarsus ♀ 0.22–0.23 × 0.05 (4.40–4.60) ♂ 0.19–0.20 × 0.04 (4.75–5.00); Leg IV: femoropatella ♀ 0.40–0.44 × 0.12–0.13 (3.08–3.67) ♂ 0.32–0.33 × 0.10–0.11 (2.91–3.30), tibia ♀ 0.29–0.32 × 0.08–0.09 (3.22–4.00) ♂ 0.24–0.26 × 0.06–0.07 (3.43–4.33), metatarsus ♀ 0.14–0.16 × 0.05 (2.80–3.20) ♂ 0.12–0.13 × 0.05 (2.40–2.60), tarsus ♀ 0.14–0.15 × 0.04 (3.50–3.75) ♂ 0.12–0.13 × 0.03 (4.00–4.33).

Remarks. *Afrogarypus foordi* sp. nov. represents the second geogarypid species in South Africa that both exhibits the absence of trichobothrium *isb* on the fixed chelal finger, as well as monotarsate legs I and II. With the discovery of this species, a correction has to be made to the distribution data presented in Neethling and Haddad (2016), since the specimens identified in this study were erroneously identified, and presented as *Afrogarypus subimpressus* in the 2016 study. Thus, the distribution of *Afrogarypus subimpressus* no longer has any inland specimens, with the remaining distributions being along the coast of the Western Cape Province.

Please also note in this context that these two species are not the only geogarypid species with reductive features. Other geogarypids outside of South Africa are also known to have seven trichobothria on the fixed chelal finger and these include *Geogarypus conatus* Harvey, 1986 from Australia, and the Neotropical species *G. bucculentus* Beier, 1955 and *G. pustulatus* Beier, 1959 (Harvey, 1987).

Ecology. *Afrogarypus foordi* sp. nov. is currently known to inhabit the shaded leaf litter found under indigenous shrub and tree stands in the veld of the Free State, as well as those of larger Karoo bushes. Its known distribution (Fig. 5) falls outside of both the Maputaland-Pondoland-Albany hotspot, as well as the Cape Floristic Region, where the majority of South Africa's Geogarypidae diversity is found (Neethling and Haddad 2016; Neethling 2024). In contrast to the arboreal lifestyle of *Afrogarypus castigatus*, the other South African geogarypid that exhibits the absence of trichobothrium *isb* and monotarsate

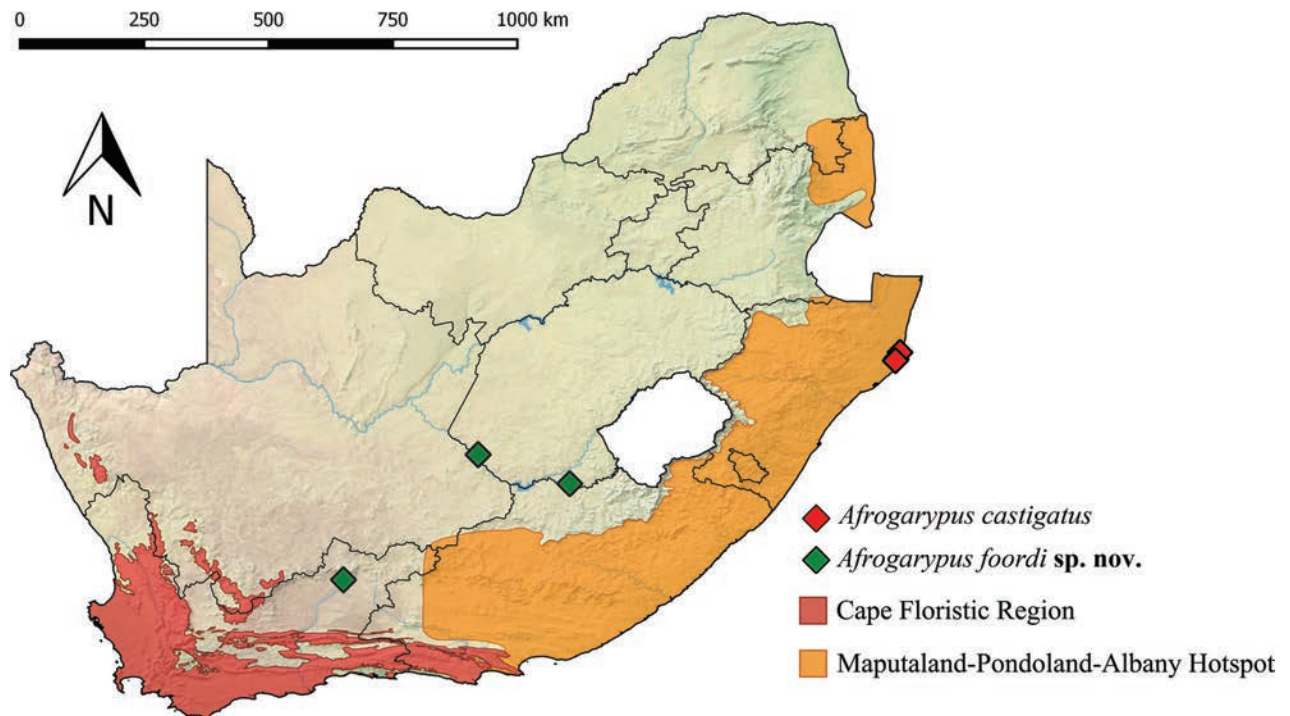


Figure 5. Topographical map of South Africa displaying the distribution of *Afrogarypus foordi* sp. nov., as well as the morphologically similar *A. castigatus* Neethling & Haddad, 2016. Also highlighted are the distributions of the Cape Floristic Region and the Maputaland-Pondoland-Albany hotspots. Shapefile acquired from http://www.conservation.org/where/priority_areas/hotspots/Pages/hotspots_main.aspx (accessed 20.XI.2020).

legs I and II, all specimens of *A. foordi* sp. nov. have been found in leaf litter. *Afrogarypus castigatus* furthermore possess much more compact bodies with comparatively shorter, more stout appendages, while *A. foordi* sp. nov. exhibits body proportions that are much less compact and more reminiscent of other ground-dwelling Geogarypidae. Specimens were collected during the months of April, October and November. Elevation: 1187–1286 m.

Additional information

Conflict of interest

The authors have declared that no competing interests exist.

Ethical statement

No ethical statement was reported.

Funding

No funding was reported.

Author contributions

All authors have contributed equally.

Author ORCIDs

Jan Andries Neethling  <https://orcid.org/0000-0003-1702-9566>

Danilo Harms  <https://orcid.org/0009-0006-7437-6897>

Data availability

All of the data that support the findings of this study are available in the main text.

References

- Battirola LD, Brizzola dos Santos G, Meurer E, Castilho ACC, Mahnert V, Brescovit AD, Marques MI (2017) Soil and canopy Pseudoscorpiones (Arthropoda, Arachnida) in a monodominant forest of *Attalea phalerata* Mart. (Arecaceae) in the Brazilian Pantanal. *Studies on Neotropical Fauna and Environment* 52(2): 1–8. <https://doi.org/10.1080/01650521.2017.1282210>
- Beier M (1931) Neue Pseudoscorpione der U. O. Neobisiinea. *Mitteilungen aus dem Zoologischen Museum in Berlin* 17: 299–318.
- Beier M (1932) Pseudoscorpionidea I. Subord. Chthoniinea et Neobisiinea. *Tierreich* 57: 1–258. <https://doi.org/10.1515/9783111435107.1>
- Beier M (1947) Zur Kenntnis der Pseudoscorpionidenfauna des südlichen Afrika, insbesondere der südwest- und südafrikanischen Trockengebiete. *Eos (Washington, D.C.)* 23: 285–339.
- Beier M (1955) Pseudoscorpionidea. In: Hanstrom B, Brinck P, Rudebeck G (Eds) *South African Animal Life: Results of the Lund University Expedition in 1950–1951*.
- Beier M (1964) Weiteres zur Kenntnis der Pseudoscorpioniden-Fauna des südlichen Afrika. *Annals of the Natal Museum* 16: 30–90.
- Chamberlin JC (1930) A synoptic classification of the false scorpions or chela-spinners, with a report on a cosmopolitan collection of the same. Part II. The Diplosphyronida (Arachnida-Chelonethida). *Annals & Magazine of Natural History* 10(30): 585–620. <https://doi.org/10.1080/00222933008673173>
- Cullen KE, Harvey MS (2021) New species of the pseudoscorpion genus *Synsphyronus* (Pseudoscorpiones: Garypidae) from Australia. *Records of the Western Australian Museum* 36(1): 33–65. <https://doi.org/10.18195/issn.0312-3162.36.2021.033-065>
- Ellingsen E (1912) The pseudoscorpions of South Africa based on the collections of the South African Museum, Cape Town. *Annals of the South African Museum* 10: 75–128. <https://doi.org/10.5962/bhl.part.9312>
- Harvey MS (1986) The Australian Geogarypidae, new status, with a review of the generic classification (Arachnida: Pseudoscorpiones). *Australian Journal of Zoology* 34(5): 753–778. <https://doi.org/10.1071/ZO9860753>
- Harvey MS (1987) Redescriptions of *Geogarypus bucculentus* Beier and *Geogarypus pustulatus* Beier (Geogarypidae: Pseudoscorpionida). *Bulletin - British Arachnological Society* 7: 137–141.
- Harvey MS (1991) *Catalogue of the Pseudoscorpionida*. Manchester University Press, Manchester.
- Harvey MS (1992) The phylogeny and classification of the Pseudoscorpionida (Chelicerata: Arachnida). *Invertebrate Systematics* 6(6): 1373–1435. <https://doi.org/10.1071/IT9921373>
- Harvey MS (2010) Redescription of *Geogarypus irrugatus* from Sumatra (Pseudoscorpiones: Geogarypidae). *The Journal of Arachnology* 38(2): 383–386. <https://doi.org/10.1636/A08-101SC.1>
- Harvey MS (2023) A preliminary phylogeny for the pseudoscorpion family Garypinidae (Pseudoscorpiones: Garypinoidea), with new taxa and remarks on the Australasian fauna. *Invertebrate Systematics* 37(9): 623–676. <https://doi.org/10.1071/IS23029>

- Henderickx H (2005) A new *Geogarypus* from Baltic amber (Pseudoscorpiones: Geogarypidae). *Phegea* 33: 87–92.
- Heurtault J (1970) Pseudoscorpions du Tibesti (Tchad). II. Garypidae. *Bulletin du Muséum National d'Histoire Naturelle* 41(2): 1361–1366.
- Hu JF, Zhang F (2012) Description of two new *Stenohya* species from China (Pseudoscorpiones, Neobisiidae). *ZooKeys* 213: 79–91. <https://doi.org/10.3897/zookeys.213.2237>
- Judson MLI (2007) A new and endangered species of the pseudoscorpion genus *Lagynochthonius* from a cave in Vietnam, with notes on chelal morphology and the composition of the Tyrannochthoniini (Arachnida, Chelonethi, Chthoniidae). *Zootaxa* 1627(1): 53–68. <https://doi.org/10.11646/zootaxa.1627.1.4>
- Nassirkhani M (2014) A new pseudoscorpion species of the genus *Geogarypus* (Arachnida: Pseudoscorpiones) from Iran. *Acta Arachnologica* 63(2): 99–103. <https://doi.org/10.2476/asjaa.63.99>
- Neethling JA (2024) Three new Geogarypidae (Pseudoscorpiones: Garypoidea) from South Africa, with an updated key to the country's geogarypid species. *Zootaxa* 5443(3): 387–405. <https://doi.org/10.11646/zootaxa.5443.3.4>
- Neethling JA, Haddad CR (2016) A systematic revision of the South African pseudoscorpions of the family Geogarypidae (Arachnida: Pseudoscorpiones). *Indago* 32: 1–80.
- QGIS Development Team (2020) QGIS Geographic Information System. Open Source Geospatial Foundation. <http://qgis.org>
- Tullgren A (1907a) Zur Kenntnis außereuropäischer Chelonethiden des Naturhistorischen Museums in Hamburg. *Mitteilungen aus dem Naturhistorischen Museum in Hamburg* 24: 21–75.
- Tullgren A (1907b) Chelonethiden aus Natal und Zululand. In: Wirén A (Ed.) *Zoologiska studier tillagnade Professor T. Tullberg*. Almquist and Wiksells, Uppsala. 216–236.
- WPC [World Pseudoscorpion Catalog] (2022) World Pseudoscorpiones Catalog. Natural History Museum Bern. <http://wac.nmbe.ch> [accessed on 13/09/2024]

On some new and poorly-known Chrysillini from arid western South Africa (Araneae, Salticidae)

Charles Richard Haddad¹, Wanda Wesółowska²

¹ Department of Zoology & Entomology, University of the Free State, Nelson Mandela Drive, Bloemfontein 9300, South Africa

² Department of Biodiversity and Evolutionary Taxonomy, University of Wrocław, Przybyszewskiego 65, 51-148 Wrocław, Poland

Corresponding author: Charles Richard Haddad (haddadcr@ufs.ac.za)

Abstract

Following a rapid biodiversity assessment of spiders in the arid western interior of South Africa, we report on the occurrence of some poorly known and new species of chrysilline jumping spiders. *Helafricanus patellaris* (Simon, 1901), *Heliocapensis capensis* (Wesółowska, 1986), *H. mirabilis* (Wesółowska, 1986) and *Menemerus lesserti* Lawrence, 1927 are recorded from the Northern Cape Province for the first time, and *Heliocapensis maluti* (Wesółowska & Haddad, 2014) (Lesotho) and *Heliophanus deformis* Wesółowska, 1986 (Angola) are recorded from South Africa for the first time, both also from the Northern Cape. The hitherto unknown females of *Heliocapensis mirabilis* (Wesółowska, 1986) and *Icius pulchellus* Haddad & Wesółowska, 2011 and the male of *M. lesserti* are described for the first time. Three new species are described: *Icius jacksoni* **sp. nov.** (♂), *Menemerus foordi* **sp. nov.** (♂) and *Natta triguttata* **sp. nov.** (♂♀). One new combination, *Afraflacilla matabelensis* (Wesółowska, 2011), **comb. nov.** (ex *Pseudicius* Simon, 1885), is proposed. We present the first comprehensive molecular analysis of South Africa Chrysillini jumping spiders, based on the cytochrome oxidase I (COI) gene, which supports the monophyly of all but two genera (*Helafricanus* Wesółowska, 1986 and *Heliophanus* C.L. Koch, 1833), which we briefly discuss.

Key words: Cytochrome oxidase subunit I, desert, jumping spiders, Salticinae, Salticoida, succulent karoo



This article is part of:

Gedenkschrift for Prof. Stefan H. Foord

Edited by Galina Azarkina, Ansie

Dippenaar-Schoeman, Charles Haddad,

Robin Lyle, John Mldgley, Caswell Munyai

Academic editor: Galina N. Azarkina

Received: 1 September 2024

Accepted: 4 November 2024

Published: 19 November 2024

ZooBank: <https://zoobank.org/CC028E33-8418-4345-950E-72E977FEE66C>

Citation: Haddad CR, Wesółowska W (2024) On some new and poorly-known Chrysillini from arid western South Africa (Araneae, Salticidae). African Invertebrates 65(2): 127–159. <https://doi.org/10.3897/AfrInvertebr.65.136083>

Copyright: ©

Charles Richard Haddad & Wanda Wesółowska.

This is an open access article distributed under

terms of the Creative Commons Attribution

License (Attribution 4.0 International – CC BY 4.0).

Introduction

South Africa includes three global biodiversity hotspots (Myers et al. 2000), of which the Succulent Karoo hotspot in the west, which includes most of the extent of the Succulent Karoo Biome (SKB), is shared with southern Namibia. The SKB is globally recognised for its exceptional richness and endemism of dwarf succulents, but the invertebrate fauna remains poorly known for most orders (e.g. Janion-Scheepers et al. 2016). Coupled with the SKB, large parts of arid western South Africa and southern Namibia are characterised by Nama Karoo vegetation and, to a lesser extent, Desert Biome (DB) surrounding the lower section of the Orange River and pockets of Fynbos further south (Mucina and Rutherford 2006).

The arid western parts of South Africa remain the most unexplored concerning spider biodiversity, with the majority of quarter-degree cells being either severely undersampled or never having been sampled at all (Foord et al. 2011,

2020; Janion-Scheepers et al. 2016; Dippenaar-Schoeman et al. 2023). This has been primarily influenced by the distribution of arachnologists in the eastern and southern parts of the country, perceived logistical challenges associated with the rural west and the expected lower species richness of arid versus mesic biotopes, which would be expected to yield lower species richness and abundance for the sampling effort. The majority of spiders recorded from this region were described by Purcell (1908) and Simon (1910), with specific details of the original localities provided in Haddad and Marusik (2019).

To help address this, the first author and colleagues collected in five historically poorly sampled degree squares along a north–south transect in the arid western interior of the country during 2021 and 2022, including the DB of the Richtersveld National Park and four sites to the south in the SKB (Fig. 1). Here, we present data on some new and poorly-known jumping spiders of the tribe Chrysillini that were collected during this study, supplemented by specimens from the area sourced from natural history collections, to improve knowledge of this group in the arid zone of South Africa. Three new species are described, two unknown sexes are described for the first time and new distribution data are provided for several poorly-known species.

Material and methods

Morphology

All of the material examined in this study is preserved in 70% ethanol and deposited in the National Collection of Arachnida, ARC – Plant Health and Protection, Pretoria (**NCA**), National Museum, Bloemfontein (**NMBA**) and KwaZulu-Natal Museum, Pietermaritzburg (**NMSA**). Digital microscope photographs of the habitus and genitalic morphology were taken by the second author with a Nikon Coolpix 8400 mounted on a Nikon SMZ 1500 and Zeiss Stemi 2000 stereomicroscope, with a series of extended focal range images taken and stacked using Helicon Focus software to increase the depth of field. For *Icius insolidus* (Wesolowska, 1999) (♂♀) and *Menemerus transvaalicus* Wesolowska, 1999 (♀), specimens were photographed with a Nikon D5-L3 camera system attached to a Nikon SMZ800 stereomicroscope, with the series of images stacked using the CombineZM imaging software (<http://www.hadleyweb.pwp.blueyonder.co.uk>) to increase the depth of field.

Genitalic structures were illustrated with the aid of a reticular eyepiece on a binocular microscope (Nikon and MBS-10). Detailed examination of the male pedipalps and female epigynes were done following dissection, with the epigynes cleared in 5% hot potassium hydroxide (KOH) solution for a few minutes, dehydrated with 100% ethanol, cleared in xylene and drawn in temporary eugenol mounts. All genitalia were placed in microvials containing 70% ethanol together with the specimens from which they were dissected.

All measurements are provided in millimetres and were determined with an eyepiece micrometer on a binocular microscope (Nikon and MBS-10). The carapace length was measured along the mid-line of the carapace from the base of the anterior median eyes (i.e. excluding the lenses) to the posterior margin of the carapace medially. The abdomen length was measured from the anterior margin of the abdomen to the anal tubercle, i.e. excluding the petiole and spinnerets.

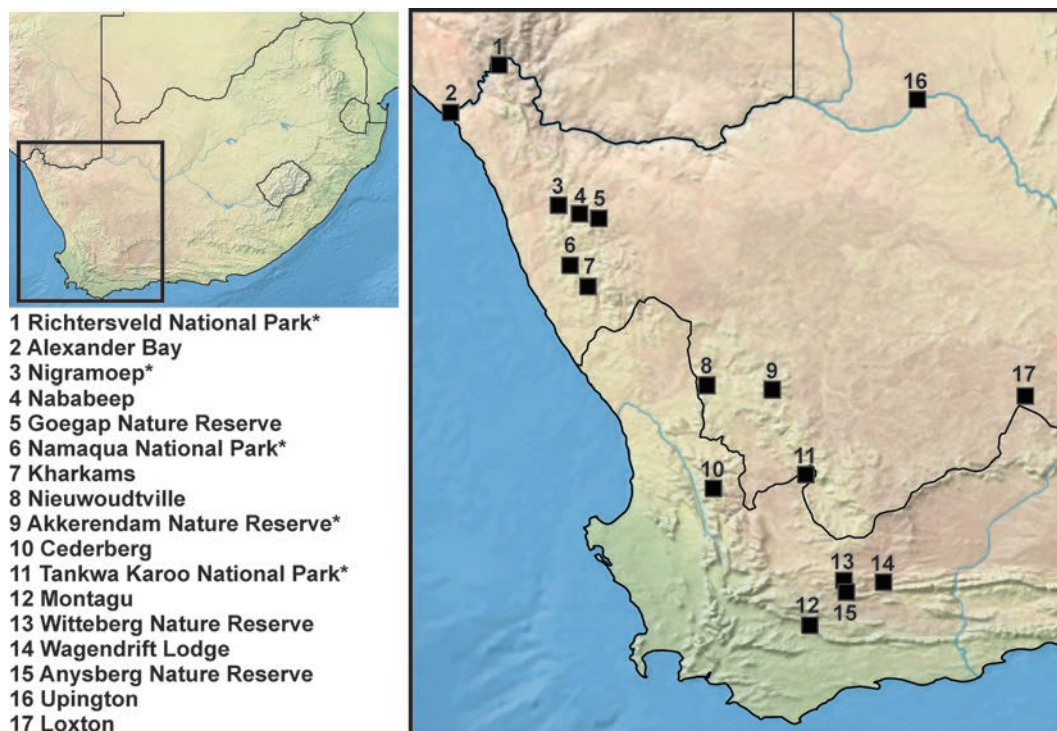


Figure 1. Map of South Africa, with enlargement indicating the 17 localities from which the Chrysillini examined in this study originated. Localities marked with * were sampled during the transect study.

Molecular analysis

As part of the deliverables for the transect project, leg tissues of representative specimens of all species collected in each of the five degree-squares were prepared for DNA barcoding (cytochrome oxidase subunit I, COI) by the Canadian Centre for DNA Barcoding, which conducted the extraction and sequencing following their standard protocols for arthropods (CCDB 2019). All the sequence data have been uploaded to the SPIZA (Spiders of South Africa) project on the Barcode of Life Data System (BOLD, www.boldsystems.org; Ratnasingham and Hebert 2007, 2013).

To assess the conspecificity of males and females of the species treated herein and support their taxonomic distinctness, we performed a phylogenetic analysis of COI sequences on the complete set of South African Chrysillini species on SPIZA, using *Massagris honesta* Wesolowska, 1993 (Hisponinae) to root the tree. All relevant data related to the specimens included in the phylogenetic analysis are presented in Appendix 1 (species, sex and process IDs of specimens, locality, depository number and sequence length), with the full collecting details of the specimens from western South Africa provided in the main text. To avoid excessively large clades in the tree, we only included a single male and female (wherever possible) for all described South African Chrysillini species not specifically treated in this paper. All individuals assigned to the species treated in this paper that were sequenced (marked with * in Appendix 1) were included, together with all their sequenced conspecifics from other localities in the country, to confirm their conspecificity. For all terminals, the species name, SPIZA sample ID, institutional depository and sampling location are provided in the tree (Fig. 2).

We used the “Sequence analysis” tool in BOLD to analyse the selected sequences (68 terminals in total), selecting the Kimura 2 Parameter distance model, Neigh-

bour-joining algorithm, aligning the sequences using Muscle (Edgar 2004) and a minimum overall overlap of 200 bp between sequences. To optimise the results, we only included sequences more than 500 bp in length, preferably those with the optimal length of 658 bp. The tree produced was further modified in Corel Draw X7.

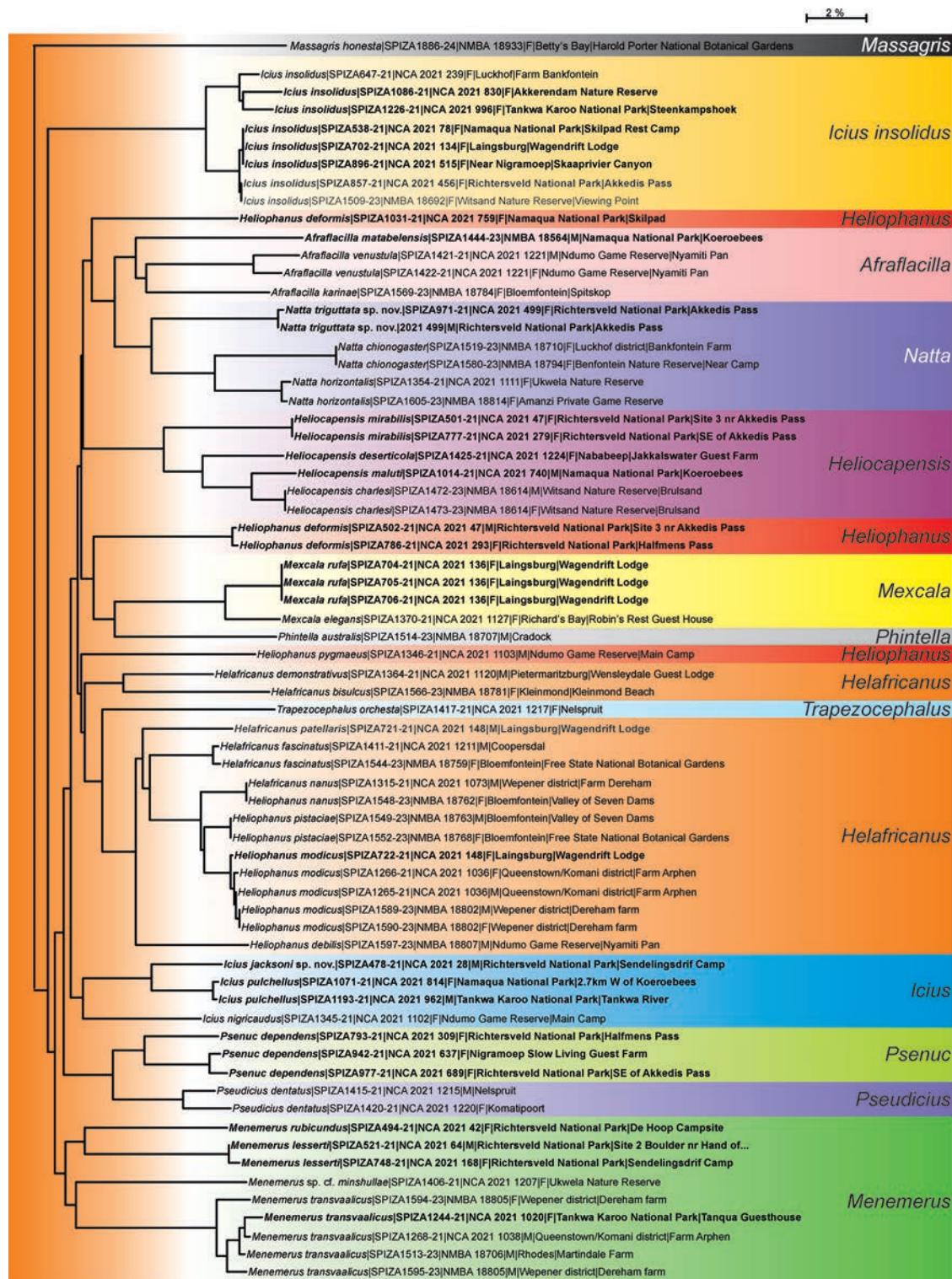


Figure 2. Phylogenetic tree of South African Chrysilini, based on cytochrome c oxidase subunit 1 (COI) sequences, with genera indicated in different colours. *Massagris honesta* (Hisponinae) was used as the outgroup to root the tree. Specimens in bold are treated in this paper. * - genus with possible contaminated sequence(s); ** possibly paraphyletic genus.

Phylogenetics

The analysis, based on the COI gene, found all of the genera of South African Chrysillini monophyletic based on the terminals included, with two exceptions (Fig. 2). *Heliophanus* C.L. Koch, 1833 *sensu stricto* (indicated by * in the tree), represented by two species (*H. deformis* Wesolowska, 1986 and *H. pygmaeus* Wesolowska & Russell-Smith, 2000) was polyphyletic, with two *H. deformis* forming a clade sister to *Mexcala* G. W. Peckham & E. G. Peckham, 1902 and one specimen as sister to a clade including *Afraflacilla* Berland & Millot, 1941 and *H. pygmaeus* as sister to a clade containing *Helaffricanus* and *Trapezocephalus* Berland & Millot, 1941. Considering the disparate placement of the specimen from Namaqua National Park (SPIZA1031-21), it is plausible that this sequence may have been contaminated.

Helaffricanus itself (indicated by ** in the tree) was represented by two clades, separated by *T. orchestra* (Simon, 1886); this result is not entirely surprising, as the first clade is represented by *H. bisulcus* (Wesolowska, 1986) and *H. demonstrativus* (Wesolowska, 1986), two species that are considerably larger than most other *Helaffricanus* and with a modified embolus and epigyne structure, similar to other members of the *marshalli* species group (Wesolowska 1986). It is quite plausible that these two species and other close relatives may represent another genus, but any decisions on their systematics and that of *Heliophanus sensu stricto* should be based on a more comprehensive molecular dataset.

Our results also support the placement of *Pseudicius matabelensis* Wesolowska, 2011 in a clade containing two *Afraflacilla* Berland & Millot, 1941 species, *A. karinae* (Haddad & Wesolowska, 2011) and *A. venustula* (Wesolowska & Haddad, 2009). As such, we propose the transfer of this species below. When Prószyński (2017) partially revised *Pseudicius* Simon, 1885, he transferred numerous African species to *Afraflacilla* and *Psenec* Prószyński, 2017, but a considerable proportion of species remaining unresolved and were retained in *Pseudicius*. As such, this proposed transfer here is only one step in resolving the placement of many of these untreated species.

Our tree also supports the placement of the three new species described in this paper in their respective genera, i.e. *Icius jacksoni* sp. nov., *Menemerus foordi* sp. nov. and *Natta triguttata* sp. nov. (Fig. 2). As such, we show that even a single gene (COI) can provide valuable information regarding the monophyly of genera and the placement of new species described therein.

Taxonomy

Family Salticidae Blackwall, 1841

Afraflacilla matabelensis (Wesolowska, 2011), comb. nov.

Pseudicius matabelensis Wesolowska, 2011: 338, figs 73–78.

Material examined. SOUTH AFRICA • Northern Cape Province; 2♂; Upington, Duine-in-die-Weg Guest Farm; -28.57, 21.77; 840 m a.s.l.; 24 Oct 2017; H. Badenhorst leg.; hand collecting; NCA 2020/18 • 1♀; same collection data as for preceding; -28.58, 21.78, 875 m a.s.l.; NCA 2020/21 • 1♂; Namaqua National Park,

Koeroebees; -30.1447, 17.7029; 240 m a.s.l.; 27 Mar 2022, C. Haddad et al. leg.; beating shrubs, dry river bed; NMBA 18564.

Distribution. A species described from Zimbabwe (Wesolowska 2011) and recently recorded from the KwaZulu-Natal and Northern Cape provinces of South Africa (Dippenaar-Schoeman et al. 2023). Recorded from two additional localities in the latter province here, indicating a broad distribution in southern Africa.

***Helafricanus modicus* (G. W. Peckham & E. G. Peckham, 1903)**

Heliophanus modicus Peckham & Peckham, 1903: 193, pl. 20, fig. 2; Wesolowska 1986: 25, figs 215–225.

Helafricanus modicus Wesolowska 2024: 82.

Material examined. SOUTH AFRICA • Western Cape Province; 1♀, together with 1♂ *H. patellaris*; Laingsburg District, Wagendrift Lodge; 33°22.782'S, 20°56.566'E; 510 m a.s.l.; 22 Jan 2021; C. Haddad et al. leg.; hand collecting, in garden; NCA 2021/148.

Distribution. A species previously known from Madagascar (Wesolowska 1986), Lesotho (Wesolowska and Haddad 2014) and the Eastern Cape, Free State and Western Cape provinces of South Africa (Dippenaar-Schoeman et al. 2023; World Spider Catalog 2024).

***Helafricanus patellaris* (Simon, 1901)**

Heliophanus patellaris Simon, 1901a: 541, fig. 667; Simon 1901b: 58, fig. 11; Wesolowska 1986: 22, figs 163–175; Wesolowska and Haddad 2014: 242, figs 30, 31, 49–55.

Helafricanus patellaris Wesolowska 2024: 81, fig. 1A–H.

Material examined. SOUTH AFRICA • Northern Cape Province; 1♂; Alexander Bay; 28°35'S, 16°29'E; 1 Nov 1970; M. Meyer leg.; hand collection; NCA 78/1688 • Western Cape Province • 1♂, together with 1♀ *H. modicus*; Laingsburg District, Wagendrift Lodge; 33°22.782'S, 20°56.566'E; 510 m a.s.l.; 22 Jan 2021; C. Haddad et al. leg.; hand collecting, in garden; NCA 2021/148.

Distribution. A species previously known from Lesotho (Wesolowska and Haddad 2014) and all the South African provinces, excluding Limpopo and North West (Dippenaar-Schoeman et al. 2023).

***Heliocapensis capensis* (Wesolowska, 1986)**

Heliophanus capensis Wesolowska, 1986: 12, figs 12–17.

Heliocapensis capensis Wesolowska 2024: 84.

Material examined. SOUTH AFRICA • Northern Cape Province; 2♀; Nieuwoudtville, Farm Papkuilsfontein; 31°22'S, 19°06'E; 26 Aug 2008; A. Russell-Smith leg.; under shrubs; NCA 2016/28.

Distribution. A species previously known from several localities in the Northern and Western Cape in South Africa (Dippenaar-Schoeman et al. 2023).

***Heliocapensis deserticola* (Simon, 1901)**

Heliophanus deserticola Simon, 1901b: 59, fig. 13; Wesolowska 1986: 12, figs 4–9; Prószyński 2017: 31, fig. 13H.

Heliocapensis deserticola Wesolowska 2024: 84.

Material examined. SOUTH AFRICA • Northern Cape Province; 1♀; Goegap Nature Reserve, Reception Office; 29°39.905'S, 17°59.827'E; 16 Jul 2017; R. Booysen leg.; beating; NCA 2017/1284 • 1♀; Namaqua National Park, Near Skilpad Rest Camp; -30.1661, 17.7685; 610 m a.s.l.; 28 Mar 2023; C. Haddad et al. leg.; leaf litter, north-facing hillside; NMBA 18551 • 1♀; Near Nababeep, Jakkalswater Guest Farm; 29°37'S, 17°48'E; 910 m a.s.l.; 22 Aug 2020; P. Webb leg.; hand collecting; NCA 2021/1224.

Distribution. Previously recorded from the Eastern Cape, Northern Cape and Mpumalanga provinces of South Africa (Dippenaar-Schoeman et al. 2023).

***Heliocapensis maluti* (Wesolowska & Haddad, 2014)**

Fig. 3A, D

Heliophanus maluti Wesolowska & Haddad, 2014: 241, figs 28, 29, 41–47.

Heliocapensis maluti Wesolowska 2024: 84.

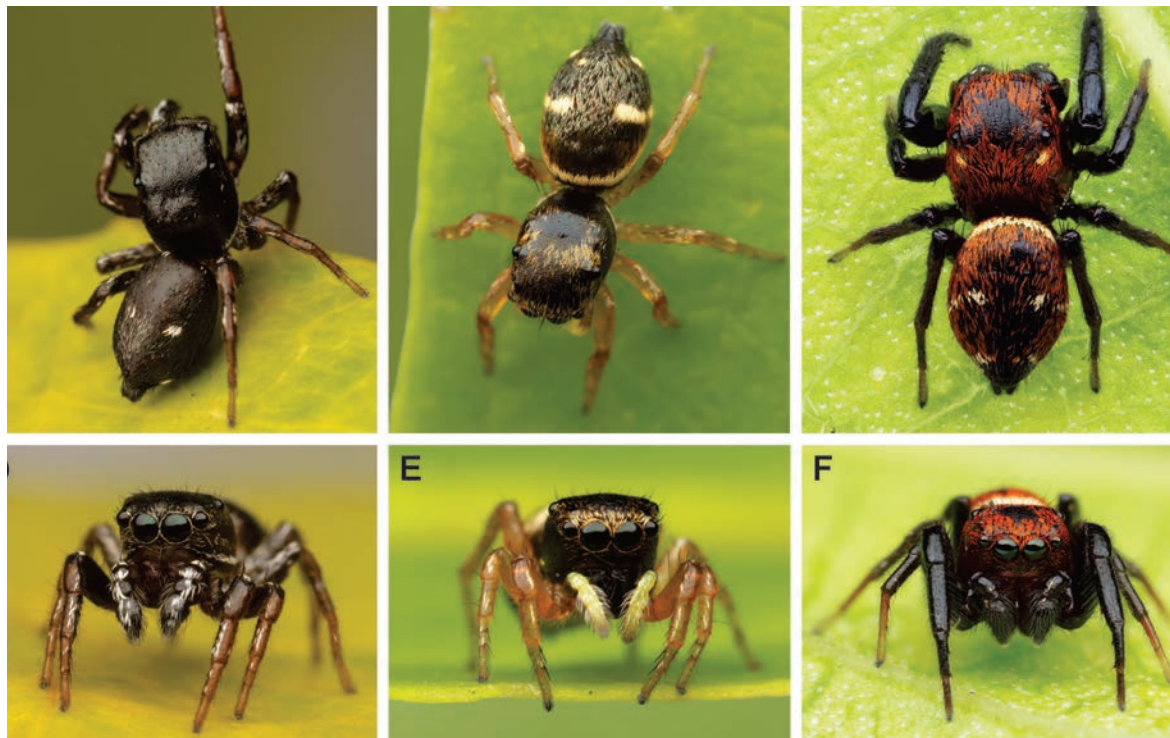


Figure 3. Dorsal habitus (A–C) and anterior view (D–F) of living *Heliocapensis maluti* Wesolowska & Haddad, 2014 male (A, D), *H. mirabilis* (Wesolowska, 1986) female (B, E) and *Heliophanus deformis* Wesolowska, 1986 male (C, F).

Material examined. SOUTH AFRICA • Northern Cape Province; 1 ♂; Namaqua National Park, Koeroebees; 30°08.683'S, 17°42.177'E; 240 m a.s.l.; 14 Jan 2021; C. Haddad et al. leg.; beating short shrubs, dry river bed; NCA 2021/740 • 1 ♂; same collection data as for preceding; NMBA 19849.

Description. See Wesolowska and Haddad (2014) for a description of both sexes. General appearance of live male as in Fig. 3A, D.

Distribution. A species previously known only from the montane enclave of Lesotho, recorded from South Africa for the first time (Wesolowska and Haddad 2014; Dippenaar-Schoeman et al. 2023).

***Heliocapensis mirabilis* (Wesolowska, 1986)**

Figs 3B, E, 4, 5

Heliophanus mirabilis Wesolowska, 1986: 14, figs 50–53; Haddad and Wesolowska 2013: 480, figs 44–47, 53.

Heliocapensis mirabilis Wesolowska 2024: 85.

Material examined. SOUTH AFRICA • Northern Cape Province; 1 ♂ 5 ♀; Richtersveld National Park, Halfmens Pass; 28°07.789'S, 16°57.667'E; 235 m a.s.l.; 8 Jan 2021; C. Haddad et al. leg.; leaf litter, open plain; NCA 2021/292 • 2 ♀; same collection data as for preceding; NCA 2021/304 • 2 ♂ 3 ♀; same locality; 10 Jul 2021; C. Haddad et al. leg.; beating short shrubs, open plain; NCA 2021/414 • 4 ♀; Richtersveld National Park, near Akkedis Pass; 28°07.884'S, 16°59.700'E; 330 m a.s.l.; 6 Jan 2021; C. Haddad et al. leg.; beating, karroid bushes; NCA 2024/17 • 1 ♀; Richtersveld National Park, Near Hand of God; 28°05.874'S, 16°58.736'E; 35 m a.s.l.; 6 Jan 2021; C. Haddad et al. leg.; hand collecting, under rocks; NCA 2021/66 • 3 ♂ 3 ♀ Richtersveld National Park, SE of Akkedis Pass; 28°11.123'S, 17°02.543'E; 535 m a.s.l.; 7 Jul 2021; C. Haddad et al. leg.; leaf litter, dry river bed; NCA 2021/354 • 1 ♂ 1 ♀; same collection data as for preceding; NCA 2021/389 • 7 ♀; same collection data as for preceding; 7 Jan 2021; NCA 2021/279 • 1 ♀; same collection data as for preceding; NCA 2021/267 • 4 ♂; same collection data as for preceding; NCA 2021/280 • 5 ♀ (together with 1 ♂ *Heliophanus deformis*); Richtersveld National Park, Site 3 near Akkedis Pass; 28°07.882'S, 16°59.700'E; 330 m a.s.l.; 6 Jan 2021; C. Haddad et al. leg.; beating, karroid bushes; NCA 2021/471 • 1 ♀; Richtersveld National Park, Sendelingsdrif Camp, 28°07.496'S, 16°53.445'E; 40 m a.s.l.; 8 Jan 2021; C. Haddad & R. Booyesen leg.; hand collecting at night; NCA 2021/34.

Diagnosis of female. The female can be distinguished from its congeners by the course of the seminal ducts, which initially run anteriorly from the epigynal depressions (Fig. 5E), while posteriorly in other species.

Description. For description of the male, see Haddad and Wesolowska (2013). General appearance of male in alcohol as in Fig. 4A, B; palpal organ in Figs 4C–E, 5A–C.

Female: Measurements: Cephalothorax length 1.6–1.8, width 1.1–1.2, height 0.5–0.6. Abdomen length 1.6–2.5, width 1.1–1.7. Eye field length 0.6, anterior width 1.0, posterior width 1.1. General appearance of live female as in Fig. 3B, E, of female in alcohol in Fig. 4F. Carapace dark brown, clothed in yellowish-grey scale-like hairs, eye field black, amongst scales some long brown bristles. Mouthparts and sternum dark brown. Abdomen black, covered with

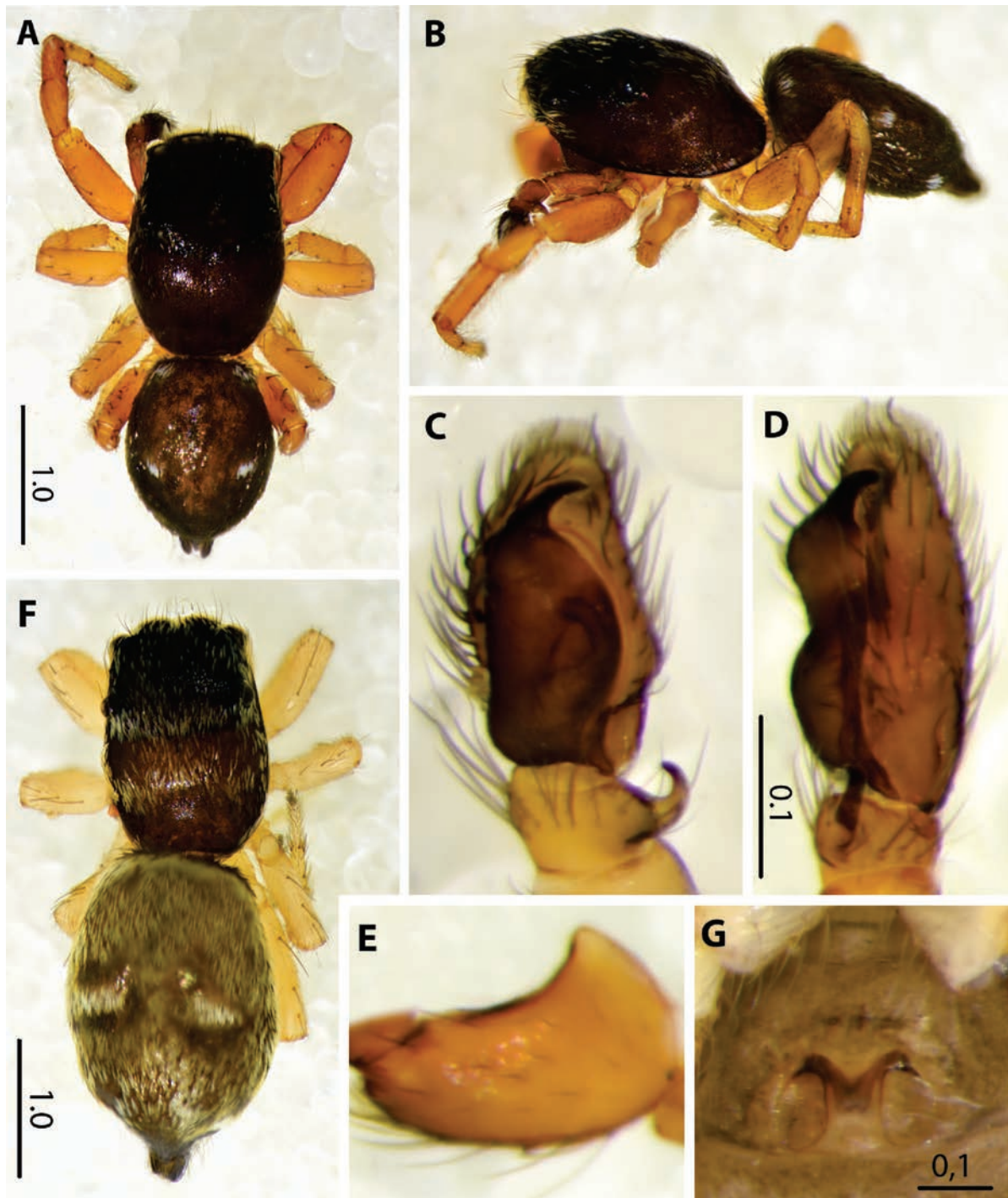


Figure 4. *Heliocapensis mirabilis* (Wesolowska, 1986), male (A–E) and female (F, G): A, F general appearance, dorsal view B same, lateral view C palpal organ, ventral view D same, retrolateral view E palpal femur G epigyne, ventral view.

greyish scales, pair of diagonal or rounded white spots at mid-point, some specimens also with single pair of small spots posteriorly. Venter dark grey, spinnerets black. Legs yellow. Epigyne with pair of large, rounded depressions (Figs 4G, 5D). Internal structure as in Fig. 5E.

Distribution. Species previously known from the Western Cape in South Africa (Dippenaar-Schoeman et al. 2023), recorded from the Northern Cape for the first time.

Remark. The female of this species is described here for the first time.

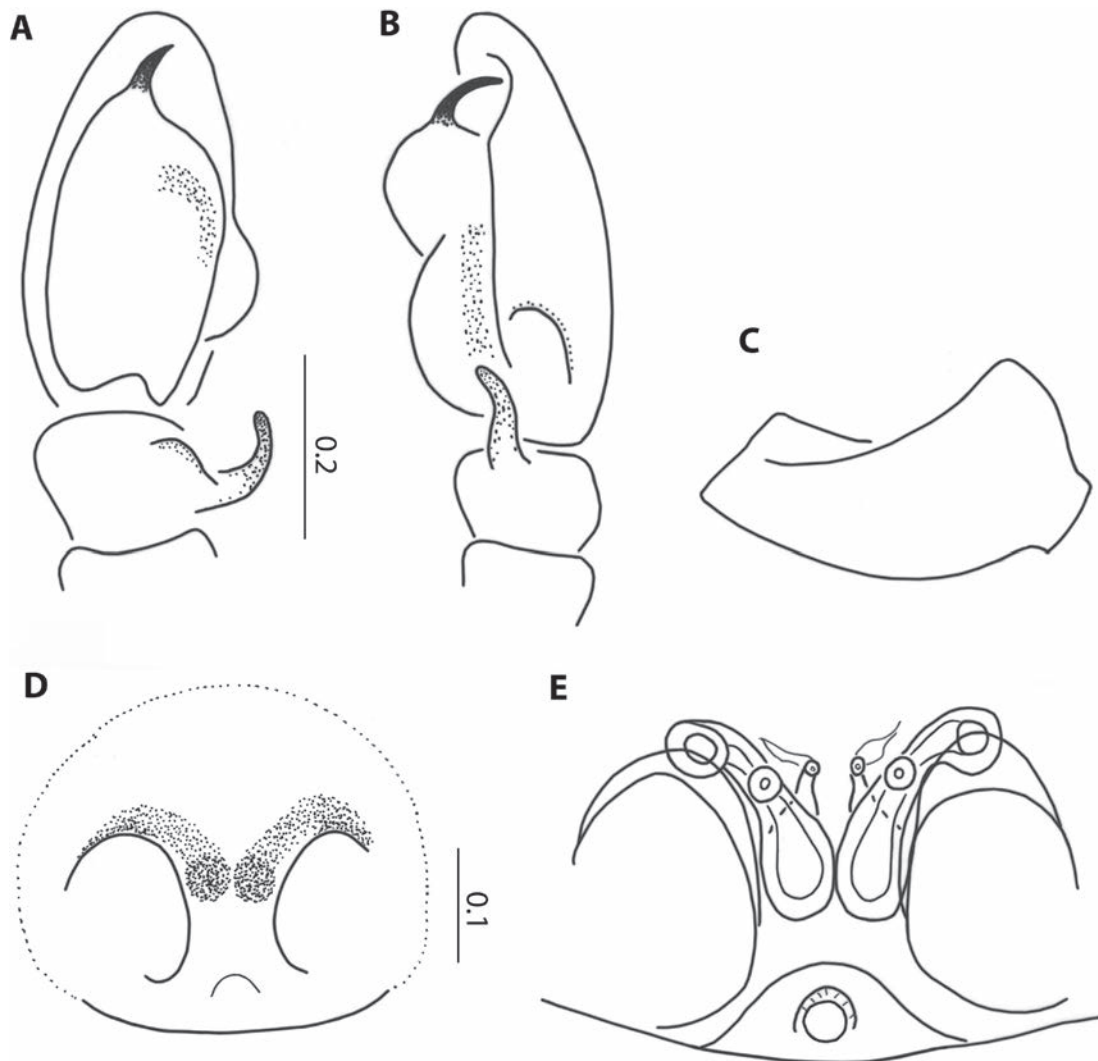


Figure 5. *Heliocapensis mirabilis* (Wesołowska, 1986), male (**A–C**) and female (**D, E**): **A** palpal organ, ventral view **B** same, retrolateral view **C** palpal femur **D** epigyne, ventral view **E** internal structure of epigyne.

***Heliocapensis redimitus* (Simon, 1910)**

Fig. 6

Heliophanus redimitus Simon, 1910: 216; Wesołowska 1986: 12, figs 10, 11.

Heliocapensis redimitus Wesołowska 2024: 85.

Material examined. SOUTH AFRICA • Northern Cape Province; 1♀; Goegap Nature Reserve; 29°41'18"S, 17°57'57"E; 16 Jul 2017; R. Booysen leg.; beating shrubs; NCA 2017/1284.

Re-description. Female: Measurements: Cephalothorax length 1.7, width 1.2, height 0.6. Abdomen length 2.2, width 1.5. Eye field length 0.7, anterior width 1.1, posterior width 1.2. General appearance in alcohol as in Fig. 6A. Carapace dark brown, clothed in whitish hairs and brown bristles, thin white line along lateral edges of carapace, eye field black, reticulate punctured, anterior eyes rounded by white scales. Sternum and mouthparts brown. Abdomen brown, covered with dark hairs, with thin white streak along anterior edge, pair of round white stains in middle of abdomen. Venter brownish, spinnerets black.

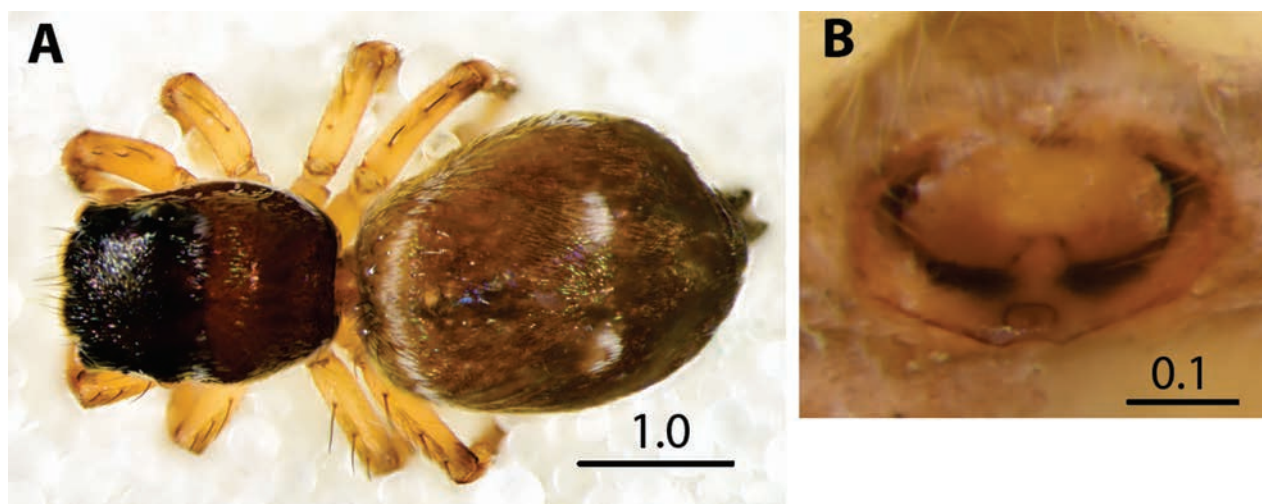


Figure 6. *Heliocapensis redimitus* (Simon, 1910), female: **A** general appearance of female, dorsal view **B** epigyne, ventral view.

Legs dark yellow, spines and hairs brown. Epigyne oval, wide and short, with large central depression (Fig. 6B). Copulatory openings placed laterally, at borders of depression, internal structure simple (see fig. 11 in Wesolowska 1986).

Distribution. This species was previously known from the type locality, Komaggas (Wesolowska 1986; Haddad and Marusik 2019), approximately 45 km west of this recently collected specimen. This is only the second record of the species.

***Heliophanus deformis* Wesolowska, 1986**

Figs 3C, F, 7, 8

Heliophanus deformis Wesolowska, 1986: 226, figs 819–824.

Material examined. SOUTH AFRICA • Northern Cape Province; 1♀; Namaqua National Park, Skilpad; 30°09.868'S, 17°47.282'E; 730 m a.s.l.; 13 Jan 2021; C. Haddad et al. leg.; beating shrubs; NCA 2021/759 • 1♂ 3♀; Richtersveld National Park, Halfmens Pass; 28°07.789'S, 16°57.667'E; 235 m a.s.l.; 8 Jan 2021, C. Haddad et al. leg.; open area; NCA 2021/305 • 1♂ 1♀; same collection data as for preceding; NCA 2021/293 • 5♂ 1♀; same collection data as for preceding; 10 Jul 2021; NCA 2021/423 • 2♂; Richtersveld National Park, SE of Akkedis Pass; 28°11.123'S, 17°02.543'E; 535 m a.s.l.; 7 Jan 2021; C. Haddad et al. leg.; beating short shrubs; NCA 2021/283 • 1♂ same collection data as for preceding; 7 Jul 2021; NCA 2021/501 • 1♂ (together with 5♀ *Heliocapensis mirabilis*); Richtersveld National Park, Site 3 near Akkedis Pass; 28°07.882'S, 16°59.700'E; 330 m a.s.l.; 6 Jan 2021; C. Haddad et al. leg.; beating, karoid bushes; NCA 2021/47.

Re-description. Male: Cephalothorax length 1.5, width 1.3, height 0.8. Abdomen length 1.6, width 1.3. Eye field length 0.7, anterior and posterior width 1.0. General appearance of live male as in Fig. 3C, F, of male in alcohol Fig. 7A, B. Carapace brown, covered with dense reddish-orange scale-like hairs, white scales on lateral slopes and behind eye field, with long brown bristles near anterior eyes. Mouthparts and sternum brown. Abdomen also clothed in dense

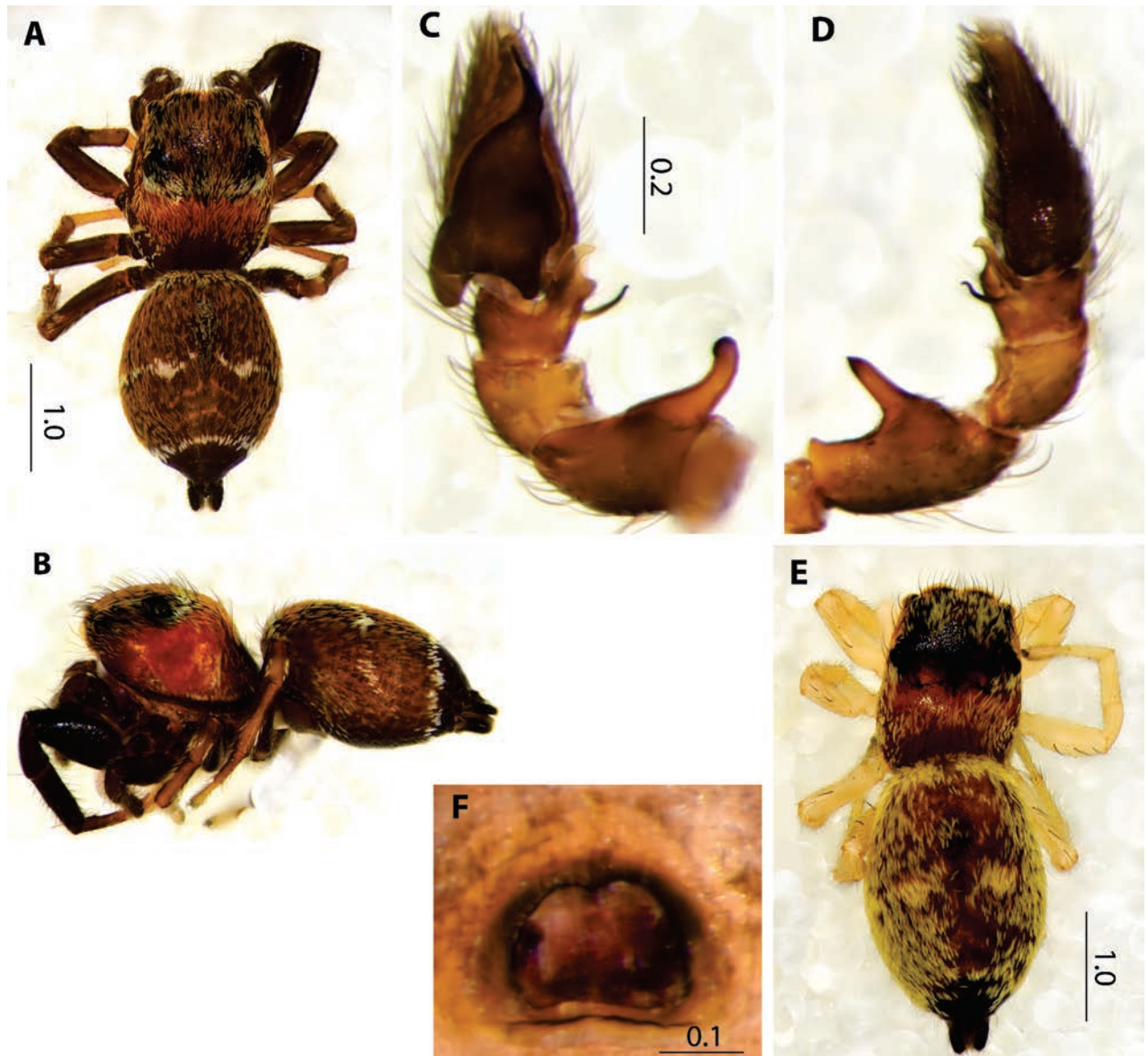


Figure 7. *Heliophanus deformis* Wesolowska, 1986, male (A–D) and female (E, F): A, E general appearance, dorsal view B same, lateral view C palpal organ, ventral view D same, retrolateral view F epigyne, ventral view.

reddish scales, with three narrow white streaks; first along anterior edge, second at middle and last near abdominal end. Posterior part of abdomen dark brown, without hairs, spinnerets black. Venter of abdomen brown. First pair of legs black, others brown with darker femora. Palps brown, some white scales on cymbium. Palpal organ as in Figs 7C, D, 8A–C, femur with large apophysis. Tibia with two apophyses, one of them very thin (Figs 7C, 8A).

Female: Cephalothorax length 1.5, width 1.3, height 0.6. Abdomen length 2.0, width 1.5. Eye field length 0.7, anterior and posterior width 1.0. General appearance as in Fig. 7E. Colouration similar to male, body clothed in dense golden orange scale-like hairs. No white scales on dorsum, but present on ventral surface of abdomen. Legs yellow. Epigyne with deep large heart-shaped depression (Figs 7F, 8D). Internal structure simple, as in Fig. 8E.

Distribution. A species previously only known from Angola (Wesolowska 1986); recorded from South Africa for the first time.

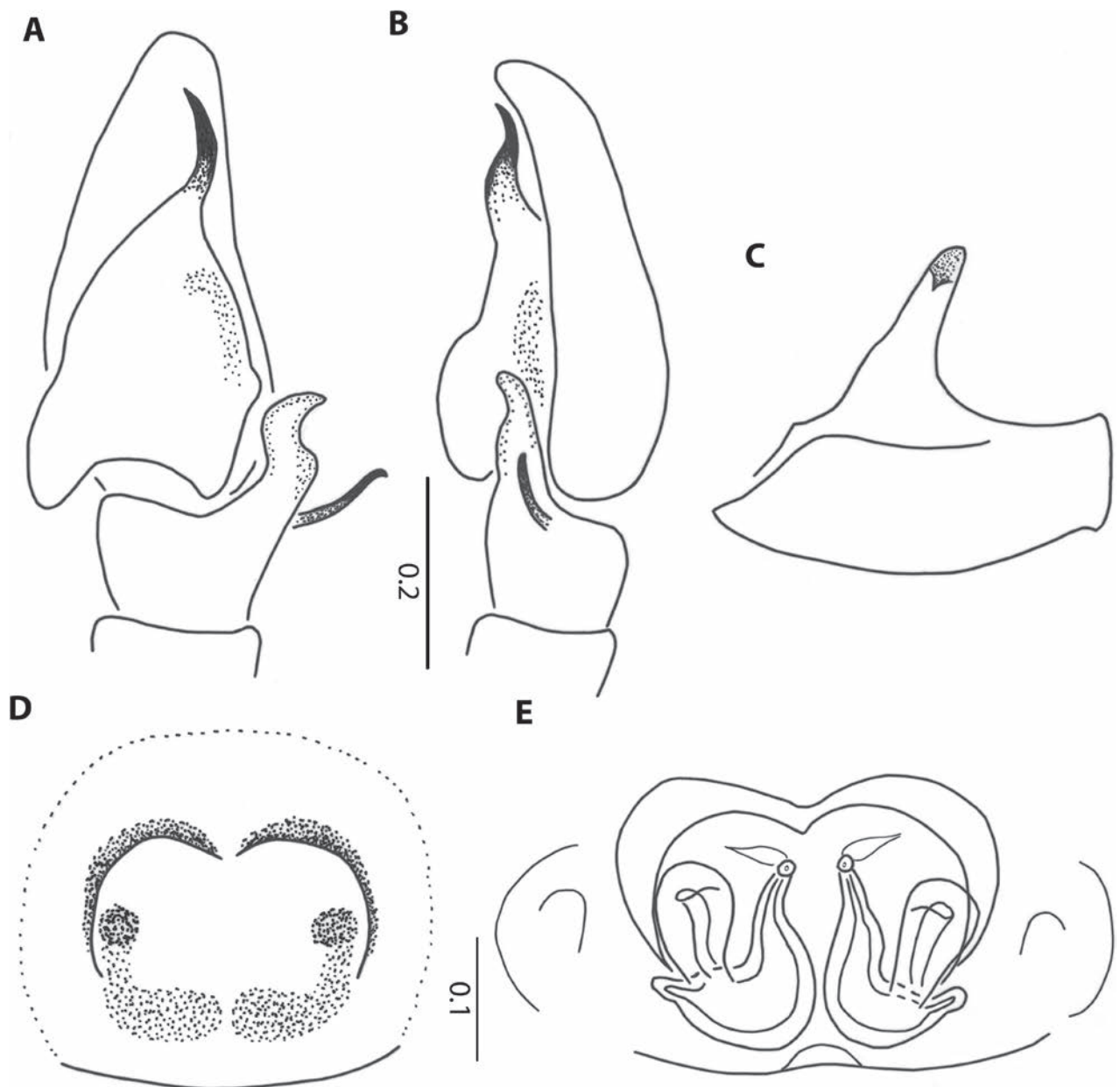


Figure 8. *Heliophanus deformis* Wesolowska, 1986, male (A–C) and female (D, E): A palpal organ, ventral view B same, lateral view C palpal femur D epigyne, ventral view E internal structure of epigyne.

***Icius insolidus* (Wesolowska, 1999)**

Fig. 9

Menemerus insolidus Wesolowska, 1999: 299, figs 158–161.

Icius insolidus Wesolowska 2006: 234, figs 43–52; Haddad and Wesolowska 2011: 75, figs 45–46, 55–56.

Material examined. SOUTH AFRICA • Northern Cape Province; 1♀; Calvinia, Akkerendam Nature Reserve; 31°24.896'S, 19°46.728'E; 1095 m a.s.l.; 16 Jan 2021; C. Haddad et al. leg.; leaf litter, dry river bed; NCA 2021/830 • 1♂; Same locality; 31°24.643'S, 19°46.077'E; 1235 m a.s.l.; 17 Jan 2021; C. Haddad et

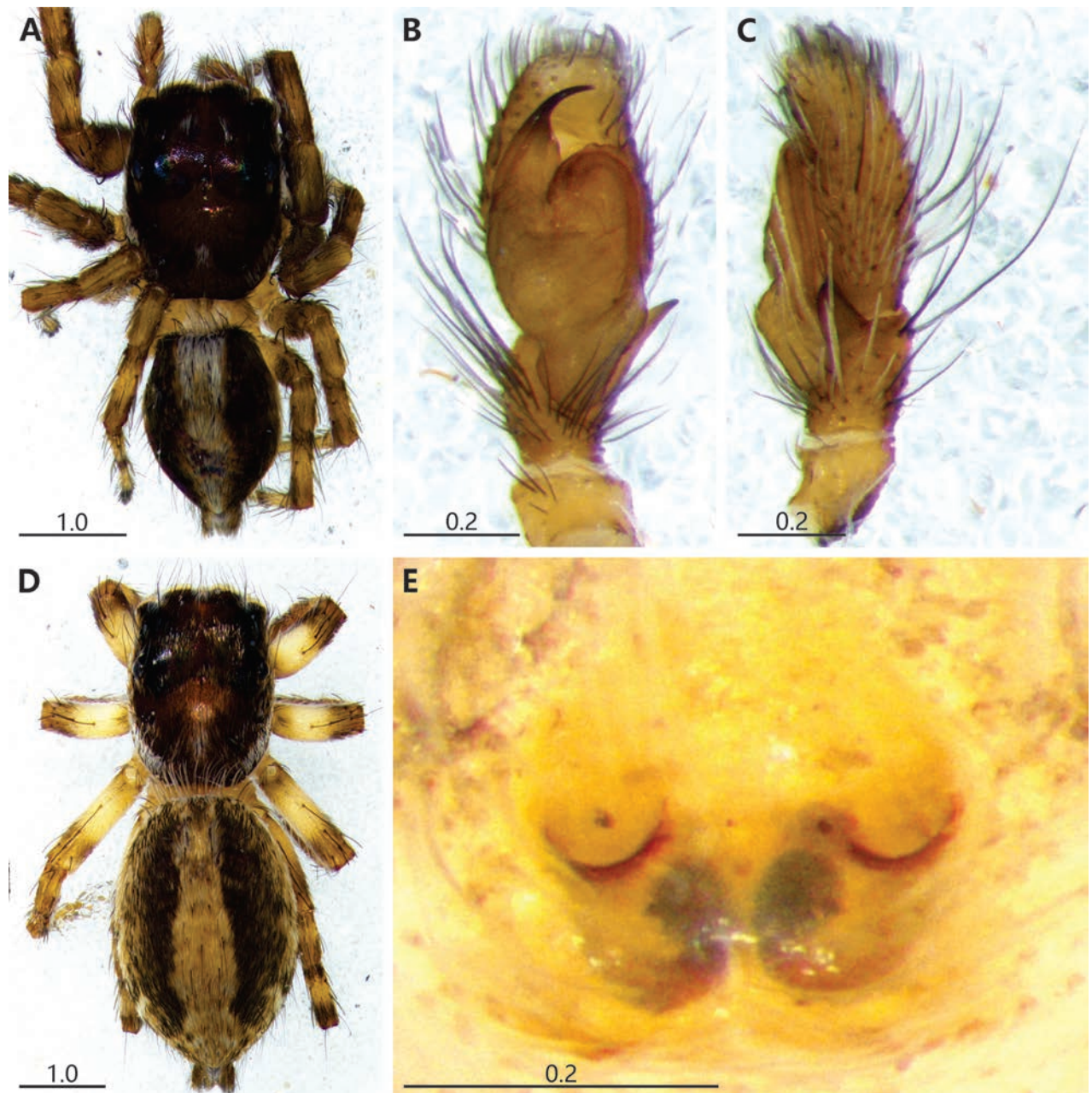


Figure 9. *Icius insolidus* (Wesolowska, 1999), male (A–C) and female (D, E): **A, D** general appearance, dorsal view **B** palpal organ, ventral view **C** same, retrolateral view **E** epigyne, ventral view.

al. leg.; beating shrubs, east-facing slope; NCA 2021/896 • 1♀; Kharkams, Kharkams High School; 30°21.665'S, 17°53.201'E; 735 m a.s.l. ; 5 Jul 2021; C. Haddad leg.; hand collecting, under rocks; NMBA 19882 • 1♀; Namaqua National Park, 1.7 km WSW of Skilpad Rest Camp; 30°10.044'S, 17°45.674'E; 575 m a.s.l.; 13 Jan 2021; C. Haddad et al. leg.; beating short shrubs, east-facing slope; NCA 2021/795 • 1♂; Namaqua National Park, Koeroebes; 30°08.683'S, 17°42.177'E; 240 m a.s.l.; Apr 2022; C. Haddad & R. Booysen leg.; hand collecting; NMBA 19921 • 1♀; Namaqua National Park, Skilpad Rest Camp; 30°09.802'S, 17°46.671'E; 725 m a.s.l.; 14 Jan 2021; C. Haddad & R. Booysen leg.; hand collecting, at night around houses; NCA 2021/78 • 1♀;

near Nigramoep, Skaaprivier Canyon; 29°33.130'S, 17°39.135'E; 690 m a.s.l.; 10 Jan 2021; C. Haddad et al. leg.; beating shrubs, river bed; NCA 2021/515 • 1♀; Nigramoep Slow Living Guest Farm; 29°31.869'S, 17°35.150'E; 745 m a.s.l.; 9 Jan 2021; C. Haddad et al. leg.; leaf litter, open plain; NCA 2021/532 • 1♀; Richtersveld National Park, Akkedis Pass; 28°10.772'S, 17°02.173'E; 600 m a.s.l.; 8 Jan 2021; C. Haddad et al. leg.; under rocks, west-facing slope; NCA 2021/342 • 1♀; Richtersveld National Park, Akkedis Pass; 28°10.673'S, 17°01.863'E; 540 m a.s.l.; 8 Jul 2021; C. Haddad et al. leg.; beating short shrubs, east-facing slope; NCA 2021/456 • 1♀; Richtersveld National Park, Akkedis Pass; 28°10.577'S, 17°02.069'E; 645 m a.s.l.; 9 Jul 2021; C. Haddad et al. leg.; under rocks, west-facing slope; NCA 2021/489 • 1♀; Tankwa Karoo National Park, Steenkampshoek; 32°16.737'S, 20°09.622'E; 860 m a.s.l.; 19 Jan 2021; C. Haddad et al. leg.; leaf litter, east-facing slope; NCA 2021/996 • 1♂ 1♀; 12 miles W of Upington; 28°27'S, 21°15'E; 12 Apr 1970; B. Lamoral leg.; NMSA 26500 • Western Cape Province; 1♂; Laingsburg District, Wagendrift Lodge; 33°22.446'S, 20°54.247'E; 580 m a.s.l.; 6 Oct 2015; Z. Mbo leg.; hand collecting, under rocks; NCA 2016/2692 • 1♀; Same locality; 33°22.943'S, 20°54.711'E; 530 m a.s.l.; 5 Oct 2015; Z. Mbo leg.; hand collecting, under rocks; NCA 2016/2703 • 3♀; Same locality; 33°22.861'S, 20°56.910'E; 520 m a.s.l.; 22 Jan 2021; C. Haddad et al. leg.; hand collecting, under rocks in veld; NCA 2021/134.

Description. For description of male, see Wesolowska (2006); for female, see Wesolowska (1999). General appearance of male in alcohol in Fig. 9A, palp in ventral and retrolateral views in Fig. 9B, C, respectively; general habitus of female in Fig. 9D, ventral epigyne in Fig. 9E.

Distribution. A common species widespread in South Africa, having been recorded from all the provinces except the Western Cape (Dippenaar-Schoeman et al. 2023), from which it is recorded here for the first time.

***Icius jacksoni* sp. nov.**

<https://zoobank.org/89040F85-2AC6-48BA-9B1D-265D0E26BE93>

Figs 10, 11

Material examined. Holotype: SOUTH AFRICA • ♂; Northern Cape Province; Richtersveld National Park, Sendelingsdrift camp; 28°07.494'S, 16°35.454'E; 40 m a.s.l.; 8 Jan 2021; C. Haddad & R. Booysen leg.; hand collecting; NCA 2021/28.

Diagnosis. This species has a male palp similar to that of *Icius hamatus* (C.L. Koch, 1846), but differs in the absence of the anterior lobe of the bulb at the base of the embolus (present in *I. hamatus*), as well as the notch between the two branches of the apophysis, which is V-shaped in *I. jacksoni* sp. nov., while U-shaped in *I. hamatus* (cf. Fig. 10B with fig. 2 in Andreeva et al. 1984). *Icius jacksoni* (Fig. 10B) also differs by the shape of the tibial apophysis from *I. pulchellus* Haddad & Wesolowska, 2011 (fig. 61 in Haddad and Wesolowska 2011) and *I. minimus* Wesolowska & Tomasiewicz, 2008 from Ethiopia (fig. 73 in Wesolowska and Tomasiewicz 2008). *Icius jacksoni* sp. nov. is one of the smallest species in the genus.

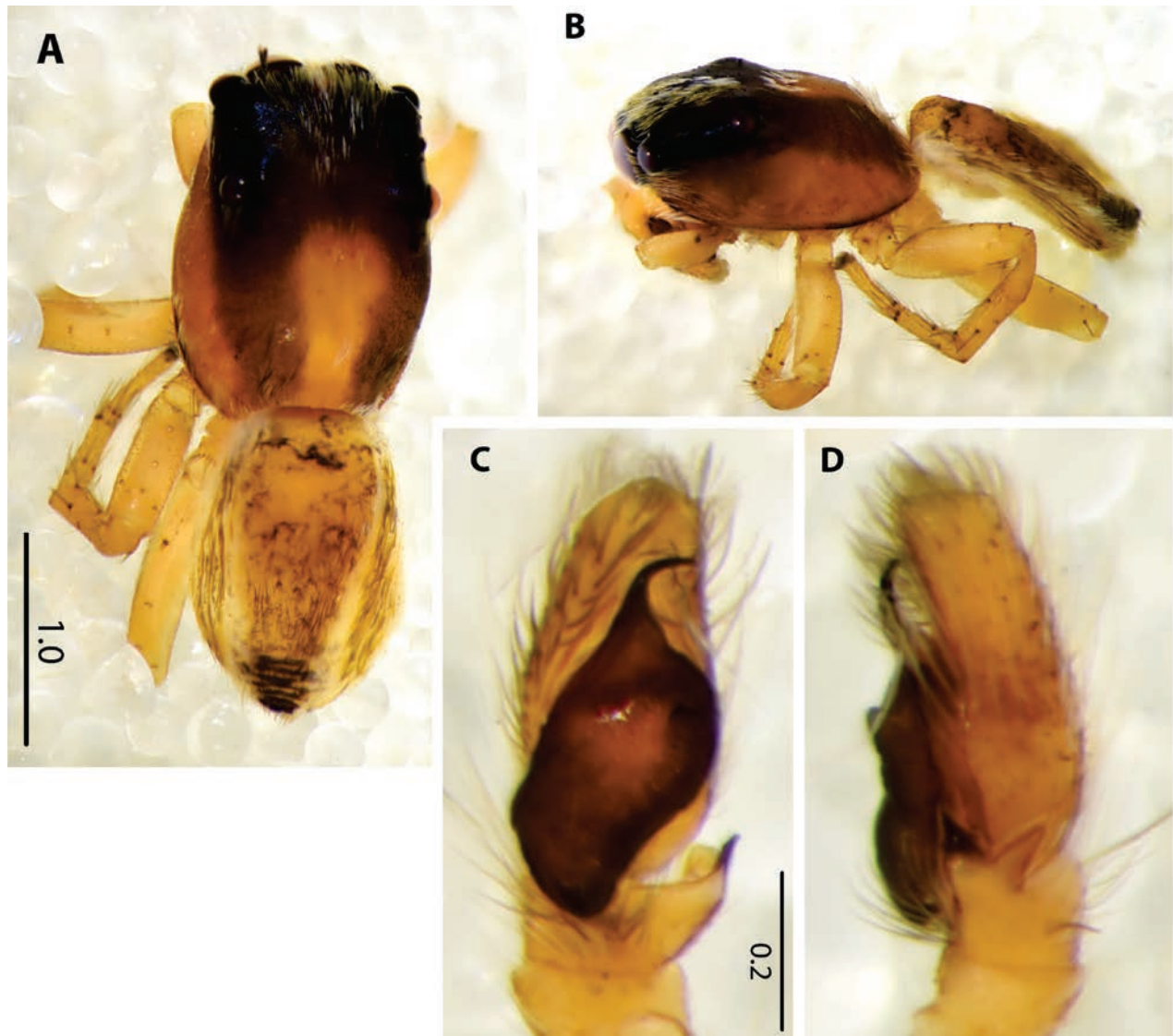


Figure 10. *Icius jacksoni* sp. nov., male, holotype: **A** general appearance, dorsal view **B** same, lateral view **C** palpal organ, ventral view **D** same, retrolateral view.

Description. Male: Measurements: Cephalothorax length 1.7, width 1.3, height 0.6. Abdomen length 1.3, width 1.1. Eye field length 0.8, anterior width 1.1, posterior width 1.2. General appearance in alcohol as in Fig. 10A, B, diminutive spider. Carapace light brown with two darker streaks on thoracic part, eye field black, clothed in white hairs. Anterior median eyes surrounded by white hairs from bottom, clypeus also with white hairs. Mouthparts light brown, sternum yellow. Abdomen oval, brownish, with two thin white strips laterally, sides brownish with light marks, end of abdomen blackish, venter and spinnerets light yellow. Legs yellow. Palpal organ as in Figs 10C, D, 11A, B, bulb oval, embolus short, tibial apophysis wide, with deep V-shaped notch.

Female: Unknown.

Etymology. This species is named for Robert Jackson, in recognition of his unparalleled contribution to our understanding of jumping spider biology over a career spanning five decades.

Distribution. Only known from the type locality.

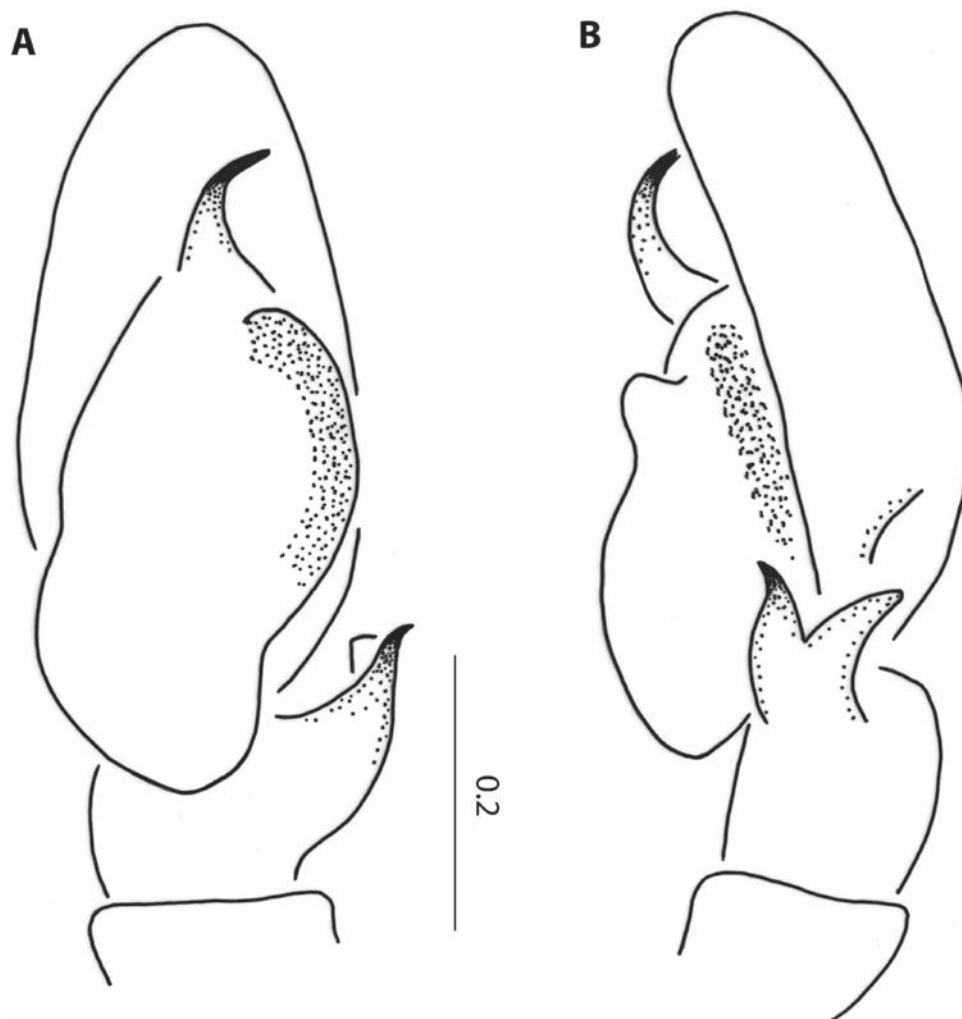


Figure 11. *Icius jacksoni* sp. nov., male, holotype: **A** palpal organ, ventral view **B** same, lateral view.

***Icius pulchellus* Haddad & Wesolowska, 2011**

Figs 12A, B, D, E, 13, 14

Icius pulchellus Haddad & Wesolowska, 2011: 76, figs 47 and 57–62.

Material examined. SOUTH AFRICA • Northern Cape Province; 2♀; Namaqua National Park, 2.7 km W of Koeroebees; 30°08.683'S, 17°42.177'E; 345 m a.s.l.; 14 Jan 2021; C. Haddad et al. leg.; beating short shrubs; NCA 2021/814 • 3♂ 8♀; Tankwa Karoo National Park, Paulshoek; 32°16.556'S, 20°06.626'E; 500 m a.s.l.; 20 Jan 2021; C. Haddad et al. leg.; beating shrubs, open plain; NCA 2021/976 • 2♂ 3♀; Tankwa Karoo National Park, Tankwa River; 32°24.598'S, 20°20.215'E; 375 m a.s.l.; 20 Jan 2021; C. Haddad et al. leg.; beating shrubs, river bed; NCA 2021/962.

Diagnosis of female. The female of this species has an epigyne somewhat similar to that in *Icius minimus* but has the spermathecae placed parallel to the posterior edge of the epigyne, while in *I. minimus* they lie obliquely (compare Fig. 14B with fig. 81 in Wesolowska and Tomasiewicz 2008). These species also differ in carapace colour: in *I. minimus*, white hairs create a cross pattern in the eye field (fig. 78 in Wesolowska and Tomasiewicz 2008), while *I. pulchellus* has a dark eye field (Fig. 13D–G).

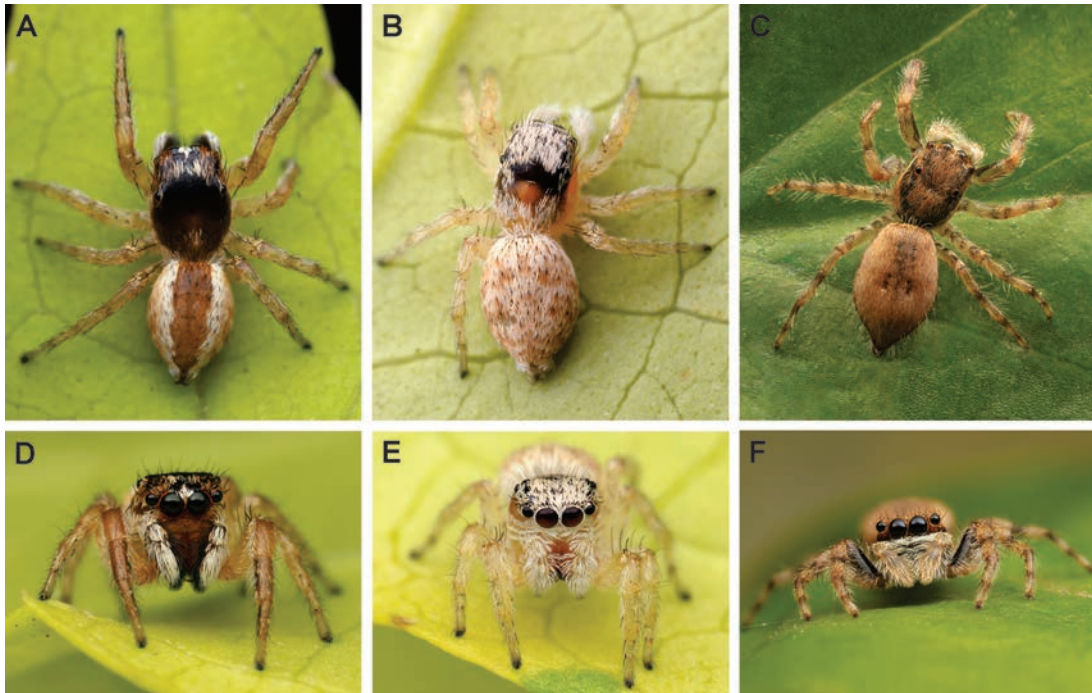


Figure 12. Dorsal habitus (A–C) and anterior view (D–F) of living *Icius pulchellus* Haddad & Wesolowska, 2013 female (A, D) and male (B, E) and *Menemerus foordi* sp. nov. subadult male (C, F).

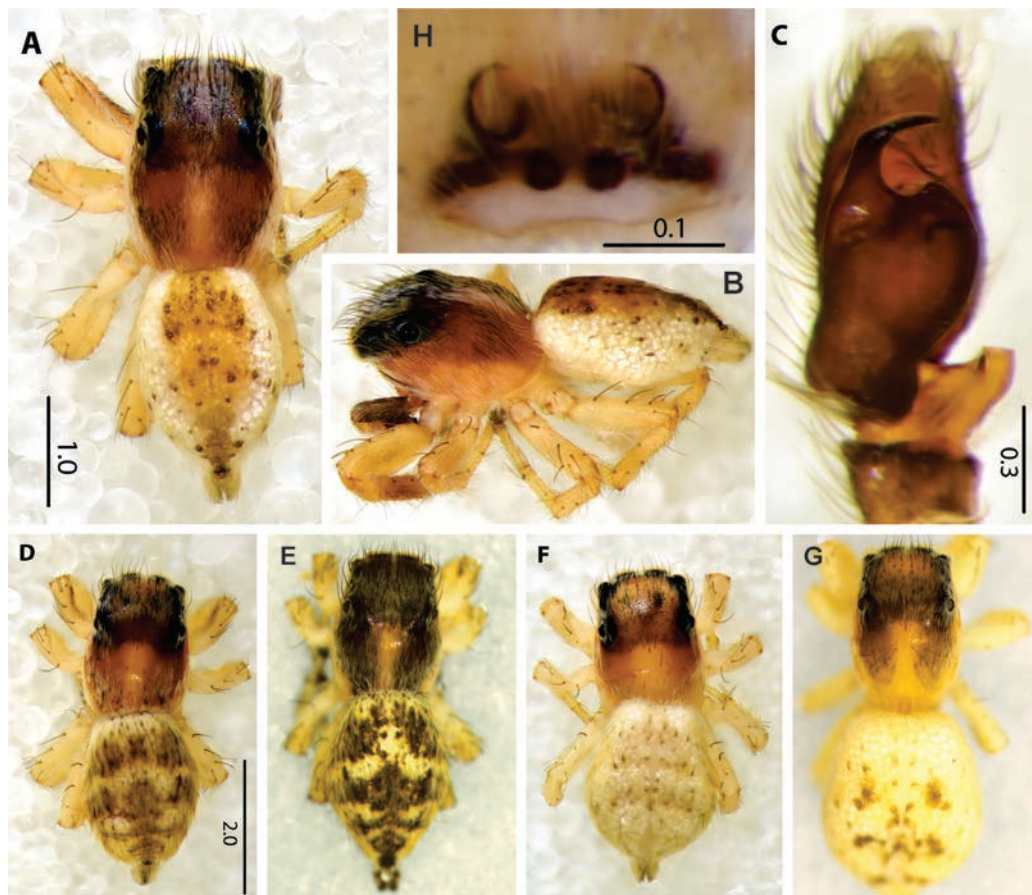


Figure 13. *Icius pulchellus* Haddad & Wesolowska, 2011, male (A–C) and female (D–H): A, D–G general appearance, dorsal view B same, lateral view C palpal organ, ventral view H epigyne, ventral view D, E are dark variants of the female and F, G are pale variants.

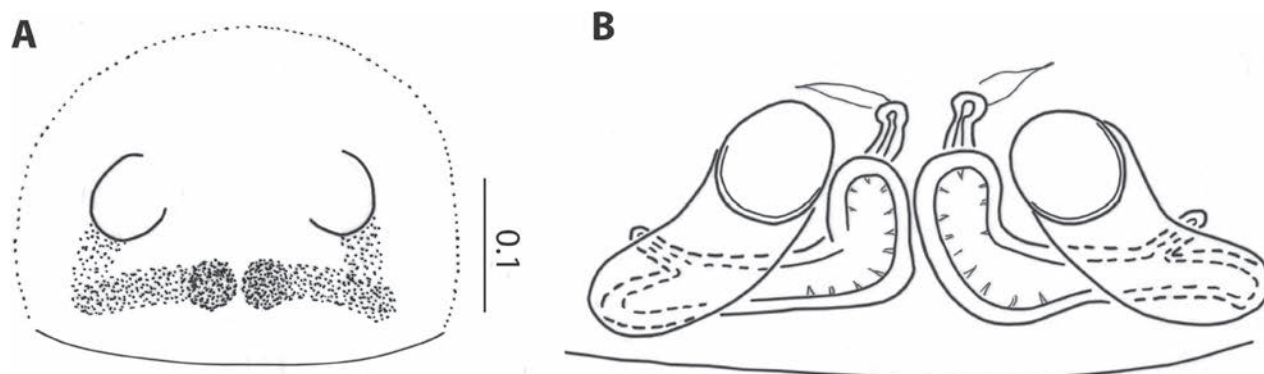


Figure 14. *Icius pulchellus* Haddad & Wesolowska, 2011, female: **A** epigyne, ventral view **B** internal structure of epigyne.

Description. Male: See Haddad and Wesolowska (2011). General appearance of living male as in Fig. 12A, D, in alcohol as in Fig. 13A, B; palpal organ as in Fig. 13C.

Female: Measurements: Cephalothorax length 2.0–2.4, width 1.4–1.7, height 0.8–0.9. Abdomen length 2.3–2.7, width 1.6–1.9. Eye field length 0.8–0.9, anterior width 1.1–1.2, posterior width 1.3–1.4. General appearance of living female as in Fig. 12B, E, in alcohol as in Fig. 13D–G. Carapace brown, with lighter median streak on thoracic part, lateral sides dark yellow, eye field black. Dense light grey hairs on carapace, amongst them long brown bristles, more numerous on eye field. Chelicerae unidentati, light brown. Sternum, labium and endites yellow. Abdomen ovoid, yellow, with leaf-shaped brownish pattern (Fig. 13D, E). In some specimens, abdomen light, creamy-yellow (Fig. 13F), sometimes with brownish marks (Fig. 13G). Venter covered with silver spots (translucent guanine). Spinnerets light. Legs yellow, their hairs faint, spines long, brown. Epigyne short and wide (Figs 13H, 14A). Copulatory openings large, widely separated. Internal structure simple (Fig. 14B), seminal ducts tubuliform, spermathecae elongated, accessory glands present.

Distribution. Species previously known only from the Free State Province, recorded from the Northern Cape for the first time based on this material (Dipenaar-Schoeman et al. 2023).

Remark. The female of this species is described here for the first time.

***Menemerus foordi* sp. nov.**

<https://zoobank.org/F94D1325-B96D-41DC-8D4E-9D51E8AA8622>

Figs 12C, F, 15, 16

Material examined. Holotype: SOUTH AFRICA • ♂; Northern Cape Province; Richtersveld National Park, Kokerboomkloof; 28°18.434'S, 17°17.476'E; 15 Sep 1994; A. Leroy leg.; on grass; NCA 2007/2503.

Other material. SOUTH AFRICA • Northern Cape Province; 1 subadult ♂; Richtersveld National Park, Akkedis Pass; 28°10.577'S, 17°02.069'E; 645 m a.s.l.; 9 Jul 2021; C. Haddad et al. leg.; under rocks, west-facing slope; NMBA 19095.

Diagnosis. The palpal organ of this species is similar to that of *Menemerus lesnei* Lessert, 1936 but differs by the presence of a ventral apophysis (absent in *M. lesnei*), narrower retrolateral apophysis and the shape of the embolus (with small membranous conductor in *M. foordi* sp. nov., while with a distal lamella in *M. lesnei*). Compare Fig. 16A with fig. 162 in Wesolowska (1999).

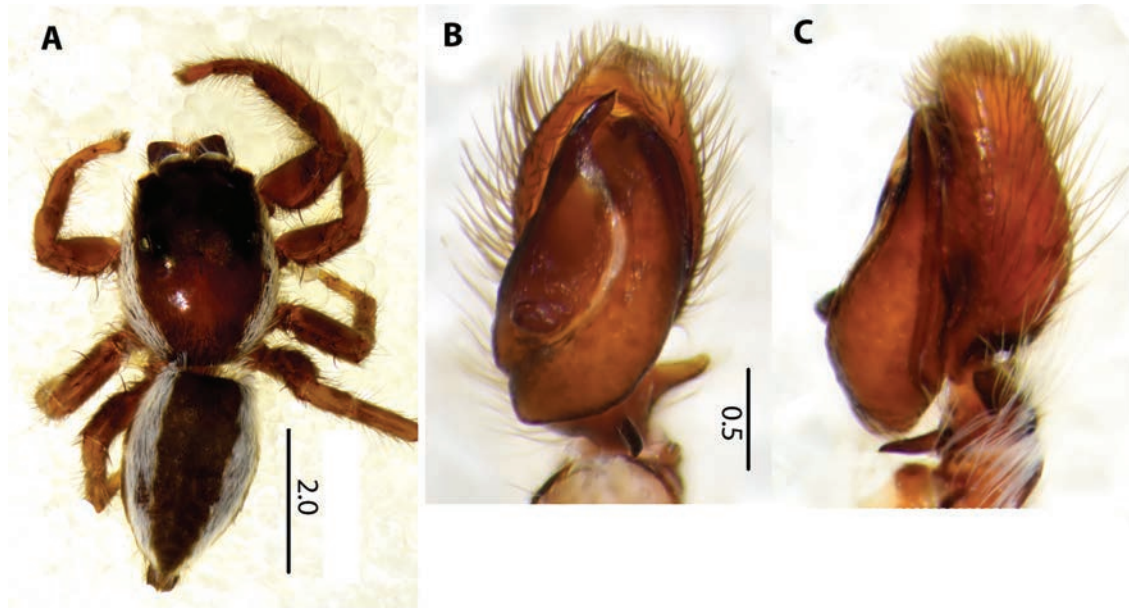


Figure 15. *Menemerus foordi* sp. nov., male, holotype: **A** general appearance of male **B** palpal organ, ventral view **C** same, retrolateral view.

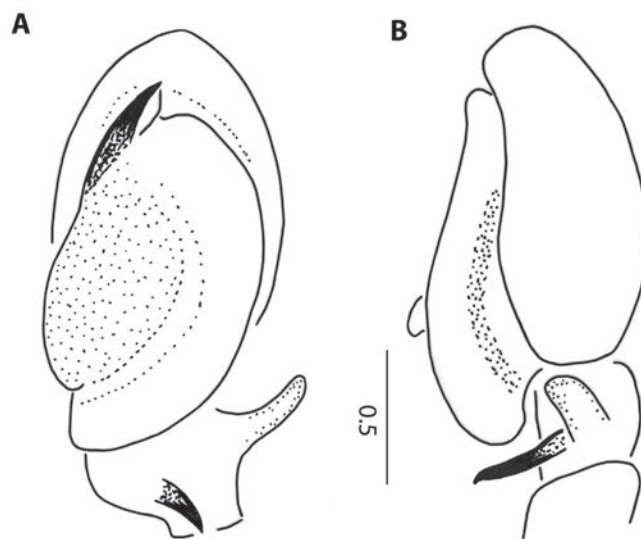


Figure 16. *Menemerus foordi* sp. nov., male, holotype: **A** palpal organ, ventral view **B** same, retrolateral view.

Description. Male: Measurements: Cephalothorax length 2.8, width 2.2, height 1.0. Abdomen length 2.8, width 1.7. Eye field length 1.2, anterior width 1.6, posterior width 1.8. General appearance of live subadult male as in Fig. 12C, F, of adult male in alcohol as in Fig. 15A. Carapace dark brown, eye field black, with wide streaks composed of white hairs along lateral margins. Clypeus with white hairs. Mouthparts dark brown, only tips of endites pale. Sternum dark brown. Abdomen black, with broad white streaks laterally, venter dark brown, spinnerets black. Legs brown, hairy. Palps dark brown, femur and tibia clothed in white hairs. Palpal tibia with two long apophyses; retrolateral blunt and ventral sharpened (Figs 15B, C, 16A, B). Bulb oval, tegular furrow wide, embolus short, with small membranous functional conductor (Figs 15B, 16A).

Female: Unknown.

Etymology. The new species is a patronym in honour of the late Stefan Hendrik Foord, in recognition of his distinguished career and contributions to the development of arachnology in Africa.

Distribution. Only known from the type locality.

***Menemerus lesserti* Lawrence, 1927**

Figs 17A, B, D, E, 18, 19

Menemerus lesserti Lawrence, 1927: 60, pl. 2, fig. 45; Wesolowska 1999: 302, figs 171–176.

Material examined. SOUTH AFRICA • Northern Cape Province; 1♂; Richtersveld National Park, near Hand of God; 28°05.874'S, 16°58.736'E; 35 m a.s.l.; 6 Jan 2021; C. Haddad et al. leg.; hand collecting, under rocks; NCA 2021/64 • 2♀; Richtersveld National Park, Research Accommodation; 28°07.122'S, 16°53.480'E; 9 Jul 2021; C. Haddad & R. Booysen leg.; on rocky outcrop, hand collection; NCA 2021/190 • 1♀; same collection data as for preceding; NCA 2021/168 • 1♀; same collection data as for preceding; NMBA 19844 • 1♂; same collection data as for preceding; NMBA 19845.

Diagnosis of male. The palpal organ of this species is similar to that of *Menemerus meridionalis* Wesolowska, 1999, as both share a similar shape of the tibia, but it can be distinguished by a more robust ventral apophysis, clearly longer embolus and the shape of retrolateral apophysis, which is triangular in *M. lesserti* while rounded in *M. meridionalis* (cf. Fig. 19A, B with fig. 188 in Wesolowska 1999).

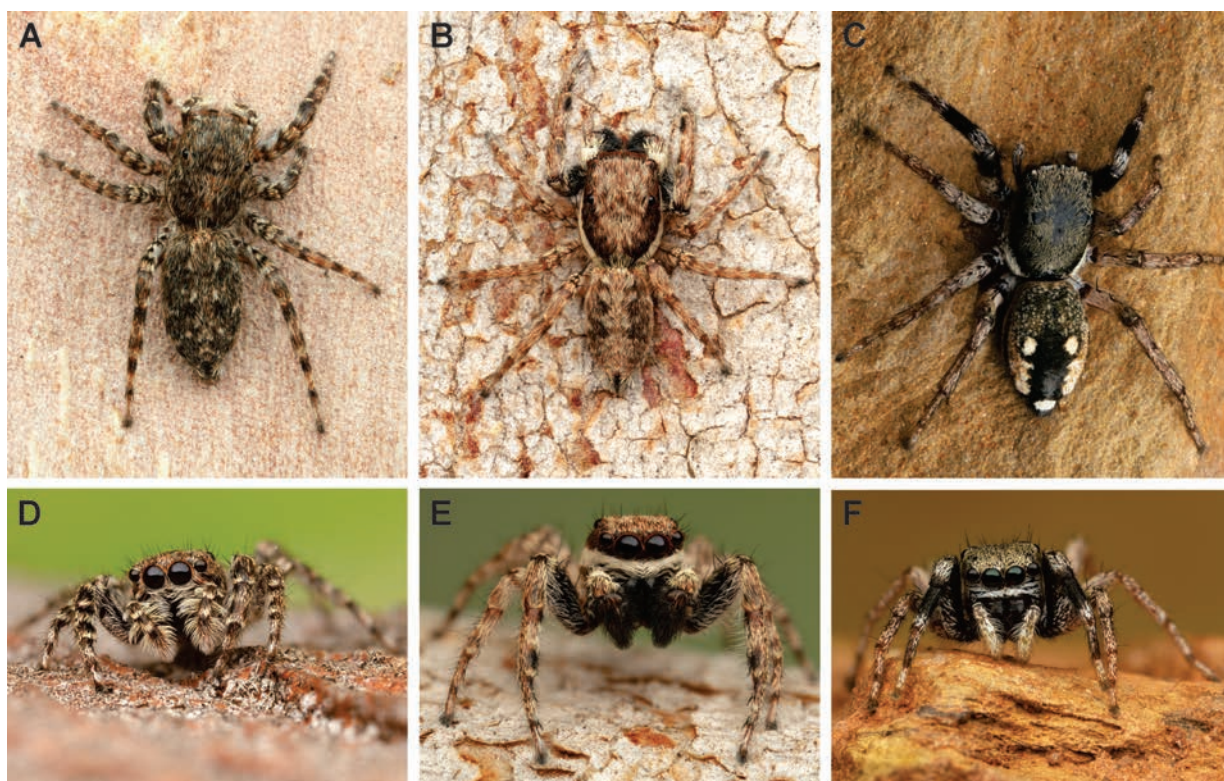


Figure 17. Dorsal habitus (A–C) and anterior view (D–F) of living *Menemerus lesserti* Lawrence, 1927 female (A, D) and male (B, E) and *Natta triguttata* sp. nov. female (C, F).

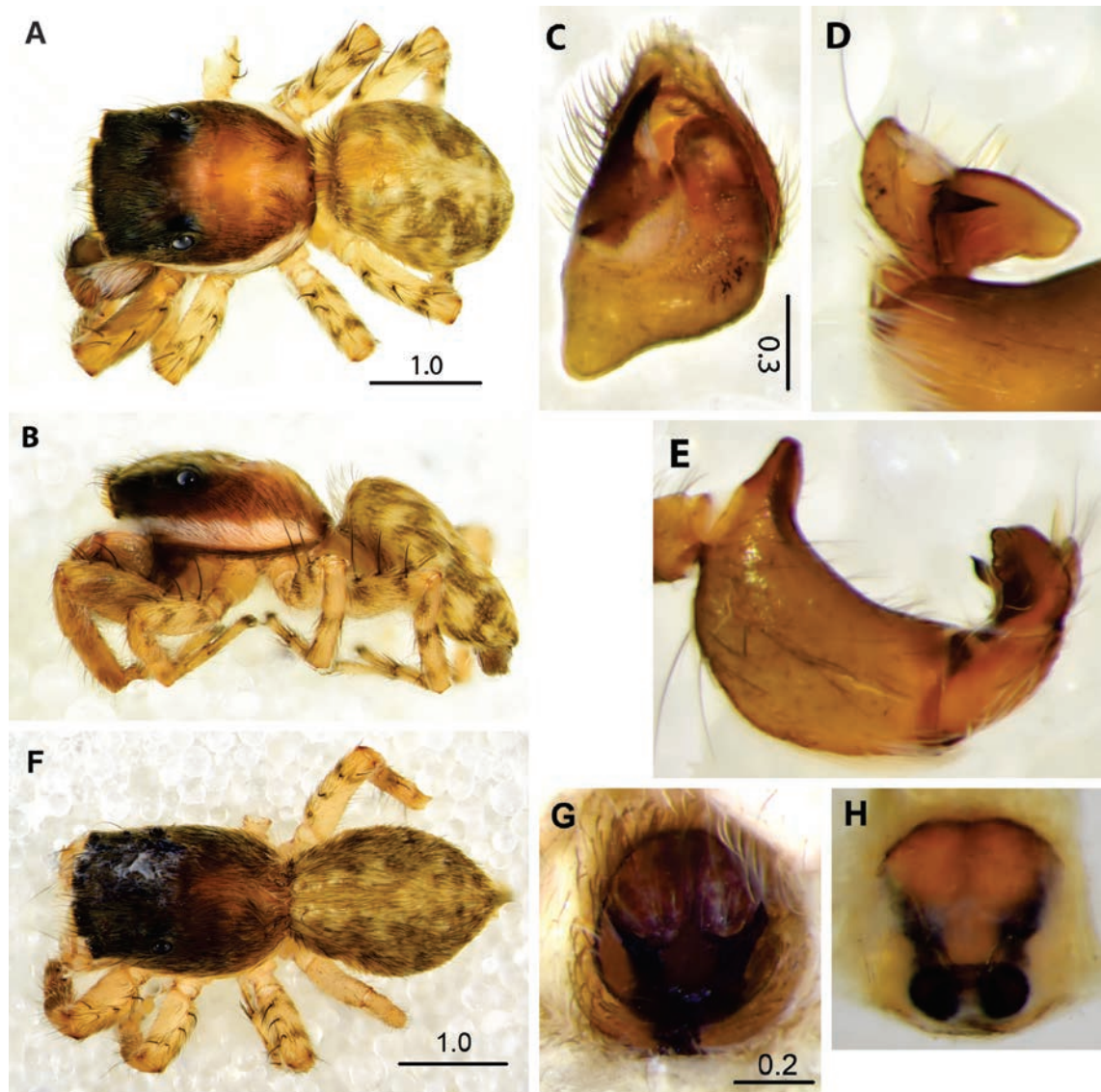


Figure 18. *Menemerus lesserti* Lawrence, 1927, male (A–E) and female (D–H): **A, F** general appearance, dorsal view **B** same, lateral view **C** palpal organ, ventral view of bulb **D** palpal tibia, ventral view **E** palpal tibia, patella and femur, retro-lateral view **G** epigyne, ventral view **H** same, dorsal view.

Description. See Wesolowska (1999) for description of female. Live habitus of female in Fig. 17A, D, of female in alcohol in Fig. 18F, epigyne in Fig. 18G, H.

Male: Measurements: Cephalothorax length 2.1, width 1.6, height 0.6. Abdomen length 2.0, width 1.5. Eye field length 0.9, anterior and posterior width 1.3. General appearance of live male as in Fig. 17B, E, of male in alcohol in Fig. 18A, B, body flattened. Carapace brown, with black eye field. Dense whitish hairs on eye field, amongst them long brown bristles. White hairs form broad streak along lateral margins of carapace (Fig. 18A, B). Clypeus low, with white hairs. Mouthparts dark brown, endites with whitish tips. Sternum yellow. Abdomen oval, light, greyish, with broad median whitish-yellow serrated streak and light patches laterally. White and brown hairs on abdomen. Venter light, spinnerets grey. Legs yellow, with brownish marks formed by brown hairs. Other leg hairs white, spines brown. Palps brown, femur clothed in white hairs. Tibia with large lobate retrolateral apophysis and spiked ventral apophysis (Figs 18D, E, 19B–D). Embolus straight, accompanied by membranous functional conductor (Figs 18C, 19A).

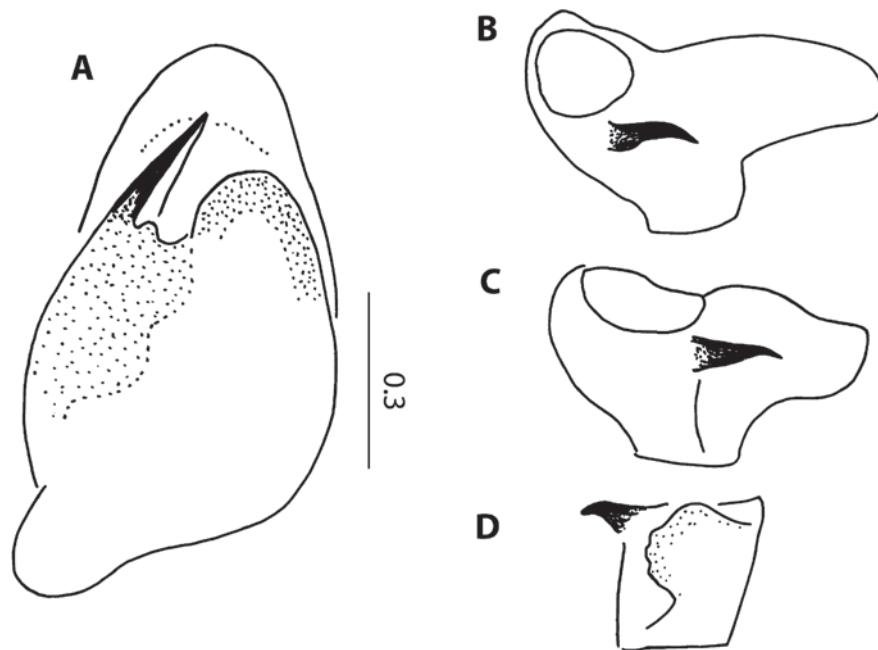


Figure 19. *Menemerus lesserti* Lawrence, 1928, male: **A** palpal organ, ventral view of bulb **B, C** palpal tibia, ventral view **D** same, retrolateral view.

Distribution. A species known from Namibia, Zimbabwe and South Africa (Limpopo and Northern Cape) (Wesolowska 1999; Dippenaar-Schoeman et al. 2023).

Remarks. The male of this species is described here for the first time. It was matched to the female of *M. lesserti*, based on DNA barcodes of the specimens sequenced (Fig. 2).

Menemerus rubicundus Lawrence, 1928

Fig. 20

Menemerus rubicundus Lawrence, 1928: 259, pl. 22, fig. 41; Wesolowska 1999: 329, figs 252–255; Wesolowska and Haddad 2018: 896, figs 65, 96 and 102–106.

Material examined. SOUTH AFRICA • Northern Cape Province; 1♀; Alexander Bay; 28°35'S, 16°29'E; 4 Apr 1988; A. Leroy leg.; hand collection; NCA 88/861.

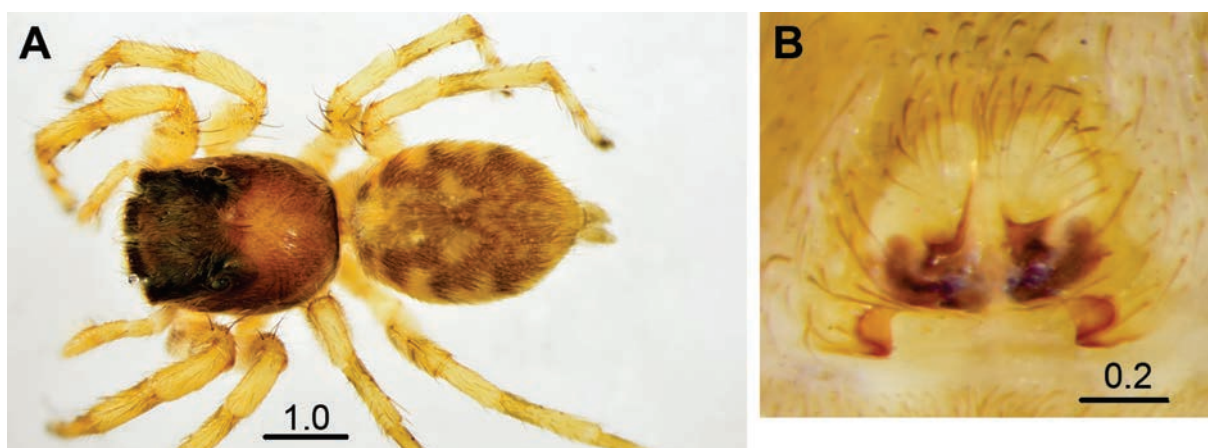


Figure 20. *Menemerus rubicundus* Lawrence, 1928, female: **A** general appearance, dorsal view **B** epigyne, ventral view.

Description. For male, see in Wesolowska and Haddad (2018); for female, see Wesolowska (1999). General appearance of female in alcohol as in Fig. 20A, epigyne in Fig. 20B.

Distribution. A species known from Namibia and South Africa (Free State and Northern Cape) (Wesolowska 1999; Wesolowska and Haddad 2018).

***Menemerus transvaalicus* Wesolowska, 1999**

Fig. 21

Menemerus transvaalicus Wesolowska, 1999: 339, figs 284–296; Haddad and Wesolowska 2011: 86, figs 71, 72; Wesolowska and Haddad 2014: 253.

Material examined. SOUTH AFRICA • Western Cape Province; 1♀; Tankwa Karoo National Park, Tanqua Guesthouse; 32°23.911'S, 19°50.713'E; 355 m a.s.l.; 19 Jan 2021; C. Haddad & R. Booyesen leg.; hand collecting, at night around houses; NCA 2021/1020.

Description. See Wesolowska (1999) for a description of both sexes. General appearance of female in alcohol as in Fig. 21A, epigyne in Fig. 21B.

Distribution. A species widespread in South Africa, also recorded from Lesotho (Wesolowska and Haddad 2014; Dippenaar-Schoeman et al. 2023).

***Mexcala rufa* G. Peckham & E. Peckham, 1902**

Mexcala rufa G. Peckham & E. Peckham, 1902: 333; G. Peckham & E. Peckham 1903: 247, pl. 29, fig. 1; Prószyński 1984: figs on p. 83; Wesolowska 2009: 176, figs 95–99.

Material examined. SOUTH AFRICA • Northern Cape Province; 2 imm. 1♂; near Nababeep, Jakkalswater Guest Farm; 29°37'S, 17°48'E; 895 m a.s.l.; 23 Aug 2020; P. Webb leg.; NCA 2020/208 • 1♂; Richtersveld National Park, Kokerboomkloof;

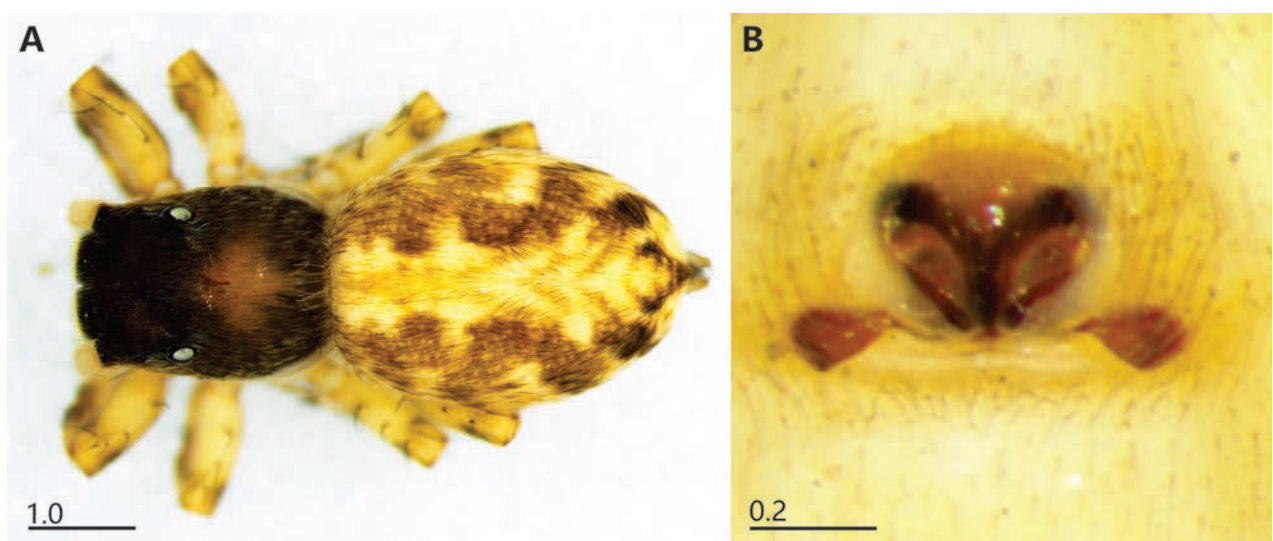


Figure 21. *Menemerus transvaalicus* Wesolowska, 1999, female: **A** general appearance, dorsal view **B** epigyne, ventral view.

28°18.434'S, 17°17.476'E; 15 Sep 2007; A. Leroy leg.; on grass; NCA 2007/25 • Western Cape Province • 2 imm. 1♂; Anysberg Nature Reserve, Road between Vrede and Allemorgens; 33°28.627'S, 20°31.499'E; 23 Sep 2007; C. Haddad leg.; under rocks; NCA 2007/3970 • 2 imm. 2♂; Same locality, Landsekloof; 33°29.493'S, 20°34.078'E; 24 Sep 2007, C. Haddad & R. Lyle leg.; under rocks; NCA 2007/3772 • 1♂ 1♀; Cederberg Tourist Park, Kromrivier, 72 km SSE of Clanwilliam, 32°32'S, 19°17'E; 3100 ft a.s.l.; 1–7 Nov 1985; C. Griswold et al. leg.; with *Camponotus* ant; NMSA 26403 • 4♀; Laingsburg District, Wagendrift Lodge; 33°22.861'S, 20°56.910'E; 520 m a.s.l.; 22 Jan 2021; C. Haddad et al. leg.; hand collecting, under rocks in veld; NCA 2021/136 • 1♂; Montagu, Les Hauts de Montagu; 33°48.915'S, 20°09.076'E; 360 m a.s.l.; Jul–Dec 2016; W. Jubber leg.; hand collecting; NCA 2017/545 • 1♂; Witteberg Nature Reserve; 33°21.462'S, 20°29.929'E; 905 m a.s.l.; 20 Oct 2015; Z. Mbo leg.; hand collecting, under rocks; NCA 2016/2613.

Distribution. A rare species known from Namibia and South Africa (Free State, Limpopo, Northern Cape and Western Cape) (Wesolowska 2009; Haddad 2021; Dippenaar-Schoeman et al. 2023).

***Natta chionogastra* (Simon, 1901)**

Cyllobelus chionogaster Simon, 1901a: 541, 549, fig. 665; Simon 1901c: 151; G. Peckham & E. Peckham 1903: 195, pl. 21, fig. 1.

Cyllobelus australis G. Peckham & E. Peckham, 1902: 334; G. Peckham & E. Peckham 1903: 194, pl. 21, fig. 2.

Natta chionogastra Prószyński 1984: figs on pp. 87–88; Prószyński 1985: 80, figs 39–41, 45, 47; Wesolowska 1993: 19, figs 1–16; Haddad and Wesolowska 2011: 89, figs 74, 75.

Material examined. SOUTH AFRICA • Northern Cape Province; 1♂; Loxton; 31°28'23"S, 22°21'07"E; 15 Mar 2001; C. Stuart leg.; hand collection; NCA 2010/713 • Western Cape • 2♂ 1♀; Cederberg Mountains, 17 km SE of Algeria; 32°25'S, 19°10'E; 3000 ft a.s.l.; 1 Nov 1985; C. Griswold et al. leg.; fynbos; NMSA 26466.

Distribution. Species widely distributed in Africa. Recorded from all the South African provinces (Dippenaar-Schoeman et al. 2023).

***Natta triguttata* sp. nov.**

<https://zoobank.org/C8C35C71-FE03-41A2-B5A7-78C1CE8FB4CB>

Figs 17C, F, 22, 23

Material examined. Holotype: SOUTH AFRICA • ♂; Northern Cape; Richtersveld National Park, Akkedis Pass; 28°10.577'S, 17°02.069'E; 645 m a.s.l.; 9 Jul 2021, C. Haddad et al. leg.; leaf litter, dry river bed; NCA 2021/499.

Paratype: SOUTH AFRICA • 1♀; together with holotype.

Diagnosis. The new species differs from congeners in colouration: the presence of a pair of round white spots near the middle of the abdominal dorsum and a single white spot above the spinnerets differs from the other species, which have many orange or yellow spots. The palpal organ is similar to that in *Natta horizontalis* Karsch, 1979, but can be recognised by the thin, pointed tibial

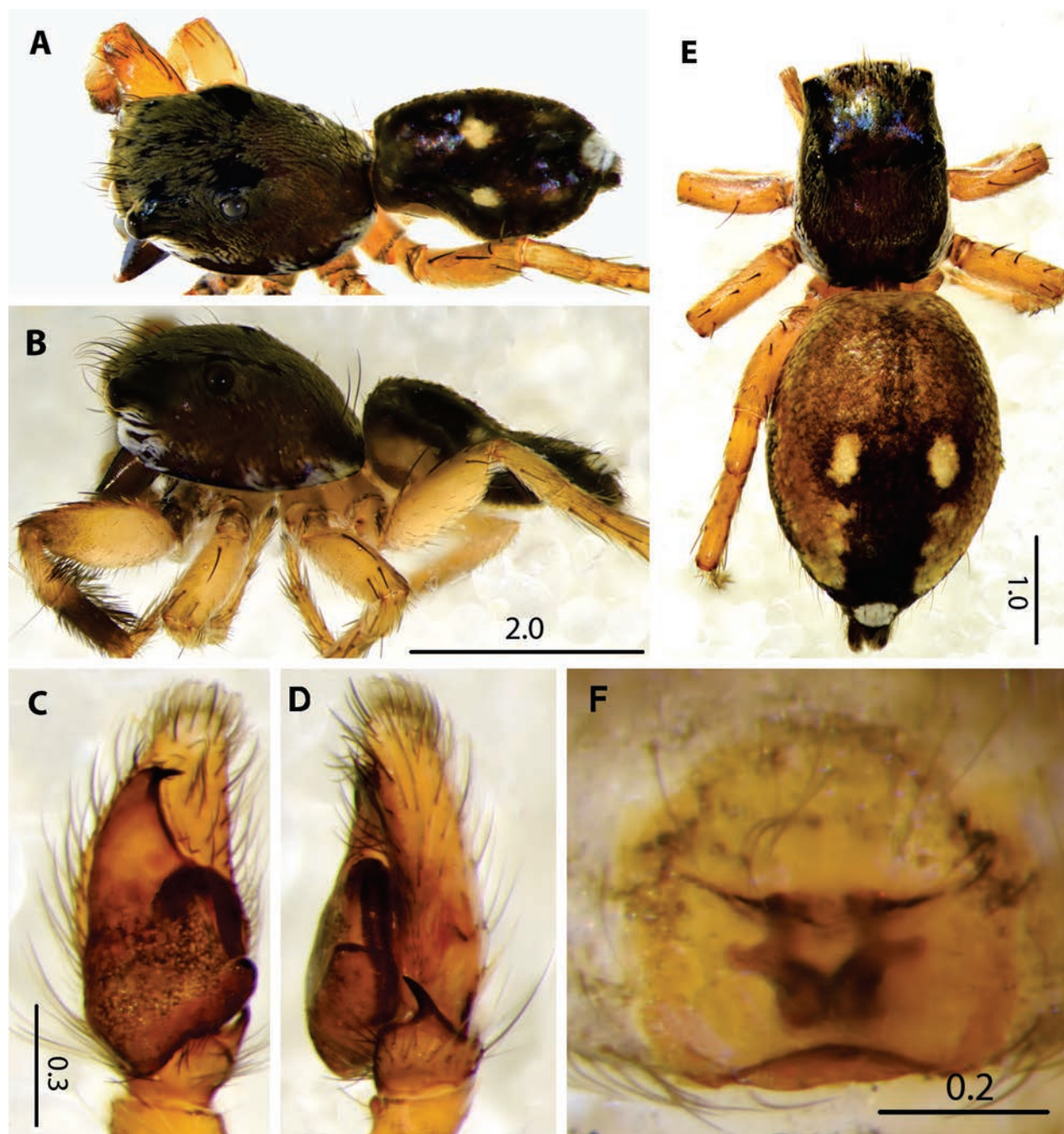


Figure 22. *Natta triguttata* sp. nov., holotype male (A–D) and paratype female (E, F): A, E general appearance, dorsolateral view B same, lateral view C palpal organ, ventral view D same, lateral view F epigyne, ventral view.

apophysis (Figs 22C, D, 23A, B), whereas it is shorter, wide and truncated in the latter species (Wesołowska 1993: figs 23, 28, 33). The female differs from congeners by the absence of an epigynal depression (Figs 22F, 23C).

Description. Male: Measurements: Cephalothorax length 2.1, width 1.5, height 0.8. Abdomen length 2.0, width 1.5. Eye field length 1.0, anterior width 1.2, posterior width 1.3. General appearance in alcohol as in Fig. 22A, B. Carapace black, clothed in dense greyish scales, amongst them some long brown bristles. Some white scales on lateral slopes, same scales form two lines below anterior lateral eyes (Fig. 22B). Chelicerae unidentati. Mouthparts and sternum blackish. Abdomen black, with pair of white round spots near mid-point and single white spot

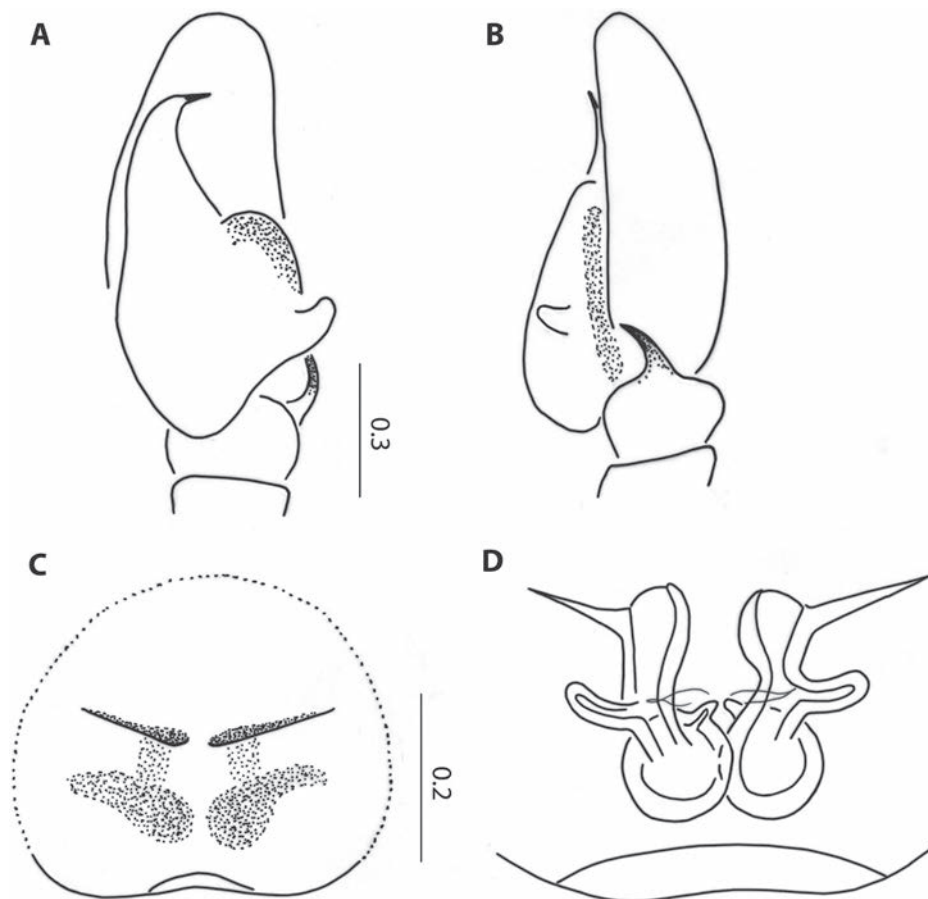


Figure 23. *Natta triguttata* sp. nov., holotype male (**A, B**) and paratype female (**C, D**): **A** palpal organ, ventral view **B** same, lateral view **C** epigyne, ventral view **D** internal structure of epigyne.

at end of abdomen above spinnerets, spinnerets black. Venter black, shining. Legs dark yellow, hairs and spines brown, long sharp bristles on ventral surface of femur I. Palpal organ as in Figs 22C, D, 23A, B, bulb triangular, embolus very short, tip orientated transversely towards retrolateral side, tibial apophysis thin.

Female: Measurements: Cephalothorax length 2.2, width 1.5, height 0.9. Abdomen length 3.1, width 2.3. Eye field length 1.0, anterior width 1.2, posterior width 1.3. General appearance of live female as in Fig. 17C, F, in alcohol as in Fig. 22E. Larger than male, similarly coloured. White streak composed of scales along lateral margins of carapace. Abdomen slightly lighter, brown with black wide median streak in posterior half, white spots as in male. Dorsum of abdomen covered with transparent scales, venter light brown. Epigyne as in Figs 22B, 23C, with wide posterior pocket, copulatory openings placed centrally, their outer edges with long sclerotised flange. Internal structure simple, large accessory glands connected to seminal ducts, spermathecae spherical (Fig. 23D).

Etymology. The species name is derived from the Latin tri- (three) and guttatus (spotted), referring to the three distinct spots on the abdomen of both sexes.

Distribution. Only known from the type locality.

Remarks. This is the first new species of *Natta* to be described in more than 120 years. The placement of the species was confirmed through the molecular results (Fig. 2), as well as the consistency in somatic morphology of the new species with *N. chionogaster* and *N. horizontalis*, particularly the presence of iridescent scales all over the body (Fig. 18C).

***Psenuc dependens* (Haddad & Wesolowska, 2011)**

Pseudicius dependens Haddad & Wesolowska, 2011: 109, figs 141, 142 and 166–170.

Psenuc dependens Prószyński 2016: 23.

Material examined. SOUTH AFRICA • Northern Cape Province; 2♀; Nigramoep Slow Living Guest Farm; 29°32.385'S, 17°34.746'E; 765 m a.s.l.; 9 Jan 2021; C. Haddad et al. leg.; beating short shrubs, east-facing slope; NCA 2021/637 • 1♀; Richtersveld National Park, Akkedis Pass; 28°10.673'S, 17°01.863'E; 540 m a.s.l.; 8 Jul 2021; C. Haddad et al. leg.; beating short shrubs, east-facing slope; NCA 2021/457 • 1♀; Richtersveld National Park, Halfmens Pass; 28°07.789'S, 16°57.667'E; 235 m a.s.l.; 8 Jan 2021; C. Haddad et al. leg.; beating short shrubs, open plain; NCA 2021/309 • 1♀; same collection data as for preceding; 10 Jul 2021; C. Haddad et al. leg.; NCA 2021/422 • 1♀; Richtersveld National Park, SE of Akkedis Pass; 28°11.123'S, 17°02.543'E; 535 m a.s.l.; 7 Jul 2021; C. Haddad et al. leg.; beating short shrubs, dry river bed; NCA 2021/689.

Distribution. Previously recorded from the Free State, Limpopo, Northern Cape and Western Cape Provinces (Dippenaar-Schoeman et al. 2023), but for the first time from the western parts of the Northern Cape.

Discussion

This paper presents the results of the first focused treatment of a spider group from the arid western interior of South Africa, based on freshly sampled material supplemented by numerous historical museum records. Our survey uncovered three new species and several new provincial and country records from the region, highlighting the poor state of knowledge of jumping spiders in this part of South Africa. This is not surprising, as several studies have emphasised the poor historical collecting effort in this part of the country and the need to focus resources on sampling here to improve knowledge of its fauna (Foord et al. 2011; Janion-Scheepers et al. 2016; Dippenaar-Schoeman et al. 2023).

Considering these results, it is plausible that taxonomic studies of other salticid clades will also show how poorly studied its fauna is. For example, of the eight species of Euophryini collected along the transect, only one species (*Euophrys leipoldti* G. W. Peckham & E. G. Peckham, 1903), is described. Only through a concerted taxonomic effort on Salticidae and other families can the fauna of this region be properly documented, although there is still great potential for intensive sampling in the arid zone to address the massive geographical gaps that persist.

Acknowledgements

This paper pays tribute to our late colleague Stefan Foord, who was involved in the transect project as the data analyst. Unfortunately, he was unable to see his contribution to this work to completion. We are grateful to Reginald Christiaan, Ruan Booyesen, Michael Vickers, Adriaan Stander, Lancelot Malope and Siphephelo Sibisi for assistance in the field and Pheladi Chuene (Nam-

aqua N.P.), Brent Whittington (Richtersveld N.P.), Kennet Mkhondo (Tankwa Karoo N.P.) and the Louw family (Nigramoep) for allowing us to sample at these sites. Collecting permits were kindly provided by SANParks and the Northern Cape Department of Environment and Nature Conservation. Vida van der Walt kindly provided her excellent photographs of the live habitus of numerous species treated in this paper. Robin Lyle (NCA), Trudie Peyper (NMBA) and Matabaro Ziganira (NMSA) are thanked for accessioning and/or loaning the specimens included in this study.

Additional information

Conflict of interest

The authors have declared that no competing interests exist.

Ethical statement

No ethical statement was reported.

Funding

The fieldwork and DNA barcoding were funded through a grant from the National Research Foundation of South Africa in the Foundational Biodiversity Information Programme (#129108).

Author contributions

Charles Haddad – Field sampling, sorting and processing of material, DNA barcoding tissue preparation and data recording, microscope photography, wrote part of manuscript, edited final manuscript. Wanda Wesołowska – Descriptions, illustrations, microscope photography, preparation of figure plates.

Author ORCIDs

Charles Richard Haddad  <https://orcid.org/0000-0002-2317-7760>

Wanda Wesołowska  <https://orcid.org/0000-0002-4411-1058>

Data availability

All of the data that support the findings of this study are available in the main text or Supplementary Information.

References

- Andreeva EM, Hęciak S, Prószyński J (1984) Remarks on *Icius* and *Pseudicius* (Araneae, Salticidae) mainly from central Asia. *Annales Zoologici, Warszawa* 37: 349–375.
- CCDB [Canadian Centre for DNA Barcoding] (2019) CCDB Protocols. CCDB [Internet], Guelph. http://ccdb.ca/site/wp-content/uploads/2016/09/CCDB_Amplification.pdf [accessed 19 December 2023]
- Dippenaar-Schoeman AS, Haddad CR, Lotz LN, Booysen R, Steenkamp RC, Foord SH (2023) Checklist of the spiders (Araneae) of South Africa. *African Invertebrates* 64(3): 221–281. <https://doi.org/10.3897/AfrInvertebr.64.111047>
- Edgar RC (2004) MUSCLE: A multiple sequence alignment method with reduced time and space complexity. *BMC Bioinformatics* 5(1): 113. <https://doi.org/10.1186/1471-2105-5-113>

- Foord SH, Dippenaar-Schoeman AS, Haddad CR (2011) Chapter 8 – South African spider diversity: African perspectives on the conservation of a mega-diverse group. In: Grillo O, Venora G (Eds) *Changing Diversity in Changing Environment*. InTech Publishing, Rijeka, Croatia, 163–182.
- Foord SH, Dippenaar-Schoeman AS, Haddad CR, Lyle R, Lotz L, Sethusa T, Raimondo D (2020) The South African National Red List of spiders: Patterns, threats, and conservation. *The Journal of Arachnology* 48(2): 110–118. <https://doi.org/10.1636/0161-8202-48.2.110>
- Haddad CR (2021) Undergraduate entomology field excursions are a valuable source of biodiversity data: A case for spider (Araneae) bycatches in ecological studies. *Biodiversity and Conservation* 30(14): 4199–4222. <https://doi.org/10.1007/s10531-021-02301-9>
- Haddad CR, Marusik YM (2019) Clarifying the taxonomic status and distributions of the spider species collected during the Leonhard Schultze expeditions in western and central southern Africa (Arachnida: Araneae). *Zootaxa* 4608(3): 451–483. <https://doi.org/10.11646/zootaxa.4608.3.3>
- Haddad CR, Wesolowska W (2013) Additions to the jumping spider fauna of South Africa (Araneae: Salticidae). *Genus* 24: 459–501.
- Janion-Scheepers C, Measey J, Braschler B, Chown SL, Coetzee L, Colville J, Dames J, Davies AB, Davies S, Davis A, Dippenaar-Schoeman AS, Duffy G, Fourie D, Griffiths C, Haddad CR, Hamer M, Herbert D, Hugo-Coetzee LEA, Jacobs A, Jansen Van Rensburg C, Lamani S, Lotz LN, Louw Svd M, Lyle R, Malan A, Marais M, Neethling JA, Nxele T, Plisko D, Prendini L, Rink AN, Swart A, Theron P, Truter M, Ueckermann E, Uys VM, Villet MH, Willows-Munrow S, Wilson JRU (2016) Soil biota in a megadiverse country: Current knowledge and future research directions in South Africa. *Pedobiologia* 59(3): 129–174. <https://doi.org/10.1016/j.pedobi.2016.03.004>
- Lawrence R (1927) Contributions to a knowledge of the fauna of South-West Africa V. Arachnida. *Annals of the South African Museum* 25: 1–75 [pl. 1–4].
- Lawrence R (1928) Contributions to a knowledge of the fauna of South-West Africa VII. Arachnida (part 2). *Annals of the South African Museum* 25: 217–312 [pl. 21–24].
- Mucina L, Rutherford MC (2006) The vegetation of South Africa, Lesotho and Swaziland. *Strelitzia* 19: 1–807.
- Myers N, Mittermeier RA, Mittermeier CG, Da Fonseca GAB, Kent J (2000) Biodiversity hotspots for conservation priorities. *Nature* 403(6772): 853–858. <https://doi.org/10.1038/35002501>
- Peckham GW, Peckham EG (1902) Some new genera and species of Attidae from South Africa. *Psyche* (Cambridge, Massachusetts) 9(312): 330–335. <https://doi.org/10.1155/1902/13502>
- Peckham GW, Peckham EG (1903) New species of the family Attidae from South Africa, with notes on the distribution of the genera found in the Ethiopian region. *Transactions of the Wisconsin Academy of Sciences, Arts and Letters* 14: 173–278 [pl. 19–29].
- Prószyński J (1984) Atlas rysunków diagnostycznych mniej znanych Salticidae (Araneae). *Zeszyty Naukowe Wyższej Szkoły Rolniczo-Pedagogicznej, Siedlce*, 177 pp.
- Prószyński J (1985) On *Siler*, *Silerella*, *Cylobelus* and *Natta* (Araneae, Salticidae). *Annales Zoologici, Warszawa* 39: 69–85.
- Prószyński J (2016) Delimitation and description of 19 new genera, a subgenus and a species of Salticidae (Araneae) of the world. *Ecologica Montenegrina* 7: 4–32. <https://doi.org/10.37828/em.2016.7.1>
- Prószyński J (2017) Pragmatic classification of the world's Salticidae (Araneae). *Ecologica Montenegrina* 12: 1–133. <https://doi.org/10.37828/em.2017.12.1>

- Purcell WF (1908) Araneae (I). In: Schultze L (Ed.) Zoologische und anthropologische Ergebnisse einer Forschungsreise im westlichen und zentralen Südafrika. Erster Band: Systematik und Tiergeographie. Zweite Lieferung. Denkschriften der Medizinisch-Naturwissenschaftlichen Gesellschaft zu Jena 13: 203–246.
- Ratnasingham S, Hebert PDN (2007) BOLD: The Barcode of Life Data System (www.barcodinglife.org). Molecular Ecology Notes 7(3): 355–364. <https://doi.org/10.1111/j.1471-8286.2007.01678.x>
- Ratnasingham S, Hebert PDN (2013) A DNA-based registry for all animal species: The Barcode Index Number (BIN) system. PLoS One 8(7): e66213. <https://doi.org/10.1371/journal.pone.0066213>
- Simon E (1901a) Histoire naturelle des araignées. Deuxième édition, tome second. Roret, Paris, 381–668. <https://doi.org/10.5962/bhl.title.51973>
- Simon E (1901b) Etudes arachnologiques. 31e Mémoire. XLVIII. Etude sur les *Heliophanus* d'Afrique et de Madagascar. Annales de la Société Entomologique de France 70(1): 52–61. <https://doi.org/10.1080/21686351.1901.12279316>
- Simon E (1901c) Descriptions d'araignées nouveaux de la famille des Attidae (suite). Annales de la Société Entomologique de Belgique 45: 141–161.
- Simon E (1910) Arachnoidea: Araneae (II). In: Schultze L (Ed.) Zoologische und anthropologische Ergebnisse einer Forschungsreise im westlichen und zentralen Südafrika. Vierter Band. Systematik und Tiergeographie. Denkschriften der Medizinisch-Naturwissenschaftlichen Gesellschaft zu Jena 16: 175–218.
- Wesołowska W (1986) A revision of the genus *Heliophanus* C. L. Koch, 1833 (Aranei: Salticidae). Annales Zoologici, Warszawa 40: 1–254.
- Wesołowska W (1993) Notes on the genus *Natta* Karsch, 1879 (Araneae, Salticidae). Genus 4: 17–32.
- Wesołowska W (1999) A revision of the spider genus *Menemerus* in Africa (Araneae: Salticidae). Genus 10: 251–353.
- Wesołowska W (2006) Jumping spiders from the Brandberg massif in Namibia (Araneae: Salticidae). African Entomology 14: 225–256.
- Wesołowska W (2009) A revision of the spider genus *Mexcala* Peckham et Peckham, 1902 (Araneae: Salticidae). Genus 20: 149–186.
- Wesołowska W (2011) New species and new records of jumping spiders from Botswana, Namibia and Zimbabwe (Araneae: Salticidae). Genus 22: 307–346.
- Wesołowska W (2024) Taxonomic notes on the genus *Heliophanus* C.L. Koch, 1833, with description of three additional genera (Araneae: Salticidae: Chrysillini). Zootaxa 5405(1): 80–92. <https://doi.org/10.11646/zootaxa.5405.1.3>
- Wesołowska W, Haddad CR (2014) An overview of the jumping spiders of Lesotho (Araneae: Salticidae), with descriptions of six new species. African Invertebrates 55: 229–268.
- Wesołowska W, Haddad CR (2018) Further additions to the jumping spider fauna of South Africa (Araneae: Salticidae). Annales Zoologici 68(4): 879–908. <https://doi.org/10.3161/00034541ANZ2018.68.4.011>
- Wesołowska W, Russell-Smith A (2000) Jumping spiders from Mkomazi Game Reserve in Tanzania (Araneae Salticidae). Tropical Zoology 13(1): 11–127. <https://doi.org/10.1080/03946975.2000.10531126>
- Wesołowska W, Tomasiewicz B (2008) New species and records of Ethiopian jumping spiders (Araneae, Salticidae). Journal of Afrotropical Zoology 4: 3–59.
- World Spider Catalog (2024) World Spider Catalog. Version 25.5. Natural History Museum Bern. <https://doi.org/10.24436/2> [accessed on 14 October 2024]

Appendix 1

Table A1. Summary of Chrysillini specimens from western South Africa for which DNA barcodes (cytochrome oxidase subunit I) have been generated (indicated with *), with additional Chrysillini from South Africa and *Massagris honesta* Wesolowska, 1993 (Hisponinae) as the outgroup used for the molecular analysis. All sequences are included in the SPIZA project on BOLD (Barcode of Life Data Systems). The *Heliocapensis mirabilis* specimen marked with a dash did not sequence successfully.

| Species | Sex | BOLD Sample ID | Locality | Depository | Length |
|------------------------------------|-----|----------------|------------------|---------------|--------|
| <i>Afraflacilla karinae</i> | ♂ | SPIZA1444-23 | *Namaqua | NMBA 18564 | 657 bp |
| <i>Afraflacilla venustula</i> | ♂ | SPIZA1421-21 | Ndumo | NCA 2021/1221 | 658 bp |
| | ♀ | SPIZA1422-21 | Ndumo | NCA 2021/1221 | 658 bp |
| <i>Helafricanus bisulcus</i> | ♀ | SPIZA1566-23 | Kleinmond | NMBA 18781 | 657 bp |
| <i>Helafricanus debilis</i> | ♂ | SPIZA1531-23 | Amanzi | NMBA 18732 | 657 bp |
| <i>Helafricanus demonstrativus</i> | ♂ | SPIZA1364-21 | Pietermaritzburg | NCA 2021/1120 | 658 bp |
| <i>Helafricanus fasciatus</i> | ♂ | SPIZA1411-21 | Coopersdal | NCA 2021/1211 | 658 bp |
| | ♀ | SPIZA1544-23 | Bloemfontein | NMBA 18759 | 657 bp |
| <i>Helafricanus modicus</i> | ♀ | SPIZA722-21 | *Wagendrift | NCA 2021/148 | 658 bp |
| | ♂ | SPIZA1265-21 | Queenstown | NCA 2021/1036 | 658 bp |
| <i>Helafricanus nanus</i> | ♀ | SPIZA1315-21 | Wepener | NCA 2021/1073 | 658 bp |
| | ♂ | SPIZA1548-23 | Bloemfontein | NMBA 18762 | 657 bp |
| <i>Helafricanus patellaris</i> | ♂ | SPIZA721-21 | *Wagendrift | NCA 2021/148 | 658 bp |
| <i>Helafricanus pistaciae</i> | ♂ | SPIZA1549-23 | Bloemfontein | NMBA 18763 | 657 bp |
| | ♀ | SPIZA1552-23 | Bloemfontein | NMBA 18768 | 657 bp |
| <i>Helafricanus trepidus</i> | ♀ | SPIZA1267-21 | Queenstown | NCA 2021/1037 | 658 bp |
| <i>Heliocapensis charlesi</i> | ♂ | SPIZA1472-23 | Witsand | NMBA 18614 | 658 bp |
| | ♀ | SPIZA1473-23 | Witsand | NMBA 18614 | 658 bp |
| <i>Heliocapensis deserticola</i> | ♀ | SPIZA1425-21 | *Nababeep | NCA 2021/1224 | 658 bp |
| <i>Heliocapensis maluti</i> | ♂ | SPIZA1014-21 | *Namaqua | NCA 2021/740 | 658 bp |
| <i>Heliocapensis mirabilis</i> | ♀ | SPIZA485-21 | *Richtersveld | NCA 2021/34 | 599 bp |
| | ♀ | SPIZA501-21 | *Richtersveld | NCA 2021/47 | 639 bp |
| | ♀ | SPIZA777-21 | *Richtersveld | NCA 2021/279 | 658 bp |
| | ♂ | SPIZA778-21 | *Richtersveld | NCA 2021/280 | – |
| <i>Heliophanus deformis</i> | ♀ | SPIZA502-21 | *Richtersveld | NCA 2021/47 | 658 bp |
| | ♀ | SPIZA786-21 | *Richtersveld | NCA 2021/293 | 658 bp |
| | ♂ | SPIZA1031-21 | *Namaqua | NCA 2021/759 | 658 bp |
| <i>Heliophanus gramineus</i> | ♂ | SPIZA1802-23 | Jonkershoek | NMBA 18891 | 658 bp |
| | ♀ | SPIZA1887-23 | Betty's Bay | NMBA 18934 | 658 bp |
| <i>Heliophanus pygmaeus</i> | ♂ | SPIZA1346-21 | Ndumo | NCA 2021/1103 | 658 bp |
| <i>Icius insolitus</i> | ♀ | SPIZA1086-21 | *Akkerendam | NCA 2021/830 | 658 bp |
| | ♀ | SPIZA1226-21 | *Tankwa | NCA 2021/996 | 631 bp |
| | ♀ | SPIZA538-21 | *Namaqua | NCA 2021/78 | 658 bp |
| | ♀ | SPIZA702-21 | *Wagendrift | NCA 2021/134 | 658 bp |
| | ♀ | SPIZA896-21 | *Nigramoep | NCA 2021/515 | 658 bp |
| | ♀ | SPIZA857-21 | *Richtersveld | NCA 2021/456 | 658 bp |
| | ♀ | SPIZA702-21 | *Wagendrift | NCA 2021/134 | 658 bp |
| | ♀ | SPIZA647-21 | Bankfontein | NCA 2021/239 | 658 bp |
| <i>Icius jacksoni</i> sp. nov. | ♂ | SPIZA478-21 | *Richtersveld | NCA 2021/28 | 658 bp |
| <i>Icius nigricaudus</i> | ♀ | SPIZA1345-21 | Ndumo | NCA 2021/1102 | 658 bp |
| <i>Icius pulchellus</i> | ♀ | SPIZA1070-21 | *Namaqua | NCA 2021/814 | 561 bp |
| | ♀ | SPIZA1071-21 | *Namaqua | NCA 2021/814 | 658 bp |
| | ♂ | SPIZA1193-21 | *Tankwa | NCA 2021/962 | 658 bp |
| | ♀ | SPIZA1194-21 | *Tankwa | NCA 2021/962 | 598 bp |

| Species | Sex | BOLD Sample ID | Locality | Depository | Length |
|--|-------|----------------|---------------|---------------|--------|
| <i>Massagris honesta</i> | ♀ | SPIZA1678-21 | Hermanus | NMBA 19027 | 657 bp |
| <i>Mememerus</i> sp. cf. <i>minshullae</i> | ♀ | SPIZA1406-21 | Ukwela | NCA 2021/1207 | 658 bp |
| <i>Menemerus foordi</i> sp. nov. | s/a ♂ | SPIZA2148-24 | *Richtersveld | NMBA 19095 | 658 bp |
| <i>Menemerus lesserti</i> | ♂ | SPIZA521-21 | *Richtersveld | NCA 2021/64 | 658 bp |
| | ♀ | SPIZA748-21 | *Richtersveld | NCA 2021/168 | 632 bp |
| | ♂ | SPIZA521-21 | *Richtersveld | NCA 2021/64 | 658 bp |
| <i>Menemerus rubicundus</i> | ♀ | SPIZA494-21 | *Richtersveld | NCA 2021/42 | 658 bp |
| <i>Menemerus transvaalicus</i> | ♀ | SPIZA1244-21 | *Tankwa | NCA 2021/1020 | 658 bp |
| | ♂ | SPIZA1268-21 | Queenstown | NCA 2021/1038 | 658 bp |
| | ♂ | SPIZA1513-23 | Rhodes | NMBA 18706 | 658 bp |
| | ♀ | SPIZA1594-23 | Wepener | NMBA 18805 | 657 bp |
| | ♂ | SPIZA1595-23 | Wepener | NMBA 18805 | 657 bp |
| <i>Mexcala elegans</i> | ♀ | SPIZA1370-21 | Richard's Bay | NCA 2021/1127 | 658 bp |
| <i>Mexcala rufa</i> | ♀ | SPIZA704-21 | *Wagendrift | NCA 2021/136 | 658 bp |
| | ♀ | SPIZA705-21 | *Wagendrift | NCA 2021/136 | 658 bp |
| | ♀ | SPIZA706-21 | *Wagendrift | NCA 2021/136 | 658 bp |
| <i>Natta chionogaster</i> | ♀ | SPIZA1519-23 | Bankfontein | NMBA 18710 | 658 bp |
| | ♀ | SPIZA1580-23 | Amanzi | NMBA 18794 | 657 bp |
| <i>Natta horizontalis</i> | ♀ | SPIZA1354-21 | Ukwela | NCA 2021/1111 | 658 bp |
| | ♂ | SPIZA1423-21 | Ndumo | NCA 2021/1222 | 658 bp |
| <i>Natta triguttata</i> sp. nov. | ♀ | SPIZA971-21 | *Richtersveld | NCA 2021/499 | 658 bp |
| | ♂ | SPIZA972-21 | *Richtersveld | NCA 2021/499 | 658 bp |
| <i>Phintella australis</i> | ♂ | SPIZA1514-23 | Cradock | NMBA 18707 | 658 bp |
| <i>Pseudicius dentatus</i> | ♂ | SPIZA1415-21 | Nelspruit | NCA 2021/1215 | 658 bp |
| | ♀ | SPIZA1420-21 | Komatipoort | NCA 2021/1220 | 658 bp |
| <i>Pseudicius matabelensis</i> | ♂ | SPIZA1444-21 | *Namaqua | NMBA 18564 | 658 bp |
| <i>Psenuc dependens</i> | ♀ | SPIZA793-21 | *Richtersveld | NCA 2021/309 | 658 bp |
| | ♀ | SPIZA942-21 | *Nigramoep | NCA 2021/637 | 658 bp |
| | ♀ | SPIZA977-21 | *Richtersveld | NCA 2021/689 | 658 bp |
| <i>Trapezocephalus orchestra</i> | ♀ | SPIZA1417-21 | Nelspruit | NCA 2021/1217 | 658 bp |

Supplementary material 1

Details of collecting data of Chrysillini jumping spiders from western South Africa

Authors: Charles Richard Haddad, Wanda Wesolowska

Data type: xlsx

Explanation note: This spreadsheet contains all of the specimen data presented in the main document text.

Copyright notice: This dataset is made available under the Open Database License (<http://opendatacommons.org/licenses/odbl/1.0/>). The Open Database License (ODbL) is a license agreement intended to allow users to freely share, modify, and use this Dataset while maintaining this same freedom for others, provided that the original source and author(s) are credited.

Link: <https://doi.org/10.3897/AfrInvertebr.65.136083.suppl1>

A revision of Afrotropical *Asceua* (Araneae, Zodariidae), ant-eating spiders with puzzling distributions

Rudy Jocqué¹ , Arnaud Henrard¹ 

¹ Royal Museum for Central Africa, Leuvensesteenweg 13, B-3080 Tervuren, Belgium
Corresponding author: Rudy Jocqué (debarst@telenet.be)

Abstract

The Afrotropical representatives of the zodariid spider genus *Asceua* Thorell, 1889 are revised. Apart from the known species *A. radiosa* Jocqué, 1986 (Comoros, Mayotte) and *A. lejeunei* Jocqué, 1991 (DR Congo, Ethiopia, Ghana, Guinea, Ivory Coast, Nigeria), six new species are recognized and described: *A. arborivaga* **sp. nov.** (♀, Guinea), *A. foordi* **sp. nov.**, (♂♀, DR Congo, Guinea, South Africa), *A. incensa* **sp. nov.** (♂♀, DR Congo), *A. luki* **sp. nov.** (♂♀, DR Congo), *A. palustris* **sp. nov.** (♀, DR Congo) and *A. ventrofigurata* **sp. nov.** (♂♀, Tanzania). A key to the species is provided. Some of the species have a very large distribution, which is unusual in the Zodariidae. The phenomenon is probably linked to the canopy dwelling behaviour, which appears common in the genus but unique for this spider family.

Key words: Africa, ant-eating spider, ant mimicry, canopy dwellers, ecology, taxonomy



This article is part of:

Gedenkschrift for Prof. Stefan H. Foord

Edited by Galina Azarkina, Ansie Dippenaar-Schoeman, Charles Haddad, Robin Lyle, John Mldgley, Caswell Munyai

Academic editor: Robin Lyle
Received: 27 September 2024
Accepted: 30 October 2024
Published: 27 November 2024

ZooBank: <https://zoobank.org/9230378F-8FE3-4785-9FDE-E78FA65002BE>

Citation: Jocqué R, Henrard A (2024)
A revision of Afrotropical *Asceua* (Araneae, Zodariidae), ant-eating spiders with puzzling distributions. African Invertebrates 65(2): 161–198. <https://doi.org/10.3897/AfrInvertebr.65.138029>

Copyright: © Rudy Jocqué & Arnaud Henrard.
This is an open access article distributed under terms of the Creative Commons Attribution License (Attribution 4.0 International – CC BY 4.0).

Introduction

Zodariidae is among the larger spider families, and are commonly known as ant-eating or burrowing spiders. Although a few genera in the Cryptothelinae such as *Thaumastochilus* Simon, 1897, *Storenomorpha* Simon, 1884 and *Chariobas* Simon, 1893 live in burrows in wood (Jocqué 1994; Jocqué and Bosmans 1989) or rolled grass leaves (Leroy and Jocqué 1993), the majority of the species are ground dwelling (Jocqué 1991; Dippenaar-Schoeman 2023). Apart from an odd specimen of *Mallinella* Strand, 1906 (personal observation), representatives of *Asceua* Thorell, 1889, are the only zodariids appearing regularly in canopy samples, indicating an arboreal lifestyle (e.g. Komatsu 2016). There is no doubt that these spiders belong in the canopy fauna, but strangely enough they are also often found in the litter layer of forest and woodland. This peculiar mixed lifestyle may be part of the explanation of the puzzling distribution of the African species in the genus. So far only two species (*A. radiosa* Jocqué, 1986 and *A. lejeunei* Jocqué, 1991) were known from Africa. In the present paper we describe six more species, some of which have a remarkable distribution. We provide a key to the African species and discuss the distributions.

Materials and methods

Specimens were observed and drawn with a WILD M 10 stereomicroscope. Photographs of the habitus, details of mouthparts, detached male palps, female genitalia and measurements were taken with a DFC500 camera mounted on a Leica MZ16A and piloted with the Leica Application Suite automontage software (LAS ver. 4.13). The epigynes were dissected and digested using half a tablet of Total Care Enzima product (protein removal system originally for cleaning contact lenses and containing subtilisin A-0,4 mg per tablet; Abbott Medical Optics, Santa Ana, CA) in a few millilitres of distilled water overnight, then immersed in 75% ethanol to be photographed and stored. Some detached epigynes were not digested but temporarily mounted in a clearing mixture of methyl salicylate and cedukol (Merck, Darmstadt) and photographed as explained above. Photographs of specimens of the Royal Museum for Central Africa (**RMCA**) are accessible through the RMCA Virtual Collection website (<https://virtualcol.africanmuseum.be>). For scanning electron micrographs (**SEM**), specimens were first transferred to fresh 100% ethanol overnight, then to acetone overnight, and finally air dried on a heated plate set at 50 °C. The dried samples were glued to aluminium stubs using double-sided copper tape, and sputter coated with gold then examined and photographed with a JEOL 6480 LV scanning electron microscope at 5 to 12 kV. All measurements are in millimetres. The distribution map was prepared with the online software SimpleMappr (Shorthouse 2010).

Abbreviations: **ALE** = anterior lateral eyes; **AME** = anterior median eyes; **C** = conductor; **CF** = cymbial fold; **CL** = carapace length; **DP** = dorsal prong of palpal tibial apophysis; **Ex** = small prolateral extension of the median prong; **Fe** = femur; **P** = patella; **MOQ** = median ocular quadrangle; **MA** = median apophysis; **MP** = median prong of palpal tibial apophysis; **Mt** = metatarsus; **O** = copulatory opening; **PLE** = posterior lateral eyes; **PME** = posterior median eyes; **Sc** = epigynal scape; **t** = tarsus; **Ti** = tibia; **TL** = total body length; **TT** = tegular tooth; **VP** = ventral prong of palpal tibial apophysis.

Repositories: **NCA** = National Collection of Arachnida (non-Acari) of the Agricultural Research Council, Pretoria, South Africa (R. Lyle); **RMCA** = Royal Museum for Central Africa, Tervuren, Belgium (D. Van den Spiegel).

Remark: The arachnological collection of the RMCA is identified by the acronym "BE_RMCA_ARA.Ara.". This acronym is followed by a unique code for each recorded sample, and, for the sake of clarity, it is simplified by RMCA_XXXXXX in the text.

Taxonomy

Zodariidae Thorell, 1881

Zodariinae Simon, 1893

***Asceua* Thorell, 1887**

Diagnosis (modified from Jocqué 1991). *Asceua* belongs to the dual femoral organ clade (Henrard and Jocqué 2015) which only contains *Suffasia* Jocqué, 1991, *Suffrica* Henrard & Jocqué, 2015 and *Suffascar* Henrard & Jocqué, 2017.

Asceua are recognized by the narrow, compressed cymbium (male), the superficially intricately wound ducts in the epigyne (female) and the presence of only one or two spines on the femora.

Description (modified from Jocqué 1991). Small spiders (2.5–4.5), with relatively high, oval carapace, without cervical grooves, widest at level of coxae II; narrowed in front to 0.65 maximum width in males and to about 0.75 times maximum carapace width in females. Highest point in profile between PME and fovea. Tegument smooth or finely granulated. Colour: Carapace, chelicerae, and sternum orange to dark brown; legs basically yellow to brown with dark stripes, femora usually with pale base. Abdomen dark grey with pale dorsal patches; venter pale or grey, rarely with pattern. Eyes in two procurved rows; ALE dark, circular; remainder pale, circular; eyes subequal. AME less than their diameter apart and at similar distance from ALE. PME about their diameter apart and slightly further from PLE, which are close to ALE. MOQ wider in back than in front and slightly longer than posterior width. Clypeus about three times as high as width of ALE, convex and protruding. Chilum single triangular sclerite, approximately as high as wide, rarely wider and oval. Chelicerae promargin with two small teeth; retromargin with one tooth near fang base (Fig. 11A, B); with patch of pores on inner face at anterior half (Fig. 11A, C). Endites and labium typical for subfamily (Fig. 11D); meso-apical part of the endites with modified, biseriate setae with dorsal tooth (Fig. 11E). Sternum bulging; roughly triangular with slight lateral triangles, corresponding with coxal concavities. Legs: Formula 4123 or 4132. Spination very poor; at most 1 or 2 dorsal spines on femora. Distoventral tuft of hairs poorly developed on Mt III and IV, but with clearly chisel-shaped setae (Fig. 11H, I). Hinged setae absent. Three claws: paired ones with about 10 teeth on legs I and II, with 4 or 5 teeth on legs III and IV. Inferior claw very small or vestigial, on protruding support. Tarsi I and II fusiform, III and IV laterally compressed. Legs beset with indented setae, which may be flat. Trichobothria in two rows on T, in one row on Mt and t; distal trichobothrium on Mt long (Fig. 11J). Femora provided with two femoral organs (Fig. 11K, L): a shallow perforated depression, with few curved, undivided setae. Abdomen oval, with dorsal scutum and epiandrum in male. Spinnerets 4 in male, 6 in female. Colulus represented by transverse row of few setae. Tracheal spiracle narrow, slightly procurved, anterior rim slightly sclerotized. Male palp with short tibia, provided with one or more short lateral and/or dorsal apophyses; cymbium very narrow as seen from above, due to wide lateral fold. Embolus thread-like, originating on mesoproximal side of tegulum, the latter with small median apophysis and membranous conductor. Female palp with finely pectinate claw, turned inward over 90° (Fig. 11F). Tarsus slightly fusiform. Epigyne often with transparent scape; copulatory ducts long, coiled, leading to tubular, rarely spherical, spermathecae.

Key to the Afrotropical species of *Asceua*

Species included:

A. arborivaga sp. nov. ♀

A. foordi sp. nov. ♂♀

A. incensa sp. nov. ♂♀

- A. lejeunei* Jocqué, 1991 ♂♀
A. luki sp. nov. ♂♀
A. palustris sp. nov. ♀
A. radiosa Jocqué, 1986 ♂♀
A. ventrofigurata sp. nov. ♂♀

| | | |
|---|---|--|
| 1 | Males..... | 2 |
| – | Females..... | 7 |
| 2 | Palp with cymbial retrolateral fold narrow, extended over 2/3 of cymbium length (Figs 19D, 20C); palpal tibia with two apophyses; (Figs 19D, 20C); embolus slightly curved, not sinuous (Figs 19B, C, 20B)..... | A. radiosa Jocqué, 1986 |
| – | Palp with cymbial retrolateral fold wide, extended over almost entire cymbium length (Figs 4B, 5B, 8C, 9B, 12C, 13B); palpal tibia with three apophysis (Figs 4B, 5B, 8C, 9B, 12C, 13B); embolus strongly curved and sinuous (Figs 4A, 5A, 8A, B, 9A, 12A, B, 13B)..... | 3 |
| 3 | Distal part of cymbial retrolateral fold deep and curved upwards (Figs 4B, 5B)..... | A. foordi sp. nov. |
| – | Cymbial retrolateral fold smoothly curved to distal tip (Figs 8C, 9B, 12C, 13B, 15B, C, 16B)..... | 4 |
| 4 | Dark species with dark abdominal venter (Fig. 7B); chilum much wider than high..... | A. incensa sp. nov. |
| – | Abdominal venter pale or with dark pattern on pale background (Figs 14C, 21D); chillum triangular, as wide as high..... | 5 |
| 5 | AME large (diameter 1.5 times ALE); venter of abdomen with dark pattern on pale background (Fig. 21B); dorsal prong on palpal tibia broad, its spine implanted subdistally directed forward at an angle of 90° with the base (Figs 22B, C, 23B); MA with three small teeth (Figs 22B, D, E, 23B)..... | A. ventrofigurata |
| – | AME of similar size as ALE; abdominal venter uniform pale; dorsal prong of palpal tibial apophysis slender, with spine at extremity..... | 6 |
| 6 | Cymbium without retrobasal button like process (Fig. 12C); Dorsal prong of palpal tibial apophysis parallel-sided up to distal tip (Figs 12C, 13 B); tegular tooth subdistal and visible from both sides (Fig. 13A, B)..... | A. lejeunei Jocqué, 1991 |
| – | Cymbium with retrobasal button-like process fitting DP concavity (Fig. 15B); Dorsal prong of palpal tibial apophysis tapered up to distal tip (Fig. 16B); (Fig. 15D, E); tegular tooth distal and visible from retrolateral side only (Figs 15B, C, 16B)..... | A. luki |
| 7 | Dorsum of abdomen with intricate dark and pale pattern (Figs 18F, G, H); epigyne without scape (Figs 19E, 20E); spermathecae well defined, rounded (Fig. 19F)..... | A. radiosa |
| – | Dorsum of abdomen with pale spots on dark background (Figs 3D, 6A, B, 7C, 10A, H, 13C, 14E, 21D); epigyne with scape (most often transparent and inconspicuous); spermathecae tubular..... | 8 |
| 8 | Scape narrow and long, main part widest in the middle, tip almost reaching the epigastric furrow (Fig. 2A–C, H)..... | A. arborivaga |
| – | Scape either parallel sided or widened at posterior tip..... | 9 |

- 9 Dark species with dark abdominal venter (Fig. 7F); chilum much wider than high ***A. incensa***
- Abdominal venter pale or with dark pattern on pale background (Figs 3E, 21E); chilum triangular, as wide as high..... **10**
- 10 Scape with parallel sides (Figs 22F, 23D), copulatory ducts wider (Figs 8F–H, 12F, G) **11**
- Scape strongly widened at posterior tip (Figs 4C, D, 5C, 15D, 16C), copulatory ducts narrower (Figs 4C–E, 17D–F) **13**
- 11 Scape long, about 4/5 of epigyne length (Fig. 23D); less than five copulatory duct coils visible in transparency..... **12**
- Scape shorter, 3/4 of epigyne length, indented at tip (Fig. 13D); six copulatory duct coils visible in transparency..... ***A. lejeunei***
- 12 Venter of abdomen with dark pattern on pale background (Fig. 21E); vulva anteriorly with two copulatory duct coils (Fig. 22G, H)..... ***A. ventrofigurata***
- Venter of abdomen uniform pale (Fig. 14F); vulva anteriorly with three copulatory duct coils (Fig. 15G, H) ***A. luki***
- 13 Epigyne with at least six coils of copulatory ducts visible in transparency (Figs 4C, 5C); beginning of copulatory ducts not crossing (Fig. 4E)..... ***A. foordi***
- Less than six copulatory ducts visible in transparency (Fig. 17D); beginning of copulatory ducts crossing (Fig. 17D, G) ***A. palustris***

Descriptions

***Asceua arborivaga* sp. nov.**

<https://zoobank.org/7B3154FF-B078-4C11-8215-0D550FBE5A61>

Figs 1, 2, 24

Material examined. Holotype: GUINEA • ♀; Mount Nimba, Fouenyi Forest; 7°40'00.0"N, 8°28'00.0"W; 1.III.2012; sieving litter under trees; A. Henrard, C. Allard, P. Bimou, and M. Sidibé leg., RMCA_247163.

Paratypes: GUINEA • 1♀; same data as holotype; RMCA_247298; • 2♀♀; Mount Nimba, Nzérékoré, Gouan Forest (mid one) near SMFG camp site; 7°42'02.9"N, 8°23'57.8"W; 6.X.2011; litter in trees and shrubs; at 1.5–3 m above the floor; A. Henrard, and D. VandenSpiegel leg.; RMCA_247161.

Diagnosis. Females of this species are recognised by the dark dorsum of the abdomen with two V-shaped pairs of pale spots (Fig. 1A, B), by the epigyne with a long, narrow, tapered scape (Fig. 2A–D, H) and by the duct conformation of the vulva (Fig. 2E–G).

Etymology. The specific name, *arborivaga* means ‘active in trees’, refers to the ecology of the species, which has been found in litter but also in trees.

Description. Female Holotype. Fig. 1A–E. TL 3.91. Colour in ethanol: carapace with dark thoracic area and medium brown cephalic area with faint darker ‘V’ in front of fovea and narrow dark rings around eyes; chelicerae uniform medium brown; endites and labium pale brown with pale anterior margin; sternum dark brown, paler in the centre; legs: coxae white, trochanters dark brown, femora with narrow proximal dark ring, wider pale ring and distal 2/3 dark brown, patellae pale with pro- and retrolateral dark patch, tibiae pale with ventral dark stripe;



Figure 1. *Asceua arborivaga* sp. nov., Holotype female habitus **A** dorsal view **B** idem, air dried (out of alcohol for a few minutes) **C** ventral view **D** frontal view **E** lateral view. Scale bars: 1 mm.

dorsum of abdomen black with two pairs of white blotches arranged in V-shape, and tiny white spot in front of spinnerets; sides uniform black extended on venter in front of pale yellow spinnerets, remainder of venter pale. Carapace 1.70 long, 1.14 wide, 0.78 high. Eye sizes and interdistances: AME: 0.10; ALE: 0.08; AME–AME: 0.03; AME–ALE: 0.05; PME: 0.09; PLE: 0.12; PME–PME: 0.12; PME–PLE: 0.13. MOQ: frontal width 0.23, posterior width 0.30, length 0.30. Clypeus 0.36 high. Chilum: small triangle 0.12 wide, 0.10 high. Sternum shield-shaped, 0.85 long, 0.78 wide. All femora with one short, dorsal spine in proximal half.

Legs: measurements in Table 1.

Table 1. Female leg measurements.

| Leg | Fe | P | Ti | Mt | t | tot |
|-----|------|------|------|------|------|------|
| I | 1.05 | 0.42 | 0.77 | 1.12 | 0.63 | 3.99 |
| II | 0.91 | 0.42 | 0.70 | 0.84 | 0.56 | 3.43 |
| III | 0.84 | 0.42 | 0.77 | 1.05 | 0.56 | 3.64 |
| IV | 1.05 | 0.42 | 0.84 | 1.40 | 0.56 | 4.27 |

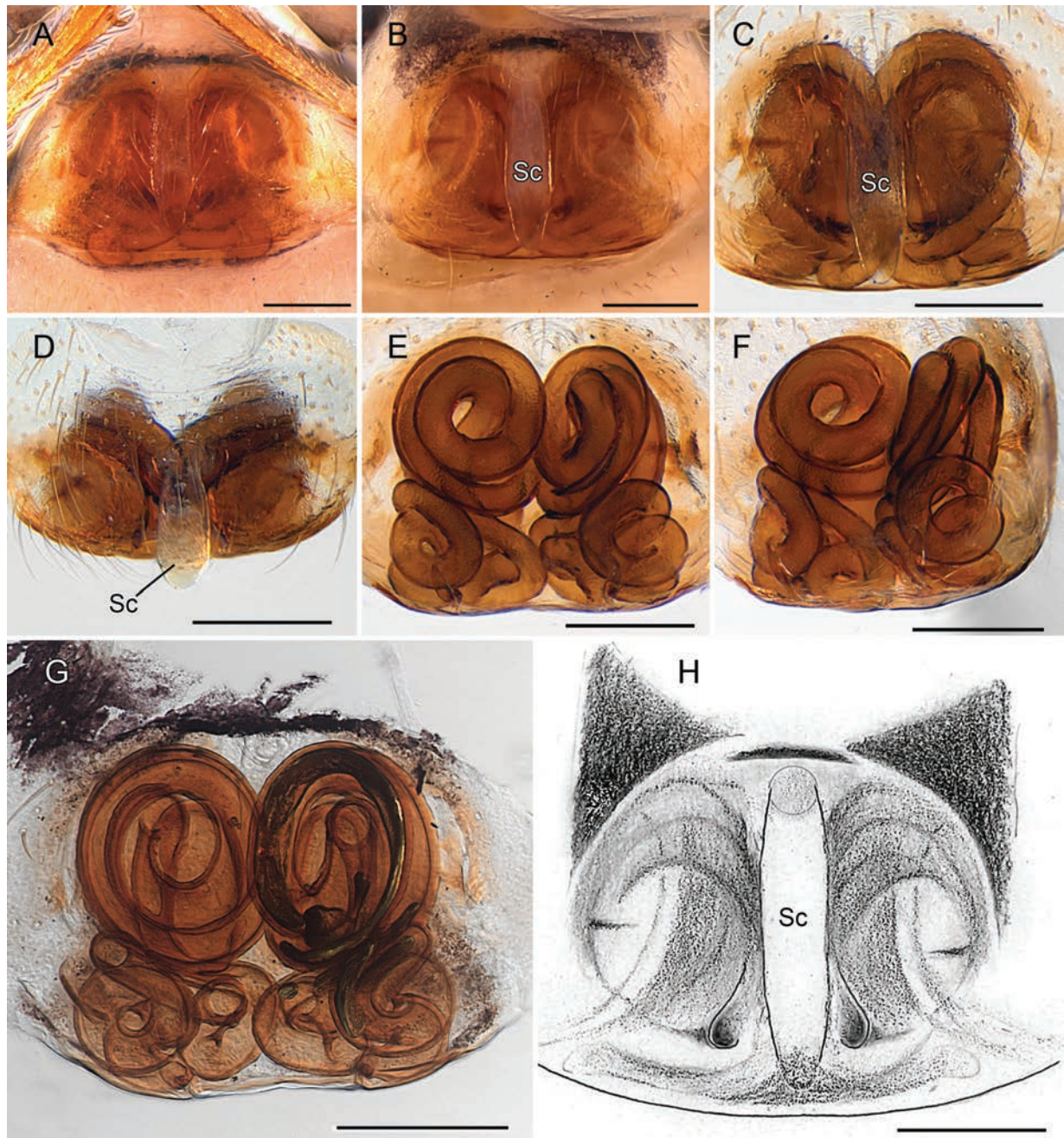


Figure 2. *Asceua arborivaga* sp. nov., female genitalia **A** holotype female **B–F, H** paratype female (RMCA_247163) **G** paratype female (RMCA_247161) **A, B** epigynes, ventral view **C** idem, cleared **D** idem, antero-ventral view **E** vulva, cleared, dorsal view **F** idem, slightly lateral **G** idem, transmitted light **H** Drawing of epigyne, ventral view. Abbreviation: Sc = scape. Scale bars: 0.2 mm.

Epigyne (Fig. 2A–H): Scape (Sc) long, narrow, with widest part in the middle, distally tapered and rounded; copulatory ducts in transparency vague, longitudinal; copulatory ducts in posterior part, mainly transverse, intricately wound, in dense, wide spirals in anterior part.

Male. Unknown.

Variation. Females (n = 2). TL 4.19–4.47, CL 1.56–1.70. White patches on abdominal dorsum may be less strongly inclined and sometimes anastomosing.

Distribution. The species is known from the Mount Nimba area in Guinea (Fig. 24).

***Asceua foordi* sp. nov.**

<https://zoobank.org/9A41E803-50F3-47DF-BB89-577DF441D7A5>

Figs 3–6, 24

Type material. Holotype: SOUTH AFRICA • ♂; Eastern Cape Province, Mazeppa Bay; 32°28.476'S, 28°38.873'E; 28.X.2006; grassy litter, *Acacia* thicket, behind dunes; C. Haddad leg.; NCA 2007/206.

Paratypes: SOUTH AFRICA • 3♂♂ 1♀; Eastern Cape Province, Mazeppa Bay, 32°28.734'S, 28°39.118'E; 28.X.2006; C. Haddad leg.; NCA 2007/219; • 1♂, Eastern Cape Province, Mazeppa Bay; 32°26.495'S, 28°36.968'E; 28.X.2006; leaf litter, *Eucalyptus* plantation; C. Haddad leg.; NCA 2007/280; • 2♀♀; Eastern Cape Province, Coffee Bay; 31°58.862'S, 29°09.119'E; 2.XI.2006; leaf litter coastal dune forest; C. Haddad leg.; NCA 2007/168; • 1♂ 3♀♀; KwaZulu-Natal, Vernon Crookes Nature Reserve; 30°16.250'S, 30°36.400'E; 486 m a.s.l.; 9–12.X.2020; Hand collecting; R. Booysen and R. Steenkamp leg.; NCA 2020/782; • 2♀♀ (DNA Z015); Eastern Cape Province, Coffee Bay; 31°59.148'S, 29°09.076'E; 5 m a.s.l.; 9.I.2011; base of grass tussocks; C. Haddad leg.; RMCA_245369; • 1♀ (drawing epigyne); Kwazulu Natal Province, Alfred District, Oribi Gorge; 30°42'S, 30°16'E; XI.1961, N. Leleup leg., RMCA_1326311; • 1♂ 3♀♀; Eastern Cape Province, Kei Mouth; 32°41'S, 28°23'E; 12.XII.2002; C. Haddad leg.; RMCA_215900; • 1♂; Kwazulu Natal Province, Krantzkloof, Krantzkloof Nature reserve; 28°51'S, 30°43'E; 25.VI.2002, forest, sieved litter; R. Jocqué leg.; RMCA_212169; • 3 juv.; as previous; winker extraction from sieved litter; R. Jocqué leg.; RMCA_212323; • 1♂; Kwazulu Natal Province, Mtunzini; 28°57'S, 31°45'E; 26.VI.2002; coastal forest, sieved litter; R. Jocqué leg.; RMCA_212282; • 3♂♂ 1♀; Eastern Cape Province, Silaka N.R.; 31°39'S, 29°30'E; 1.XI.2011; 43 m a.s.l.; base of grasses and ferns; C. Haddad leg.; RMCA_239310; • 2♀♀; Eastern Cape Province, Port St Johns, Cremorne Estate: 31°36'S, 29°32'E; 1.X.2011; 43 m ; sifting leaf litter, coastal forest, C. Haddad leg., RMCA_239309; • 1♀; Eastern Cape Province, Coffee Bay; 31°58.862'S, 29°09.119'E; 10.I.2011; 15 m a.s.l.; sifting leaf litter coastal dune forest; C. Haddad leg.; RMCA_239312; • 2♀; Kwazulu Natal Province, Eshowe District, Dhlinda forest; 28°53'S, 31°27'E; X.1960; dans l'humus; N. Leleup leg. RMCA_132650.

Other material examined. GUINEA • 1♂; Mount Nimba, Pierré Richaud; 7°39'N, 8°22'W; 10–7.X. 2011; fogging 04, top of gallery forest, open area, canopy of trees; 1625 a.s.l.; Van den Spiegel Didier, et al. RMCA_238012); DR CONGO • 1♀; Parc National Salonga, 505 m a.s.l.; 2.28766S 21.02188E, 3.XII.2022, B. Pett, and M. Jocque leg. RMCA_247696; • 1♂; as previous; RMCA_247694) • 1♂; as previous; RMCA_247695.

Diagnosis. Males of this species are characterised by details of the palp (Figs 4A, B, 5A, B): the distal spine-shaped part of the dorsal tibial prong is directed forward at an angle of 90° with the base of the apophysis; the cymbium has a wide, S-shaped fold of which the distal part is particularly deep and curved upwards; females are recognized by the epigyne with scape strongly widened apically ending in the middle and the complex copulatory duct with six loops visible in transparency along its course (Figs 4C–E, 5C).

Etymology. The specific name is a patronym in honour of our friend and colleague, the late Stefan Foord, who was a dynamic arachnologist and driving force for arachnology in South Africa and beyond.

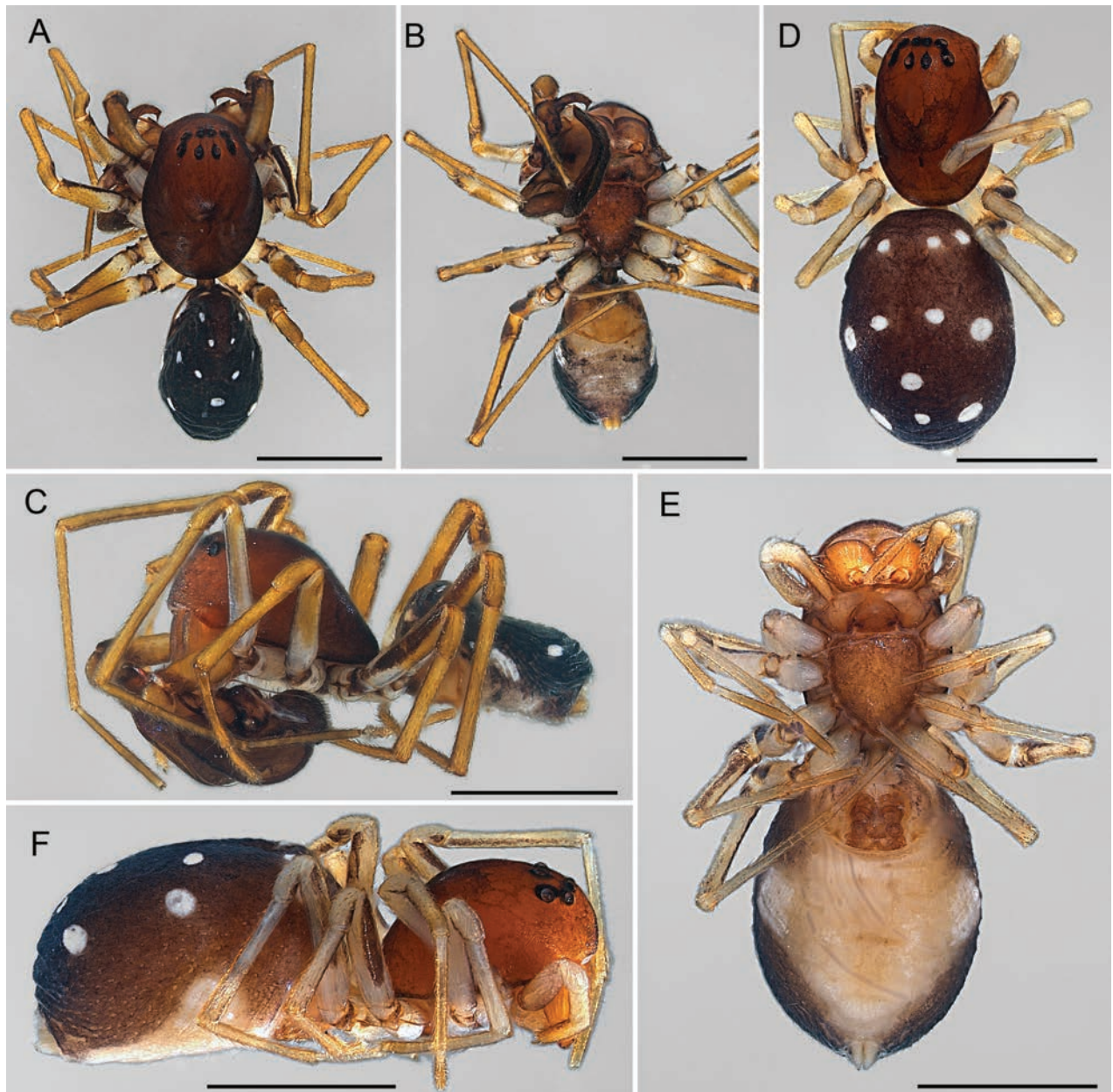


Figure 3. *Asceua foordi* sp. nov., male and female habitus **A–D** holotype male **D–F** paratype female (RMCA_132631) **A, D** dorsal view **B, E** ventral view **C, F** lateral view. Scale bars: 1 mm.

Description. Male Holotype. Figs 3A–C, 6C–E. Total body length 2.77. Colour in ethanol: carapace uniform medium brown with narrow dark rings around eyes and W-shaped dark area in front of fovea; chelicerae, endites and labium medium brown; sternum medium brown with darker margin; legs: femora pale with dark anterior stripes on Fe I–IV and dark posterior stripe on Fe III and IV in distal two thirds; abdomen: dorsum dark grey with narrow dark brown scutum in anterior half, 13 tiny white spots (Fig. x); sides dark with oblique white streak; venter pale, narrow yellowish patch in front of white spinnerets and yellow in front of epigastric fold. Carapace 1.28 long, 0.92 wide, 0.64 high. Eye sizes and interdistances: AME: 0.07; ALE: 0.08; AME–AME: 0.03; AME–ALE: 0.05; PME: 0.07; PLE: 0.10; PME–PME: 0.07; PME–PLE: 0.08. MOQ: frontal width 0.16, posterior width 0.21, length 0.24. Clypeus 0.34 high. Chilum: small triangle 0.08

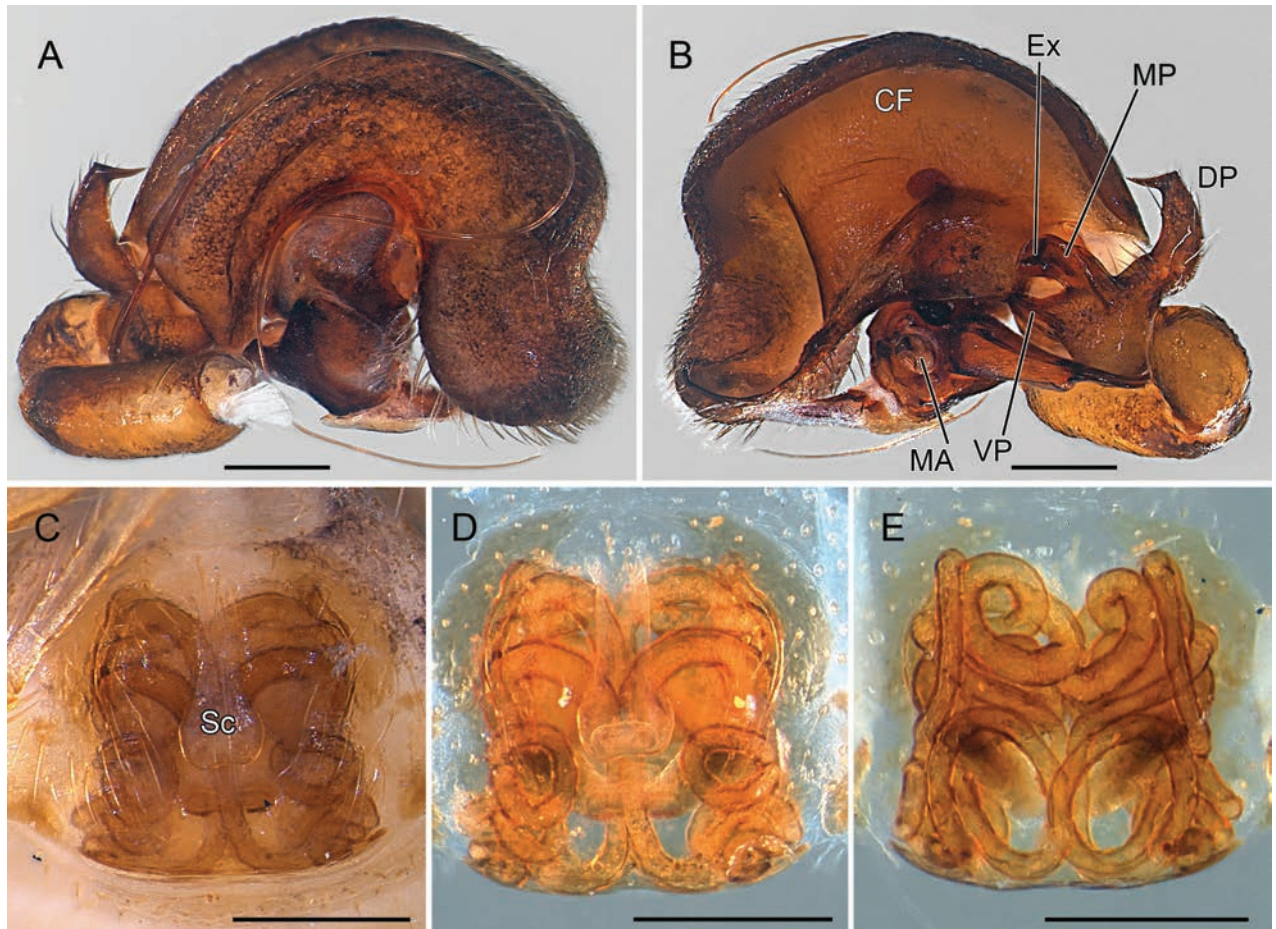


Figure 4. *Asceua foordi* sp. nov., male and female genitalia **A, B** holotype male **C–E** paratype female (RMCA_132631) **A** palp, retrolateral view **B** idem, prolateral view **C** epigyne, ventral view **D** idem, cleared **E** vulva, dorsal view. Abbreviations: CF = cymbial fold; DP = dorsal prong of palpal tibial apophysis; Ex = small prolateral extension of the median prong; MA = median apophysis; MP = median prong of palpal tibial apophysis; Sc = scape; VP = ventral prong of palpal tibial apophysis. Scale bars: 0.2 mm.

wide and as high. Sternum shield-shaped, 0.57 long, 0.54 wide. All femora with one short dorsal spine in proximal half.

Legs: measurements in Table 2.

Palp (Figs 4A, B, 5A, B): very large: length including Ti 0.8 times carapace length. Tibia with three apophyses: dorsal prong (DP) broad, directed up, slightly curved forward, with distal spine shaped tip pointing forward at an angle of 90°; median prong (MP) shorter, curved downward with rounded extremity, with sharp triangular extension visible by transparency (Ex); inferior one (VP) short, straight with rounded extremity; cymbium laterally compressed with large lateral S-shaped fold (CF), its distal curve deep and directed upwards; tegulum

Table 2. Male leg measurements.

| Leg | Fe | P | Ti | Mt | t | tot |
|-----|------|------|------|------|------|------|
| I | 1.12 | 0.35 | 1.05 | 1.12 | 0.70 | 4.34 |
| II | 0.91 | 0.35 | 0.70 | 0.91 | 0.56 | 3.43 |
| III | 0.77 | 0.35 | 0.63 | 0.91 | 0.42 | 3.08 |
| IV | 1.05 | 0.35 | 0.84 | 1.26 | 0.56 | 4.06 |

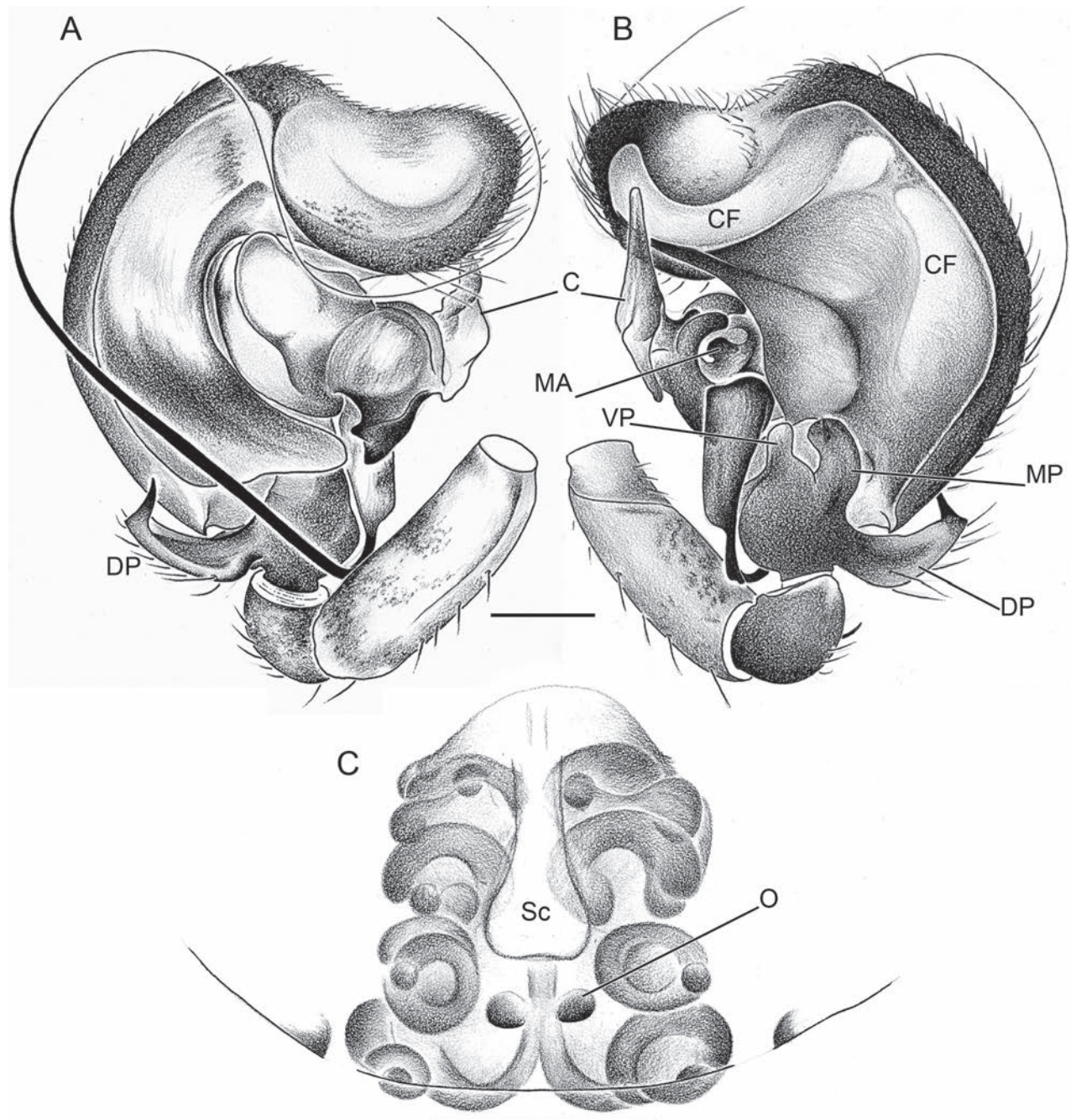


Figure 5. *Asceua foordi* sp. nov., genitalia drawings **A, B** paratype male (RMCA_212282) **C** paratype female (RMCA_132631) **A** palp, retrolateral view **B** idem, prolateral view **C** epigyne, ventral view. Abbreviations: C = conductor; CF = cymbial fold; DP = dorsal prong of palpal tibial apophysis; MA = median apophysis; MP = median prong of palpal tibial apophysis; O = copulatory opening; Sc = scape; VP = ventral prong of palpal tibial apophysis. Scale bars: 0.2 mm.

with two appendages: largest one, mainly visible prolaterally; second one pear-shaped with long tapered forward directed prong; median apophysis (MA) sub-circular with short rounded lip directed forward; conductor (C) large, directed forward; embolus long and whip-shaped originating on dorsal side of tapered posterior end of roughly triangular base.

Female (paratype NCA 2007/219). Figs 3D–F, 6A, B. Total body length 3.20. Colour as in male; dorsum with 15 white spots; lateral spot rounded. Carapace 1.42 long, 0.78 wide, 0.71 high. Eye sizes and interdistances: AME: 0.07; ALE:

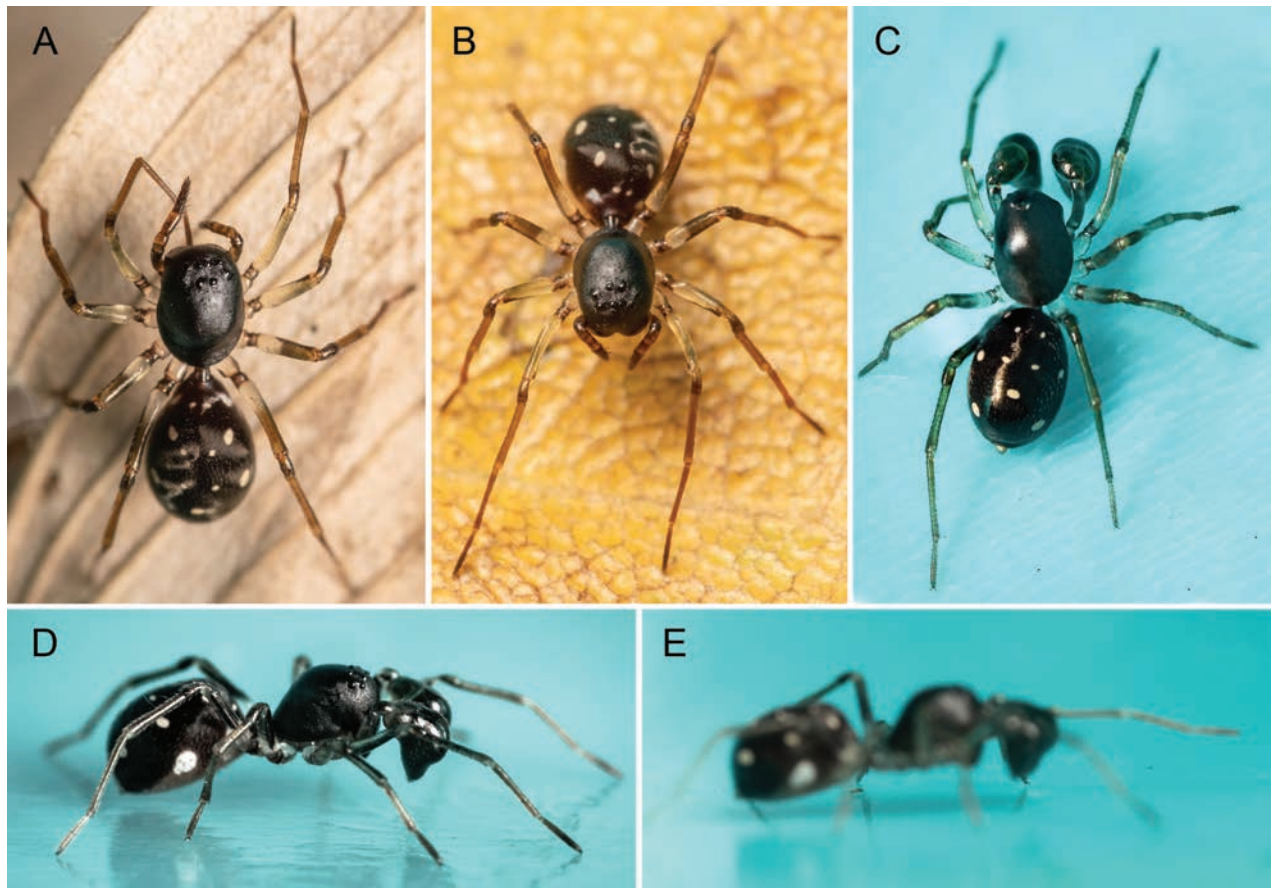


Figure 6. *Asceua foordi* sp. nov., photographs of specimens *in vivo* (NCA 2020/782) **A, B** females **C–E** male subadult. Note the ant-looking appearance in the blurred photo (E). Photos by Rudolph Steenkamp.

0.07; AME–AME: 0.03; AME–ALE: 0.07; PME: 0.07; PLE: 0.08; PME–PME: 0.07; PME–PLE: 0.10. MOQ: frontal width 0.16, posterior width 0.20, length 0.26. Clypeus 0.30 high. Chilum: small triangle 0.08 wide and as high. Sternum shield-shaped, 0.64 long, 0.57 wide. Legs without spines; measurements in Table 3.

Epigyne (Figs 4C–E, 5C): rectangular area slightly wider behind than in front; scape (Sc) widened towards posterior part situated in the centre of the epigyne, its tip slightly indented, copulatory openings (O) situated in posterior half; copulatory ducts narrow, strongly wound, with six loops visible in transparency; very complex internal structure with many loops mainly longitudinal in posterior part, mainly transverse in anterior part.

Variation. South Africa: Males ($n = 5$): TL 2.77–3.00, CL 1.28–1.50; white spots on dorsum 11–13. Females ($n = 11$): TL 2.70–3.83, CL 1.21–1.68; white spots on dorsum 13–16. The shape of the small spots may vary from circular to elongate oval.

Table 3. Female leg measurements.

| Leg | Fe | P | Ti | Mt | t | tot |
|-----|------|------|------|------|------|------|
| I | 0.84 | 0.35 | 0.84 | 0.77 | 0.49 | 3.29 |
| II | 0.70 | 0.35 | 0.56 | 0.70 | 0.49 | 2.80 |
| III | 0.70 | 0.35 | 0.56 | 0.63 | 0.42 | 2.66 |
| IV | 0.91 | 0.35 | 0.70 | 0.98 | 0.49 | 3.43 |

DR Congo: Males (n = 2): TL 2.63–2.77, CL 1.35–1.42; dorsum in the centre with two transverse rectangular white spots. Female (n = 1): TL 2.51, CL 1.21; dorsum as in males. Guinea: Male (n = 1): TL 2.59; CL 1.44. Abdominal pattern as in type series.

Distribution. The species is known from South Africa, DR Congo and Guinea (Fig. 24).

***Asceua incensa* sp. nov.**

<https://zoobank.org/9120A2D9-26E5-498B-8ACD-80F70FD73408>

Figs 7–9, 24

Type material. Holotype: D.R. CONGO • ♂; Mayombe, Luki Biosphere Reserve; 5°38'S, 13°04'E; 23.IX.2007; canopy fogging, secondary rainforest; D. De Bakker and J.P. Michiels leg; RMCA_247724.

Paratypes: • 1♀; same data as holotype; RMCA_234808; • 3♂♂ 1♀; 19.IX.2007; secondary rainforest; further as previous; RMCA_235127; • 2♂♂ 1♀; 18.IX.2007; canopy fogging, secondary rainforest; further as previous; RMCA_235126.

Diagnosis. Both sexes are recognised by the wide chilum and the dark colour including the venter of the abdomen (Fig. 7B–D). Males are further characterised by the palp (Figs 8A–E, 9A, B) with stout median apophysis with pear-shaped base and claw-shaped tip, cymbial fold not strongly narrowed towards the extremity, stopping short of the cymbium tip. Females are recognised by the epigyne scape with widened tip ending at posterior half in front of copulatory openings (Figs 8F, 9C), and the genitalia with anterior loops tight and obliquely transverse (Fig. 8G, H).

Etymology. The species name is an adjective (Latin *incensus* = burnt) referring to the dark colour of the species.

Description. Male Holotype. Fig. 7A–C. TL 2.68. Colour in ethanol: carapace dark brown, cephalic area slightly paler with faint darker 'V' in front of fovea; chelicerae medium brown; endites medium brown with lateral margins darkened; labium medium brown with pale frontal margin; sternum dark brown, darker towards lateral margins; legs: coxae pale cream with narrow prolateral dark stripe; femora pale cream in proximal third, dark brown in distal two thirds; patellae, tibiae and metatarsi yellow with dark brown ventral stripe; abdomen: dorsum almost black with black scutum, on either side with small oval pale spot; sides and venter dark grey, lighter in front of epigastric fold, at its extremities with rounded white spot.

Carapace 1.32 long, 0.99 wide, 0.70 high. Eye sizes and interdistances: AME: 0.10; ALE: 0.10; AME–AME: 0.03; AME–ALE: 0.03; PME: 0.08; PLE: 0.08; PME–PME: 0.10; PME–PLE: 0.15. MOQ: frontal width 0.23, posterior width 0.26, length 0.28. Clypeus 0.34 high. Chilum: wide sclerite 0.28 wide, 0.08 high, dorsal margin procurved, ventral margin almost straight. Sternum shield-shaped, 0.71 long, 0.64 wide. All femora with one short dorsal spine in proximal half.

Legs: measurements in Table 4.

Palp (Figs 8A–E, 9A, B): large: length including Ti 0.75 times carapace length. Tibia with three apophyses: dorsal one (DP) narrow, slightly concave in prolateral view, slightly curved forward, with distal spine shaped prong smoothly following curve of basal part; median tibial apophysis (MP) parallel sided with

Table 4. Male leg measurements.

| Leg | Fe | P | Ti | Mt | t | tot |
|-----|------|------|------|------|------|------|
| I | 0.93 | 0.32 | 0.77 | 0.96 | 0.61 | 3.58 |
| II | 0.83 | 0.32 | 0.54 | 0.90 | 0.54 | 3.14 |
| III | 0.86 | 0.32 | 0.58 | 0.93 | 0.45 | 3.14 |
| IV | 0.96 | 0.32 | 0.70 | 1.12 | 0.54 | 3.65 |

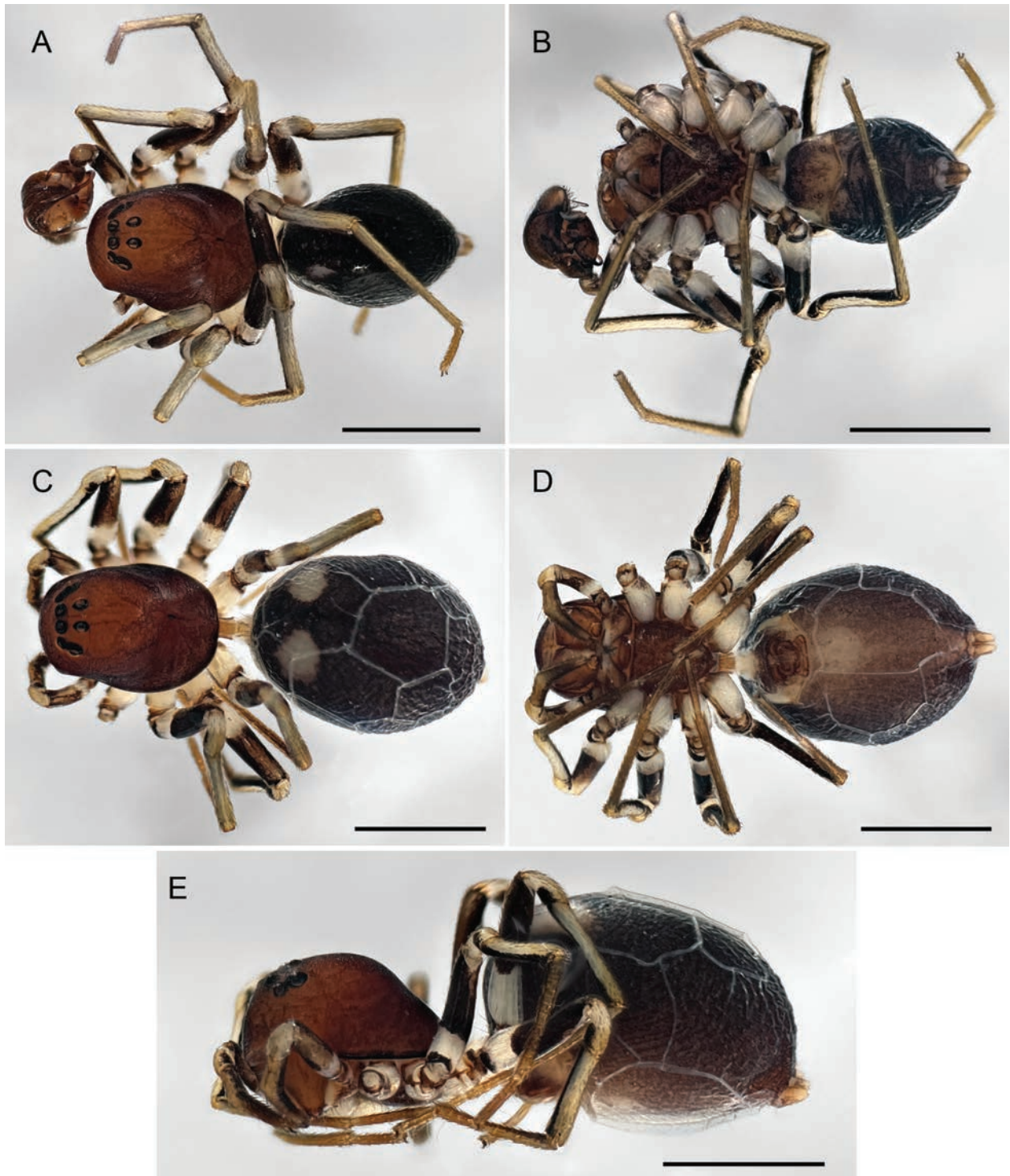


Figure 7. *Asceua incensa* sp. nov., male and female habitus **A, B** male holotype **C-E** female paratype (RMCA_234808) **A, C** dorsal view **B, D** ventral view **E** lateral view.

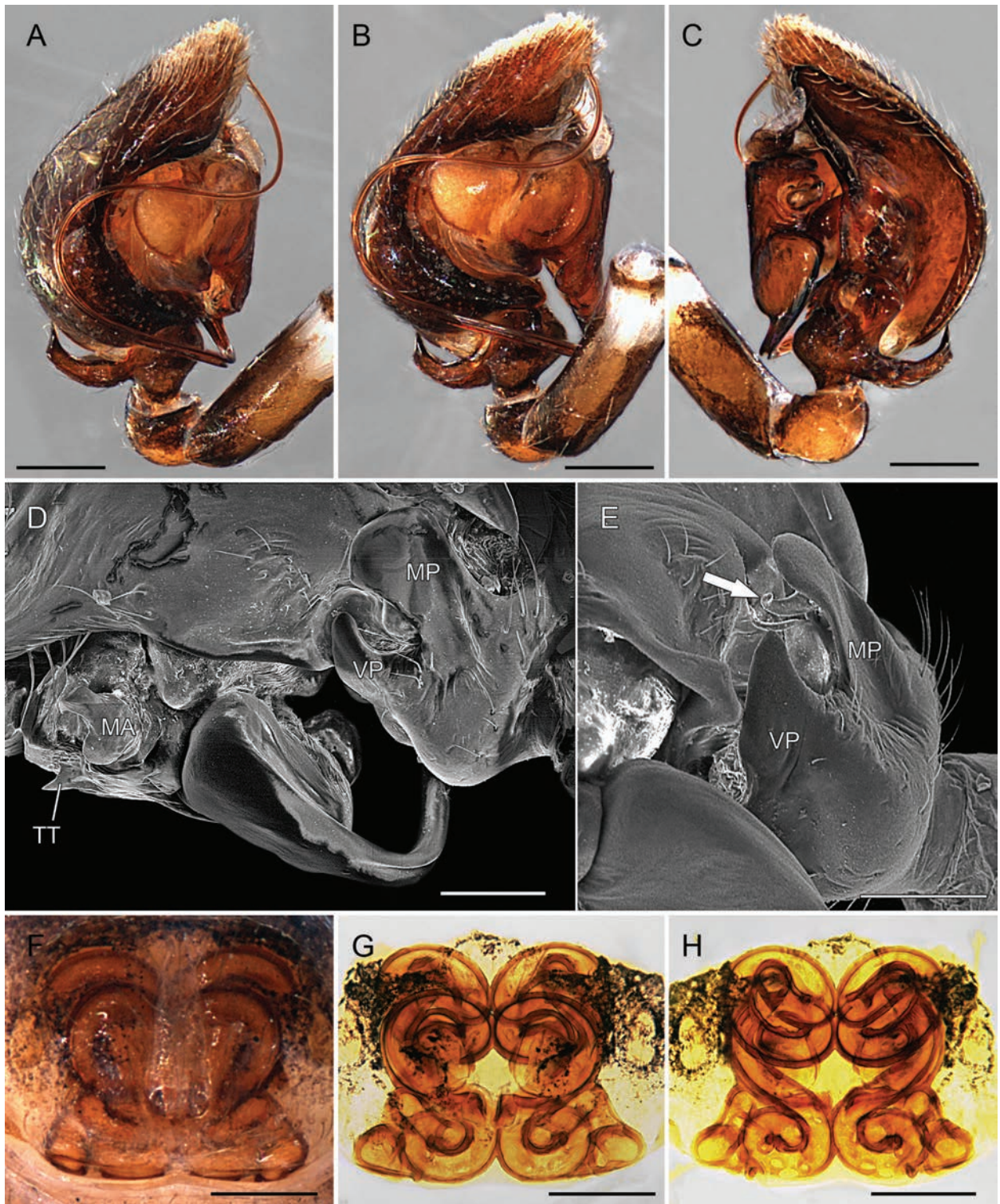


Figure 8. *Asceua incensa* sp. nov., genitalia **A–C** male holotype **D, E** male paratype (RMCA_235127) **F–H** female paratype (RMCA_234808) **A** palp, prolateral view **B** idem, slightly ventral **C** idem, retrolateral view **D** idem, SEM view, details **E** idem, detail of palpal tibial apophyses **F** epigyne, ventral view **G** idem, cleared **H** vulva, dorsal view. Abbreviations: MA = median apophysis; MP = median prong of palpal tibial apophysis; TT = tegular triangular tooth; VP = ventral prong of palpal tibial apophysis. Scales bars: 0.2 mm (**A–C**); 0.1 mm (**D–H**).

rounded extremity, with thin extension behind it (Ex); inferior one (VP) short, curved upward with rounded extremity; cymbium laterally compressed with large lateral semicircular fold, not strongly narrowed towards the extremity,

stopping short of the cymbium tip; tegulum with three appendages: largest one voluminous mainly visible prolaterally with smoothly rounded posterior tip pointing back; median apophysis (MA) pear-shaped with small tapered, rounded, upward directed prong; one extra small triangular tooth sub apically (TT); conductor membranous, directed forward; embolus long and whip shaped with large triangular base directed backward.

Female Paratype (RMCA_234808). Fig. 7D, E. TL 3.43. Colour as in male but for the absence of a scutum, pale dorsal spots larger and rounded, venter with small paler area behind epigastric fold. Carapace 1.73 long, 1.20 wide, 0.91 high. Eye sizes and interdistances: AME: 0.08; ALE: 0.08; AME–AME: 0.05; AME–ALE: 0.05; PME: 0.08; PLE: 0.08; PME–PME: 0.10; PME–PLE: 0.13. MOQ: frontal width 0.21, posterior width 0.26, length 0.30. Clypeus 0.31 high. Chilum: 0.39 wide, 0.08 high, shape as in male. Sternum shield-shaped, 0.66 long, 0.59 wide.

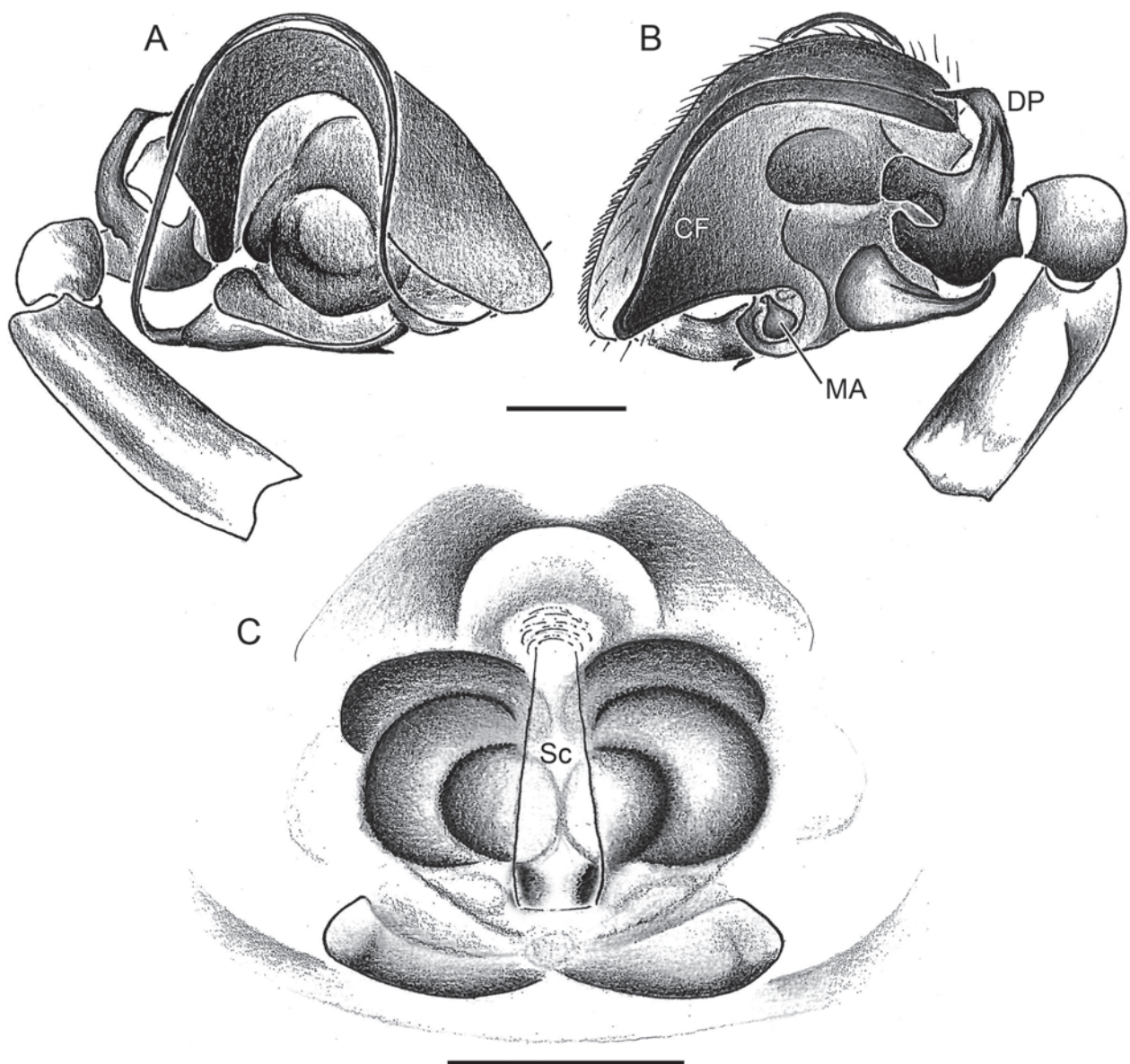


Figure 9. *Asceua incensa* sp. nov., genitalia drawings **A**, **B** male holotype **C** female paratype (RMCA_234808) **A** palp, retro-lateral view **B** idem, prolateral view **C** epigyne, ventral view. Abbreviations: CF = cymbial fold; DP = dorsal prong of palpal tibial apophysis MA = median prong of palpal tibial apophysis; Sc = scape. Scale bars: 0.2 mm.

Table 5. Female leg measurements.

| Leg | Fe | P | Ti | Mt | t | tot |
|-----|------|------|------|------|------|-------|
| I | 0.86 | 0.32 | 0.70 | 0.90 | 0.54 | 3.33 |
| II | 0.83 | 0.32 | 0.61 | 0.83 | 0.48 | 3.07 |
| III | 0.74 | 0.32 | 0.61 | 0.86 | 0.48 | 3.01 |
| IV | 0.96 | 0.32 | 0.83 | 1.09 | 0.51 | 3.371 |

Legs: All femora with one short dorsal spine in proximal half. Leg measurements in Table 5.

Epigyne (Figs 8C–E, 9C): quadrangular area, as wide as long; scape (Sc) moderately long (0.75 time epigyne height), with widened tip; copulatory openings in front of scape tip; ducts relatively wide, strongly wound, posterior part with short dense spires, anterior part with three densely superposed, obliquely transverse loops.

Variation. Males (n = 6): TL 2.68–2.94, CL 1.32–1.41; dorsum of abdomen with spots sometimes slightly larger. Females (n = 3): TL 3.43–3.84, CL 1.47–1.73; dorsum with spots sometimes slightly more oval.

Distribution. The species is known from the type locality in western DR Congo (Fig. 24).

***Asceua lejeunei* Jocqué, 1991**

Figs 10–13, 24

Asceua lejeunei Jocqué, 1991: 41.

Type material. Holotype: D.R. CONGO • ♂; Kivu-N, Ruindi, vallée de la Ruindi; 0°48'S, 29°18'E; 10.VII.1972 battage, Lejeune M. RMCA_144436).

Paratypes: 4♀♀, 2. juv. together with holotype.

Other material examined. CÔTE D'IVOIRE • 1♂; Taï forest, 5°52'N, 7°27'W; 1.IX.2010; 185 m a.s.l.; beating, D. Van den Spiegel, and A. Kablan leg.; RMCA_233436; ETHIOPIA: • 1♂; Yayu Coffee Forest; 8°23'N, 35°48'E; 30.XII.2003; 1476 m a.s.l.; forest, beating, N. Akililu leg., RMCA_229444; • 1♂; Yayu Coffee Forest; 8°23'N, 35°48'E; 15.I.2004; 1476 m a.s.l.: secondary forest, beating; N. Akililu leg.; RMCA_229446; GHANA: • 1♀; Kakum forest; 5°20'N, 1°23'W; 14.XI.2005; primary forest; L. Baert, R. Jocqué, and D. De Bakker leg.; RMCA_217241; • 2♂♂ 1♀; as previous; RMCA_218341; • 9♂♂ 9♀♀; 18.XI.2005, further as previous RMCA_218343; • 2♂♂ 1♀; 19.XI.2005; secondary forest, further as previous; RMCA_218344; • 3♂♂; 17.XI.2005; further as previous; RMCA_218342; GUINEA: • 1♂ 1♀; Mount Nimba, Forest of Gbié reserve; 7°38.707'N; 8°20.46'W; 21.XI.2017; 579 m a.s.l.; A. Henrard, D. Van den Spiegel, C. Allard, Samoura Aboubacar Mr, P. Bimou, Bamba Mr leg.; RMCA_247165; • 1♂ 1♀; Mount Nimba, Seringbara near camp 1; 7°38.975'N, 8°25.393'W; 29.XI.2017; 674 m a.s.l.: A. Henrard, D. Van den Spiegel, C. Allard, Samoura Aboubacar (Mr), P. Bimou, Bamba (Mr) leg.; RMCA_247530; • 1♀; Mount Nimba, Gouan Forest (Mid-one); 7°42'N, 8°24'W; 29.I.2012; sieving litter, secondary forest: D. Van den Spiegel et al. leg.: RMCA_238794; • 1♀; Mount Nimba, Fouenyi forest; 7°40'N, 8°28'W; 1.III.2012, 573 m a.s.l.: sieving litter under trees; M. Sidibé, A. Henrard, C. Allard,

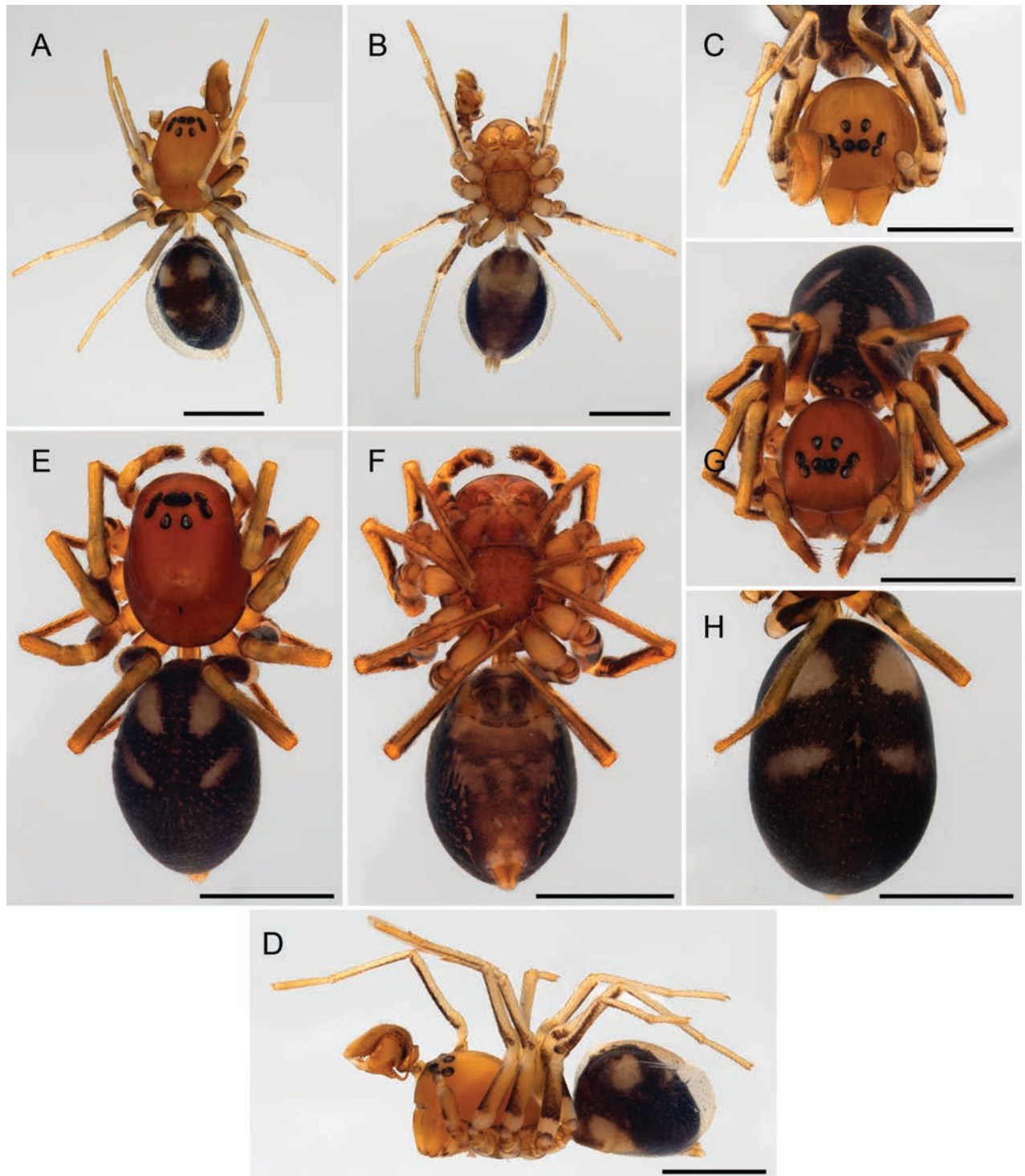


Figure 10. *Asceua lejeunei* Jocqué, 1991, male and female habitus **A–D** holotype male **E–H** paratype female (RMCA_144436) **A, E** dorsal view **B, F** ventral view **C, G** frontal view **D** lateral view **H** abdomen, dorsal view. Scale bars: 1 mm.

P. Bimou leg.; RMCA_239733; • 1♀; Mount Nimba, Freton, Seringbara; 7°38'N, 8°27'W; 2.III.2012, 586 m a.s.l.; sieving humid litter, primary forest; M. Sidibé, A. Henrard, C. Allard, P. Bimou leg.; RMCA_239254; • 1♀; Mount Nimba, Gbié forest, Deguelou; 7°40'N, 8°19'W; 18.III.2012; 595 m a.s.l.; sieving soil litter, near river Deguelou; M. Sidibé, A. Henrard, C. Allard, P. Bimou leg.; RMCA_239141; • 2♂♂

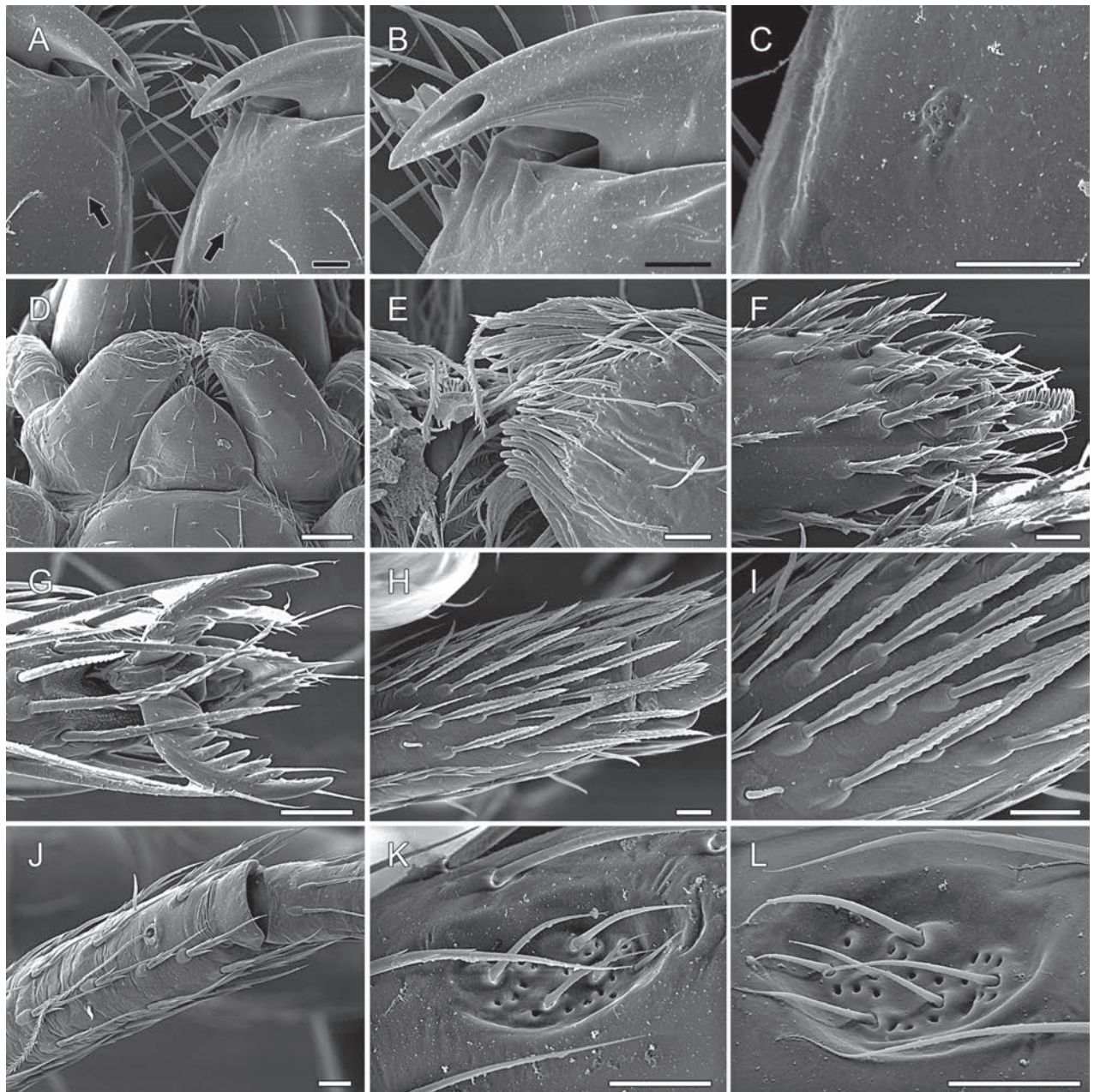


Figure 11. *Asceua lejeunei* Jocqué, 1991, SEM views of somatic characters, female (RMCA_ 245370) **A** cheliceral fangs and promargins, ventral view. Arrows pointing to cheliceral pores **B** idem, detail of fang and promargin teeth **C** detail of cheliceral pores on proventral face **D** endites and labium, ventral view **E** apex of endites, detail of setae **F** apex of palpal tarsus, ventral view **G** claws of leg IV **H** apex of metatarsus III, ventral view **I** idem, detail of chisel-shaped setae **J** apex of metatarsus IV **K** Femoral organ of leg I, retrolateral side **L** idem, proteral side. Scale bars: 20 μm (**A–C**, **E–L**); 0.1 mm (**D**).

1 ♀; Mount Nimba, Seringbara Forest; 7°39'N, 8°26'W; 13.III.2012; 606 m a.s.l.; fogging, secondary forest, canopy, no wind; M. Sidibé, A. Henrard, C. Allard, P. Bimou leg.; RMCA_239640; • 2 ♀♀; Mount Nimba, Fouenyi Forest; 7°40'N, 8°28'W; 1.III.2012; 573 m a.s.l.; sieving soil litter; Sidibé M., A. Henrard, C. Allard, P. Bimou leg.; RMCA_238797; • 1 ♂; Mount Nimba, Forêt Gouan (Mid-one), 7°42'N, 8°24'W, 8.X.2011, sieving litter, secondary forest, A. Henrard, D. Van den Spiegel leg. RMCA_245370; • 2 ♂♂; Mount Nimba, Gouan forest (Mid-one) 7°42'N, 8°24'W, 8.X.2011, beating, litter in trees and shrubs, at 1.5–3 m above the floor, A. Henrard and Van den Spiegel leg.; RMCA_247162; • 1 ♂; Mount Nimba, Gouan For-

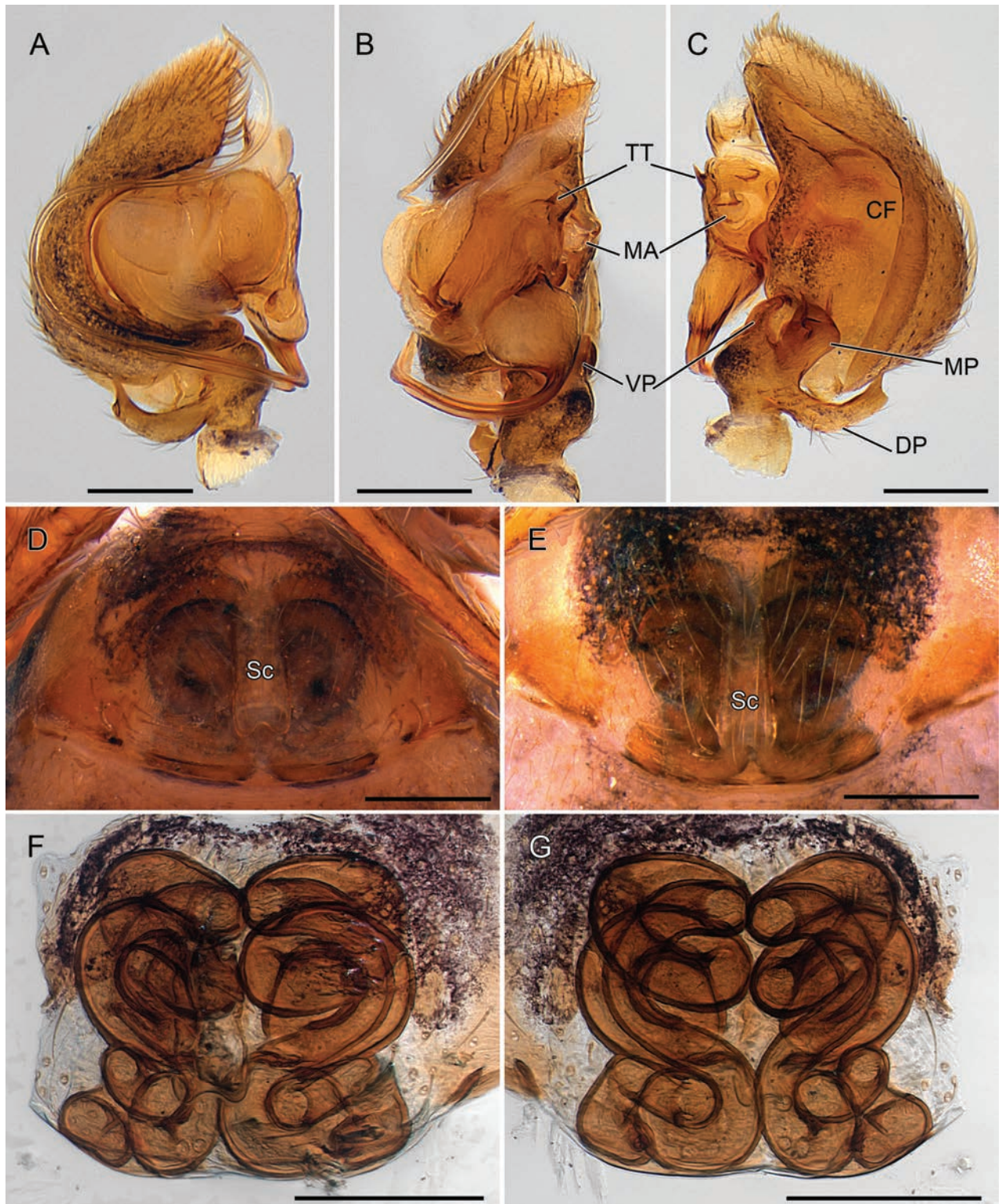


Figure 12. *Asceua lejeunei* Jocqué, 1991, male and female genitalia **A–C** holotype male **D–G** paratype females (RMCA_144436) **A** palp, prolateral view **B** idem, ventral view **C** idem, retrolateral view **D** epigyne, ventral view **E** idem, another female **F** idem, cleared **G** vulva, dorsal view. Abbreviations: CF = cymbial fold; DP = dorsal prong of palpal tibial apophysis; MA = median apophysis; MP = median prong of palpal tibial apophysis; Sc = scape; TT = tegular tooth; VP = ventral prong of palpal tibial apophysis. Scale bars: 0.2 mm.

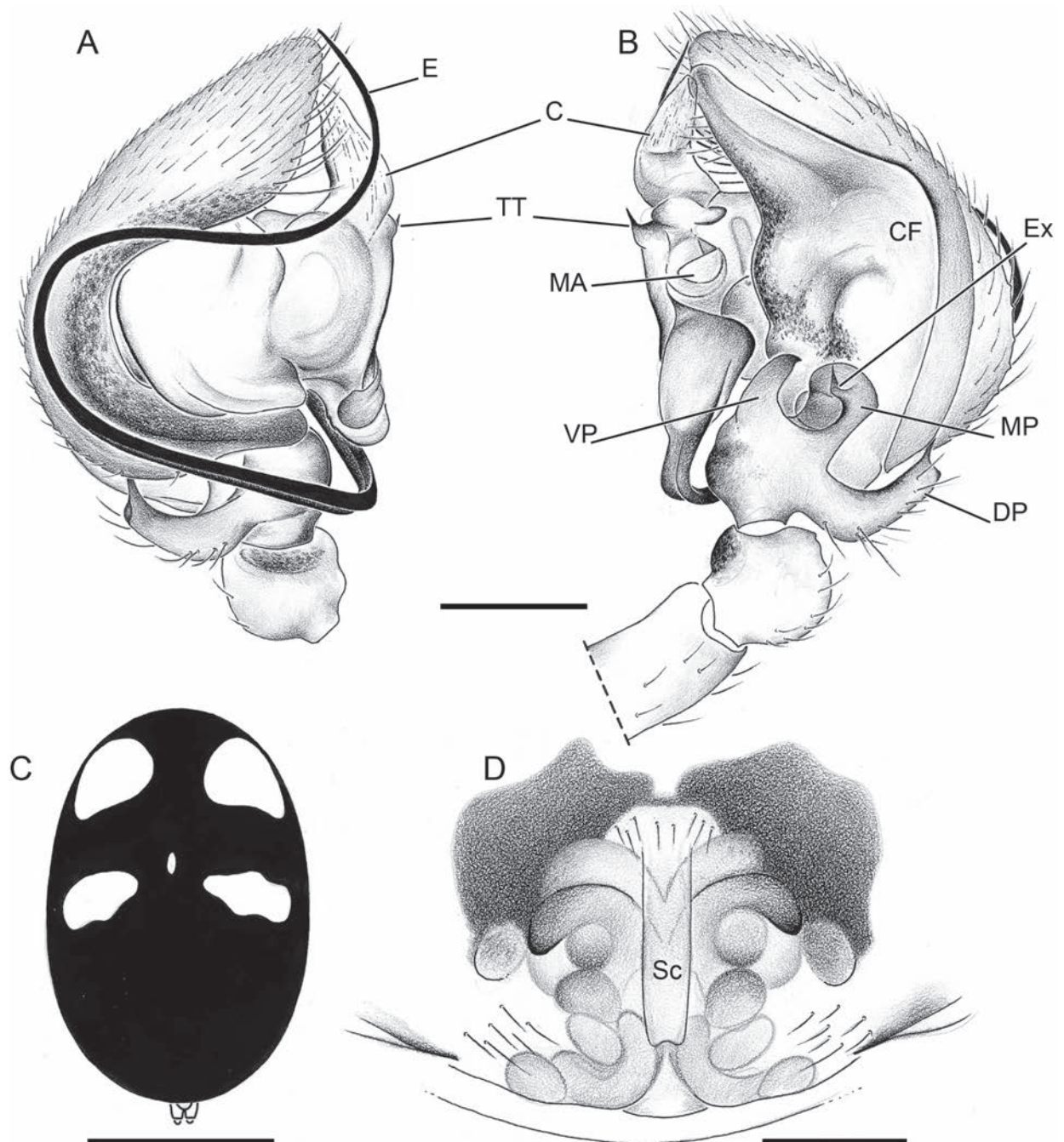


Figure 13. *Asceua lejeunei* Jocqué, 1991, drawings **A, B** holotype male **C, D** paratype females (RMCA_144436) **A** palp, prolateral view **B** idem, retrolateral view **C** female abdomen, dorsal view **D** epigyne, ventral view. Abbreviations: C = conductor; CF = cymbial fold; E = embolus; Ex = small prolateral extension of the median prong; DP = dorsal prong of palpal tibial apophysis; MA = median apophysis; MP = median prong of palpal tibial apophysis; TT = tegular tooth; Sc = scape; VP = ventral prong of palpal tibial apophysis. Scale bars: 0.2 mm (**A, B, D**); 1 mm (**C**).

est (Mid-one); 7°42'3"N, 8°23'5"W; 8.X.2011; beating, litter in trees and shrubs, at 1.5–3 m above the floor, D. Van den Spiegel, A. Henrard leg.; RMCA_245358; • 1♂; Mount Nimba, Seringbara Forest; 7°39'N, 8°26'E; 12.III.2012; 584 m a.s.l.; canopy fogging; M. Sidibé, A. Henrard, C. Allard, P. Bimou leg.; RMCA_239747;

• 1♂: Mount Nimba, Seringbara Forest; 7°39'N, 8°26'W; 13.III.2012; 606 m a.s.l.: fogging, secondary forest, canopy fogging, no wind; M. Sidibé, A. Henrard, C. Allard, P. Bimou leg.; RMCA_239602; • 1♂; Mount Nimba, Seringbara parking; 7°38'N, 8°27'W; 2.III.2012; 586 m a.s.l.: sieving soil litter, primary forest; M. Sidibé, A. Henrard, C. Allard, P. Bimou leg.; RMCA_238681; • 1♂; Mount Nimba, Middle valley of Zougoué, near Gbakoré mine camp; 7°42'N, 8°24'W; 5.X.2011; Fogging 3, secondary gallery forest, canopy fogging; D. Van den Spiegel and A. Henrard leg.; RMCA_238943; NIGERIA: • 1♀; Western, Ibadan, Ibadan, IITA; 7°14'N, 3°30'E; 22–29.V.1981; pitfall 5, secondary forest; A. Russell-Smith leg.; RMCA_235840.

Diagnosis. Males of this species are recognised by the cymbium without retrobasal button like process (Fig. 12C), by the dorsal prong of palpal tibial apophysis parallel-sided up to distal tip (Figs 12C, 13 B) and by the well-developed tegular subdistal tooth visible from both sides (Fig. 13A, B). Females are characterised by the epigyne scape with parallel sides, indented at posterior tip and reaching 0.75 of epigyne length.

Description. For description, see Jocqué (1991: 41).

Distribution. Known from areas across the African continent, from Ethiopia in the east, to Guinea in the west (Fig. 24).

***Asceua luki* sp. nov.**

<https://zoobank.org/AE640F71-ECEF-45E5-9009-4FF508F86CE0>

Figs 14–16, 24

Type material. Holotype: D.R. CONGO • ♂: Bas-Congo, Mayombe, Luki Biosphere Reserve; 5°38'S, 13°04'E; 22.IX.2007; canopy fogging, secondary rainforest; D. De Bakker, and J.P. Michiels leg.; RMCA_247723. **Paratypes:** • 4♂♂ 3♀♀; as holotype; RMCA_235130; • 1♂ 1♀; 21.IX.2007; further as holotype; RMCA_235129; • 3♂♂ 1♀; 20.IX.2007; further as previous; RMCA_235128.

Diagnosis. Males and females of this species differ from those of *A. incensa* by the pale venter of the abdomen (Fig. 14C, F) and the triangular shape, as wide as high, of the chilum. In the male palp of *A. luki* the cymbial fold reaches the very tip of the cymbium and is strongly narrowed at the extremity (Figs 15B, C, 16B), but it does not in *A. incensa* (Figs 8C, 9B). In addition, the palp of *A. luki* is similar to that of *A. lejeunei* but differs by some details: in *A. luki*, the median prong of the tibial apophysis is provided with a prolateral triangular tooth visible in transparency (Fig. 15D, E); in *A. lejeunei* the tooth on the slightly wider median prong of the tibial apophysis is thinner and curved (Figs 12C, 13B). Females are recognised by the structure of the epigyne similar to that of *A. palustris*: in *A. luki* the scapus is longer and narrower and not strongly widened at the posterior tip, and the copulatory openings are in front of the scapus tip, whereas behind it in *A. palustris* (Figs 15F, 16C vs. Fig. 17D, G); the posterior copulatory ducts are large and tightly wound, in *A. luki* they are narrower, loosely wound and crossing at the start in *A. palustris* (Fig. 15G, H vs. Fig. 17E, F). Females of *A. luki* differ from *A. lejeunei* by the scape, which is not indented (Fig. 16C vs. Fig. 13D).

Etymology. The species name is a noun in apposition taken from the type locality.

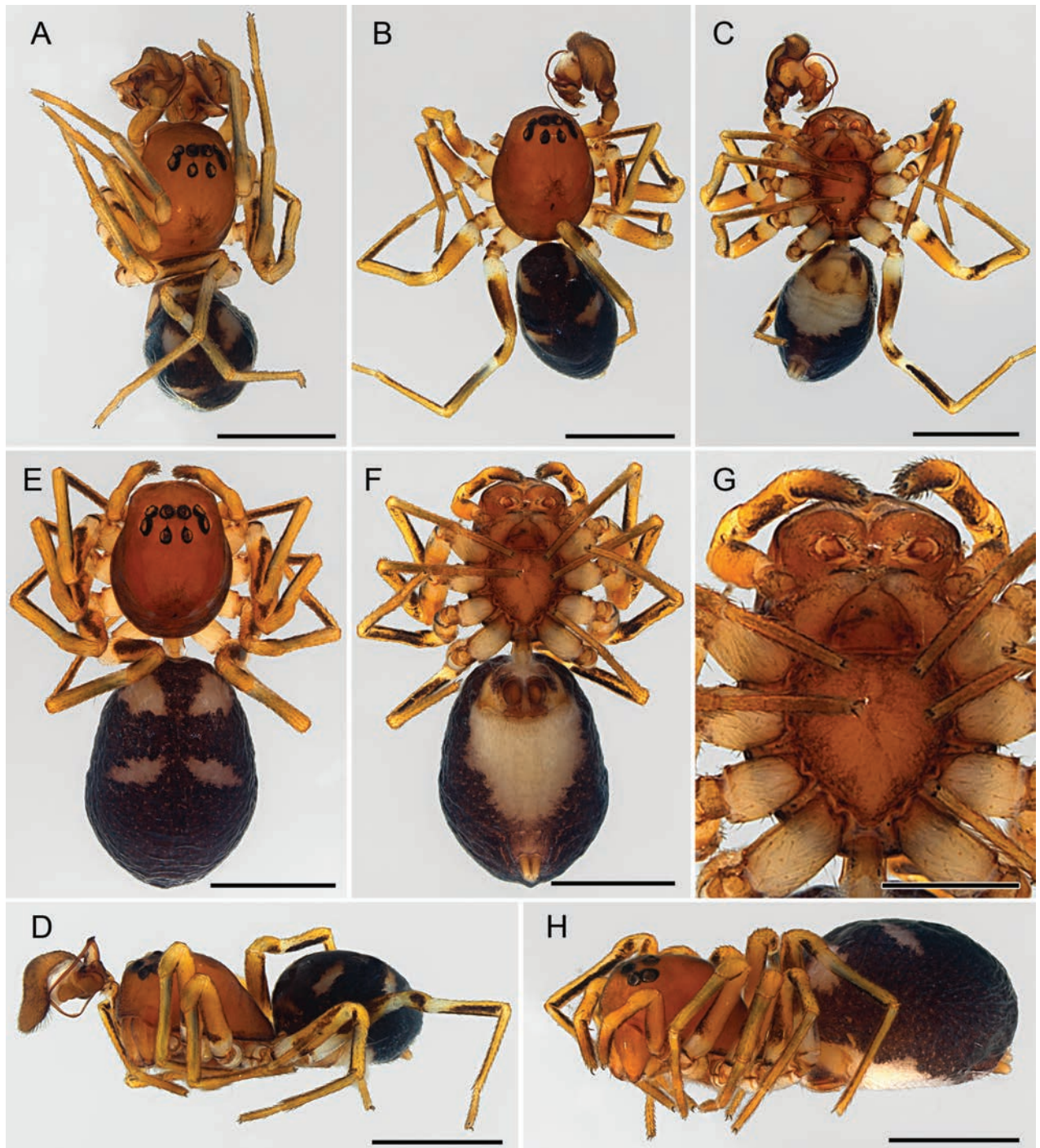


Figure 14. *Asceua luki* sp. nov., male and female habitus **A** holotype male **B–D** paratype male (RMCA_235130) **E–H** paratype female (RMCA_235130). **A, B, E.** dorsal view. **C, F, G.** ventral view **D, H** lateral view. Scale bars: 1 mm.

Description. Male Holotype. Fig. 14A–D. Total body length 2.68. Colour in ethanol: carapace brownish orange, with faint darker 'X' in front of fovea, dark rings around eyes and dark clypeus; chelicerae pale brown; endites and labium medium brown with pale frontal margin; sternum yellowish brown with darker margins; legs: femora proximal third of Fe white, distal 2/3 yellow with dark prolateral stripe and extra retrolateral stripe on Fe IV; remainder of legs yellow with dark ventral stripe on patellae, tibiae and metatarsi; abdomen: dorsum sepia with transparent brown scutum, two longitudinal, oval pale spots in anterior

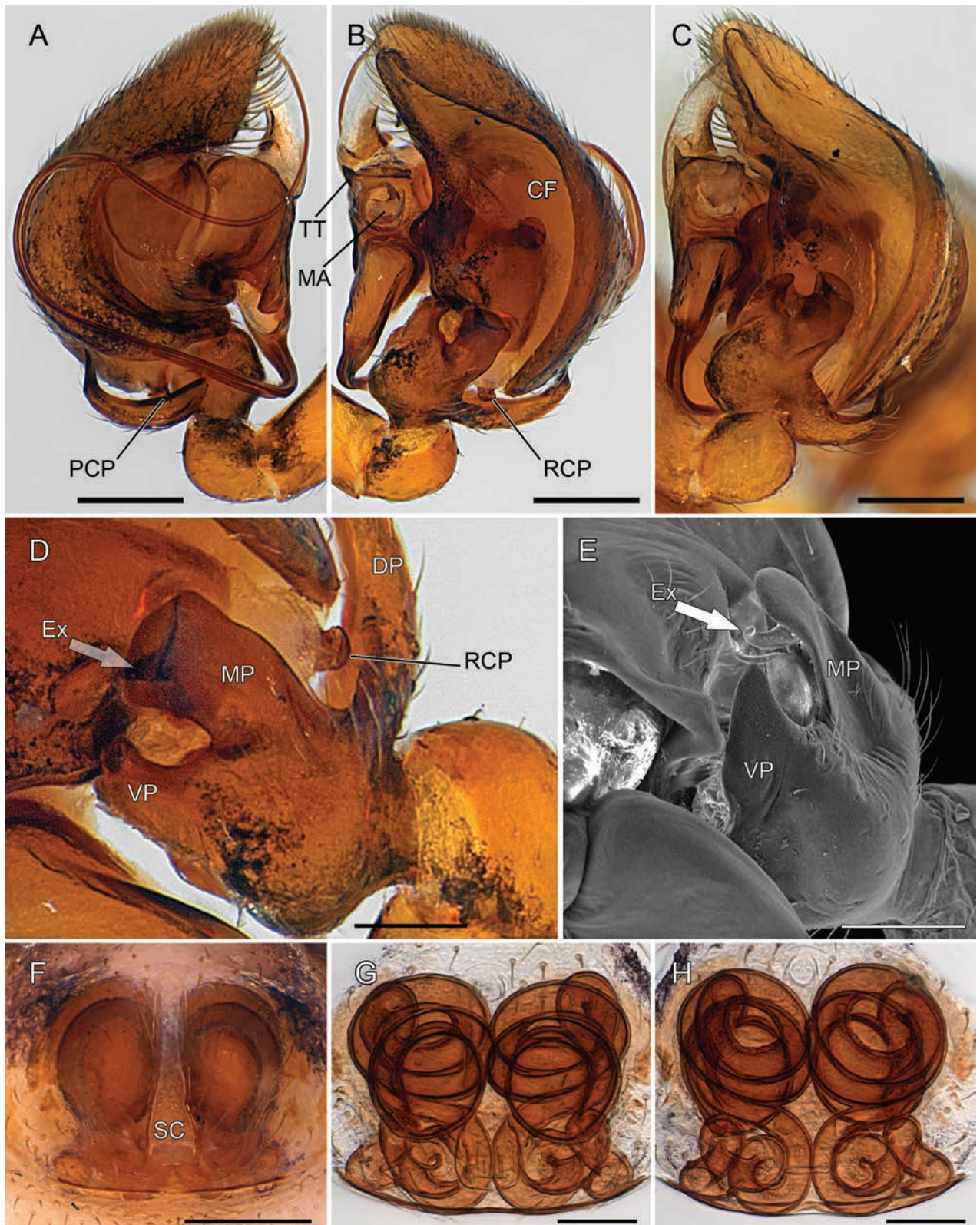


Figure 15. *Asceua luki* sp. nov., male and female genitalia **A, B** paratype male (RMCA_235130) **C** holotype male **D–F** paratype female (RMCA_235130) **A** palp, prolateral view **B, C** idem, retrolateral view **D** detail of the palpal tibial apophyses **E** idem, SEM view **F** epigyne, ventral view **G** idem, cleared **H** vulva, dorsal view. The arrows point to Ex. Abbreviations: CF = cymbial fold; DP = dorsal prong of palpal tibial apophysis; Ex = small prolateral extension of the median prong; MA = median apophysis; MP = median prong of palpal tibial apophysis; PCP = probasal cymbial process; RCP = retrobasal cymbial process; TT = tegular tooth; Sc = scape; VP = ventral prong of palpal tibial apophysis. Scale bars: 0.2 mm (**A, B, F**); 0.1 mm (**D, E, G, H**).

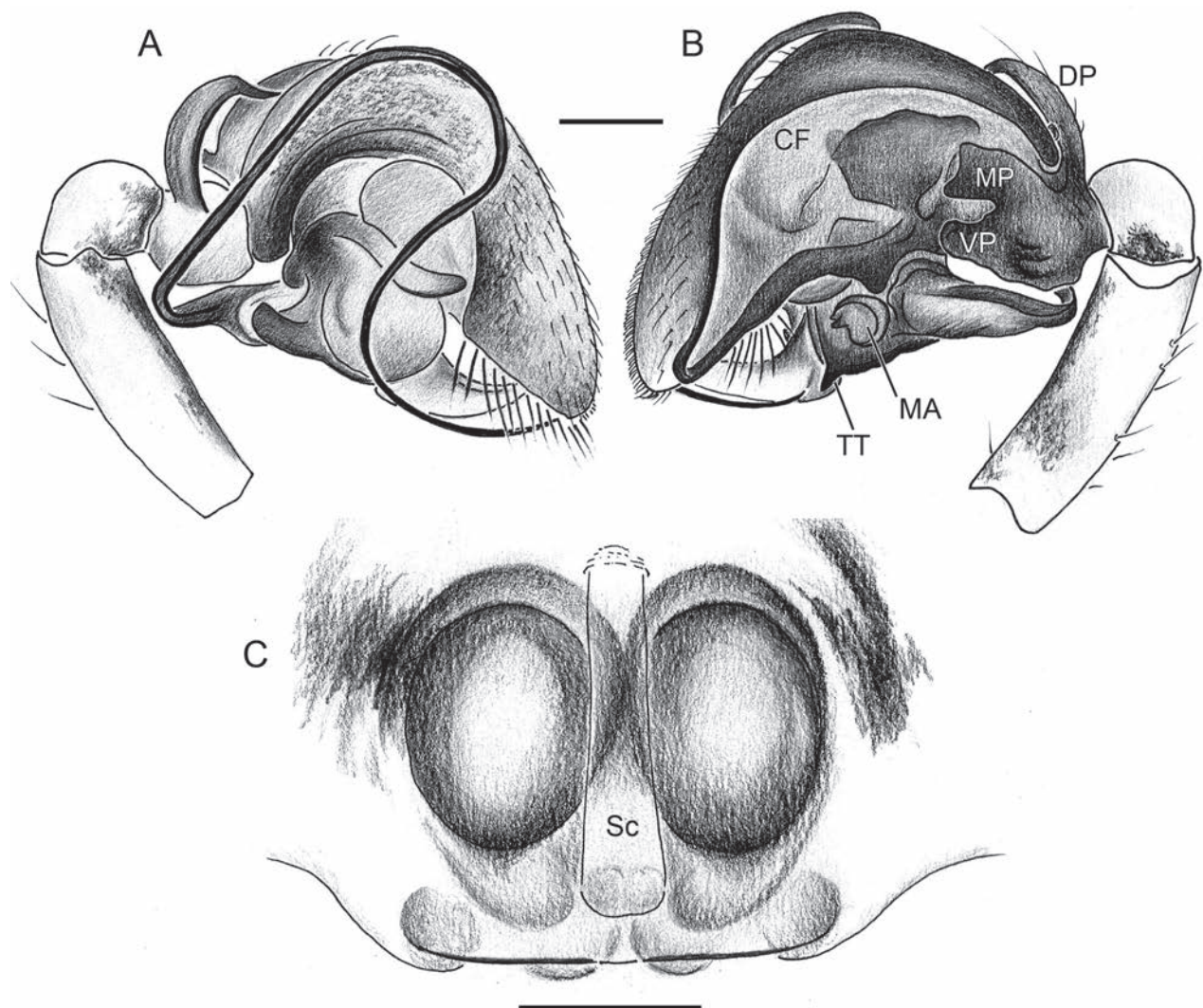


Figure 16. *Asceua luki* sp. nov., drawings **A, B** paratype male (RMCA_235130) **C** paratype female (RMCA_235130) **A** palp, retrolateral view **B** idem, prolateral view **C** epigyne, ventral view. Abbreviations: CF = cymbial fold; DP = dorsal prong of palpal tibial apophysis; MA = median apophysis; MP = median prong of palpal tibial apophysis; Sc = scape; VP = ventral prong of palpal tibial apophysis. Scale bars: 0.1 mm.

half and two transverse oval spots in the middle; sides dark as dorsum; venter pale in anterior 2/3; spinnerets yellow surrounded by dark area continuing from dorsum. Carapace 1.32 long, 0.99 wide, 0.92 high. Eye sizes and interdistances: AME: 0.09; ALE: 0.10; AME–AME: 0.07; AME–ALE: 0.02; PME: 0.10; PLE: 0.12; PME–PME: 0.07; PME–PLE: 0.11. MOQ: frontal width 0.25, posterior width 0.26, length 0.28. Clypeus 0.30 high. Chilum: triangular poorly defined sclerite 0.07 wide and as high. Sternum shield-shaped, 0.64 long, 0.61 wide. Legs: all femora with one short dorsal spine in proximal half; ; measurements in Table 6.

Palp (Figs 15A–C, 16A, B): large: length including Ti 0.61 times carapace length. Tibia with three apophyses: dorsal prong (DP) wide, concave in prolateral view, curved forward, with distal, spine-shaped prong pointing forward at an angle of 45°, inserted on apophysis tip; median prong (MD) roughly square with prolateral tooth (Ex); ventral prong (VP) short, straight with rounded extremity; cymbium laterally compressed with large retrolateral semicircular fold (CF), strongly narrowed at extremity reaching cymbial tip, with small, retrobasal button-like process (RCP) fitting DP concavity and sharp conical prolateral

Table 6. Male leg measurements.

| Leg | Fe | P | Ti | Mt | t | tot |
|-----|------|------|------|------|------|------|
| I | 0.86 | 0.32 | 0.70 | 0.80 | 0.54 | 3.23 |
| II | 0.80 | 0.32 | 0.64 | 0.70 | 0.48 | 2.94 |
| III | 0.70 | 0.32 | 0.51 | 0.77 | 0.48 | 2.78 |
| IV | 0.83 | 0.32 | 0.67 | 0.96 | 0.51 | 3.30 |

Table 7. Female leg measurements.

| Leg | Fe | P | Ti | Mt | t | tot |
|-----|------|------|------|------|------|------|
| I | 0.83 | 0.32 | 0.64 | 0.83 | 0.48 | 3.10 |
| II | 0.77 | 0.32 | 0.61 | 0.77 | 0.48 | 2.94 |
| III | 0.83 | 0.32 | 0.54 | 0.83 | 0.45 | 2.98 |
| IV | 0.96 | 0.32 | 0.70 | 1.06 | 0.38 | 3.42 |

extension (PCP); tegulum with ventral part provided with small tooth (TT) anteriorly; median apophysis (MA) rounded and concave opening towards the front; embolus long and whip shaped, its base smoothly tapered in retrolateral view, a broad triangle in ventral view.

Female Paratype (RMCA_235130). Fig. 14E–H. Total body length 3.43. Colour as in male but for the absence of a scutum, pale dorsal spots larger and rounded, venter with smaller paler area behind epigastric fold. Carapace 1.73 long, 1.20 wide, 0.91 high. Eye sizes and interdistances: AME: 0.09; ALE: 0.10; AME–AME: 0.05; AME–ALE: 0.05; PME: 0.10; PLE: 0.10; PME–PME: 0.07; PME–PLE: 0.12. MOQ: frontal width 0.23, posterior width 0.26, length 0.31. Clypeus 0.28 high. Chilum: triangular, 0.10 wide and as high; shape as in male. Sternum shield-shaped, 0.67 long, 0.58 wide. Legs: all femora with one short dorsal spine in proximal half; measurements in Table 7.

Epigyne (Figs 15F–H, 16C): quadrangular area, as wide as long; scape (Sc) long, slightly narrower in anterior half, clearly widened at tip; copulatory openings in front of scape tip; ducts relatively wide, strongly wound, posterior part a short dense spire, anterior part with three densely superposed loops.

Variation. Males (n = 8): TL 2.16–2.77; CL 1.28–1.73; white spots on dorsum sometimes narrower. Females (n = 4): TL 2.92–3.43, CL 1.21–1.68; white spots on dorsum wide.

Distribution. The species is known from the type locality in western DR Congo (Fig. 24).

***Asceua palustris* sp. nov.**

<https://zoobank.org/2D09FE33-F891-4DE6-8B10-21DC2048E6B9>

Figs 17, 24

Type material. Holotype D.R. CONGO • ♀; Kwango. territoire de Feshi. rive gauche de la Kwenge; 4°50'S, 18°54'E; 840 m a.s.l.; IV.1959; îlot de forêt marécageux inondée; J. Leleup leg.; RMCA_113670. **Paratype**: • 1 ♀; II.1959; further as Ht; RMCA_113489.

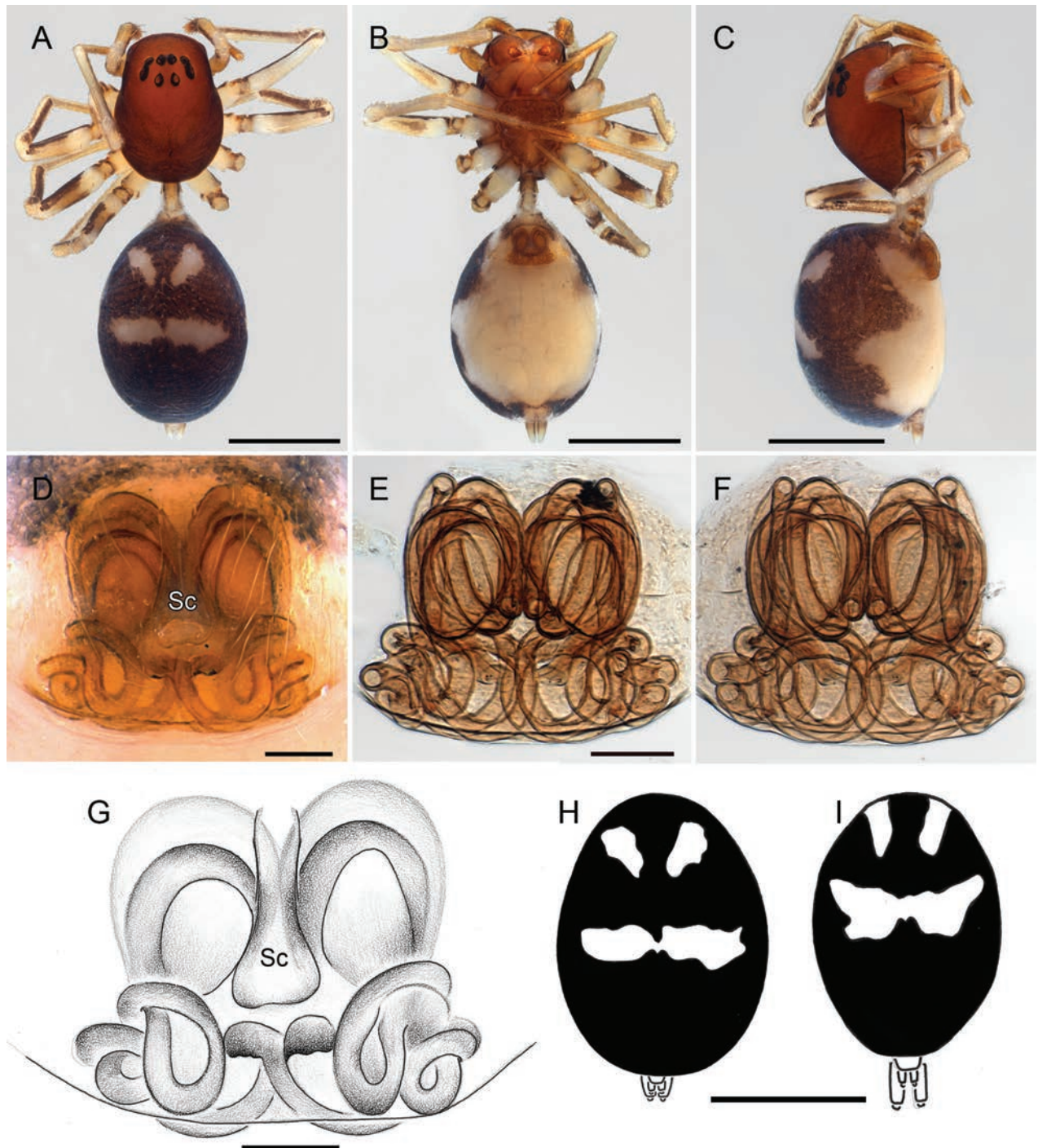


Figure 17. *Asceua palustris* sp. nov. **A–D, G, H** holotype female (RMCA_113670). **E, F, I.** paratype female (RMCA_113489) **A** habitus, dorsal view **B** idem, ventral view **C** idem, lateral view **D, G** epigyne, ventral view **E** idem, cleared **F** vulva, dorsal view **H, I** abdomen, dorsal view. Abbreviations: Sc = scape. Scale bars: 1 mm (**A–C, H, I**); 0.1 mm (**D–G**).

Other material examined. D.R. CONGO • 1♀; Kivu-N., Visiki, forêt de Visiki; 0°12'N, 29°15'E ; 23.XII.1971; M. Lejeune leg. ;RMCA_140837; • 1 subadult ♂: Kwango, Feshi, tête de source de la Mvula myeji, rive gauche de la Kwenge; 4°50'S 18°54'E; 840 m a.s.l.; III.1959; forêt de terre ferme; J. Leleup leg.; RMCA_113520; 1 subadult ♂: as previous ; RMCA_113523.

Diagnosis. Females of this species are recognised by the ventral aspect of the epigyne with two central smooth areas, surrounded by loops of the copu-

Table 8. Female leg measurements.

| Leg | Fe | P | Ti | Mt | t | total |
|-----|------|------|------|------|------|-------|
| I | 0.92 | 0.28 | 0.69 | 0.89 | 0.66 | 3.43 |
| II | 0.87 | 0.31 | 0.61 | 0.74 | 0.52 | 3.05 |
| III | 0.52 | 0.28 | 0.66 | 0.84 | 0.62 | 2.92 |
| IV | 0.90 | 0.28 | 0.79 | 0.98 | 0.62 | 3.58 |

latory ducts visible in transparency; the crossing of the copulatory ducts at the beginning is unique in the Afrotropical species; the dorsum of the abdomen is provided with two pairs of spots.

Etymology. The specific name refers to the type of habitat.

Description. Female Holotype. Fig. 17A–C, H, I. Total body length 3.52. Colour in ethanol: carapace and chelicerae uniform medium brown with narrow dark rings around eyes; endites and labium medium brown with pale anterior margin; sternum medium brown with pale central longitudinal triangle in posterior half; legs pale with narrow, pro- and retrolateral dark stripes; dorsum of abdomen dark sepia with sinuous margin on sides, provided with two oblique pale triangles in anterior half and two transverse rectangular spots, touching in the middle; venter pale, spinnerets pale yellow. Carapace 1.52 long, 0.96 wide, 0.60 high. Eye sizes and interdistances: AME: 0.07; ALE: 0.08; AME–AME: 0.05; AME–ALE: 0.02; PME: 0.07; PLE: 0.13; PME–PME: 0.08; PME–PLE: 0.07. MOQ: frontal width 0.18, posterior width 0.23, length 0.26. Clypeus 0.33 high. Chilum: small triangle 0.10 wide and as high. Sternum shield-shaped, 0.72 long, 0.60 wide. Spination: all femora with short proximal dorsal spine; measurements in Table 8.

Epigyne (Fig. 17D–G): Scape (Sc) short reaching centre of epigyne, widened near posterior tip; with smooth area on either side of scape, surrounded by looped copulatory ducts visible in transparency; copulatory openings posterior of scape tip; copulatory ducts crossing near the entrances; anterior part of ducts looped in longitudinal direction, posterior parts occupying a wider area than the frontal part.

Male. Unknown.

Distribution. The species is known from south-western and eastern D.R. Congo (Fig. 24).

***Asceua radiosa* Jocqué, 1986**

Figs 18–21, 24

Asceua radiosa Jocqué, 1986: 309.

Type material. Holotype: COMOROS • ♂; Grande Comore, Moroni; 12°15'S, 43°45'E; 4.VIII.1981; litière de jardin, (radio Comores); R. Jocqué leg.; RMCA_164051.

Paratypes: • 4 ♀♀; same data as for holotype; RMCA_155294.

Other material examined. COMOROS: • 1 ♀; Mohéli, Hagnamouada; 12°15'S, 43°45'E, 25.V.2003; forest edge, under rocks; D. Van den Spiegel, and R. Jocqué leg.; RMCA_213294; • 1 ♂; Grande Comore, en face de l'île des Tortues; 11°35'S, 43°20'E; 31.X.1983; sous pierres; R. Jocqué leg.; RMCA_160659; • 2 ♂♂; Mayotte, Mbouanatsa, pick-nick place near beach; 12°56'32"S, 45°6'5"E; 15.II.1999; concrete slab with small dead leaves and gravel; R. Jocqué and G. De Smet leg.; RMCA_208557.

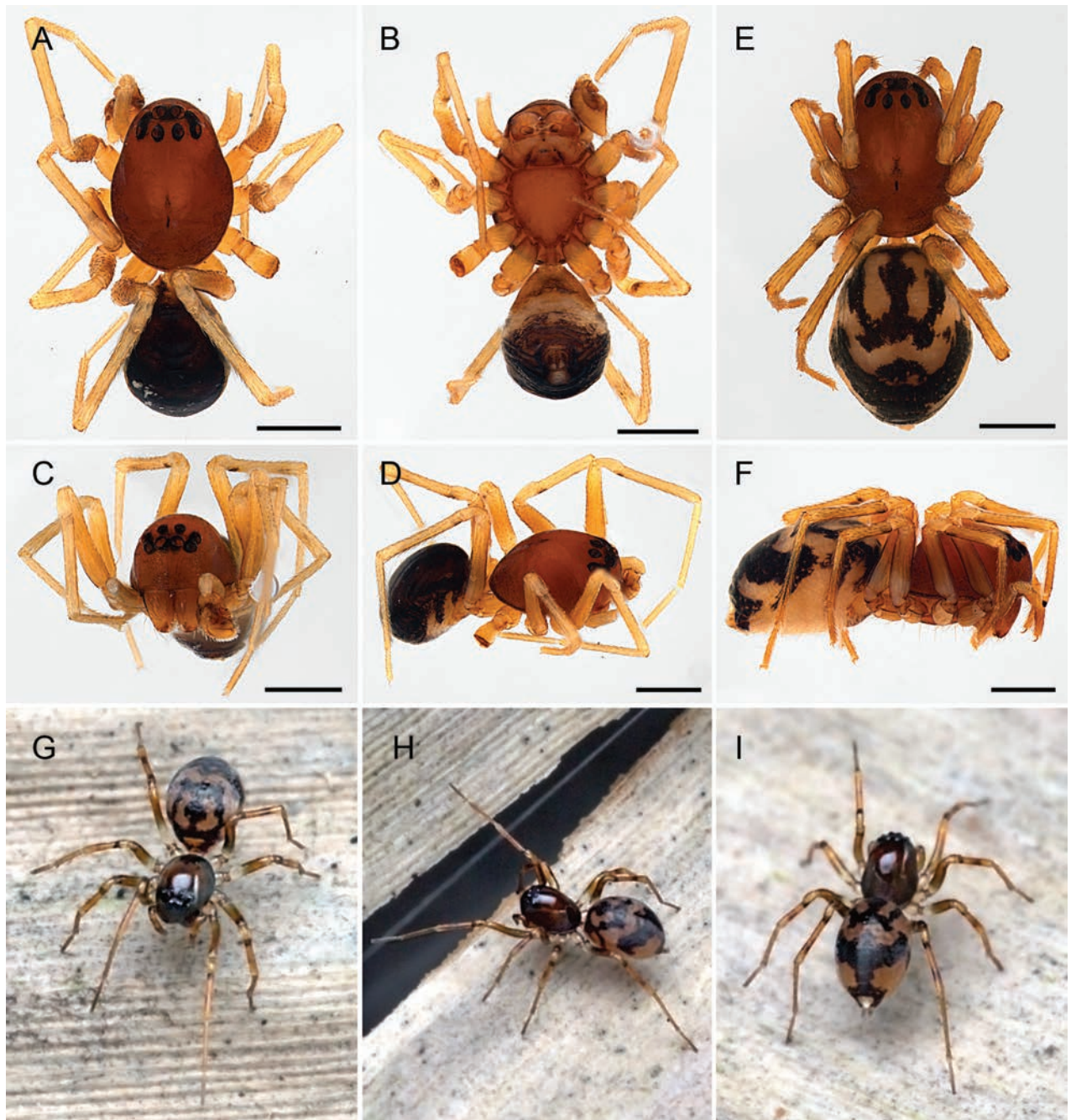


Figure 18. *Asceua radiosa* Jocqué, 1986, male and female habitus **A–D** holotype male **E, F** paratype female (RMCA_155294) **A, E** dorsal view **B** ventral view **C** frontal view **D, F** lateral view **G, H** female specimen photographed *in vivo* on Mayotte (Photo by Arnaud Henrard). Scale bars: 0.5 mm.

Diagnosis. Males and females of *A. radiosa* are easily recognised by the intricate abdominal pattern (Figs 18A, F, 20D, 21A–C). Males are further recognised by the cymbial fold reaching only half the length of the cymbium and the relatively short, non-sinuuous embolus (Figs 19A–D, 20A–C); females are characterised by the absence of a scape in the epigyne, the relatively short copulatory ducts and the spherical spermathecae (Figs 19E, F, 20E).

Description. For description see Jocqué (1986: 309).

Distribution. Known from three islands of the Comoro Archipelago: Grande Comore, Mohéli, Mayotte (Fig. 24).

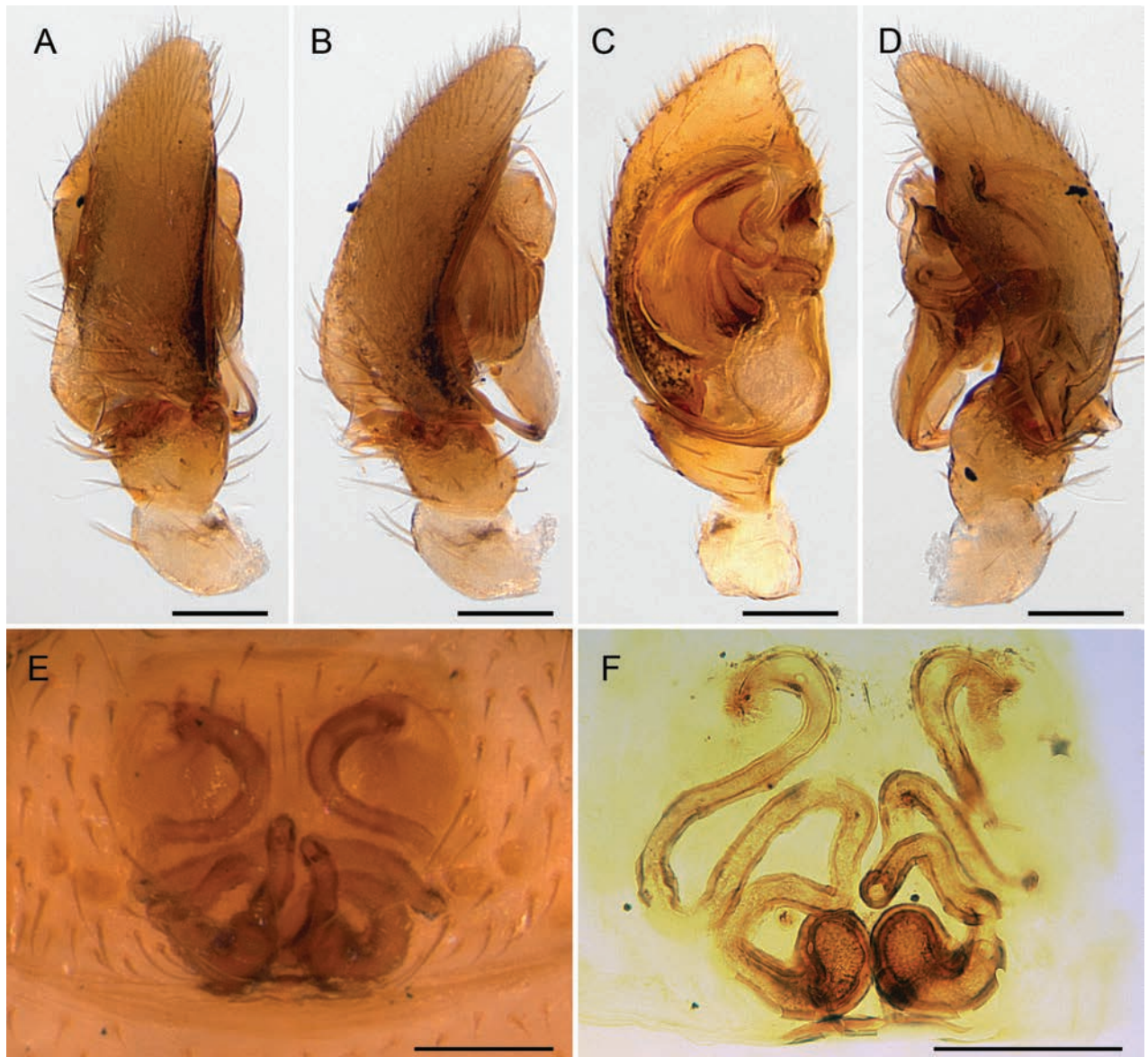


Figure 19. *Asceua radiosus* Jocqué, 1986, male and female genitalia **A–D** holotype male (right palp mirrored) **E, F** paratype female (RMCA_155294) **A** palp, dorsal view **B** idem, prolateral view **C** idem, ventral view **D** idem, retrolateral view **E** epigyne, ventral view **F** vulva, dorsal view. Scale bars: 0.1 mm.

***Asceua ventrofigurata* sp. nov.**

<https://zoobank.org/A7AD9403-BAE4-48B7-9162-80FFC0DAD89A>

Figs 21–24

Type material. Holotype: TANZANIA • ♂; Mbeya Region, Igaya, Road to Ileje, Kabulu Forest Reserve; -9.8533, 33.5; 28.XI.1991; miombo woodland, sieved litter; R. Jocqué leg.; RMCA_247697.

Paratypes: • 1♂ 2♀♀; together with holotype; RMCA_173229; • 5♂♂ 7♀♀; same data as holotype; RMCA_173168.

Etymology. The species name is an adjective referring to the abdominal venter provided with a dark pattern on pale background.

Diagnosis. Males of this species are characterised by the uniform medium brown carapace, the relatively large AME and details of the male palp: the distal

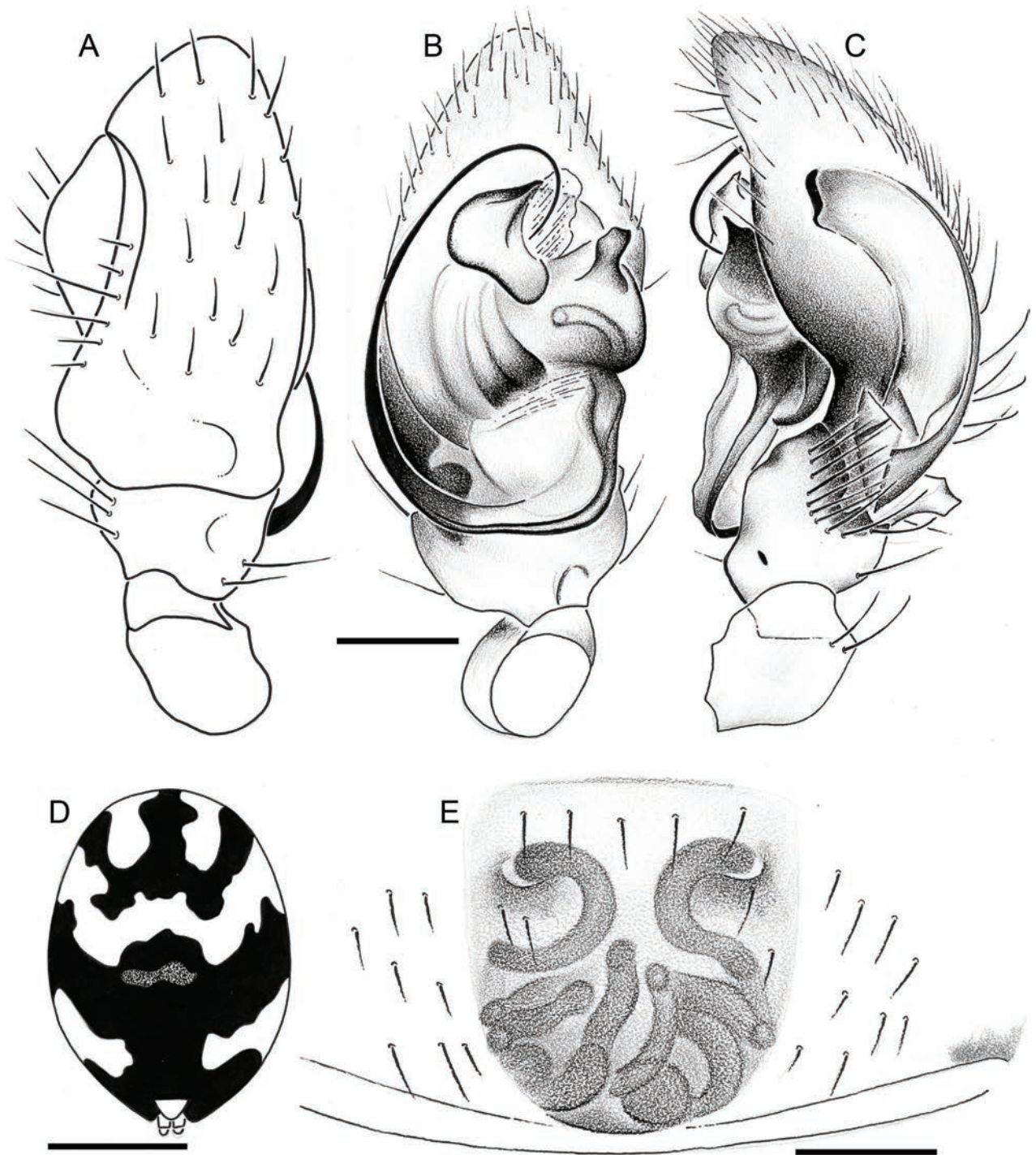


Figure 20. *Asceua radiosa* Jocqué, 1986, drawings **A–C** holotype male (right palp mirrored) **D, E** paratype female (RMCA_155294) **A** palp, dorsal view **B** idem, ventral view **C** idem, retrolateral view **D** Abdomen, dorsal view **E** epigyne, ventral view. Scale bars: 0.1 mm (**A–C, E**); 0.5 mm (**D**).

spine-shaped part of the dorsal tibial apophysis is implanted slightly before the tip directed forward at an angle of 90° with the base of the apophysis which is broad and concave in prolateral view; females are recognized by fairly large AME and the epigyne with narrow parallel sided scape and copulatory ducts hardly visible in transparency.

Description. Male Holotype. Fig. 21A–C. Total body length 3.27. Colour in ethanol: carapace uniform medium brown with narrow darker margin, narrow

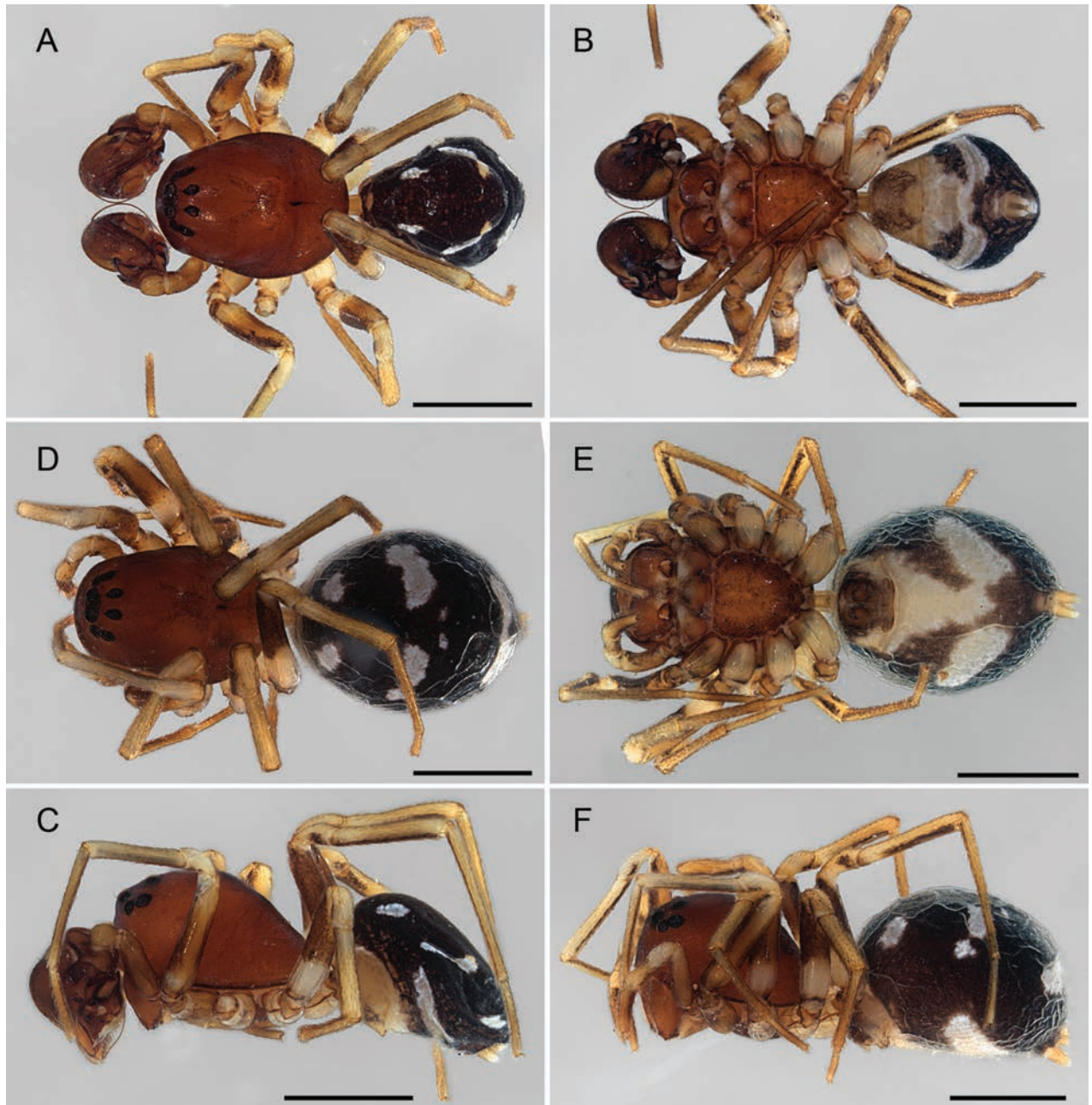


Figure 21. *Asceua ventrofigurata* sp. nov, male and female habitus (paratypes RMCA_173168) A–C male D–F female A, D dorsal view B, E ventral view C, F lateral view. Scale bars: 1 mm.

dark rings around eyes and rectangular dark area in front of AME; chelicerae and sternum pale brown; endites and labium medium brown with pale frontal margin; legs: femora pale with dark anterior stripes on Fe I–IV and dark posterior stripe on Fe III and IV in distal two thirds; abdomen: dorsum dark grey with dark sepia scutum covering 2/3 of abdomen length; with four pale spots adjacent to scutum: pair of short, longitudinal ones in anterior half, a pair of pro-curved longer ones in posterior half; sides dark with narrow longitudinal pale lines; venter pale with dark patch on each side and dark area around pale yellow spinnerets, yellow in front of epigastric fold. Carapace 1.70 long, 1.21 wide, 1.14 high. Eye sizes and interdistances: AME: 0.12; ALE: 0.08; AME–AME: 0.07; AME–ALE: 0.03; PME: 0.08; PLE: 0.10; PME–PME: 0.13; PME–PLE: 0.12. MOQ:

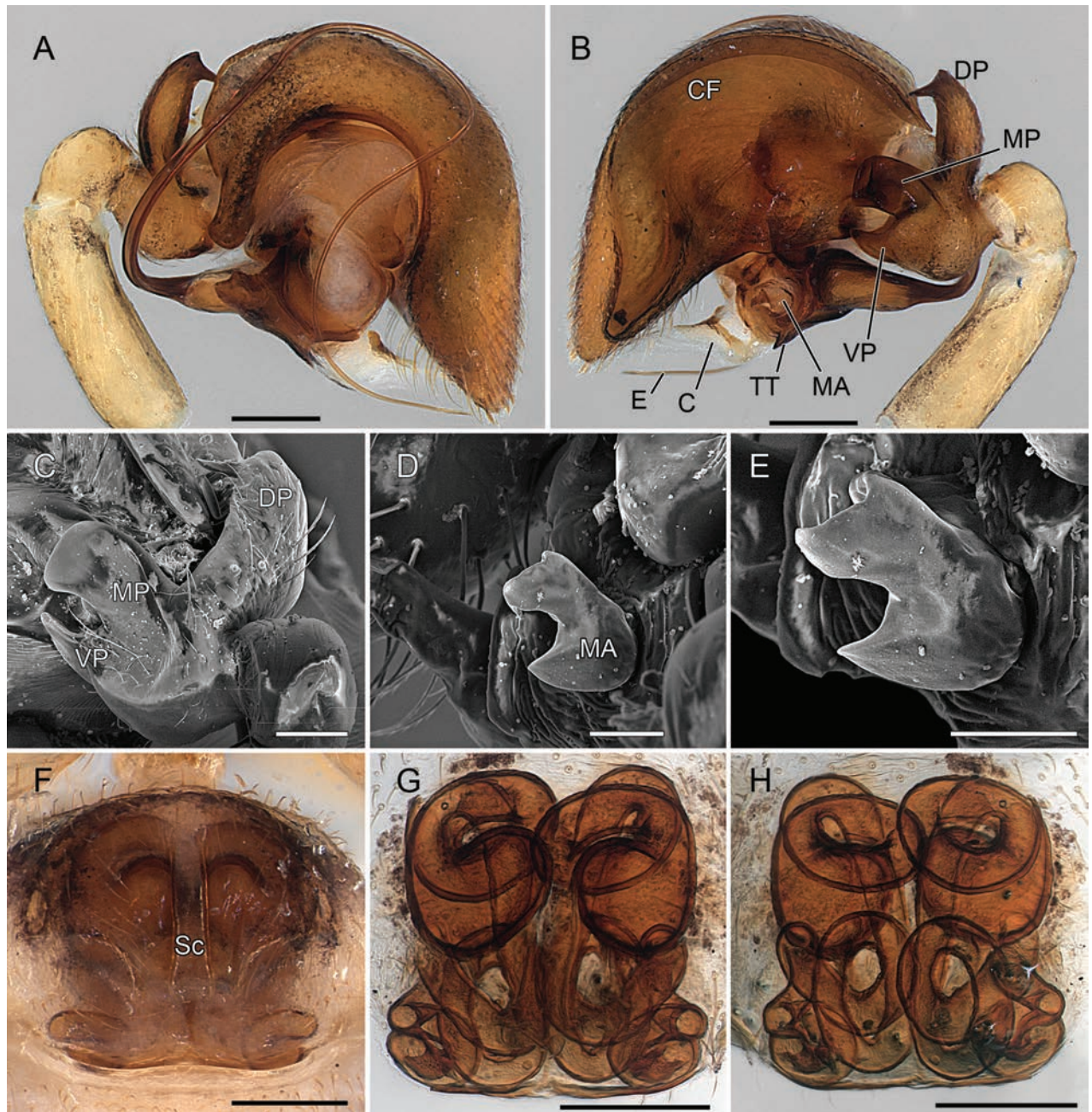


Figure 22. *Asceua ventrofigurata* sp. nov., male and female genitalia **A, B** holotype male (RMCA_173229) **C–E** paratype male (RMCA_173168) **F–H** paratype female (RMCA_173168) **A** palp, prolateral view **B** idem, retrolateral view **C** SEM view of palpal tibial apophyses **D** idem, showing median apophysis **E** idem, detail view. Abbreviations: C = conductor; CF = cymbial fold; E = embolus; DP = dorsal prong of palpal tibial apophysis; MA = median apophysis; MP = median prong of palpal tibial apophysis; TT = tegular tooth; Sc = scape; VP = ventral prong of palpal tibial apophysis. Scale bars: 0.2 mm (**A, B, F–H**); 0.1 mm (**C**); 50 μ m (**D, E**).

frontal width 0.30, posterior width 0.31, length 0.31. Clypeus 0.39 high. Chilum: small triangle 0.08 wide and as high. Sternum shield-shaped, 1.14 long, 0.75 wide. All femora with one short dorsal spine in proximal half; measurements in Table 9.

Palp (Figs 22A–E, 23A, B): very large: length including Ti 0.75 times carapace length. Tibia with three apophyses: dorsal one broad (DP), concave in prolateral view, slightly curved forward, with distal spine shaped prong pointing forward

Table 9. Male leg measurements.

| Leg | Fe | P | Ti | Mt | t | tot |
|-----|------|------|------|------|------|------|
| I | 1.26 | 0.42 | 0.98 | 1.12 | 0.63 | 4.41 |
| II | 0.98 | 0.35 | 0.77 | 0.91 | 0.49 | 3.50 |
| III | 0.91 | 0.42 | 0.70 | 1.05 | 0.49 | 3.57 |
| IV | 1.19 | 0.42 | 0.98 | 1.47 | 0.56 | 4.62 |

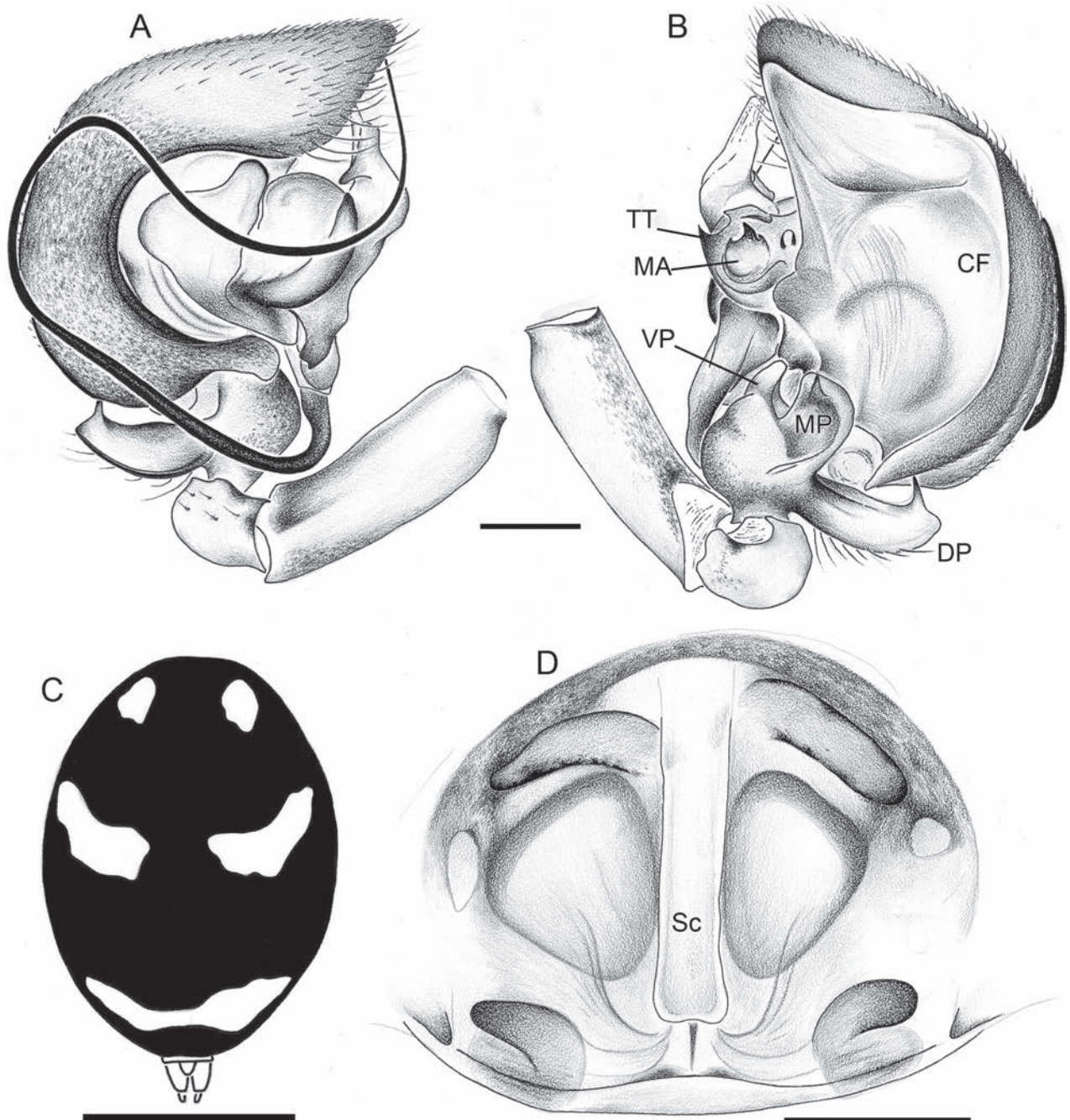


Figure 23. *Asceua ventrofigurata* sp. nov., drawings **A, B** holotype male **C, D** paratype female (RMCA_173168) **A** palp, prolateral view **B** idem, retrolateral view **C** Abdomen, dorsal view **D** epigyne, ventral view. Abbreviations: CF = cymbial fold; DP = dorsal prong of palpal tibial apophysis; MA = median apophysis; MP = median prong of palpal tibial apophysis; TT = tegular tooth; Sc = scape; VP = ventral prong of palpal tibial apophysis. Scale bars: 0.2 mm (**A, B, D**); 1 mm (**C**).

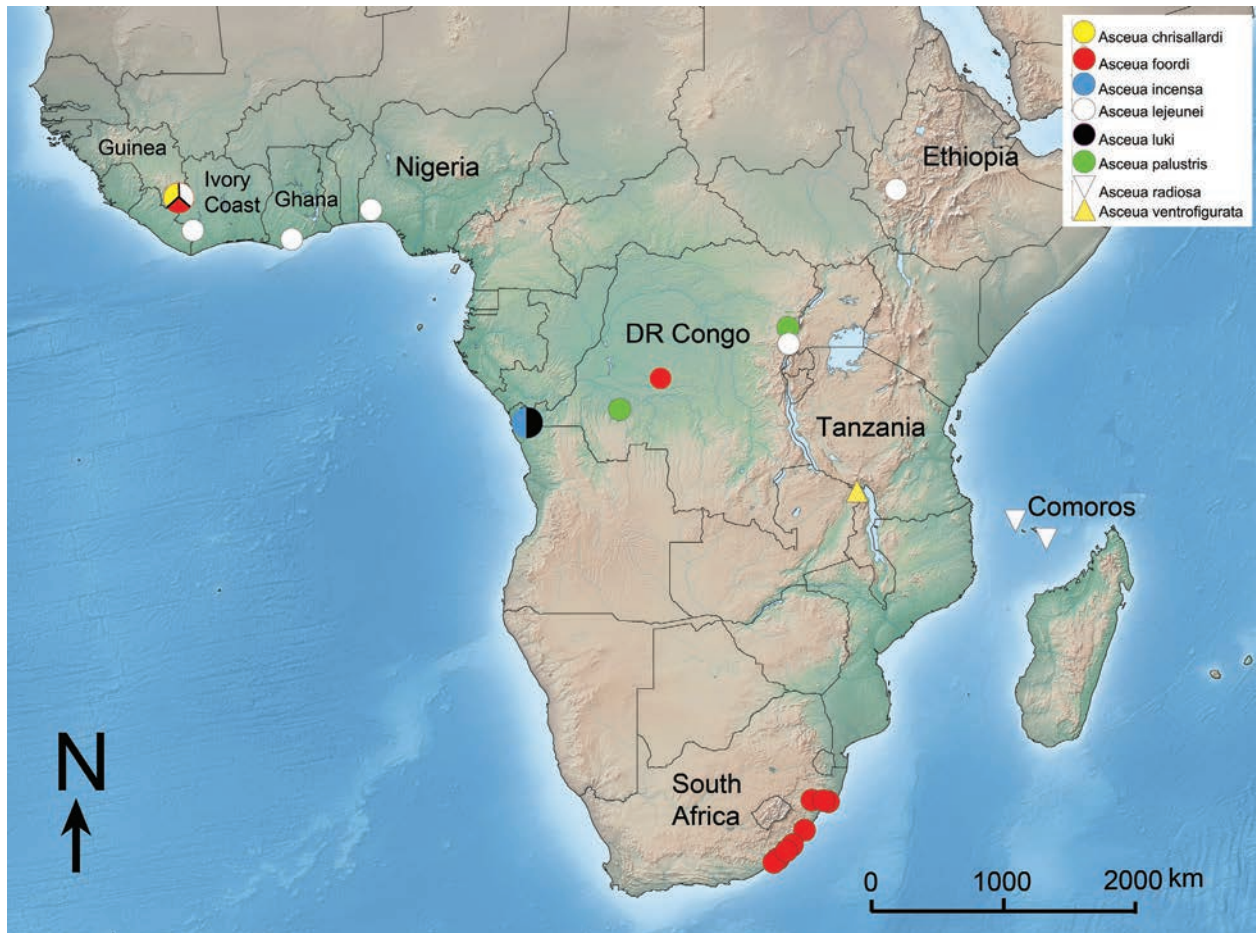


Figure 24. Distribution map of *Asceua* species occurring in the Afrotropics.

at an angle of 90° , inserted just under apophysis tip; median prong (MP) roughly square; inferior one (VP) short, straight with rounded extremity; cymbium laterally compressed with large lateral semicircular fold (CF); tegulum with three appendages: largest one voluminous mainly visible prolaterally, retrolateral one pear-shaped with small tapered forward directed prong, ventral one membranous, directed forward with small prolateral prong directed backward, tegular tooth sharp (TT); embolus long and whip-shaped with large triangular base directed backward, frontal margin concave.

Female Paratype (RMCA_173229). Figs 21D–F, 23C. Total body length 3.80. Colour as in male but for the absence of a scutum and presence of two extra dorsal abdominal spots: a transverse pale bar in posterior half followed by a small spot in front of spinnerets. Carapace 1.73 long, 1.20 wide, 0.91 high. Eye sizes and interdistances: AME: 0.13; ALE: 0.10; AME–AME: 0.05; AME–ALE: 0.05; PME: 0.10; PLE: 0.10; PME–PME: 0.10; PME–PLE: 0.13. MOQ: frontal width 0.31, posterior width 0.30, length 0.33. Clypeus 0.33 high. Chilum: small triangle 0.08 wide and as high. Sternum shield-shaped, 0.92 long, 0.78 wide. All femora with one short dorsal spine in proximal half; measurements in Table 10.

Epigyne (Figs 22F–H, 23D): rectangular area slightly wider behind than in front; scape widened towards posterior part situated in the centre of the epigyne; copulatory duct strongly wound, with six loops visible in transparency,

Table 10. Female leg measurements.

| Leg | Fe | P | Ti | Mt | t | tot |
|-----|------|------|------|------|------|------|
| I | 0.98 | 0.35 | 1.33 | 0.98 | 0.63 | 4.27 |
| II | 0.91 | 0.35 | 0.63 | 0.84 | 0.56 | 3.29 |
| III | 0.98 | 0.35 | 0.70 | 0.98 | 0.56 | 3.57 |
| IV | 1.12 | 0.35 | 0.98 | 1.47 | 0.56 | 4.48 |

Variation. Males (n = 7): TL 3.00–3.36, CL 1.40–1.68; white spots on dorsum 11–13. Females (n = 9): TL 3.40–4.04 CL 1.64–1.80. The shape and configuration of the dorsal spots varies to some extent: the frontal pair may be circular or oval; the second pair comma-shaped or transverse and straight, rarely with a tiny spot behind them; the posterior spot covers the entire width, sometimes narrower, rarely divided,

Distribution. The species is known from the type locality in south-western Tanzania (Fig. 24).

Discussion

Zodariidae are among the few families for which no ballooning behaviour has been observed (Jocqué 1991). This is probably linked to their ground-dwelling behaviour. It is therefore not surprising that most species in the family have relatively small distributions as witnessed by the distribution maps of *Zodarion* Walckenaer in the Iberian Peninsula (Bosmans 1994) and of South African zodariids (Dippenaar-Schoeman 2014). In this context, the distribution patterns of *Asceua* are strange: some of them are extremely large as is the case for *A. foordi* found from Kwazulu-Natal in South Africa, through central DR Congo to as far north as Guinea in West Africa. *A. lejeunei* spans the width of the African continent as it is found from Ethiopia to Ivory Coast. It is also remarkable that some of the species are found sympatrically: *A. luki* and *A. incensa* in western DR Congo, and even three species, *A. arborivaga*, *A. lejeunei* and *A. foordi*, together on Mount Nimba in Guinea, although they are apparently found at different altitudes. Part of the explanation may be due to the fact that these species are found to be the only canopy-dwelling Zodariidae, a behaviour already mentioned by Komatsu (2016) and by Ono and Ogata (2018) for *Asceua japonica* (Bösenberg & Strand, 1906). The genus has a remarkably large distribution and is apparently the genus with the largest distribution in the Zodariidae (from South Africa and West Africa to Japan). Although there are no observations so far, it would not be surprising that these Zodariidae do indeed balloon, a behaviour linked to their arboreal lifestyle.

It is also puzzling that the species are often found in forest leaf litter on the ground, even the same species found in canopy samples as it is the case for *A. lejeunei*. It is possible that adults (juveniles are rarely collected) migrate from the canopy to the soil where it is easier to find a mate, certainly for a spider with poor eyesight that does not construct a web. If confirmed, this behaviour may be an example of the importance of whereabouts at mating time.

Since at least some of the species are canopy dwelling it can be expected that more species will be collected when more canopy studies are carried out.

A remarkable feature of the males in this genus is the similarity of their habitus to that of an ant. This is particularly obvious on the blurred picture of a live

male specimen in Fig. 6E, the palps showing great similarity to an ant's head. Many Zodariidae are known to prey on ants (Pekár et al. 2005). Observations on the biology of *Asceua* (Komatsu 2016; Ono and Ogata 2018) have revealed that these spiders prefer ants as prey. In this context it makes perfect sense that they mimic ants. This phenomenon reminds us of that of *Pranburia mahannopi* Deeleman-Reinhold, 1993, in which the habitus of an ant is obtained when the hair brushes on the frontal femora are kept together (Deeleman-Reinhold 1993). In this case, the large palps of *Asceua* males play the role of the ant's head but the effect is permanent and therefore not entirely similar to the Asiatic corinnid.

Acknowledgments

We are indebted to Charles Haddad for material from South Africa and to BINCO (Biodiversity Inventories for Conservation) for specimens from DR Congo. We are grateful for photos of live specimens of *A. foordi* provided by Rudolf Steenkamp. We thank Alain Reygel for the drawings he prepared between 2002 and 2024 on our request. We thank Leon Lotz and Alireza Zamani for welcome comments on the submission.

Additional information

Conflict of interest

The authors have declared that no competing interests exist.

Ethical statement

No ethical statement was reported.

Funding

This work was supported by Belspo (Belgian Science Policy).

Author contributions

Both authors carried out fieldwork, provided illustrations and prepared the text.

Author ORCIDs

Rudy Jocqué  <https://orcid.org/0000-0003-1776-0121>

Arnaud Henrard  <https://orcid.org/0000-0003-3270-7193>

Data availability

All of the data that support the findings of this study are available in the main text.

References

- Bosmans R (1994) Revision of the genus *Zodarion* Walckenaer, 1833 in the Iberian Peninsula and Balearic Islands (Araneae, Zodariidae). *Eos* (Washington, D.C.) 69: 115–142.
- Deeleman-Reinhold CL (1993) A new spider genus from Thailand with a unique ant-mimicking device, with description of some other castianeirine spiders (Araneae: Corinnidae: Castianeirinae). *The Natural History Bulletin of the Siam Society* 40: 167–184.
- Dippenaar-Schoeman A (2014) *Field guide to the spiders of South Africa*. LAPA publishers, Pretoria, 432 pp.

- Dippenaar-Schoeman A (2023) Field guide to the spiders of South Africa. Struik Nature, Pretoria, 400 pp.
- Henrard A, Jocqué R (2015) On the new Afrotropical genus *Suffrica* with discovery of an abdominal gland and a dual femoral organ (Araneae, Zodariidae). *Zootaxa* 3972: 1–25. <https://doi.org/10.11646/zootaxa.3972.1.1>
- Jocqué R (1986) Ant-eating spiders from the Comoros (Araneae, Zodariidae). *Revue de Zoologie Africaine* 100: 307–312.
- Jocqué R (1991) A generic revision of the spider family Zodariidae (Araneae). *Bulletin of the American Museum of Natural History* 201: 1–160.
- Jocqué R (1994) A termite mimicking spider: *Thaumastochilus termitomimus* n. sp. (Araneae, Zodariidae). *Journal of African Zoology* 108: 321–327.
- Jocqué R, Bosmans R (1989). A revision of the genus *Storenomorpha* Simon (Araneae, Zodariidae). *Spixiana* 12: 125–134.
- Komatsu T (2016) Diet and predatory behavior of the Asian ant-eating spider, *Asceua* (formerly *Doosia*) *japonica* (Araneae: Zodariidae). *SpringerPlus* 5(1): 577. <https://doi.org/10.1186/s40064-016-2234-1>
- Leroy A, Jocqué R (1993) A note on the stitching habit of *Chariobas* sp. (Araneae, Zodariidae). *Journal of African Zoology* 107: 189–190.
- Ono H, Ogata K (2018) Spiders of Japan: their natural history and diversity. Tokai University Press, Kanagawa, 713 pp.
- Pekár S, Král J, Lubin Y (2005) Natural history and karyotype of some ant-eating zodariid spiders (Araneae, Zodariidae) from Israel. *The Journal of Arachnology* 33(1): 50–62. <https://doi.org/10.1636/S03-2>
- Shorthouse DP (2010) SimpleMappr, an online tool to produce publication-quality point maps. <https://www.simplemappr.net>

Research Article

Metalacurbs foordi sp. nov., a new Lacurbsinae (Opiliones, Laniatores, Biantidae) from Ankasa National Park, Ghana

Abel Pérez-González^{1*}, Vanesa Mamani^{1,2*}

¹ División Aracnología, Museo Argentino de Ciencias Naturales “Bernardino Rivadavia” – CONICET, Av. Ángel Gallardo 470, C1405DJR, Buenos Aires, Argentina

² Departamento de Biodiversidad y Biología Experimental, Facultad de Ciencias Exactas y Naturales, Universidad de Buenos Aires, Av. Int. Güiraldes s/n, Ciudad Universitaria, C1428EHA, Buenos Aires, Argentina

Corresponding author: Abel Pérez-González (abelaracno@gmail.com)



This article is part of:

Gedenkschrift for Prof. Stefan H. Foord

Edited by Galina Azarkina, Ansie

Dippenaar-Schoeman, Charles Haddad,

Robin Lyle, John Mldgley, Caswell Munyai

Academic editor: Robin Lyle

Received: 3 October 2024

Accepted: 20 November 2024

Published: 4 December 2024

ZooBank: <https://zoobank.org/45BDCA97-EB71-44AF-AFE4-47CD13CFD787>

Citation: Pérez-González A, Mamani V (2024) *Metalacurbs foordi* sp. nov., a new Lacurbsinae (Opiliones, Laniatores, Biantidae) from Ankasa National Park, Ghana. African Invertebrates 65(2): 199–211. <https://doi.org/10.3897/AfrInvertebr.65.138398>

Copyright:

© Abel Pérez-González & Vanesa Mamani.

This is an open access article distributed under terms of the Creative Commons Attribution License (Attribution 4.0 International – CC BY 4.0).

Abstract

Despite being one of the most conspicuous African opilionids, the members of Lacurbsinae remain one of the least known groups of harvestmen species. All eight previously-known species of Lacurbsinae are inadequately described and poorly illustrated, leaving the morphological characteristics of this subfamily obscure. After more than half a century, we describe a new species of Lacurbsinae. *Metalacurbs foordi* sp. nov. is described, based on a male specimen collected in Ankasa National Park, Ghana, with a detailed description and illustration of its external and genital morphology. This marks the first modern taxonomic description of a species within Lacurbsinae, including an illustration and description of the male genital morphology, a crucial modern taxonomic characteristic for Opiliones and represents a starting point for the taxonomic revision of the subfamily.

Key words: Afrotropical Region, genitalia, harvestmen, taxonomy, new species

Introduction

There are many African nations with fewer described Opiliones species than might be expected, given their large number of ecoregions and the rich biodiversity of this arachnid order in the continent. This pattern is particularly remarkable in certain parts of tropical Africa, where there are huge and rich humid forests, but much of the Opiliofauna is undescribed. The Republic of Ghana is one of these countries with only 16 opilionid records (Kury et al. 2024). These low numbers contrast with the 41 species in the neighbouring Republic of Côte d'Ivoire, the 31 species of the much smaller Republic of Equatorial Guinea or the more than 200 species recorded in the Republic of South Africa (Kury et al. 2024).

Roewer (1949) described *Eulacurbs paradoxa* Roewer, 1949 and *Prolacurbs singularis* Roewer, 1949, from Aburi, in the Eastern Region of south Ghana and, to date, these remain the only representatives of Biantidae in the country. These two species belong to the small and poorly-known subfamily Lacurbsinae Lawrence, 1959. Thanks to the collection effort of our friend and colleague Dr Bernhard Huber, head of the Arachnida Section and Curator of the Zoologisches

* These authors contributed equally.

Forschungsmuseum Alexander Koenig in Bonn, Germany, we had the opportunity to study one Lacurbsinae specimen from the Western Region of south Ghana, which results in a new species that we describe and illustrate in this work.

Materials and methods

The specimen examined for this work was borrowed from the Zoologisches Forschungsmuseum Alexander Koenig (ZFMK), Bonn, Germany (Bernhard A. Huber, Head of Arachnida Section and Curator).

The specimen was examined using a Leica M205A stereomicroscope and different focal plane pictures were taken with a Leica DF295 digital camera. Illustrations were performed on a Leica M165C stereoscopic microscope with a *camera lucida*. Male genitalia were prepared using glycerine as a clearing agent following Acosta et al. (2007) and were drawn using a *camera lucida* attached to an Olympus BH2 microscope. Morphological nomenclature follows Kury and Pérez-González (2007), Gnaspini and Rodrigues (2011), Kury and Medrano (2016) and Wolff et al. (2016). Measurements are given in millimetres (mm). Descriptions of colours follow Kury and Orrico (2006) using the standard names of the 267 Colour Centroids of the NBS/IBCC Colour System (<http://people.csail.mit.edu/jaffer/Color/Dictionaries#nbs-iscs>). Drawings were vectorised and plates were prepared in CorelDRAW Graphics Suite 2023 (24.3.0). The distribution map was created by SimpleMappr (Shorthouse 2010).

Taxonomy

Opiliones Sundevall, 1833

Laniatores Thorell, 1876

Biantidae Thorell, 1889

Lacurbsinae Lawrence, 1959

***Metalacurbs* Roewer, 1915**

***Metalacurbs foordi* sp. nov.**

<https://zoobank.org/BA6B8F87-B420-41F2-B99A-0D45FC8D6EAF>

Figs 1–7

Material examined. Type material: *Holotype*: GHANA • 1 ♂; Western Region, Ankasa National Park; [5.2172, -2.6514]; 180 m a.s.l.; 22 Feb 2013; B.A. Huber leg.; forest near entrance, day collecting; (ZFMK Op835).

Etymology. Patronym in honour of our dear and long-time good friend, the late Stefan Foord (1971–2023), in recognition of a productive, passionate and dedicated life to the research and development of African Arachnology; name in the genitive case.

Diagnosis. The new species can be easily distinguished not only from the other species in the genus, but also from all species of Lacurbsinae by the presence, in males, of basally enlarged metatarsus II (Fig. 4D) and a dorsal spiniform apophysis on femur IV (Fig. 6A–D). Only *Metalacurbs oedipus* (Roewer, 1958) and *Metalacurbs villiersi* (Roewer, 1953) exhibit a tibia IV stout and enlarged as in *Metalacurbs foordi* sp. nov., but the tibia IV outline and armature are completely different amongst these three species (compare Fig. 6A–C, E versus Roewer 1953: 620, fig. 5 and Roewer 1958: 236, fig. 4).



Figure 1. *Metalacurbs foordi* sp. nov., holotype male (ZFMK Op835), habitus photos **A** dorsal view **B** ventral view **C** ventral view with detail of coxae I–III **D** ventral view with detail of coxa IV and free sternites **E** lateral view **F** posterior view **G** detail of free tergites I–III and anal operculum. Black arrows indicate spiniform apophyses. Scale bars: 1 mm (**A**, **B**, **E**); 500 μ m (**C**, **D**, **F**, **G**).

Description. Male holotype (ZFMK Op835). Body measurements: Total body length 2.78, carapace length 0.73, *scutum magnum* length 2.30, carapace maximum width 1.14, abdominal *scutum* maximum width 1.81. Appendage measurements in Table 1.

Dorsum: Outline with a theta (θ) shape, campaniform (bell-shaped) (Figs 1A, 2A). Carapace wider than long, with a small and rounded frontal hump; anterior

Table 1. Appendage measurements (in mm) of *Metalacurbs foordi* sp. nov., holotype male (ZFMK Op835). Tr–Trochanter, Fe–Femur, Pa–Patella, Ti–Tibia, Mt–Metatarsus, Ta–Tarsus, T–Total.

| | Tr | Fe | Pa | Ti | Mt | Ta | T |
|-----------------|------|------|------|------|------|------|--------------|
| Pedipalp | 0.34 | 1.88 | 1.29 | 0.86 | – | 0.55 | 4.92 |
| Leg I | 0.31 | 1.30 | 0.48 | 1.01 | 1.76 | 1.07 | 5.93 |
| Leg II | 0.42 | 2.77 | 0.76 | 2.13 | 3.22 | 2.45 | 11.76 |
| Leg III | 0.35 | 1.68 | 0.53 | 1.22 | 2.31 | 1.26 | 7.35 |
| Leg IV | 0.63 | 2.97 | 0.86 | 2.42 | 2.43 | 1.57 | 10.88 |

border slightly convex (Figs 1A, 2A). Cheliceral sockets not marked (Fig. 2A). Eyes separated, eye mounds high along the mid-line of the carapace; interocular area is smooth with a small transversal elevation (Figs 1A, E, 2A). Carapace straight in lateral view (Fig. 1E). Abdominal **scutum** convex in lateral view (Fig. 1E). Sulcus I deep and well-marked, in dorsal view medially slightly curved to posterior body region (Fig. 2A). Mesotergal areas defined; sulci II–V notably wide, shallow and complete (Figs 1A, 2A). Mesotergal area I larger than mesotergal areas II–IV (Figs 1A, 2A). Mesotergal areas I–II with two lateral tubercles; mesotergal area IV with two medial tubercles; tubercles of mesotergal area II longer than tubercles of mesotergal areas I and IV; mesotergal area III with two medial long spiniform apophyses (Figs 1A, E, F, 2A). Mesotergal area V with a row of five small pointed tubercles (Figs 1G, 2A). Lateral borders of abdominal **scutum** with a row of rounded granules, but at level of posterior mesotergal area II and anterior mesotergal area III with larger tubercles (Figs 1A, 2A). Free tergite I with a row of six tubercles, with the two most lateral tubercles longer than medial ones; free tergite II with a row of seven tubercles; free tergite III with a row of lateral tubercles and one medial spiniform apophysis [broken] (Figs 1A, E–G, 2A).

Venter: Coxa I with setiferous granules (Fig. 1B, C); anterior and posterior borders of coxa III with a row of granules connecting with coxae II and IV, respectively; posterior granules of coxa III larger than anterior granules (Fig. 1B–D); free sternites with a row of setiferous granules (Fig. 1D, F, G); anal operculum with two small tubercles (Fig. 1E–G). Spiracles not concealed (Fig. 1D).

Chelicerae: Basichelicerite unarmed, with an elongated and slightly marked **bulla** (Fig. 2B). Cheliceral hand with sparse setae and rounded frontal setiferous granules (Fig. 2B, C). Fixed and movable finger with a row of conical teeth (Fig. 2C).

Pedipalps: Raptorial, with spines concentrated on tibia and tarsus (Fig. 2D, E). Coxa elongated, slightly shorter than basichelicerite; proximally with one dorsomesal and one dorsoectal granule; ventrally with small granules (Figs 1A–C, 2A). Trochanter rounded. Femur straight; ventrally with a row of four proximo-medial pointed tubercles and one mesal spine in the third proximal region (Fig. 2D–F). Patella elongated ventrodistally with one ectal pointed tubercle and one mesal spine (Fig. 2D, E). Tibia ventrally with four ectal spines followed by a pointed setiferous tubercle (Fig. 2E) and three mesal spines (Fig. 2D). Tarsus shorter than tibia; ventrally armed with two ectal and two mesal spines (Fig. 2D, E). Claw elongated and pointed (Fig. 2D).

Legs: Coxa IV with prolateral pointed setiferous tubercles and two spiniform apophyses, one distal and one subdistal (Figs 1A, B, D, F, 2A). Trochanter II with

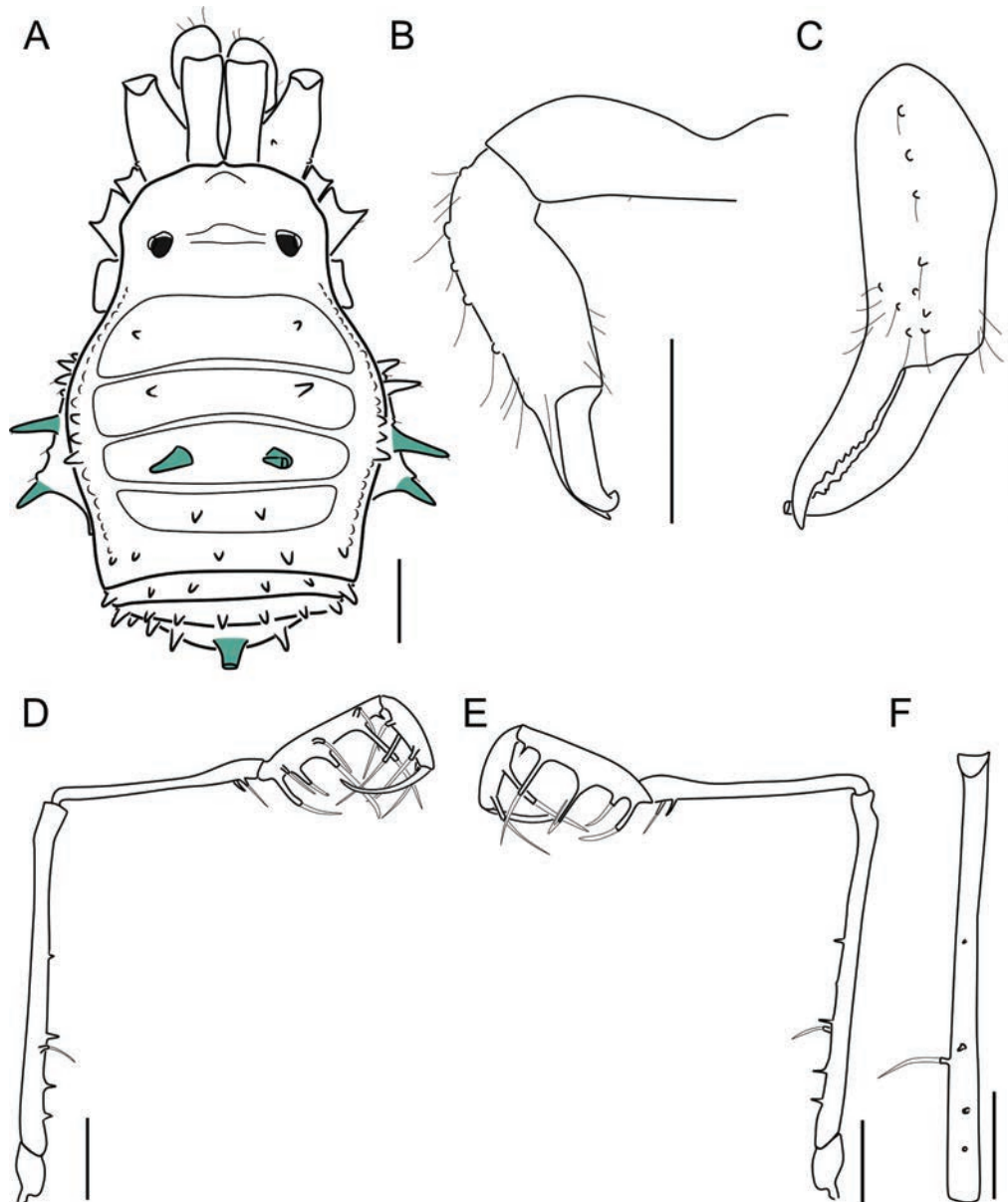


Figure 2. *Metalacurbs foordi* sp. nov., holotype male (ZFMK Op835), drawings of habitus, chelicera and pedipalp **A** habitus, dorsal view **B, C** left chelicera **B** ectal view **C** frontal view **D–F** left pedipalp **D** mesal view **E** ectal view **F** femur, ventral view. Spiniform apophyses in green. Scale bars: 500 µm.

one dorsal tubercle (Fig. 4A, B); trochanter IV apically with one retrolateral and one proteral spiniform apophysis (Figs 1F, 6A–D). Femur I unarmed (Fig. 3A, B); femur II with a dorsal row of short tubercles (Fig. 4B); femur III with a row of longer dorsal pointed tubercles than in femur II (Fig. 5B); femur IV distally slightly thickened, armed with longitudinal rows of pointed tubercles on all surfaces; ventrodistal tubercles longer; dorsally with one spiniform apophysis at the beginning of the distal third and one spiniform apophysis on the distal edge; ventrally with a proteral subdistal spiniform apophysis (Fig. 6A–D). Patellae I–II unarmed (Figs 3A, B, 4A, B); patella III with dorsal tubercles, the most distal longer and sharp-pointed (Fig. 5A–C); patella IV with sharp-pointed tubercles, the most distal tubercles longer (Fig. 6A–E). Tibiae I–II unarmed (Figs 3C, 4C); tibia III with a dorsoproximal tubercle (Fig. 5C); tibia IV ventrally enlarged, dorsally with four proximal tubercles, followed by small tubercles decreasing in size, distally with a proteral and retro-

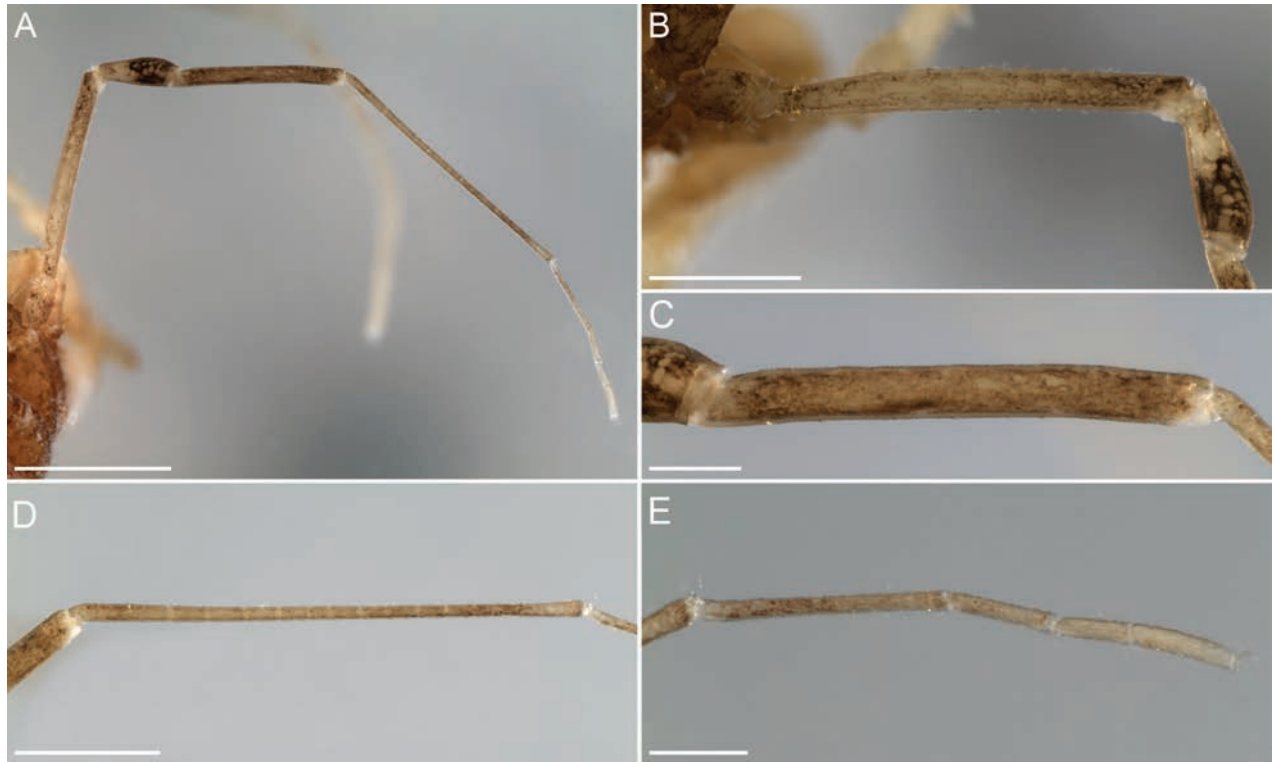


Figure 3. *Metalacurbs foordi* sp. nov., holotype male (ZFMK Op835), right leg I, photos **A** retrolateral view **B** detail of trochanter, femur and patella **C** detail of tibia **D** detail of metatarsus **E** detail of tarsus. Scale bars: 1 mm (**A**); 500 μ m (**B**, **D**); 200 μ m (**C**, **E**).



Figure 4. *Metalacurbs foordi* sp. nov., holotype male (ZFMK Op835), right leg II, photos **A** retrolateral view **B** detail of trochanter, femur and patella **C** detail of tibia **D** detail of metatarsus **E** detail of tarsus. Arrow indicates the proximally swollen metatarsus II. Scale bars: 1 mm (**A**, **D**); 500 μ m (**B**, **C**, **E**).



Figure 5. *Metalacurbs foordi* sp. nov., holotype male (ZFMK Op835), right leg III, photos **A** retrolateral view **B** detail of trochanter, femur and patella **C** detail of tibia **D** detail of metatarsus **E** detail of tarsus. Scale bars: 1 mm (**A**); 500 μ m (**B–D**); 200 μ m (**E**).

lateral pointed tubercle; ventral surface with a row of prolateral tubercles increasing in size, followed by a curved, strong and pointed prolateral apophysis and by a short conical and blunt-tipped apophysis; ventrodistally with two retrolateral short blunt-tipped apophyses (Fig. 6A–C, E). Metatarsi I and III thin and unarmed, with pseudoarticular rings (Figs 3D, 5D); metatarsus II unarmed, proximally swollen (obclavate) and distally thin with pseudoarticular rings (Fig. 4D); metatarsus IV proximally broadened, ventroproximally with conical tubercles; dorsoproximally with three pointed tubercles (Fig. 6A–C, F). Tarsi III–IV with a dense scopula (Figs 5E, 6G). Tarsal formula: 4(2):9–10(3):5:6 (Figs 3E, 4E, 5E, 6G).

Colour (specimen preserved in 80% ethanol): General body appearance yellowish-brown; carapace and coxae I–III with dark reticulations; mesotergal areas I–IV, lateral border of **scutum magnum**, posterior border of area V and free tergites I–III darker; posterior border of stigmatic area and free sternites dark yellowish-brown (Fig. 1A–G); lighter colouration at the level of cheliceral insertion, creating a false appearance of a marked cheliceral socket; pseudoarticular rings lighter (Fig. 1A). Appendages light yellowish-brown (Fig. 1A); trochanters I–IV, distal portion of femora I–IV, patellae I–IV and tibiae IV with dark brown reticulations (Figs 3A, B, 4A, B, 5A, B, 6C–E); tibia I–III, proximal portion of metatarsi II, IV dark brown (Figs 3C, 4C, D, 5F, 6F).

Genitalia: General shape of penis tubular (Fig. 7A, E) apically enlarged (Fig. 7C, D), making the **pars basalis** and **pars distalis** clearly defined (Fig. 7C). **Pars distalis** with a ventral enlarged, rounded and laterally compressed portion, that connects to a ventral thin and wide **lamina apicalis**; the junction between these two regions forms a semicircular edge (Fig. 7D). **Lamina apicalis** with a dorsal pseudotubular-shaped

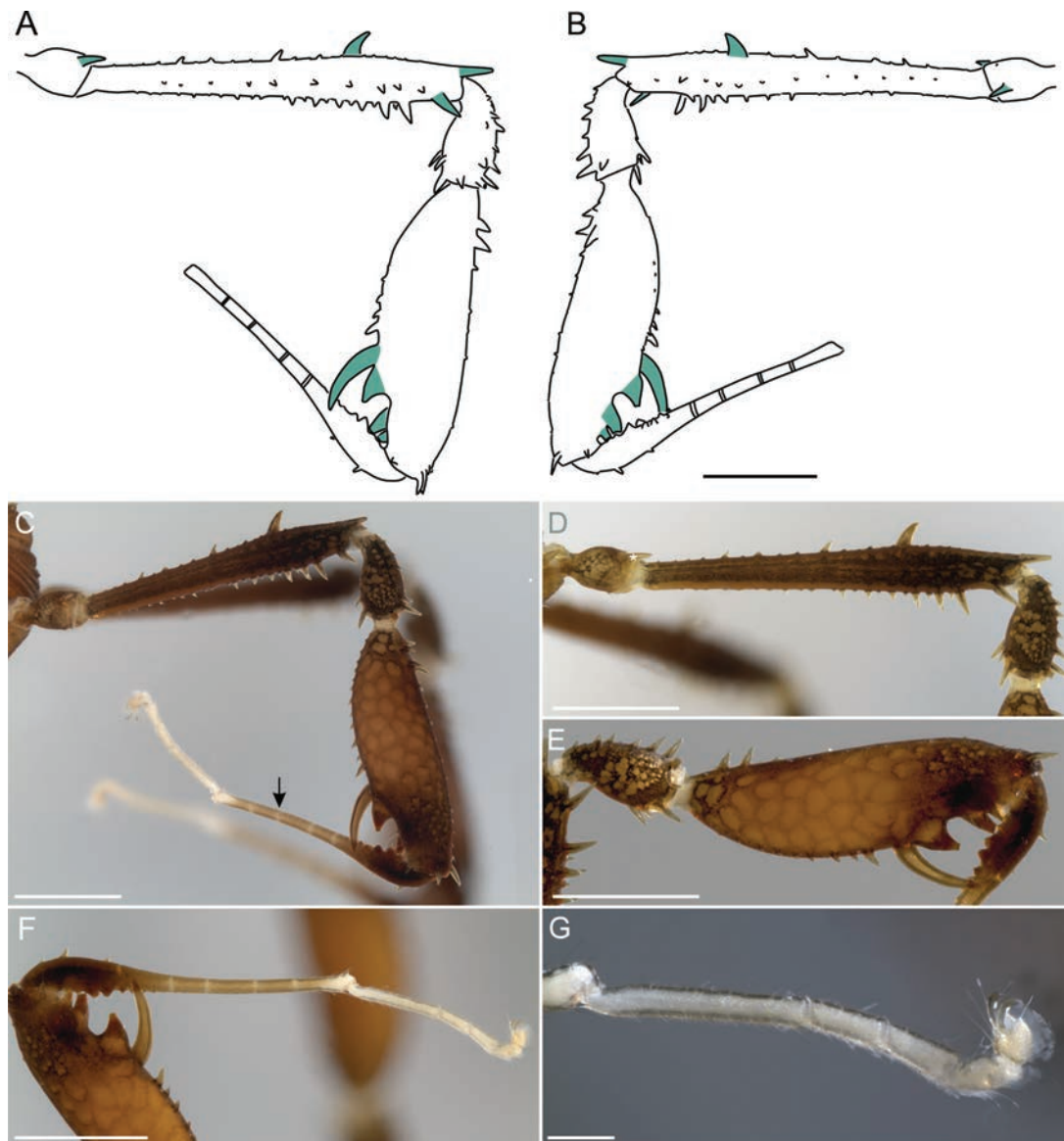


Figure 6. *Metalacurbs foordi* sp. nov., holotype male (ZFMK Op835), drawings and photos of left leg IV **A** prolateral view **B** retrolateral view **C** prolateral view **D** detail of trochanter, femur and patella **E** detail of tibia **F** detail of metatarsus **G** detail of tarsus. Spiniform apophysis in green. Arrow indicates a pseudoarticular ring. Scale bars: 1 mm (**A–C**); 500 µm (**D–F**); 200 µm (**G**).

fold (Fig. 7B, D); **lamina apicalis** with two ventral pairs of small and acute macrosetae (Fig. 7F). **Pars distalis** with a basal pair of lateral small and acute macrosetae, pointed to the apical region, located just below the narrow-rounded portion (Fig. 7D). Narrow-rounded portion of **pars distalis** with two ventral and one ventrolateral pair of small, acute macrosetae (Fig. 7F). Glans with basal **capsula externa** articulated with the truncus and with a jack-knife movement during the hydraulic expansion. **Capsula externa** as a rigid sclerite (similar to the **stragulum** in Zalmoxoidea) with two long and curved projections basally fused; apically, each projection with an enlarged laminar portion tapering to a pointing end, extending laterally over the rounded portion of the **pars distalis** (Fig. 7A, D); dorsally with a wide mediobasal cleft (leaving part of the **capsula interna** exposed) becoming mediolaterally very narrow so that the curved projections are in contact (Fig. 7B). **Capsula interna**, barely visible through transparency, rigid, with a stylus and conductors largely fused, only

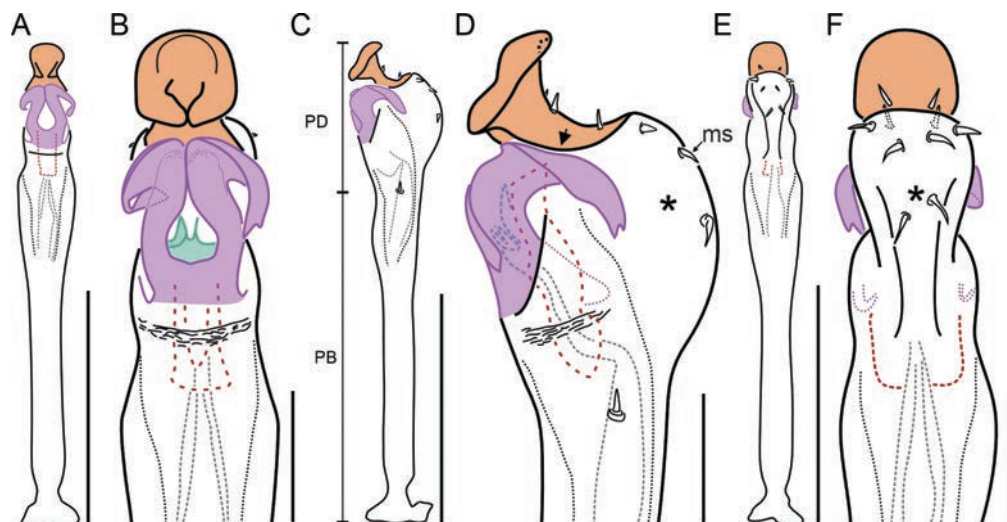


Figure 7. *Metalacurbs foordi* sp. nov., holotype male (ZFMK Op835), penis drawings **A, B** dorsal view **C, D** lateral view **E, F** ventral view. *Lamina apicalis* in orange; *Capsula externa* in magenta; conductors in red (dashed line); stylus in green (solid and dashed line). Abbreviation: PB (*pars basalis*), PD (*pars distalis*), ms (macroseta). Arrow indicates the semi-circular edge formed by the junction between *lamina apicalis* and the narrow-rounded portion of *pars distalis*. Asterisk indicates the narrow-rounded portion of *pars distalis*. Scale bars: 500 μ m (**A, C, E**); 100 μ m (**B, D, F**).

separated at the apical end; conductors with straight apical margin; stylus pointed with a subapical opening of *ductus ejaculatorius* (Fig. 7B, D).

Female. Unknown.

Distribution. Known only from the type locality (Fig. 8).

Discussion

Metalacurbs foordi sp. nov., is the ninth species known of the small biantid subfamily Lacurbsinae. Lacurbsinae has a fuzzy taxonomic history since its very beginning. It was cryptically proposed by Lawrence (1959) when dealing with the Biantinae fauna of Madagascar, without detailed explanations or proper taxonomic treatment. Lawrence (1959) just cited the type genus, made reference to the number of tarsomeres of leg I and referred to the possibility that the genus *Lacurbs* Sørensen, 1896, could be segregated in its own subfamily Lacurbsinae, which was enough for the subfamilial nomen to become available (Kury 2018). It seems as though Lawrence was not fully convinced about his proposal because, shortly after, Lawrence (1965) did not recognise his own subfamily and referred to the lacurbsines as the “*Lacurbs* group” (within Biantinae). After that, the name Lacurbsinae was largely ignored until it was resurrected by Kury (2003), but without further definitions or explanations. Only Kury and Pérez-González (2007) highlight some Lacurbsinae morphological features in a general Biantidae characterisation and include the subfamily in a dichotomous key. Therefore, Lacurbsinae remains poorly characterised and defined. A taxonomic revision of all the genera and previous species is needed.

The present contribution is a starting milestone in this goal and represents the first time a Lacurbsinae species has been described under modern standards as well as the first time male genitalia have been properly characterised in this subfamily. Regarding the external morphology, lacurbsines are a cohesive group that could be easily recognised from other Biantidae, mainly by the

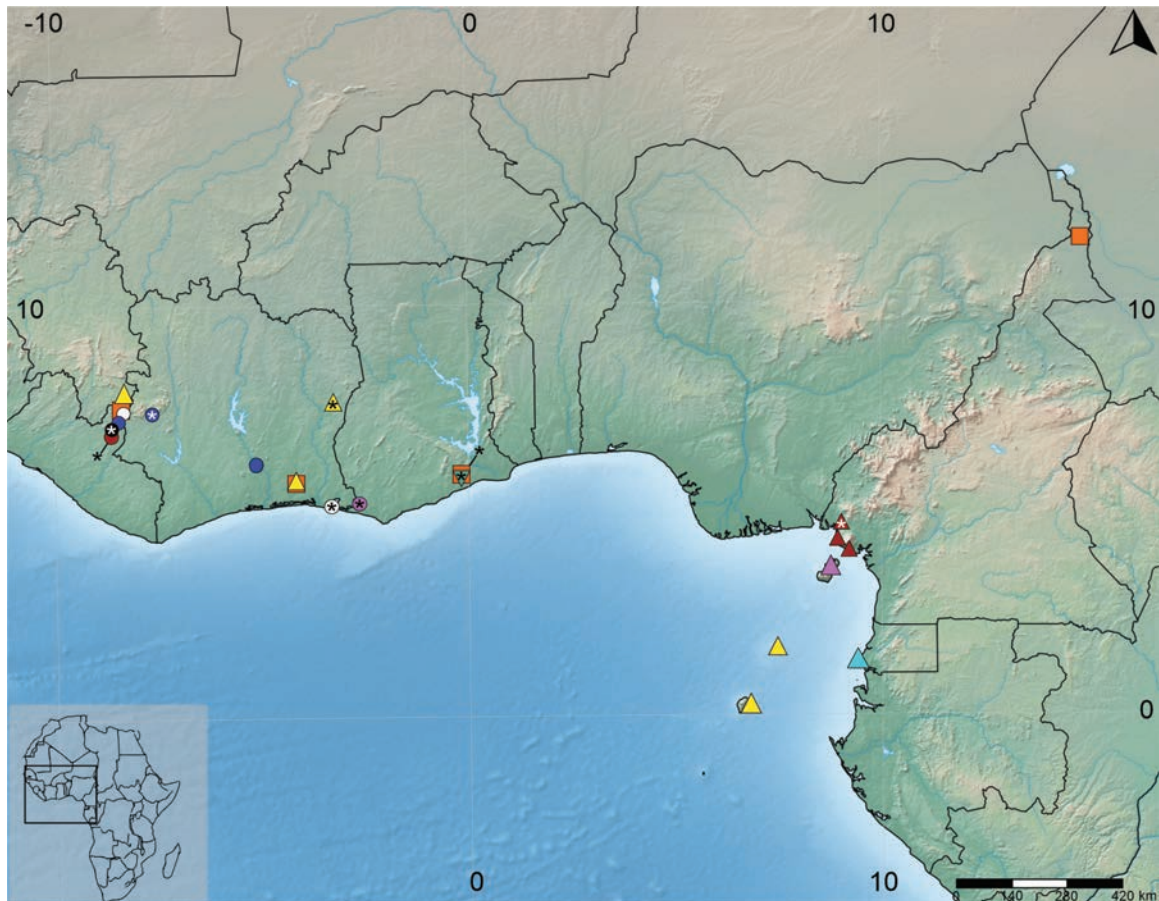


Figure 8. Geographical distribution of Lacurbsinae. *Eulacurbs paradoxa* (orange square). *Lacurbs* (triangles): *Lacurbs nigrimana* (yellow), *L. spinosa* (red), *L. fernandopoensis nomen nudum* (magenta), *Lacurbs* sp. (bright-cyan). *Metalacurbs* (circles): *Metalacurbs cornipes* (black), *M. foordi* sp. nov. (magenta), *M. oedipus* (red), *M. simoni* (white), *M. villiersi* (blue). *Prolacurbs singularis* (green inverted triangle). Asterisks indicate the type localities.

combination of an abdominal **scutum** which is much wider in the middle with convergent posterior margins and a tibia and metatarsus IV heavily armed and/or swollen in males (Kury and Pérez-González 2007).

The male genital morphology is distinctive in lacurbsines and remarkably different from other biantids. The **pars distalis** morphology and glans hydraulic functioning convergently share some similarities to those of Zalmoxoidea. First, the **capsula externa** does not exhibit the typical biantinae soft titillators (e.g. Martens 1978) and is modified in a rigid sclerite similar to the **stragulum** in Zalmoxoidea. This rigid **capsula externa** also appears in other biantids such as Antillean Stenostygninae (e.g. Alegre et al. 2019; Alegre-Barroso and Pérez-González 2024) and the Mexican *Stygnomma teapense* Goodnight & Goodnight, 1951 (obs. pers.). Second, the ventral **pars distalis** is tagmatized, also similar to those in Zalmoxoidea. It ends in a thin **lamina apicalis** dorsally folded that somewhat resembles the zalmoxoidean **rutrum** and basally with a kind of rounded **pergula**. The complex **pergula/rutrum** somewhat resembles those of *Phalangodella* sp. and *Hevelia crucis* Kury, García and Ahumada-C., 2023. The **capsula interna** in *Metalacurbs foordi* sp. nov. is also rigid and basally fused with the **capsula externa**. Once the glans (i.e. **capsula externa** + **capsula interna**) are conformed by rigid sclerites, the only way of functioning during the hydraulic expansion is unfolding the **capsula externa** from the truncus as a jack-knife to expose

the *casula interna* with the stylus, similar to the mode of function in Zalmoxoidea (e.g. Kury and Pérez-González 2002). That means that the jack-knife movement of the glans in *Metalacurbs foordi* sp. nov. is completely different from the typical “in-out of truncus” expansion movement in biantines (see Martens 1978, 1986). In fact, the markedly different glans structure and mode of function during the hydraulic expansion of *Lacurbs* and *Metalacurbs* was pointed out by Martens (1978) to justify the exclusion of both genera from his Biantidae concept.

Unfortunately, none of the previous lacurbsine species has been re-described to date and their penial morphology still remains unpublished. Given this context, we refrain from a critical assignment of the new species to a lacurbsine genus, considering also the male genital morphology. Instead, we follow the traditional approach and include the new species in the genus *Metalacurbs* because of its major congruence (excepting only the armature of free tergite II) with this genus according to Lawrence’s (1965) dichotomous key. Therefore, the combination under *Metalacurbs* adopted herein is merely tentative. Further taxonomic and systematic studies are needed in order to provide stronger evidence for generic allocation of the new species described.

Lacurbsines, to date, are restricted to western tropical Africa (Fig. 8). They are recorded mainly from continental localities (Sørensen 1896; Roewer 1912, 1915, 1923, 1949, 1953, 1958, 1959; Lawrence 1947, 1965; Staręga 1992), with particularly high sympatry in Mount Nimba, but also on islands, as is the case of *Lacurbs nigrimana* Roewer, 1912, in the Democratic Republic of São Tomé and Príncipe (Roewer 1927) and *Lacurbs fernandopoensis nomen nudum* in Bioko (Fernando Po during the colonial era), Republic of Equatorial Guinea (Andrés Cobeta 2001; Santos and Prieto 2010). The geographic distribution of the subfamily exhibits enormous distributional gaps where no lacurbsines are recorded. It is highly probable that new species will be detected once lacurbsines specimens from these areas are studied.

Acknowledgments

We are indebted to Dr Bernhard Huber, who kindly collected and lent us the specimen studied. We are indebted to Dr John Midgley and Dra. Galina Azarkina for the kind invitation to participate in the “Gedenkschrift” (memorial volume) in honour of Stefan Foord and for including our manuscript in the sponsored articles. We are grateful to Adriano B. Kury for maintaining the essential online resources for Opiliones taxonomic work: the Omnipaper Project and the World Opiliones Catalogue. We’d like to thank Ella Frigyik for performing the language review on an early version of the manuscript. We are grateful to the subject editor, Robin Lyle, for the kindness during the editorial process and to Gonzalo Giribet and one anonymous reviewer for the thorough revision of the manuscript and useful suggestions.

Additional information

Conflict of interest

The authors have declared that no competing interests exist.

Ethical statement

No ethical statement was reported.

Funding

This research received support from Fondo para la Investigación Científica y Tecnológica (grants numbers: PICT 2019-2745 and PICT 2020-1907) and Consejo Nacional de Investigaciones Científicas y Técnicas (grant number: PUE 098). VM is deeply grateful for the Doctoral Fellowship awarded by the "Consejo Nacional de Investigaciones Científicas y Técnicas – CONICET," Argentina.

Author contributions

Both authors have equal contribution in this article.

Author ORCIDs

Abel Pérez-González  <https://orcid.org/0000-0002-4245-3302>

Vanesa Mamani  <https://orcid.org/0000-0001-9748-5339>

Data availability

All of the data that support the findings of this study are available in the main text.

References

- Acosta LE, Pérez-González AP, Tourinho AL (2007) Methods for taxonomic study. In: Pinto-da-Rocha R, Machado G, Giribet G (Eds) *Harvestmen: The Biology of Opiliones*. Harvard University Press, Cambridge, 494–510.
- Alegre A, Gainett G, López Iborra G, Giribet G (2019) Two new species of *Manahunca*, redescription of its type species, current conservation status of the genus and a survey of male glands in Stenostyginae (Opiliones: Laniatores: Biantidae). *Zootaxa* 4686(1): 83–111. <https://doi.org/10.11646/zootaxa.4686.1.4>
- Alegre-Barroso A, Pérez-González A (2024) Two new species of *Caribbiantes*, with the redescription of the type species and a review of male genital patterns in Antillean Stenostyginae (Opiliones: Laniatores: Biantidae). *Zootaxa* 5514(5): 401–430. <https://doi.org/10.11646/zootaxa.5514.5.1>
- Andrés Cobeta FJ de (2001) Catálogo de las colecciones zoológicas de Guinea Ecuatorial del Museo de Ciencias Naturales. Vol. I. Invertebrados no insectos. Serie de Manuales Técnicos de Museología. Número 10. Museo Nacional de Ciencias Naturales and Consejo Superior de Investigaciones Científicas, Madrid, 159 pp.
- Gnaspini P, Rodrigues GCS (2011) Comparative study of the morphology of the gland opening area among Grassatores harvestmen (Arachnida, Opiliones, Laniatores). *Journal of Zoological Systematics and Evolutionary Research* 49(4): 273–284. <https://doi.org/10.1111/j.1439-0469.2011.00626.x>
- Kury AB (2003) Annotated catalogue of the Laniatores of the New World (Arachnida, Opiliones). *Revista Iberica de Aracnología*, vol. especial monográfico 1: 1–337.
- Kury AB (2018) Familial nomina in harvestmen (Arachnida, Opiliones). *Bionomina* 13(1): 1–27. <https://doi.org/10.11646/bionomina.13.1.1>
- Kury AB, Medrano M (2016) Review of terminology for the outline of dorsal scutum in Laniatores (Arachnida, Opiliones). *Zootaxa* 4097(1): 130–134. <https://doi.org/10.11646/zootaxa.4097.1.9>
- Kury AB, Orrico VGD (2006) A new species of *Lacronia* Strand, 1942 from the highlands of Rio de Janeiro (Opiliones, Gonyleptidae, Pachylinae). *Revista Iberica de Aracnología* 13: 147–153.
- Kury AB, Pérez-González A (2002) A new family of Laniatores from northwestern South America (Arachnida, Opiliones). *Revista Iberica de Aracnología* 6: 3–11.

- Kury AB, Pérez-González A (2007) Zalmoxidae Sørensen, 1886. In: Pinto-da-Rocha R, Machado G, Giribet G (Eds) *Harvestmen: The Biology of Opiliones*. Harvard University Press, Cambridge, 243–246.
- Kury AB, Kury IS, de Oliveira ABR (2024) Checklists of extant harvestman (Arachnida: Opiliones) species for all the countries of the world. *Zootaxa* 5515(1): 1–162. <https://doi.org/10.11646/zootaxa.5515.1.1>
- Lawrence RF (1947) Opiliones from the Ivory Coast of West Africa collected by R. Paulian and C. Delamare-Deboutteville. *Revue Française d'Entomologie* 14(1): 34–46.
- Lawrence RF (1959) Arachnides-Opilions. *Faune de Madagascar* 9. Publications de L'Institut de Recherche Scientifique Tananarive, Tsimbazaza, 1–121.
- Lawrence RF (1965) A small collection of Opiliones from the Ivory Coast of West Africa. *Bulletin du Muséum National d'Histoire Naturelle* 36: 797–811.
- Martens J (1978) Opiliones aus dem Nepal-Himalaya. IV. Biantidae (Arachnida). *Senckenbergiana Biologica* 58(5/6): 347–414.
- Martens J (1986) Die Grossgliederung der Opiliones und die Evolution der Ordnung (Arachnida). In: Barrientos JA (Ed.) *Actas del X Congreso Internacional de Aracnología* (Jaca, Spain, September 1986). v. 1. Juvenil, Barcelona, 289–310.
- Roewer CF (1912) Die Familien der Assamiiden und Phalangodiden der Opiliones-Laniatores. (= Assamiden, Dampetriden, Phalangodiden, Epedaniden, Biantiden, Zalmoxiden, Samoiden, Palpipediden anderer Autoren). *Archiv für Naturgeschichte*, Berlin, Abt. A, Original-Arbeiten 78(3): 1–242.
- Roewer CF (1915) Fünfzehn neue Opilioniden. *Archiv für Naturgeschichte*, Berlin, Abt. A, Original-Arbeiten 80(9): 106–132.
- Roewer CF (1923) Die Weberknechte der Erde. Systematische Bearbeitung der bisher bekannten Opiliones. Gustav Fischer, Jena, 1116 pp.
- Roewer CF (1927) Weitere Weberknechte I. (1. Ergänzung der: "Weberknechte der Erde," 1923). *Abhandlungen der Naturwissenschaftlichen Verein zu Bremen* 26(2): 261–402.
- Roewer CF (1949) Über Phalangodidae II. Weitere Weberknechte XIV. *Senckenbergiana* 30(4/6): 247–289.
- Roewer CF (1953) Opiliones aus Französisch-Westafrika, gesammelt durch Herrn Dr. A. Villiers. *Bulletin de l'Institut Français d'Afrique Noire* 15(2): 610–630.
- Roewer CF (1958) XI. Opilions. La Réserve naturelle intégrale du Mont Nimba. *Mémoires de l'Institut Français d'Afrique Noire* 53(11): 229–240.
- Roewer CF (1959) Opiliones der II. Mont Nimba-Collection von Prof. M. Lamotte. *Bulletin du Muséum National d'Histoire Naturelle*, 2^e Série (2)31: 355–358
- Santos R, Prieto CE (2010) Los Assamiidae (Opiliones: Assamiidae) de Río Muni (Guinea Ecuatorial), con la descripción de ocho nuevas especies. *Revista de Biología Tropical* 58(1): 203–243. <https://doi.org/10.15517/rbt.v58i1.5205>
- Shorthouse DP (2010) SimpleMappr, an online tool to produce publication-quality point maps. <http://www.simplemappr.net> [Date of access: 10 September 2024]
- Sørensen WE (1896) Opiliones Laniatores a cl. Dr. Yngve Sjöstedt in Kamerun (Africa Centrali) collectos. *Entomologisk Tidskrift* 17(2–3): 177–202.
- Staręga W (1992) An annotated check-list of harvestmen, excluding Phalangiidae, of the Afrotropical Region (Opiliones). *Annals of the Natal Museum* 33(2): 271–336.
- Wolff JO, Schönhofer AL, Martens J, Wijnhoven H, Taylor CK, Gorb SN (2016) The evolution of pedipalps and glandular hairs as predatory devices in harvestmen (Arachnida, Opiliones). *Zoological Journal of the Linnean Society* 177(3): 1–44. <https://doi.org/10.1111/zoj.12375>

Short Communication

The rare siphonophore *Rhizophysa eysenhardtii* Gegenbaur, 1859 (Hydrozoa, Siphonophora, Cystonectae) from False Bay, South Africa

Gillian M. Mapstone¹ , Jannes Landschoff^{2,3} 

¹ Department of Life Sciences, The Natural History Museum, London, UK

² Sea Change Project, Sea Change Trust, 6 Buxton Avenue, Oranjezicht, 8001, Cape Town, South Africa

³ Department of Botany and Zoology, Stellenbosch University, Private Bag X1, Matieland, 7602, South Africa

Corresponding author: Jannes Landschoff (jannes@landschoff.net)

Abstract

From June to September 2022, five colonies of the rare hydrozoan siphonophore *Rhizophysa eysenhardtii* were observed for the first time near the surface in False Bay, South Africa. The two colonies in June/July were small with all tentacles contracted, while the September colonies were larger, the largest up to 0.8 m long (in video), with most of its tentacles extended for feeding. In this species, tentacles are typically pink and each arises from the proximal end of a gastrozoid, which engulfs and digests the prey. Fish larvae were noted in the gastrozooids and counted and a chaetognath was observed stuck to one of the tentacles. The pneumatophore was prominent in all specimens and gonodendra bearing sexual gonophores were visible between the gastrozooids of the larger specimens.

Key words: Benguela ecosystem, cystonect, diet, Great African Seaforest, *in situ* observation, photo and video identification



Academic editor: Sean Porter

Received: 4 September 2024

Accepted: 28 October 2024

Published: 10 December 2024

ZooBank: <https://zoobank.org/601C2EC6-98A6-42A0-AEAF-D37E7C7A1C86>

Citation: Mapstone GM, Landschoff J (2024) The rare siphonophore *Rhizophysa eysenhardtii* Gegenbaur, 1859 (Hydrozoa, Siphonophora, Cystonectae) from False Bay, South Africa. African Invertebrates 65(2): 213–221. <https://doi.org/10.3897/AfrInvertebr.65.136267>

Copyright: ©

Gillian M. Mapstone & Jannes Landschoff.

This is an open access article distributed under

terms of the Creative Commons Attribution

License (Attribution 4.0 International – CC BY 4.0).

Introduction

Rhizophysa is a cystonect siphonophore, with a float, or pneumatophore, at the apex of the stem, but no nectophores (swimming bells). There are only five currently recognised cystonect species, which are distributed between two families: the Physaliidae and the Rhizophysidae (Dunn et al. 2005, fig. 6). The Physaliidae is monotypic for the Portuguese Man of War, *Physalia physalis*, which has a large float, but no stem. The Rhizophysidae have a smaller float and a long stem which bears repeated cormidial units each comprising a gastrozoid or feeding zooid, with tentacle and, when mature, a gonodendron or reproductive zooid. This family includes two genera: the bathypelagic *Bathypphysa* and the mostly epipelagic *Rhizophysa*, which morphologically differ only in the presence or absence of ptera or wings on the gastrozooids. Ptera are present in the gastrozooids of *Bathypphysa* species (Mapstone et al. 2021) and are thought to increase the surface area of the colony and slow down its sinking rate (Biggs and Harbison 1976). In *Rhizophysa*, sinking is slowed by constant contraction and relaxation of the stem to maintain its position in the water column (Totton 1965; Munro et al. 2018) and colonies have been observed peacefully drifting

and writhing about at the surface in a calm sea, while their tentacles hang down below like long fishing lines to catch prey (Gegenbaur 1853).

This study reports the first occurrence of *Rhizophysa eysenhardtii* Gegenbaur, 1859 from False Bay, Cape Town, South Africa from snorkelling observations at shallow near shore depths of 1–3 m.

Materials and methods

Elongate cystonect specimens were observed swimming near the surface (Table 1) by JL on the western side of False Bay around Simon's Town (34°12.6'S, 18°28.05'E), South Africa: one on 19 and two more on 25 September 2022. Multiple videos and numerous still images were taken *in situ* and sent to GM for more detailed examination. Images were taken adjacent to a head of the Bamboo kelp *Ecklonia maxima* using an Olympus TG6 with FCON-T01 Fish-eye converter. Natural sunlight was complemented by using a BigBlue VLT4200P video light. Colony length was estimated, based on the distance of the specimen from the camera and varied between more than 0.4–0.5 m to 0.8 m, depending on whether the colony was expanded or contracted. The gas-filled space in the gas chamber of the pneumatophore was particularly prominent in all images due to the reflection of light rays from it.

Using an Olympus TG6 with natural sunlight, two more long-stemmed cystonects were also imaged by Catherine Corder: one near the water surface at Long Beach, Simon's Town (34°11.20'S, 18°25.59'E) on 27 June 2022 and one at Smitswinkel Bay (34°16.00'S, 18°28.01'E) and sent to JL on 7 October 2023. Both were also identified as a rhizophysid.

Using the available images, we counted the number of caught fish larvae per colony by counting the eye-pairs that were visible inside the gastrozooids.

Glossary of terminology used in this paper:

| | |
|--------------------------|--|
| Cormidial unit | serially repeated (iterative) group of zooids on the main stem of siphonophores, each including, in cystonects, a gastrozoid and one or more gonophores. |
| Gastrozoid | asexual feeding zooid in a cormidium, with tentacle arising from the proximal end. |
| Gonophore | sexual medusoid zooid arising from a branched complex called a gonodendron; each gonophore releases gametes of one sex only. |
| Hypocystic cavity | surrounds the pneumatosaccus of the pneumatophore. |
| Nectophore | asexual swimming bell. |
| Pneumatosaccus | gas bladder within the pneumatophore. |
| Pneumatophore | anterior gas-filled float. |
| Tentillum | side-branch of a tentacle bearing nematocysts (stinging cells). |

Results

Two species are referred to the genus *Rhizophysa*: *R. filiformis* Forskal, 1775 and *R. eysenhardtii* Gegenbaur, 1859. These are distinguished mainly on differences between the side branches (tentilla) of their tentacles. In *R. filiformis*, the side branches terminate in swollen tips where the nematocysts for prey capture

occur (Totton 1965), whereas in *R. eysenhardtii*, the side branches lack swollen tips and, instead, the nematocysts are distributed along the whole length of the side branch, as well shown by Kawamura (1910, fig. 5c). There are also specific differences in the overall colour of the colony (Pugh 2019) and in the maximum size attained by the pneumatophore (Totton 1965).

The larger specimens imaged in False Bay (specimens 3–5, Table 1) had only simple side branches (tentilla) on the tentacles and, in those specimens with contracted tentacles, the tentacles were pink (Fig. 1). They were therefore concluded to be *R. eysenhardtii*. Specimen 1, for which we only had a picture with tentacles contracted, showed the same pink colouration (Fig. 2). Specimen 2 was small, contracted, with no clear visible colour and also photographed in a rock pool, so the identification of this specimen was based on coincidence of timing and event with specimen 1. The length of the pneumatophore of specimen 5 was estimated at ca.13 mm (Fig. 1B). The *Rhizophysa eysenhardtii* colonies described in this paper varied in colour from an overall rose in the small specimens (Fig. 2), to more translucent throughout, with pink tentacles and a yellow stem in the large specimen (Fig. 1).

The specimens had fed on fish larvae of unknown identity. Per colony, the number of gastrozooids containing captured fish larvae ranged from 0 to 8 (see Table 1). Furthermore, the largest Specimen 5 had captured a fish larva, as well as an unknown chaetognath (Phylum Chaetognatha), in its tentacles and both were not yet ingested by the gastrozooids.

Discussion

Two species in the genus *Rhizophysa* are currently known. Based on shape of the tentilla of the tentacles and on the colour, we identified the specimens presented in this paper as *R. eysenhardtii*. Our observations add biological information to a rarely documented siphonophore, which also presents a new record of the species for the location of False Bay, South Africa. Although probably common and potentially playing important ecological roles in the pelagic zones, published accounts of rhizophysids remain limited and, therefore, add valuable knowledge on the species' biology and distribution. Totton (1965, p.40) notes that "None of the Rhizophysidae commonly come into the hands of systematists, though the hands of fishermen suffer from their stings, since their tentacles adhere to cordage and nets by their nematocysts. No doubt these animals are abundant in deep water".

Table 1. Occurrence events of *Rhizophysa eysenhardtii* on the western shore of False Bay, Cape Town, South Africa.

| Specimen | Size | Date | Remarks | Captured fish larvae (No. of gastrozooids) | Location | GPS | Photographer |
|----------|--------------------|-------------|----------------------|---|--------------------------|------------------------|---------------|
| 1 | 0.1 m, contracted | 27 Jun 2022 | surface | 8 (11) | Long Beach, Simon's Town | 34°11.20'S, 18°25.59'E | C. Corder |
| 2 | 0.05 m, contracted | 05 Jul 2022 | rock pool | 0 (4) | Smitswinkel Bay | 34°16.00'S, 18°28.01'E | C. Corder |
| 3 | 0.6 m, extended | 19 Sep 2022 | surface to 2 m depth | 6 (7) | A-Frame, Simon's Town | 34°12.46'S, 18°27.74'E | J. Landschoff |
| 4 | 0.4 m, extended | 25 Sep 2022 | 1, 2 m depth | 2 (9) | A-Frame, Simon's Town | 34°12.46'S, 18°27.74'E | J. Landschoff |
| 5 | 0.8 m, extended | 25 Sep 2022 | surface to 3 m depth | 8 (19) + 1 fish and 1 chaetognath in tentacle | A-Frame, Simon's Town | 34°12.46'S, 18°27.74'E | J. Landschoff |

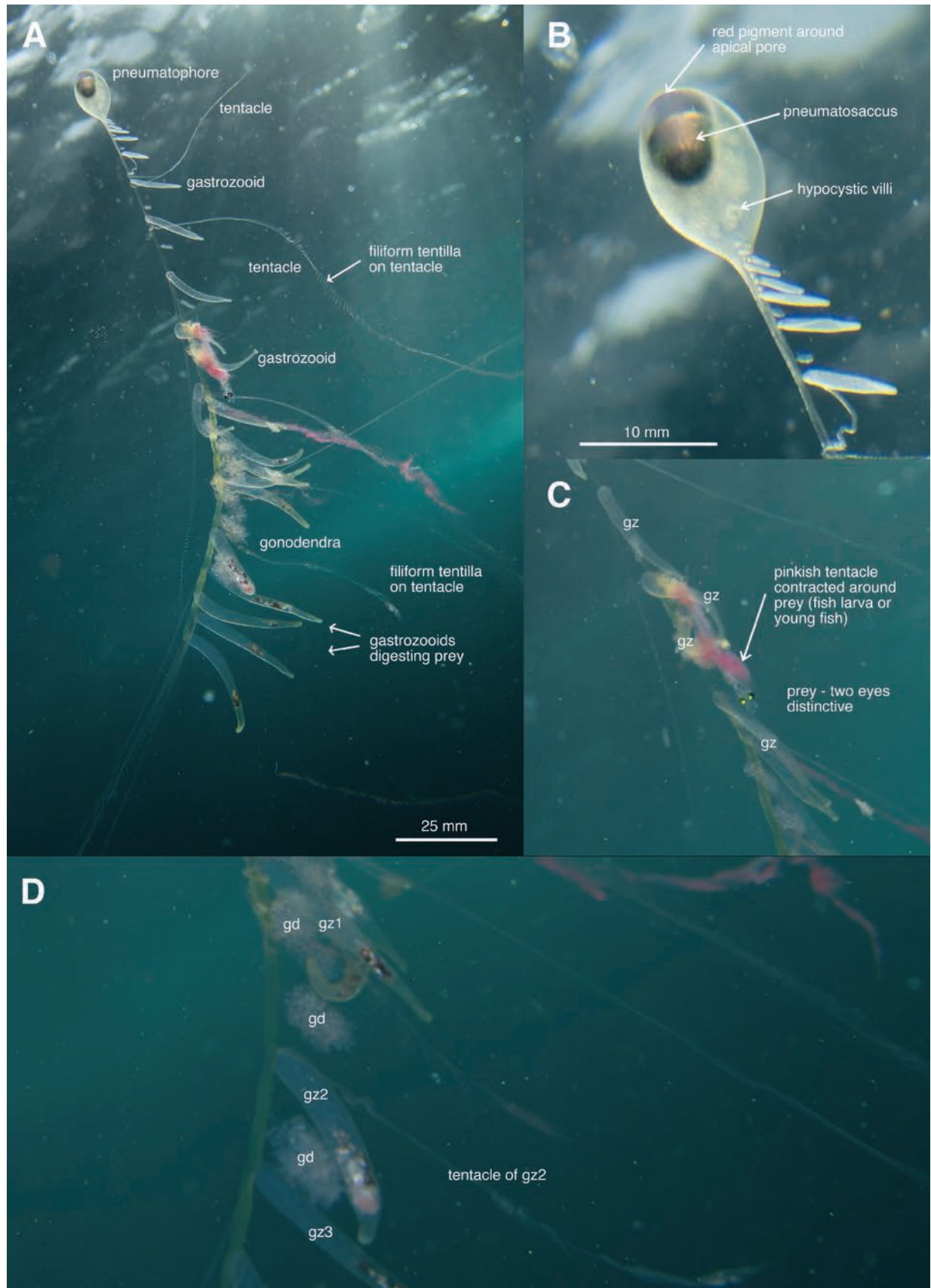


Figure 1. *Rhizophysa eyenhardtii* in shallow waters of False Bay, South Africa **A** whole colony **B** components of the pneumatophore **C** detail showing prey in contracted tentacle **D** detail showing three gonodendra (gz1–3) and nearby gastrozooids (gz – gastrozoid, gd – gonodendron). Pictures Jannes Landschoff, Sea Change Project.

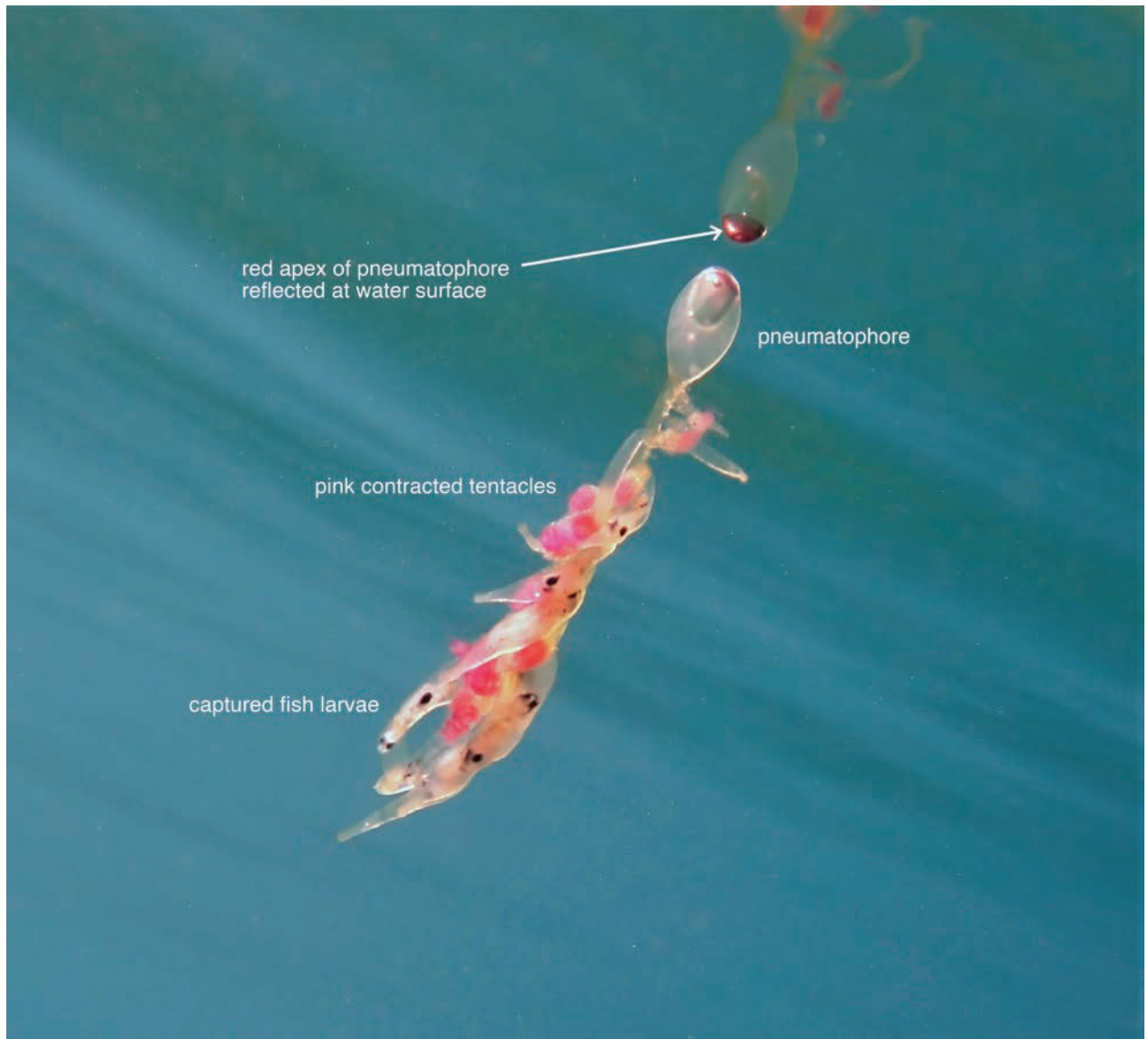


Figure 2. *R. eysenhardtii* smaller specimen near water surface with several captured fish larvae. Picture Catherine Corder.

The pneumatophore of rhizophysids is relatively larger than that of physonect siphonophores and, in the present specimens, a prominent gas bladder or pneumatosaccus, is identifiable, surrounded by a hypocystic cavity confluent with the gastrovascular cavity of the stem. Hypocystic villi arise from the base of the pneumatosaccus and contain gas-producing cells which secrete carbon monoxide into the gas bladder. The latter is lined with a layer of chitin which prevents the gas escaping, except via an apical pore that is controlled by a sphincter muscle (Pugh 2019). A good figure of a section through a rhizophysid pneumatophore is given by Chun (1897) for *R. filiformis* and the pneumatophore of a small specimen of *R. eysenhardtii* is well illustrated by Pagès and Gili (1992, fig. 2). Pugh (2019) notes that the pneumatophore of *R. eysenhardtii* tends to be larger than that of *R. filiformis* and the number and size of the hypocystic villi increase with age. Pneumatophores of the *Rhizophysa* specimens described by Totton (1965) were 12 mm in length for *R. filiformis* and < 18 mm long for *R. eysenhardtii* and the estimate of the pneumatophore of the present specimens falls within this range.

Furthermore, the colouring of the specimens in this study agrees with that described by Kawamura (1910) and Pugh (2019) for this species. Notable is the red circle of pigment surrounding the apical pore of the pneumatophore (Pugh 2019) and this shows particularly well in the smaller colony of specimen 1 (Fig. 2). The pink tentacles are characteristic of *R. eysenhardtii* (Pugh 2019, p. 75) and are well displayed in both present colonies (Figs 1A, C, 2). In contrast, the tentacles of *R. filiformis* are, in general, greenish (Pugh 2019).

A single gonodendron occurs between two gastrozooids in the larger specimen and gonodendra increase considerably in size as they mature towards the posterior end of the specimen, although none is evident in the last three cormidia of the present large specimen (Fig. 1). Pugh (2019) comments that in some specimens there may be two gonodendra per cormidium, but this was not found in the present larger specimens. Perhaps they are released once mature, as has been described for *Bathypphysa sibogae* by Dunn and Wagner (2006).

Rhizophysa eysenhardtii has been shown by Purcell (1981a, b, 1985) to feed almost exclusively on fish larvae. Our observations confirmed that a main source of prey are fish larvae, although one colony had also captured a chaetognath with one of its tentacles. We counted the ingested fish larvae by visual inspection of single to multiple images per colony for the presence of pairs of eyes in the gastrozooids. With this method, we would miss any other ingested prey, such as arrow worms (chaetognaths) that do not have prominent large eyes. Haddock and Dunn (2015) have found that prey of *R. eysenhardtii* is attracted to the colony by a strip of green fluorescence along the length of each gastrozoid, as well shown in their fig. 6B. Such prey attraction is also well demonstrated in fluorescent lures on the tentilla of all five species of the physonect genus *Erenna*, whose diet also comprises exclusively fish (Pugh and Haddock 2016). This finding, therefore, is added evidence for the use of fluorescent lures to attract fish prey in some siphonophores.

Northern and southern limits for published records of *Rhizophysa eysenhardtii* in the three oceans range from Bermuda (32°19'59"N) in the North Atlantic (Fewkes 1883) to previously 'slightly SW of Hondeklip Bay' (31°01'S), South Africa (Pagès and Gili 1992). This record is now extended to False Bay, South Africa. In the Pacific, the species ranges from 35°07'N off Misaki, Japan (Kawamura 1910, 1954) to 23°06'S Mejillones Bay, Chile (Palma and Apablaza 2004) and in the Indian Ocean from 18°N to 32°S (Daniel 1985, maps 3-4). These illustrate that *R. eysenhardtii* has a relatively warm water distribution, but there are no records of this species from the Mediterranean. In contrast, *R. filiformis* has been recorded in both warm and temperate regions (Pagès and Gili 1992) and recently also from the Mediterranean (Pastor-Prieto et al. 2024). From worldwide records, it does appear that *R. eysenhardtii* can be found at a range of depths, from shallow waters at or near the surface (Daniel and Daniel 1963; Purcell 1981a, b; Pagès and Gili 1991; Palma and Apablaza 2004; Dunn et al. 2005; Dunn and Wagner 2006) to deep water from 1901 m, 1886 m and 701 m (Lens and van Riemsdijk 1908).

The *Rhizophysa eysenhardtii* specimens from False Bay presented in this study are the first records of this species in the Bay. This is a considerable range extension record and about 450 km further south than the only previously reported distribution of *Rhizophysa eysenhardtii* southwest of Hondeklip Bay on the west coast of South Africa. As discussed by Mapstone et al. (2022) for the prajid siphonophore *Lilyopsis*, it seems likely that *Rhizophysa eysenhardtii* may have

arrived in False Bay via the variability of the Agulhas Current at Cape Hangklip during the winter and spring of 2022. Although its congeneric species *R. filiformis* has been sequenced by Munro et al (2018), so far *R. eyenhardtii* has not.

Acknowledgements

We would like to thank Catherine Corder for providing two additional photographic records. GMM expresses gratitude to Clare Valentine and The Natural History Museum, London, for their support in facilities and research encouragement. JL extends his deepest gratitude to the Seaforest for ongoing inspiration and to the team at the Sea Change Project for their support. Special thanks go to Pippa Ehrlich, who first noticed the colonies of *Rhizophysa* and brought them to JL's attention, sparking this research. JL would like to thank his funders and project collaborators from the Save Our Seas Foundation for their ongoing motivational support. We also thank Elena Guerrero and Mark Gibbons for their valuable reviews that helped improve the manuscript.

Additional information

Conflict of interest

The authors have declared that no competing interests exist.

Ethical statement

No ethical statement was reported.

Funding

This project was conducted with the support and as part of the Keystone Grant 542 - 1001 Seaforest Species - from the Save Our Seas Foundation.

Author contributions

JL provided the observational records. Both authors conceived the idea for the manuscript. GMM wrote the initial draft. JL provided the figures. Both authors edited the final versions.

Author ORCIDs

Gillian M. Mapstone  <https://orcid.org/0000-0001-5405-167X>

Jannes Landschoff  <https://orcid.org/0000-0001-9836-1530>

Data availability

All of the data that support the findings of this study are available in the main text.

References

- Biggs DC, Harbison GR (1976) The siphonophore *Bathypphysa sibogae* (Lens and van Riemsdijk 1908) in the Sargasso Sea, with notes on its natural history. *Bulletin of Marine Science* 24: 14–18.
- Chun C (1897) Die Siphonophoren der Plankton-Expedition. Band II. Ergebnisse der Plankton-Expedition der Humboldt-Stiftung. Lipsius and Tischer, Kiel and Leipzig, Germany, 126 pp.

- Daniel R (1985) The fauna of India and the adjacent countries. Coelenterata: Hydrozoa, Siphonophora. Zoological Survey of India Publication, Calcutta, India, 440 pp.
- Daniel R, Daniel A (1963) On the siphonophores of the Bay of Bengal. 1. Madras coast. *Journal of the Marine Biological Association of India* 5(2): 185–220.
- Dunn CW, Wagner GP (2006) The evolution of colony-level development in the Siphonophora (Cnidaria: Hydrozoa). *Development Genes and Evolution* 216(12): 743–775. <https://doi.org/10.1007/s00427-006-0101-8>
- Dunn CW, Pugh PR, Haddock SHD (2005) Molecular phylogenetics of the Siphonophora (Cnidaria), with implications for the evolution of functional specialisation. *Systematic Biology* 54(6): 916–935. <https://doi.org/10.1080/10635150500354837>
- Fewkes JW (1883) Explorations of the surface fauna of the Gulf Stream, under the auspices of the United States Coast Survey. IV. On a few medusae from Bermuda. *Bulletin of the Museum of Comparative Zoölogy at Harvard College* 11: 79–90. <https://www.biodiversitylibrary.org/item/26401>
- Gegenbaur C (1853) Beiträge zur näheren Kenntniss der Schwimmpolypen (Siphonophoren). *Zeitschrift für Wissenschaftliche Zoologie* 5(2/3): 285–344.
- Haddock SHD, Dunn CD (2015) Fluorescent proteins function as a prey attractant: Experimental evidence from the hydromedusa *Olindias formosus* and other marine organisms. *Biology Open* 4(9): 1094–1104. <https://doi.org/10.1242/bio.012138>
- Kawamura T (1910) “Bozunira” and “Katsuwo no Eboshi” *Rhizophysa* and *Physalia*. *Zoological Magazine (Tokyo)* 22: 445–454. [Dobutsugaku zasshi]
- Kawamura T (1954) A report on Japanese siphonophores with special reference to new and rare species. *Journal of the Shiga Prefectural Junior College Series A* 2(4): 99–129.
- Lens AD, van Riemsdijk T (1908) The Siphonophora of the “Siboga” Expedition. *Siboga Expedition* 9: 1–130.
- Mapstone GM, Diosdado G, Guerrero E (2021) First shallow record of *Bathypphysa conifera* (Studer, 1878) (Siphonophora, Cystonectae), a live specimen in the Strait of Gibraltar. *Worldwide species distribution review. Mediterranean Marine Science* 22(1): 51–58. <https://doi.org/10.12681/mms.23575>
- Mapstone GM, Foster CN, Gibbons MJ (2022) First occurrence of the rare siphonophore *Lilyopsis* Chun, 1885 (Hydrozoa, Siphonophora, Prayinae) in South Africa. *African Invertebrates* 63(2): 121–130. <https://doi.org/10.3897/afrinvertebr.63.94095>
- Munro C, Siebert S, Zapata F, Howison M, Serrano AD, Church SH, Goetz FE, Pugh PR, Haddock SHD, Dunn CW (2018) Improved phylogenetic resolution within Siphonophora (Cnidaria) with implications for trait evolution. *Molecular Phylogenetics and Evolution* 127: 823–833. <https://doi.org/10.1016/j.ympev.2018.06.030>
- Pagès F, Gili J-M (1991) Vertical distribution of epipelagic siphonophores at the confluence between Benguela waters and the Angola Current over 48 hours. *Hydrobiologia* 216/217: 355–362. <https://doi.org/10.1007/BF00026486>
- Pagès F, Gili J-M (1992) Siphonophores (Cnidaria, Hydrozoa) of the Benguela Current (southeastern Atlantic). *Scientia Marina* 56(Supplement 1): 65–112.
- Palma GS, Apablaza P (2004) Abundancia estacional y distribución vertical del zooplancton gelatinoso carnívoro en una área de surgencia en el norte del Sistema de la Corriente de Humboldt. *Investigaciones Marinas* 32(1): 49–70. <https://doi.org/10.4067/S0717-71782004000100005>
- Pastor-Prieto M, Raya V, Sabatés A, Guerrero E, Mir-Arguimbau J, Gili J-P (2024) Assemblages of planktonic cnidarians in winter and their relationship to environmental conditions in the NW Mediterranean Sea. *Journal of Marine Systems* 245: 103987. <https://doi.org/10.1016/j.jmarsys.2024.103987>

- Pugh PR (2019) A history of the sub-order Cystonectae (Hydrozoa: Siphonophorae). *Zootaxa* 4669: 001–091. <https://doi.org/10.11646/zootaxa.4669.1.1>
- Pugh PR, Haddock SHD (2016) A description of two new species of the genus *Erenna* (Siphonophora: Physonectae: Erennidae), with notes on recently collected specimens of other *Erenna* species. *Zootaxa* 4189(3): 401–446. <https://doi.org/10.11646/zootaxa.4189.3.1>
- Purcell JE (1981a) Feeding ecology of *Rhizophysa eysenhardti*, a siphonophore predator of fish larvae. *Limnology and Oceanography* 26(3): 424–432. <https://doi.org/10.4319/lo.1981.26.3.0424>
- Purcell JE (1981b) Dietary composition and diel feeding patterns of epipelagic siphonophores. *Marine Biology* 65(1): 83–90. <https://doi.org/10.1007/BF00397071>
- Purcell JE (1985) Predation on fish eggs and larvae by pelagic cnidarians and ctenophores. *Bulletin of Marine Science* 37(2): 739–755.
- Totton AK (1965) A Synopsis of the Siphonophora. British Museum (Natural History), London, 232 pp.

Completing the web: identifying sampling bias and knowledge gaps within South African spider surveys (Arachnida, Araneae)

Aileen C. van der Mescht¹, Charles R. Haddad¹, Stefan H. Foord^{2†}, Ansie S. Dippenaar-Schoeman²

¹ University of the Free State, Bloemfontein, South Africa

² University of Venda, Thohoyandou, South Africa

Corresponding author: Aileen C. van der Mescht (aileenvandermescht@gmail.com)



This article is part of:

Gedenkschrift for Prof. Stefan H. Foord

Edited by Galina Azarkina, Ansie Dippenaar-Schoeman, Charles Haddad, Robin Lyle, John Midgley, Caswell Munyai

Academic editor: John Midgley

Received: 9 October 2024

Accepted: 19 November 2024

Published: 18 December 2024

ZooBank: <https://zoobank.org/9EB46EAD-718C-493C-A4D9-8FB713112730>

Citation: van der Mescht AC, Haddad CR, Foord SH, Dippenaar-Schoeman AS (2024) Completing the web: identifying sampling bias and knowledge gaps within South African spider surveys (Arachnida, Araneae). *African Invertebrates* 65(2): 223–246. <https://doi.org/10.3897/AfrInvertebr.65.138881>

Copyright: © Aileen C. van der Mescht et al. This is an open access article distributed under terms of the Creative Commons Attribution License (Attribution 4.0 International – CC BY 4.0).

Abstract

Species distribution datasets are fundamental for macroecological studies, although there is an overarching need to ensure that these datasets are representative of the entire community. Shortfalls, or knowledge gaps, within biodiversity datasets originate for a range of reasons, and can lead to incorrect conclusions or recommendations being drawn. Spatial scale influences the interpretations of diversity patterns and thus is an important aspect to consider. South Africa has a rich history of spider sampling and as such, it is possible to investigate the influence that scale, both spatial and taxonomic, has on the overall interpretations of how complete the spider knowledge base is in the country. To do this, we draw on curated natural history spider collections and determine how complete the spider assemblages are across twelve unique combinations of taxonomic and spatial scales. Overall, we received 121 605 usable records from seven collections, with spider records and diversity, being concentrated along the eastern and coastal regions of South Africa. We show that assemblage completeness increases with both increasing taxonomic and spatial scales, and as such, knowledge of the distribution of spider families at the biome level is largely complete. Moreover, we show that our fine-scale knowledge of spider assemblages in South Africa is relatively poor, yet we do identify, even at fine scales, assemblages in South Africa that can be considered complete. We identify under-sampled regions of the country, which in turn are congruent with the distribution of under-sampled regions found in other South African invertebrate groups. We show that the scaling of completeness can only be interpreted in one direction: as scale increases so does completeness. These findings will have important implications for spider research and conservation in South Africa, given that regions where completeness is highest correspond strongly to areas in South Africa with the highest threats to biodiversity.

Key words: Museum records, spatial scale, species accumulation, taxonomic scale

Introduction

Species distribution datasets form the fundamental building blocks for many macroecological studies (Wüest et al. 2020; Cornford et al. 2021). Primary data sourced from natural history collections provide extremely valuable biodiversity information (Robertson et al. 2010; Scoble 2010), with much of the information

† Deceased.

regarding South Africa's biodiversity being provided by the country's natural history collections (Drinkrow et al. 1994; Hamer 2012). Beyond natural history collections, data can be sourced from published taxonomic descriptions and checklists, to citizen science databases such as iNaturalist (Dippenaar-Schoeman et al. 2012; Callaghan et al. 2020; Wolf et al. 2022; Garretson et al. 2023). Although the quality and reliability of curated versus untrained citizen science data can be debated (Aceves-Bueno et al. 2017; Jacobs and Zipf 2017; Fraisl et al. 2022), there is an overarching need to ensure that all datasets used in macroecological studies are a representative whole of the community (Qian 2020; Kusumoto et al. 2023; Alves-Martins et al. 2024). Sampling bias impacting species to geographic regions of interest will result in inherent biases within databases (Dippenaar-Schoeman et al. 2012), and thus unbiased interpretations based on these data are impossible (Yang et al. 2013).

Within large biodiversity datasets, various shortfalls regarding the completeness of these databases exist (Hortal et al. 2015). Inevitably named after prominent taxonomists or ecologists, the main shortfalls encountered in many datasets impact a range of biodiversity aspects. Arguably, the two most apparent shortfalls are firstly the Linnean, where most of the species on earth are neither described nor catalogued, and secondly, the Wallacean shortfall, which refers to the fact that the geographic and temporal distribution of many species is incomplete (Hortal et al. 2015). Wallacean shortfalls have been identified in many datasets (Mora et al. 2008; Yang et al. 2013; Troia and McManamy 2016). In many cases, though, incomplete datasets for a region are because of a combination of both Wallacean and Linnean shortfalls, with knowledge gaps representing both the lack of distributional knowledge of a species, as well as the presence of undescribed species at the site (Oliveira et al. 2016).

These knowledge gaps and biodiversity shortfalls can result from a plethora of reasons (Whittaker et al. 2005; Foord et al. 2011a, 2011b; Hortal et al. 2015; Oliveira et al. 2016; Ramírez et al. 2022; Vergara-Asenjo et al. 2023). Beyond the obvious constraints regarding the time taken to collect, store, sort and identify samples (Cardoso et al. 2011; Foord et al. 2013; Janion-Scheepers et al. 2016; Wilkinson et al. 2021), the idiosyncrasies and personal preferences of "unbiased" collectors can result in geographical bias within databases. This occurs either when research or collections are undertaken at preferential sites, such as nature reserves and scenic areas (Sánchez-Fernández et al. 2022), or close to access routes, or when higher rates of sampling occur in regions expected to be more diverse (Oliveira et al. 2016), such as the global biodiversity hotspots (Myers et al. 2000). Furthermore, in many cases sampling locations are highly correlated to the locations of research institutes and universities (Oliveira et al. 2016; Sánchez-Fernández et al. 2022). As such, species richness estimators and species accumulation curves are traditionally used to identify regions where sampling is complete (Chao and Jost 2012; Chao et al. 2020).

Diversity patterns, and the interpretations thereof, are highly influenced by scale (Whittaker et al. 2005; Foord et al. 2008), with challenges arising when attempting to extrapolate from one scale to another (Teng et al. 2020). Alpha diversity (α) describes diversity at a local scale, whereas beta (β) and gamma (γ) diversity describe the turnover of diversity between sites, and thus both describe diversity across larger scales (Burley et al. 2016; Foord and Dippenaar-Schoeman

2016). At a local scale, species responses to the landscape can be modulated either by local factors, such as the presence of suitable habitats leading to habitat filtration of species (Pärtel et al. 2016), or by biogeographical factors that occur across larger spatial scales (Banks-Leite et al. 2022). Thus, the interpretation of local and regional patterns of biodiversity may vary considerably depending on the scale at which patterns are observed (Pärtel et al. 2016; Banks-Leite et al. 2022), with variable functional relationships existing between ecological variables at different scales (Teng et al. 2020).

Variation in environmental drivers at local sites (Pärtel et al. 2016) and differing responses of species across different regions and biomes (Foord et al. 2011b; Haddad et al. 2013; Banks-Leite et al. 2022) leads to complex and varied interactions between factors at local and regional scales. For example, local α -diversity can be the result of local responses to habitat availability and filtration (Pärtel et al. 2016), yet this α -diversity is also dependent of the regional pool of species (β - and γ -diversity), yet the degree of specialisation and diversity (or lack thereof) of species at a local site can also be as a result of interactions of various spatiotemporal factors, species dispersal abilities or even geographical barriers (Burley et al. 2016).

Scale is essential to consider when investigating the distribution of diversity, be it local or regional, as differing mechanisms may emerge as drivers of species distributions (Gómez-Rodríguez and Baselga 2018; Martín-Devasa et al. 2024). Considering spiders in particular, local richness and composition are positively driven by local ecological factors such as habitat heterogeneity (Clough et al. 2005; Jiménez-Valverde and Lobo 2007; De Mas et al. 2009; Haddad et al. 2019), site context and local landscape configuration (Clough et al. 2005) and vegetation complexity (Clough et al. 2005). Furthermore, habitat (between plant types) and microhabitat (within the same plant type) have been shown to variably impact the colonisation and specialisation (phylogenetic variation) of the associated spider communities. When considering the habitat level, spider size and shape are filtered, whereas spider evolutionary adaptations as well as size and shape are selected on at the microhabitat level (Gonçalves-Souza et al. 2014; Wilson et al. 2023).

When model performance is considered, explained variation, as well as the environmental variables identified, will vary across different local scales. Thus, a larger scale model may suggest an ecological variable of importance, that when applied to local conservation or management protocols may in fact be less appropriate and less effective at managing and protecting spider communities. For example, at a local scale spanning 230 × 230 m (the model with the highest explained variance) and all other smaller scales considered up to this point, the rock terrain, percentage sclerophyllous vegetation and the standard deviation of NDVI best predicted spider species richness (De Mas et al. 2009). Yet, at larger scales, the variation explained by the models decreased, as well as the number of significant explanatory variables, until only percentage sclerophyllous vegetation explained half the variance of the best model (De Mas et al. 2009). Furthermore, species-specific responses vary across different local scales (Schmidt et al. 2008).

The extrapolation of the local scale models attempting to predict the distribution of spider diversity to larger scales fail largely due to the lack of structural environmental variable(s) for the area (Jiménez-Valverde and

Lobo 2007; De Mas et al. 2009; Joseph et al. 2018). At a continental scale, spider assemblages across Europe are shaped by the dispersal limitation of individual species. Yet, when southern and northern Europe are considered as individual units (sub-continental scale), dispersal limitation is the principle shaping force of spider assemblages in southern Europe, while no causal force can be isolated for northern European spider assemblages (Martín-Devasa et al. 2024).

The history of spider sampling in South Africa spans over 300 years, with the first two spiders to be described in South Africa in the 1700's. From then on, the number of described species rapidly increased up until the early 1900's, with peak rates of descriptions up until the 1920's. This was followed by a relative slowing in the rate at which species were described until 1997 (Dippenaar-Schoeman et al. 2023). In 1997, the South African National Survey of Arachnida (SANSA) was initiated to determine the extent of the South African Arachnida biodiversity, as well as identify gaps in the geographic distribution of species (Dippenaar-Schoeman et al. 2015). Since then, the rate of species descriptions has increased remarkably (Dippenaar-Schoeman et al. 2023). The First Atlas of South African Spiders was published in 2010 (Dippenaar-Schoeman et al. 2010), which provided maps for 2010 species of spiders from 71 families. This geographical data was essential in preparing the first Red List of the South African spiders (Foord et al. 2020), as well as a National Spider Checklist of 2265 spider species (Dippenaar-Schoeman et al. 2023), an increase of 255 species from 2010. The checklist breaks down the distribution of species richness and number of records per province in South Africa (Dippenaar-Schoeman et al. 2023), with ascensions functioning as a proxy for sampling effort. Given that this latest checklist makes a start at describing knowledge gaps, and sampling bias within the spider distributions in South Africa, quantification of these gaps through empirical means is the logical next step.

Thus, this study aims to quantify sample completeness within the South African spider assemblages. To achieve this, our first objective is to compile as comprehensive a database as possible using curated data from various sources. Secondly, we determine how completeness of the spider database varies in accordance to both spatial and taxonomic scales. We quantify completeness by comparing estimated species richness to observed species richness across the scales, accounting for the number of specimen records. We vary spatial scale by using both arbitrarily defined geographical boundaries (quarter and degree grid cells), as well as ecological boundaries (bioregion and biome) to do this. Taxonomic scale is varied across species, genus, and family level. We hypothesise that at both finer spatial and taxonomic levels, completeness within the database will be relatively low given how diverse spiders are known to be. However, as the scales become coarser, we hypothesise that the completeness will increase as sampling effort per taxonomic/geographic region increases, effectively reducing the accumulation of diversity as the sample size increases. Beyond identifying areas to target for further sampling, this study forms the basis upon which further macroecological spider studies in South Africa can be built by identifying bias and possible shortfalls within the already existing data, thus ensuring that these shortfalls can be addressed and bias reduced in any other study going forward.

Methods

Data collection

The majority of spider specimen records for South Africa ($n = 73\,649$) used for this study were sourced from the National Collection of Arachnida (NCA) at the Agricultural Research Council in Pretoria. We did not include any records from partial enclave of eSwatini. We received spider specimen accession records from local and international collections, namely the Albany Museum, Grahamstown ($n = 1\,77$); National Museum, Bloemfontein ($n = 16\,061$); KwaZulu-Natal Museum, Pietermaritzburg ($n = 10\,517$); Iziko South African Museum, Cape Town ($n = 9\,763$); Ditsong National Museum of Natural History, Pretoria ($n = 5\,837$) and Royal Museum of Central Africa, Tervuren, Belgium ($n = 4\,001$). Only specimen records where the spiders were identified to either species, genus or family level were retained. Subspecies identifications were absorbed into the species level identification.

To ensure that species names across all data sources were accurate and valid, and to prevent duplication where individual samples may have been identified with old nomenclature, all species names were validated against the Spider Checklist of South Africa (Dippenaar-Schoeman et al. 2023). Where species names did not match with the checklist, CH validated each name, correcting for nomenclatural changes as well as spelling mistakes using the World Spider Catalog (2024).

A fundamental requirement of the data is that each spider record needed to be georeferenced with complete coordinates. Thus, the number of records received across all data sources was always greater than the number of records that we retained. All samples were plotted in QGIS (QGIS Development Team 2020), and sites where the coordinates did not match the provided location information were identified. Where possible, these coordinates were corrected, either by swapping the x and y coordinate or where location information was specific enough, coordinates for the location were used. Otherwise, incorrectly georeferenced sample records were excluded from the final database. The final spider sample database was saved as a shapefile. It must be noted that older specimens and records often have rudimentary descriptions attached or lack detailed morphological descriptions or collecting data (e.g. described from South Africa, Transvaal or Cape), so could not be included. Furthermore, some species remain known from the original descriptions only and have never been resampled and definitively identified, and as their type material resides in international collections not included in this study, such species were also omitted.

The SANSA database used in the production of the national checklist include all the NCA records as well as all published species records from local and international collections from the taxonomic literature. Considering the issues discussed above, the restricted number of collection databases used in our study, and the exclusion of published records not in the seven institutional databases were used, our final database contains approximately 180 fewer species than were recorded from South Africa by Dippenaar-Schoeman et al. (2023).

Mapping

South Africa was divided at four different spatial scales ranging from fine to coarse, namely 1) quarter degree and 2) degree grid cells, and then at the 3) bioregion and 4) biome levels. QGIS was used to create the two grid cell levels,

South Africa was divided first by a grid measuring $0.25^\circ \times 0.25^\circ$ (approximately 24 km longitudinally \times 27 km latitudinally), thus dividing the country into 1995 quarter degree grid cells (QDGC), using the WGS84 projection for South Africa. Each cell was named according to convention. This procedure was repeated a second time, where grids measuring $1^\circ \times 1^\circ$ (approximately 97 km longitudinally \times 110 km latitudinally) divided the country into 151 degree grid cells (DGC). Here, each cell was named according to the latitude and longitude comprising the intersection of the top left corner of each cell.

Bioregion and biome levels were extracted from the vegetation map of South Africa (South African National Biodiversity Institute 2006), with bioregion being a finer scale than biome (Rutherford et al. 2005). The spider sample shapefile was then overlaid on the two grid cell layers, as well as the vegetation map in R (R Core Team 2020). To determine in which QDGC, DGC, bioregion and biome individual spider samples occurred, the *st_join* function in the *sf* package (Pebesma 2018) was used. All further analyses were conducted on the resultant spider database containing both the taxonomic information relating to each spider sample, as well as spatial information relating its location.

Statistical analysis

Sample completeness was determined at three taxonomic levels, namely species-, genus- and family-level identifications. Four spatial scales were used to delimit spider communities, two arbitrary (QDGC and DGC grids) and two ecological (bioregion and biome). Thus, there were 12 unique combinations between taxonomic and spatial levels across which sample completeness was determined. As such, the spider database was first split by spatial level, and input matrices were then generated where individual spider samples were rows and either species, genus or family names were columns, depending on the spatial-taxonomic combination being assessed.

Biodiversity sample completeness of a site or region is often estimated using a rarefied species accumulation curve and determining whether the curve reaches an asymptote (Chao et al. 2014). The issue here is that in many cases an eyeball measure of completeness is then employed to state that the asymptote has been reached or that the sample completeness is approaching the asymptote without directly determining the asymptotic value, or how far the curve is away from the asymptote. With an asymptotic value, which functions as an estimate of the expected species richness of a sample (S_{est}), as well as observed species richness value (S_{obs}), it is possible to determine the percentage completeness of a sample such that:

$$Percentage\ completeness = \frac{S_{obs}}{S_{est}} \times 100$$

To calculate the percentage completeness, we used the function *iNEXT* in the package *iNEXT* (Chao et al. 2014; Hsieh et al. 2020) to calculate the asymptotic values for each spatial-taxonomic scale combination. Incidence-based frequencies of each species at a spatial scale were used. We then calculated the percentage completeness for each unit based on these first-order species richness estimators. In addition to percentage completeness, we then calculated the number of accession records per spatial-taxonomic combination. As the accuracy of

extrapolation methods on small sample sizes is often inaccurate and can result in a high occurrence of false positives, the number of accession records allowed us to filter these false positives out. In addition, we also calculated the completeness of the species, genus and family records of South Africa as a whole.

We defined four threshold levels of total sampling completeness based on cut-off values for the percentage completeness and number of accession records per unit. Under-sampled regions had a percentage completeness < 0.6 and < 10 accession records. Moderately well-sampled regions had a percentage ≥ 0.6 but ≤ 0.75 and ≥ 10 accession records. Relatively well-sampled regions had a percentage completeness of ≥ 0.76 but ≤ 0.9 and ≥ 25 accession records. Finally, well-sampled regions had a percentage completeness of ≥ 0.91 and ≥ 50 accession records. Accession record cut-off values were based on Troia and McManamay (2016) who used these values as cutoffs for a range of groups such as amphibians, plants, insect and fishes. The percentage completeness cut-off values were based on Sánchez-Fernández et al. (2022). Yang et al. (2013) calculated the slope of the accumulation curve based on the last 10% of the data to determine how complete a sample is, with Troia and McManamay (2016) doing the same and then adding a third threshold class based on slope values, with the assumption that a slope closer to 0 is almost at its asymptote. However, as this method relies on fitting a linear function to a non-linear curve – a somewhat mathematically dubious approach – we chose to use percentage completeness and the number of accession records only.

To quantify changes in sample completeness across increasing taxonomic levels (species $<$ genus $<$ family), we used an ordinal regression approach with the calculated sample completeness (described above) as the response variables in the models. We modelled each spatial scale separately, as the spatial boundaries of the QDGCs, DGCs, bioregions and biomes do not correspond. We used cumulative link mixed effect models (CLMMs), where we ranked sample completeness as under-sampled $<$ moderately well-sampled $<$ relatively well-sampled $<$ well-sampled. Taxonomic level and grid cell identity were used as the categorical fixed effect term and random effect of the model, respectively, as there were three repeated measures of sample completeness for each modelled spatial scale. For the QDGC and DGC models, two iterations were run, one excluding and one including all grid cells that contained no data as the lowest level of completeness (no data $<$ under-sampled $<$ moderately well-sampled $<$ relatively well-sampled $<$ well-sampled). This was done to ensure that interpretations were not biased by empty grid cells. Thus, in total, six individual models were run. All models were fitted with Laplace approximations using the *clmm* function in the *ordinal* (Christensen 2023) package in R. As ordinal models will make the first fixed effect the model intercept (in the first model repeat “species”), the model iterations were repeated with “genus” as the intercept term so that all three pair-wise model estimates were obtained (species–genus, genus–family and species–family), thus allowing us to compare the effect size changes in sample completeness as taxonomic level increases. Furthermore, these paired effect sizes can be contrasted across the different spatial scales, thus allowing us to indirectly determine changes in sample completeness as spatial scale increases (QDGC $<$ DGC $<$ bioregion $<$ biome).

It must be noted that with our procedure to quantify sample completeness there are multiple permutations that can result in the same outcome. An under-sampled

region may be the result of a region with few samples, even if the projected asymptote is reached (Fig. 1A), or as the result of a region with many samples, but whose asymptote is far from being reached (Fig. 1B). We do not try to differentiate between the sample or percentage completeness thresholds that are crossed, nor do we attribute different weights to these thresholds. These disparities between sample size and percentage completeness are larger at the lower sampling completeness levels, whereas at the higher sampling completeness levels, these disparities decrease, as well-sampled regions need to have many samples with an observed species richness within 10% of the estimated species richness (Fig. 1G).

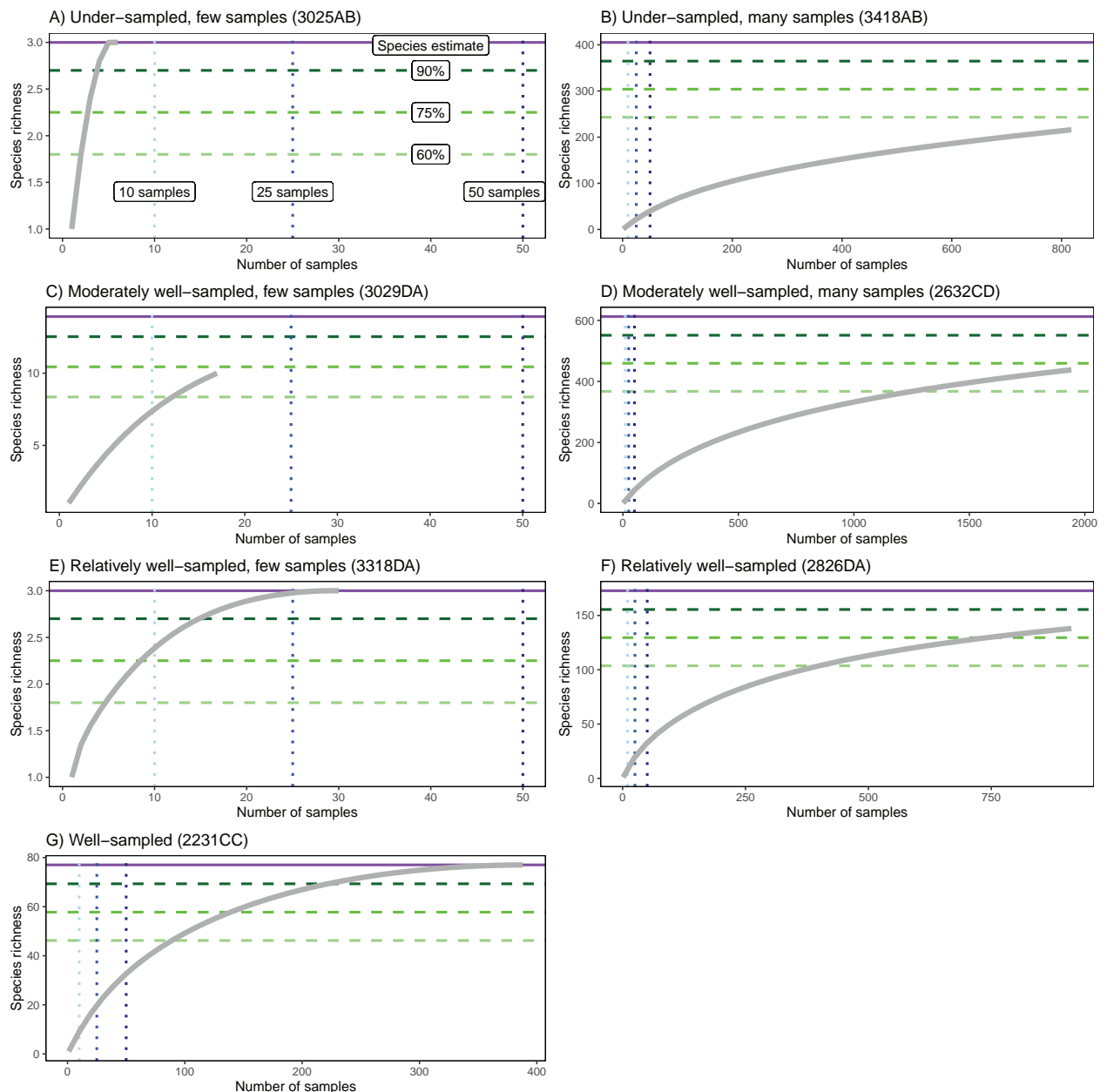


Figure 1. Example rarefaction curves (grey lines) for species level assemblages of select quarter degree grid cells. The horizontal purple line indicates the estimated species richness of the sample, while the dashed horizontal lines indicate the percentage completeness cut-off values, and the vertical dashed lines indicate the cut-off values for the accession numbers. For clarity, cut-off values are only annotated in plot A. Individual plots A–G show how different combinations of threshold values combine and result in under-sampled, moderately well-sampled, relatively well-sampled and well-sampled spatial units.

Results

Overall, 121 605 usable records were entered into our database (Table 1). Records identified to species level are the most predominant in the database, followed by genus- then family-level records (Table 1). When considering the completeness of our database, the species and genus records are relatively well-sampled, with 89.2% and 86.6% completeness percentage respectively, while the family records are well-sampled, with 100% completeness percentage calculated (Table 2).

The distribution of records across the country is somewhat uneven 41.3% of all QDGC in South Africa are lacking records, but this percentage decreases as the spatial scale increases, with only 5.3% of the DGCs lacking data, while neither the bioregions nor biomes are without spider records (Table 3). Spatially, records are distributed across the country, although there is an apparent concentration of records towards the eastern regions of South Africa, as well as along the coast from the eastern border with Mozambique, to north of Langebaan (Fig. 2). In the drier western regions of the country records are sparse, but where they do occur, they seemingly follow river courses. For example, the Orange River course is easily identifiable (Fig. 2). Consequently, spider diversity across species, genus and family level follows similar trends when considered

Table 1. Diversity summary of family, genus and species richness contained in each database, with total diversity counts shown in the last row. The last column indicates the number of records obtained from the individual databases.

| Source database | Family richness | Genus richness | Species richness | Number of records |
|--|-----------------|----------------|------------------|-------------------|
| National Collection of Arachnida | 72 | 557 | 1 718 | 73 649 |
| Albany Museum | 43 | 118 | 180 | 1 777 |
| National Museum | 65 | 404 | 643 | 16 061 |
| KwaZulu-Natal Museum | 66 | 342 | 680 | 10 517 |
| Royal Museum of Central Africa | 68 | 300 | 471 | 4 001 |
| Iziko South African Museum | 65 | 299 | 670 | 9 763 |
| Ditsong National Museum of Natural History | 66 | 256 | 266 | 5 837 |
| Overall database | 74 | 639 | 2087 | 121 605 |

Table 2. Sampling completeness of the South African spider fauna as a whole, the observed richness as well as estimated richness and standard error for each taxonomic level, as well as completeness percentages are shown.

| Taxonomic level | Number of records | Observed richness | Estimated richness | SE | Completeness percentage (%) | Level of sampling completeness |
|-----------------|-------------------|-------------------|--------------------|-------|-----------------------------|--------------------------------|
| Species | 63 007 | 2086 | 2338.5 | 37.94 | 89.20 | Relatively well |
| Genus | 98 905 | 638 | 739 | 31.5 | 86.6 | Relatively well |
| Family | 121 605 | 74 | 74 | 0.6 | 100 | Well |

Table 3. Number of units per spatial scale, with the total number of sampled and unsampled units shown. Values in brackets indicate percentage of the total number either sampled or not.

| Spatial scale | Total sampled | Not sampled | Total |
|--------------------------|---------------|-------------|-------|
| Quarter degree grid cell | 1172 (58.7) | 823 (41.3) | 1995 |
| Degree grid cell | 143 (94.7) | 8 (5.3) | 151 |
| Bioregion | 44 (100) | 0 | 44 |
| Biome | 11 (100) | 0 | 11 |

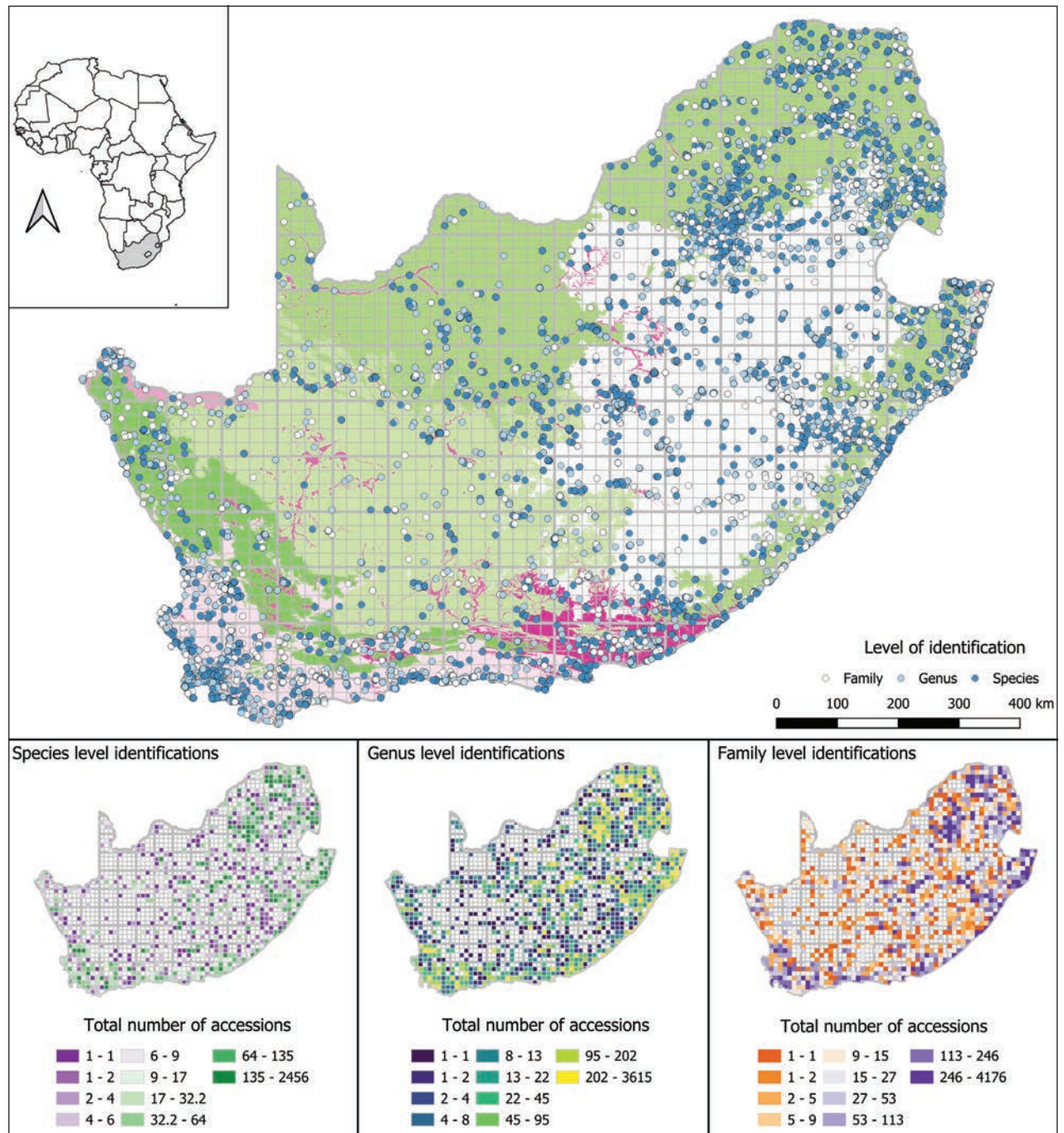


Figure 2. Distribution of the individual spider database records across South Africa. Colours indicate the lowest level individuals are identified to (family, genus or species level). For reference, the biomes are shown in green-pink fill. The map inserts show the total number of record accession in each Quarter Degree Grid Cell for records identified to family, genus and family levels.

across the four spatial levels (Fig. 3). Richness is highest in the eastern and coastal regions and lowest in the drier interior western regions of South Africa.

As we hypothesised, sample completeness scales up as both the spatial and taxonomic levels increase. Firstly, the most obvious of these completeness increases is when taxonomic scale is considered alone, at the same spatial scale (rows in Fig. 4). Here, the proportion of spatial units at higher completeness levels steadily increase as taxonomic level increases (Table 4, Fig. 4 rows). Secondly, as

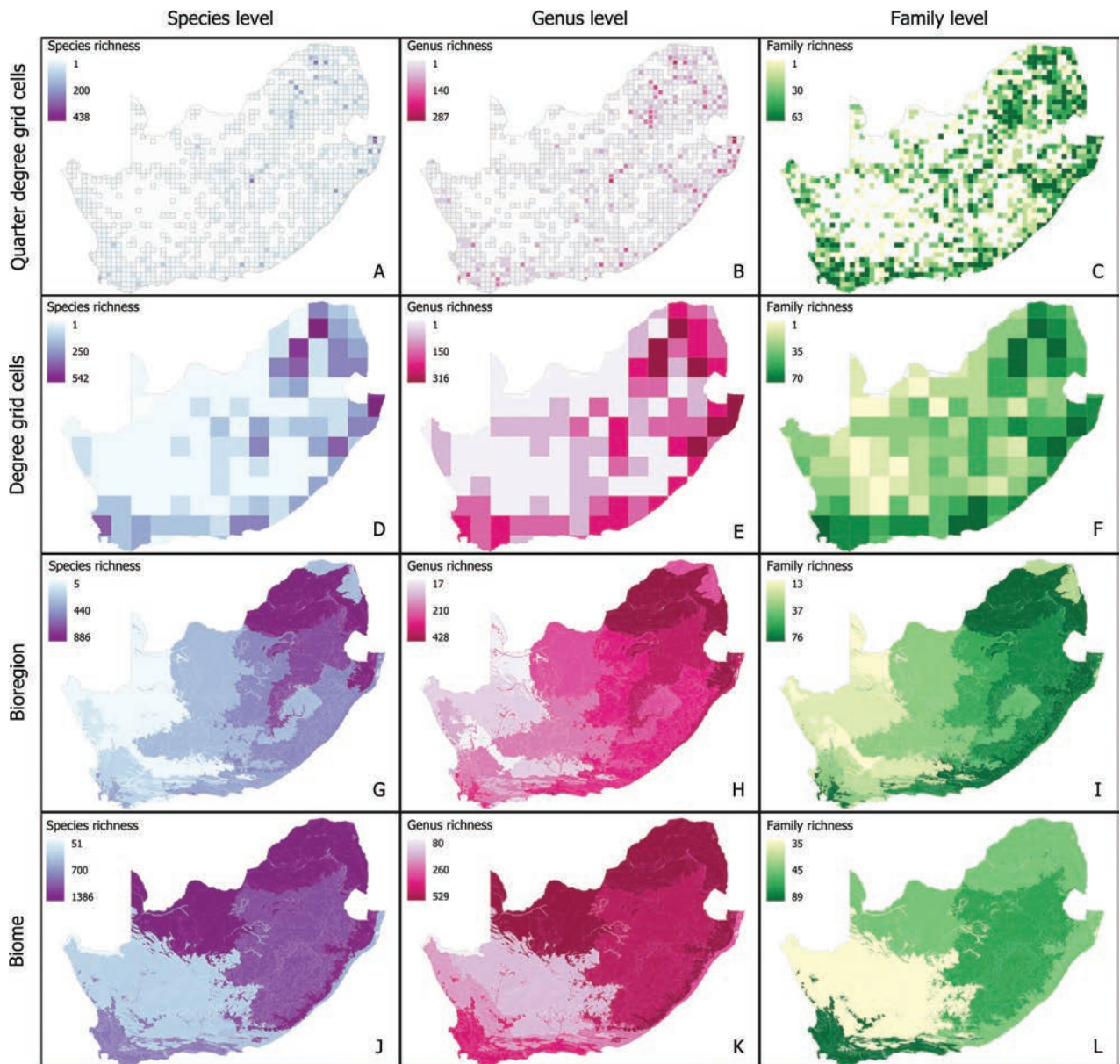


Figure 3. Distribution of spider diversity across the three taxonomic and four spatial levels considered. Darker colours indicate higher levels of diversity, with scales pertinent to each plot shown. Individual plots A–L show richness at all possible combinations of taxonomic and spatial scale.

spatial scale increases, but taxonomic scale remains constant (columns in Fig. 4), overall completeness increases. For example, spatial units that are well-sampled in terms of family level completeness increase from 3.7% to 33.77% to 47.72% to 63.64% when moving from the QDGC to biome level (Table 4, Fig. 4C, E, I, L). Although genus and species levels do not reach the well-sampled level at either the bioregion or biome scale, this pattern of increase holds true throughout the other levels of completeness (Table 4, Fig. 4). Finally, the combination of the increasing taxonomic and spatial scale results in the highest degree of sample completeness. At the lowest taxonomic and spatial scales, QDGC–species level, samples are the least complete, with only 0.15% of all QDGCs considered well-sampled and found in the northeastern and southern regions of the country (Table 4, Fig. 4A). As we hypothesized, sample completeness scales up as

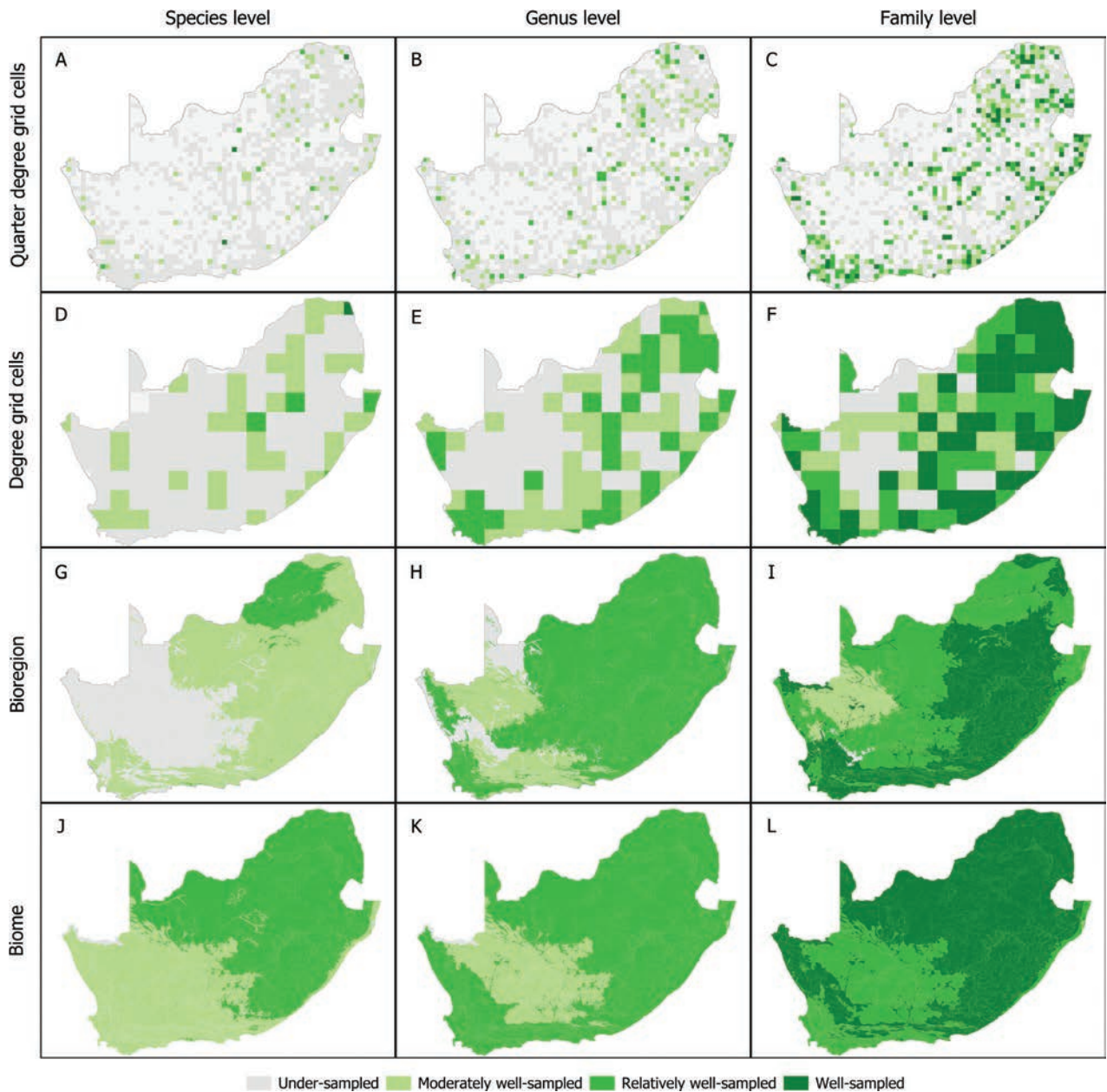


Figure 4. Changes in spider sampling completeness across both taxonomic level and spatial scale. Darker greens indicate a higher level of completeness per spatial unit. Individual plots **A–L** show sampling completeness at each combination of taxonomic and spatial scale.

both the spatial and taxonomic scales increase, such that at the highest scale combination, biome–family, sample completeness is the highest observed at 63.64% of all biomes being considered well-sampled (Table 4, Fig. 4L).

The CLMM results show that these positive changes in spider sample completeness are significant across all taxonomic and spatial levels (Table 5). The same patterns emerge both with and without the empty cells at the QDGC and DGC levels (Table 5, Fig. 4). When the magnitude and direction of the model estimates are plotted, it becomes evident that the level of spider sample completeness increases with spatial and taxonomic scale. When comparing the estimate size between genus to family (Fig. 5B) and species to family (Fig. 5C), there is a larger positive change in completeness than observed from species

Table 4. Distribution of well, relatively well, moderately well and under-sampled units across both the spatial and taxonomic scales considered. Numbers in brackets indicate the total percentage of units per criteria in relation to the total number of units in each spatial scale.

| Spatial scale | Taxonomic scale | Well- sampled | Relatively well-sampled | Moderately well-sampled | Under-sampled | No data |
|----------------------------------|-----------------|---------------|-------------------------|-------------------------|---------------|---------|
| Quarter degree grid cells | Species | 3 | 8 | 81 | 890 | 1 013 |
| | Genus | 3 | 44 | 167 | 894 | 887 |
| | Family | 73 | 176 | 206 | 717 | 823 |
| Degree grid cells | Species | 1 | 4 | 36 | 99 | 11 |
| | Genus | 0 | 37 | 46 | 60 | 8 |
| | Family | 51 | 39 | 24 | 29 | 8 |
| Bioregion | Species | 0 | 2 | 17 | 25 | |
| | Genus | 0 | 23 | 9 | 12 | - |
| | Family | 21 | 16 | 5 | 2 | |
| Biome | Species | 0 | 3 | 6 | 2 | |
| | Genus | 0 | 8 | 2 | 1 | - |
| | Family | 7 | 3 | 1 | 0 | |

Table 5. Cumulative linked mixed effect model results *Italics indicate significant comparisons. Rows with grey fill indicate models where empty cells were excluded.*

| Model iteration | n | Term comparison | Estimate | SE | z- value |
|---|------|------------------|----------|--------|----------|
| Quarter degree grid cells (empty cells excluded) | 3309 | Species – Genus | 1.73 | 0.19 | 9.35 |
| | | Genus – Family | 2.64 | 0.19 | 14.17 |
| | | Species – Family | 4.37 | 0.26 | 16.62 |
| Quarter degree grid cells (empty cells included) | 5985 | Species – Genus | 0.56 | 0.001 | 527.4 |
| | | Genus – Family | 1.65 | 0.0001 | 14 711 |
| | | Species – Family | 1.634 | 0.001 | 1632.7 |
| Degree grid cells (empty cells excluded) | 426 | Species – Genus | 2.57 | 0.34 | 7.5 |
| | | Genus – Family | 3.63 | 0.37 | 9.69 |
| | | Species – Family | 6.17 | 0.51 | 12.04 |
| Degree grid cells (empty cells included) | 453 | Species – Genus | 2.55 | 0.36 | 7.12 |
| | | Genus – Family | 3.7 | 0.39 | 9.48 |
| | | Species – Family | 6.25 | 0.57 | 10.9 |
| Bioregion | 132 | Species – Genus | 3.71 | 0.74 | 5 |
| | | Genus – Family | 4.79 | 0.86 | 5.56 |
| | | Species – Family | 8.51 | 1.33 | 6.4 |
| Biome | 33 | Species – Genus | 2.56 | 1.15 | 2.22 |
| | | Genus – Family | 4.6 | 1.59 | 2.9 |
| | | Species – Family | 7.18 | 2.09 | 3.44 |

to genus (Fig. 5A) at the QDGC and DGC levels. This, again, is what we hypothesised: the larger the difference in taxonomic scale, the larger the change in completeness. Furthermore, when comparing within taxonomic level combinations (Fig. 5A–C) individually, there is a positively larger change in completeness as spatial scale increases from QDGC to bioregion. At the biome level, this increase is not as apparent, but remains positive, which suggests that the chance of being considered at a higher level of sample completeness is still greater at these higher spatial scales.

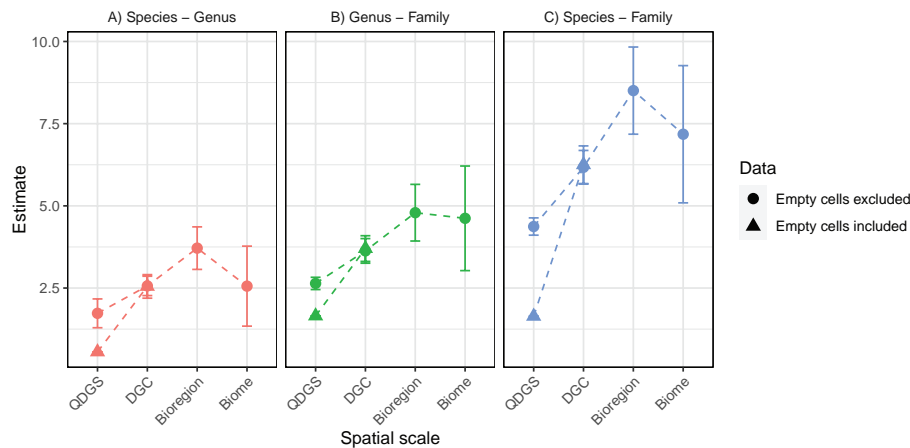


Figure 5. Cumulative linked mixed effect model estimates and standard errors shown for changes in spider sampling completeness as taxonomic level changes from **A** species to genus **B** genus to family and **C** species to family level. Within each panel, the direction and magnitude of the estimate change in spider sample completeness across spatial scale is shown. Model estimates for the quarter and degree grid cell levels with and without empty cells are also shown and indicated by the point shape.

Discussion

We show that, even for such an extensively studied taxon in South Africa, our fine-scale knowledge regarding spider assemblages in the country is relatively poor, and that extensive geographical bias exists within the database studied here. Although these biases exist, we have been able to identify regions within South Africa where spider assemblages can be considered complete, even at the finest scales considered. As scale becomes coarser, the overall completeness of the spider assemblages increases. Our demonstration that completeness of spider assemblages increases as both taxonomic and spatial scale increases is important, as it shows that the considerable amount of sampling that has been conducted on spiders in South Africa has been vital in determining a highly complete list of species. Interestingly, the estimated number of species within South Africa is 2338.5, which equates to 73 needing to be added for it to be considered complete based on the current rates of sampling and distribution of spider samples. However, based on the results of taxonomic revisions of Afrotropical spiders in recent decades (see World Spider Catalog 2024), particularly including South African taxa, many new species still await description, so this is itself a gross under-estimation of the country's spider diversity. This is exacerbated by the large parts of the country that remain unsampled.

Spider database

Spiders are mega-diverse in South Africa (Dippenaar-Schoeman et al. 2023), from which approximately 4% of the world's spiders have been recorded, with almost 59% of species considered country endemics (Dippenaar-Schoeman et al. 2023), although it is suggested that the lack of intensive sampling of spiders in neighbouring countries may artificially inflate the number of species considered as endemic (Foord et al. 2011a), which is a good example of a Wallacean shortfall within the database (Yang et al. 2013; Hortal et al. 2015). Although samples are incomplete in many areas, we have established a relatively com-

prehensive database of spatially referenced spider records from South Africa. There are fewer species represented here (2086) versus the 2265 species of the Checklist of Spiders (Dippenaar-Schoeman et al. 2023) given that these two studies draw from different data sources, differences in the total number of species can be expected. For example, the type material of the 187 spider species sampled by E. Simon between 1893 and 1910 are housed in overseas museums and were not included here. In addition to species-level records, our database contains records identified to genus or family level only, and as such, is representative of more spider genera than the Checklist (641 versus 495), this increase in numbers is due the new records being included after the publication of the checklist. The family diversity reported here represents 53% of the global family diversity of spiders (Foord et al. 2011a; World Spider Catalog 2024).

With regards to taxonomic accuracy, this database is likely the most accurate and relatively comprehensive, having combined the records of various curated natural history collections across the country. Nomenclature of the species level identification were verified so that species were not duplicated with old and new names following taxonomic transfers and synonymies. We do not include morphospecies identifications or pseudo-taxonomic records, and as such, diversity estimates are more likely to be a true reflection of the diversity at sites. Diversity estimates that are derived from morphospecies identifications are more likely to over- or under-estimate diversity, particularly in invertebrates, as most species-level identifications are based on obscure morphological features that are often overlooked when less trained individuals assign individual samples to morphospecies (Foord et al. 2013). In particular, the taxonomic resolution of the mega-diversity of spiders within South Africa is not available for other invertebrate taxa (Foord et al. 2011a).

Completeness

South Africa is a megadiverse country (Mittermeier et al. 2011; Colville et al. 2020), thus the finding of low levels of completeness in the spider assemblages is not surprising, nor is it a new hypothesis. Foord et al. (2011a) suggested that “South African spider systematics and ecology are in an exploratory phase” and further highlight biases in the distribution of records across the country. Our study further supports these findings, and in turn quantifies the completeness of the sampled spider communities. For example, 13 years ago Foord et al. (2011a) describe the Nama and Succulent Karoo as well as the Thicket biomes as poorly sampled in terms of species richness, while we in turn show that the two karoo biomes are moderately well-sampled and that the thicket is relatively well-sampled. This highlights the importance of maintaining up-to-date databases of species records, as well as the value of an integrated approach blending taxonomic and quantitative methodologies.

Abundance-based asymptotic estimators of species richness, such as Chao1 used here, are reliable estimators for species richness (Chao et al. 2014), with little variation in estimates when the sample grain size is reduced while maintaining area constant (Hortal et al. 2006). Even though we hold sample grain size constant across all scales by treating each spider record as a sample, the Chao1 estimate remains a feasible approach (Hortal et al. 2006; Chao and Jost 2012). At low sample sizes, Chao1 loses accuracy (Hortal et al. 2006), but with the inclusion

of the record thresholds here we avoid mis-classifying under-sampled regions as any higher class. Furthermore, it is well known that species richness correlates to sample size (Melo et al. 2003), yet this does not provide a species richness estimate, nor can it be used to calculate completeness of the spider assemblages.

Scale

Completeness of the spider assemblages is driven by scale. As taxonomic and geographic scale increase from fine to coarse scales, the overall completeness of the spider assemblages also increases. Considering that the increase in scale increases the size of the samples of each spatial unit, this is expected. What this highlights though, is that the larger scales absorb the sampling bias of the finer-scale samples. The western interior is a good example of this. At the finer scales, many QDGCs have no spider samples, but when looking at the completeness of the bioregions and biomes of this region, the spider assemblage is more often than not considered as moderately well-sampled. This does not mean that these determined completeness levels of the higher spatial and taxonomic scales are incorrect, but rather that completeness cannot be interpreted in the reverse direction. For example, the moderately well-sampled Nama Karoo is linked to the biome scale, but this completeness category cannot be applied to all the QDGC grid cells that fall within the region of the Nama Karoo, as many of these grid cells do not have any reported spider samples.

The difference between the estimated and observed species richness is the number of not yet sampled species (Chao et al. 2014). With regards to knowledge gaps, these “missing” species are not necessarily undescribed species (i.e. Linnean shortfall), but also species that are under-sampled and whose ranges are poorly understood (i.e. a Wallacean shortfall) (Bini et al. 2006; Hortal et al. 2015; Assis 2018; Diniz-Filho et al. 2023). Thus, as completeness of the spider knowledge base increases with spatial and taxonomic scales, the size of both the Linnean and Wallacean gaps incrementally decreases, such that at large spatial (biome) and taxonomic (family) scales, the number of families not yet sampled are all less than 40% of the estimated family diversity, with more biomes being represented by a unknown proportion of less than 25% (inverses of the threshold cutoff values).

It must be noted, though, that the estimates of richness depend on the input data and will constantly change as more and more samples are added (Chao and Jost 2012; Chao et al. 2020; Kusumoto et al. 2023). Standard errors are calculated for each richness estimate, and here we have used the mean estimate to determine the sample completeness. Thus, there is inherent variation in these estimates, and they are not a singular and perfect estimate of richness. This point is exemplified by the fact that our total species richness observed here is less than that of the Spider Checklist, yet our estimated species richness is greater than that of the Spider Checklist. Given that this study draws on a different set of data than that of the Spider Checklist, differences in observed as well as expected richness will vary, as each data source would contain a different cohort of species. However, the variation in estimates and richness should not detract from the fact that here we have shown explicitly how the knowledge gaps within the South African spiders vary across both spatial and taxonomic scales. Even though at larger scales, our understanding of spider

distributions and occurrences across the country is relatively incomplete given the sheer diversity of spiders in the country, the investment in sampling over the 300 years of spider research in the country has been hugely successful and cannot be overlooked. However, much still needs to be done to remedy the under-sampling in the western half of the country, particularly, to improve species-level distribution data, and taxonomic inputs to relieve the considerable Linnean shortfall. A suggestion, going forward and considering both limited funding and time, would be to systematically sample at the centroid of each DGC with little to no samples in the interior western regions to fill in these gaps in species-level distributions. Sampling at the QDGC would be unadvisable as there would be too many sites to feasibly sample in the short term, while deciding on sampling sites at the bioregion and biome region will not capture finer scale variation in species-level distributions. Collecting using rapid sampling protocols has been shown to generate large numbers of specimens and species-level records in sampling intervals less than a week (Haddad and Dippenaar-Schoeman 2015; Booysen and Haddad 2021; Haddad 2021), so applying this approach would enable to generation of sizable datasets in the under-sampled DGCs using the limited human resources available.

Bias

The distribution of spider records within South Africa is congruent with that of many invertebrate groups within South Africa, such as dragonflies (records from all families in the order) (Simaika and Samways 2009; Basel et al. 2021; 2024), dung beetles (records from all families in the order) (Davis and Scholtz 2020), and katydids (records only from the Tettigoniidae family) (Bazelet et al. 2016), where records are concentrated along the coastal regions of the country, and comparatively fewer in the interior drier regions of South Africa. For all these invertebrate groups, ecological drivers are suggested as the reason for the diversity distribution, although no mention of sampling bias is made. Spider records were under-sampled in the Northern Cape and North-West province of South Africa (Foord et al. 2020) and remain so here. As evidenced here by the large number of QDGC grids still unsampled, which remain concentrated in the Northern Cape and North-West provinces even though at higher scales these regions appear to be moderately, relatively and well-sampled (Fig. 3).

Bias in sample completeness will also scale with taxonomic and spatial scale of the study in question. Bazelet et al. (2016) compared katydid diversity between biodiversity hotspots and non-hotspots in South Africa and considered katydid assemblages as complete, having constructed and compared two accumulation curves for hotspots and non-hotspots. They did not consider finer scales across South Africa. Notably, there are an estimated 169 species of katydid known in South Africa (Thompson et al. 2017), so a large-scale analysis (hotspot versus non-hotspot) of katydids is likely to quickly reach an asymptote. Conversely, here we have a list of more than 2000 species, and at the smaller spatial scales sample completeness is very low. The lower spider species completeness levels at the bioregion and biome levels are justifiable when compared to the coarse level of Bazelet et al. (2016), as the spider diversity here is of an order magnitude greater than the diversity of katydids considered, as the katydids represent a single family only.

We have not distinguished between sample origins or sampling methods, but rather treated each record equally. Systematic and opportunistic surveys and sampling methods will lead to different numbers of samples. Given that the records here span a range of collection trips, the duration, methods and approaches employed will differ markedly. Record keeping between institutions and individuals will also result in bias within datasets, particularly in cases where taxonomic expertise is available to improve the resolution of identifications and keep this updated in line with global taxonomic changes (World Spider Catalog 2024). Here we set out stringent requirements for data to be retained in order to minimize record keeping errors in our dataset.

Conclusions and implications

Spider assemblage completeness is a direct result of both the spatial and taxonomic scales being considered. Furthermore, the scaling of completeness can only be interpreted in one direction, from fine to coarse and not the other way around. As scale increases, so too does the overall completeness of the spider assemblages. This will have important implications for future spider research and conservation. Given that the regions where completeness is highest across all scales correspond strongly to metropolitan areas and the areas with the highest threats to biodiversity in South Africa, and that there is a notable global decline in insect and invertebrate diversity (Cardoso et al. 2020), the determination of trends in invertebrate diversity across regions and at different scales is of paramount importance. Without understanding the underlying patterns of diversity and distributions, conservation efforts are likely to be ineffective.

Additional information

Conflict of interest

The authors have declared that no competing interests exist.

Ethical statement

No ethical clearance required as this study is based on existing museum collections.

Funding

AvdM was funded through her postdoctoral host's (Daryl Codron) National Research Foundation Competitive Grant for Rated Researcher (UID 137968). CRH and SHF were funded through the National Research Foundations Incentive Funding for Rated Researchers (grants #132687 and #87311 respectively).

Author contributions

AvdM conceptualized the study, performed data collection and cleaning, as well as the analyses and wrote the first draft of the manuscript. CRH collected and cleaned data, as well as verified species identification and contributed to the first draft of the manuscript. ASD performed identifications and established the NCA database from which much of the data originated, as well as contributing to the first draft of the manuscript. SHF was the inspiration for the study having provided over half the database freely and without hesitation, having compiled the SANSA database, his input in the final draft of the manuscript was sorely missed.

Author ORCIDs

Aileen C. van der Mescht  <https://orcid.org/0000-0003-3849-8636>

Charles R. Haddad  <https://orcid.org/0000-0002-2317-7760>

Stefan H. Foord  <https://orcid.org/0000-0002-9195-2562>

Ansie S. Dippenaar-Schoeman  <https://orcid.org/0000-0003-1532-1379>

Data availability

The full dataset is not publicly available, but will be made available upon reasonable request.

References

- Aceves-Bueno E, Adeleye AS, Feraud M, Huang Y, Tao M, Yang Y, Anderson SE (2017) The accuracy of citizen science data: A quantitative review. *Bulletin of the Ecological Society of America* 98(4): 278–290. <https://doi.org/10.1002/bes2.1336>
- Alves-Martins F, Stropp J, Juen L, Ladle RJ, Lobo JM, Martinez-Arribas J, Júnior PDM, Brasil LS, Ferreira VRS, Bastos RC, Córdoba-Aguilar A, Medina-Espinoza EF, Dutra S, Vilela DS, Cordero-Rivera A, del Palacio A, Ramírez A, Carvalho-Soares AA, Farias ABS, de Resende BO, dos Santos B, Bota-Sierra CA, Mendoza-Penagos CC, Veras DS, Anjos-Santos D, Périco E, González-Soriano E, de Oliveira Roque F, Lozano F, de Carvalho FG, Lencioni FAA, Palacino-Rodríguez F, Ortega-Salas H, Venâncio H, Sanmartín-Villar I, Muzón J, Santos JC, Montes-Fontalvo J, da Silva Brito J, da Silva Pereira JL, Oliveira-Junior JMB, Dias-Silva K, Ferreira KG, Calvão LB, Pérez-Gutiérrez LA, Rodrigues ME, Dalzochio MS, Rocha-Ortega M, von Ellenrieder N, Hamada N, Pessacq P, Rodríguez P, Martins RT, Guillermo-Ferreira R, Koroiva R, Miguel TB, Mendes TP, Neiss UG, de Almeida WR, Hortal J (2024) Sampling completeness changes perceptions of continental scale climate–species richness relationships in odonates. *Journal of Biogeography* 00(7): 1–15. <https://doi.org/10.1111/jbi.14810>
- Assis LCS (2018) Revisiting the Darwinian shortfall in biodiversity conservation. *Biodiversity and Conservation* 27(11): 2859–2875. <https://doi.org/10.1007/s10531-018-1573-3>
- Banks-Leite C, Betts MG, Ewers RM, Orme CDL, Pigot AL (2022) The macroecology of landscape ecology. *Trends in Ecology & Evolution* 37(6): 480–487. <https://doi.org/10.1016/j.tree.2022.01.005>
- Basel AM, Simaika JP, Samways MJ, Midgley GF, MacFadyen S, Hui C (2021) Assemblage reorganization of South African dragonflies due to climate change. *Diversity & Distributions* 27(12): 2542–2558. <https://doi.org/10.1111/ddi.13422>
- Basel AM, Simaika JP, Samways MJ, Midgley GF, Latombe G, MacFadyen S, Hui C (2024) Drivers of compositional turnover in narrow-ranged and widespread dragonflies and damselflies in Africa. *Insect Conservation and Diversity* 17(3): 1–11. <https://doi.org/10.1111/icad.12718>
- Bazelet CS, Thompson AC, Naskrecki P (2016) Testing the efficacy of global biodiversity hotspots for insect conservation: The case of South African katydids. *PLoS ONE* 11(9): 1–17. <https://doi.org/10.1371/journal.pone.0160630>
- Bini LM, Diniz-Filho JAF, Rangel TFLVB, Bastos RP, Pinto MP (2006) Challenging Wallacean and Linnean shortfalls: Knowledge gradients and conservation planning in a biodiversity hotspot. *Diversity & Distributions* 12(5): 475–482. <https://doi.org/10.1111/j.1366-9516.2006.00286.x>
- Booyesen R, Haddad CH (2021) Season determines the efficiency of a rapid sampling protocol for non-acarine arachnids (Chelicerata: Arachnida) in Afrotropical grassland biotopes. *Austral Entomology* 60(4): 682–697. <https://doi.org/10.1111/aen.12573>

- Burley HM, Mokany K, Ferrier S, Laffan SW, Williams KJ, Harwood TD (2016) Macroecological scale effects of biodiversity on ecosystem functions under environmental change. *Ecology and Evolution* 6(8): 2579–2593. <https://doi.org/10.1002/ece3.2036>
- Callaghan CT, Ozeroff I, Hitchcock C, Chandler M (2020) Capitalizing on opportunistic citizen science data to monitor urban biodiversity: A multi-taxa framework. *Biological Conservation* 251: 108753. <https://doi.org/10.1016/j.biocon.2020.108753>
- Cardoso P, Erwin TL, Borges PAV, New TR (2011) The seven impediments in invertebrate conservation and how to overcome them. *Biological Conservation* 144(11): 2647–2655. <https://doi.org/10.1016/j.biocon.2011.07.024>
- Cardoso P, Barton PS, Birkhofer K, Chichorro F, Deacon C, Fartmann T, Fukushima CS, Gaigher R, Habel JC, Hallmann CA, Hill MJ, Hochkirch A, Kwak ML, Mammola S, Ari Noriega J, Orfinger AB, Pedraza F, Pryke JS, Roque FO, Settele J, Simaika JP, Stork NE, Suhling F, Vorster C, Samways MJ (2020) Scientists' warning to humanity on insect extinctions. *Biological Conservation* 242: 108426. <https://doi.org/10.1016/j.biocon.2020.108426>
- Chao A, Jost L (2012) Coverage-based rarefaction and extrapolation: Standardizing samples by completeness rather than size. *Ecology* 93(12): 2533–2547. <https://doi.org/10.1890/11-1952.1>
- Chao A, Gotelli NJ, Hsieh TC, Sander EL, Ma KH, Colwell RK, Ellison AM (2014) Rarefaction and extrapolation with Hill numbers: A framework for sampling and estimation in species diversity studies. *Ecological Monographs* 84(1): 45–67. <https://doi.org/10.1890/13-0133.1>
- Chao A, Kubota Y, Zelený D, Chiu CH, Li CF, Kusumoto B, Yasuhara M, Thorn S, Wei CL, Costello MJ, Colwell RK (2020) Quantifying sample completeness and comparing diversities among assemblages. *Ecological Research* 35(2): 292–314. <https://doi.org/10.1111/1440-1703.12102>
- Christensen R (2023) ordinal - Regression Models for Ordinal Data.
- Clough Y, Kruess A, Kleijn D, Tschamtker T (2005) Spider diversity in cereal fields: Comparing factors at local, landscape and regional scales. *Journal of Biogeography* 32(11): 2007–2014. <https://doi.org/10.1111/j.1365-2699.2005.01367.x>
- Colville JF, Beale CM, Forest F, Altwegg R, Huntley B, Cowling RM, Ackerly DD, Latimer AM, Proches S (2020) Plant richness, turnover, and evolutionary diversity track gradients of stability and ecological opportunity in a megadiversity center. *Proceedings of the National Academy of Sciences of the United States of America* 117(33): 20027–20037. <https://doi.org/10.1073/pnas.1915646117>
- Cornford R, Deinet S, De Palma A, Hill SLL, McRae L, Pettit B, Marconi V, Purvis A, Freeman R (2021) Fast, scalable, and automated identification of articles for biodiversity and macroecological datasets. *Global Ecology and Biogeography* 30(1): 339–347. <https://doi.org/10.1111/geb.13219>
- Davis ALV, Scholtz CH (2020) Dung beetle conservation biogeography in southern Africa: Current challenges and potential effects of climatic change. *Biodiversity and Conservation* 29(3): 667–693. <https://doi.org/10.1007/s10531-019-01904-7>
- De Mas E, Chust G, Pretus JL, Ribera C (2009) Spatial modelling of spider biodiversity: Matters of scale. *Biodiversity and Conservation* 18(7): 1945–1962. <https://doi.org/10.1007/s10531-008-9566-2>
- Diniz-Filho JAF, Jardim L, Guedes JJM, Meyer L, Stropp J, Frateles LEF, Pinto RB, Lohmann LG, Tessarolo G, De Carvalho CJB, Ladle RJ, Hortal J (2023) Macroecological links between the Linnean, Wallacean, and Darwinian shortfalls. *Frontiers of Biogeography* 15(2): e59566. <https://doi.org/10.21425/F5FBG59566>

- Dippenaar-Schoeman AS, Haddad CR, Foord S, Lyle R, Lotz L, Helberg L, Mathebula S, Van Den Berg A, Marais P, Van Den Berg AM, Van Niekerk E, Jocqué R (2010) The First Atlas of the Spiders of South Africa (Arachnida: Araneae). South African National Survey of Arachnida Technical Report. <https://doi.org/10.5281/zenodo.7628809> [October 8, 2024]
- Dippenaar-Schoeman AS, Haddad CR, Foord S, Lyle R, Lotz L, Marais P (2015) South African National Survey of Arachnida (SANSA): Review of Current Knowledge, Constraints and Future Needs For Documenting Spider Diversity (Arachnida: Araneae). *Transaction of the Royal Society of South Africa* 70(3): 245–275. <https://doi.org/10.1080/0035919X.2015.1088486>
- Dippenaar-Schoeman A, Lyle R, van den Berg A (2012) Bioinformatics on the spiders of South Africa. *Serket = Sarkat* 13: 121–127.
- Dippenaar-Schoeman AS, Haddad CR, Lotz LN, Booysen R, Steenkamp RC, Foord SH (2023) Checklist of the spiders (Araneae) of South Africa. *African Invertebrates* 64(3): 221–289. <https://doi.org/10.3897/AfrInvertebr.64.111047>
- Drinkrow DR, Cherry MI, Siegfried WR (1994) The role of natural history museums in preserving biodiversity in South Africa. *South African Journal of Science* 90: 470–479.
- Foord SH, Dippenaar-Schoeman AS (2016) The effect of elevation and time on mountain spider diversity: A view of two aspects in the Cederberg mountains of South Africa. *Journal of Biogeography* 43(12): 2354–2365. <https://doi.org/10.1111/jbi.12817>
- Foord SH, Mafadza MM, Dippenaar-Schoeman AS, Van Rensburg BJ (2008) Micro-scale heterogeneity of spiders (Arachnida:Araneae) in the Soutpansberg, South Africa: a comparative survey and inventory in representative habitats. *African Zoology* 43(2): 156–174. <https://doi.org/10.1080/15627020.2008.11657233>
- Foord S, Dippenaar-Schoeman A, Haddad C (2011a) South African spider diversity: African perspectives on the conservation of a Mega-diverse group. In: Grillo O, Venora G (Eds) *Changing diversity in changing environment*. INTECH Open Access Publisher, Rijeka, Croatia, 163–182.
- Foord SF, Dippenaar-Schoeman AS, Haddad CR, Lotz LN, Lyle R (2011b) The faunistic diversity of spiders (Arachnida: Araneae) of the savanna biome in South Africa. *Transactions of the Royal Society of South Africa* 66(3): 170–201. <https://doi.org/10.1080/0035919X.2011.639406>
- Foord SH, Dippenaar-Schoeman AS, Stam EM (2013) Surrogates of spider diversity, leveraging the conservation of a poorly known group in the Savanna Biome of South Africa. *Biological Conservation* 161: 203–212. <https://doi.org/10.1016/j.biocon.2013.02.011>
- Foord SH, Dippenaar-Schoeman AS, Haddad CR, Lyle R, Lotz LN, Sethusa T, Raimondo D (2020) The South African National Red List of spiders: Patterns, threats, and conservation. *The Journal of Arachnology* 48(2): 110–118. <https://doi.org/10.1636/0161-8202-48.2.110>
- Fraisl D, Hager G, Bedessem B, Gold M, Hsing PY, Danielsen F, Hitchcock CB, Hulbert JM, Piera J, Spiers H, Thiel M, Haklay M (2022) Citizen science in environmental and ecological sciences. *Nature Reviews. Methods Primers* 2(1): 64. <https://doi.org/10.1038/s43586-022-00144-4>
- Garretson A, Cuddy T, Duffy AG, Forkner RE (2023) Citizen science data reveal regional heterogeneity in phenological response to climate in the large milkweed bug, *Oncopeltus fasciatus*. *Ecology and Evolution* 13(7): e10213. <https://doi.org/10.1002/ece3.10213>
- Gómez-Rodríguez C, Baselga A (2018) Variation among European beetle taxa in patterns of distance decay of similarity suggests a major role of dispersal processes. *Ecography* 41(11): 1825–1834. <https://doi.org/10.1111/ecog.03693>

- Gonçalves-Souza T, Diniz-Filho JAF, Romero GQ (2014) Disentangling the phylogenetic and ecological components of spider phenotypic variation. *PLoS ONE* 9(2): e89314. <https://doi.org/10.1371/journal.pone.0089314>
- Haddad CR (2021) Undergraduate entomology field excursions are a valuable source of biodiversity data: A case study for spider (Araneae) bycatches in ecological studies. *Biodiversity and Conservation* 30(14): 4199–4222. <https://doi.org/10.1007/s10531-021-02301-9>
- Haddad CR, Dippenaar-Schoeman AS (2015) Diversity of non-acarine arachnids of the Ophathe Game Reserve, South Africa: Testing a rapid sampling protocol. *Koedoe* 57(1): 1–15. <https://doi.org/10.4102/koedoe.v57i1.1255>
- Haddad CR, Dippenaar-Schoeman AS, Lyle R, Foord SH, Lotz LN (2013) The faunistic diversity of spiders (Arachnida: Araneae) of the South African Grassland Biome. *Transactions of the Royal Society of South Africa* 68(2): 97–122. <https://doi.org/10.1080/0035919X.2013.773267>
- Haddad CR, de Jager LJC, Foord SH (2019) Habitats and cardinal directions are key variables structuring spider leaf litter assemblages under *Searsia lancea*. *Pedobiologia* 73: 10–19. <https://doi.org/10.1016/j.pedobi.2019.01.002>
- Hamer M (2012) An assessment of zoological research collections in South Africa. *South African Journal of Science* 108(11/12): 1–11. <https://doi.org/10.4102/sajs.v108i11/12.1090>
- Hortal J, Borges PAV, Gaspar C (2006) Evaluating the performance of species richness estimators: Sensitivity to sample grain size. *Journal of Animal Ecology* 75(1): 274–287. <https://doi.org/10.1111/j.1365-2656.2006.01048.x>
- Hortal J, De Bello F, Diniz-Filho JAF, Lewinsohn TM, Lobo JM, Ladle RJ (2015) Seven shortfalls that beset large-scale knowledge of biodiversity. *Annual Review of Ecology, Evolution, and Systematics* 46(1): 523–549. <https://doi.org/10.1146/annurev-ecolsys-112414-054400>
- Hsieh TC, Ma KH, Chao A (2020) iNEXT: iNterpolation and EXTrapolation for species diversity. R package version 2.0.20. <http://chao.stat.nthu.edu.tw/wordpress/software-download/>
- Jacobs C, Zipf A (2017) Completeness of citizen science biodiversity data from a volunteered geographic information perspective. *Geo-Spatial Information Science* 20(1): 3–13. <https://doi.org/10.1080/10095020.2017.1288424>
- Janion-Scheepers C, Measey J, Braschler B, Chown SL, Coetsee L, Colville JF, Dames J, Davies AB, Davies SJ, Davis ALV, Dippenaar-Schoeman AS, Duffy GA, Fourie D, Griffiths C, Haddad CR, Hamer M, Herbert DG, Hugo-Coetsee EA, Jacobs A, Jacobs K, Rensburg CJ, van, Lamani S, Lotz LN (2016) Soil biota in a megadiverse country: Current knowledge and future research directions in South Africa. *Pedobiologia* 59(3): 129–174. <https://doi.org/10.1016/j.pedobi.2016.03.004>
- Jiménez-Valverde A, Lobo JM (2007) Determinants of local spider (Araneidae and Thomisidae) species richness on a regional scale: Climate and altitude vs. habitat structure. *Ecological Entomology* 32(1): 113–122. <https://doi.org/10.1111/j.1365-2311.2006.00848.x>
- Joseph GS, Mauda EV, Seymour CL, Munyai TC, Dippenaar-Schoeman A, Foord SH (2018) Landuse Change in Savannas Disproportionately Reduces Functional Diversity of Invertebrate Predators at the Highest Trophic Levels: Spiders as an Example. *Ecosystems* 21(5): 930–942. <https://doi.org/10.1007/s10021-017-0194-0>
- Kusumoto B, Chao A, Eiserhardt WL, Svenning J-C, Shiono T, Kubota Y (2023) Occurrence-based diversity estimation reveals macroecological and conservation knowledge gaps for global woody plants. *Science Advances*, eadh9719. <https://www.science.org>

- Martín-Devasa R, Jiménez-Valverde A, Leprieur F, Baselga A, Gómez-Rodríguez C (2024) Dispersal limitation shapes distance-decay patterns of European spiders at the continental scale. *Global Ecology and Biogeography* 33(4): e13810. <https://doi.org/10.1111/geb.13810>
- Melo AS, S Pereira RA, Santos AJ, Shepherd GJ, Machado G, et al. (2003) Comparing species richness among assemblages using sample units: why not use extrapolation methods to standardize different sample sizes? *IKOS* 101: 398–410. <https://doi.org/10.1034/j.1600-0706.2003.11893.x>
- Mittermeier RA, Turner WR, Larsen FW, Brooks TM, Gascon C (2011) Global Biodiversity Conservation: The Critical Role of Hotspots. In: *Biodiversity Hotspots*. Springer Berlin Heidelberg, Berlin, Heidelberg, 3–22. https://doi.org/10.1007/978-3-642-20992-5_1
- Mora C, Tittensor DP, Myers RA (2008) The completeness of taxonomic inventories for describing the global diversity and distribution of marine fishes. *Proceedings. Biological Sciences* 275(1631): 149–155. <https://doi.org/10.1098/rspb.2007.1315>
- Myers N, Mittermeier RA, Mittermeier CG, da Fonseca GAB, Kent J (2000) Biodiversity hotspots for conservation priorities. *Nature* 403(6772): 853–858. <https://doi.org/10.1038/35002501>
- Oliveira U, Paglia AP, Brescovit AD, de Carvalho CJB, Silva DP, Rezende DT, Leite FSF, Batista JAN, Barbosa JPPP, Stehmann JR, Ascher JS, de Vasconcelos MF, De Marco Jr P, Löwenberg-Neto P, Dias PG, Ferro VG, Santos AJ (2016) The strong influence of collection bias on biodiversity knowledge shortfalls of Brazilian terrestrial biodiversity. *Diversity & Distributions* 22(12): 1232–1244. <https://doi.org/10.1111/ddi.12489>
- Pärtel M, Bennett JA, Zobel M (2016) Macroecology of biodiversity: Disentangling local and regional effects. *The New Phytologist* 211(2): 404–410. <https://doi.org/10.1111/nph.13943>
- Pebesma E (2018) Simple Features for R: Standardized Support for Spatial Vector Data. *The R Journal* 10(1): 439. <https://doi.org/10.32614/RJ-2018-009>
- QGIS Development Team (2020) QGIS Geographic. Information Systems.
- Qian H (2020) Are species lists derived from modeled species range maps appropriate for macroecological studies? A case study on data from BIEN. *Basic and Applied Ecology* 48: 146–156. <https://doi.org/10.1016/j.baae.2020.08.003>
- R Core Team (2020) R: a language and environment for statistical computing.
- Ramírez F, Sbragaglia V, Soacha K, Coll M, Piera J (2022) Challenges for Marine Ecological Assessments: Completeness of Findable, Accessible, Interoperable, and Reusable Biodiversity Data in European Seas. *Frontiers in Marine Science* 8: 802235. <https://doi.org/10.3389/fmars.2021.802235>
- Robertson MP, Cumming GS, Erasmus BFN (2010) Getting the most out of atlas data. *Diversity & Distributions* 16(3): 363–375. <https://doi.org/10.1111/j.1472-4642.2010.00639.x>
- Rutherford MC, Mucina L, Powrie LW (2005) Biomes and bioregions of Southern Africa. *Vegetation of South Africa, Lesotho and Swaziland*. South African National Biodiversity Institute, Pretoria.
- Sánchez-Fernández D, Yela JL, Acosta R, Bonada N, García-Barros E, Guisande C, Heine J, Millán A, Munguira ML, Romo H, Zamora-Muñoz C, Lobo JM (2022) Are patterns of sampling effort and completeness of inventories congruent? A test using databases for five insect taxa in the Iberian Peninsula. *Insect Conservation and Diversity* 15(4): 406–415. <https://doi.org/10.1111/icad.12566>
- Schmidt MH, Thies C, Nentwig W, Tscharnkte T (2008) Contrasting responses of arable spiders to the landscape matrix at different spatial scales. *Journal of Biogeography* 35(1): 157–166. <https://doi.org/10.1111/j.1365-2699.2007.01774.x>

- Scoble MJ (2010) Natural history collections digitization: Rationale and value. *Biodiversity Informatics* 7: 77–80. <http://data.gbif.org>. <https://doi.org/10.17161/bi.v7i2.3994>
- Simaika JP, Samways MJ (2009) Reserve selection using Red Listed taxa in three global biodiversity hotspots: Dragonflies in South Africa. *Biological Conservation* 142(3): 638–651. <https://doi.org/10.1016/j.biocon.2008.11.012>
- South African National Biodiversity Institute (2006) The vegetation map of South Africa, Lesotho and Swaziland.
- Teng SN, Svenning J-C, Santana J, Reino L, Abades S, Xu C (2020) Linking Landscape Ecology and Macroecology by Scaling Biodiversity in Space and Time. *Current Landscape Ecology Reports* 5(2): 25–34. <https://doi.org/10.1007/s40823-020-00050-z>
- Thompson AC, Bazelet CS, Naskrecki P, Samways MJ (2017) Adapting the dragonfly biotic index to a katydid (tettigoniidae) rapid assessment technique: Case study of a biodiversity hotspot, the Cape Floristic Region, South Africa. *Journal of Orthoptera Research* 26: 63–71. <https://doi.org/10.3897/jor.26.14552>
- Troia MJ, McManamay RA (2016) Filling in the GAPS: Evaluating completeness and coverage of open-access biodiversity databases in the United States. *Ecology and Evolution* 6(14): 4654–4669. <https://doi.org/10.1002/ece3.2225>
- Vergara-Asenjo G, Alfaro FM, Pizarro-Araya J (2023) Linnean and Wallacean shortfalls in the knowledge of arthropod species in Chile: Challenges and implications for regional conservation. *Biological Conservation* 281: 110027. <https://doi.org/10.1016/j.biocon.2023.110027>
- Whittaker RJ, Araújo MB, Jepson P, Ladle RJ, Watson JEM, Willis KJ (2005) Conservation biogeography: Assessment and prospect. *Diversity & Distributions* 11(1): 3–23. <https://doi.org/10.1111/j.1366-9516.2005.00143.x>
- Wilkinson BH, Ivany LC, Drummond CN (2021) Estimating vertebrate biodiversity using the tempo of taxonomy—a view from Hubbert’s peak. *Biological Journal of the Linnean Society. Linnean Society of London* 134(2): 402–422. www.mammaldiversity.org. <https://doi.org/10.1093/biolinnean/blab080>
- Wilson JD, Bond JE, Harvey MS, Ramírez MJ, Rix MG (2023) Correlation with a limited set of behavioral niches explains the convergence of somatic morphology in mygalomorph spiders. *Ecology and Evolution* 13(1): e9706. <https://doi.org/10.1002/ece3.9706>
- Wolf S, Mahecha MD, Sabatini FM, Wirth C, Bruelheide H, Kattge J, Moreno Martínez Á, Mora K, Kattenborn T (2022) Citizen science plant observations encode global trait patterns. *Nature Ecology & Evolution* 6(12): 1850–1859. <https://doi.org/10.1038/s41559-022-01904-x>
- World Spider Catalog (2024) World Spider Catalog.
- Wüest RO, Zimmermann NE, Zurell D, Alexander JM, Fritz SA, Hof C, Kreft H, Normand S, Cabral JS, Szekely E, Thuiller W, Wikelski M, Karger DN (2020) Macroecology in the age of Big Data – Where to go from here? *Journal of Biogeography* 47(1): 1–12. <https://doi.org/10.1111/jbi.13633>
- Yang W, Ma K, Kreft H (2013) Geographical sampling bias in a large distributional database and its effects on species richness-environment models. *Journal of Biogeography* 40(8): 1415–1426. <https://doi.org/10.1111/jbi.12108>

Research Article

Revision of Afrotropical *Suragina* Walker, 1859 (Diptera, Athericidae)

Burgert S. Muller^{1,2}, Vaughn R. Swart², Louwrens P. Snyman^{3,4}

1 Department Terrestrial Invertebrates, National Museum, 36 Aliwal Street, Bloemfontein, 9301, South Africa

2 Department Zoology & Entomology, University of the Free State, P.O. Box 339, Bloemfontein, 9300, South Africa

3 Invertebrate Zoology, Royal Alberta Museum, 9810 103A Avenue NW, Edmonton, Alberta, T5J 0G2, Canada

4 Department of Veterinary Microbiology, University of Saskatchewan, 52 Campus Drive, Saskatoon, Saskatchewan, S7N 5B4, Canada

Corresponding author: Burgert S. Muller (burgert.muller@nasmus.co.za)

Abstract

Suragina Walker, 1859 of the Afrotropical Region are revised. Nineteen species are recognised and treated within. The species *Suragina bilobata* Muller, **sp. nov.**, *S. copelandi* Muller, **sp. nov.**, *S. freidbergi* Muller, **sp. nov.**, *S. liberiaensis* Muller, **sp. nov.**, *S. malavaensis* Muller, **sp. nov.**, *S. mulanjeensis* Muller, **sp. nov.**, *S. semiobscura* Muller, **sp. nov.** and *S. zombaensis* Muller, **sp. nov.** are described as new. A key to the known males and females of 17 Afrotropical species, excluding *S. disciclara* (Speiser, 1914) and *S. pilitarsis* (Lindner, 1925), is provided. Additionally, *S. bivittata* (Bezzi, 1926) is designated as junior synonym of *S. binominata* (Bequaert, 1921). Similarly, *S. varicolor* (Brunetti, 1929) is designated as junior synonym of *Suragina bezzii* (Curran, 1928). The distribution of Afrotropical *Suragina* is expanded with six new distribution records of three species: *S. agramma* (Bezzi, 1926): Kenya and Malawi; *S. bezzii*: Burundi, Kenya, and Uganda; *S. binominata*: Malawi.

Key words: Distribution, identification key, systematics, taxonomy, Water Snipe Flies



Academic editor: Kirstin Williams

Received: 29 October 2024

Accepted: 2 December 2024

Published: 23 December 2024

ZooBank: <https://zoobank.org/BCB49D2E-F772-49EB-A17A-47EB21194212>

Citation: Muller BS, Swart VR, Snyman LP (2024) Revision of Afrotropical *Suragina* Walker, 1859 (Diptera, Athericidae). African Invertebrates 65(2): 247–327. <https://doi.org/10.3897/AfrInvertebr.65.140524>

Copyright: This is an open access article distributed under the terms of the CC0 Public Domain Dedication.

Introduction

Suragina Walker, 1859 is a haematophagous genus of athericine water snipe flies. The genus has a cosmopolitan distribution, occurring in all regions except the Antarctic. At present, there are 57 recognised species of *Suragina*, including those treated in this paper. The species are distributed as follows: the Oriental Region has 27 species, the Afrotropical Region 19, the Neotropical Region five, the Australasian Region three, the Palearctic Region two, and the Nearctic Region just one (Yang et al. 2016).

While *Suragina* has not been shown to be a vector of bloodborne diseases in general, it may be considered of some limited veterinary importance as it has been observed and recorded feeding on several species of mammals and avians (Stuckenberg 2000). Knab (1912: 108, 110) noted *Suragina longipes* (Bellardi, 1861) feeding on humans and horses in Mexico, stating that it is "...a fierce biter and blood-sucker" and that the observer described the bite as "...exceedingly painful and caused more alarm among the horses in my outfit than any other fly". It can be inferred that this kind of biting behaviour could lead to irritation and stress in livestock, which in turn could potentially lead to similar weight loss in livestock as

caused by Tabanidae bites (Perich et al. 1986; Desquesnes and Lamine Dia 2004; Baldachhino et al. 2014). Stuckenberg (2000) listed and expanded on records provided by Nagatomi (1962), including records for *Suragina satsumana* (Matsumura, 1916) on cattle in Japan, and *Suragina bivittata* (Bezzi, 1926) – herein designated as junior synonym of *Suragina binominata* (Bequaert, 1921) – on Giant Eagle Owl, *Bubo lacteus* (Temminck, 1820) in South Africa (Stuckenberg and Young 1973).

Afrotropical *Suragina* are typically found in forested habitats, but some species of *Suragina*, such as *Suragina monogramma* (Bezzi, 1926), are known to occur in riverine woodland along mature, slow-flowing rivers (pers. obs.; Stuckenberg 2000).

Athericidae has, in recent years, had some revisionary work done, with Muller et al. (2023) revising the *Atrichops* Verrall, 1909 of the Afrotropical Region, Yang et al. (2016) describing seven new species of *Suragina* from the Oriental Region and Woodley (2007) describing a new species of *Dasyomma* Macquart, 1840 from Chile. Additionally, González et al. (2019) produced a catalogue of Neotropical and Andean Athericidae.

Stuckenberg (2000) noted that the generic status of the Neotropical “*Suragina*-like athericids” requires reassessment. This should be a future focus, as fresh samples are needed from as many Regions as possible to elucidate the phylogenetic relationships among the species within the genus.

This study revises the *Suragina* of the Afrotropical Region, describing eight new species, and designating two as junior synonyms. An identification key to the males and females of all Afrotropical species, except for *Suragina disciulara* (Speiser, 1914) and *S. pilitarsis* (Lindner, 1925), is provided (see remarks of both species), along with distribution maps (Figs 88, 89) for all species.

Materials and methods

Preparation methods

Morphological terminology follows that of Cumming and Wood (2017). Terminalia were macerated in heated 10% KOH for approximately 20 minutes or until clear, and examined using a Novel compound microscope with an attached Canon 850D DSLR camera. The same camera, with a 105 mm lens and extension tubes, was used for habitus photos of specimens. Specimen photos were stacked using Helicon Focus 7. Photographic images, illustrations of terminalia, as well as plates were prepared using Adobe Photoshop CC 2024 and Adobe Illustrator CC 2024. The species distribution maps (Figs 88, 89) were generated using QGIS 3.28.6 and Africa Terrestrial Ecosystems (Sayre 2023).

Material citations and collections

Any additional information added to the materials examined sections is placed within square brackets. Citations for type specimens are interpreted from the specimen labels, and images of type labels are provided where possible.

The following collection codens are used:

- AMNH** American Museum of Natural History, New York, USA
- BMSA** National Museum, Bloemfontein, South Africa
- CSCA** California State Collection of Arthropods, Sacramento, USA

- ICIPE** International Centre of Insect Physiology and Ecology, Nairobi, Kenya
NHMUK Natural History Museum, London, United Kingdom
MLUH Zentralmagazin Naturwissenschaftlicher Sammlungen (ZNS), Martin-Luther Universität Halle-Wittenberg, Halle, Germany
MNHN Muséum national d'Histoire naturelle, Paris, France
NMSA KwaZulu-Natal Museum, Pietermaritzburg, South Africa
PBZT Parc Botanique et Zoologique de Tsimbazaza, Antananarivo, Madagascar
SAMC Iziko South African Museum, Cape Town, South Africa

Taxonomy

Suragina Walker, 1859

Suragina Walker, 1859: 110.

Type species. *Suragina illucens* Walker, 1859 by monotypy.

Diagnosis. *Suragina* is most similar to the genus *Atrichops* with which it shares elongated legs and the hind coxa with a stout apical point or spine-like projection on its anteroventral surface. Similarly, *Atrichops* is also haematophagous, with well-developed mandibles. However, *Atrichops* has a knoblike proepimeral process (somewhat reduced in Afrotropical species) that is absent in *Suragina*. Additionally, *Suragina* has its frons usually contrasting velvety-black on the upper half and silvery-grey on the lower half (especially evident in ♀), whereas the frons in *Atrichops* is more concolorous. The antennal bases are comparatively widely separated in *Suragina*, and close together in *Atrichops*. *Suragina* typically has a tibial spur ratio of 0:2:2 (1:2:2 in some specimens of *S. binominata* (Bequaert, 1921)), while *Atrichops* has a ratio of 0:1:2. There is also a substantial difference in the morphology of the male terminalia, with *Suragina* having the gonostylus inserted apically and the parameral sheath simple apically, compared to *Atrichops* having the gonostylus inserted subapically, sometimes even medially on the gonocoxite (e.g. *Atrichops intermedius* Muller, 2023 in Muller et al. 2023) and the parameral sheath ending with outward projections. Woodley (2017: 887) provided a key to the known genera of Afrotropical Athericidae.

Key to the Afrotropical species of *Suragina* Walker (excluding *S. disciclara* and *S. pilitarsis*)

- 1 Scutum and pleura with ground colour mostly orange-yellow (e.g. Fig. 1), if scutum with prominent dark median vitta (e.g. Fig. 2) then pleura darker in colouration (Figs 14, 15) **2**
- Scutum and pleura with majority of surface brown to almost black (e.g. Figs 3, 6), limited orange-yellow colouration **8**
- 2 Notopleural area posterior to postpronotal lobe and anterior to transverse suture orange-yellow (e.g. Fig. 2), at most with a thin brown band along posterior edge of postpronotal lobe, no pruinosity in area **3**
- Notopleural area posterior to postpronotal lobe and anterior to transverse suture with a brownish marking on surface (e.g. Fig. 4), appearing bluish-to silver-grey pruinose in dorsal view, brown in lateral view (dependent on viewing angle) **5**

- 3 Scutum with a prominent dark median vitta (Fig. 2).....**S. binominata (Bequaert)** (in part, ♀)
- Scutum without a median vitta (Fig. 1).....**4**
- 4 Fore and hind tibiae dark brown to black; lateral margins of tergites 2–4 dark (Figs 16, 17).....**S. copelandi Muller, sp. nov.**
- Fore and hind tibiae yellow to orange-yellow, some specimens with apical half of front tibia darker; lateral margins of tergites 2–4 concolorous with rest of abdomen or only lateral margin of tergite 2 a slightly darker colour (Figs 9, 10).....**S. agramma (Bezzi)**
- 5 Scutum with a prominent dark median vitta, sometimes with additional dark markings on pre- and postsutural lateral areas**6**
- Scutum at most with two feint dorsocentral bluish-grey pruinose vittae (e.g. Fig. 5).....**7**
- 6 Scutum with additional dark markings on pre- and postsutural lateral areas in addition to notopleural marking (Fig. 4); fore tibia dark brown to almost black**S. falsa (Oldroyd)**
- Scutum without any additional pre- or postsutural dark markings apart from central vitta; fore and hind tibiae light brownish-yellow to orange-yellow (Figs 27, 28)..... **S. monogramma (Bezzi)**
- 7 Wing stigma dark brown with similarly dark substigmal mark running down to base of cell m_3 (Fig. 48); prescutellar area orange-yellow without any pruinosity; Madagascan endemic**S. milloti (Séguy)**
- Wing stigma light brown, with only some darker suffusions over posterior cells (Fig. 50); prescutellar area with bluish-grey pruinosity similar to that of notopleuron (Fig. 5); mainland Africa **S. mulanjeensis Muller, sp. nov.**
- 8 Wing stigma dark brown with similarly dark, but irregularly shaped substigmal mark running down to base of cell m_3 ; at least apical third of wing with brown suffused appearance, area between substigmal mark and suffusion appearing to form a hyaline band (e.g. Figs 39, 45–47)**9**
- Wing stigma variable, darker substigmal mark present or absent, if present, then brown suffusion runs up to or near it, not visually forming a clear hyaline band (e.g. Figs 38, 54).....**12**
- 9 Antennal 1st flagellomere bilobate, c-shaped (Fig. 13a); Madagascan endemic.....**S. bilobata Muller, sp. nov.**
- Antennal 1st flagellomere typical subreniform shape; mainland Africa...**10**
- 10 Upper occiput with a pair of well-developed dark markings that run down to occipital foramen (Fig. 7); mid femur dark brown, only yellow at extreme base and apex (Fig. 22); all abdominal tergites dark brown, without any posterior grey pruinose bands.....**S. liberiaensis Muller, sp. nov.**
- Upper occiput with narrower dark markings, either subrectangular or subtriangular; mid femur yellow, at most brownish on extreme base; tergite 1 with subtriangular dark marking, appearance of other tergites variable..... **11**
- 11 Upper occiput with a pair of narrow subrectangular dark markings (Fig. 8); mid femur yellow (Figs 20, 21); abdominal tergites yellowish-brown to dark brown, tergite 1 with a subtriangular marking, tergite 2 in some specimens with a fenestrated appearance, at least tergites 3–5 with posterior grey pruinose bands.....**S. freidbergi Muller, sp. nov.**
- Upper occiput with a subtriangular pair of well-developed dark markings (Fig. 6); mid femur yellow, at most with extreme base dark; abdomen with

- orange-yellow appearance; elongated dark median and lateral markings on tergites 2 and 3, remaining tergites orange-yellow without external markings ***S. malavaensis* Muller, sp. nov.**
- 12 Mid femur brown on at least two-thirds of surface, fore femur yellow on over two-thirds of surface **13**
- Fore and mid femora yellow, at most brown on extreme apex and base..... **14**
- 13 Wing with dark brown suffusion more pronounced on anterior half, lighter on posterior half (Fig. 53); postpronotal lobe pale yellow; fore femur yellow on at least basal half to two-thirds, remaining apical third to half dark brown ***S. semiobscura* Muller, sp. nov.**
- Wing with brownish suffusion uniformly distributed over anterior and posterior half (Fig. 38); postpronotal lobe dark brown, at most with a slight orange-yellow colouration on lateral margin; fore femur dark brown on basal third or almost entirely yellow with only extreme apex and base brown ***S. bezzii* (Curran)**
- 14 All coxae orange-yellow; hind femur orange-yellow on majority of surface, with small anterior apical dark mark, hind tibia and tarsi orange-yellow; occiput with pair of narrow dark subtriangular markings; ♂ cercus orange-yellow (♀ unknown) ***S. nigromaculata* (Brunetti)**
- Fore coxa variable, mid and hind coxae brown with some greyish pruinosity on at least anterior surface; hind femur with middle third with some degree of light infuscation to being blackish-brown, hind tibia and tarsi with some degree of overall infuscation; ♂♀ cercus darkened **15**
- 15 Antenna with 1st flagellomere brown (Figs 32, 33); postpronotal lobe and postalar callus pale orange-yellow, without pruinosity; at least tergites 1–5 with dark subtriangular medial markings; wing overall light brown suffused (Fig. 52) apparent darker suffused substigmal mark in ♂; Madagascar endemic ***S. pauliani* (Stuckenberg)**
- Antenna with 1st flagellomere orange-yellow; postpronotal lobe orange-brown to brown with greyish pruinosity, or dark brown without pruinosity, postalar callus colour variable; abdominal tergite markings variable, if dark, subtriangular then wing without apparent dark substigmal mark in ♂♀; mainland Africa **16**
- 16 Hind femur with median third only slightly infuscated, if at all; wing with light brown stigma, wing membrane lightly and evenly brown suffused (Figs 41, 42); abdominal tergites orange-yellow with blackish subtriangular median markings and similarly coloured lateral markings ***S. binominata* (Bequaert) (in part, ♂)**
- Hind femur with median third blackish; wing with dark brown stigma, wing membrane darker brown suffused on apical half, with some cells having a small hyaline patch at their centres; abdominal tergite colour variable, but never with subtriangular markings..... **17**
- 17 Upper occiput with narrow subrectangular markings not reaching down past upper third of occiput (Fig. 36); tergites 1–5 each with a median longitudinal blackish marking flanked for most part by bluish-grey pruinosity, additionally tergites 3–5 each with a grey pruinose posterior band..... ***S. zombaensis* Muller, sp. nov.**
- Upper occiput with wide subrectangular markings running down to occipital foramen; tergite 1 appearing orange-yellow without any pruinosity,

tergites 2 and 3 with a light brown dorsal marking appearing to cover most of dorsal surfaces; tergites 4 and 5 orange-yellow, with tergites 6 and 7 appearing to have brownish posterior margins, all tergites without apparent pruinosity (Fig. 18) ***S. dimidiatipennis* (Brunetti)**

***Suragina agramma* (Bezzi, 1926)**

Figs 1, 9, 10, 37, 55, 59, 75

Atrichops monogramma var. *agramma* Bezzi, 1926: 306.

Suragina agramma: Stuckenberg 1960: 291, fig. 87; Stuckenberg 1980: 312.

Type. Assumed lost by Stuckenberg (1960: 285). However a specimen matching the specimen locality data provided by Bezzi (1926: 306) was identified in the collection of the KwaZulu-Natal Museum (NMSA). It also has a label written by Bezzi affixed to it, identifying it as the female type of *S. agramma*. No additional information available.

Type material examined. Holotype: [SOUTH AFRICA] • 1 ♀; [Mpumalanga]; Baberton, De Kaap [Valley], B. 50; [25°35.2533'S, 30°58.4200'E]; 5 Oct. 1919; H.K. Munro leg.; (NMSA-DIP 028199).

Additional material examined. KENYA • 1 ♀; Coast Province; Shimba Hills Nat. Pk. [National Park], just inside Longomwagandi Forest; 04°14.0736'S, 39°24.1012'E; 389 masl; 27 Aug.–10 Sep. 2008; R. Copeland leg.; Malaise trap; (ICIPE) • 1 ♀; Shimba Hills Nat. Pk. [National Park], just inside Longomwagandi Forest; 04°14.0736'S, 39°24.1012'E; 389 masl; 24 Sep.–8 Oct. 2008; R. Copeland leg.; Malaise trap; (ICIPE) • 1 ♀; Shimba Hills Nat. Pk. [National Park], just inside Longomwagandi Forest; 04°14.0736'S, 39°24.1012'E; 389 masl; 19 Nov.–3 Dec. 2008; R. Copeland leg.; Malaise trap; (ICIPE) • 1 ♂2 ♀; Coast Province; Taita Hills, Nwatate area, below Bura Bluff; 03°29.066'S, 38°19.951'E; 1011 masl; 27 Jul.–10 Aug. 2011; R. Copeland leg.; riverine forest; Malaise trap; (ICIPE) • 1 ♀; Coast Province; Taita Hills, Chawia; 03°28.745'S, 38°20.497'E; 1614 masl; 23 Jan.–6 Feb. 2012; R. Copeland leg.; next to small forest pond; Malaise trap; (ICIPE: 20993AtherG11) • 1 ♀; Coast Province; Taita Hills, Chawia; 03°28.745'S, 38°20.497'E; 1614 masl; 8–22 Mar. 2012; R. Copeland leg.; next to small forest pond; Malaise trap; (ICIPE: 20993AtherG10) • 1 ♀; Coast Province; Taita Hills, Nwatate area, below Bura Bluff; 03°29.066'S, 38°19.951'E; 1011 masl; 24 Aug.–7 Sep. 2011; R. Copeland leg.; riverine forest; Malaise trap; (ICIPE) • 1 ♂; Coast Province; Taita Hills, Chawia; 03°28.745'S, 38°20.497'E; 1614 masl; 24 Aug.–7 Sep. 2012; R. Copeland leg.; next to small forest pond; Malaise trap; (ICIPE) • 1 ♂; Coast Province; Taita Hills, Nwatate area, below Bura Bluff; 03°29.066'S, 38°19.951'E; 1011 masl; 7–21 Sep. 2011; R. Copeland leg.; riverine forest; Malaise trap; (ICIPE) • 3 ♂3 ♀; Coast Province; Taita Hills, Nwatate area, below Bura Bluff; 03°29.066'S, 38°19.951'E; 1011 masl; 10–24 Aug. 2011; R. Copeland leg.; riverine forest; Malaise trap; (ICIPE) • 1 ♀; Coast Province; Taita Hills, Nwatate area, below Bura Bluff; 03°29.066'S, 38°19.951'E; 1011 masl; 27 Dec. 2011–10 Jan. 2012; R. Copeland leg.; riverine forest; Malaise trap; (ICIPE) • 4 ♀; Eastern Province; Njuki-ini Forest, nr. Forest station; 00°30.9978'S, 37°25.1112'E; 1471 masl; 30 May–13 Jun. 2016; R. Copeland leg.; inside indigenous forest; Malaise trap; (ICIPE) • 1 ♀; Eastern Province; Njuki-ini Forest, nr. Forest station;



Figures 1–8. Dorsal view of thorax (1–4) and head and thorax (5–8) of *Suragina* Walker spp. 1 *S. agramma* (Bezzi) ♀ (NMSA-DIP 028177) 2 *S. binominata* ♀ (NMSA-DIP 158408) 3 *S. bilobata* Muller, sp. nov. ♀ (CSCA) 4 *S. falsa* ♀ holotype (NHMUK014064160) 5 *S. mulanjeensis* Muller, sp. nov. ♂ paratype (NMSA-DIP 162049) 6 *S. malavaensis* Muller, sp. nov. ♀ paratype (ICIPE) 7 *S. liberiaensis* Muller, sp. nov. ♀ paratype (NMSA-DIP 158442) 8 *S. freidbergi* Muller, sp. nov. ♀ paratype (NMSA-DIP 158425). 4 Copyright NHMUK under CC BY 4.0. Not to scale.

00°30.9960'S, 37°25.1058'E; 1455 masl; 12–26 Feb. 2006; R. Copeland leg.; inside indigenous forest; Malaise trap; (ICIPE). MALAWI • 1♀; [Southern Region]; Zomba; 1535Ad [15°23.00'S, 35°20.00'E]; 1100 masl; 24–27 Sep. 1980; J.G.H. Londt & B.R. Stuckenberg leg.; (NMSA-DIP 028177). SOUTH AFRICA • 1♂; Limpopo; Blouberg, Northern side, Glenferness; [23°49.236'S, 29°47.374'E] 16–21 Jan. 1965; Transvaal Museum Expedition; (NMSA-DIP 028189) • 3♀; Mpumalanga; Mariepskop State Forest, Motlasedi River at.; 24°35.7333'S, 30°53.2833'E; 850 masl; 20–24 Jan. 2017; B.S. Muller & A.H. Kirk-Spriggs leg.; streambed and grassy floodplain, Legogote Sour Bushveld, Malaise trap; (BMSA(D)124062, BMSA(D)124621, BMSA(D)124627). ZIMBABWE • 4♀; [Manicaland Province]; Umtali District; S. Rhodesia; [18°58.00'S, 32°38.00'E]; 12 Apr. 1931; P.A. Sheppard leg.; (♀: NMSA-DIP 028202; NMSA-DIP 158390; NMSA-DIP 158389; NMSA-DIP 209061) • 1♀; [Manicaland Province]; Umtali District; S. Rhodesia; [18°58.00'S, 32°38.00'E]; 24 Feb. 1931; P.A. Sheppard leg.; (NMSA-DIP 028197) • 1♀; [Manicaland Province]; Umtali District; S. Rhodesia;

[18°58.00'S, 32°38.00'E]; 16 Feb. 1930; P.A. Sheppard leg.; (NMSA-DIP 028198) • 1♀; [Manicaland Province]; S. Rhodesia, N. Vumba; [19°06.00'S, 32°47.00'E]; 7 Mar. 1965; D. Cookson leg.; (NMSA-DIP 028191) • 1♂; [Manicaland Province]; S. Rhodesia, Vumba Mount[ain]., near Umtali; [19°06.00'S, 32°47'E]; 18 Jan. 1955; B.R. Stuckenberg & P. Stuckenberg leg.; (NMSA-DIP 028196) • 1♀; N. Vumba; S. Rhodesia; [19°06.00'S, 32°47.00'E]; 11 Mar. 1965; D. Cookson leg. (NMSA-DIP 028181) • 1♀; N. Vumba; S. Rhodesia; [19°06.00'S, 32°47.00'E]; 14 Oct. 1965; D. Cookson leg. (NMSA-DIP 028195) • 1♀; N. Vumba; S. Rhodesia; [19°06.00'S, 32°47.00'E]; 13 Mar. 1965; D. Cookson leg.; (NMSA-DIP 028193) • 1♀; N. Vumba; S. Rhodesia; [19°06.00'S, 32°47.00'E]; 29 Mar. 1965; D. Cookson leg.; (NMSA-DIP 028194).

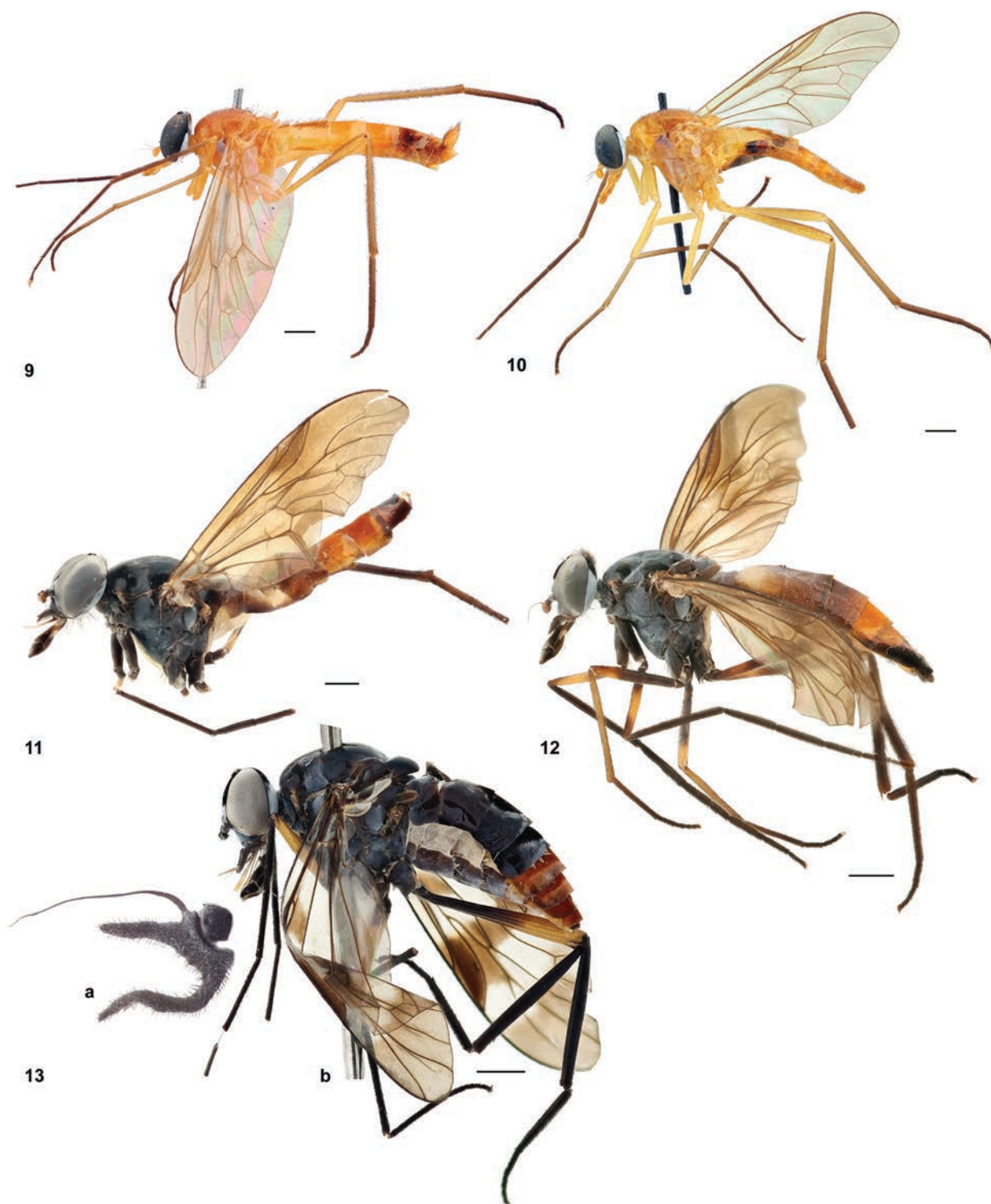
Diagnosis. *Suragina agramma* has an overall orange-yellow appearance (Figs 9, 10), the thorax without a presutural darkened spot or median vitta on the scutum (Fig. 1). Wing uniformly light brown suffused without apparent darkened substigmatal marking (Fig. 37). It is most similar to *S. copelandi* Muller, sp. nov., however, it differs from it by having the fore and hind tibiae yellow to orange-yellow, whereas *S. copelandi* Muller, sp. nov. has the tibia dark brown to black. Additionally, *S. agramma* has the lateral margins of tergites 2–4 concolorous to the rest of the abdomen compared (apart from a slightly darkened margin on tergite 2 in some specimens) to the dark lateral margins in *S. copelandi* Muller, sp. nov.

Remarks. Stuckenberg (1960) notes “eyes not contiguous” for the male from Vumba, but upon examination, the said specimen has eyes touching briefly, not “very narrowly separated” throughout. The Vumba specimen has markings on tergites 1 and 2, these are absent from the Eshowe specimen of Stuckenberg (1960). Similarly, the current Kenyan specimens examined also have tergites 1 and 2 with some slight markings similar to that of the Vumba specimen as described by Stuckenberg (1960).

Redescription. Measurements (♂ n = 5, ♀ n = 5): Wing span: ♂ 7.0–8.2 mm (avg. 7.9 mm); ♀ 8.3–8.6 mm (avg. 8.4 mm); body length: ♂ 9.0–10.1 mm (avg. 9.6 mm); ♀ 8.7–9.5 mm (avg. 8.9 mm); wing span to body length ratio (avg.): ♂ 0.82; ♀ 0.94.

Male (Fig. 9).

Head: Orange-yellow colour, with silver-white pruinosity on majority of head; eye bare; holoptic; ommatidia of similar size; lateral edge of eye with slight indentation (absent in ♀); ocellar tubercle slightly more elevated than frons, bare, colour black; vertex silver-white pruinose, with long pale setulae; anterior ocellus larger than posterior pair; ocellar tubercle in front of dorsal margin of eye, margin less indented than in ♀; vertex narrower than in ♀; dorsal inner edge of eye without discernible paired dark markings; occiput with same silver-white pruinosity as rest of head, except for paired narrow dark brown, almost black (taller in ♀) markings with pale setulae on upper occiput, abutting posterior margin of eyes, flanking vertex; upper occiput with short, pale setulae on dorsal margin and on rest of upper surface, lower occiput with long pale setulae, these continue ventrally on head to mouthparts that have similar pale ventral setulae; frons silver-white up to narrow area before eyes touch when viewed dorsally, dark velvety-brown when viewed anteriorly; frons at narrowest where eyes touch, widening towards antennal base; frons bare; face and gena silver-white with pale setulae, clypeus orange with silver-white



Figures 9–13. *Suragina* Walker spp. lateral habitus: *S. agramma* (Bezzi): **9** ♂ (NMSA-DIP 028196) **10** ♀ holotype (NM-SA-DIP 028199); *S. bezzii* (Curran): **11** ♂ (SAM-DIP-A018382) **12** ♀ (SAM-DIP-A018410); *S. bilobata* Muller, sp. nov.: **13a** ♀ paratype 1st flagellomere (CSCA) **13b** ♀ holotype (CSCA). Scale bars: 1 mm.

pruinosity, bare; face separated from clypeus by a prominent, deep suture on anterior and lateral edges; face not appearing to bulge laterally when viewed in profile; clypeus visible in profile, face not; antennal bases separated ca 0.5× width of scape, with slight longitudinal groove; scape, pedicel, 1st flagellomere orange-yellow, 2nd flagellomere brownish; 1st flagellomere reniform,

only slightly larger than pedicel and scape; 2nd flagellomere arista-like; scape and pedicel with pale dorsal and ventral setulae of similar size, palpus orange-yellow, well-developed, ca 0.5× length of proboscis; proboscis comparatively same size as that of ♀ in relation to head; proboscis orange-yellow with long pale setulae, shorter setulae ventrally; some scattered small dark setulae on proboscis and palpus.

Thorax: Majority of surface orange-yellow, median dorsal surface of scutum and scutellum with short dark setulae, remainder of thorax with longer pale setulae, especially on pleura and lateral surface of scutellum; postsutural setulae similar to presutural setulae, except for longer prescutellar setulae; postpronotal lobe slightly lighter orange-yellow in colour compared to rest of thorax, with pale setulae; scutum and scutellum uniformly orange-yellow without any vittae; pleura generally orange-yellow in colour with except for anepisternum that has a dark brown marking; anepisternum, katepisternum and katatergite lightly silver-white dusted; notopleuron with long pale setulae; area surrounding posterior spiracle orange-yellow, postspiracular scale orange-yellow, same colour as rest of thorax; proepisternum, pronotum orange-yellow; anterior spiracle bare posteriorly; proepimeron, proepisternum with pale setulae, anepisternum with pale setulae; katatergite with pale setulae; rest of pleura bare.

Legs: Coxae orange-yellow; fore and mid coxae with long pale setulae on surface, hind coxa with long pale setulae on anterior and lateral apical edges, and with well-developed anterior apical point; all trochanters same orange-yellow colour as rest of body with some scattered short pale setulae; all femora uniformly orange-yellow; mid and hind femora with small anterior apical dark mark; fore tibia darker orange-brown except for proximal area which is orange-yellow, mid and hind tibiae orange-yellow; all tarsi with somewhat darker appearance, similar in colour to fore tibia, middle basal tarsomere lighter; fore tarsal claws asymmetrical, outer claw much larger than inner claw, foreleg empodium ca 2× size of inner pulvillus, outer pulvillus ca 2× length of inner, approaching size of outer claw; fore and mid femora covered with pale setulae on all surfaces except for dorso-apical surface with short dark setulae, hind femur with mixed long pale and dark setulae on dorsal and ventral surface, basally with long pale setulae, anteriorly with short setulae and posteriorly with longer setulae; hind leg overall stouter than remaining legs; fore tarsi covered with long sensory setulae along antero- and posteroventral surfaces, sensory setulae ca 2× as long as tarsal segment is wide; fore and mid tibiae covered in short dark setulae, hind tibia with longer dark setulae; hind tarsal segments 0.97–1.05× as long as hind tibia; tibial spur formula 1:2:2.

Wing: Slight light brown suffused appearance; with a slightly yellow-brown stigma over area of veins R_1 and R_{2+3} and cell r_1 ; veins light brown; costa without distinct downward flexure over stigma; cell *cua* closed a short distance from wing margin; cell m_3 open, veins M_1 , M_2 , M_3 present; haltere almost entirely orange-yellow, with very short dark setulae and slightly infuscated apically.

Abdomen: Orange-yellow, tergites and sternites without apparent dark markings (some specimens may appear darkened due to discolouration due to dried gut contents); tergites and sternites similar in colour with short black setulae on median-dorsal surface of tergites, rest of surface of abdomen covered in long pale setulae; tergite 1 with weak median longitudinal suture.

Terminalia (Figs 55, 59): Entirely orange-yellow in colour; epandrium and cercus with dark setulae, hypoproct and hypandrium with pale setulae; gonostylus tapering with truncated apex, outer ventral surface of gonostylus base with 3 short setulae, rest of gonostylus appearing bare; gonocoxite widening and appearing more rounded on apical half, apex somewhat flattened, gonocoxite outer and ventral medial surface with long setulae, inner surface of upper half with short setulae; parameral apodeme short, not reaching base of gonocoxite in ventral view, parameral sheath including parameral apodeme ca 0.7× length of gonocoxite; gonocoxal apodeme ca 1.2× length of gonocoxite and similar in length to ejaculatory apodeme; aedeagal tine curvature extending down past gonocoxites.

Female (Fig. 10): Similar to ♂ except for the following:

Head: Dichoptic; lateral edge of eye without indentation (slight in ♂); ocellar tubercle with short dark setulae; dorsal margin of eye more indented than in ♂; vertex wider than in ♂, dark directly behind ocellar tubercle up to posterior of eye margin (in anterior view), appearing silver-white when viewed dorsally; dorsal inner edge of eye with paired dark markings but only visible when viewed anteriorly, otherwise area similarly silver-white pruinose; occiput with same silver-white pruinosity as rest of head, except for paired dark brown, almost black (taller than in ♂) markings on upper occiput, abutting posterior margin of eyes, flanking vertex; frons velvety-black from ocellar tubercle down to lower half of eye, silver-white down to antennal base; frons dark setulose on velvety-black area, pale setulose on silver-white pruinose area (♂ bare), at narrowest 1.8× width of ocellar tubercle, widening slightly towards antennal base; face separated anteriorly from clypeus by shallow transverse suture, deeper sutures laterally; 1st flagellomere comparatively much larger than in ♂.

Thorax (Fig 1): Scutum more densely setulose than in ♂.

Legs: Fore tarsi symmetrical; setulae of femora overall shorter (compared to ♂) except for preapical area of fore femur that has long pale setulae; hind femur with mix of short pale and dark setulae; hind tarsal segments 0.92–1.02× as long as hind tibia.

Wing (Fig. 37): Similar to ♂.

Abdomen: Dark dorsal setulae on tergites appearing longer towards posterior of abdomen.

Terminalia (Fig. 75): Cercus orange-yellow with pale setulae; genital fork with distal apodeme broad, forked; median lobe with shallow apical emargination; paired apical lobes with slender appearance and inner surface gradually rounded with clustered microtrichia at apex; arms gradually rounded; three ovate-shaped and sclerotised spermathecae.

Distribution. Kenya (new record), Malawi (new record), South Africa, Zimbabwe.

Behaviour. David Cookson wrote on a specimen label, collected in 1964 from Northern Vumba: "This dabs at water-surface like a tabanid and settles on bushes with a blob of water on its mouth parts".

***Suragina bezzii* (Curran, 1928)**

Figs 11, 12, 38, 57, 56, 60, 76

Atrichops bezzii Curran, 1928: 172.

Suragina bezzii: Stuckenberg 1980: 312.

Atrichops varicolor Brunetti, 1929: 2. syn. nov.
Suragina varicolor: Stuckenberg 1980: 313.

Synonymy of *Suragina varicolor* (Brunetti, 1929). Images of both the holotypes of *S. bezzii* and *S. varicolor*, as well as identified material from Uganda, Kenya and Burundi were examined and compared. There is no marked difference between the two species, apart from slight variation in colour intensity due to different preservation methods. Thus, *S. varicolor* is hereby designated as junior synonym of *S. bezzii*.

Type material examined. [from digital photographs] **Holotype:** ♀; [DEMOCRATIC REPUBLIC OF CONGO] • Bengamisa, Belgian Congo; [0°58.21'N, 25°12.64'E]; 29 Sep. 1914; (AMNH). Type photos accessible at: <https://emu-prod.amnh.org/imulive/iz/iz.html#details=ecatalogue.10021491>.

Other type material examined. *S. varicolor* syn. nov. type [from digital photographs]: **Holotype:** UGANDA • 1 ♀; Southern Region; Kampala; [0°18.8167'N, 32°34.8667'E]; 13 Aug. 1911; Presented by the Imperial Bureau of Entomology, British Museum 1929–48; (NHMUK 014064157).

Other material examined. BURUNDI • 1 ♀; Ruvubu National Park, nr. Ruvubu River; [3°10.00'S, 30°20.00'E]; 1382 masl; 21 Feb.–8 Mar. 2010; R. Copeland leg.; edge of forest; Malaise trap. KENYA • 1 ♀; Western Province; Kakamega Forest, nr. Rondo Guest House; 00°13.6602'N, 34°53.1198'E; 1630 masl; 22 Oct.–5 Nov. 2006; R. Copeland leg.; across small permanent stream; Malaise trap; (ICIPE) • 1 ♀; Western Province; Kakamega Forest, nr. Rondo Guest House; 00°13.6602'N, 34°53.1198'E; 1630 masl; 24 Sep.–8 Oct. 2006; R. Copeland leg.; across small permanent stream; Malaise trap; (ICIPE). UGANDA • 1 ♂48 ♀; Kibale National Park, Kanyawara, Makerere University Biological Field Station; 00°33.823'N, 30°21.490'E; 1505 masl; 12–26 Oct. 2008; S van Noort leg.; UG08-KF3-M13; Malaise trap; primary mid-altitude Rainforest (♂: SAM-DIP-A018410; ♀: SAM-DIP-A018378, A018379, A018380, A018381, A018383, A018384, A018386, A018387, A018388, A018389, A018391, A018392, A018393, A018394, A018395, A018396, A018397, A018398, A018399, A018400, A018401, A018402, A018403, A018404, A018405, A018406, A018407, A018408, A018409, A018411, A018412, A018413, A018414, A018416, A018417, A018418, A018419, A018420, A018421, A018422, A018423, A018424, A018425, A018426, A018427, A018428, A018429, A018432).

The female material from Kibale National Park agrees entirely with that of the original type description as well as with the publically available photos of the holotype female.

Diagnosis. *Suragina bezzii* has an overall dark appearance (Figs 11, 12), with its entire thorax dark brown to blackish with varying levels of bluish-grey pruinosity throughout. The wings are light brown suffused with a dark brown stigma and a brown suffused substigmatal marking (Fig. 38). The abdomen has tergite 2 with a fenestrated appearance and the tergites 4–6 orange, contrasting with the otherwise dark brown abdomen. The species is most similar to *S. semiobscura* Muller, sp. nov. but differs from it by having the postpronotal lobes dark brown as opposed to pale yellow. *Suragina semiobscura* Muller, sp. nov., most strikingly, has the upper half of the wing dark brown suffused, the lower half appearing lighter, creating a two-toned appearance (Fig. 53) compared to that of *S. bezzii* that has the wing uniformly brown suffused.

Remarks. Curran (1928: 172) remarked that it was possible that the “black undescribed” specimen mentioned by Bezzi (1926: 304) is in fact *S. bezzii*. That is however just conjecture at this point in time as no further information is available regarding the whereabouts of the specimen mentioned by Bezzi, nor was it ever described. There are several dark species from west and central African countries. Bezzi’s comment: “This last species, like *A. disciclara* Speiser, 1914, shows a deep longitudinal median furrow on the fore part of the frons.” is not diagnostic, as all known Afrotropical *Suragina* have a longitudinal median groove or “furrow” running up from between the antennal bases, with varying degrees of depth.

Description. Measurements (♂ n = 1, ♀ n = 5): Wing span: ♂ 7.4 mm; ♀ 8.6–9.1 mm (avg. 8.4 mm); body length: ♂ 9.3 mm; ♀ 9.0–9.8 mm (avg. 9.5 mm); wing span to body length ratio (avg.): ♂ 0.80; ♀ 0.94.

Male (Fig. 11).

Head: Black ground colour, with bluish-grey pruinosity on majority of head; eye bare; holoptic; ommatidia of similar size; lateral edge of eye with slight indentation; ocellar tubercle barely visible in profile, black in colour (appears to be rubbed bare in both sexes due to degradation from preservation method); vertex with slight grey pruinosity, otherwise appearing black in colour and dark setulose; anterior ocellus similar in size to posterior pair; ocellar tubercle in front of dorsal margin of eye, not placed as deeply towards middle of head as in ♀; dorsal inner edge of eye abutting ocellar tubercle; occiput with same bluish-grey pruinosity as rest of head; paired large rectangular black markings with dark setulae on upper occiput widening towards lateral margin of head, abutting posterior margin of eyes, flanking vertex; upper occiput with similar dark setulae; lower occiput with long pale setulae medially, dark setulae laterally; genal area bluish-grey with dark setulae, these dark setulae continue ventrally on head to mouthparts that have similar dark ventral setulae; frons bluish-grey pruinose, velvety-black from ocellar tubercle to lower half of eye; frons widening from velvety-black patch towards antennal base; frons bare; face with pale setulae; clypeus black with bluish-grey pruinosity, bare; face separated anteriorly from clypeus by a deep transverse suture, similar to lateral sutures; face not appearing to bulge laterally when viewed in profile; clypeus visible in profile, face not; antennal bases separated ca 0.5× width of scape, with slight longitudinal groove running between; scape, pedicel dark brown with whitish pruinosity; 1st flagellomere orange, with some slight darker markings and with similar pruinosity as other segments, 2nd flagellomere dark brown; scape and pedicel of similar size; 1st flagellomere reniform, ca 1.5× size of pedicel; 2nd flagellomere arista-like; pedicel with dark dorsal and ventral setulae, similar in size, scape with only dark dorsal setulae; palpus black on majority of surface with scattered white pruinosity, orange-yellow on basal third, with dark setulae throughout; palpus ca 0.5× length of proboscis; proboscis ca same length as head height; proboscis mostly brown, basally more orange-yellow, entire structure interspersed with some dark setulae and some shorter pale setulae.

Thorax: Scutum rubbed bare due to degradation from preservation method (♀ with two feint dorsocentral bluish-grey pruinose vittae running from pronotum and joining before scutellum), otherwise dark brown with bluish-grey pruinosity; pronotum bluish-grey pruinose with long pale setulae; postpronotal lobe same dark brown as rest of scutum, slight bluish-grey pruinose, setation

unknown, anterolateral margin of lobe lighter yellowish- to orange-brown (♀ colouring more apparent); notopleuron appearing slight bluish-grey pruinose when viewed in profile, however, when viewed dorsally pruinosity shifts into a silver-grey pruinose appearance, running up towards edge of mesonotum (notopleuron mostly rubbed bare except for anterior edge with long dark setulae); postalar wall and postalar callus dark brown with slight bluish-grey pruinosity, anterior of postalar callus orange-yellow; scutellum dark brown with bluish-grey pruinosity, entire margin orange-yellow from base to apex; supra-alar area, postalar wall and postalar callus with patches of dark setulae (less apparent and numerous than in ♀); majority of pleura bluish-grey pruinose, except for anterior of anepimeron and meron shiny blackish-brown; all pleura that are bluish-grey pruinose have pale setulae (only some remnant setulae remain due to damage from preservation method), except for katatergite that has long dark setulae; anatergite and meron bare; proepisternum and proepimeron with long pale setulae; anterior and posterior spiracles whitish-yellow and surroundings yellowish-brown, bare; postspiracular scale dark brown.

Legs: All coxae entirely blackish-brown with only some scattered white pruinosity; fore coxa with mostly pale setulae except for some dark setulae apically; mid coxa with long dark setulae on anterior surface, posterior margin appearing bare; hind coxa with a mix of long pale and dark setulae on anterior edge surrounding well-developed anterior apical point, lateral apical edges with long dark setulae; all trochanters reddish dark brown, all trochanters with short pale setulae; fore femur almost entirely yellow, except for blackish-brown apex and base; mid femur missing; hind femur dark brown except for yellow basal and apical quarters; fore tibia and 1st and 2nd tarsal segments dark brown almost black, rest of fore tarsi missing; mid tibia and tarsi missing; hind tibia and basitarsus blackish-brown, with base and apex of hind tibia yellowish-brown, rest of hind tarsi missing; fore and hind femora rubbed clean, setation unknown; fore tibia with short dark setulae; hind tibia with dark setulae that are at least as long as segment is wide; hind leg overall stouter than remaining legs; combined length of hind tarsal segments subequal to hind tibia; tibial spur formula 0:2:2; fore tibial spur weaker than that of hind tibia.

Wing (Fig. 38): Light brown suffused on majority of surface except for cell *cua* and anal lobe; dark brown stigma over cell r_1 ; darker suffused substigmal marking running down from stigma over crossvein *r-m*, bases of discal cell, cell m_3 and apex of cell *br*; veins dark brown, with additional darker brown suffusion around vein *CuA*; costa without distinct downward flexure over stigma; cell *cua* closed at wing margin, cell m_3 open, veins M_1 , M_2 , M_3 present; haltere stalk dirty yellow, knob darker yellowish-brown, with a few short and dark setulae.

Abdomen: Tergite 1 entirely blackish-brown, with dark setulae (pale setulae in ♀); tergite 2 pale, with dark brown median marking, giving it a fenestrated appearance; tergite 3 dark brown, tergites 4 and 5 orange, with tergite 5 with dark brown posterior band; tergite 6 with orange markings anteriorly, otherwise dark brown; remaining tergites dark brown; all tergites rubbed bare except for tergite 1; tergite 1 medially without a longitudinal suture; sternites 1–3 cream coloured, sternite 3 with posterior margin brown; rest of sternites orange-yellow; all sternites with pale setulae.

Terminalia (Figs 56, 60): Epandrium and cercus dark brown with dark setulae; gonocoxite, hypoproct and hypandrium with pale setulae; gonostylus ta-

pering with truncated apex, outer edge of gonostylus with short setulae, inner edge with a protrusion with 4 setulae, apical third of gonostylus with microtrichia; gonocoxite widening and appearing more rounded on apical half, apex somewhat flattened, gonocoxite outer and ventral surface down to parameral apodeme with long setulae, inner surface of upper half with short setulae, lower half with long inward-facing setulae; parameral apodeme well-developed, not reaching base of gonocoxite in ventral view, parameral sheath including parameral apodeme ca 0.7× length of gonocoxite; gonocoxal apodeme about same length as gonocoxite and slightly shorter than ejaculatory apodeme; aedeagal tine curvature extending down past gonocoxites; endoaedeagal process apically truncated and widened.

Female (Fig. 12).

Redescription. (Based on ♀ holotype photographs and additional ♀ material from Uganda.) **Head:** Black ground colour, with bluish-grey pruinosity on majority of head; eye bare; dichoptic; ommatidia of similar size; lateral edge of eye without any indentation; ocellar tubercle barely visible in profile, dark setulose (rubbed bare in ♂ due to damage from preservation method), bluish-grey pruinose medially when viewed dorsally, otherwise appearing black; vertex grey pruinose and dark setulose; anterior ocellus similar in size to posterior pair; ocellar tubercle placed deeper in front of dorsal margin of eye compared to ♂; dorsal inner edge of eye separated from ocellar tubercle by paired silver-grey markings; occiput with same bluish-grey pruinosity as rest of head; paired large rectangular black markings on upper occiput widening towards lateral margin of head with dark setulae, abutting posterior margin of eyes, flanking vertex; rest of upper occiput with pale setulae; lower occiput with long pale setulae medially and laterally; genal area with dark setulae, rest of ventral head setulae pale, these continue ventrally on head to mouthparts that have long pale ventral setulae and some shorter dark setulae; frons bluish-grey pruinose between lower half of eye down to antennal base, velvety-black from ocellar tubercle to lower half of eye; frons widening only slightly from velvety-black patch towards antennal bases; frons with dark setulae on velvety-black area; face, gena and clypeus with bluish-grey pruinosity; face sparsely populated with long pale setulae; clypeus black with bluish-grey pruinosity, bare; face separated anteriorly from clypeus by transverse suture, (less prominent than in ♂) similar to lateral sutures; antennal bases separated ca 0.5×–0.75× width of scape, with slight longitudinal groove running between; scape dark brown with whitish pruinosity and with yellowish lateral margins; pedicel dark brown with whitish pruinosity; 1st flagellomere orange to orange-brown with similar pruinosity as other segments, scape ca 1.5–2× length of pedicel; 1st flagellomere ca 2× size of pedicel; 2nd flagellomere, brown, arista-like; pedicel with dark dorsal and ventral setulae, similar in size, scape with only dark dorsal setulae; palpus black on majority of surface with scattered white pruinosity, orange-yellow on at most basal half, with dark setulae throughout; palpus ca 0.5× length of proboscis; proboscis ca same length as head height; proboscis mostly brown, basally more orange-yellow, entire structure interspersed with some pale and dark setulae of varying length.

Thorax: Scutum shining black with two feint dorsocentral bluish-grey pruinose vittae running from pronotum to before scutellum; pronotum bluish-grey pruinose with long pale setulae; postpronotal lobe dark brown, slight bluish-

grey pruinose with long pale setulae, anterolateral margin of lobe lighter yellowish- to orange-brown (more apparent than in ♂); scutum with paired, black almost velvety, rectangular marking behind postpronotal lobe (not visible in ♂ due to damage); notopleuron with same colouration as in ♂, however, ♀ notopleuron with scattered pale setulae interspersed with some dark setulae, anteriorly with pale setulae compared to dark group of setulae in ♂; postalar wall and postalar callus dark brown with slight bluish-grey pruinosity, anterior of postalar callus orange-yellow; supra-alar area, postalar wall and postalar callus with patches of dark setulae (more apparent and numerous than in ♂); scutellum dark brown with bluish-grey pruinosity, apical margin orange-yellow; scutum generally with short dark setulae with postsutural setulae longer than presutural setulae, especially prescutellar setulae; majority of pleura bluish-grey pruinose, except for anterior of anepimeron and meron shiny blackish-brown; all pleura that are bluish-grey pruinose have some pale setulae; katatergite with long pale setulae, in contrast to ♂ that has long dark setulae; anatergite and meron bare; proepisternum and proepimeron with long pale setulae; anterior and posterior spiracles yellowish-brown to whitish-yellow (due to damage from preservation method) and surroundings yellowish-brown, bare; postspiracular scale dark brown.

Legs: All coxae brown to blackish-brown with some bluish-grey pruinosity; fore coxa with mostly pale setulae except for some dark setulae apically; mid coxa with long dark setulae on anterior apical surface, otherwise with pale setulae, and sparsely setulose along posterior margin (♂ with only dark setulae); hind coxa with dark setulae on anterior edge surrounding well-developed anterior apical point, lateral apical edges with long pale setulae; all trochanters reddish dark brown, some more yellowish apically, all trochanters with short pale setulae; fore femur in most specimens yellow with extreme base and apex dark brown, some individuals with fore femur dark brown on basal half and apical quarter to third with remainder of segment yellow; mid femur dark brown except for ca apical third that is yellow; hind femur dark brown except for yellow basal and apical quarters; fore tibia and tarsi dark brown to blackish; mid tibia and tarsi yellow, tarsi appearing somewhat darker yellow; hind tibia and basitarsus blackish-brown, with apex of tibia yellowish-brown in some specimens; fore tarsal claws and pulvilli symmetrical, pulvillus and empodium of similar size; fore tarsi with long, somewhat curved along antero- and posteroventral surfaces, sensory setulae ca 2× as long as tarsal segment is wide; fore femur dorsally with short dark setulae, except for several scattered short pale setulae, apically and medioventrally with long pale setulae, and with a group of 1–3 dark setulae located in middle of femur; mid femur covered in short pale setulae, but with longer pale setulae ventrally and short dark setulae apically; hind femur with mix of short pale and dark setulae, with apex having somewhat longer pale and dark setulae ventrally; hind leg overall stouter than remaining legs; all tibiae with short dark setulae; hind tarsal segments 0.9–1.0× as long as hind tibia; tibial spur formula 0:2:2.

Wing: Light brown suffused on majority of surface, except for cells *bm* and *cua*, and anal lobe, overall appearing darker on apical half; dark brown stigma over cell *r*₁; darker suffused substigmal marking running down from stigma over crossvein *r-m*, bases of discal cell, cell *m*₃ and apex of cell *br*; veins dark brown, with additional darker brown suffusion around vein *CuA*; costa without distinct

downward flexure over stigma; cell *cua* closed at wing margin or at a short distance from wing margin; cell m_3 open, veins M_1 , M_2 , M_3 present; haltere stalk dirty yellow, knob darker yellowish-brown, with a few short and dark setulae.

Abdomen: Tergite 1 dark to blackish-brown, with basal margin of some specimens more orange-brown, tergite 1 with pale setulae; tergite 2 mostly pale to orange-yellow, with brown to dark brown median marking running down to brown to dark brown band along posterior margin of tergite, giving it a fenestrated appearance, lateral margins of tergite similar brown colour to rest of tergite; tergites 3 and 4 dark brown with tergite 4 with some specimens also having orange markings posteriorly, tergites 5–7 orange, each with a dark brown posterior band; lateral margins of tergites 4–7 with blackish markings; some specimens have tergite 7 entirely dark brown; dark brown parts of tergites with pale setulae, and orange parts with dark setulae; tergite 1 medially with a longitudinal suture; sternites 1 and 2 cream coloured, sternites 3 and 4 dark brown with posterior margins darker; rest of sternites orange-yellow, ending in dark brown terminalia; all sternites with pale setulae.

Terminalia (Fig. 76): Cercus dark brown with pale setulae; genital fork has distal apodeme slender, forked; median lobe with deep apical emargination, paired apical lobes with a slender appearance, inner surface inward projecting with clustered microtrichia at apex, arms gradually rounded; three ovate-shaped and sclerotised spermathecae.

Distribution. Burundi (new record), Democratic Republic of Congo, Kenya (new record), Uganda (new record).

***Suragina bilobata* Muller, sp. nov.**

<https://zoobank.org/2526571B-58F7-4EA6-A1D4-F48D0FDFA13C>

Figs 3, 13, 39, 77

On the material. The type series of specimens available for this new species are in poor condition as these come from long-term Malaise samples, with the most complete specimen missing its 1st flagellomere (present in other more damaged specimens), and all specimens exhibiting some loss of setation on the head, body and legs. In the description missing setulae are recorded as unknown (referring to the unknown characteristics such as length or colour), but the alveoli are present. While it is not ideal to designate a holotype and paratypes from material in this state, it should be taken into account that procurement of additional material from Madagascar is not viable due to the highly seasonal nature of Athericidae adults and the prohibitively expensive nature of performing fieldwork in Madagascar. The forests of Madagascar are threatened by deforestation (e.g. Harper et al. 2007), with Ranomafana National Park being one of the largest remaining primary rainforests in Madagascar (Torppa et al. 2020). Describing and identifying endemic species could contribute to its conservation. This species is thus far the only species of *Suragina* that does not have a reniform 1st flagellomere, instead it is bilobate and c-shaped (Fig. 13a). It was also briefly mentioned by Woodley (2017: 888). Woodley regarded the specimens as *Suragina*, and viewed the 1st flagellomere shape as “a highly autapomorphic antennal flagellum”. In all other regards, *S. bilobata* Muller, sp. nov. possesses characters unique to *Suragina*: the frons velvety-black on upper half

and silver-grey on lower half in combination with hind coxa having a well-developed anterior apical point, and generally slender and elongated legs. Given the unique antennal characters and contrasting black and orange colouration of this species, there is little doubt that any future specimens collected will be easily attributable to *S. bilobata* Muller, sp. nov.

Type material examined. Holotype: MADAGASCAR • 1♀; Fianarantsoa Province; Ranomafana National Park, radio tower; 21°15.05'S, 47°24.43'E; 1127 masl; 23–30 Apr. 2002; M.E. Irwin, R. Harin'Hala leg.; Malaise in open area nr forest edge; CSCA.

Paratypes: 2♀; same data as Holotype; CSCA.

Holotype and paratypes deposited in CSCA.

Diagnosis. *Suragina bilobata* Muller, sp. nov. has its 1st antennal flagellomere uniquely bilobed, or c-shaped (Fig. 13a), contrasting to the typical reniform shape found in other Afrotropical Athericidae. The overall appearance of the species is reminiscent of other dark Afrotropical species (e.g. *Suragina bezzii*), but the combination of the antennal shape, and wing with a dark stigma, sub-stigmatal marking, and hyaline band before apical brown suffusion makes it easy to distinguish from all other known species.

Description. Measurements (♀ n = 1): Wing span: 8.1 mm; body length: 8.9 mm; wing span to body length ratio: 1.03.

Male. Unknown.

Female (Fig. 13).

Head: Black ground colour, with bluish-grey pruinosity on majority of head; eye bare; dichoptic; ommatidia of similar size; lateral edge of eye without any indentation; ocellar tubercle elevated, visible in profile, same velvety-black as upper half of frons, surface setulae unknown; vertex bluish-grey pruinose, with dark setulae; anterior ocellus similar in size to posterior pair; ocellar tubercle in front of dorsal margin of eye; dorsal inner edge of eye with paired dark markings; occiput with same bluish-grey pruinosity as rest of head; paired black markings with unknown setulae on upper occiput running down to near occipital foramen, abutting posterior margin of eyes, flanking vertex; upper occiput otherwise with pale setulae; lower occiput lateral marginal setulae unknown, with long pale setulae medially, these continue ventrally on head to mouthparts that have mix of pale and dark ventral setulae; frons bluish-grey pruinose, velvety-black from ocellar tubercle to lower half of eye; frons running almost parallel, widening towards antennal base; frons setulae unknown; face with silver-white pruinosity and gena bluish-grey, face with a mix of pale and dark setulae, genal setulae unknown; clypeus with bluish-grey pruinosity, bare; face separated anteriorly from clypeus by shallow transverse suture, with deeper sutures laterally; face not appearing to bulge laterally when viewed in profile; clypeus visible in profile, face not; antennal bases separated ca 0.5–0.75× width of scape, with slight longitudinal groove running between; scape, pedicel, and 1st flagellomere dark brown with some whitish pruinosity, 2nd flagellomere dark brown; scape and pedicel of similar size; 1st flagellomere bilobate, c-shaped (Fig. 13a), upper lobe ca 2× length of scape and pedicel combined, lower lobe ca 3× length of scape and pedicel combined; 1st flagellomere lobes covered on all surfaces with pale setulae that are as long as lobes are wide; 2nd flagellomere arista-like; pedicel with dark dorsal and ventral setulae, similar in size, scape with only dark dorsal setulae; palpus brown with bluish-grey

pruinosity, with dark setulae throughout, ca 0.5× length of proboscis; proboscis ca same length as head height; proboscis dark brown with some whitish pruinosity on prementum, dorsal setulae unknown, ventrally with short dark setulae and some scattered longer pale setulae.

Thorax (Fig. 3): Scutum shining black with two feint dorsocentral bluish-grey pruinose vittae running from pronotum to before scutellum, ending in a large bluish-grey pruinose posterior patch; pronotum bluish-grey pruinose with long pale setulae; postpronotal lobe dark brown, slightly bluish-grey pruinose with long pale setulae; notopleuron bluish-grey pruinose with long pale setulae just behind postpronotal lobe and rest of surface with dark setulae; postalar wall and postalar callus brown with bluish-grey pruinosity; scutellum uniform black with slight bluish-grey pruinosity; scutum setulae unknown; majority of pleura bluish-grey pruinose, except for anatergite and anepimeron yellowish-brown; all pleura that are bluish-grey pruinose have long pale setulae; anepimeron with long pale setulae, anatergite and meron bare; proepisternum and proepimeron with long pale setulae; anterior and posterior spiracles and surroundings brownish-yellow, bare; postspiracular scale dark brown; postscutellum black with slight bluish-grey pruinosity.

Legs: All coxae dark brown bluish-grey pruinosity on surface; fore and hind coxae with pale setulae, fore coxa with short dark setulae at apex, mid coxa with dark setulae on anterior apical surface, and inner and outer lateral surfaces, interspersed with some pale setulae; hind coxa with pale setulae on anterior edge surrounding well-developed anterior apical point, lateral apical edges with longer pale setulae; all trochanters glossy black with short pale setulae; fore femur yellow with extreme basal and apical margins appearing shiny dark brown to black; mid femur similar to fore femur, except basal area dark brown, this basal area similar in length to trochanter; hind femur dark brown on basal half to two-thirds; all tibiae and tarsi dark brown to black; fore tarsal claws, empodium and pulvilli unknown; fore tarsi with long, somewhat curved sensory setulae along antero- and posteroventral surfaces, sensory setulae ca 2× as long as tarsal segment is wide; leg setation mostly unknown; all femora apparently with a mix of short pale and dark setulae; all tibiae with short dark setulae; hind leg overall stouter than remaining legs; combined length of hind tarsal segments subequal to hind tibia; tibial spur formula 0:2:2.

Wing (Fig. 39): Dark brown stigma over apex of veins R_1 and R_{2+3} and cells sc , r_1 , base of cell r_{2+3} , crossvein $r-m$, bases of discal cell, cell m_3 and apex of cell br ; cell bm with similar dark substigmal marking medially and apically, otherwise hyaline; vein CuA with a dark marking along length; entirety of cells m_1 and m_2 , apex of cell m_3 , apical half of cell r_5 , apical two-thirds of cell r_4 and apical half of cell r_{2+3} brown suffused; rest of wing hyaline; veins dark brown; costa without distinct downward flexure over stigma; cell cua closed a short distance from wing margin; cell m_3 open, veins M_1 , M_2 , M_3 present; haltere stalk light brown, knob darker brown, with some short and dark setulae.

Abdomen: Tergite 1 with bluish-grey pruinosity on anterolateral margins, medially with a dark marking and a longitudinal suture; tergites 2–4 with a triangular dark marking, narrowing towards posterior with posterior and lateral margins of each segment with bluish-grey pruinosity; tergite 5 and onwards a deep orange colour, with posterior margin appearing darker; sternites 1–4 dark brown with bluish-grey pruinosity, sternites 5 and onwards orange-yellow; setation unknown.

Terminalia (Fig. 77): Cercus dark orange-brown with pale setulae; genital fork has distal apodeme apically expanded with truncated appearance, without a clear fork, median lobe with shallow apical emargination, paired apical lobes with expanded appearance, inner edge with clustered microtrichia at apex; arms gradually rounded; three oval-shaped, apically rounded spermathecae, sclerotised, short and stout.

Etymology. From the Latin “bi”, two and “lobatus”, having lobes; named for the unique bilobed or c-shaped 1st flagellomere. Feminine noun in the nominative singular case.

Distribution. Madagascar.

***Suragina binominata* (Bequaert, 1921)**

Figs 2, 14, 15, 41, 42, 57, 61, 78

Atherix longipes Loew, 1863: 12 (Junior homonym, preoccupied. by *Ath. longipes* Bellardi, 1861).

Atrichops binominata Bequaert, 1921: 6 (replacement name for *Ath. longipes* Loew); Bezzi 1926: 310.

Suragina binominata: Stuckenberg 1960: 285, fig. 87; Stuckenberg 1980: 312.

Atrichops bivittata Bezzi, 1926: 308; syn. nov.

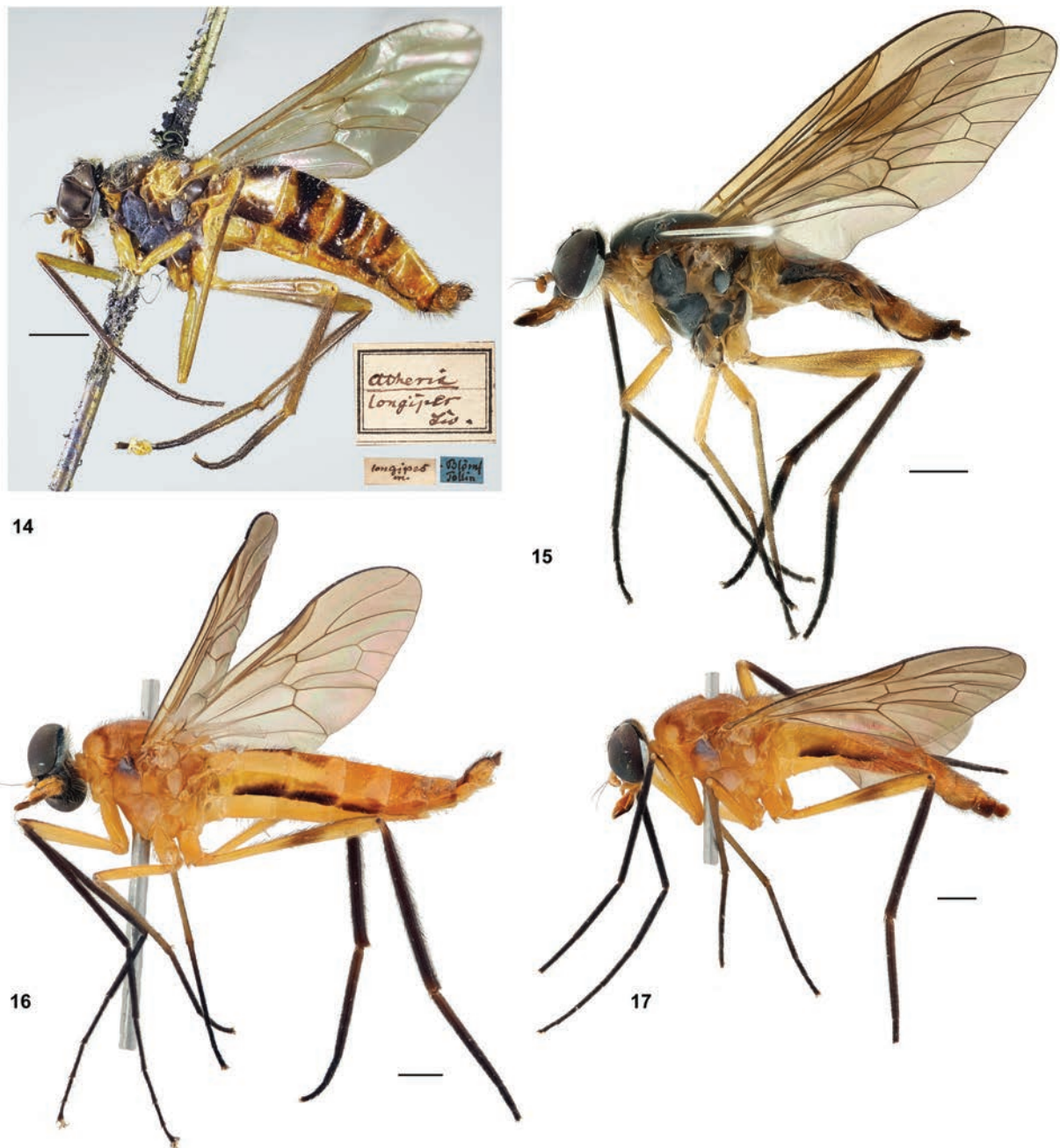
Suragina bivittata: Stuckenberg 1960: 286, fig. 87; Stuckenberg 1980: 312.

Synonymy of *Suragina bivittata* Bezzi. *Suragina binominata* is only known from the male holotype of *Atherix longipes* Loew, 1863. Stuckenberg (1960: 285) briefly discussed the possibility that *S. bivittata* is a junior synonym of *S. binominata*.

He stated that out of a series of four females of *S. bivittata* which he had collected from near the Nhlavini River (KwaZulu-Natal, South Africa), one female matched the female description of *S. binominata* by Bezzi (1926: 310) perfectly, with the others being very similar as well, taking into account the known degrees of variation within the species. Stuckenberg compared these to the type female of *S. bivittata* and found no significant differences between the female specimens of the two species. Additionally, Bezzi's descriptions of both the species' female specimens are based on material collected at the same locality, only seven days apart, which, coupled with Bezzi never stating that he did examine the holotype of *Ath. longipes*, complicated matters. Stuckenberg further stated that *S. bivittata* could only be synonymised with *S. binominata* after future examination and comparison of the male holotype of *Ath. longipes* Loew, 1863 with his described males of *S. bivittata*. Here we compare the type male of *Ath. longipes* with that of the males of *S. bivittata* as described by Stuckenberg (1960). There are no significant differences between the males or females of the two species, apart from minor colour differences that fall within the known variation previously exhibited by *S. bivittata*. Thus, we designate *S. bivittata* as a junior synonym of *S. binominata*.

Type material examined. [from digital photographs] **Holotype:** SOUTH AFRICA • 1♂; Free State; Bloemfontein; [29°07.00'S, 26°13.00'E]; Tollin leg.; (MLUH).

Other type material examined. *Atherix bivittata* syn. nov. type: SOUTH AFRICA • 1♀; [KwaZulu-Natal], Bulwer, Greene; [29°47.85'S, 29°46.16'E]; Sep. 1916.



Figures 14–17. *Suragina* Walker spp. lateral habitus: *S. binominata* (Bequaert): 14 ♂ holotype (MLUH) 15 ♀ (BMSA(D)124083); *S. copelandi* Muller, sp. nov.: 16 ♂ holotype (BMSA(D)83426) 17 ♀ paratype (BMSA(D)84688). 14 Copyright ZNS Halle, January 30, 2024. Scale bars: 1 mm.

Other material examined. MALAWI • 1 ♀; [Southern Region]; Mulanje Mt. [Mulanje Massif] nr Likabula; [15°56.983'S, 35°35.617'E]; 26–28 Oct. 1983; A. Freidberg leg.; (NMSA-DIP 194746) • 1 ♀; [Southern Region]; Mulanje District; Mulanje mt. [Mulanje Massif], Likabula; 15°56.2667'S, 35°30.0667'E; 786 masl; 12–15 Nov. 2016; A.H. Kirk-Spriggs & B.S. Muller leg.; Malaise trap, stream, montane evergreen forest; (BMSA(D)92592). SOUTH AFRICA • 1 ♀; Gauteng; Pretoria; [25°45.441'S, 28°12.618'E]; 4 Oct. 1910; Hardenberg leg.; (NMSA-DIP 028192) • 1 ♀; Eastern Cape; Hillside Farm, Pot River nr. Maclear; [31°19.933'S, 28°26.742'E]; 21 Jan. 1963; B.R. Stuckenberg & P. Stuckenberg leg.; (NMSA-DIP 028163) • 5 ♀; Western Cape; Littlestone Cottage, Robinson's Pass, R328; 33°57.756'S, 22°05.184'E; 99

masl; 7–8 Dec. 2022; B.S. Muller & M.J.J. Magoai leg.; on rock face over stream pool, hand collected; (BMSA(D)119797, 124009, 124055, 124083, 124088) • 1♀; Western Cape; Knysna, Caplant; [33°56.879'S, 23°09.575'E]; Mar. 1913; Brauns leg.; (NMSA-DIP 028161) • 1♀; North West Province; Ottoshoop; [25°48.929'S, 26°46.154'E] Apr. 1916; H.G. Breyer leg.; (NMSA-DIP 028190) • 1♀; Mpumalanga; 20 km E Nelspruit, Noordkaap River; 2530Db [25°36.579'S, 30°58.579'E]; 23 Sep. 1980; R.M. Miller leg.; NMSA-DIP 158408) • 2♀; Mpumalanga; Echo caves; [24°33.733'S, 30°36.208'E]; 6 Mar. 2000; M. Picker leg.; (NMSA-DIP 158446, 158447) • 9♀; Mpumalanga; K.N.P. [Kruger National park] Survey, Skukuza; [24°59.75'S, 31°35.52'E]; 21–24 Nov. 1972; J. van Reenen leg.; (NMSA-DIP 028164, 028167, 158434, 158435, 158436, 158437, 158438, 158439, 158440) • 1♀; North West Province; Rietspruit, Marico [Sehubyane stream]; [25°02.85'S, 26°23.90'E]; Jan. 1918; J.C. Faure leg.; (NMSA-DIP 028200) • 1♀; Mpumalanga; Mariepskop State Forest, Klaserie river at.; 24°35.5667'S, 30°56.1333'E; 736 masl; 24–26 Jan. 2017; B.S. Muller & A.H. Kirk-Spriggs leg.; Streambed & marginal vegetation, Legogote Sour Bushveld; Malaise trap; (BMSA(D)125145) • 1♀; KwaZulu-Natal; Ashburton; [29°40.335'S, 30°27.119'E]; 18 Dec. 1990; R.M. Miller leg.; at light; (NMSA-DIP 158441) • 1♀; KwaZulu-Natal; Ashburton; [29°40.335'S, 30°27.119'E]; 15 Dec. 1991; R.M. Miller leg.; (NMSA-DIP 158410) • 1♀; KwaZulu-Natal; Ashburton; [29°40.335'S, 30°27.119'E]; 17 Apr. 1992; R.M. Miller leg.; on window; (NMSA-DIP 158409) • 4♂4♀; KwaZulu-Natal; Nhlavini River, Ixopo Dist.; [30°07.783'S, 30°12.614'E]; 17 Mar. 1957; B.R. Stuckenberg leg.; (♂: NMSA-DIP 028165, 158427, 158428, 158430; ♀: NMSA-DIP 158429, 158431, 158432, 158433) • 1♀; KwaZulu-Natal; Ukulinga Research Farm, 10 km SE Pietermaritzburg; [29°37.76'S, 30°24.29'E]; 20–26 Nov. 1985; R.M. Miller leg.; grassland impoundment, Malaise trap; (NMSA-DIP 194744).

Comment. Holotype ♂: middle left leg missing, left wing missing, left fore tibia and tarsi missing, right fore apical tarsus missing.

Diagnosis. A variably coloured species with the scutum ranging from orange-yellow to brown ground colour with darker pleura and heavily patterned tergites. *Suragina binominata* males are most similar to the holotype male of *Suragina nigromaculata* (Brunetti, 1929) in general appearance, but differ from it in having the lateral margins of all abdominal tergites dark brown compared to *S. nigromaculata* that has darkened lateral margins only on tergites 1 and 2. Additionally, males of *S. binominata* have the scutellum bicoloured, being orange-yellow apically and dark brown on basal half. Conversely, the holotype male of *S. nigromaculata* has the scutellum almost entirely orange-yellow except for the basal margin, being somewhat darker in appearance. The females of *S. binominata* have the scutellum similar to that of the holotype male of *S. nigromaculata*, but its scutum has a much more prominent central black vitta (Fig. 2) and similar abdominal markings to that of the *S. binominata* male.

Redescription. Measurements (♂ n = 1, ♀ n = 5): Wing span: ♂ 5.7 mm; ♀ 5.8–6.9 mm (avg. 6.6 mm); body length: ♂ 7.5 mm; ♀ 6.7–7.7 mm (avg. 7.3 mm); wing span to body length ratio (avg.): ♂ 0.76; ♀ 0.91.

Male (Fig. 14).

Head: Brown colour, with silver-grey pruinosity on majority of head; eye bare; holoptic; ommatidia of similar size; lateral edge of eye with slight indentation; ocellar tubercle slightly more elevated than frons, with some dark setulae and surface colour dark brown with slight pruinescence; vertex silver-grey pruinose

with long pale setulae; ocellar tubercle in front of dorsal margin of eye (♀ unknown); dorsal inner edge of eye without discernible paired dark markings; occiput with same silver-grey pruinosity as rest of head, except for paired subrectangular dark brown, almost black markings with pale setulae on upper occiput, abutting posterior margin of eyes, flanking vertex and running down to occipital foramen; upper occiput with short pale setulae, lower occiput with long pale setulae, these continue ventrally on head to mouthparts that have dark ventral setulae; frons silver-white running up to narrow area before eyes converge when viewed dorsally, at which point frons is velvety-black in appearance; lower part of frons dark brown when viewed anteriorly; frons at narrowest ca 0.5× width of anterior ocellus, widening towards antennal bases; frons bare; face and gena silver-grey with pale setulae, clypeus dark brown with silver-grey pruinosity, bare; face separated from clypeus by a prominent, deep suture on anterior and lateral edges; face not appearing to bulge laterally when viewed in profile; clypeus visible in profile, face not; antennal bases separated ca 0.5× width of scape, with slight longitudinal groove; scape, pedicel brown, appearing darker in dorsal view; 1st flagellomere orange-yellow, 2nd flagellomere brownish; 1st flagellomere reniform, only slightly larger than pedicel and scape; 2nd flagellomere arista-like; scape and pedicel with dark setulae; scape with only dorsal setulae, pedicel with dorsal and ventral setulae, setulae of similar size; palpus orange-yellow, but darker orange-brown on apical half, well-developed, ca 0.5× length of proboscis; proboscis orange-yellow at base but orange-brown on majority of surface with long dark setulae, some scattered small dark setulae on proboscis and palpus.

Thorax: Dark brown ground colour; median dorsal surface of scutum and scutellum with short pale setulae, remainder of thorax with longer pale setulae, especially on pleura and lateral surface of scutellum; postsutural setulae similar to presutural setulae, except for longer prescutellar setulae; postpronotal lobe dark brown on majority of surface except for yellow-brown anterolateral surface; with long pale setulae.

Scutum mostly dark brown with slight median greyish pruinosity; postalar wall and callus appearing orange-yellow; scutellum bicoloured, with apical half being orange-yellow and basal half dark brown, scutellar setulae long and pale; all pleura dark brown in colour with greyish pruinosity, except for anepimeron that is yellowish-brown dorsomedially; notopleuron dark brown with long pale setulae; area surrounding posterior spiracle brown, postspiracular scale brown, lighter than colour of pleura; proepisternum, pronotum dark brown; anterior spiracle and surrounds yellow, bare; proepimeron, proepisternum with pale setulae, anepisternum with pale setulae; katatergite with pale setulae; rest of pleura bare.

Legs: Fore coxa orange-yellow; mid coxa more brownish-yellow with orange-yellow lower anterior surface; hind coxa orange-yellow with brownish markings on anterodorsal surface; fore coxa with long pale setulae on surface and shorter dark setulae apically, mid coxa with long dark setulae on surface, hind coxa with long dark setulae on anterior and lateral apical edges, and with well-developed anterior apical point; all trochanters same orange-yellow colour as rest of body with some scattered short dark setulae; all femora uniformly orange-yellow with hind femur slightly darker on middle third; fore tibia and tarsi dark brown, mid tibia orange-yellow; hind tibia dark brown with apex more yellowish; mid and hind tarsi dark brown with basitarsus same yellowish-brown on basal half as that of apex of hind tibia; fore and mid femora with covered in

dark setulae, fore femur with long pale setulae on median ventral surface and long dark setulae toward apex, mid femur with similar long dark setulae on ventral surface; hind femur with long dark setulae on dorsal and ventral surfaces, basally with long pale setulae, anteriorly with short dark setulae and posteriorly with longer dark setulae; hind leg overall stouter than remaining legs; fore tarsi covered with long sensory setulae along antero- and posteroventral surfaces, sensory setulae ca 2× as long as tarsal segment is wide; fore and mid tibiae covered in short dark setulae, hind tibia with longer dark setulae, especially on dorsal surface; combined length of hind tarsal segments subequal to hind tibia; tibial spur formula 0:2:2.

Wing (Fig. 41): Overall slight light brown suffused appearance except for discal cell and cell *cua* that are lighter; crossveins *r-m* and *bm-cu* with darker suffusions and with brown stigma over area of veins R_1 and R_{2+3} and cell r_1 ; veins brown; costa without distinct downward flexure over stigma; cell *cua* closed a short distance from wing margin; cell m_3 open, veins M_1 , M_2 , M_3 present; haltere orange-yellow, with very short dark setulae and slightly darker apically.

Abdomen: Overall orange-yellow colour; tergite 1 dark brown with orange-yellow posterior and lateral margins; tergite 2 with a dark brown subtriangular marking that runs down to posterior margin, and additional dark marking on lateral margin; tergites 3 and 4 each with dark brown marking that runs transversely across entire segment to lateral margin; tergite 5 similar to tergites 3 and 4, but marking much narrower and connection between median and lateral markings lighter brown; tergites 6 and 7 with only dark brown lateral markings; tergite covered in a mix of pale and dark setulae, lateral margins with long dark setulae; sternites all orange-yellow without any apparent dark markings, all segments with similar long pale setulae as on lateral margins of tergites; tergite 1 without median longitudinal suture.

Terminalia (Figs 57, 61): Mostly dark orange-yellow in colour; epandrium with some darker brown markings at base, cercus dark brown; epandrium, hypandrium and cercus with dark setulae; gonostylus tapering with truncated apex, outer edge of gonostylus with short setulae, inner edge with protrusion with 4 setulae, apical third of gonostylus sparsely covered in microtrichia; gonocoxite widening and appearing more rounded on apical half, apex somewhat flattened, gonocoxite outer and ventral medial surface with long setulae, inner surface of upper half with short setulae, lower ventral surface comparatively less setulose; gonocoxite with microtrichia between setulae; parameral apodeme with truncated apex, not reaching base of gonocoxite in ventral view, parameral sheath including parameral apodeme ca 0.7× length of gonocoxite; gonocoxal apodeme similar in length to gonocoxite and slightly longer than ejaculatory apodeme; aedeagal tine curvature extending down past gonocoxites, apex of tines extending out past parameral sheath; endoaedeagal process apically truncated and widened.

Female (Fig. 15).

Head: Dark brownish-black ground colour, with bluish-grey pruinosity on majority of occiput; eye bare; dichoptic; ommatidia of similar size; lateral edge of eye without any indentation; ocellar tubercle slightly elevated, visible in profile, dark setulose, bluish-grey pruinose, much more apparent when viewed posterodorsally, more blackish when viewed anteriorly; vertex bluish-grey pruinose, with pale setulae, vertex appearing blackish dark brown when viewed posteriorly; anterior ocellus similar in size to posterior pair; ocellar tubercle in front of dorsal margin

of eye; dorsal inner edge of eye without discernible paired dark markings, same bluish-grey pruinose as rest of head; occiput similarly bluish-grey pruinose; paired subrectangular blackish-brown markings with pale setulae on upper occiput running down to occipital foramen, abutting posterior margin of eyes, flanking vertex; upper occiput with similar pale setulae; lower occiput with lateral margins and medial area with long pale setulae, these continue ventrally on head to mouthparts that have pale ventral setulae; frons shining bluish-grey pruinose on lower half, velvety-black from ocellar tubercle to lower half of eye; frons running almost parallel, widening only very slightly towards antennal base; frons with short dark setulae on velvety-black upper half, with scattered pale setulae at posterior of lower half of frons; face and gena grey pruinose, gena with several long pale setulae; clypeus with lighter brown ground colour similar to mouthparts (some non-type specimens have clypeus appearing almost black anteriorly), with less dense bluish-grey pruinosity, bare; face separated anteriorly from clypeus by shallow transverse suture, deeper sutures laterally; face not appearing to bulge laterally when viewed in profile; clypeus visible in profile, face not; antennal bases separated ca 1× width of scape, with slight longitudinal groove running between; scape, pedicel mostly orange-yellow, dorsally more brown, with some whitish pruinosity; 1st flagellomere entirely orange-yellow; 2nd flagellomere brown; scape ca 1.5× size of pedicel; 1st flagellomere reniform, 2× size of pedicel; 2nd flagellomere arista-like; pedicel with dark dorsal and ventral setulae, similar in size, scape with only dark dorsal setulae; palpus orange-yellow with mostly dark setulae, some interspersed pale setulae; palpus ca 0.5× length of proboscis; proboscis ca same length as head height; proboscis darker brownish-orange on apical half, orange on basal half with some long pale setulae dorsally, short and long dark setulae ventrally.

Thorax (Fig. 2): Scutum orange-yellow with central shining black vitta with bluish-grey pruinosity running from just behind pronotum to before scutellum; scutum with presutural area with darker orange-yellow colour, some specimens with darker mark; notopleuron orange-yellow; postsutural area with blackish-brown on dorsal surface up to before supra-alar and postalar areas that are orange-yellow; pronotum orange-yellow with pale setulae; postpronotal lobe yellow, with short pale setulae; notopleuron orange-yellow, setulae pale; postalar wall and postalar callus orange-yellow; scutellum almost entirely orange-yellow with pale setulae, basal anterior margin blackish with bluish-grey pruinosity, appearing as run-on from scutum; scutum generally with short pale setulae, postsutural setulae somewhat longer, with some dark setulae as well; majority of pleura brownish with some bluish-grey pruinosity, except for anepimeron and proepisternum that are orange-yellow; pleura with pale setulae; anepimeron and katepisternum with long pale setulae, anatergite and meron bare; proepisternum and proepimeron with long pale setulae; anterior and posterior spiracles and surroundings orange-yellow, bare; postspiracular scale orange-yellow; postnotum blackish.

Legs: Coxae orange-yellow, some specimens with slightly darker orange-yellow posterior surfaces on mid and hind coxae; fore coxa with long pale setulae on anterior and posterior surfaces; mid coxa with long pale setulae on anterior surface; hind coxa with pale setulae on anterior surface as well as surrounding well-developed anterior apical point, lateral apical edges with long pale setulae; all trochanters orange-yellow with short dark setulae; fore, middle and hind femora yellow; fore tibia brown with orange-yellow base, middle and hind tibia

orange-yellow; fore tarsi dark brown, mid and hind tarsi dark brown except for orange-yellow basal half of basitarsus; fore tarsal claws and pulvilli symmetrical, pulvillus and empodium of similar size; fore tarsi with long, somewhat curved sensory setulae along antero- and posteroventral surfaces, sensory setulae ca 2× as long as tarsal segment is wide; fore femur with short dark setulae on anterodorsal surface and long pale setulae on apical half of posteroventral surface; mid femur with long pale setulae on anteroventral surface, otherwise with a mix of short pale and dark setulae; hind femur mostly with short dark setulae, apically with some longer dark setulae; all tibiae with short dark setulae; hind leg overall stouter than remaining legs; hind tarsal segments 0.92–1.18× as long as hind tibia; tibial spur formula 0:2:2.

Wing (Fig. 42): Very lightly brown suffused, almost appearing hyaline; lighter towards basal part of wing; brown stigma over apex of veins R_1 and R_{2+3} and cells sc , r_1 ; slightly darker brown suffused over base of discal cell and cell m_3 ; veins brown, and crossveins $r-m$ and $bm-cu$ (intensity differs between specimens); costa without distinct downward flexure over stigma; cell cua closed a short distance from wing margin; cell m_3 open, veins M_1 , M_2 , M_3 present; haltere stalk orange-yellow, knob light brown, with some short and dark setulae.

Abdomen: Overall orange-yellow with blackish-brown markings; tergite 1 with dark median marking; tergite 2 with median longitudinal dark marking and paired dark lateral markings; tergite 3 with a median longitudinal dark marking on anterior half of tergite and with similar paired dark lateral markings; tergite 4 with a dark marking along anterior margin (very light or absent on some specimens); tergites 4–7 orange-yellow to brownish-orange, with tergite 6 posterior margin and tergite 7 lateral and dorsal surface much darker than preceding segments, in some specimens displaying as dark markings; some specimens with dark lateral markings extending down from tergites 3–7, and tergite 5 with similar anterior marginal markings as tergite 4; sternites orange-yellow in colour; all tergites with short dark setulae dorsally; tergites 1 and 2 additionally with long pale setulae on dorsal surface; lateral margins of tergites 1–4 with pale setulae and some interspersed dark setulae; remaining tergites with dark lateral marginal setulae; sternites with pale setulae, longer on sternites 1–4 compared to remaining sternites; tergite 1 medially with a longitudinal suture.

Terminalia (Fig. 78): Cercus orange to dark orange-brown with pale setulae; genital fork with distal apodeme ending broadly forked; median lobe with wide, moderate emargination; paired apical lobes with somewhat slender appearance, inner surface with clustered microtrichia at apex above a conspicuous, bare toothlike projection; arms gradually rounded; three oblong and sclerotized spermathecae.

Distribution. Malawi (new record), South Africa.

***Suragina copelandi* Muller, sp. nov.**

<https://zoobank.org/256E33E2-9B8F-4226-9F25-A35370E86929>

Figs 16, 17, 40, 58, 62, 79

Type material examined. Holotype: TOGO • 1♂: Plateaux; Kuma Tokpli; 06°58.30'N, 00°34.15'E; 486 masl; 21–24 Jan. 2016; A.H. Kirk-Spriggs leg.; well-vegetated stream bed; Malaise trap; (BMSA(D)83426) (BMSA).

Paratypes: 9♂8♀; same data as holotype; (♂: BMSA(D)83421, 83425, 83427, 83428, 83429, 83430, 83431, 83432, 83435; ♀: BMSA(D)83422, 83423, 83424, 83433, 83434, 83436, 83437, 83438). Togo • 3♂9♀; Plateaux; Dzogbegan Monastery; 07°14.27'N, 00°41.56'E; 762 masl; 24–25 Jan. 2016; A.H. Kirk-Spriggs leg.; vegetated stream bed; Malaise trap (♂: BMSA(D)84681, 84682, 84691; ♀: BMSA(D)84684, 84683, 84685, 84686, 84689, 84690, 84687, 84688, 84697) • 2♀; Plateaux: Zogbégan-Carrière, (SE von Badou), Région des Plateaux; 07°34.8333'N, 00°40.05'E; 650 masl; 23–26 Apr. 2008; A. Ssymank leg.; NN MF, FO: 7093 (CSCA). KENYA • 3♀; Western Province; Kakamega Forest, nr. Rondo Guest House; 00°13.6602'N, 34°53.1198'E; 1630 masl; 13–27 Aug. 2006; R. Copeland leg.; across small permanent stream; Malaise trap; (ICIPE) • 1♀; Western Province; Kakamega Forest, nr. Rondo Guest House; 00°13.6602'N, 34°53.1198'E; 1630 masl; 24. Sep–8. Oct. 2006; R. Copeland leg.; across small permanent stream; Malaise trap; (ICIPE) • 1♀; Western Province; Kakamega Forest, nr. Rondo Guest House; 00°13.6602'N, 34°53.1198'E; 1630 masl; 8–22 Oct. 2006; R. Copeland leg.; across small permanent stream; Malaise trap; (ICIPE) • 1♀; Western Province; Kakamega Forest, behind W. Okeka house; 00°14.13'N, 34°51.87'E; 1550 masl; 10–24 Feb. 2007; R. Copeland leg.; just inside forest; Malaise trap; (ICIPE) • 1♀; Western Province; Kakamega Forest, behind W. Okeka house; 00°14.13'N, 34°51.87'E; 1550 masl; 24 Feb.–10 Oct. 2007; R. Copeland leg.; just inside forest; Malaise trap (ICIPE) • 1♀; Western Province; Mt Elgon Lodge; [1°23.309'S, 34°48.322'E]; 1–6 Nov. 1983; A. Freidberg leg.; Malaise trap (NMSA-DIP 158399). UGANDA • 1♀; Kibale National Park, Kanyawara Makerere University Biological Field Station; 00°33.823'N, 30°21.490'E; 1505 masl; 12–26 Aug. 2008; S. van Noort leg.; UG08-KF3-M13; Malaise trap, primary mid-altitude Rainforest; (SAM-DIP-A018415) • 1♀; Kibale National Park, Kanyawara Makerere University Biological Field Station; 00°34.806'N, 30°21.874'E; 1491 masl; 2–12 Aug. 2008; S. van Noort leg.; UG08-KF6-M06; Malaise trap, secondary mid-altitude Rainforest, marshy area; (SAM-DIP-A018390).

Holotype deposited in BMSA and paratypes deposited as per listed institutional codens in citations above: CSCA, ICIPE and SAM.

Diagnosis. *Suragina copelandi* Muller, sp. nov., is most similar to *S. agramma* (see *S. agramma* diagnosis) in its general appearance. It differs from it by having the fore and hind tibiae dark brown to black compared to the mostly yellow to orange-yellow appearance of *S. agramma*. Additionally, *S. agramma* has the lateral margins of tergites 2–4 concolorous to the rest of the abdomen compared (apart from a slight darkened margin on tergite 2 in some specimens) to the dark lateral margins in *S. copelandi* Muller, sp. nov. It is widely distributed from western Kenya to Togo, compared to *S. agramma* which occurs from eastern Kenya down to northeastern South Africa, seemingly without any known overlap in distribution.

Description. Measurements (♂ n = 2, ♀ n = 2): Wing span: ♂ 7.0–7.4 mm (avg. 7.2 mm); ♀ 8.8–9.4 mm (avg. 9.2 mm); body length: ♂ 9.4–9.5 mm (avg. 9.5 mm); ♀ 10.0–10.6 mm (avg. 10.3 mm); wing span to body length ratio (avg.): ♂ 0.76; ♀ 0.90.

Male (Fig. 16).

Head: Orange-yellow colour, with silver-white pruinosity on majority of head; eye bare; holoptic; ommatidia of similar size; lateral edge of eye with slight indentation (absent in ♀); ocellar tubercle slightly more elevated than frons,

black with dark setulae, shorter than pale setulae on vertex; vertex silver-white pruinose, with long pale setulae; ocelli similar in size; ocellar tubercle in front of dorsal margin of eye, margin less indented than in ♀; vertex narrower than in ♀; dorsal inner edge of eye without discernible paired dark markings; occiput with same silver-white pruinosity as rest of head, except for paired narrow dark brown, almost black (taller in ♀) markings with extreme dorsal edge with short dark setulae on upper occiput, abutting posterior margin of eyes, flanking vertex; upper occiput with short pale setulae on dorsal margin and on rest of upper surface, lower occiput with long pale setulae, these continue ventrally on head to mouthparts that have similar pale ventral setulae (with some scattered dark setulae); frons silver-white up to narrow area before eyes touch, when viewed dorsally, dark velvety-brown when viewed anteriorly; frons at narrowest where eyes touch, widening towards antennal base; frons bare; face and gena silver-white with pale setulae, clypeus orange with silver-white pruinosity, bare; face separated from clypeus by a prominent, deep suture on anterior and lateral edges; face not appearing to bulge laterally when viewed in profile; clypeus visible in profile, face not; antennal bases separated ca 0.5× width of scape, with slight longitudinal groove; scape, pedicel, 1st flagellomere orange-yellow, 2nd flagellomere brownish; 1st flagellomere reniform, only slightly larger than pedicel and scape; 2nd flagellomere arista-like; scape with pale dorsal setulae, pedicel with dark dorsal and ventral setulae, similar in size, palpus orange-yellow, well-developed, ca 0.5× length of proboscis; proboscis more slender than that of ♀, comparatively same length as that of ♀ in relation to head; proboscis mostly orange-yellow, except for ventral surface that is light brown, proboscis with long pale setulae, with some setulae ventrally; some scattered small dark setulae on proboscis and palpus.

Thorax: Majority of surface orange-yellow, dorsal surface of scutum and scutellum with dark setulae, pleura with longer pale setulae; scutum with post-sutural setulae similar to presutural setulae, except for longer prescutellar setulae; postpronotal lobe slightly lighter orange-yellow colour compared to rest of thorax, with pale setulae; area behind postpronotal lobe brownish; scutum and scutellum uniformly orange-yellow without any vittae; pleura generally orange-yellow in colour with except for anepisternum that has a dark brown marking; anepisternum, katepisternum and katatergite lightly silver-white dusted; notopleuron with long pale and dark setulae; area surrounding posterior spiracle orange-yellow, postspiracular scale orange-yellow, same colour as rest of thorax; proepisternum, pronotum orange-yellow; anterior spiracle bare posteriorly; proepimeron, proepisternum with pale setulae, anepisternum with pale setulae; katatergite with pale setulae; rest of pleura bare.

Legs: Coxae orange-yellow; fore and mid coxae with long pale setulae on surface, hind coxa with long pale setulae on anterior and lateral apical edges, and with well-developed anterior apical point; all trochanters same orange-yellow colour as rest of body with some scattered short pale setulae; all femora uniformly orange-yellow, with hind femur with darker colouration medially; mid and hind femora with small anterior apical dark mark; fore and hind tibiae dark brown, mid tibia darker orange-yellow than mid femur; hind basal tarsus proximally and hind tibia apically lighter orange-brown; fore and hind tarsi dark brown, similar in colour to respective tibia, mid tarsi darker orange-yellow than mid tibia; fore tarsal claws asymmetrical, outer claw much larger than inner claw, foreleg empodium

ca 2× size of inner pulvillus, outer pulvillus ca 2× length of inner, approaching size of outer claw; fore and mid femora covered with pale setulae on all surfaces except for dorso-apical surface with short dark setulae, hind femur with mixed long pale and dark setulae on dorsal and ventral surfaces, distoventrally with long pale setulae; hind leg overall stouter than remaining legs; fore tarsi covered with long sensory setulae along antero- and posteroventral surfaces, sensory setulae ca 2× as long as tarsal segment is wide; fore and mid tibiae covered in short dark setulae, hind tibia with longer dark dorsal setulae; hind tarsal segments 0.9–1.0× as long as hind tibia; tibial spur formula 1:2:2.

Wing: Slight light brown suffused appearance; with a slightly yellow-brown stigma over area of veins R_1 and R_{2+3} and cell r_1 ; veins dark brown; costa without distinct downward flexure over stigma; cell *cua* closed a short distance from wing margin; cell m_3 open, veins M_1 , M_2 , M_3 present; haltere almost entirely orange-yellow, with very short dark setulae.

Abdomen: Orange-yellow, tergites 2–4 with dark lateral margin, rest unmarked; sternites without any markings; tergites with black setulae on median-dorsal surface, with long pale setulae on lateral surface; sternites covered in long pale setulae; tergite 1 with weak median longitudinal suture.

Terminalia (Figs 58, 62): Epandrium and cercus orange-yellow with dark setulae, epandrium with a dark brown dorsal mark; cercus dark brown dorsally; hypoproct and hypandrium with pale setulae, gonostylus tapering with truncated apex, outer ventral surface of gonostylus base with 3 short setulae, inner edge with a protrusion with 4 setulae, apical third of gonostylus with microtrichia; gonocoxite widening and appearing more rounded on apical half, apex somewhat flattened, gonocoxite outer and ventral medial surface with long setulae, inner surface of upper half with short setulae; gonocoxite with microtrichia between setulae; parameral apodeme short, not reaching base of gonocoxite in ventral view, parameral sheath including parameral apodeme ca 0.7× length of gonocoxite; gonocoxal apodeme ca 1.2× length of gonocoxite and similar in length to ejaculatory apodeme; aedeagal tine curvature extending down past gonocoxites, endoaedeagal process widening apically with a slight bilobed appearance.

Female (Fig. 17): Similar to ♂ except for the following:

Head: Dichoptic; lateral edge of eye without indentation (slight in ♂); ocellar tubercle with shorter dark setulae than in ♂; dorsal margin of eye more indented than in ♂; vertex wider than in ♂, dark directly behind ocellar tubercle up to posterior of eye margin (in anterior view), appearing silver-white when viewed dorsally; dorsal inner edge of eye with paired dark markings, but only visible when viewed anteriorly, otherwise area similarly silver-white pruinose; occiput with same silver-white pruinosity as rest of head, except for paired dark brown, almost black (taller than in ♂) markings on upper occiput, abutting posterior margin of eyes, flanking vertex, running down to occipital foramen; frons velvety-black from ocellar tubercle down to lower half of eye, silver-white down to antennal base; frons dark setulose on velvety-black area, pale setulose on silver-white pruinose area (♂ bare), at narrowest 1.86× width of ocellar tubercle, widening slightly towards antennal base; face separated anteriorly from clypeus by shallow transverse suture, deeper sutures laterally; proboscis stout compared to ♂, with dark ventral colour; 1st flagellomere comparatively much larger than in ♂.

Thorax: Scutum more densely setulose than in ♂.

Legs: Fore tarsi symmetrical; setulae of femora overall shorter (compared to ♂) except for preapical area of fore femur that has long pale setulae; hind femur with mix of short pale and dark setulae; hind tarsal segments 0.9× as long as hind tibia.

Wing (Fig. 40): Slightly darker suffused compared to ♂; vein CuA with some slightly darker suffusion around it.

Abdomen: Tergites with short dark setulae more widely spread, including on later setulae, interspersed between long pale setulae; tergites 2–8 with a dark lateral marking, much darker on terminal segments; tergites 7 and 8 densely dark setulose.

Terminalia (Fig. 79): Cercus orange-yellow with pale setulae; genital fork with distal apodeme narrow, forked; median lobe with gradual emargination; paired apical lobes with somewhat slender appearance, widening towards apex, inner surface with clustered microtrichia at apex; arms gradually rounded; three oval and sclerotized spermathecae.

Etymology. Named after the collector Dr Robert (Bob) Copeland, for his contribution to Dipterology in the Afrotropical Region. Noun in the genitive case.

Distribution. Kenya, Togo, Uganda.

***Suragina dimidiatipennis* (Brunetti, 1929)**

Figs 18, 43

Atrichops dimidiatipennis Brunetti, 1929: 3.

Suragina dimidiatipennis: Stuckenberg 1980: 313.

Type material examined. [from digital photographs] **Holotype:** NIGERIA • 1♀; Ibadan; [07°23.78'N, 03°55'E]; 27 Mar. 1923; Presented by Imperial Bureau of Entomology British Museum; 1484, 1929–48; (NHMUK 014064158).

Paratype: NIGERIA • 1♀; So [Southern] Nigeria; Ibadan; [07°23.78'N, 03°55'E]; 10 Aug. 1920; Presented by Imperial Bureau of Entomology British Museum; 1484, 1929–48; (NHMUK 014064159).

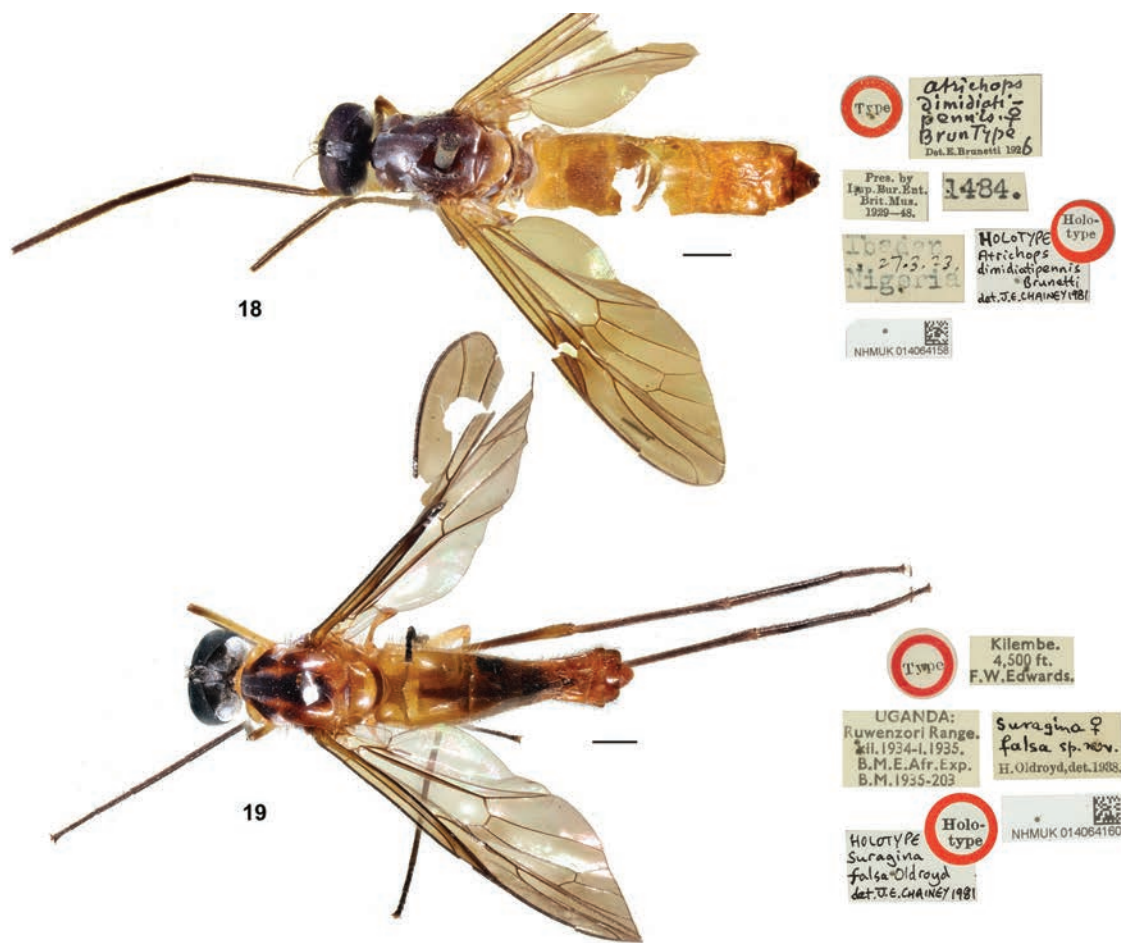
Diagnosis. Head and thorax with dark brown ground colour and silver-grey pruinosity. Abdomen is orange-yellow to dark orange, brown on terminal segments. Tergites 2 and 3 with large brown markings. Wing brown suffused on apical half with dark brown stigma and substigmal marking (Fig. 43), in this regard, it is most similar to *S. zombaensis* Muller, sp. nov., but differs from it by having wide subrectangular markings on the upper occiput compared to narrow markings in *S. zombaensis* Muller, sp. nov., and a marked difference in abdominal colour and patterning, with the latter having medial longitudinal blackish markings with bluish-grey pruinosity that are completely absent in *S. dimidiatipennis*.

Redescription. (Based on digital photographs of ♀ Holotype and ♀ paratype)

Measurements (♀ n = 2): Wing span: 7.9–8.8 mm (avg. 8.4 mm); body length: 10.3 (avg. 10.3 mm); wing span to body length ratio (avg.): 0.81.

Female (Fig. 18).

Head: Dark brown ground colour, with silvery-grey pruinosity on majority of head; eye bare; dichoptic; ommatidia of similar size; lateral edge of eye without any visible indentation; ocellar tubercle slightly elevated, visible in profile, dark setulose, silvery-grey pruinose; vertex silvery-grey pruinose, with dark setulae; anterior ocellus similar in size to posterior pair; ocellar tubercle in front of dorsal



Figures 18, 19. *Suragina* Walker spp. dorsal habitus: *S. dimidiatipennis* (Brunetti): 18 ♀ holotype (NHMUK 014064158); *S. falsa* Oldroyd: 19 ♀ holotype (NHMUK 014064160). 18, 19 Copyright NHMUK under CC BY 4.0. Scale bars: 1 mm.

margin of eye; dorsal inner edge of eye without discernible paired dark markings, same silvery-grey pruinose as rest of head; occiput with same silvery-grey pruinosity; paired widely-shaped blackish-brown subrectangular markings with dark setulae on upper occiput running down to occipital foramen, abutting posterior margin of eyes, flanking vertex; upper occiput otherwise with pale setulae; lower occiput with lateral margins and medial area with long pale setulae, these continue ventrally on head to mouthparts that have pale ventral setulae; frons silvery-grey pruinose with short dark setulae on lower half, velvety-black from ocellar tubercle to lower half of eye; frons running almost parallel, widening only very slightly towards antennal base; frons with long dark setulae; face and gena silvery-grey pruinose, with pale setulae; clypeus with silvery-grey pruinosity, bare; face separated anteriorly from clypeus by shallow transverse suture, deeper sutures laterally; face not appearing to bulge laterally when viewed in profile; clypeus visible in profile, face not; antennal bases separated ca 1× width of scape, with obvious longitudinal groove running up into lower frons; scape, pedicel mostly orange, dorsally orange-brown, otherwise with some silvery-grey pruinosity; 1st flagellomere entirely orange; 2nd flagellomere brown; scape appearing larger than pedicel when viewed dorsally; 1st flagellomere reniform, 2× size of pedicel; 2nd flagellomere arista-like; pedicel with dark dorsal and ventral setulae, similar in size, scape with only dark dorsal setulae; palpus orange with mostly darker setulae, and some interspersed pale setulae; palpus

ca 0.5× length of proboscis; proboscis ca same length as head height; proboscis orange-yellow with dark setulae and some paler shorter setulae.

Thorax: Scutum dark brown with central vitta, delineated by silver-grey pruinosity on presutural surface; central vitta ending before scutellum; scutum with large paired presutural dark brown markings behind postprontal lobe; pronotum yellowish-brown with pale setulae; postpronotal lobe brown, base same dark brown as preceding presutural scutal area; scutellum with short dark setulae; notopleuron appearing silver-grey pruinose when viewed dorsally, setulae dark; postalar wall and postalar callus orange-brown; scutellum orange-yellow with short dark setulae; scutum generally with short dark setulae with postsutural setulae somewhat longer; majority of pleura dark brown, except for anepisternum, katepisternum and meron with silver white pruinosity; pruinose pleura have long pale setulae; anepimeron setulae unknown; anatergite and meron bare; proepisternum and proepimeron with long pale setulae; anterior and posterior spiracles and surroundings yellow, bare; postspiracular scale brownish; postnotum dark brown, silver-grey pruinose on lateral margins.

Legs: Fore coxa orange-yellow, mid and hind coxae dark brown; fore coxa with long pale setulae on anterior and posterior surfaces, anterior apex with short dark setulae; mid coxa with dark setulae on anterior surface; hind coxa with dark setulae on anterior surface as well as dark setulae surrounding well-developed anterior apical point, lateral apical edges also with long dark setulae; fore trochanter orange-yellow with short pale setulae, mid trochanter dark brown, hind trochanter missing; fore and mid femora orange-yellow; hind femur missing (original description has hind femur with basal and apical third “brownish-yellow” interpreted here as orange-yellow, and middle third “black” interpreted here as blackish-brown); fore tibia blackish-brown; mid tibia darker orange-yellow than that of mid femur; hind tibia and tarsi missing (original description has hind tibia and tarsi “black”, interpreted here dark brown based of photos); fore tarsi dark brown, mid tarsi yellowish-brown; fore tarsal claws and pulvilli missing, not described; fore tarsi with long, somewhat curved sensory setulae along antero- and posteroventral surfaces, sensory setulae ca 2× as long as tarsal segment is wide; fore and hind femora with pale setulae, some darker setulae on apical dorsal surface of fore femur; fore and hind femora with long pale setulae on apical ventral and posteroventral surfaces; mid femur with long pale setulae on ventral surface; fore and mid tibiae with short dark setulae; hind leg overall stouter than remaining legs; hind tarsi missing not measured; tibial spur formula unknown.

Wing (Fig. 43): Brown suffused on apical half; darker brown stigma over apex of veins R_1 and R_{2+3} and cells sc , r_1 ; darker suffused substigmatal marking over crossvein $r-m$, bases of discal cell, cell m_3 and apex of cell br ; cell bm hyaline; veins dark brown; costa without distinct downward flexure over stigma; cell cua closed a short distance from wing margin; cell m_3 open, veins M_1 , M_2 , M_3 present; haltere stalk yellow, knob light brown, with some short and dark setulae. Holotype (NHMUK014064158) with an elongated hyaline marking in cell $r_{2+3'}$, paratype (NHMUK014064159) without such a hyaline marking.

Abdomen: Overall orange-yellow to dark orange colour; tergite 1 orange-yellow; tergites 2 and 3 with large brown markings taking up majority of surface, somewhat darker on lateral margins as well; tergites 4 and 5 orange-yellow; remaining tergites orange-brown, with posterior margins of especially tergites

7 and 8 darker; sternites orange-yellow, with sternites 3 and 4 covered in darker marking; rest of sternites orange-yellow; tergites with short dark setulae dorsally, and long pale setulae laterally; sternites with short pale setulae; tergite 1 medially with a longitudinal suture.

Terminalia: Cercus dark brown with pale setulae; internal structures unknown, type material not dissected.

Distribution. Nigeria.

***Suragina disciclara* (Speiser, 1914)**

Atherix disciclara Speiser, 1914: 3.

Suragina disciclara: Stuckenberg 1980: 313.

Type material. Not examined (see remarks), no additional material available.

Remarks. The type of *S. disciclara* (Speiser, 1914) was held in the collection of Paul Speiser and was subsequently destroyed in 1945 during the World War II bombing of Dresden, Germany by Allied forces (Evenhuis 2024). The only associated data with it is that it was female and collected on 25 February 1913 from Tiko near Viktoria [now Limbe] in Cameroon.

The characters mentioned in the original description, especially that of the frons having a "sammetschwarz" velvety-black upper half and the lower half "glänzend" interpreted as shiny or silvery, in combination with the general *Suragina*-like combination of characteristics leaves no doubt that the species belongs in the genus. However, the original description in German is not sufficient to distinguish the species from other Afrotropical species based on the text alone and subsequently the species is excluded from the identification key in this paper. Additional material will need to be collected from the type locality Tiko.

***Suragina falsa* Oldroyd, 1939**

Figs 4, 19, 44

Suragina falsa Oldroyd, 1939: 15; Stuckenberg 1980: 313.

Type material examined. [from digital photographs] **Holotype:** 1♀; UGANDA; Western Region; Ruwenzori [Rwenzori] Range, Kilembe; [00°11.8833'N, 30°00.8167'E]; 4500 ft [1372 masl]; Dec. 1934–Jan. 1935; F.W. Edwards leg.; B.M.E. Afr.Exp.; BM135-203; NHMUK 014064160 (NHMUK).

Paratypes: 1♀; same data as holotype; NHMUK014064161 (NHMUK); 2♀; Western Region; Ruwenzori [Rwenzori] Range, Namwamba Valley; [0°14.245'N, 29°58.13'E]; 6500 ft [1981 masl]; Dec. 1934–Jan. 1935; F.W. Edwards leg.; B.M.E. Afr.Exp.; BM135-203; (2♀: NHMUK014064162, 014064163) (NHMUK).

Diagnosis. An orange-yellow species, the scutum with central blackish-brown vitta, and additional pre- and postsutural dark brown markings. Notopleural area with a brown marking and silver-grey pruinosity (Fig. 4). It is most similar to *S. monogramma* (Bezzi, 1926), but that species has only a single central vitta without any additional pre- or postsutural dark markings. *Suragina monogramma*

also has its tibia brownish-yellow to orange-yellow compared to *S. falsa* that has its tibia dark brown, almost black.

Redescription. (Based on digital photographs of ♀ Holotype and 3♀ paratypes.)

Measurements (♀ n = 3): Wing span: 8.0–10.5 mm (avg. 9.3 mm); body length: 8.6–10.4 mm (avg. 9.5 mm); wing span to body length ratio (avg.): 0.98.

Male. Unknown.

Female (Fig. 19).

Head: Dark brownish-black ground colour, with silvery-grey pruinosity on majority of head; eye bare; dichoptic; ommatidia of similar size; lateral edge of eye without any indentation; ocellar tubercle slightly elevated, visible in profile, dark setulose, silvery-grey pruinose; vertex silvery-grey pruinose, with dark setulae, vertex appearing blackish dark brown when viewed posteriorly; anterior ocellus similar in size to posterior pair; ocellar tubercle in front of dorsal margin of eye; dorsal inner edge of eye without discernible paired dark markings, same silvery-grey pruinose as rest of head; occiput with same silvery-grey pruinosity; paired subrectangular blackish-brown markings with dark setulae on upper occiput running down to occipital foramen, abutting posterior margin of eyes, flanking vertex; upper occiput otherwise with pale setulae; lower occiput with lateral margins and medial area with long pale setulae, these continue ventrally on head to mouthparts that have pale ventral setulae; frons silvery-grey pruinose, velvety-black from ocellar tubercle to lower half of eye; frons running almost parallel, widening only very slightly towards antennal base in paratypes; frons with dark setulae; face and gena silvery-grey pruinose, with pale setulae; clypeus with silvery-grey pruinosity, bare; face separated anteriorly from clypeus by shallow transverse suture, deeper sutures laterally; face not appearing to bulge laterally when viewed in profile; clypeus visible in profile, face not; antennal bases separated ca 1× width of scape, with slight longitudinal groove running between; scape, pedicel mostly orange, dorsally orange-brown, otherwise with some whitish pruinosity; 1st flagellomere entirely orange; 2nd flagellomere brown; scape and pedicel of similar size; 1st flagellomere reniform, 2× size of pedicel; 2nd flagellomere arista-like; pedicel with dark dorsal and ventral setulae, similar in size, scape with only dark dorsal setulae; palpus orange with mostly darker setulae, and some interspersed pale setulae (Namwamba Valley paratype has outer lateral margins of palpus black with some white pruinosity and with dark setulae throughout, apical half of proboscis darker than in other specimens); palpus ca 0.5× length of proboscis; proboscis ca same length as head height; proboscis darker brownish-orange on apical half, orange on basal half with long pale setulae dorsally, dark setulae ventrally.

Thorax (Fig. 4): Scutum dark orange-yellow with central blackish-brown vitta with silver-grey pruinosity on presutural surface; central vitta extends to before and sometimes reaching scutellum (especially pronounced in paratype from Namwamba Valley); scutum with large paired presutural dark brown markings that do not extend into notopleuron; scutum also with smaller postsutural dark brown markings (more elongated appearance in paratype from Namwamba Valley), taking up half of posterior surface of scutum, with remaining posterior surface orange-yellow; scutum generally with short dark setulae with postsutural setulae somewhat longer; pronotum yellow with pale setulae; postpronotal

lobe yellow, with short dark setulae; notopleuron appearing silver-grey pruinose when viewed dorsally, more yellow when viewed in profile; notopleural setulae dark; postalar wall and postalar callus orange-yellow; scutellum orange-yellow with short dark setulae; majority of pleura orange-yellow with some whitish pruinosity, except for anepisternum and katepisternum that is blackish-grey with white pruinosity and meron that is dark brown with similar pruinosity; pruinose pleura with long pale setulae; anepimeron with long pale setulae, anatergite and meron bare; proepisternum and proepimeron with long pale setulae; anterior and posterior spiracles and surroundings yellow, bare; postspiracular scale orange-yellow; postnotum brown, yellow on lateral margins.

Legs: Coxae orange-yellow with mid coxa brown on inner anterior surface; fore coxa with long pale setulae on anterior and posterior surfaces; mid coxa with dark setulae on anterior surface; hind coxa with dark setulae on anterior surface as well as dark setulae surrounding well-developed anterior apical point, lateral apical edges with long pale setulae; all trochanters orange-yellow with short pale setulae, mid trochanter with dark hind margin; fore and mid femora yellow, fore femur with apical dorsal surface dark brown; hind femur yellow on apical and basal third, dark brown medially (Namwamba Valley paratypes with larger dark brown medial section); fore and hind tibiae entirely blackish-brown; mid tibia and first two tarsal segments yellow, rest of tarsi blackish-brown; fore tarsal claws and pulvilli symmetrical, pulvilus and empodium of similar size; fore tarsi with long, somewhat curved sensory setulae along antero- and posteroventral surfaces, sensory setulae ca 2× as long as tarsal segment is wide; all femora with pale setulae, some darker setulae on apical dorsal surface of fore femur; all femora with long pale setulae on apical ventral and posteroventral surfaces; mid femur with long pale setulae on ventral surface; all tibiae with short dark setulae; hind leg overall stouter than remaining legs; hind tarsal segments 1.1× as long as hind tibia; tibial spur formula 0:2:2.

Wing (Fig. 44): Brown suffused on apical half; darker brown stigma over apex of veins R_1 and R_{2+3} and cells sc , r_1 ; darker suffused substigmal marking over crossvein $r-m$, bases of discal cell, cell m_3 and apex of cell br ; cell bm hyaline; veins dark brown; costa without distinct downward flexure over stigma; cell cua closed a short distance from wing margin; cell m_3 open, veins M_1 , M_2 , M_3 present; haltere stalk yellow, knob light brown, with some short and dark setulae; paratype NHMUK014064163 from Namwamba Valley with wing appearing uniformly dark brown, whereas paratype NHMUK014064162 from same locality has similar wings except centres of each wing cell are hyaline.

Abdomen: Overall orange-yellow to dark orange colour; tergites 1–3 with a brown median marking, tergites 2 and 3 with narrow, weakly developed lateral markings; tergites 4 and less so 5 with a much darker dorsal appearance compared to preceding segments; remaining tergites dark orange; sternites with similar colour to tergites, except for sternites 4 and 5 that are distinctly dark brown; tergites with short dark setulae dorsally, and long pale setulae laterally; sternites with short pale setulae; tergite 1 medially with a longitudinal suture.

Terminalia: Cercus dark orange with dark setulae; internal structures unknown, type material not dissected.

Distribution. Uganda.

***Suragina freidbergi* Muller, sp. nov.**

<https://zoobank.org/A55946FD-E8CC-49A8-9EAD-F67317C9BA11>

Figs 8, 20, 21, 45, 63, 67, 80

Type material examined. Holotype: MALAWI • 1♂; Southern Region; Mulanje Mountain [Mulanje Massif] nr. Likabula; [15°56.983'S, 35°35.617'E]; 26–27 Oct. 1983; A. Freidberg leg.; (NMSA-DIP 158423).

Paratypes: • 3♀; same data as holotype; (NMSA-DIP 158426, 158425, 158424) • 2♀; Southern Region; Zomba Plateau, Kuchawe Trout Farm; 15°21.2333'S, 35°18.1'E; 1530 masl; 8–11 Nov. 2016; A.H. Kirk-Spriggs & B.S. Muller leg.; stream, montane evergreen forest; Malaise trap; (BMSA(D)91210, 91208) • 5♀; Southern Region; Zomba Plateau, William's Falls; 15°20.85'S, 35°17.9167'E; 1583 masl; 15–19 Nov. 2016; A.H. Kirk-Spriggs & B.S. Muller leg.; stream bed, montane evergreen forest; Malaise trap; (BMSA(D)92158, 92159, 92162, 92160, 92161) • 1♂; Southern Region; Mulanje Dist. Mulanje mnt. at.; 15°56.1667'S, 35°31.2'E; 1061 masl; 12–14 Oct. 2016; A.H. Kirk-Spriggs & B.S. Muller leg.; stream bed, miombo woodland; Malaise trap; (BMSA(D)92376).

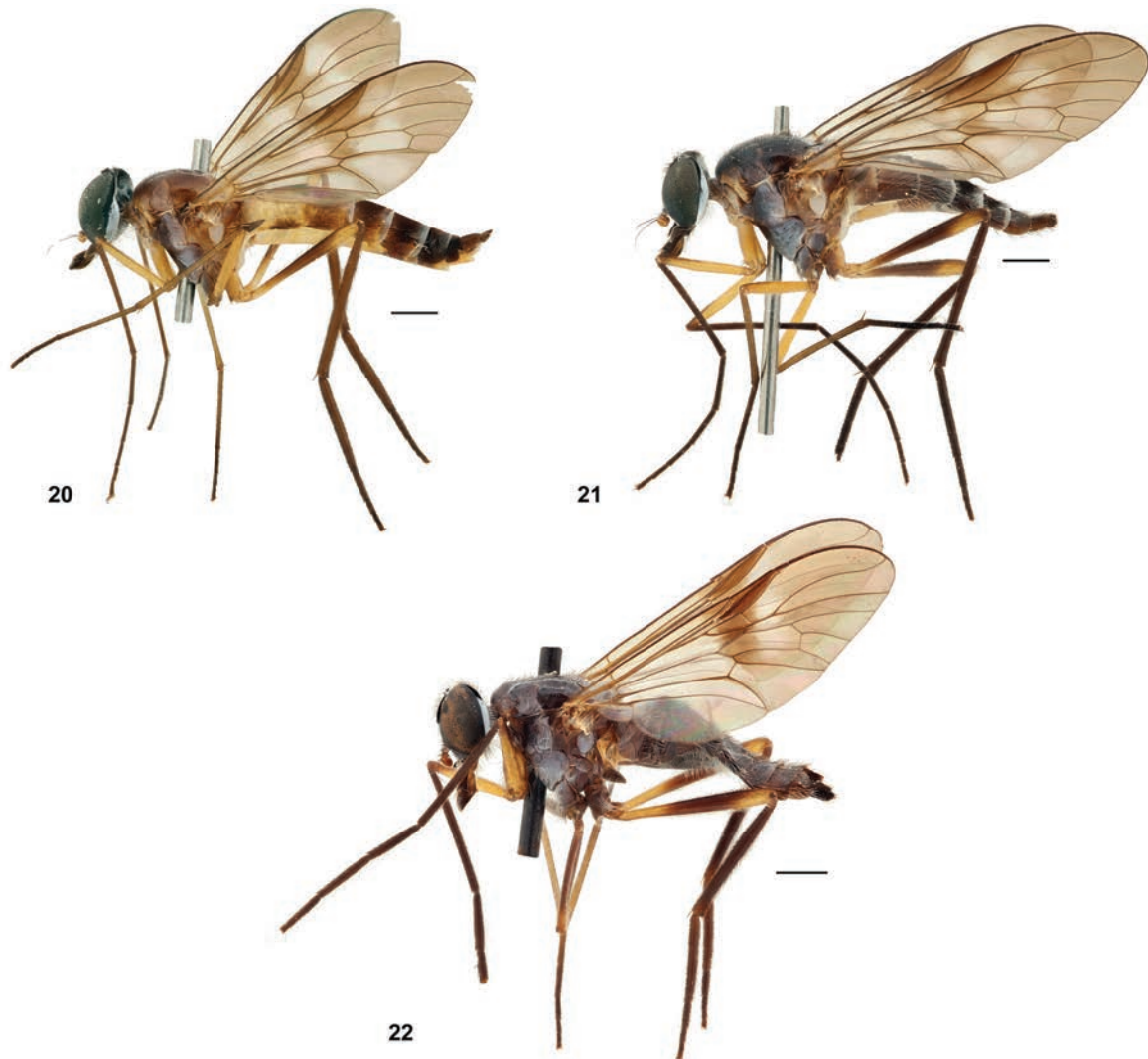
Holotype deposited in NMSA and paratypes deposited as per listed institutional codens in citations above: BMSA and NMSA.

Diagnosis. *Suragina freidbergi* Muller, sp. nov. has an overall yellowish-brown to brown appearance, with the males typically lighter in colour than the females (Fig. 20 vs Fig. 21). The pleura are brown with mostly bluish-grey pruinosity, the scutum dark brown to black with two bluish-grey pruinose dorsocentral vittae, the notopleuron with similar pruinosity (Fig. 8). The prescutellar area bluish-grey pruinose. It is most similar to *S. zombaensis* Muller, sp. nov. in its general appearance, but differs from it in having at most the apical third of the wing brown suffused, the preceding area with hyaline patches (Fig. 45), compared to *S. zombaensis* Muller, sp. nov. that has the majority of the apical half of the wing brown suffused (Fig. 54). Additionally, *S. freidbergi* Muller, sp. nov. has the scutellum yellow on at least apical half (Fig. 8) compared to *S. zombaensis* Muller, sp. nov. that has the scutellum dark brown with only the apical margin yellow.

Description. Measurements (♂ n = 2, ♀ n = 2): Wing span: ♂ 7.2–7.5 mm (avg. 7.35 mm); ♀ 8.6–9.3 mm (avg. 8.95 mm); body length: ♂ 8.9–9.0 mm (avg. 8.95 mm); ♀ 9.0–9.5 mm (avg. 9.25 mm); wing span to body length ratio (avg.): ♂ 0.94; ♀ 0.97.

Male (Fig. 20).

Head: Blackish-brown ground colour, with bluish-grey pruinosity on majority of head; eye bare; holoptic; ommatidia on lower and upper quarter of eye smaller than those on rest of eye; lateral edge of eye with slight indentation, and an apparent tubercle next to indentation; ocellar tubercle barely visible in profile, blackish-brown in colour with slight bluish-grey pruinosity and short dark setulae; vertex blackish-brown with bluish-grey pruinosity and long dark setulose; anterior ocellus larger than posterior pair; ocellar tubercle in front of dorsal margin of eye, not placed as deeply towards middle of head as in ♀; dorsal inner edge of eye abutting ocellar tubercle; occiput with same bluish-grey pruinosity as rest of head; paired narrow rectangular black markings with short dark setulae on upper occiput widening towards lateral margin of head, abutting posterior margin of eyes, flanking vertex; upper occiput with pale setulae; lower occiput with long pale setulae; genal area bluish-grey with long pale setulae,



Figures 20–22. *Suragina* Walker spp. lateral habitus: *S. freidbergi* Muller, sp. nov.: **20** ♂ holotype (NMSA-DIP 158423) **21** ♀ paratype (NMSA-DIP 158424); *S. liberiaensis* Muller, sp. nov.: **22** ♂ holotype (NMSA-DIP 158443). Scale bars: 1 mm.

these continue ventrally on head to mouthparts that have similar long ventral setulae; frons bluish-grey pruinose, velvety-black from ocellar tubercle to before lower half of eye when viewed anteriorly, when viewed anteroventrally entire frons appears blackish-brown with a slight velvety appearance; frons widening from where eyes touch down to antennal base; frons with short pale setulae; face bluish-grey with pale setulae; clypeus dark brown with bluish-grey pruinosity, bare; face separated anteriorly from clypeus by a deep transverse suture, similar to lateral sutures; face not appearing to bulge laterally when viewed in profile; clypeus visible in profile, face not; antennal bases separated ca 0.75× width of scape, with slight longitudinal groove running between; scape dark brown and pedicel orange-brown, both with silvery pruinosity; 1st flagellomere orange-yellow, with sparse silvery pruinosity; 2nd flagellomere dark brown; scape and pedicel of similar size; 1st flagellomere reniform, ca 1.5× size of pedicel; 2nd flagellomere arista-like; pedicel with dark dorsal and ventral setulae, similar in size, scape with only pale dorsal setulae; palpus brown with dense bluish-grey pruinosity, with dark setulae throughout; palpus ca 0.5× length of proboscis; proboscis slightly shorter than head height; proboscis dark orange-brown in co-

lour, prementum orange-yellow, proboscis with long pale setulae ventrally and darker setulae dorsally.

Thorax: Scutum brown, mostly with short dark setulae, with two feint dorso-central bluish-grey pruinose vittae in some specimens running from pronotum to before scutellum, joining to form a bluish-grey pruinose patch, in other specimens vittae are diffused, ending before transverse suture (Fig. 8); pronotum orange-brown with bluish-grey pruinosity and short pale setulae; postpronotal lobe orange-yellow and appearing slightly browner dorsally, with sparse grey pruinosity; setulae short pale; notopleuron bluish-grey pruinose with pale setulae anteriorly and longer dark setulae posteriorly; postalar wall and postalar callus orange-brown with slight bluish-grey pruinosity supra-alar area with dark setulae, postalar callus with some short pale setulae interspersed between dark setulae; scutellum yellow with long dark setulae; majority of pleura brown with bluish-grey pruinosity, except for anepimeron, anatergite, katatergite and katepimeron orange-yellow; proepisternum, proepimeron, katatergite and katepisternum with long pale setulae; anatergite and meron bare; anterior and posterior spiracles whitish-yellow, bare; postspiracular scale dark brown; postscutellum orange-brown.

Legs: Fore coxa yellow, mid coxa brown, blackish-brown anteriorly with a slight greyish pruinosity, hind coxa brownish-yellow; all coxae with mostly long pale setulae; fore coxal setulae entirely pale or with at most a couple of dark setulae apically; mid coxal setulae mixed pale and dark; hind coxal setulae long, and pale or dark on anterior edge surrounding well-developed anterior apical point, lateral apical edges with long pale setulae; all trochanters brownish-yellow with short pale and dark setulae; fore and mid femora almost entirely yellow, except for slightly brown apex; hind femur yellow with light brown to brown median band; fore and hind tibiae brownish-yellow, mid tibia yellow; fore and hind tarsi brown, mid basitarsus yellow; with remaining tarsi brown; fore tarsal claws asymmetrical, outer claw much larger than inner claw, foreleg empodium ca 2× size of inner pulvillus, outer pulvillus ca 2× length of inner, approaching size of outer claw; fore femur overall with short pale setulae, with long pale setulae on posteroventral surface; mid femur with long pale setulae on ventral surface, otherwise with short pale setulae; hind femur with a mix of pale and dark setulae on dorsal and ventral surfaces, base of femur with pale setulae; fore tarsi covered with long sensory setulae along antero- and posteroventral surfaces, sensory setulae ca 2× as long as tarsal segment is wide; hind leg overall stouter than remaining legs; hind tarsal segments 0.8–1.0× as long as hind tibia tibial spur formula 0:2:2.

Wing: Hyaline; dark brown stigma over area of veins R_1 and R_{2+3} and cell r_1 ; dark suffused substigmal marking running down from stigma over crossvein $r-m$, bases of discal cell, cell m_3 and apex of cell br ; apical half of wing suffused with hyaline patches in cells r_{2+3} , $r_{4'}$, $r_{5'}$, discal cell, cells m_3 and $m_{4'}$; some dark suffusion over veins CuA and CuP ; veins dark brown; costa without distinct downward flexure over stigma; cell cua closed at wing margin, cell m_3 open, veins M_1 , M_2 , M_3 present; haltere stalk yellow, knob dark brown, with a few short and dark setulae.

Abdomen: Overall brownish-yellow in colour; tergite 1 light brownish-yellow with a dark subtriangular dorsal marking surrounded by bluish-grey pruinosity; tergites 2–5 each with a dark dorsal marking covering majority of dorsal surface, less prominent on tergite 2 giving it a slight fenestrated appearance con-

trasting to brownish-yellow colour; tergites 2–5 also with lateral marginal dark marking; tergites 3–5 with grey pruinose band along posterior margin; tergite 1 medially without a longitudinal suture; tergites with dark setulae dorsally, and long pale setulae on lateral margins; sternites yellowish, with some irregular dark markings towards terminal segments; sternites with long pale setulae.

Terminalia (Figs 63, 67): Epandrium and cercus dark brown with dark setulae; gonocoxite, hypoproct and hypandrium with pale setulae; gonostylus tapering with truncated apex, outer edge of gonostylus with short setulae, inner edge with protrusion with 4 setulae, apical third of gonostylus sparsely covered in microtrichia; gonocoxite widening and appearing more rounded on apical half, apex somewhat flattened, gonocoxite outer and ventral medial surface with long setulae, inner surface of upper half with short setulae, lower ventral surface similarly long setulose; gonocoxite with microtrichia between setulae; parameral apodeme with rounded apex, not reaching base of gonocoxite in ventral view, parameral sheath including parameral apodeme ca 0.7× length of gonocoxite; gonocoxal apodeme similar in length to gonocoxite and slightly longer than ejaculatory apodeme; aedeagal tine curvature extending down past gonocoxites, apex of tines not extending out past parameral sheath; endo-aedeagal process apically truncated and widened.

Female (Fig. 21): Similar to ♂ except for the following:

Head (Fig. 8): Dichoptic; ommatidia of similar size; lateral edge of eye without any indentation, but also with apparent tubercle as in ♂; ocellar tubercle blackish-brown with brownish-grey pruinosity (bluish-grey in ♂); anterior ocellus slightly larger in size than posterior pair; ocellar tubercle placed deeper in front of dorsal margin of eye compared to ♂; dorsal inner edge of eye separated from ocellar tubercle by paired silver-grey markings, appearing to extend down from vertex; genal area with long pale setulae and one or two interspersed dark setulae (all pale in ♂) these continue ventrally on head to mouthparts that have a mix of similarly long pale and dark ventral setulae; frons bluish-grey pruinose between lower half of eye down to antennal base, velvety-black from ocellar tubercle to lower half of eye when viewed anteriorly; frons widening only slightly from velvety-black patch towards antennal bases; frons with dark setulae on velvety-black upper half and pale setulae on lower grey half; face, gena and clypeus with bluish-grey pruinosity; face sparsely populated with long pale setulae, face separated anteriorly from clypeus by transverse suture, (less prominent than in ♂); antennal bases separated ca 0.5–0.8× width of scape, with slight longitudinal groove running between; 1st flagellomere ca 1.75× size of pedicel; proboscis ca same length as head height; proboscis ventrally with both long pale and dark setulae.

Thorax (Fig. 8): Scutum blackish-brown and overall darker than in ♂ and more setulose, posterior half of scutum additionally with long pale setulae; pronotum dark brown with bluish-grey pruinosity and short pale setulae; postpronotal lobe dark brown with greyish pruinosity on anterior surface (compared to ♂ with dorsal surface also slightly pruinose), pale setulose; notopleuron with same colouration as in ♂, however, more densely setulose in comparison; postalar wall and postalar callus dark brown compared to orange-brown in ♂, and more setulose; scutellum entirely orange-yellow, or orange-yellow on apical half up to margin, and basally dark brown with slight bluish-grey pruinosity, with dark setulae; pleura similar to that of ♂.

Legs: Fore coxa yellow as in ♂ but browner anteriorly and sparsely greyish pruinose; hind coxa more widely brown in comparison to ♂; coxal setulae similar to ♂; femora similar in patterning as ♂, but markings dark brown, almost black instead of light brown to brown; fore and hind tibiae, as well as tarsi blackish, mid tibia brownish-yellow, mid basitarsus brownish-yellow; with remaining tarsi dark brown to blackish (tibia and tarsi similar in patterning to ♂, just darker); fore tarsal claws symmetrical; overall leg setation similar to ♂ except generally shorter; hind tarsal segments 0.9–1.0× as long as hind tibia.

Wing (Fig. 45): Similar to ♂.

Abdomen: Tergite 1 more densely bluish-grey pruinose than in ♂, medially with a longitudinal suture; tergite 2 in some specimens similar to ♂ with dark longitudinal marking, but surrounded by bluish-grey pruinosity instead of brownish-yellow ground colour, in others (NMSA-DIP 158425) entirely dark brown, as proceeding tergites; tergites 3–7 dark brown with dark dorsal markings barely discernible, posterior margins with similar grey pruinose bands as in ♂; tergite 1 with long pale setulae on pruinose surface, and short dark setulae on dark brown surfaces, tergites 2–6 with short pale setulae on posterior pruinose bands and short dark setulae on rest of surface; tergite 7 with short dark setulae; tergites 1–4 with long pale setulae on lateral margins, tergites 5–7 with dark setulae laterally; sternites similar to ♂ but with shorter pale setulae on surface.

Terminalia (Fig. 80): Cercus dark brown with pale setulae; genital fork with distal apodeme slender, apex truncated, unforked; median lobe with u-shaped emargination; paired apical lobes with somewhat slender appearance, widening toward apex, inner surface with clustered microtrichia at apex; arms gradually rounded; three oval and sclerotized spermathecae.

Etymology. Named after the late Dr Amnon Freidberg, in recognition of his contribution to Dipterology and as collector of much of the type material from Malawi. Noun in the genitive case.

Distribution. Malawi.

***Suragina liberiaensis* Muller, sp. nov.**

<https://zoobank.org/2015C4F4-2088-4FCF-9A5E-644DB0C1844C>

Figs 7, 22, 46, 81

Type material examined. Holotype: LIBERIA • 1♀; [Margibi]; [Harbel], Roberts Field; [6°04.91'N, 10°20.96'W]; 23 Jul. 1945; R.F Lawrence leg.; Briscoe Collection; (NMSA-DIP 158443).

Paratypes: • 1♀; same data as holotype; (NMSA-DIP 158445) • 1♀; [Margibi]; [Harbel], Roberts Field; [6°04.91'N, 10°20.96'W]; 9 Jul. 1945; R.F Lawrence leg.; Briscoe Collection; (NMSA-DIP 158442) • 1♀; [Margibi]; [Harbel], Roberts Field; [6°04.91'N, 10°20.96'W]; 10 Jul. 1945; R.F Lawrence leg.; Briscoe Collection; (NMSA-DIP 158444).

Holotype and paratypes deposited in NMSA.

Diagnosis. An overall dark brown almost black species with only the legs partially yellow (Fig. 22). The upper occiput of head with large black markings running down to occipital foramen (Fig. 7). The thorax pruinosity and wing colouration similar to species such as *S. freidbergi* Muller, sp. nov. and

S. zombaensis Muller, sp. nov., but differs by the scutellum being blackish without any yellow margins (Fig. 7). Abdomen dark brown, somewhat more yellowish from sternite 5 onwards.

Description. Measurements (♀ n = 3): Wing span: 7.1–7.9 mm (avg. 7.6 mm); body length: 8.3–9.0 mm (avg. 8.7 mm); wing span to body length ratio (avg.): 0.87.

Male. Unknown.

Female (Fig. 22).

Head (Fig. 7): Black ground colour, with bluish-grey pruinosity on majority of head; eye bare; dichoptic; ommatidia of similar size; lateral edge of eye without any indentation; ocellar tubercle elevated, visible in profile, dark setulose, bluish-grey pruinose; vertex bluish-grey pruinose, with pale setulae; anterior ocellus similar in size to posterior pair; ocellar tubercle in front of dorsal margin of eye; dorsal inner edge of eye without discernible paired dark markings, same bluish-grey pruinose as rest of head; occiput similarly bluish-grey pruinose; paired black markings with dark setulae on upper occiput running down to occipital foramen, abutting posterior margin of eyes, flanking vertex; upper occiput otherwise with pale setulae; lower occiput with lateral margins with long dark setulae, and long pale setulae medially, these continue ventrally on head to mouthparts that have mix of pale and dark ventral setulae; frons bluish-grey pruinose, velvety-black from ocellar tubercle to lower half of eye; frons running almost parallel, widening only slightly towards antennal base; frons with mixed pale and dark setulae; face and gena bluish-grey with pale and darker setulae respectively; clypeus black with bluish-grey pruinosity, bare; face separated anteriorly from clypeus by shallow transverse suture, deeper sutures laterally; face not appearing to bulge laterally when viewed in profile; clypeus visible in profile, face not; antennal bases separated ca 1× width of scape, with slight longitudinal groove running between; scape, pedicel orange to orange-brown with white pruinosity; 1st flagellomere entirely orange or at least orange at base, brown apically, 2nd flagellomere brown; scape and pedicel of similar size; 1st flagellomere reniform, 2× size of pedicel; 2nd flagellomere arista-like; pedicel with dark dorsal and ventral setulae, similar in size, scape with only dark dorsal setulae; palpus velvety-black on apical half with scattered white pruinosity, orange on basal half, with dark setulae throughout; palpus ca 0.5× length of proboscis; proboscis ca same length as head height; proboscis brownish on apical half, orange on basal half with long pale setulae dorsally, dark setulae ventrally.

Thorax (Figs 7): Scutum shining black with two feint dorsocentral bluish-grey pruinose vittae running from pronotum to before scutellum; pronotum bluish-grey pruinose with long pale setulae; postpronotal lobe orange-brown, slight bluish-grey pruinose with long pale setulae; notopleuron bluish-grey pruinose with long pale setulae just behind postpronotal lobe and rest of surface with dark setulae; postalar wall and postalar callus brown with bluish-grey pruinosity; scutellum brown with bluish-grey pruinosity, apical margin yellow; scutum generally with short dark setulae with postsutural setulae longer than presutural setulae, especially prescutellar setulae; majority of pleura bluish-grey pruinose, except for anatergite, anepimeron, part of meron brown; all pleura that are bluish-grey pruinose have long pale setulae; anepimeron with long pale setulae, anatergite and meron bare; proepisternum and proepimeron with long pale setulae; anterior and posterior spiracles and surroundings brownish-yellow, bare; postspiracular scale yellow-brown; postscutellum brown.

Legs: Fore coxa yellow with brown anterior surface, mid and hind coxae brown, all coxae with some degree of bluish-grey pruinosity on surface; fore coxa with dark setulae anteriorly and some interspersed with some pale setulae especially on posterior surface; mid coxa with long dark setulae on anterior surface, sparsely setulose along posterior margin; hind coxa with long dark setulae on anterior edge surrounding well-developed anterior apical point, lateral apical edges with long pale setulae; all trochanters yellow-brown with short pale setulae; fore femur yellow with apical dorsal surface dark brown, some brown markings at base; mid and hind femora dark brown, both yellow at extreme base and apex; fore and hind tibiae and tarsi dark brown, mid tibia and tarsi yellow; fore tarsal claws and pulvilli symmetrical, pulvillus and empodium of similar size; fore tarsi with long, somewhat curved sensory setulae along antero- and posteroventral surfaces, sensory setulae ca 2× as long as tarsal segment is wide; all femora with pale setulae, some darker setulae on dorsal surface of fore femur; all femora with long pale setulae on apical ventral and posteroventral surfaces; mid femur with long pale setulae on ventral surface; all tibiae with short dark setulae; hind leg overall stouter than remaining legs; hind tarsal segments 0.9–1.0× as long as hind tibia; tibial spur formula 0:2:2.

Wing (Fig. 46): Brown suffused on apical half starting at R_{4+5} fork, continuing along edge of wing to anal lobe; darker brown stigma and substigmal marking over apex of veins R_1 and R_{2+3} and cells sc , r_1 , base of cell $r_{2+3'}$, crossvein $r-m$, bases of discal cell, cell m_3 and apex of cell br ; cell bm hyaline; veins dark brown; costa without distinct downward flexure over stigma; cell cua closed a short distance from wing margin; cell m_3 open, veins M_1 , M_2 , M_3 present; haltere stalk yellow, knob brown, with some short and dark setulae.

Abdomen: Entirely dark brown, tergites and sternites without apparent darker markings; tergites with short black setulae on dorsal surface, long pale setulae laterally; tergite 1 with bluish-grey pruinosity, medially with a longitudinal suture, remaining tergites with similar pruinosity when viewed at an angle; sternites with long pale setulae similar to those on tergites.

Terminalia (Fig. 81): Cercus dark brown with dark setulae; genital fork with distal apodeme ending broadly with shallow fork; median lobe with evenly curved edge; paired apical lobes slender, wider than arms, inner surface with clustered microtrichia at apex; arms gradually rounded; three shortly oval and sclerotized spermathecae.

Etymology. Named after the type locality country, Liberia. Feminine adjective in the nominative singular case.

Distribution. Liberia.

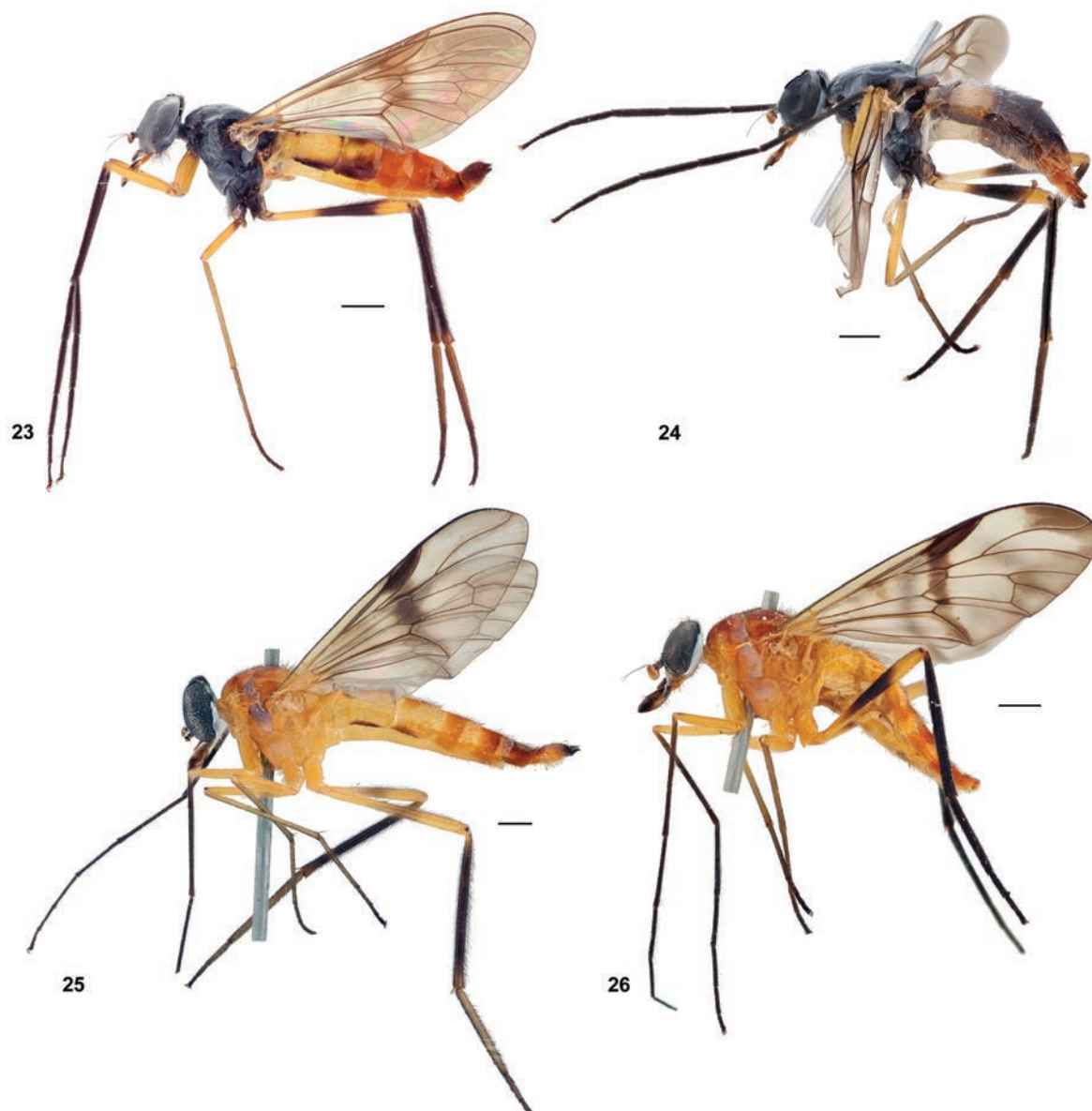
***Suragina malavaensis* Muller, sp. nov.**

<https://zoobank.org/24B5E1A6-667A-49A8-A0BB-F6CBFE1DC162>

Figs 6, 23, 24, 47, 64, 68, 82

Type material examined. Holotype: KENYA • 1♂; Western Province; Malava Forest; 00°27.8232'N, 34°51.4362'E; 1619 masl; 4–18 May 2017; R. Copeland leg.; Indigenous forest; Malaise trap; (ICIPE 3863-72).

Paratypes: • 1♂; same data as holotype; (ICIPE) • 1♂; same data as holotype; 20 Apr.–4 May 2017; (ICIPE) • 1♀; same data as holotype; 1–15 Jun. 2017; (ICIPE).



Figures 23–26. *Suragina* Walker spp. lateral habitus: *S. malavaensis* Muller, sp. nov.: 23 ♂ holotype (ICIPE 3863-72) 24 ♀ paratype (ICIPE); *S. milloti* (Séguy): 25 ♂ (BMSA(D)58540) 26 ♀ (BMSA(D)58882). Scale bars: 1 mm.

Holotype and paratypes deposited at ICIPE.

Diagnosis. A species with well-developed subtriangular upper occipital markings (Fig. 6). The wing with a hyaline band between brown suffused apical third of wing and substigmal markings (Fig. 47). The species is most similar to *S. freidbergi* Muller, sp. nov., however the latter has the upper occipital marking more rectangular (Fig. 8) than triangular, and the mid femur entirely yellow compared to that of *S. malavaensis* Muller, sp. nov. that has its mid femur yellow with the base dark. Additionally, *S. malavaensis* Muller, sp. nov. has tergites 4 and onwards orange-yellow compared to that of *S. freidbergi* Muller, sp. nov. that has tergites 3–5 with posterior grey pruinose bands.

Description. Measurements (♂ n = 2, ♀ n = 1): Wing span: ♂ 7.1–7.6 mm (avg. 7.3 mm); ♀ 8.4 mm; body length: ♂ 8.2–8.4 mm (avg. 8.3 mm); ♀ 8.9 mm; wing span to body length ratio (avg.): ♂ 0.88; ♀ 0.94.

Male (Fig. 23).

Head: Black ground colour, with bluish-grey pruinosity on majority of head; eye bare; holoptic, eyes touching; ommatidia of similar size; lateral edge of eye with indentation; ocellar tubercle elevated, visible in profile, pale setulose (rubbed bare in ♀), black in colour; vertex bluish-grey pruinose, with only pale setulae; anterior ocellus similar in size to posterior pair; ocellar tubercle in front of dorsal margin of eye, not placed as deeply towards middle of head as in ♀; dorsal inner edge of eye abutting ocellar tubercle; occiput with same bluish-grey pruinosity as rest of head; paired black markings with dark setulae on upper occiput widening towards lateral margin of head, abutting posterior margin of eyes, flanking vertex; upper occiput with similar dark setulae; lower occiput with long pale setulae, only genal area with dark setulae, these continue ventrally on head to mouthparts that have mix of pale and dark ventral setulae; frons bluish-grey pruinose, velvety-black from ocellar tubercle to lower half of eye; frons widening from velvety-black patch towards antennal base; frons bare; face and gena bluish-grey, face with pale setulae; clypeus black with bluish-grey pruinosity, bare; face separated anteriorly from clypeus by a deep transverse suture, similar to lateral sutures; face not appearing to bulge laterally when viewed in profile; clypeus visible in profile, face not; antennal bases separated ca 0.5× width of scape, with slight longitudinal groove running between; scape, pedicel same dark brown to blackish colour as rest of head, with white pruinosity; 1st flagellomere darker orange with similar pruinosity as other segments, 2nd flagellomere brown; scape and pedicel of similar size; 1st flagellomere reniform, ca 1.5× size of pedicel; 2nd flagellomere arista-like; pedicel with dark dorsal and ventral setulae, similar in size, scape with only dark dorsal setulae; palpus black on apical half with scattered white pruinosity, orange-yellow on basal half, with dark setulae throughout; palpus ca 0.5× length of proboscis; proboscis ca same length as head height; proboscis mostly orange-yellow, with some infuscation on labellum, entire structure interspersed with some long pale and dark setulae.

Thorax: Scutum shining black with two feint dorsocentral bluish-grey pruinose vittae running from pronotum to before scutellum; pronotum bluish-grey pruinose with long pale setulae; postpronotal lobe dark brown, slight bluish-grey pruinose with long pale setulae, anterolateral margin of lobe lighter yellowish to orange-brown (♀ colouring more apparent); notopleuron bluish-grey pruinose with long dark setulae and some pale setulae anteriorly; postalar wall and postalar callus dark brown with slight bluish-grey pruinosity, anterior of postalar callus orange-yellow; scutellum dark brown with bluish-grey pruinosity, entire margin orange-yellow from base to apex; scutum generally with short dark setulae with postsutural setulae longer than presutural setulae, especially prescutellar setulae; majority of pleura bluish-grey pruinose, except for anatergite, posterior of anepimeron, part of meron shiny blackish-brown; all pleura that are bluish-grey pruinose have long pale setulae; anepimeron with long pale setulae, anatergite and meron bare; proepisternum and proepimeron with long pale setulae; anterior and posterior spiracles and surroundings brownish-yellow, bare; postspiracular scale dark brown.

Legs: Fore coxa entirely yellow with only some scattered white pruinosity, mid and hind coxae blackish-brown, with bluish-grey pruinosity on surface; fore coxa with mostly pale setulae except for some dark setulae apically; mid coxa with long pale setulae on anterior surface, sparsely setulose along posterior margin; hind coxa with a mix of long pale and dark setulae on anterior edge

surrounding well-developed anterior apical point, lateral apical edges with long pale setulae; fore and hind trochanters mostly dirty yellow with edges brown, mid trochanter dark brown with yellow edges, all trochanters with short pale setulae; fore femur entirely yellow; mid femur yellow with extreme base in some specimens shiny dark brown, otherwise yellow; hind femur dark brown except for yellow basal and apical sections; fore tibia and tarsi dark brown almost black; mid tibia and basitarsus yellow, apical tarsal segments appearing darker; hind tibia blackish-brown, with apex dark yellow; hind tarsi dark brown except for dark yellow basal part of basitarsus; fore tarsal claws asymmetrical, outer claw much larger than inner claw, foreleg empodium ca 2× size of inner pulvillus, outer pulvillus ca 2× length of inner, approaching size of outer claw; fore tarsi with long, somewhat curved sensory setulae along antero- and postero-ventral surfaces, sensory setulae ca 2× as long as tarsal segment is wide; fore femur with 2–3 long pale setulae grouped together on ventral surface, similar in appearance as rest of setulae; all femora with a mix of short pale and dark and long pale setulae on dorsal surfaces; fore femur with long pale setulae on apical ventral and posteroventral surfaces; mid femur with long pale setulae on ventral surface, without dark setulae dorso-apically (present in ♀); hind femur with setulae throughout, longer pale setulae dorsally, darker surface areas with dark setulae; fore and mid tibiae with short dark setulae; hind tibia with dark setulae that are at least as long as segment is wide; hind leg overall stouter than remaining legs; combined length of hind tarsal segments subequal to hind tibia; tibial spur formula 0:2:2.

Wing (Fig. 47): Brown suffused on apical half except for middle of discal cell, base of cells r_{2+3} and r_5 that appears lighter; dark brown stigma over cell r_1 ; darker suffused substigmal marking running down from stigma over crossvein $r-m$, bases of discal cell, cell m_3 and apex of cell br ; cells bm and cua hyaline; veins dark brown, with additional brown suffusion around vein CuA ; costa without distinct downward flexure over stigma; cell cua closed a short distance from wing margin; cell m_3 open, veins M_1 , M_2 , M_3 present; haltere stalk dirty yellow, knob darker yellowish-brown, with a few short and dark setulae.

Abdomen: Tergite 1 orange-yellow with anterior and posterior margins dark brown, lateral margins orange-yellow; tergites 2 and 3 mostly orange-yellow, lateral margins also dark brown; a dark median vitta runs from anterior of tergite 1 to posterior of tergite 3; rest of tergites orange-brown without darker colouring; tergites covered in short dark setulae with longer pale setulae on lateral margins; tergite 1 medially with a longitudinal suture; sternites all orange-yellow.

Terminalia (Fig. 64, 68): Epandrium and cercus dark brown with dark setulae; gonocoxite, hypoproct and hypandrium with pale setulae; gonostylus tapering to a point, outer edge of gonostylus with some scattered short setulae, inner edge with protrusion with some short setulae, apical third of gonostylus sparsely covered in microtrichia; gonocoxite widening and appearing more rounded on apical half, apex somewhat flattened, gonocoxite outer and ventral medial surface densely covered with long setulae, inner surface of upper half bare except for a patch of short setulae on upper marginal area, lower ventral surface similarly setulose as rest of gonocoxite; gonocoxite with microtrichia between setulae; parameral apodeme with pointed apex, not reaching base of gonocoxite in ventral view, parameral sheath including parameral apodeme ca 0.9× length of gonocoxite; gonocoxal apodeme 0.8× length of gonocoxite and

of similar length as ejaculatory apodeme; aedeagal tine curvature barely extending down past gonocoxites, apex of tines not extending out past parameral sheath; endoaedeagal process ending widely bilobed apically.

Female (Fig. 24).

Head (Fig. 6): Black ground colour, with bluish-grey pruinosity on majority of head; eye bare; dichoptic; ommatidia of similar size; lateral edge of eye without any indentation; ocellar tubercle elevated, visible in profile, rubbed bare in ♀ (♂ pale setulose), bluish-grey pruinose medially when viewed dorsally, otherwise appearing black; vertex bluish-grey pruinose, with only pale setulae; anterior ocellus similar in size to posterior pair; ocellar tubercle in front of dorsal margin of eye; dorsal inner edge of eye without discernible paired dark markings, same bluish-grey pruinose as rest of head; occiput similarly bluish-grey pruinose; paired black markings with dark setulae on upper occiput widening towards lateral margin of head, abutting posterior margin of eyes, flanking vertex; upper occiput with similar dark setulae; lower occiput with long pale setulae, only genal area with dark setulae, these continue ventrally on head to mouthparts that have mix of pale and dark ventral setulae; frons bluish-grey pruinose, velvety-black from ocellar tubercle to lower half of eye; frons running almost parallel, widening only slightly towards antennal base; frons with dark setulae on velvety-black upper half and pale setulae on lower half; face bluish-grey with pale setulae; clypeus black with bluish-grey pruinosity, bare; face separated anteriorly from clypeus by shallow transverse emargination, with deeper sutures laterally; face not appearing to bulge laterally when viewed in profile; clypeus visible in profile, face not; antennal bases separated ca 0.5× width of scape, with slight longitudinal groove running between; scape, pedicel same dark brown to blackish colour as rest of head, with white pruinosity; 1st flagellomere darker orange with similar pruinosity as other segments, 2nd flagellomere brown; scape ca 2× size of pedicel; 1st flagellomere reniform, 2× size of pedicel; 2nd flagellomere arista-like; pedicel with dark dorsal and ventral setulae, similar in size, scape with only dark dorsal setulae; palpus black on apical half with scattered white pruinosity, orange-yellow on basal half, with dark setulae throughout; palpus ca 0.5× length of proboscis; proboscis approximately same length as head height; proboscis mostly orange-yellow, with some infuscation on labellum, entire structure interspersed with some long pale and dark setulae.

Thorax (Fig. 6): Scutum shining black with two feint dorsocentral bluish-grey pruinose vittae running from pronotum to before scutellum; pronotum bluish-grey pruinose with long pale setulae; postpronotal lobe dark brown, slight bluish-grey pruinose with long pale setulae, anterolateral margin of lobe a lighter yellowish- to orange-brown; notopleuron bluish-grey pruinose with long dark setulae and some pale setulae anteriorly; postalar wall and postalar callus dark brown with slight bluish-grey pruinosity, anterior of postalar callus orange-yellow; scutellum dark brown with bluish-grey pruinosity, apical margin orange-yellow, with laterobasal section appearing to have orange-yellow spot; scutum generally with short dark setulae with postsutural setulae longer than presutural setulae, especially prescutellar setulae; majority of pleura bluish-grey pruinose, except for anatergite, posterior of anepimeron, part of meron shiny blackish-brown; all pleura that are bluish-grey pruinose have long pale setulae; anepimeron with long pale setulae, anatergite and meron bare; proepisternum and proepimeron with long pale setulae; anterior and posterior spiracles and surroundings brownish-yellow, bare; postspiracular scale dark brown.

Legs: Fore coxa entirely yellow with only some scattered white pruinosity, mid and hind coxae blackish-brown, with bluish-grey pruinosity on surface; fore coxa with mostly pale setulae except for some dark setulae apically; mid coxa with long pale setulae on anterior surface, sparsely setulose along posterior margin; hind coxa with a mix of long pale and dark setulae on anterior edge surrounding well-developed anterior apical point, lateral apical edges with long pale setulae; fore and hind trochanters mostly dirty yellow with edges brown, mid trochanter dark brown with yellow edges, all trochanters with short pale setulae; fore femur entirely yellow; mid femur yellow with anteroventral basal quarter a shiny dark brown; hind femur dark brown except for yellow basal and apical sections; fore tibia and tarsi dark brown almost black; mid tibia and basitarsus yellow, apical tarsal segments appearing darker; hind tibia blackish-brown, with apex dark yellow; hind tarsi dark brown except for dark yellow basal part of basitarsus; fore tarsal claws and pulvilli symmetrical, pulvillus and empodium of similar size; fore tarsi with long, somewhat curved sensory setulae along antero- and posteroventral surfaces, sensory setulae ca 2× as long as tarsal segment is wide; fore femur with 2–3 long pale setulae grouped together on ventral surface, similar in appearance as rest of setulae; all femora with a mix of short pale and dark setulae on dorsal surfaces; fore femur with long pale setulae on apical ventral and posteroventral surfaces; mid femur with long pale setulae on ventral surface, some dark setulae dorso-apically; hind femur with short setulae throughout except for longer pale setulae towards apex; all tibiae with short dark setulae; hind leg overall stouter than remaining legs; hind tarsal segments 0.9× (♀) as long as hind tibia; tibial spur formula 0:2:2.

Wing: Brown suffused on apical half except for middle of discal cell, base of cells r_{2+3} and r_5 that is hyaline; dark brown stigma over cell r_1 ; darker suffused substigmatal marking running down from stigma over crossvein $r-m$, bases of discal cell, cell m_3 and apex of cell br ; cells bm and cua hyaline; veins dark brown, with additional brown suffusion around vein CuA ; costa without distinct downward flexure over stigma; cell cua closed a short distance from wing margin; cell m_3 open, veins M_1 , M_2 , M_3 present; haltere stalk dirty yellow, knob brown, with a few short and dark setulae.

Abdomen: Tergite 1 dark brown to black, basal margin produced anteriorly, orange-yellow with slight grey pruinosity and black edge; tergite 2 mostly orange-yellow with a dark brown median vitta running towards a narrow brown posterior margin, lateral margins also dark brown; tergites 3 and 4 dark brown, tergite 4 orange-brown along posterior margin except for dark brown median vitta which runs down tergite 5 as well; tergites 5–7 orange-yellow for most part with lateral margins same colour; abdomen covered in short dark setulae with longer pale setulae on lateral margins; pale setulae on orange-yellow sections of tergite 2; tergite 1 medially with a longitudinal suture; sternites with long pale setulae similar to those on tergites; sternites 1 and 2 pale yellow, sternite 3 brown, and rest of sternites darker orange ending in black terminalia.

Terminalia (Fig. 82): Cercus dark brown with pale setulae; sternite 8 blackish-brown; genital fork with distal apodeme narrow, ending broadly, but shallowly bifurcated; median lobe with narrow emargination; paired apical lobes with somewhat slender appearance, inner surface with clustered microtrichia at apex; arms gradually rounded; three oval and sclerotized spermathecae.

Etymology. Named after the type locality, Malava Forest, Kenya. Feminine adjective in the nominative singular case.

Distribution. Kenya.

***Suragina milloti* (Séguy, 1951)**

Figs 25, 26, 48, 65, 69, 83

Atrichops milloti Séguy, 1951: 395.

Suragina milloti: Stuckenberg 1965: 93, figs 3, 4, 7, 8; Stuckenberg 1980: 313.

Type material not examined. Holotype: MADAGASCAR • 1♂; Tsaratanana mountains; Oct. 1949; (MNHN – Séguy 1951: 395).

Other material examined. MADAGASCAR • 1♂4♀; Diégo-Suarez District [Antsiranana Province]; Madagascar-Nord, Montagne d'Ambre [National Park]; [12°30.132'S, 49°09.966'E]; 1000 masl; 23 Nov.–4 Dec. 1957; B.R. Stuckenberg leg.; (♂: NMSA-DIP 158381; ♀: NMSA-DIP 158379, 158380, 028165) (NMSA) • 1♀; Madagascar-Nord, Analamerana [Special Reserve], 50 km SE Diégo-Suarez [Antsiranana], [12°48.00'S, 49°30.00'E]; 80 masl; Jan. 1959; R. Andria leg.; NMSA-DIP 028166 • 1♀; Antsiranana [Province]; Montagne d'Ambre NP [National Park]; 12°32.46'S, 49°10.08'E; 1190 masl; 14 Nov. 2017; M. Hausler leg.; FFP17MAD59 • 1♂1♀; [Atsinanana Region]; Torotorofotsy, Andasibe (Perinet), 22 km NW, Moramonga; 18°46.25'S, 48°25.93'E; 960 masl; 23–25 Oct. 2014; A.H. Kirk-Spriggs, R. Harin'Hala leg.; Malaise trap, primary rainforest; (♂: BMSA(D)58541; ♀: BMSA(D)58540) (BMSA) • 1♂5♀; Fianarantsoa Province; Ranomafana National Park, Talatakely, 800 m SW entrance, Ifanadiana; 21°15.48'S, 47°25.27'E; 610 masl; 16–19 Oct. 2014; A.H. Kirk-Spriggs, R. Harin'Hala leg.; Malaise trap, secondary rainforest; (♂: BMSA(D)58880; ♀: BMSA(D)58879, 58878, 58879, 58881, 58882) (BMSA) • 2♂13♀; Ranomafana National Park, radio tower; 21°15.05'S, 47°24.43'E; 1127 masl; 23–30 Apr. 2002; M.E. Irwin, R. Harin'Hala leg.; Malaise trap in open area nr forest edge; (CSCA) • 1♂; Ranomafana National Park, radio tower; 21°15.05'S, 47°24.43'E; 1127 masl; 27.iv–7 May 2003; R. Harin'Hala leg.; Malaise trap in open area, forest edge; MA02-098-59; (CSCA) • 2♀; Sofia Region; Mahajanga; Amkarafa; 14°23.15'S, 47°45.45'E; 180 masl; 5–11 Nov. 2015; M. Irwin, R. Rasolondalao leg.; MG-69-11; (CSCA).

Diagnosis. *Suragina milloti* is most similar in appearance to other orange-yellow species such as *S. agramma*, *S. copelandi* Muller, sp. nov. and *S. mulanjeensis* Muller, sp. nov. However, *S. agramma* and *S. copelandi* Muller, sp. nov. have the notopleural area the same orange-yellow as the rest of the scutum (e.g. Fig. 1), whereas the notopleural area between the postpronotal lobe and suture is covered in a dark subrectangular mark with bluish-grey pruinosity in *S. milloti* and *S. mulanjeensis* Muller, sp. nov. (Fig. 6). *Suragina mulanjeensis* Muller, sp. nov., however, has its abdominal tergites with dark medial markings compared to the more uniform orange-yellow abdomen of *S. milloti*. Additionally, *S. milloti* has the substigmatal marking of the wing much darker and more apparent (Fig. 48) compared to the other species.

Redescription. Measurements (♂ n = 2, ♀ n = 2): Wing span: ♂ 8.8–9.9 mm (avg. 9.38 mm); ♀ 8.9–9.0 mm (avg. 8.94 mm); body length: ♂ 9.6–11.6 mm

(avg. 10.6 mm); ♀ 9.2–10.0 mm (avg. 9.6 mm); wing span to body length ratio (avg.): ♂ 0.89; ♀ 0.94.

Male (Fig. 25).

Head: Dark brown ground colour, with silvery-grey pruinosity on majority of head; eye bare; holoptic; ommatidia of similar size; lateral edge of eye with slight indentation (absent in ♀); ocellar tubercle slightly more elevated than frons, blackish with dark setulae; vertex grey pruinose (appearing dark brown at certain angles), with long dark setulae; anterior ocellus slightly larger than posterior pair; ocellar tubercle in front of dorsal margin of eye, margin less indented than in ♀; vertex narrower than in ♀; dorsal inner edge of eye without discernible paired dark markings; occiput with same silver-grey pruinosity as rest of head, except for paired narrow elongated subrectangular dark brown almost velvety-black markings (ca 2× as tall in ♀) with short dark setulae on upper occiput, abutting posterior margin of eyes, flanking vertex; reniform dark brown marking surrounding occipital foramen; rest of upper occiput with short pale setulae and lower occiput with long pale setulae, these continue ventrally on head to mouthparts that have similar pale ventral setulae at base; frons silver-white up to area before eyes touch when viewed dorsally, dark velvety-brown when viewed anteriorly down to before antennal bases; frons at narrowest where eyes touch, widening towards antennal base; with a longitudinal groove running from ocellar triangle down to before antennal base, narrowly separating eyes; frons bare; face and gena silver-white, appearing bare; lateral facial margins with markings that appear dark brown when viewed anteriorly from underneath, but otherwise appearing silver-grey; clypeus brown with silver-grey pruinosity, bare; face separated from clypeus by a prominent, deep suture on anterior and lateral edges; face not appearing to bulge laterally when viewed in profile; clypeus visible in profile, face not; antennal bases separated ca 0.5× width of scape, with slight longitudinal groove; scape and pedicel dark brown with silver-grey pruinosity, scape and pedicel of similar height, but pedicel somewhat thinner; 1st flagellomere orange-yellow, 2nd flagellomere dark brown; 1st flagellomere reniform, 2× as tall as pedicel; 2nd flagellomere arista-like; scape and pedicel with dark dorsal setulae, scape bare ventrally, pedicel with dark ventral setulae of similar size to dorsal setulae; palpus brownish-orange, darker ventrally, well-developed, ca 0.5× length of proboscis; palpus with long dark setulae ventrally and some shorter dark setulae dorsally; proboscis comparatively shorter than that of ♀ in relation to head; proboscis orange-yellow, with darker apex, mostly with short dark setulae, some long pale setulae basoventrally and long dark setulae on labrum; some scattered small pale ventral setulae on proboscis.

Thorax: Majority of surface, including scutum, orange-yellow, dorsal surface of scutum with short dark setulae; scutellum with long dark setulae similar to those on postsutural area of scutum; postsutural setulae, especially those on posterior half of postsutural area longer than remaining setulae of scutum; postpronotal lobe yellow with pale setulae, lighter than surroundings; almost entire notopleural area between postpronotal lobe and suture covered in a dark subrectangular mark with bluish-grey pruinosity, dark colour much more visible when viewed in profile; scutellum similarly orange-yellow as scutum, with some specimens having apical half more yellow compared to rest; postscutellum orange-yellow; all pleura yellow except for anepisternum that is similar brown

colour to notopleural area; anepisternum and katepisternum slight bluish-grey pruinose, remaining pleura with only some scattered greyish pruinosity; notopleuron with long dark setulae; area surrounding posterior spiracle yellow, postspiracular scale yellow; proepisternum, pronotum yellow; anterior spiracle bare posteriorly, area surrounding it orange-yellow; proepimeron, proepisternum, anepisternum and katatergite with pale setulae, rest of pleura bare.

Legs: All coxae yellow (sometimes lightly tinged with brown) and with pale setulae; all coxae with longer pale setulae on anterior surface, long pale setulae along posterior margin of fore and hind coxal posterolateral margins; hind coxa with well-developed anterior apical point; all trochanters yellow with some scattered short pale setulae; all femora yellow; hind femur with a light brown median band that can be difficult to observe; mid and hind femora with small anterior apical dark mark; fore and hind tibiae dark brown, mid tibia yellow; fore tarsi dark brown; mid and hind tarsi yellow, but appearing darker brown towards apex; fore tarsal claws asymmetrical, outer claw much larger than inner claw, foreleg empodium ca 2× size of inner pulvillus, outer pulvillus ca 2× length of inner, approaching size of outer claw; fore and mid femora covered with pale setulae on all surfaces, additionally dorsoapical surface of both with some very short dark setulae; hind femur with longer pale setulae at base, mostly dark setulae on dorsal surface and mostly pale setulae on ventral surface, fore and hind femora anteriorly with shorter setulae and posteriorly with longer setulae; hind leg overall stouter than remaining legs; fore tarsi covered with long sensory setulae along antero- and posteroventral surfaces, sensory setulae ca 2× as long as tarsal segment is wide; fore and mid tibiae covered in short dark setulae, hind tibia with longer dark setulae; combined length of hind tarsal segments subequal to hind tibia; tibial spur formula 0:2:2 (some specimens 1:2:2), mid spur orange-yellow, hind spur reddish-brown.

Wing: Overall light brown suffused appearance; darker stigma over area of veins R_1 and R_{2+3} and cell r_1 ; darker elongated suffused substigmal marking over base of cell r_{2+3} , apex of cell br , base of discal cell and cell m_3 ; additionally some slightly darker suffusion over basal half of cell br and vein CuA ; veins brownish; costa without distinct downward flexure over stigma; cell cua closed a short distance from wing margin; cell m_3 open, veins M_1 , M_2 , M_3 present; haltere entirely orange-yellow, with some very short dark setulae.

Abdomen: Yellow to orange-yellow; tergites 1–3 yellow, remaining tergites more orange-yellow; tergites 2–4 with a lighter yellow anterior margin; tergites 2 and 3 with brown lateral markings; tergites 1–3 with a poorly defined suffused marking running along dorsal surface; sternites yellow; tergites with short black setulae on median-dorsal surface and long pale setulae on lateral margins; sternites with long pale setulae; tergite 1 without weak median longitudinal suture.

Terminalia (Figs 65, 69): Epandrium reddish-orange, dark brown along apical margin, cercus dark brown with dark setulae; hypoproct and hypandrium with pale setulae; gonostylus somewhat tapering with truncated apex, outer edge of gonostylus with some scattered short setulae, inner edge with small protrusion with 2–4 setulae, apex of gonostylus sparsely covered in microtrichia; gonocoxite widening apically, subrectangular in shape, apex somewhat flattened, gonocoxite outer, ventral medial and lower surfaces with long setulae, inner surface

of upper half with shorter setulae; gonocoxite with microtrichia between setulae; parameral apodeme ending with a hook-like apex, almost reaching base of gonocoxite in ventral view, parameral sheath including parameral apodeme ca 0.8× length of gonocoxite; gonocoxal apodeme similar in length to gonocoxite and slightly longer than ejaculatory apodeme; aedeagal tine curvature extending down past gonocoxites, apex of tines barely extending out past parameral sheath; endoaedeagal process apically truncated and widened.

Female (Fig. 26): Similar to ♂ except for the following:

Head: Orange-brown ground colour; dichoptic; lateral edge of eye without indentation (slight in ♂); dorsal margin of eye more indented than in ♂; vertex silver-grey when viewed anteriorly, wider than in ♂ with long dark setulae that are much more apparent than in ♂, dark brown when viewed dorsally; upper frons appearing to extend up dorsal inner edge of eye with paired dark markings, but only visible when viewed anteriorly, otherwise area similarly silver-white pruinose; occiput with same silver-white pruinosity as rest of head, except for paired dark brown, almost black subrectangular markings on upper occiput that are taller than in ♂; frons velvety-black from ocellar tubercle down to lower half of eye, silver-grey down to antennal base, if viewed anteroventrally velvety-black appearance seemingly extends down to between antennal bases; short dark setulose on velvety-black upper half of frons, bare on silver-white pruinose area past middle of eye; when viewed posterodorsally there is a clear divide between velvety-black upper half and silver-grey lower half of frons; frons at narrowest ca 2× width of ocellar tubercle, widening slightly towards antennal base; face separated anteriorly from clypeus by shallow transverse emargination, deeper sutures laterally; clypeus orange base colour with slight whitish pruinosity; palpus basal segment orange-yellow with long pale setulae, apical segment black with silver-grey pruinosity and long dark setulae; proboscis with overall infuscated appearance, with ventral surface yellowish, dark setulae throughout.

Thorax: Anepisternum light brown, more apparent on upper surface; similar pruinosity as in ♂, but denser.

Legs: Same patterning as in ♂, but darker brown colour compared to lighter brown ♂, especially evident on median band of hind femur.

Wing (Fig. 48). Overall light brown suffused appearance; darker stigma over area of veins R_1 and R_{2+3} and cell r_1 compared to ♂; darker elongated suffused substigmatal marking over base of cells r_{2+3} and $r_{5'}$, apex of cell br , base of discal cell and cells m_3 and m_4 ; additionally some darker blotchy suffusion on basal half of cell br and widely suffused over vein CuA ; darker suffused over apical half of cells r_{2+3} and r_4 , apical third of cells r_4 , m_3 and m_4 and entirety of cells m_1 and m_2 ; veins dark brown.

Abdomen: Similar to ♂, lateral dark markings on tergites 2 and 3 only dark orange, not brown; suffused dorsal markings not evident on tergites.

Terminalia (Fig. 83): Cercus orange-yellow with pale setulae; genital fork with distal apodeme ending broadly truncated with a bilobed appearance; median lobe with wide, moderate emargination; paired apical lobes with somewhat slender appearance, inner surface with clustered microtrichia at apex; arms gradually rounded; three oblong and sclerotized spermathecae.

Distribution. Madagascar.

***Suragina monogramma* (Bezzi, 1926)**

Figs 27, 28, 49, 66, 70, 84

Atrichops monogramma Bezzi, 1926: 305.

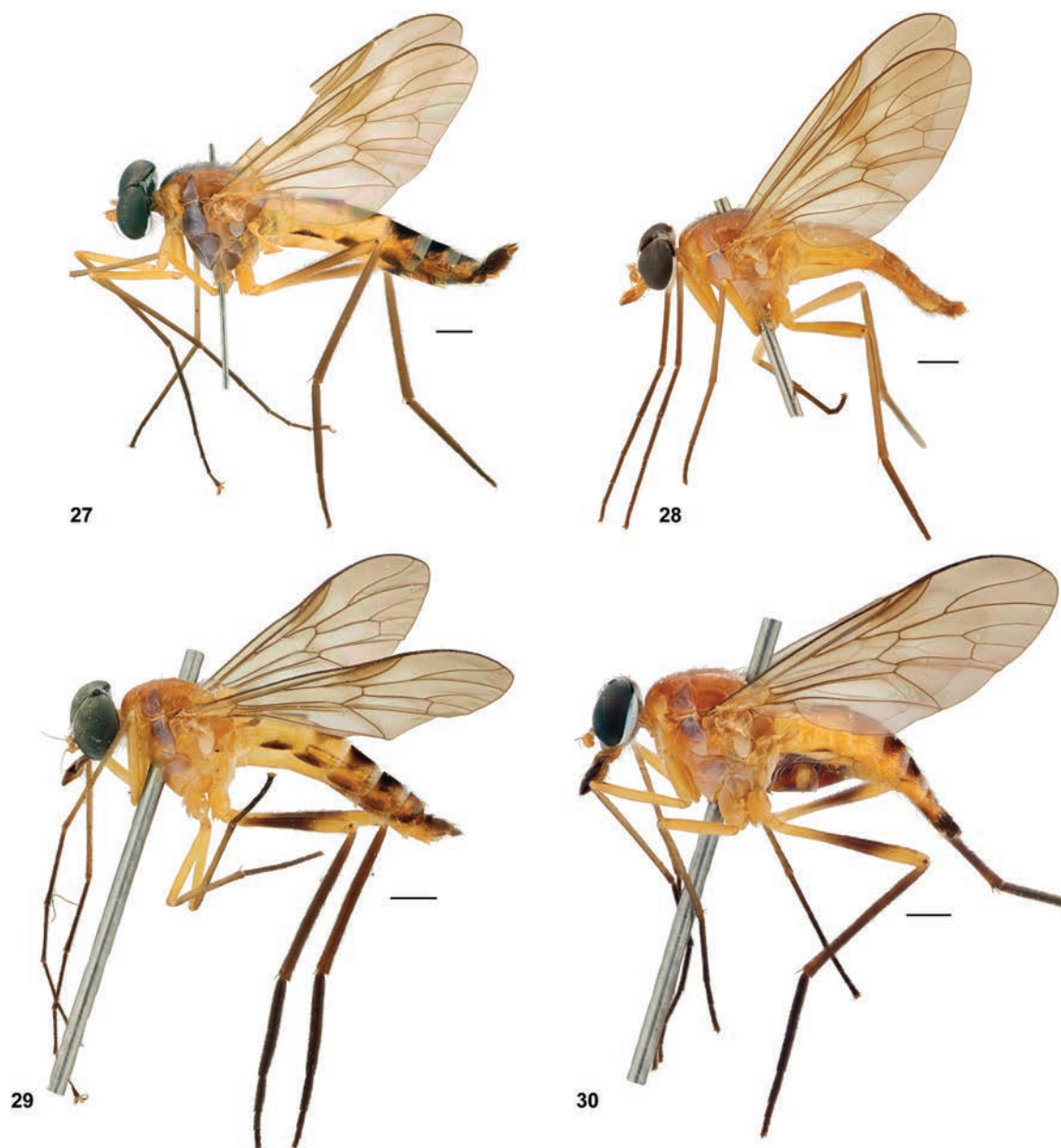
Suragina monogramma: Stuckenberg 1960: 288, fig. 87; Stuckenberg 1980: 313.

Atrichops inaequalis Bezzi, 1926: 307; synonymised by Stuckenberg 1960: 288.

Type material examined. Holotype: 1 ♀ [SOUTH AFRICA] • [KwaZulu-Natal], Mfongosi, Zulu L. [Land]; [28°42.69'S, 30°49.95'E]; W.E. Jones leg.; Dec. 1916; (SAM-DIP-A006860).

Other material examined. ♂♀ Types of *Atrichops inaequalis*: SOUTH AFRICA • KwaZulu-Natal: K. Kloof [Kranzkloof, now Kloof], [29°45.858'S, 30°51.0529'E]; Dec. 1915, Marley leg.; (SAM-DIP-A006861). MOZAMBIQUE: • 4 ♂3 ♀; [Sofala Province] Gorongoza Mountain, Manica Sofala Dist; [18°45.96'S, 34°30'E]; 840 masl; Jul. 1959; B.R. Stuckenberg leg.; Gallery Forest; (♂:NMSA-DIP 028168, 158383, 158384, 162050; ♀: NMSA-DIP 027714, 158382, 158385). SOUTH AFRICA • 1 ♂; KwaZulu-Natal; Pinetown district, Gillitts; [29°47.85'S, 30°47.20'E]; Feb. 1963; B.R. Stuckenberg & P. Stuckenberg leg.; (♂:NMSA-DIP 158416; ♀: NMSA-DIP 158412, 158413, 158414) • 1 ♂; KwaZulu-Natal; Pinetown district, Gillitts; [29°47.85'S, 30°47.20'E]; 21 Nov. 1963; B.R. Stuckenberg & P. Stuckenberg leg.; (NMSA-DIP 028180) • 1 ♀; KwaZulu-Natal; Pinetown district, Gillitts; [29°47.85'S, 30°47.20'E]; 28 Dec. 1961; B.R. Stuckenberg & P. Stuckenberg leg.; (NMSA-DIP 028176) • 1 ♀; KwaZulu-Natal; Woodgrove Retirement Village; 30°21.9167'S, 30°21.9333'E; 10 Oct. 2018; Londt, J.G.H.; in garden; (NMSA-DIP 205579) • 1 ♀; KwaZulu-Natal; Merrivale dist.; 29°30.00'S, 30°14.00'E; 14 Nov. 2006; B.R. Stuckenberg leg.; (NMSA-DIP 158391) • 1 ♀; KwaZulu-Natal; Royal Natal National Park, Thendele Camp [nr Devil's Hoek path, forest patch]; 28°42.62'S, 29°56.04'E; 14–17 Jan. 2019; J. Midgley & K. Williams leg.; Malaise trap; (NMSA-DIP 102630) • 1 ♀; KwaZulu-Natal; Mtamvuna Nature Reserve; 3130AA [31°06.00'S, 30°09.6'E]; 10–15 Jan. 1982; J.G.H. Londt leg.; Malaise trap; (NMSA-DIP 158388) • 1 ♀; KwaZulu-Natal; Pietermaritzburg, Ashburton; 29°49.3167'S, 30°27.1'E; ca 630 masl; 22 Nov. 2009; R.M. Miller leg.; in house; (NMSA-DIP 192953) • 2 ♀; KwaZulu-Natal; Royal Natal National Park; 2828DB [28°41.34'S, 28°56.7'E]; Jan. 1971; H. Townes leg.; late January; (NMSA-DIP 158448, 1588449) • 1 ♀; KwaZulu-Natal; Royal Natal National Park; [28°41.34'S, 28°56.7'E]; 6–10 Dec. 1984; J.G.H. Londt leg.; Riverine bush, Montane slopes; (NMSA-DIP 028175) • 1 ♀; KwaZulu-Natal; Shawswood, Karkloof; 29°18.1'S, 30°18.25'E; 18 Nov. 2020; L., Mva leg.; (BMSA(D)129988) • 2 ♂; KwaZulu-Natal; K. Kloof [Krantzkloof]; [29°45.858'S, 30°51.0529'E]; Dec. 1915; Marley leg.; (NMSA-DIP 028160, 158386) • 1 ♂; Mpumalanga; Gladde-spruit river, nr. Nelspruit Airfield; 2530DB [25°30.628'S, 30°53.941'E]; 2975 ft; 3 Nov. 1970; B.R. Stuckenberg leg.; Streamside bush; (NMSA-DIP 028170) • 1 ♀; Eastern Cape; Hogsback; 3226DB [32°35.88'S, 26°56.28'E]; 13–16 Dec. 1985; J.G.H. Londt & B. Londt leg.; Forest and Forest margins; (NMSA-DIP 158387).

Diagnosis. An orange-yellow species (Figs 27, 28) with a black median vitta on the scutum that contrasts with the surrounding orange-yellow colour and runs down to before the scutellum. The median vitta is also flanked by bluish-grey pruinosity. Additionally, almost the entire notopleural area is covered with a dark subrectangular mark with silver-grey pruinosity. The abdomen has dark narrow median markings. *Suragina monogramma* is most similar to *S. fal-*



Figures 27–30. *Suragina* Walker spp. lateral habitus: *S. monogramma* (Bezzi): 27 ♂ (NMSA-DIP 028180) 28 ♀ (NMSA-DIP 158385); *S. mulanjeensis* Muller, sp. nov.: 29 ♂ holotype (NMSA-DIP 158398) 30 ♀ paratype (NMSA-DIP 158394). Scale bars: 1 mm.

sa (Fig. 19), however, the latter has the scutum with central blackish-brown vitta, and additional pre- and postsutural dark brown markings (Fig. 4), whereas *S. monogramma* does not have the mentioned dark brown markings. Additionally, *S. monogramma* has its tibia brownish-yellow to orange-yellow compared to *S. falsa* that has its tibiae dark brown, almost black.

Redescription. Measurements (♂ n = 2, ♀ n = 2): Wing span: ♂ 7.0–7.6 mm (avg. 7.3 mm); ♀ 7.5–9.7 mm (avg. 8.6 mm); body length: ♂ 7.4–9.6 mm (avg. 8.5 mm); ♀ 7.2–10.7 mm (avg. 8.9 mm); wing span to body length ratio (avg.): ♂ 0.87; ♀ 0.97.

Male (Fig. 27).

Head: Dark brown colour, with silver-white pruinosity on majority of head; eye bare; holoptic; ommatidia of similar size; lateral edge of eye with slight indentation

(absent in ♀); ocellar tubercle slightly more elevated than frons, with pale setulae, colour black with slight greyish pruinosity; vertex whitish-grey pruinose, with long pale setulae; anterior ocellus same size as posterior pair; ocellar tubercle in front of dorsal margin of eye, margin less indented than in ♀; vertex narrower than in ♀; dorsal inner edge of eye without discernible paired dark markings; occiput with same silver-white pruinosity as rest of head, except for paired narrow dark brown, almost velvety-black (ca 2× as tall in ♀) markings with short dark setulae on upper occiput, abutting posterior margin of eyes, flanking vertex; small subrectangular brownish patch below vertex; upper occiput with short pale setulae on dorsal margin and rest of upper surface, lower occiput with long pale setulae, these continue ventrally on head to mouthparts that have similar pale ventral setulae at base; frons silver-white up to narrow area before eyes touch when viewed dorsally, dark velvety-brown when viewed anteriorly; frons at narrowest where eyes touch, widening towards antennal base; frons bare; face and gena silver-white with pale setulae, lateral facial margins with markings that are same dark velvety-brown as frons when viewed anteriorly; clypeus brownish with silver-white pruinosity, bare; face separated from clypeus by a prominent, deep suture on anterior and lateral edges; face not appearing to bulge laterally when viewed in profile; clypeus visible in profile, face not; antennal bases separated ca 0.75× width of scape, with slight longitudinal groove; scape and pedicel orange-yellow, sometime infuscated dorsally; 1st flagellomere orange-yellow, 2nd flagellomere brownish; 1st flagellomere reniform, only slightly larger than pedicel and scape; 2nd flagellomere arista-like; scape and pedicel with dark dorsal setulae, scape bare ventrally, pedicel with dark ventral setulae of similar size to dorsal setulae; palpus orange-yellow, well-developed, ca 0.5× length of proboscis; palpus with dark setulae on apical half and longer pale setulae on lower half; proboscis comparatively shorter than that of ♀ in relation to head; proboscis orange-yellow with long dark setulae, similar setulae ventrally; some scattered small pale setulae on proboscis.

Thorax: Majority of surface orange-yellow, dorsal surface of scutum with short dark setulae; scutellum with long dark setulae similar to those on postsutural area of scutum; postsutural setulae, especially those on posterior half of postsutural area, longer than remaining setulae of scutum; postpronotal lobe yellow, lighter than surroundings; almost entire notopleural area between postpronotal lobe and suture covered in dark subrectangular mark with silver-grey pruinosity, dark colour much more visible when viewed in profile; marking separated from median vittae in majority of specimens, but in some from Mozambique, mark is joined with median vittae which is much wider (see Stuckenberg 1960: 289); scutum with black median vitta that is sparsely grey pruinose and runs anteriorly from behind pronotum down to just before scutellum; median vittae pinched at posterior end in some specimens, ending more broadly in others; median vittae bordered by bluish-grey pruinose dorsocentral vittae that fade out posteriorly; scutellum uniformly orange-yellow with basal area dark brown, some specimens basal half dark brown; postscutellum dark brown; anepisternum, katapisternum, meron, katapimeron and katatergite dark brown with bluish-grey pruinosity, remaining pleura orange-yellow with only slight whitish pruinosity; notopleuron with long dark setulae; area surrounding posterior spiracle yellow, postspiracular scale orange-yellow; proepisternum, pronotum yellow; anterior spiracle bare posteriorly, area surrounding it orange-yellow; proepimeron, proepisternum, anepisternum and katatergite with pale setulae, rest of pleura bare.

Legs: Fore and hind coxae yellow; mid coxa sometimes brown on anterior surface and some bluish pruinosity; fore coxa with pale setulae, mid and hind coxae with pale setulae, and on anterior apical surface and margins with dark setulae; all coxae with longer pale setulae on anterior surface except for long pale setulae on posterolateral margin of hind coxa; hind coxa with well-developed anterior apical point; all trochanters same yellow as coxae, with some scattered short pale setulae; all femora yellow; hind femur with a median dark band, appearing absent or very weak in specimens from Gillets, KwaZulu-Natal; mid and hind femora with small anterior apical dark mark; fore and hind tibiae and tarsi dark brown, much lighter brown, almost dark yellow in specimens from Gillets, KwaZulu-Natal; mid tibia yellow, tarsi brownish; fore tarsal claws asymmetrical, outer claw much larger than inner claw, foreleg empodium ca 2× size of inner pulvillus, outer pulvillus ca 2× length of inner, approaching size of outer claw; fore and mid femora covered with pale setulae on all surfaces, mid femur with ventro-apical surface with some short dark setulae, hind femur with mixed long pale and dark setulae on dorsal and ventral surfaces, basally with long pale setulae, anteriorly with short setulae and posteriorly with longer setulae; hind leg overall stouter than remaining legs; fore tarsi covered with long sensory setulae along antero- and posteroventral surfaces, sensory setulae ca 2× as long as tarsal segment is wide; fore and mid tibiae covered in short dark setulae, hind tibia with longer dark setulae; combined length of hind tarsal segments subequal to hind tibia; tibial spur formula 0:2:2 or 1:2:2 in some specimens.

Wing: Appearing mostly hyaline, with light brown suffused appearance on apical half of wing, with discal cell (except for basal third), cell *cua*, parts of cells *br* and *bm* hyaline; with darker stigma over area of veins R_1 and R_{2+3} and cell r_1 ; veins brownish; costa without distinct downward flexure over stigma; cell *cua* closed a short distance from wing margin; cell m_3 open, veins M_1 , M_2 , M_3 present; haltere entirely orange-yellow, with some very short dark setulae.

Abdomen: Yellow to orange-yellow; tergite 1 without dark lateral border, tergites 2–6 always with dark brown lateral borders, but more prominent on tergites 2–4; pattern of median dark markings on dorsal surface of tergites variable but distinctive from surroundings; tergites 1–6 usually with a dark median marking, especially on tergites 1–4; dark brown marking on tergite 3 may be incomplete; each dark marking has a brown suffusion surrounding it, giving marking a posteriorly tapering subtriangular appearance in some specimens; tergite 7 dark brown; in some specimens tergites 3–6 have greyish pruinose borders; sternites yellow, but in some specimens these are discoloured and may appear darkened due to dried gut contents; tergites with short black setulae on median-dorsal surface of tergites, with long pale setulae on lateral margins; sternites with long pale setulae; tergite 1 without median longitudinal suture.

Terminalia (Figs 66, 70): Epandrium and cercus dark brown with dark setulae; hypoproct and hypandrium with pale setulae; gonostylus tapering with truncated apex, outer edge of gonostylus with short setulae, inner edge with protrusion with 2–4 setulae, apex of gonostylus sparsely covered in microtrichia; gonocoxite widening and appearing more rectangular than rounded on apical half, apex somewhat flattened, gonocoxite outer and ventral medial surface with long setulae, inner and ventral surfaces of upper half with short setulae, lower ventral surface comparatively less setulose; gonocoxite with microtrichia between setulae; parameral apodeme with truncated, rectangular

apex, not reaching base of gonocoxite in ventral view, parameral sheath including parameral apodeme ca 0.7× length of gonocoxite; gonocoxal apodeme similar in length to gonocoxite and slightly longer than ejaculatory apodeme; aedeagal tine curvature extending down past gonocoxites, apex of tines not extending out past parameral sheath; endoaedeagal process apically truncated and widened.

Female (Fig. 28): Similar to ♂ except for the following:

Head: Dichoptic; lateral edge of eye without indentation (slight in ♂); ocellar tubercle with short dark setulae; dorsal margin of eye more indented than in ♂; vertex wider than in ♂, without subrectangular mark underneath vertex; silver-white pruinose directly behind ocellar tubercle up to posterior of eye margin; dorsal inner edge of eye with paired dark markings, but only visible when viewed anteriorly, otherwise area similarly silver-white pruinose; occiput with same silver-white pruinosity as rest of head, except for paired subtriangular (ca 2× as tall as ♂) dark brown, almost black markings on upper occiput, abutting posterior margin of eyes, and flanking but not touching vertex; frons velvety-black from ocellar tubercle down to lower half of eye, silver-white down to antennal base; frons mixed pale and dark setulose on velvety-black area, bare on silver-white pruinose area past middle of eye (♂ bare), when viewed posteriorly silver-white colour shifts upwards, at narrowest ca 2× width of ocellar tubercle, widening slightly towards antennal base; face separated anteriorly from clypeus by shallow transverse emargination, deeper sutures laterally; clypeus orange base colour with slight greyish pruinosity; 1st flagellomere ca 2× size of pedicel; scape and pedicel sometimes infuscated dorsally otherwise entirely orange-yellow with some whitish pruinosity.

Thorax: Katepisternum orange-yellow compared to dark brown of ♂, but still with same bluish-grey pruinosity; meron and katepimeron orange-yellow (dark brown in ♂); postscutellum reddish-brown (♂ dark brown).

Legs: All coxae with only pale setulae; mid coxa with whitish pruinosity on anterior surface (♂ bluish-grey); fore tarsi symmetrical; setulae of femora overall shorter (compared to ♂) except for preapical ventral area of fore femur that has long pale setulae, and apical dorsal area that has short dark setulae; hind femur with mix of short pale and dark setulae.

Wing (Fig. 49): Similar to ♂.

Abdomen: Variable, much as in ♂: overall orange-yellow; tergites 1–6 with a dark median marking, tergite 1 not marked, tergites 1–3 with dark median marking, entire abdomen irregularly marked with dark brown colour, or abdomen entirely blackish-brown.

Terminalia (Fig. 84): Cercus orange-yellow with pale setulae; genital fork with distal apodeme ending broadly rounded-bilobed; median lobe with wide, moderate emargination; paired apical lobes with somewhat slender, elongated rectangular appearance, inner surface with clustered microtrichia at apex; arms gradually rounded; three oblong and sclerotized spermathecae.

Remarks. Stuckenberg (1960: 289) provides a detailed description of colour variation in a series of 12 males he examined from Gorongosa, Mozambique. Some of these males agree with and overlap in colour characters from South African specimens, highlighting the variability of the species.

Distribution. Mozambique, South Africa.

***Suragina mulanjeensis* Muller, sp. nov.**

<https://zoobank.org/27E2B0DF-D926-47D1-AFCA-EA73FCD53ED8>

Figs 5, 29, 30, 50, 71, 73, 85

Type material examined. Holotype: MALAWI • 1♂; [Southern Region]; Mulanje Mt. [Mulanje Massif] nr Likabula; [15°56.983'S, 35°35.617'E]; 26–27 Oct. 1983; A. Freidberg leg.; (NMSA-DIP 158398) (NMSA).

Paratypes: 1♂6♀; same data as holotype (♂: NMSA-DIP 162049; ♀: NMSA-DIP 158392, 158393, 158394, 158395, 158396, 158397) (NMSA) • 1♂4♀; Southern Region; Mulanje Mountain [Mulanje Massif] at.; 15°56.1667'S, 35°31.1982'E; 1061 masl; 12–14 Oct. 2016, A.H. Kirk-Spriggs & B.S. Muller leg.; Malaise trap, stream bed; Miombo woodland; (♂: BMSA(D)92379; ♀: BMSA(D)92374, 92375, 92377, 92378) (BMSA).

Holotype deposited in NMSA and paratypes deposited as per listed institutional codens in citations above: BMSA and NMSA.

Diagnosis. An orange-yellow species (Figs 29, 30), without apparent dark substigmatal markings on the wing (Fig. 50). The abdomen in most specimens has subtriangular markings on the majority of segments. It is most similar to *S. milloti* (Figs 25, 26), which is a Madagascan endemic. Apart from distribution, *S. milloti* differs from *S. mulanjeensis* Muller, sp. nov. in having its abdominal tergites more uniformly orange-yellow and a much more prominent dark substigmatal mark.

Description. Measurements (♂ n = 2, ♀ n = 2): Wing span: ♂ 7.3–7.6 mm (avg. 7.4 mm); ♀ 7.9–8.5 mm (avg. 8.2 mm); body length: ♂ 8.4–9.2 mm (avg. 8.8 mm); ♀ 7.6–10.0 mm (avg. 8.8 mm); wing span to body length ratio (avg.): ♂ 0.85; ♀ 0.94.

Male (Fig. 29).

Head (Fig. 5): Orange-brown ground colour, with silver-grey pruinosity on majority of head; eye bare; holoptic, some specimens' eyes separated 0.5× width of anterior ocellus; ommatidia on lower quarter of eye smaller than those on rest of eye; lateral edge of eye with indentation, and an apparent weak, dark tubercle just above indentation (more apparent in some specimens than others); ocellar tubercle clearly visible in profile, blackish-brown in colour with only slight grey pruinosity, with short dark setulae; vertex dark brown with greyish pruinosity and long dark setulose; anterior ocellus larger than posterior pair; ocellar tubercle in front of dorsal margin of eye, not placed as deeply towards middle of head as in ♀; dorsal inner edge of eye abutting ocellar tubercle; occiput with same silver-grey pruinosity as rest of head; paired very narrow subrectangular black markings with short dark setulae on upper occiput, abutting posterior margin of eyes, flanking vertex; upper occiput with short pale setulae; lower occiput with long pale setulae, these continue ventrally on head to premental area of mouthparts that have similar long ventral setulae; frons entirely bluish-grey pruinose when viewed dorsally, velvety-black from ocellar tubercle down to before antennal bases when viewed anteriorly; frons widening from where eyes touch down to antennal base; frons with short pale setulae up to two-thirds of frons towards ocellar tubercle; face and gena silver-grey, both with pale setulae; clypeus orange-brown with bluish-grey pruinosity, bare; face separated anteriorly from clypeus by a deep transverse suture, similar to lateral sutures; face not appearing to bulge laterally when viewed in profile; clypeus visible in profile, face not; antennal

bases separated ca 0.5× width of scape, with slight longitudinal groove running between; scape dark brown, pedicel orange-yellow to orange-brown, both with silvery pruinosity; 1st flagellomere orange-yellow, with sparse silvery pruinosity; 2nd flagellomere dark brown; scape slightly larger than pedicel; 1st flagellomere reniform, ca 1.4× size of pedicel; 2nd flagellomere arista-like; pedicel with dark dorsal and ventral setulae, similar in size, scape with only pale dorsal setulae; palpus orange-brown with dense grey pruinosity or orange-yellow with only slight greyish pruinosity; palpus with dark setulae throughout, ca 0.5× length of proboscis; proboscis slightly shorter than head height; proboscis orange-yellow to almost entirely dark brown in colour, specimens with orange-yellow proboscis with lateral and ventral margins dark brown; prementum orange-yellow, proboscis with long dark setulae except for those on prementum that are long pale.

Thorax (Fig. 5): Thorax predominantly orange-yellow, including majority of pleura and scutum; scutum with short dark setulae, with two feint dorsocentral brownish-grey pruinose vittae running from pronotum to before transverse suture; pronotum yellow with whitish pruinosity and pale setulae; postpronotal lobe with similar yellow colour and whitish pruinosity as pronotum; postpronotal lobe with a mix of pale and dark setulae; notopleuron brown with bluish-grey pruinosity, with a mix of long pale and dark setulae throughout; postalar wall and postalar callus orange-yellow with only slight whitish pruinosity, supra-alar area and postalar callus with short dark setulae; scutellum orange-yellow with dark setulae, prescutellar area with bluish-grey pruinosity; pleura with slight whitish pruinosity, especially evident on anepisternum, katapisternum and katatergite; majority of anepisternum dark brown and similar in appearance to notopleuron, contrasting with surrounding orange-yellow pleura; proepisternum and proepimeron, katatergite and anepisternum have long pale setulae, rest of pleura bare; anterior and posterior spiracles whitish-yellow, bare; postspiracular scale orange-yellow with brownish apical margins; postscutellum orange-yellow.

Legs: All coxae yellow to orange-yellow; fore coxal setulae entirely pale or at most with a couple of dark setulae apically; mid coxal setulae mixed pale and dark; hind coxal setulae pale with some dark setulae on anterior edge surrounding well-developed anterior apical point, lateral apical edges with long pale setulae; fore and hind trochanters yellow, mid trochanter brownish-yellow, all trochanters with short pale setulae; fore and mid femora almost entirely yellow, except for slightly brown apex in some specimens; hind femur yellow with brown to dark brown median band; fore tibia yellow except for apical third brownish, mid tibia yellow, hind tibia brown to dark brown with base and apex yellowish-brown; fore and hind tarsi brown to dark brown, mid basitarsus yellow on majority of segment except for yellowish-brown apex, with remaining mid tarsal segments brown; fore tarsal claws asymmetrical, outer claw much larger than inner claw, foreleg empodium ca 2× size of inner pulvillus, outer pulvillus ca 2× length of inner, approaching size of outer claw; fore femur overall with short pale setulae, with long pale setulae on posteroventral surface; mid femur with long pale setulae on ventral surface, otherwise with short pale setulae; hind femur with a mix of pale and dark setulae on dorsal and ventral surfaces, base of femur with pale setulae; fore tarsi covered with long sensory setulae along antero- and posteroventral surfaces, sensory setulae ca 2× as long as tarsal segment is wide; hind leg overall stouter than remaining legs; hind tarsal length subequal to hind tibia; tibial spur formula 0:2:2.

Wing: Hyaline; darker brown stigma over area of veins R_1 and R_{2+3} and cell r_1 ; apical third of wing with a brown suffused appearance, except for discal cell, and cells r_{2+3} , m_4 hyaline; cell br medially suffused; cells bm and cua hyaline apart from suffusion around surrounding veins CuA and CuP ; veins dark brown; costa without distinct downward flexure over stigma; cell cua closed near wing margin, cell m_3 open, veins M_1 , M_2 , M_3 present; haltere stalk yellow, knob yellowish-brown, with a few short and dark setulae.

Abdomen: Overall brownish-yellow to yellow in colour; tergites 1 and 2 typically without any markings, some specimens each with a dorsal longitudinal subrectangular median dark brown marking; tergite 3 always with a dorsal subtriangular brown suffused marking, some specimens with an additional longitudinal subrectangular dark brown marking over suffused marking; tergites 4–6 each with brown to dark brown suffused dorsal marking, in some specimens this is much reduced and dorsal surface is mostly brownish-yellow; tergites 3–6 with grey pruinose band along posterior margin; tergites 2–6 with elongated dark lateral markings, some specimens these markings are very light and almost indistinguishable; tergite 1 medially without a longitudinal suture; tergites 1–5 with dark setulae dorsally, and long pale setulae on lateral margins; tergite 6 with dark lateral setulae; sternites yellowish, with some irregular dark markings on sternites 4 and 5; sternites with pale setulae.

Terminalia (Figs 71, 73): Epandrium and cercus dark brown with dark setulae; hypoproct and hypandrium with pale setulae, gonocoxite with dark lateral setulae and pale inner setulae; gonostylus almost parallel shaped with a truncated apex, outer edge of gonostylus with short setulae, inner edge with protrusion with 4 setulae, apical third of gonostylus sparsely covered in microtrichia; gonocoxite widening and appearing more rounded on apical half, apex somewhat flattened, gonocoxite outer and ventral medial surface with long setulae, inner and ventral surfaces of upper half with short setulae, lower ventral surface setulose; gonocoxite with microtrichia between setulae; parameral apodeme with truncated apex, not reaching base of gonocoxite in ventral view, parameral sheath including parameral apodeme ca 0.7× length of gonocoxite; gonocoxal apodeme similar in length to gonocoxite and slightly longer than ejaculatory apodeme; aedeagal tine curvature barely extending down past gonocoxites, apex of tines not extending out past parameral sheath; endo-aedeagal process apically truncated and widened.

Female (Fig. 30): Similar to ♂ except for the following:

Head: Dichoptic; ommatidia of similar size; lateral edge of eye without any indentation, but also with apparent tubercle as in ♂; anterior ocellus similar in size to posterior pair; ocellar tubercle placed deeper in front of dorsal margin of eye compared to ♂; dorsal inner edge of eye separated from ocellar tubercle by pair of silver-grey markings, appearing to extend down from vertex, which is more bluish-grey pruinose (more greyish in ♂); occiput with paired subrectangular black markings ca 2× height of those on ♂ upper occiput; frons bluish-grey pruinose between lower half of eye down to antennal base, velvety-black from ocellar tubercle to lower half of eye when viewed dorsally, when viewed anteriorly entire frons appears blackish, although lower half is shinier than upper velvety-black half; frons widening only slightly from velvety-black patch towards antennal bases; frons with dark setulae on velvety-black upper half and pale setulae on bluish-grey lower half; face and gena silvery-grey pruinose, clypeus with

bluish-grey pruinosity; face separated anteriorly from clypeus by transverse suture, (less prominent, and angle more obtuse than in ♂); antennal bases separated ca 0.4–0.6× width of scape, with slight longitudinal groove running between; 1st flagellomere ca 1.5× size of pedicel; proboscis ca same length as head height.

Thorax: Similar to that of ♂, except whitish pruinosity is denser than in ♂.

Legs: Fore and mid coxae with a slight white pruinosity; fore coxal setulae entirely pale; all trochanters yellow; fore and mid femora entirely yellow; hind femur with similar dark median band as in ♂, but band is narrower than in ♂; rest of leg colouration similar to that of ♂; fore tarsal claws symmetrical; overall leg setation similar to ♂ except generally shorter.

Wing (Fig. 50): Similar to ♂.

Abdomen: Overall orange-yellow to yellow in colour; in some specimens tergites almost entirely unmarked except for some darker markings on tergite 7, in other specimens tergites 1–6 with subtriangular dark suffused markings, varying in intensity, tergite 7 with two dark markings and tergite 8 entirely dark; tergites 2 and 6 with elongated dark lateral markings, intensity differs between specimens; all sternites apparently yellow, some dark discolouration due to dried gut contents; tergite 1 with weak median longitudinal suture.

Terminalia (Fig. 85): Cercus yellowish-brown with pale setulae; genital fork with distal apodeme ending in a truncated broad knob; median lobe without a clear emargination; paired apical lobes with somewhat slender appearance, inner surface with inward projecting knob that has clustered microtrichia at apex; arms gradually rounded; three rounded and sclerotised spermathecae.

Etymology. Named after the type locality, the Mulanje Massif, Malawi. Feminine adjective in the nominative singular case.

Distribution. Malawi.

***Suragina nigromaculata* (Brunetti, 1929)**

Figs 31, 51

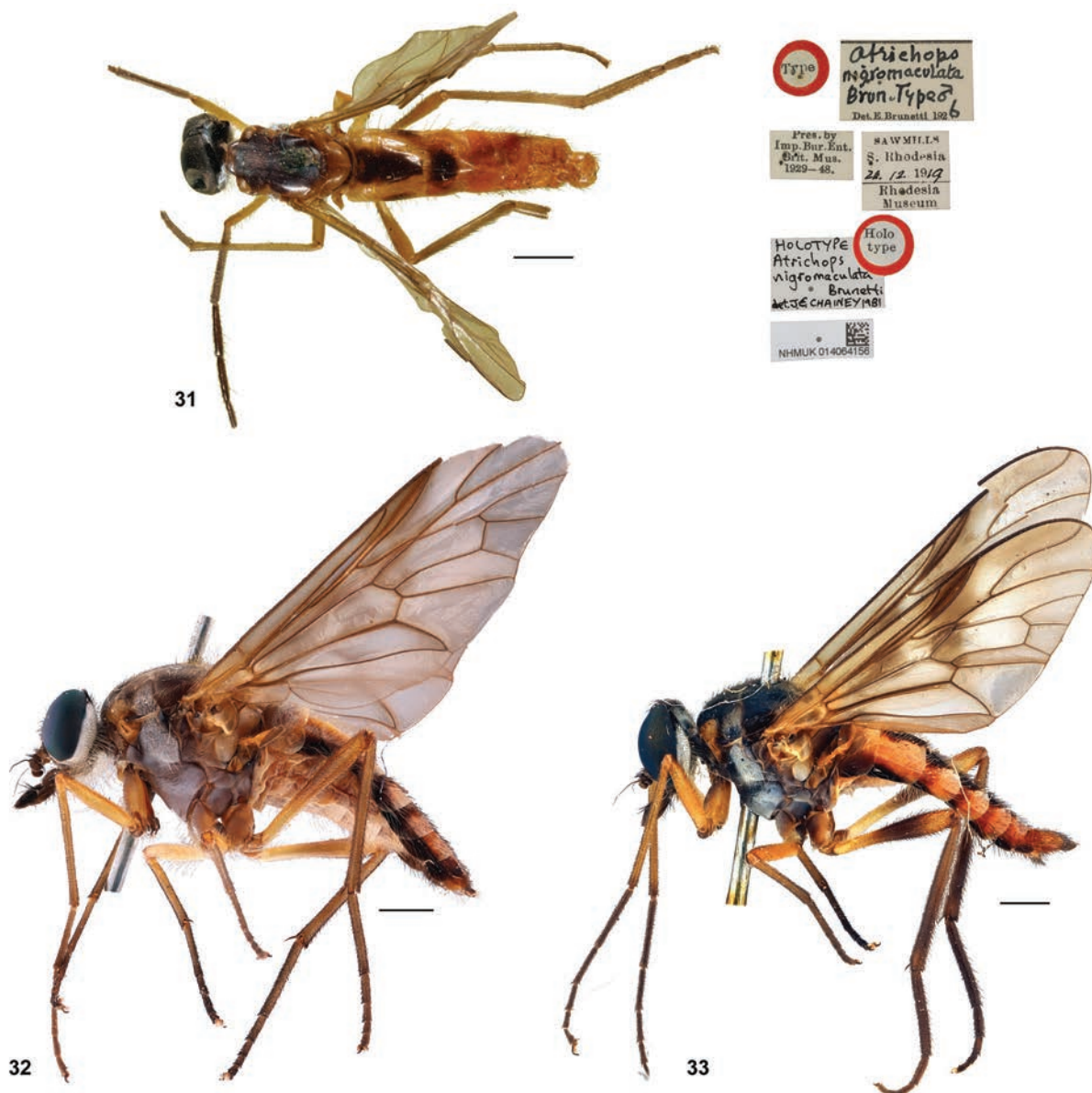
Atrichops nigromaculata Brunetti, 1929: 1.

Suragina nigromaculata: Stuckenberg 1960: 293, fig. 87; Stuckenberg 1980: 313.

Type material examined. [from digital photographs] **Holotype:** ZIMBABWE • 1♂ Sawmills, S. Rhodesia; 26 Dec. 1919; [19°34.998'S 28°01.986'E, 1059 masl] Rhodesia Museum; Presented by the Imperial Bureau of Entomology, British Museum 1929–48; *Atrichops nigromaculata* Brun Type ♂, det. E. Brunetti 1926; Holotype *Atrichops nigromaculata* Brunetti det. J.E. Chainey 1981 (NHMUK 014064156).

Diagnosis. The male (Fig. 31) of the species has a general orange-yellow appearance with darker pleura and scutum (female unknown). The abdomen is mostly orange-yellow, however, tergites 1 and 2 have dark brown median vittae, with tergites 2 and 3 with lateral markings as well. The species is most similar so *S. binominata* (see *S. binominata* diagnosis) and, to a lesser extent, *S. monogramma* (see below).

Remarks. The original description of the male by Brunetti (1929: 1) is brief, and the description was published posthumously along with other species found in his manuscript papers. The original description also lacks certain key



Figures 31–33. *Suragina* Walker spp. dorsal habitus: 31 *S. nigromaculata* ♂ holotype (NHMUK 014064156); lateral habitus, *S. pauliani* Stuckenberg: 32 ♂ paratype (NMSA-DIP 28172) 33 ♀ paratype (NMSA-DIP 028174). 31 Copyright NHMUK under CC BY 4.0. Scale bars: 1 mm.

characters, such as the presence of a presutural spot. This led to Stuckenberg (1960: 293) proposing that should the male have this spot, then *S. nigromaculata* may in fact be a synonym of *S. monogramma*.

Upon examination of the provided male type photographs during the current revision, it was found that the type does not have the aforementioned presutural spot in the notopleural area; additionally, several characters not mentioned in the original description easily distinguish it from the male of *S. monogramma* (see diagnosis), and the species is here regarded as valid. A redescription of the male type from Saw-Mills, Zimbabwe follows, based on digital photographs provided by the NHMUK.

Description. Male (Fig. 36).

Measurements (n = 1): Wing span: 5.2 mm; body length: 7.2 mm; wing span to body length ratio: 0.72.

Redescription. (Based on digital photographs of ♂ Holotype).

Head: Brown colour, with silver-white pruinosity on majority of head; eye bare; holoptic; ommatidia of similar size; lateral edge of eye with slight indentation; ocellar tubercle slightly more elevated than frons, black in colour with some short pale setulae; vertex silver-white pruinose, apparently rubbed bare; anterior ocellus larger than posterior pair; ocellar tubercle in front of dorsal margin of eye (♀ unknown); dorsal inner edge of eye without discernible paired dark markings; occiput with same silver-white pruinosity as rest of head, except for paired narrow subtriangular dark brown, almost black markings with pale setulae on upper occiput, abutting posterior margin of eyes, flanking vertex; upper occiput with short pale setulae on dorsal margin and on rest of upper surface, lower occiput with long pale setulae, these continue ventrally on head to mouthparts that have similar pale ventral setulae; frons silver-white up to narrow area before eyes touch when viewed dorsally, dark velvety-brown when viewed anteriorly; frons at narrowest ca 0.5× width of anterior ocellus, widening towards antennal base; frons bare; face and gena silver-white with pale setulae, clypeus dark brown with silver-white pruinosity, bare; face separated from clypeus by a prominent, deep suture on anterior and lateral edges; face not appearing to bulge laterally when viewed in profile; clypeus visible in profile, face not; antennal bases separated ca 1× width of scape, with slight longitudinal groove; scape, pedicel, 1st flagellomere orange-yellow, 2nd flagellomere brownish; 1st flagellomere reniform, only slightly larger than pedicel and scape; 2nd flagellomere arista-like; scape and pedicel with dark dorsal and ventral setulae of similar size, palpus orange-yellow, well-developed, ca 0.5× length of proboscis; proboscis orange-yellow with long pale setulae, some long dark setulae ventrally; some scattered small dark setulae on proboscis and palpus.

Thorax: Orange-yellow ground colour; median dorsal surface of scutum and scutellum with short pale setulae, remainder of thorax with longer pale setulae, especially on pleura and lateral surface of scutellum; postsutural setulae similar to presutural setulae, except for longer prescutellar setulae; postpronotal lobe orange-yellow with long pale setulae; scutum mostly dark brown with slight median greyish pruinosity; postalar wall and callus appearing orange-yellow; scutellum almost entirely orange-yellow except for darker basal margin; pleura brown in colour except for posterior of anepisternum that is orange-yellow; anepisternum, katapisternum and katatergite lightly silver-white dusted; notopleuron orange-yellow with long pale setulae; anterior spiracle bare posteriorly; area surrounding posterior spiracle brown, postspiracular scale brown, similar to majority of pleura; proepisternum, pronotum brownish; proepimeron, proepisternum with pale setulae, anepisternum with pale setulae; katatergite with pale setulae; rest of pleura bare.

Legs: Coxae orange-yellow; fore and mid coxae with long pale setulae on surface, hind coxa with long pale setulae on anterior and lateral apical edges, and with well-developed anterior apical point; all trochanters same orange-yellow colour as rest of body with some scattered short pale setulae; all femora uniformly orange-yellow; mid and hind femora with small anterior apical dark mark; fore tibia and tarsi reddish-brown, mid and hind tibiae orange-yellow; mid and hind tarsi orange-yellow; terminal fore tarsi missing; fore and mid femora covered with pale setulae on all surfaces except for dorso-apical surface with short dark setulae, hind femur with mixed long pale and dark setulae on dorsal

and ventral surfaces, basally with long pale setulae, anteriorly with short setulae and posteriorly with longer setulae; hind leg overall stouter than remaining legs; remaining fore tarsi covered with long sensory setulae along antero- and posteroventral surfaces, sensory setulae ca 2× as long as tarsal segment is wide; fore and mid tibiae covered in short dark setulae, hind tibia with longer dark setulae; combined length of hind tarsal segments subequal to hind tibia; tibial spur formula 0:2:2.

Wing (Fig. 51): Overall slight light brown suffused appearance; with a slightly yellow-brown stigma over area of veins R_1 and R_{2+3} and cell r_1 ; veins light brown; costa without distinct downward flexure over stigma; cell *cua* closed a short distance from wing margin; cell m_3 open, veins M_1 , M_2 , M_3 present; haltere orange-yellow, slightly infuscated apically, with very short dark setulae.

Abdomen: Overall orange-yellow colour; tergites 1 and 2 with broad dark brown median vittae, tergite 3 with dark marking on anterior two-thirds; tergite 2 additionally with dark brown lateral markings; tergites with short black setulae on medial-dorsal surfaces, laterally with longer dark setulae; sternites orange-yellow with dark markings and with pale setulae; tergite 1 with weak median longitudinal suture.

Terminalia: Entirely orange-yellow in colour; epandrium (damaged) and cercus with dark setulae, hypandrium with dark setulae; terminalia not dissected.

Female. Unknown.

Distribution. Zimbabwe.

***Suragina pauliani* Stuckenberg, 1965**

Figs 32, 33, 52

Suragina pauliani Stuckenberg, 1965: 96, figs 1, 2, 5, 6, 9–11; Stuckenberg 1980: 313.

Type material not examined. Holotype: MADAGASCAR: 1♂; [Vakinankaratra Region]; Manjakatempo Forest Station [Ankaratra Massif]; [19°21.00'S, 47°18.00'E]; 1700 masl; Jan. 1956; B.R. Stuckenberg leg.; (PBZT).

Type material examined. Paratypes: MADAGASCAR: 1♂; Ambatolampy District [Vakinankaratra]; Madagascar Centre, Col de Mahafompeno [Mahafompona Pass]; [19°23.97'S, 47°15.018'E]; 2200–2400 masl; 11–15 Dec. 1957; B.R. Stuckenberg leg.; [on yellow bordered label: Paratype *Suragina pauliani* Stuckenberg, 1965]; NMSA-DIP 028172) (NMSA). 1♂2♀; [Vakinankaratra]; Ankaratra Massif, Manjakatempo Forest Station; [19°21.00'S, 47°18.00'E]; 1700 masl; Jan. 1956; B.R. Stuckenberg leg.; (♂: NMSA-DIP 028173; 2♀: NMSA-DIP 028174, 158441) (NMSA).

Diagnosis. A more compact and hirsute species compared to other Afrotropical *Suragina*. The males have the head narrowly dichoptic, with the frons distinctly velvety-black in appearance, much like in females. *Suragina pauliani* has its thorax brown for the most part, the abdomen orange-yellow with dark subtriangular dorsal and elongated lateral markings throughout. It differs from the other two Madagascan endemics in colouration: *S. milloti* is a mostly orange-yellow species and a comparatively more slender species, whereas *S. bilobata* Muller, sp. nov. is a blackish species with a unique bilobed 1st flagellomere.

Redescription. Measurements: Wing span: ♂ 6.6–7.5 mm; ♀ 7.8–7.9 mm; body length: ♂ 7.6–8.4 mm; ♀ 7.8–8.2 mm; wing span to body length ratio (avg.): ♂ 0.88; ♀ 0.99.

Male (Fig. 32).

Head: Brown colour, with grey pruinosity on majority of head; eye bare; narrowly dichoptic, frons at narrowest as wide as anterior ocellus, widening towards antennal bases; ommatidia of similar size; lateral edge of eye without indentation; ocellar tubercle slightly more elevated than frons, dark brown to blackish with some short dark setulae; vertex grey pruinose, dark brown when viewed posterodorsally, with long dark setulae; anterior ocellus larger than posterior pair; ocellar tubercle in front of dorsal margin of eye (margin less indented than in ♀); dorsal inner edge of eye without discernible paired dark markings; occiput with same greyish pruinosity as rest of head, except for paired narrow subrectangular dark brown almost black markings with short dark setulae on upper occiput, abutting posterior margin of eyes, flanking vertex; upper occiput with short dark setulae; lateral margins of occiput with pale setulae; lower occiput with long pale setulae, these continue ventrally on head to base of mouthparts that have similar long pale ventral setulae; frons dark velvety-brown from ocellar triangle down to a small area above antennal bases that is greyish; dark part of frons with conspicuous dark proclinate setulae, lower grey part of frons with some pale setulae; face and gena silvery-grey with pale setulae; clypeus brown with some greyish pruinosity, bare; face separated from clypeus by a prominent, deep suture on anterior and lateral edges; face not appearing to bulge laterally when viewed in profile; clypeus visible in profile; antennal bases separated ca 0.5× width of scape, with slight longitudinal groove; scape, pedicel, 1st flagellomere brown with some whitish pruinosity, 2nd flagellomere brown; 1st flagellomere reniform, only slightly larger than pedicel and scape; 2nd flagellomere arista-like; scape and pedicel with dark dorsal setulae, pedicel with setulae dorsally and ventrally, scape with setulae only on dorsal surface; palpus blackish with some sparse greyish pruinosity, well-developed, ca 0.5× length of proboscis, with dark setulae; proboscis blackish-brown with long dark setulae and some scattered shorter dark setulae.

Thorax: Brown ground colour; median dorsal surface of scutum with short dark setulae, postsutural surface with long pale setulae; postsutural setulae longer than presutural setulae; postpronotal lobe orange-yellow with long dark setulae; scutum mostly dark brown with two dorsocentral brownish-grey pruinose vittae running to middle of scutum in dorsal view; postalar wall and callus appearing orange-yellow; scutellum almost entirely orange-yellow except for brown basal margin, median surface with short dark setulae, apical margin with long pale setulae; pleura mostly blackish-brown with greyish pruinosity, except for posterior surface of anepimeron and entire katatergite that are yellowish-brown with similar pruinosity; notopleuron greyish pruinose with long dark setulae; area surrounding anterior and posterior spiracle orange-yellow, postspiracular scale orange-brown; anterior spiracle bare posteriorly; proepisternum, pronotum similar in appearance to aforementioned pleura; proepimeron, proepisternum, anepisternum, parts of anepimeron and entire katatergite with pale setulae; rest of pleura bare; postscutellum dark brown.

Legs: Fore and hind coxae brown on anterior surface and orange-yellow posteriorly; mid coxa brown on majority of surface, orange-yellow on apical posterior surface; all coxae with long pale setulae on anterior surface, in addition fore

coxa has long pale setulae on posterior surface and hind coxa with long pale setulae on lateral apical edges, and with well-developed anterior apical point; all trochanters brown with short dark setulae; fore and mid femora entirely orange-yellow, hind femur orange-yellow with dark brown band on middle of hind femur; fore and mid tibiae orange-yellow and apically darker, hind tibia mostly dark brown, yellowish-brown at base and apex; fore and mid tarsi brownish, hind tarsi darker brown with more yellowish-brown terminal tarsal segments; fore and mid femora covered with pale setulae on almost all surfaces except for dorso-apical and posteroventral surface with some short dark setulae, hind femur with mixed long pale and dark setulae on dorsal and ventral surfaces, basally with long pale setulae, anteriorly with short setulae and posteriorly with longer setulae; hind leg overall stouter than remaining legs; fore tarsi covered with long sensory setulae along antero- and posteroventral surfaces, sensory setulae ca 2× as long as tarsal segment is wide; fore and mid tibiae covered in short dark setulae, hind tibia with longer dark setulae; hind basal tarsal segment with long dark posterior setulae; fore tarsal claws asymmetrical, outer claw much larger than inner claw, foreleg empodium ca 2× size of inner pulvillus, outer pulvillus ca 2× length of inner, approaching size of outer claw; hind tarsal segments 1.1× as long as hind tibia; tibial spur formula 0:2:2.

Wing: Overall slight light brown suffused appearance; with a dark brown stigma over area of veins R_1 and R_{2+3} and cell r_1 ; veins brown; substigmal marking extends down over base of cell r_{2+3} , apex of cells br and bm , base of cells r_5 and m_2 , crossvein $r-m$ and basal third of discal cell; additional darker suffusion over majority of cell br ; hyaline appearance in cell cua , apical two-thirds of discal cell, base of cell r_4 , post basal half of cell r_5 ; costa without distinct downward flexure over stigma; cell cua closed a short distance from wing margin; cell m_3 open, veins M_1 , M_2 , M_3 present; haltere orange-yellow with a brownish knob and very short dark setulae.

Abdomen: Overall orange-yellow colour; tergites 1–5 with broad dark brown subtriangular median vittae, remaining tergites with only a slight median marking; tergites 1–3 with long pale setulae, remaining tergites with shorter dark setulae; tergites 1–7 with dark lateral markings and especially on tergites 1–5 with prominent long pale setulae; sternites orange-yellow with pale setulae; tergite 1 without median longitudinal suture.

Terminalia: Epandrium orange with dark setulae, hypandrium orange-brown, cercus blackish, both with dark setulae, terminalia not dissected.

Female (Fig. 33): Similar to ♂ except for the following:

Head: Widely dichoptic; dorsal margin of eye more indented than in ♂; vertex wider than in ♂, dorsal inner edge of eye brownish-grey pruinose, appearing as an extension of vertex surrounding ocellar tubercle; occiput with paired dark brown almost black subtriangular (more narrow and subrectangular in ♂) markings on upper occiput; frons similar in colour appearance to that of ♂ but at narrowest ca 1.6× width of ocellar tubercle, widening slightly towards antennal base, gradually fading at edges into bronzy brown colour; face separated anteriorly from clypeus by shallow transverse suture, deeper sutures laterally; face slightly visible in profile; 1st flagellomere comparatively much larger than in ♂; scape ca 2× as long as pedicel; 1st flagellomere ca 2× as long as pedicel.

Thorax: Scutum slightly lighter than in ♂, otherwise with similar appearance; postpronotal lobes with similar dark setulae as in ♂ but lobe with long pale setulae

as well; pleura reddish-brown with grey pruinosity, with similar patterning as in ♂ just lighter; postspiracular scale orange in colour; scutellum with only pale setulae.

Legs: Coxae similar to ♂, just overall lighter in colour; hind femur with median band light brown; fore and mid legs yellow with tarsi brownish, but basal two-thirds of basitarsi yellowish; fore tarsal claws symmetrical; hind leg with general orange-yellow colour on segments, including tarsi; hind femur with mix of short pale and dark setulae compared to ♂; hind tarsal segments 0.9× as long as hind tibia.

Wing (Fig. 52): Overall brownish suffusion, with upper third of wing somewhat darker suffused, stigma also markedly lighter compared to ♂; no prominent dark suffused substigmatal markings running longitudinally on wing as in ♂.

Abdomen: Similar patterning and colour as ♂; lateral dark markings on tergites appearing as more uniform and continuous dark marginal line.

Terminalia: Cercus orange-brown with pale setulae; terminalia not dissected.

Distribution. Madagascar.

Suragina pilitarsis (Lindner, 1925)

Atherix pilitarsis Lindner, 1925: 22.

Suragina pilitarsis: Stuckenberg 1980: 313.

Type material not examined. See remarks, no additional material available.

Remarks. *Suragina pilitarsis* (Lindner, 1925) was regarded as “unplaced and doubtful” by Yang et al. (2016: 446), however, without justification. Based on Lindner’s description of characters, especially the characteristic velvety-black upper frons, slim body and elongated legs in combination with the overall colour characteristics, the species described is clearly a *Suragina*. The type material of *S. pilitarsis* was recorded as being in “Hamburger Museum”. The only additional data associated with it is “Gaboon, leg. Soyaux 1881”. Unfortunately, the museum was destroyed during World War II, and after communication with the staff at Museum der Natur Hamburg, the type is now recorded as destroyed. No additional material of *S. pilitarsis* is known, and the original description in German is not sufficient to distinguish the species from other Afrotropical species based on the text alone and subsequently the species is excluded from the identification key in this paper. Additional material will need to be collected from the country, but without a definitive type locality this could prove difficult.

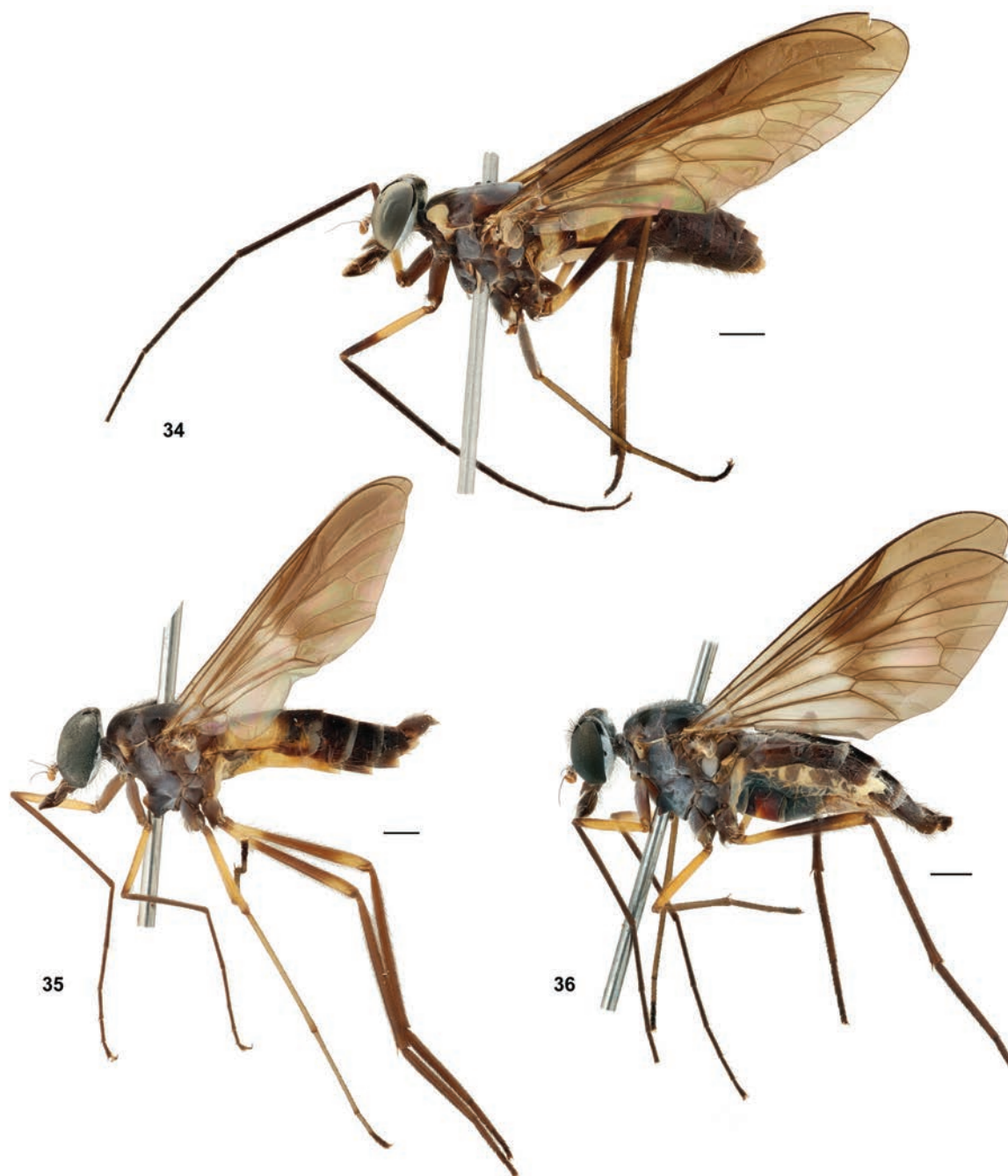
Suragina semiobscura Muller, sp. nov.

<https://zoobank.org/4C3DDF6A-3D5F-4FE0-A4C1-F1BBF48F6992>

Figs 34, 53, 86

Type material examined. Holotype: UGANDA • 1♀; Kibale National Park, Kanyawara Makerere University Biological Field Station; 00°33.960'N, 30°21.267'E; 1495 masl; 12–26 Aug. 2008; S. van Noort leg.; UG08-KF1-M11; Malaise trap, secondary mid-altitude Rainforest, marshy area; (SAM-DIP-A018385).

Paratypes: CENTRAL AFRICAN REPUBLIC • 1♀; Prefecture Sangha-Mbaéré; Réserve Spéciale de Forêt Dense de Szanga-Sangha, 12.7 km 326°NW Bayanga;



Figures 34–36. *Suragina* Walker spp. lateral habitus: **34** *S. semiobscura* Muller, sp. nov. ♀ holotype (SAM-DIP-A018385); *S. zombaensis* Muller, sp. nov.: **35** ♂ paratype (NMSA-DIP 158421) **36** ♀ paratype (NMSA-DIP 158415). Scale bars: 1 mm.

03°00.27'N, 16°11.53'E; 420 masl; 12–13 May 2001, S. van Noort leg.; Malaise trap, CAR01-M109, Lowland Rainforest; (SAM-DIP-018431). KENYA • Western Province; Kakamega Forest, nr. KFS HDQTRs; 00°14.2452'N, 34°51.9642'E; 1620 masl; 2–16 May 2017; R. Copeland leg.; Indigenous forest; Malaise trap; (ICIPE 4020-26) • Western Province; Kakamega Forest, nr. KFS HDQTRs; 00°14.2452'N, 34°51.9642'E; 1620 masl; 9 Apr.–3 May 2017; R. Copeland leg.; Indigenous forest; Malaise trap; (ICIPE) • Western Province; Kakamega Forest, nr. Rondo Guest House; 00°13.6602'N, 34°53.1198'E; 1630 masl; 13–27 Aug. 2006; R. Copeland leg.; across small permanent stream; Malaise trap; (ICIPE) • Western Province; Kakamega Forest, nr. Rondo Guest House; 00°13.6602'N,

34°53.1198'E; 1630 masl; 8–22 Oct. 2006; R. Copeland leg.; across small permanent stream; Malaise trap; (ICIPE).

Holotype deposited in SAM and paratypes deposited as per listed institutional codens in citations above: ICIPE, SAM.

Diagnosis. *Suragina semiobscura* Muller, sp. nov. has its thorax dark brown to blackish with varying levels of bluish-grey pruinosity throughout, except for a yellow scutellum. The wing, uniquely, has its anterior half dark brown suffused, and posterior half light brown suffused, giving a two-toned appearance (Fig. 53). The species is most similar to *S. bezzii* (See *S. bezzii* diagnosis), but the latter has the scutellum brown and tergites 4–6 orange, compared to dark brown in *S. semiobscura* Muller, sp. nov.

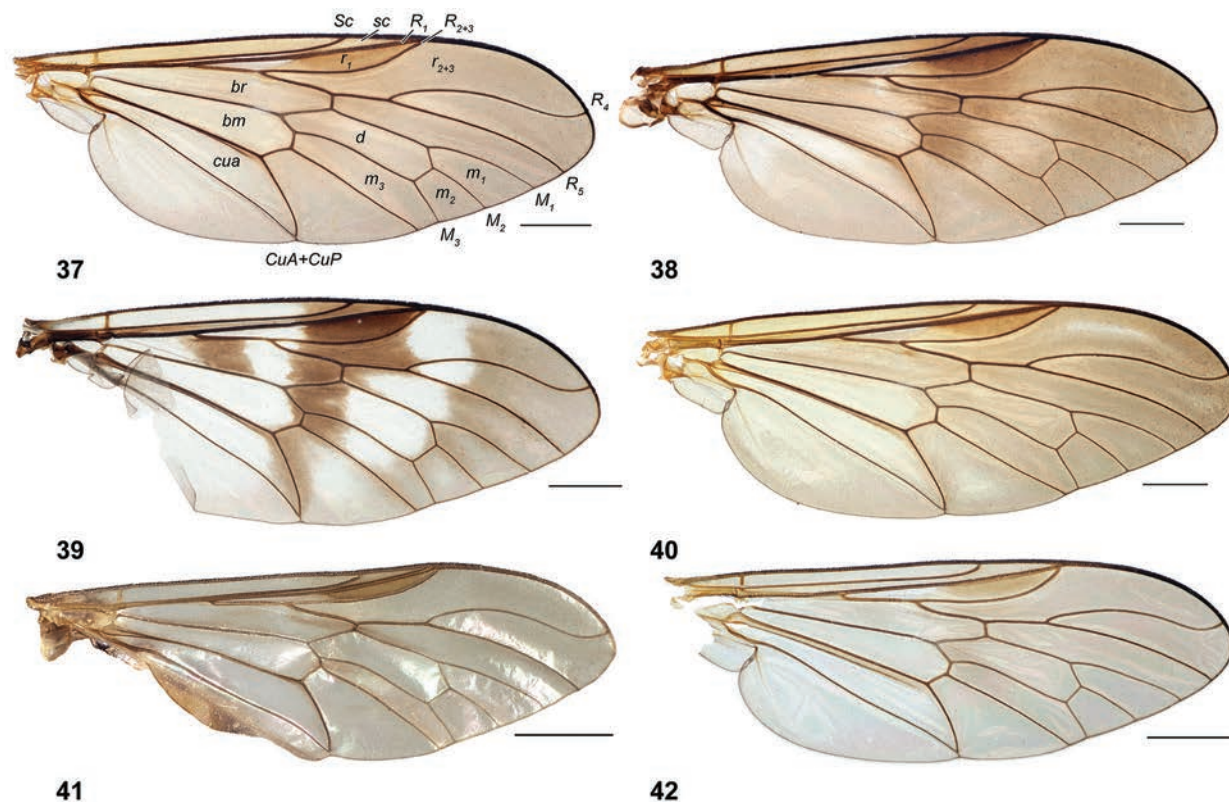
Description. Measurements (♀ n = 2): Wing span: 9.9–10.5 mm (avg. 10.2 mm); body length: 9.2–9.5 mm (avg. 9.4 mm); wing span to body length ratio (avg.): 1.1.

Male. Unknown.

Female (Fig. 34).

Head: Black ground colour, with bluish-grey pruinosity on majority of head; eye bare; dichoptic; ommatidia of similar size; lateral edge of eye without any indentation; ocellar tubercle elevated, visible in profile, same velvety-black as upper half of frons, with short dark setulae; vertex bluish-grey pruinose, with dark setulae; anterior ocellus larger than posterior pair; ocellar tubercle in front of dorsal margin of eye; dorsal inner edge of eye with bluish-grey markings; occiput with silver-grey pruinosity; paired narrow black markings with short dark setulae on upper occiput, abutting posterior margin of eyes, flanking vertex; upper occiput otherwise with pale setulae; lower occiput lateral margins and medial surface with long pale setulae, these continue ventrally on head to mouthparts that have mix of pale and dark ventral setulae; lower half of frons bluish-grey pruinose, velvety-black from ocellar tubercle to lower half of eye; frons running almost parallel, widening towards antennal base; frons setulae dark on upperhalf, pale on lower half; face and gena with silver-grey pruinosity, face with pale setulae, gena with dark setulae; clypeus with bluish-grey pruinosity, bare; face barely separated anteriorly from clypeus by shallow transverse suture, with deeper sutures laterally; face much reduced in appearance, bulging laterally when viewed in profile; clypeus visible in profile; antennal bases separated ca 1× width of scape, with slight longitudinal groove running between; scape, pedicel, and 1st flagellomere orange-yellow with some whitish pruinosity; pedicel in some specimens browner dorsally; 2nd flagellomere dark brown; scape and pedicel of similar size; 1st flagellomere reniform, ca 1.5× as tall as pedicel; 2nd flagellomere arista-like; pedicel with dark dorsal and ventral setulae, similar in size, scape with only dark dorsal setulae; palpus orange-brown with dense dark setulae ventrally and whitish pubescence dorsally; ca 0.5× length of proboscis; proboscis ca same length as head height; proboscis orange-brown to dark brown, setulae dark with some scattered short pale setulae.

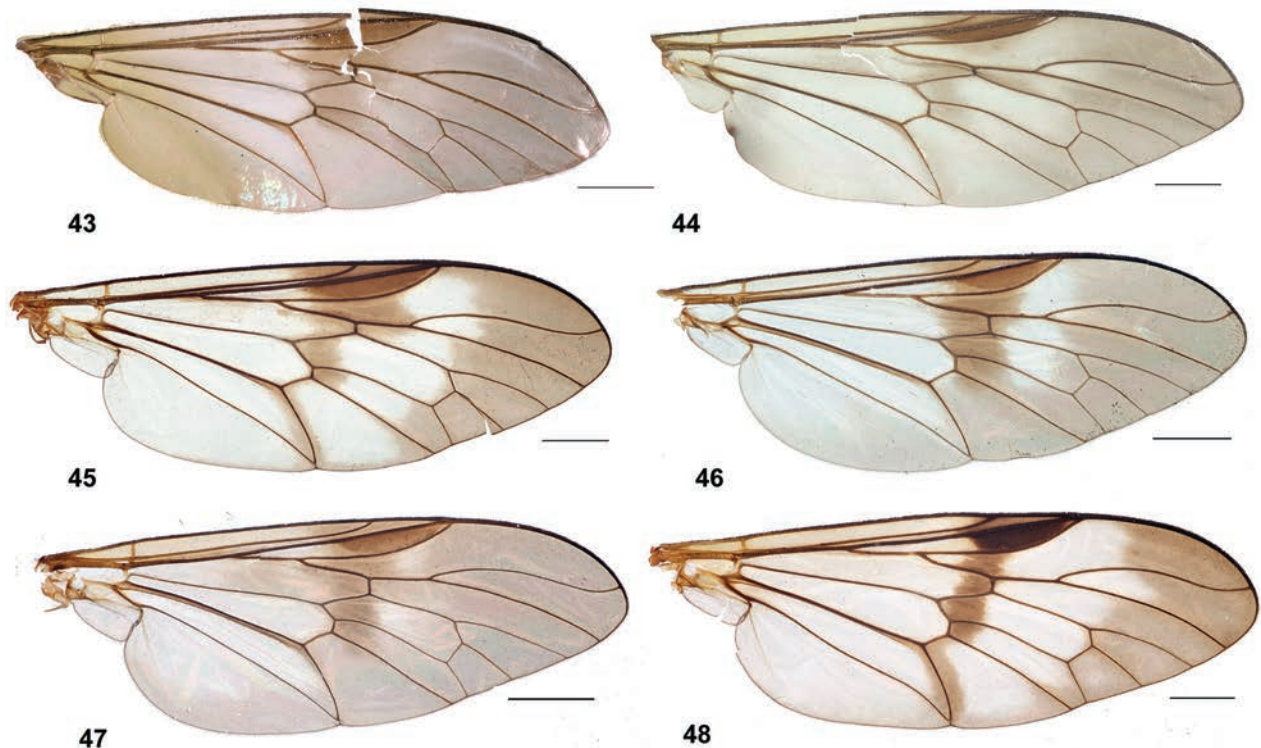
Thorax: Scutum dark brown, median vittae unknown due to damage from preservation method; pronotum orange-yellow dorsally, with lateral margins dark brown; postpronotal lobe yellow, slightly whitish pruinose, setulae pale; notopleuron dark brown with bluish-grey pruinosity with long pale setulae; postalar wall yellowish-brown with ridge dark setulose, postalar callus brown; scutellum yellow with long pale setulae, apical margin with long dark setulae;



Figures 37–42. *Suragina* Walker spp. wing dorsal view: **37** *S. agramma* (Bezzi) ♀ (BMSA(D)124627) **38** *S. bezzii* (Curran) ♂ (SAM-DIP-A018410) **39** *S. bilobata* Muller, sp. nov. ♀ paratype (CSCA) **40** *S. copelandi* Muller, sp. nov. ♀ paratype (BMSA(D)83423); *S. binominata* (Bequaert): **41** holotype ♂ (MLUH) **42** ♀ (NMSA-DIP 158446). **41** Copyright ZNS Halle, January 30, 2024. Abbreviations: *br* – basal radial cell; *bm* – basal medial cell; *cua* – anterior cubital cell; *CuA+CuP* – anterior branch of cubital vein + posterior branch of cubital vein; *d* – discal cell; *M*₁ – first branch of media; *m*₁ – first medial cell; *M*₂ – second branch of media; *m*₂ – second medial cell; *M*₃ – third branch of media; *m*₃ – third medial cell; *R*₁ – anterior branch of radius; *r*₁ – first radial cell; *R*₂₊₃ – second branch of radius; *r*₂₊₃ – second radial cell; *R*₄ – upper branch of third branch of radius; *R*₅ – lower branch of third branch of radius; *Sc* – subcostal vein; *sc* – subcostal cell. Scale bars: 1 mm.

scutum setulae unknown, rubbed bare; all pleura dark brown with bluish-grey pruinosity, except for meron and anepimeron markedly less dusted; anepimeron with long pale setulae, anatergite and meron bare; proepisternum with pale setulae and proepimeron with dark setulae; anterior and posterior spiracles and surroundings yellowish and dark brown respectively, bare; postspiracular scale dark brown; postscutellum dark brown with slight bluish-grey pruinosity.

Legs: Fore coxa yellow with apex brown, mid and hind coxae brown with slight bluish-grey pruinosity on surface; fore coxa with long pale setulae anteriorly and apically with short dark setulae apically; mid and hind coxae with dark setulae on anterior surfaces, mid coxa with pale setulae at base; hind coxa with dark setulae on anterior edge surrounding well-developed anterior apical point, lateral apical edges with longer pale setulae; all trochanters yellowish-brown with short dark setulae; fore femur yellow on at least basal half, dorsally with dark brown apex, some specimens with apical half to third dark brown; mid femur with apical third and extreme base dark brown, yellow medially; hind femur with dark brown medial band, basal quarter yellow, apical quarter orange-yellow; fore tibia dark brown, mid tibia yellow, hind tibia brown with apical third yellowish-brown; fore tarsi dark brown, mid and hind tarsi yellowish-brown with basal segments lighter; fore tarsal claws, empodium and pulvilli symmetrical;

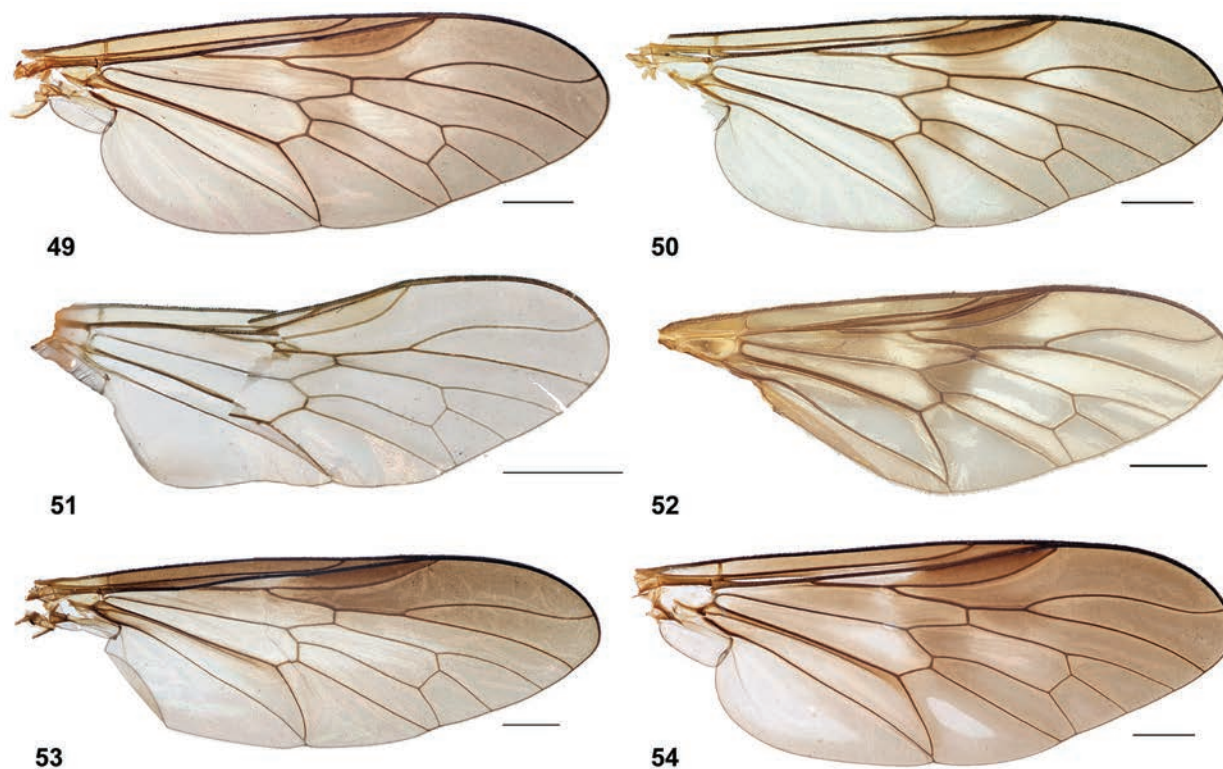


Figures 43–48. *Suragina* Walker spp. wing dorsal view: **43** *S. dimidiatipennis* (Brunetti) ♀ holotype (NHMUK 014064158) **44** *S. falsa* Oldroyd ♀ (NHMUK014064160) **45** *S. freidbergi* Muller, sp. nov. ♀ paratype (BMSA(D)92158) **46** *S. liberiaensis* Muller, sp. nov. ♀ paratype (NMSA-DIP 158445) **47** *S. malavaensis* Muller, sp. nov. ♂ (ICIPE) **48** *S. milloti* (Séguy) ♀ (CSCA). **43, 44** Copyright NHMUK under CC BY 4.0. Scale bars: 1 mm.

fore tarsi with long, somewhat curved sensory setulae along antero- and posteroventral surfaces, sensory setulae ca 2× as long as tarsal segment is wide; fore femur with long pale setulae on antero- and posteroventral surface, dorsally with short pale setulae, apically with dark setulae on dark dorsal marking; mid femur with short pale setulae and some longer pale setulae on ventral surface; hind femur with a mix of pale and dark setulae, setulae longer on ventral apex; all tibiae with short dark setulae; hind leg overall stouter than remaining legs; hind tarsal segments 0.9–1.0× as long as hind tibia; tibial spur formula 0:2:2.

Wing (Fig. 53): Upper half of wing dark brown suffused, lower half light brown suffused; dark brown stigma over apex of veins R_1 and R_{2+3} and cells sc , r_1 , base of cell r_{2+3} ; entirety of cells r_{2+3} and r_4 dark brown suffused, rest of radial and marginal cells and veins light brown suffused, including discal cell; veins dark brown; costa without distinct downward flexure over stigma; cell cua closed a short distance from wing margin; cell m_3 open, veins M_1 , M_2 , M_3 present; haltere stalk orange-brown with knob darker brown, with some short and dark setulae.

Abdomen: Tergite 1 yellow, posterior margin with a dark brown marginal band, narrowing around medial longitudinal suture; tergite 2 yellow with dark brown median longitudinal band appearing to extend from dark marginal band on tergite 1 and continuing down to tergite 3, additionally tergite 2 with paired narrow dark brown lateral markings; tergite 3 with some yellow markings on anterior margin; remaining tergites entirely dark brown; sternites 1–3 yellow, sternite 3 dark brown on posterior third, rest of sternites dark brown; tergite 1 with long pale setulae anteriorly and short dark setulae on dark posterior markings, tergite 2 with short dark setulae; remaining tergites with a mix of



Figures 49–54. *Suragina* Walker spp. wing dorsal view: 49 *S. monogramma* (Bezzi) ♀ (BMSA(D)129988) 50 *S. mulanjeensis* Muller, sp. nov. ♀ (BMSA(D)92374) 51 *S. nigromaculata* Muller, sp. nov. ♂ holotype (NHMUK 014064156) 52 *S. pauliani* ♂ paratype (NMSA-DIP 028172) 53 *S. semiobscura* Muller, sp. nov. ♀ paratype (ICIPE) 54 *S. zombaensis* Muller, sp. nov. ♀ paratype (NMSA-DIP 158451). 51 Copyright NHMUK under CC BY 4.0. Scale bars: 1 mm.

short pale and dark setulae on dorsal surfaces, all tergites laterally with long pale setulae; sternites with pale setulae on yellow segments, dark setulae on dark segments.

Terminalia (Fig. 86): Cercus dark orange-yellow with pale setulae; genital fork with distal apodeme ending broadly truncated and sharply bilobate; median lobe with deep and wide emargination; paired apical lobes with somewhat slender appearance, inner surface darkened with clustered microtrichia at apex; arms gradually rounded, wide, similar to apical lobes in width; three ovate and sclerotised spermathecae.

Etymology. From the Latin *semi* “half” and *obscurus* “dark or shady”, describing the species’ wing that has its anterior half of wing dark brown suffused, contrasting with the lighter brown suffused posterior half. Feminine noun in the nominative singular case.

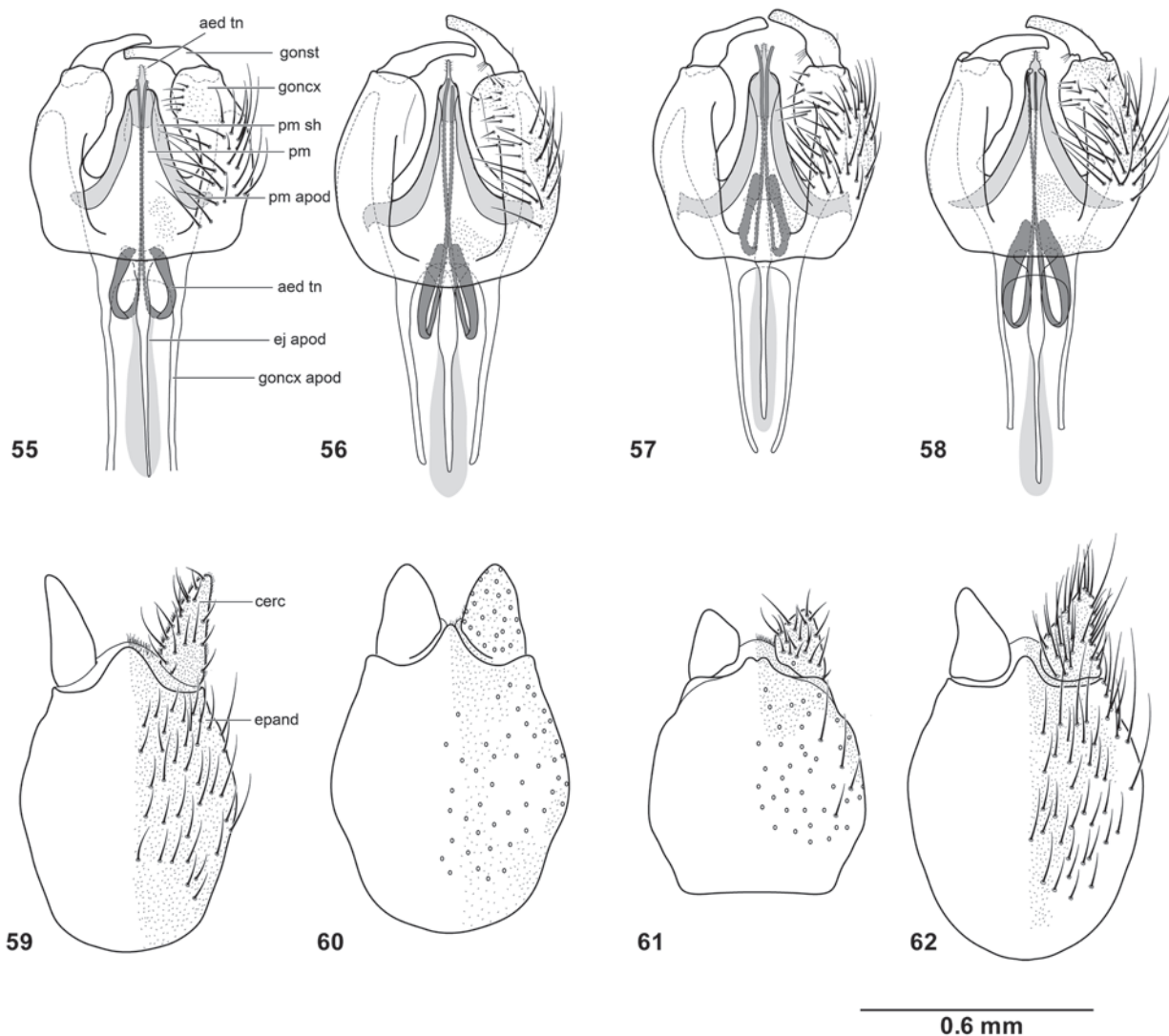
Distribution. Central African Republic, Kenya, Uganda.

***Suragina zombaensis* Muller, sp. nov.**

<https://zoobank.org/80FD6CC3-1332-469B-8FB6-0C45CD0E06A5>

Figs 35, 36, 54, 72, 74, 87

Type material examined. Holotype: MALAWI • 1 ♂; Zomba; 1535Ad; [15°23.00'S, 35°20.00'E]; 24–27 Nov. 1980; J.G.H. Londt & B.R. Stuckenberg leg.; (NMSA-DIP 158422).



Figures 55–62. *Suragina* Walker spp. male terminalia, ventral view (**55–58**) and epandrium with cerci, dorsal view (**59–62**): **55, 59** *S. agramma* (Bezzi) (ICIPE) **56, 60** *S. bezzii* (Curran) (SAM-DIP A018382) **57, 61** *S. binominata* (Bequaert) (NMSA-DIP 028165) **58, 62** *S. copelandi* Muller, sp. nov. paratype (BMSA(D)83425). Abbreviations: aed tn – aedeagal tine; cerc – cercus; ej apod – ejaculatory apodeme; epand – epandrium; goncx – gonocoxite; goncx apod – gonocoxal apodeme; gonst – gonostylus; pm – paramere; pm apod – parameral apodeme; pm sh – parameral sheath. Scale bar (applicable to all illustrations): 0.6 mm.

Paratypes: 3♂4♀; Same data as holotype; (♂: NMSA-DIP 158420, 158421, 158450; ♀: NMSA-DIP 158417, 158418, 158419, 158451) • 1♀; Ntchisi Forest reserve; 1334Ac; 13°22.00'S, 34°00.00'E]; 1500 masl; 3–4 Dec. 1980; J.G.H. Londt & B.R. Stuckenberg leg.; Montane forest, woodland; (NMSA-DIP 158415). Holotype and paratypes deposited in NMSA.

Diagnosis. *Suragina zombaensis* Muller, sp. nov. has its thorax almost entirely brown with bluish-grey pruinosity, the scutellum with apical margin yellow. The males and females are similarly coloured (Figs 35, 36), except for the males having the lateral margins of tergites 3 and 4 yellow compared to dark brown in the female. Tergite 2 in both sexes has dark vitta medially, flanked by brownish-yellow colouration, giving it a fenestrated appearance. The wing of *S. zombaensis* Muller, sp. nov. is most similar to that of *S. dimidiatipennis*, being brown suffused on apical half (Fig. 54 vs Fig. 43). *Suragina zombaensis* Muller, sp. nov.

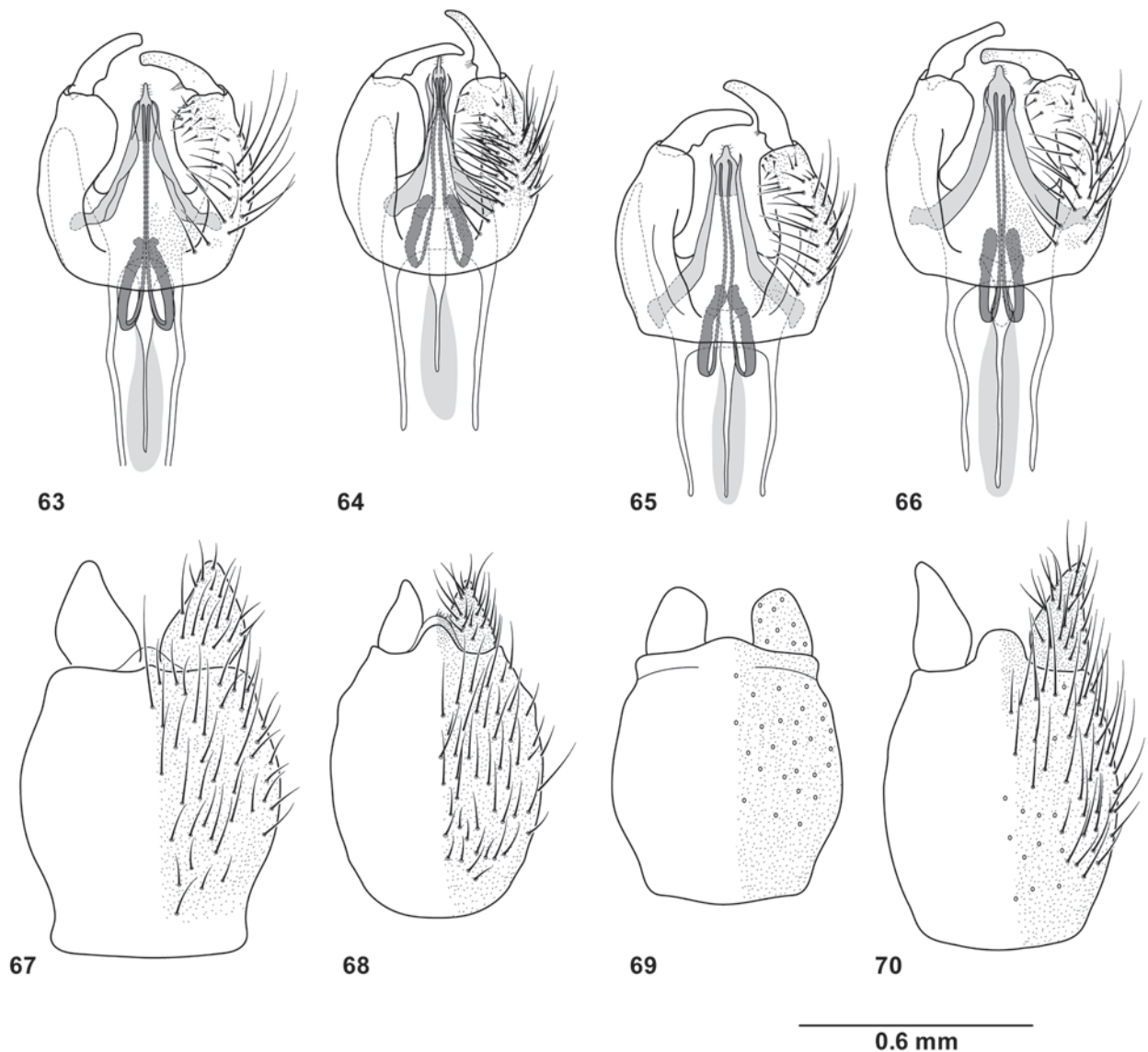
(Figs 35, 36), however, differs from *S. dimidiatipennis* (Fig. 18) in being a much darker species, with mostly dark abdominal tergites with grey dusted apical margins, compared to *S. dimidiatipennis* having a mostly orange-yellow to brown abdomen without any dark markings. *Suragina freidbergi* Muller, sp. nov. is also similar to *S. zombaensis* Muller, sp. nov. (see *S. freidbergi* Muller, sp. nov. diagnosis).

Description. Measurements (♂ n = 2, ♀ n = 2): Wing span: ♂ 7.7–8.7 mm (avg. 8.2 mm); ♀ 8.7–9.8 mm (avg. 9.3 mm); body length: ♂ 8.3–10.5 mm (avg. 9.4 mm); ♀ 8.9–9.6 mm (avg. 9.2 mm); wing span to body length ratio (avg.): ♂ 0.97; ♀ 0.99.

Male (Fig. 35).

Head: Blackish-brown ground colour, with bluish-grey pruinosity on majority of head; eye bare; holoptic; ommatidia on lower and upper quarter of eye smaller than those on rest of eye; lateral edge of eye with slight indentation, and an apparent tubercle next to indentation; ocellar tubercle barely visible in profile, blackish-brown in colour with slight brownish- to bluish-grey pruinosity and short dark setulae; vertex blackish-brown with bluish-grey pruinosity and long dark setulose; anterior ocellus larger than posterior pair; ocellar tubercle in front of dorsal margin of eye, not placed as deeply towards middle of head as in ♀; dorsal inner edge of eye abutting ocellar tubercle; occiput with same bluish-grey pruinosity as rest of head; paired narrow subrectangular black markings with short dark setulae on upper occiput, widening only slightly towards lateral margin of head in some specimens, abutting posterior margin of eyes, flanking vertex; upper occiput with pale setulae; lower occiput with long pale setulae, these continue ventrally on head to mouthparts that have similar long ventral setulae; frons bluish-grey pruinose, velvety-black from ocellar tubercle to before lower half of eye when viewed anteriorly, when viewed anteroventrally entire frons appears blackish-brown with a slight velvety appearance; frons widening from where eyes touch down to antennal base; frons with long dark setulae (setulae can appear pale depending on viewing angle); face and gena bluish-grey, lateral margins of face with long pale setulae, gena with long dark setulae; clypeus dark brown with bluish-grey pruinosity, bare; face separated anteriorly from clypeus by a deep transverse suture, similar to lateral sutures; face not appearing to bulge laterally when viewed in profile; clypeus visible in profile, face not; antennal bases separated ca 0.7× width of scape, with slight longitudinal groove running between; scape dark brown and pedicel orange-brown, both with silvery pruinosity; 1st flagellomere orange-yellow, with sparse silvery pruinosity; 2nd flagellomere dark brown; scape 1.5× length of pedicel; 1st flagellomere reniform, ca 1.5× size of pedicel; 2nd flagellomere arista-like; pedicel with dark dorsal and ventral setulae, similar in size, scape with only dark dorsal setulae; palpus orange-yellow with dense bluish-grey pruinosity, with dark setulae throughout; palpus ca 0.5× length of proboscis; proboscis slightly shorter than head height; proboscis brown to dark brown in colour, prementum brown, proboscis with long pale setulae basoventrally and dark setulae on rest of ventral and dorsal surfaces, except for short pale setulae apically.

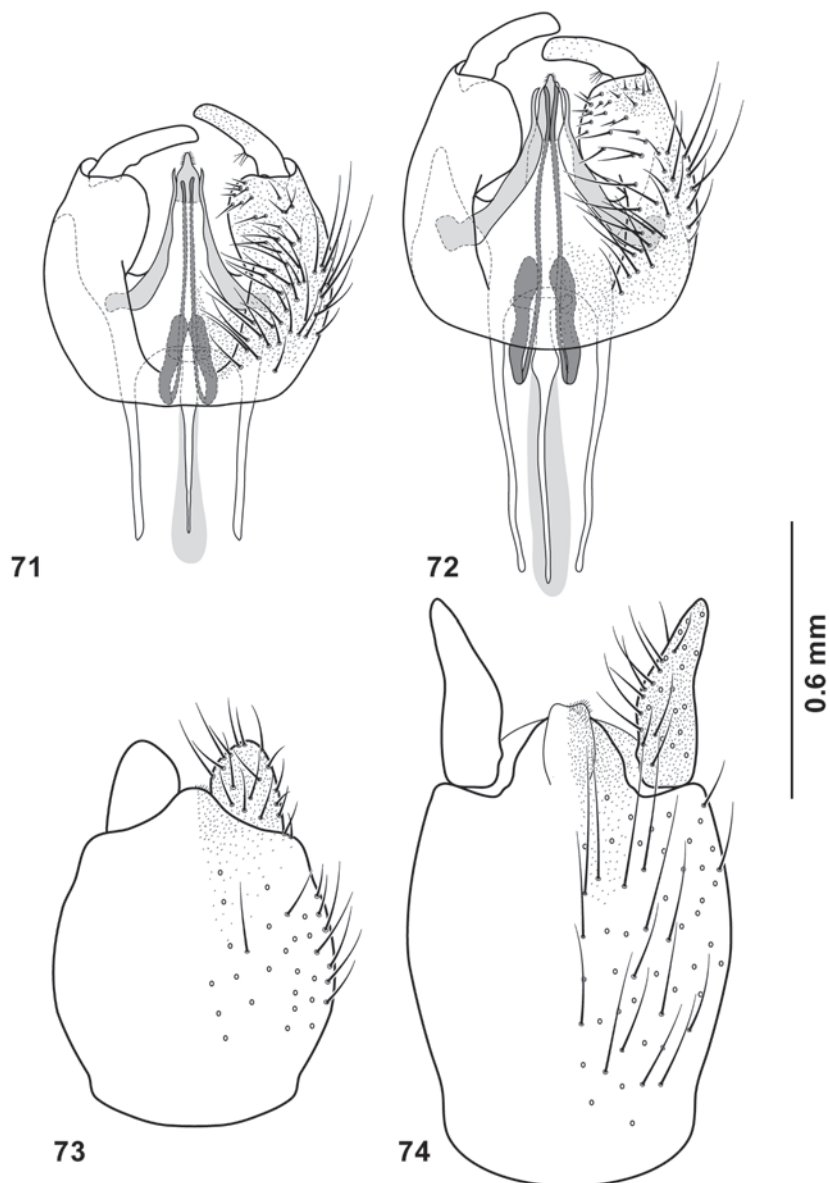
Thorax: Scutum brown, mostly with short dark setulae, with two dorsocentral whitish-brown pruinose vittae running from posterior half of postpronotal lobes to transverse suture; prescutellar area bluish-grey pruinose; pronotum brown with bluish-grey pruinosity and short pale setulae; postpronotal lobe orange-brown, appearing slightly browner dorsally, with sparse bluish-grey pruinosity, setulae



Figures 63–70. *Suragina* Walker spp. male terminalia, ventral view (63–66) and epandrium with cerci, dorsal view (67–70): **63**, **67** *S. freidbergi* Muller, sp. nov. paratype (BMSA(D)92376) **64**, **68** *S. malavaensis* Muller, sp. nov. paratype (ICIPE) **65**, **69** *S. milloti* (Séguy) (CSCA) **66**, **70** *S. monogramma* (Bezzi) (NMSA-DIP 028180). Scale bar (applicable to all illustrations): 0.6 mm.

pale; notopleuron bluish-grey pruinose with long pale setulae anteriorly and long dark setulae posteriorly; postalar wall dark brown and postalar callus orange-brown, both with slight bluish-grey pruinosity, supra-alar area with dark setulae, postalar callus with some short pale setulae interspersed between dark setulae; scutellum dark brown with a brownish- to orange-yellow apical margin with long dark setulae; majority of pleura brown with bluish-grey pruinosity, except for anepimeron, anatergite, katatergite and katepimeron orange-brown with bluish-grey pruinosity; proepisternum and proepimeron, katatergite and katepisternum with long pale setulae; anatergite and meron bare; anterior and posterior spiracles whitish-yellow, bare; postspiracular scale orange-brown; postscutellum orange-brown.

Legs: Fore coxae yellowish-brown, mid and hind coxae brown, all three coxae with bluish-grey pruinosity, hind coxa much less pronounced; fore coxal setulae long pale on anterior surface, with dark setulae apically; mid coxal setulae long



Figures 71–74. *Suragina* Walker spp. male terminalia, ventral view (**71**, **72**) and epandrium with cerci, dorsal view (**73**, **74**): **71**, **73** *S. mulanjeensis* Muller, sp. nov. paratype (NMSA-DIP 162049) **72**, **74** *S. zombaensis* Muller, sp. nov. paratype (NMSA-DIP 158450). Scale bar (applicable to all illustrations): 0.6 mm.

pale on anterior surface, dark apically; hind coxal setulae dark on anterior edge surrounding well-developed anterior apical point with some scattered short setulae, lateral apical edges with a mix of long pale and dark setulae; all trochanters yellowish-brown with short pale setulae; fore femur almost entirely yellow, except for brown apex; mid femur entirely yellow; hind femur yellow with brown to dark brown median band; fore and hind tibiae brown to dark brown, mid tibia yellow; fore and hind tarsi brown to dark brown, mid tarsi yellow except for terminal 3 segments that are brown; fore tarsal claws asymmetrical, outer claw much larger than inner claw, foreleg empodium ca 2× size of inner pulvillus, outer pulvillus ca 2× length of inner, approaching size of outer claw; fore femur overall with short pale setulae, with long pale setulae on posteroventral surface; mid femur with long pale setulae on ventral surface, otherwise with short pale setulae; hind femur with a mix of pale and dark setulae on dorsal and ventral

surfaces, base of femur with pale setulae; fore tarsi covered with long sensory setulae along antero- and posteroventral surfaces, sensory setulae ca 2× as long as tarsal segment is wide; hind leg overall stouter than remaining legs; hind tarsal segments 0.9–1.0× as long as hind tibia; tibial spur formula 0:2:2.

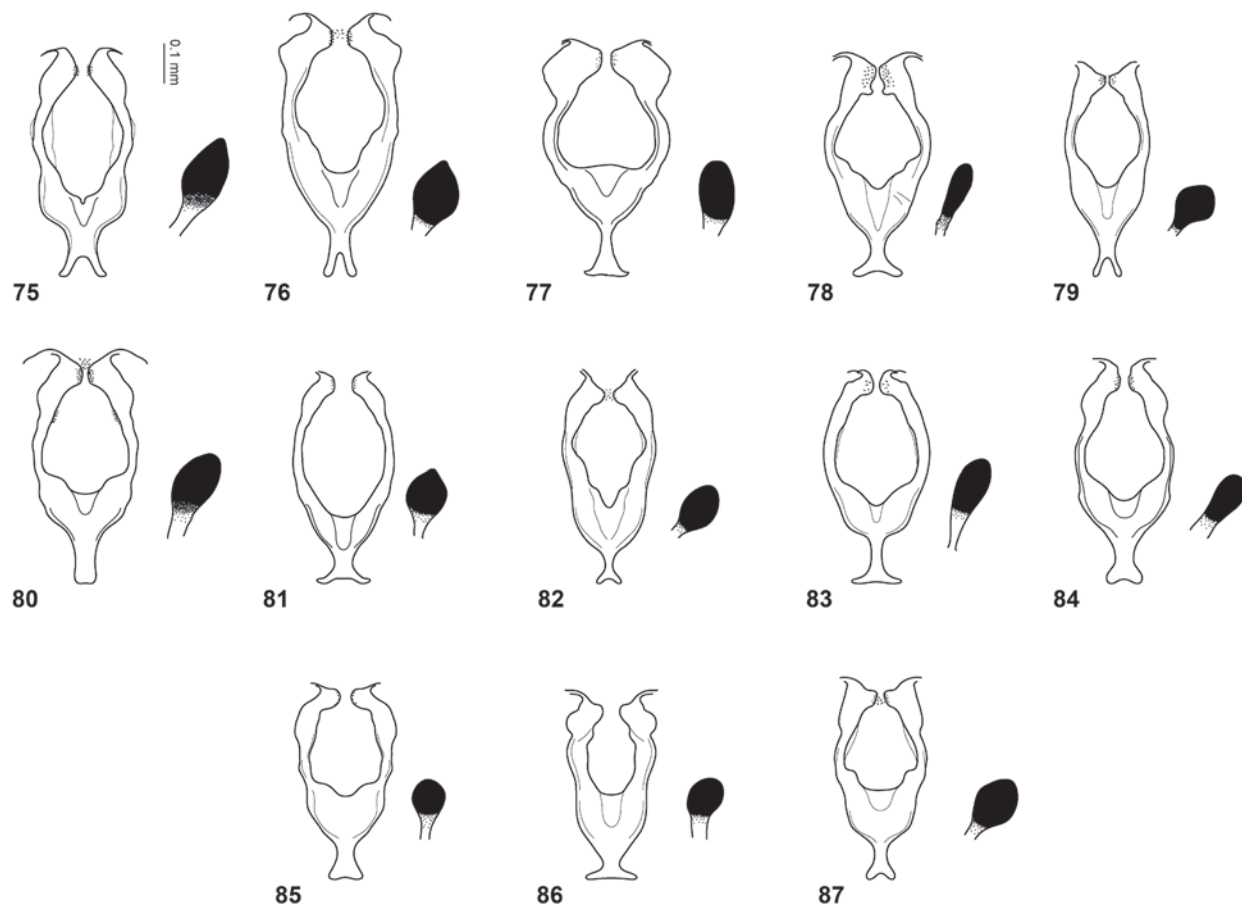
Wing: Brown suffused on majority of surface; dark brown stigma over area of veins R_1 and R_{2+3} and cell r_1 , difficult to discern due to surrounding brown suffusion on apical half of wing; preapical parts of cells br , bm hyaline, most of cell cua and anal lobe, and apical two-thirds of discal cell only lightly brown suffused; some specimens with cells r_{2+3} and m_4 having a small hyaline marking in each of their centres; veins dark brown; costa without distinct downward flexure over stigma; cell cua closed at wing margin, cell m_3 open, veins M_1 , M_2 , M_3 present; haltere stalk (except for yellow basal half) and knob dark brown, with a few short dark setulae.

Abdomen: Overall brownish-yellow colour; tergite 1 light brownish-yellow with a dark brown subtriangular dorsal marking surrounded by bluish-grey pruinosity up to lateral margins; tergites 2 and 3 with a dark brown longitudinal rectangular marking, otherwise brownish-yellow, tergite 3 also with a grey pruinose posterior band; tergite 4 with a dark brown subtriangular marking running towards a dark posterior band with greyish pruinosity; tergite 5 entirely dark brown with posterior grey pruinose band; remaining tergites dark brown; tergite 1 medially without a longitudinal suture; tergites with dark setulae dorsally, and long pale setulae laterally up to margins; sternites mostly yellowish, except sternites 4 and 5 dark brown; sternites with short and long pale setulae.

Terminalia (Figs 72, 74): Epandrium and cercus dark brown with dark setulae; gonocoxite, hypoproct and hypandrium with pale setulae; gonostylus almost parallel shaped with truncated apex, outer edge of gonostylus with short setulae, inner edge with protrusion with 4 setulae, apex of gonostylus sparsely covered in microtrichia; gonocoxite widening and appearing more rounded on apical half, apex somewhat flattened, gonocoxite outer and ventral medial surface with long setulae, inner and median surface of upper half with short setulae, lower ventral surface comparatively less setulose; gonocoxite with microtrichia between setulae; parameral apodeme with truncated apex, not reaching base of gonocoxite in ventral view, parameral sheath including parameral apodeme ca 0.7× length of gonocoxite; gonocoxal apodeme similar in length to gonocoxite and slightly shorter than ejaculatory apodeme; aedeagal tine curvature barely extending down past gonocoxites, apex of tines extending out slightly past parameral sheath; endoaedeagal process apically truncated and widened.

Female (Fig. 36): Similar to ♂ except for the following:

Head: Dichoptic; ommatidia of similar size except for those on upper quarter that are somewhat smaller; lateral edge of eye without any indentation, but also with apparent tubercle as in ♂; anterior ocellus similar in size to posterior pair; ocellar tubercle placed deeper in front of dorsal margin of eye compared to ♂; dorsal inner edge of eye separated from ocellar tubercle by paired silver-grey markings, appearing to extend down from vertex; upper occiput with some short dark setulae below black rectangular markings (♂ without); frons bluish-grey pruinose between lower half of eye down to antennal base, velvety-black from ocellar tubercle to lower half of eye when viewed anteriorly; frons running almost parallel down to antennal base; frons densely covered with dark setulae on velvety-black upper half, with dark setulae on lateral margins of lower half;



Figures 75–87. *Suragina* Walker spp. female genital fork and spermathecae, ventral view: **75** *S. agramma* (Bezzi) (ICIPE) **76** *S. bezzii* (Curran) (SAM-DIP-018403) **77** *S. bilobata* Muller, sp. nov. (CSCA) **78** *S. binominata* (Bequaert) (NMSA-DIP 158411) **79** *S. copelandi* Muller, sp. nov. paratype (BMSA(D)84686) **80** *S. freidbergi* Muller, sp. nov. paratype (BMSA(D)92158) **81** *S. liberiaensis* Muller, sp. nov. paratype (NMSA-DIP 158442) **82** *S. malavaensis* Muller, sp. nov. paratype (ICIPE) **83** *S. milloti* (Séguy) (CSCA) **84** *S. monogramma* (Bezzi) (BMSA(D)129988) **85** *S. mulanjeensis* Muller, sp. nov. paratype (NMSA-DIP 158392) **86** *S. semiobscura* Muller, sp. nov. paratype (ICIPE) **87** *S. zombaensis* Muller, sp. nov. paratype (NMSA-DIP 1584719). Scale bar (applicable to all illustrations): 0.1 mm.

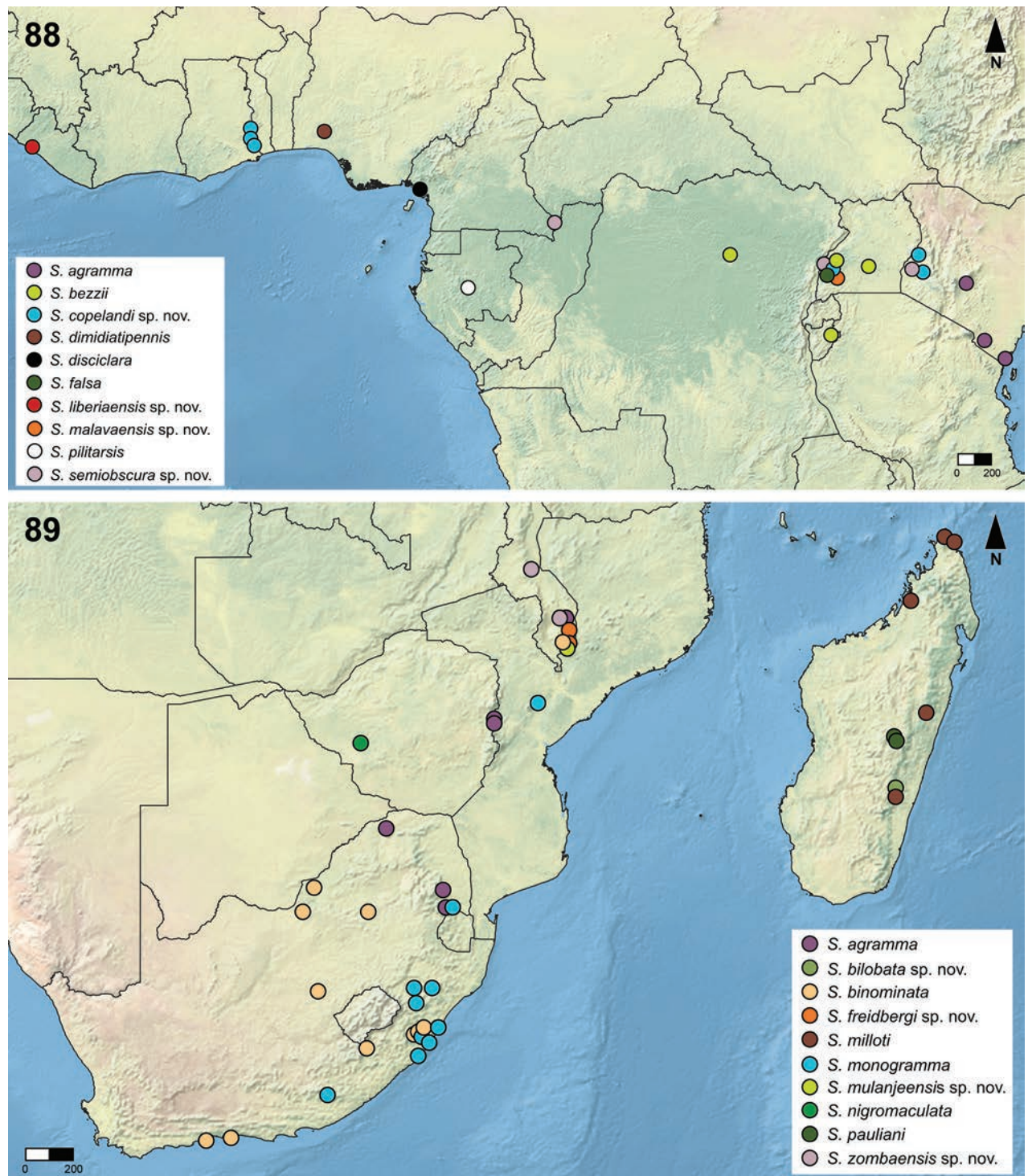
face separated anteriorly from clypeus by transverse suture, (less prominent than in ♂); antennal bases separated ca 0.6–0.8× width of scape, with slight longitudinal groove running between; scape 1.7× length of pedicel; 1st flagellomere ca 2× size of pedicel; proboscis ca same length as head height.

Thorax: Overall similar to ♂; scutum similar to that of ♂, except two dorso-central vittae are bluish-grey pruinose compared to whitish-brown in ♂.

Legs: Similar to ♂ in colour; fore tarsal claws symmetrical; overall leg setation similar to ♂ except generally shorter and coxal setulae all pale except for dark setulae surrounding anterior apical point of hind coxa; hind tarsal segments 0.98–1.01× as long as hind tibia

Wing (Fig. 54): Similar to ♂.

Abdomen: Tergite 1 with a narrower, rectangular (♂ subtriangular) dark brown marking, more widely bluish-grey pruinose than in ♂, medially with a longitudinal suture; tergite 2 with similar dark longitudinal marking, but surrounded by bluish-grey pruinosity instead of brownish-yellow ground colour; tergites 3–5 dark brown, posterior margins with similar grey pruinose bands as in ♂; tergite 1 with



Figures 88, 89. Distribution of *Suragina* Walker spp. within the Afrotropical Region.

long pale setulae on pruinose surface, and short dark setulae on dark brown surfaces, tergites 2–5 with short pale setulae on posterior pruinose bands and short dark setulae on rest of surface; tergites 6 and 7 with short dark setulae; tergites 1–5 with long pale setulae on lateral margins, tergites 6 and 7 with dark setulae laterally; sternites all yellow, compared to sternites 5 and 6 dark brown in ♂.

Terminalia (Fig. 87): Cercus yellowish-brown with some greyish pruinosity, with pale setulae; genital fork with distal apodeme ending broadly truncated; median lobe with narrow emargination; paired apical lobes with somewhat

slender appearance, inner surface with clustered microtrichia at apex; arms gradually rounded; three ovate and sclerotised spermathecae.

Etymology. Named after the type locality, the Zomba Plateau, Malawi. Feminine adjective in the nominative singular case.

Distribution. Malawi.

Acknowledgements

Martin Hauser (CSCA), Mandisa Ndlovu and Kirstin Williams (NMSA), and Robert Copeland (ICIPE) are thanked for providing study material. John Midgley and Terence Bellingan are thanked for extracting study material at the Iziko South African Museum, and Aisha Mayekiso (SAMC) for facilitating its loan. Erica McAlister (NHMUK) is thanked for providing photos of type material of several species. Western Cape material was collected using Cape Nature Permit AAA007-00032-0056. The Forestry Research Institute of Malawi, (FRIM), in particular, Dr Tembo Chanyenga, is thanked for their partnership and for providing a research permit. Sally Adam is thanked for facilitating access to Little Stone Cottage, Robinson Pass. Richard Green is thanked for facilitating the research license from the South African Department of Agriculture, Forestry and Fisheries (DAFF) for Mariepskop State Forest. Frank Menzel is thanked for assisting with information on the whereabouts of the type material of *S. disciclara*. Andreas Stark is thanked for facilitating photographs of the type material of *S. binominata*. Martin Husemann and Eileen Nguyen at Museum der Natur Hamburg are thanked for information on the whereabouts of the type material of *S. pilatarsis*. BSM acknowledges the National Museum, Bloemfontein, for its continued support of research on Afrotropical Diptera. The reviewers of the manuscript are thanked for their constructive comments and corrections.

Additional information

Conflict of interest

The authors have declared that no competing interests exist.

Ethical statement

BSM confirms ethical clearance, number NMB ECC 2019/1, forming part of project 457 of the National Museum, Bloemfontein, South Africa.

Funding

All funding provided by the National Museum, Bloemfontein.

Author contributions

Muller conceptualised the project with inputs from Swart and Snyman. Muller identified, described and revised the species, and wrote the first draft of the manuscript. Snyman and Swart commented and made additions to the final draft.

Author ORCIDs

Burgert S. Muller  <https://orcid.org/0000-0002-7304-4050>

Vaughn R. Swart  <https://orcid.org/0000-0001-7905-5298>

Louwrens P. Snyman  <https://orcid.org/0000-0002-5768-7216>

Data availability

All of the data that support the findings of this study are available in the main text.

References

- Baldachhino F, Desquesnes M, Mihok S, Foil LD, Duvall G, Jittapalapong S (2014) Tabanids: Neglected subjects of research, but important vectors of disease agents. *Infection, Genetics and Evolution* 28: 596–615. <https://doi.org/10.1016/j.mee-gid.2014.03.029>
- Bequaert J (1921) *Atherix braunsi* nov. sp., a South African leptid with gregarious habits (Diptera). *Psyche* (Cambridge, Massachusetts) 28(1): 1–7. <https://doi.org/10.1155/1921/95269>
- Bezzi M (1926) South African Rhagionidae (Diptera) in the South African Museum. *Annals of the South African Museum* 23: 297–324. <https://biostor.org/reference/128969> [Last accessed: 2024/10/29]
- Brunetti E (1929) I.—New African Diptera. *Annals & Magazine of Natural History* 4(19): 1–35. <https://doi.org/10.1080/00222932908673024>
- Cumming JM, Wood DM (2017) 3. Adult morphology and terminology. In: Kirk-Spriggs AH, Sinclair BJ (Eds) *Manual of Afrotropical Diptera*. Volume 1. Introductory chapters and keys to Diptera families. Suricata 4. South African National Biodiversity Institute, Pretoria, 89–133.
- Curran CH (1928) Diptera of the American Museum Congo Expedition. Part III. – Stratiomyidae, Rhagionidae, Therevidae, Scenopinidae, Ortalidae, Micropezidae, Piophilidae, Sepsidae and Diopsidae. *Bulletin of the American Museum of Natural History* 58: 167–187.
- Desquesnes M, Lamine Dia M (2004) Mechanical transmission of *Trypanosoma vivax* in cattle by the African tabanid *Atylotus fuscipes*. *Veterinary Parasitology* 119(1): 9–19. <https://doi.org/10.1016/j.vetpar.2003.10.015>
- Evenhuis NL (2024) The insect and spider collections of the world website. <http://hbs.bishopmuseum.org/codens/> [Last accessed: 2024/10/29]
- González C, Elgueta M, Coscarón S (2019) A catalog of Athericidae (Diptera) from Neotropical and Andean Regions. *Zootaxa* 4648(2): 287–298. <https://doi.org/10.11646/zootaxa.4648.2.5>
- Harper GJ, Steininger MK, Tucker CJ, Juhn D, Hawkins F (2007) Fifty years of deforestation and forest fragmentation in Madagascar. *Environmental Conservation* 34(4): 325–333. <https://doi.org/10.1017/S0376892907004262>
- Knab F (1912) Blood-sucking and supposedly blood-sucking Leptidae. *Proceedings of the Entomological Society of Washington* 14: 108–110.
- Lindner E (1925) Neue exotische Dipteren (Rhagionidae et Tabanidae). *Konowia* 4: 20–24. https://www.zobodat.at/pdf/KON_4_0020-0024.pdf [Last accessed: 2024/11/27]
- Loew H (1863) Enumeratio dipterorum, quae C. Tollin ex Africâ meridionali (Orangestat, Bloemfontein) misit. *Wiener entomologische Monatsschrift* 7: 9–16.
- Muller BS, Swart VR, Snyman LP (2023) Afrotropical *Atrichops* Verrall (Diptera, Athericidae) with description of a new species. *African Invertebrates* 64(3): 303–322. <https://doi.org/10.3897/afrinvertebr.64.113133>
- Nagatomi A (1962) Studies in the aquatic snipe flies of Japan. Part V. Biological notes (Diptera, Rhagionidae). *Mushi* 36: 103–149.

- Oldroyd H (1939) Rhagionidae, Tabanidae, Asilidae, Bombyliidae. Ruwenzori Expedition – 1934–5, Vol. II Nos. 1–2. Trustees of the British Museum (Natural History), London, 13–47.
- Perich MJ, Wright RE, Lusby KS (1986) Impact of Horse Flies (Diptera: Tabanidae) on Beef Cattle. *Journal of Economic Entomology* 79(1): 128–131. <https://doi.org/10.1093/jee/79.1.128>
- Sayre R (2023) Africa Terrestrial Ecosystems: U.S. Geological Survey data release. <https://doi.org/10.5066/P9BHBKA2>
- Ségué E (1951) Description d'une nouvelle espèce de Rhagionidae de Madagascar. *Mémoires de l'Institut scientifique de Madagascar. Série A.* 6: 395–397.
- Speiser P (1914) Beiträge zur Dipterenfauna von Kamerun II. *Deutsche Entomologische Zeitschrift* 1914(1): 1–16. <https://doi.org/10.1002/mmnd.191419140102>
- Stuckenberg BR (1960) Chapter XII. Diptera (Brachycera): Rhagionidae. In: Hanström B, Brinck P, Rudebeck G (Eds) *South African animal life. Results of the Lund University Expedition in 1950–1951.* V. Almqvist & Wiksell, Uppsala, 216–308.
- Stuckenberg BR (1965) The Rhagionidae of Madagascar (Diptera). *Annals of the Natal Museum* 18: 89–170. https://hdl.handle.net/10520/AJA03040798_759 [Last accessed: 2024/10/29]
- Stuckenberg BR (1980) 23. Family Athericidae. In: Crosskey RW (Ed.) *Catalogue of the Diptera of the Afrotropical Region.* British Museum (Natural History), London, 312–313.
- Stuckenberg BR (2000) A new genus and species of Athericidae (Diptera: Tabanoidea) from Cape York Peninsula. *Records of the Australian Museum* 52(2): 151–159. <https://doi.org/10.3853/j.0067-1975.52.2000.1312>
- Stuckenberg BR, Young E (1973) A record of an avian host for blood-sucking Athericidae (Diptera). *South African Journal of Science* 69: 315.
- Torppa KA, Wirta H, Hanski I (2020) Unexpectedly diverse forest dung beetle communities in degraded rain forest landscapes in Madagascar. *Biotropica* 52(2): 351–365. <https://doi.org/10.1111/btp.12767>
- Woodley NE (2007) Notes on South American Dasyomma, with the description of a remarkable new species from Chile (Diptera: Athericidae). *Zootaxa* 1443(1): 29–35. <https://doi.org/10.11646/zootaxa.1443.1.3>
- Woodley NE (2017) 38. Athericidae (Water Snipe Flies). In: Kirk-Spriggs AH, Sinclair BJ (Eds) *Manual of Afrotropical Diptera. Volume 2. Nematocerous Diptera and lower Brachycera. Suricata 5.* South African National Biodiversity Institute, Pretoria, 885–891.
- Yang D, Dong W, Zhang K (2016) 65 Fauna Sinica, Insecta, Diptera: Rhagionidae and Athericidae. Science Press, Beijing, 480 pp.

A new species and new records of *Chumma* (Araneae, Macrobonidae) from South Africa

Yuri M. Marusik^{1,2,3} , Charles R. Haddad² 

¹ Institute for Biological Problems of the North, Portovaya Str. 18, Magadan 685000, Russia

² Department of Zoology & Entomology, University of the Free State, Bloemfontein 9300, South Africa

³ Altai State University, Lenina Pr., 61, Barnaul, RF-656049, Russia

Corresponding author: Charles R. Haddad (haddadcr@ufs.ac.za)

Abstract

A new species of the genus *Chumma* Jocqué, 2001, *C. foordi* **sp. nov.**, is described from the Western Cape, South Africa. New distribution records for *C. bicolor* Jocqué & Alderweireldt, 2018, *C. foliata* Jocqué & Alderweireldt, 2018 and *C. gastroperforata* Jocqué, 2001 are presented. The genus is recorded from the Northern Cape Province for the first time, extending its range extensively to the northwest by approximately 450 km. The distribution of all *Chumma* species is mapped.

Key words: Amaurobiidae, Aranei, Chummidae, forest, fynbos, spider



This article is part of:

Gedenkschrift for Prof. Stefan H. Foord

Edited by Galina Azarkina, Ansie Dippenaar-Schoeman, Charles Haddad, Robin Lyle, John Mldgley, Caswell Munyai

Academic editor: Ansie Dippenaar

Received: 7 October 2024

Accepted: 4 December 2024

Published: 30 December 2024

ZooBank: <https://zoobank.org/68A457C7-9F92-4C49-A7DB-1E8243AE5086>

Citation: Marusik YuM, Haddad CR (2024) A new species and new records of *Chumma* (Araneae, Macrobonidae) from South Africa. African Invertebrates 65(2): 329–338. <https://doi.org/10.3897/AfrInvertebr.65.138735>

Copyright: ©

Yuri M. Marusik & Charles R. Haddad.

This is an open access article distributed under terms of the Creative Commons Attribution License (Attribution 4.0 International – CC BY 4.0).

Introduction

Chumma Jocqué, 2001 is a small genus with nine described species restricted to southern Africa. Most have been collected in the southern parts of South Africa (eight species), with one species recorded from the enclave of Lesotho. All the species were described in two publications (Jocqué 2001; Jocqué and Alderweireldt 2018). Originally, the genus was described in a monogeneric and monotypic family, Chummidae Jocqué, 2001. However, it was later synonymized with Amaurobiidae Thorell, 1869 based on a molecular analysis using six genes (Wheeler et al. 2017), with its placement in the subfamily Macroboninae Bonnet, 1957 also supported by Crews et al. (2020) and Kulkarni et al. (2023) based on analyses of multiple genes. Recently, *Chumma* was included in Macrobonidae when the subfamily was elevated to family rank based on analysis of ultraconserved elements (Gorneau et al. 2023). In all these studies, *Chumma* was clearly nested within the Macroboninae/-idae clade, usually as sister to the South African genus *Chresiona* Simon, 1903, supporting the synonymy of Chummidae with Macrobonidae, as defined by Gorneau et al. (2023).

While studying spiders collected in the Western Cape, the first author found trionychan specimens with only one pair of spinnerets visible through a compound microscope. More precise examination using photography revealed six spinnerets, with two pairs considerably reduced. Discussions with the second author revealed that these specimens belong to *Chumma*. The goal of this

paper is to provide a description of this new species, new records of the genus collected subsequent to the recent treatment of the genus by Jocqué and Alderweireldt (2018), and comments on its relationships.

Material and methods

The material examined in this study is deposited in the National Collection of Arachnida, ARC – Plant Health and Protection, Pretoria (NCA) and the National Museum, Bloemfontein (NMBA). All measurements are given in millimeters. The distribution map was prepared using SimpleMappr (www.simplemappr.net).

Photographs of specimens and their copulatory organs were obtained using an Olympus Camedia E-520 camera attached to an Olympus SZX16 stereomicroscope at the Zoological Museum of the University of Turku, Finland. Digital images of different focal planes were stacked with Helicon Focus™ 8.1.1. The palp of the paratype male was dehydrated in a series of increasing ethanol concentrations, glued to a stub, sputter-coated with gold and examined using a JEOL JSM-6490LV scanning electron microscope.

Abbreviations: **ALE** – anterior lateral eye; **ALS** – anterior lateral spinnerets; **AME** – anterior median eye; **PLE** – posterior lateral eye; **PLS** – posterior lateral spinnerets; **PME** – posterior median eye; **PMS** – posterior median spinnerets.

Taxonomy

Macrobnidae Bonnet, 1957

Remarks. The type species of *Macrobnus* Tullgren, 1901, *M. backhause-ni* (Simon, 1896) was redescribed, redefined and extensively illustrated by Almeida-Silva (2013), with an updated diagnosis of the genus provided. However, this work has never been formally published and is thus not included in the literature on the species or in the World Spider Catalog (WSC 2024). With the exception of *Chumma*, genera included in the Macrobnidae have no dorsal abdominal scuta. Almeida-Silva (2013) mentions that in several genera considered in the family the ALS are usually larger than the PMS and PLS and mentioned a vestigial form: “Males with reduced PLS may lack spigots on these” (Almeida-Silva 2013). Jocqué (2001: fig. 2a) and Almeida-Silva (2013) showed that the PMS and PLS of female *C. inqueta* Jocqué, 2001 were similar in size and both smaller than the ALS. In this paper, we image the spinnerets of male *Chumma* for the first time, showing that both posterior pairs are significantly reduced in size and can be considered vestigial (Fig. 1E).

Chumma foordi sp. nov

<https://zoobank.org/69F6393F-3C9D-4D99-A6FB-1D5925D260E9>

Figs 1–3

Material examined. Holotype. SOUTH AFRICA • ♂; *Western Cape Province*; Cape Town, Kirstenbosch Botanical Garden; 33°58'54"S, 18°25'19"E; 30 Jan. 2017; Y.M. Marusik leg.; litter in Afromontane forest (NMBA 19612).

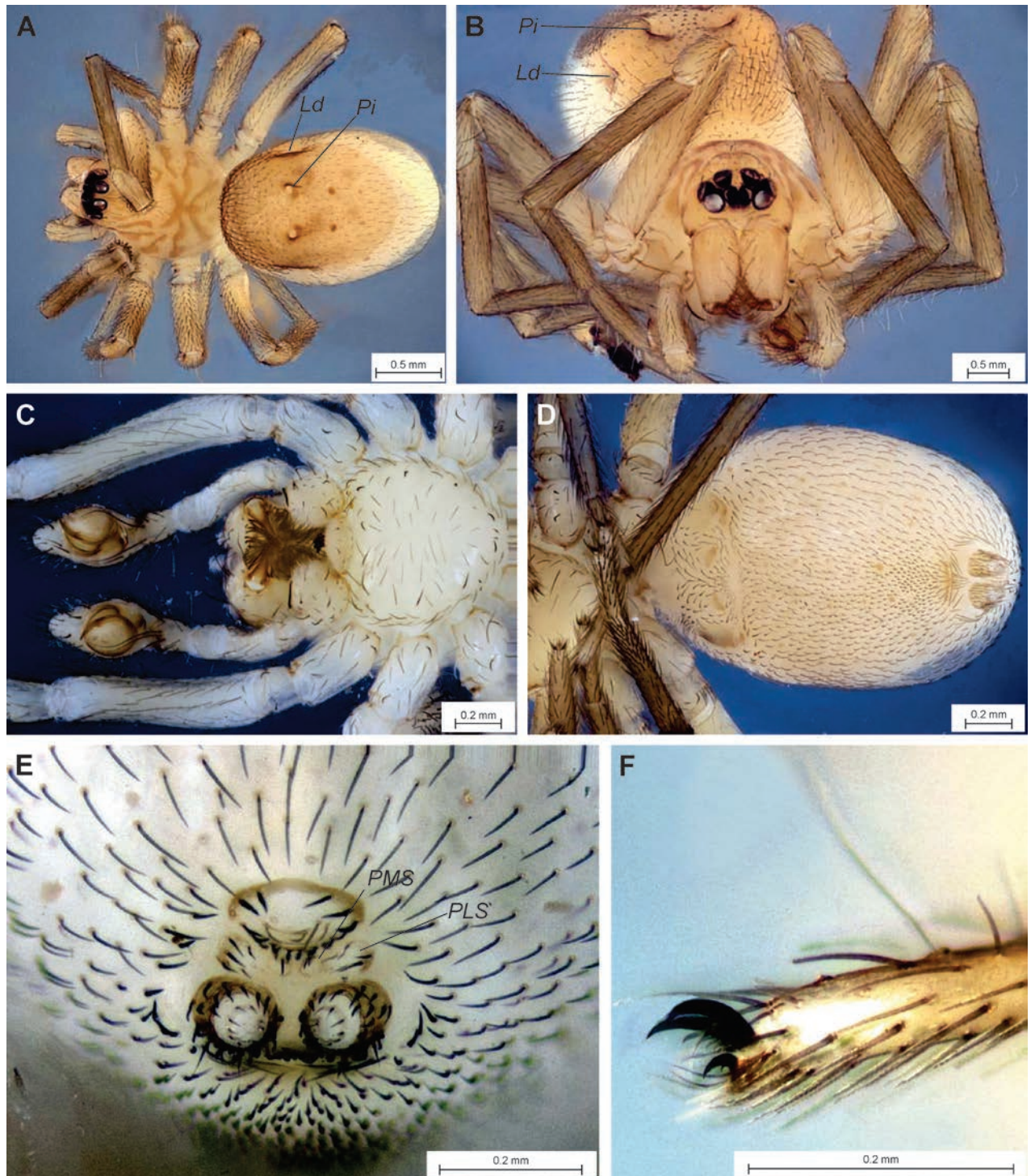


Figure 1. Holotype male of *Chumma foordi* sp. nov., somatic morphology **A** habitus, dorsal **B** same, frontal **C** prosoma, ventral **D** abdomen, ventral **E** spinnerets, caudal **F** tarsus I, dorso-lateral. Abbreviations: *Ld* lateral depression; *Pi* round pit of scutum; *PLS* posterior lateral spinneret; *PMS* posterior median spinneret.

Paratype. 1♂, same data as holotype.

Other material. 17 juveniles, same data as holotype.

Diagnosis. Males of the new species differ from all congeners by having a pair of deep round pits (*Pi*) on the scutum (vs. absent or elongate) and a lateral depression (*Ld*, lacking in all other species) (see Jocqué 2001; Jocqué and

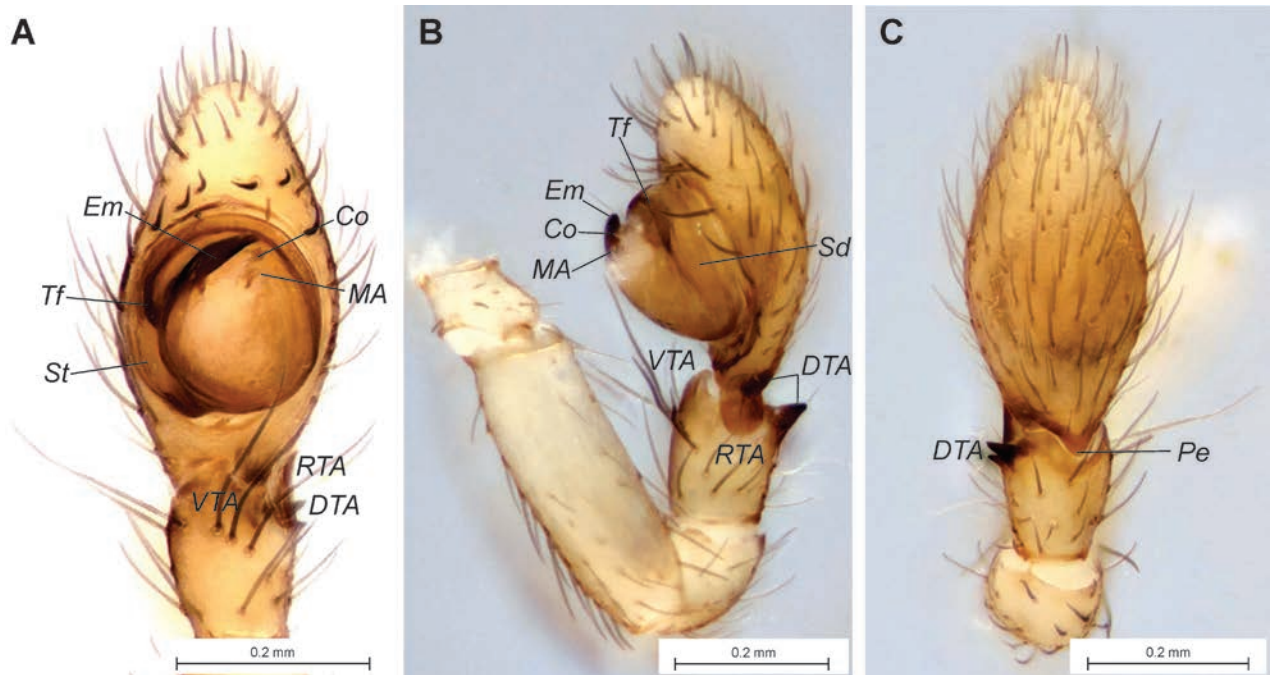


Figure 2. Holotype male of *Chumma foordi* sp. nov. **A** terminal part of left palp, ventral **B** whole left palp, retrolateral **C** left palpal patella, tibia and cymbium, dorsal. Abbreviations: *Co* conductor; *DTA* dorsal tibial apophysis; *Em* embolus; *MA* median apophysis; *Pe* proximal extension of cymbium; *RTA* retrolateral tibial apophysis; *Sd* sperm duct; *St* subtegulum; *Tf* tegular furrow; *VTA* ventral tibial apophysis.

Alderweireldt 2018). The new species also differs by the short embolus, which is somewhat similar to that in *C. interfluvialis* Jocqué & Alderweireldt, 2018 but has four rather than three tibial apophyses and a round rather than oval tegulum (cf. Figs 2, 3 with Jocqué and Alderweireldt 2018: fig. 5A–C). Coloration yellow to light brown dorsally and pale yellow ventrally; carapace with dark radial stripes. Female unknown.

Description. Male: Total length 2.83. Carapace 1.14 long, 0.93 wide, sternum 0.64 long and wide; chelicera 0.29 long; labium 0.14 long, 0.27 wide; abdomen 1.79 long, 1.19 wide, scutum 1.29 long. ALE~PLE~PME ca. 0.1, AME 0.06; AME-AME 0.02, AME-ALE 0.01, ALE-ALE 0.19, PME-PME 0.06, PME-PLE 0.05, PLE-PLE 0.41; clypeus near ALE 0.06.

Carapace cream, with yellow-brown radial stripes directed towards palps and legs (Fig. 1A). Distal part of chelicerae and maxillae with dense setae; maxillae as long as wide; labium semicircular, ca. 2.3 times wider than long; sternum as wide as long, about round. Abdomen oval, with dorsal scutum occupying ca. $\frac{3}{4}$ of abdomen length, ca. 1.4 times longer than wide, scutum darker than rest of abdomen (Fig. 1A, B), with pair of deep round pits (*Pi*) in anterior 1/3, pair of sigilla behind pits and lateral depressions (*Ld*); modified setae located only in anterior part of scutum; venter uniformly colored, with pair of scuta at epiandrus, setae on epiandrus shorter than others (Fig. 1C); short setae also concentrated anterior to tracheal spiracle (Fig. 1D); colulus represented by group of setae; under light microscopy only two spinnerets can be recognized, but three pairs actually present, with PMS and PLS vestigial (Fig. 1E); tarsi with three claws (Fig. 1F).

Leg measurements of *Chumma foordi* sp. nov. holotype male:

| | Fe | Pt | Ti | Mt | Ta | Total |
|------|------|------|------|------|------|-------|
| Palp | 0.44 | 0.2 | 0.14 | - | 0.44 | 1.22 |
| I | 1.07 | 0.4 | 0.97 | 0.86 | 0.61 | 3.91 |
| II | 0.93 | 0.36 | 0.74 | 0.71 | 0.57 | 3.31 |
| III | 0.8 | 0.31 | 0.57 | 0.69 | 0.36 | 2.73 |
| IV | 1.17 | 0.4 | 0.94 | 1.0 | 0.44 | 3.95 |

Legs spineless. Chelicera with two promarginal and three retromarginal teeth.

Palp as in Figs 2, 3: femur 3 × longer than wide, as long as cymbium; patella as long as femur wide; tibia cylindrical, 1.3 × longer than wide, with four short apophyses: ventral (VTA), retrolateral (RTA) and two spike-like subdorsal (DTA); cymbium lenticular in dorsal view, twice as long as wide, widest at middle, with proximal extension (Pe) facing towards tibial notch; tegulum round in ventral view, as long as wide, with deep distal tegular furrow (Tf); sperm duct running along lateral margin of tegulum, lacking any loops, originating at ca. 9 o'clock position; conductor (Co) small, almost indistinct; median apophysis (MA) small, membranous, finger-like; embolus (Em) small, with rounded anterior and straight posterior parts, about 4 × longer than maximal width, originating at ca. 9 o'clock position and terminating at about 0:30; subtegulum (St) exposed prolaterally.

Etymology. Named after our late friend and colleague Stefan Foord, in recognition of his contributions to the study of spider ecology and biodiversity, particularly in South Africa.

Distribution. Only known from the type locality (Fig. 4).

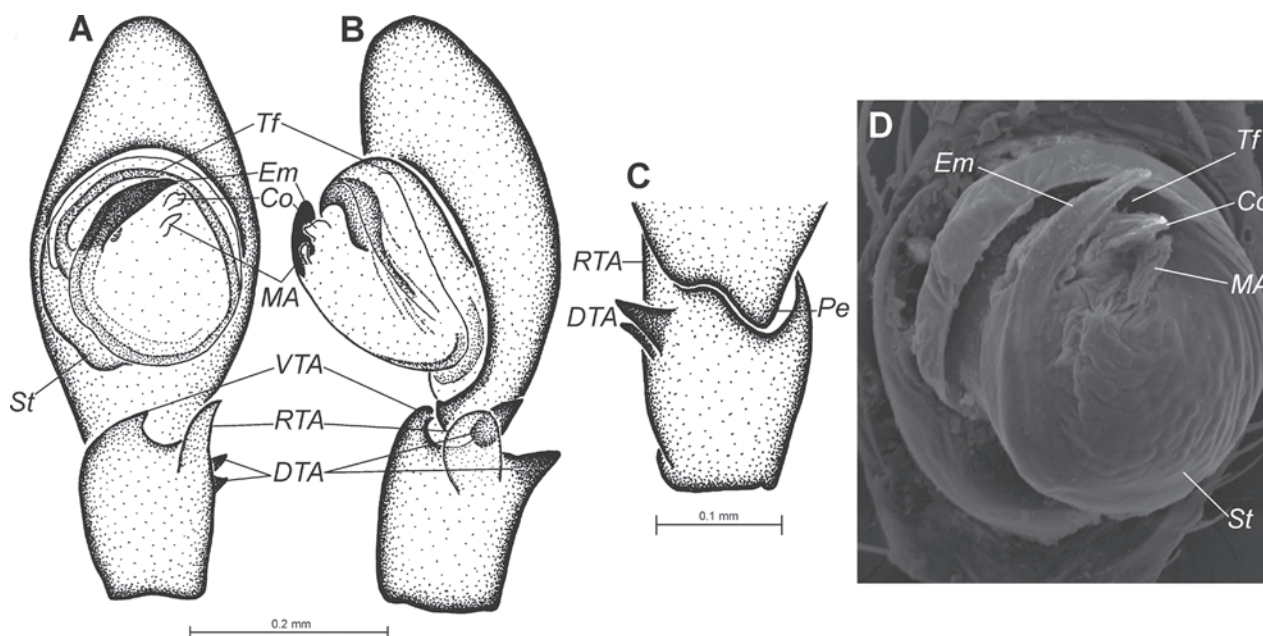


Figure 3. Line drawings of holotype male (A–C) and scanning electron microscope photo of paratype male (D) of *Chumma foordi* sp. nov. **A** left palpal tibia and tarsus, ventral **B** same, retrolateral **C** left palpal tibia and basal part of cymbium, dorsal **D** right palpal tegulum, mirrored, ventral. Abbreviations: Co conductor; DTA dorsal tibial apophysis; Em embolus; MA median apophysis; Pe proximal extension of cymbium; RTA retrolateral tibial apophysis; St subtegulum; Tf tegular furrow; VTA ventral tibial apophysis.

***Chumma bicolor* Jocqué & Alderweireldt, 2018**

Chumma bicolor Jocqué & Alderweireldt, 2018: 4, figs 1A–E, 2A (♀).

Chumma bicolor: Dippenaar-Schoeman et al. 2022: 10, 2 figs (♀).

Material examined. SOUTH AFRICA; Western Cape Province • 2 imm. 2♀; Hoekwil, Bergplaas Rd hiking trail; 33°54.706'S, 22°40.689'E; 475 m a.s.l.; 10 Oct. 2022; C. Haddad et al. leg.; sifting litter, fynbos; NMBA 19424 • 2 subadult ♂ 1♀; Plettenberg Bay, Bobbejaanskloof Private Nature Reserve; 33°57.805'S, 23°21.232'E; 175 m a.s.l.; 10 Oct. 2022; C. Haddad et al. leg.; sifting litter, Afro-montane forest; NMBA 19487 • 1 subadult ♀; Riversdale, Garcia Nature Reserve, Sleeping Beauty trail; 33°57.357'S, 21°13.255'E; 530 m a.s.l.; 8 Oct. 2023; C. Haddad et al. leg.; sifting litter, fynbos; NMBA 19276.

Distribution. Previously known from the type locality (Goukamma in the Western Cape) only. Reported from three additional localities here (Fig. 4). This species is sympatric with *C. gastroperforata* Jocqué, 2001 at Bobbejaanskloof Private Nature Reserve.

***Chumma foliata* Jocqué & Alderweireldt, 2018**

Chumma foliata Jocqué & Alderweireldt, 2018: 7, figs 2B–D, 3A–F (♂♀).

Chumma foliata: Dippenaar-Schoeman et al. 2022: 11, 3 figs (♂♀).

Material examined. SOUTH AFRICA; Eastern Cape Province • 2♂; Grahamstown, Coombs District, Clayputs Farm, New Windmill Camp; 33°19.900'S, 26°51.311'E; 12 Mar. 2020; R. Booysen & A. Marais leg.; hand collecting; NCA 2020/1107.

Distribution. Previously known from the type locality (Hogsback) only. Reported from an additional locality here (Fig. 4).

***Chumma gastroperforata* Jocque, 2001**

Chumma gastroperforata Jocqué, 2001: 486, figs 8b, 9a, b, 10a–e, 11a, b (♂♀).

Chumma gastroperforata: Jocqué & Alderweireldt, 2018: 15, fig. 7H (♂♀).

Chumma gastroperforata: Dippenaar-Schoeman et al. 2022: 12, 5 figs. (♂♀).

Material examined. SOUTH AFRICA; Western Cape Province • 2♀; George, Outeniqua Nature Reserve; 33°56.015'S, 22°25.543'E; 260 m a.s.l.; 9 Oct. 2022; C. Haddad et al. leg.; sifting litter, Afromontane forest; NMBA 19339 • 1♂; Gondwana Game Reserve; 34°02'49"S, 21°52'57"E; 25 Mar. 2005–3 Jan. 2006; M. Burger et al. leg.; pitfall and funnel traps; NCA 2011/843 • 1♂; Outeniquastrand, near George; 34°02.754'S, 22°17.037'E; 7 Jan. 2015; C. Haddad leg.; base of grass tussocks; NCA 2015/1753 • 3♂; Plettenberg Bay, Bobbejaanskloof Private Nature Reserve; 33°57.805'S, 23°21.232'E; 175 m a.s.l.; 10 Oct. 2022; C. Haddad et al. leg.; sifting litter, Afromontane forest; NMBA 19486 • 2 subadult ♂ 2♂ 1 subadult ♀; Plettenberg Bay, Keurbooms Nature Reserve; 34°00.070'S, 23°24.165'E; 220 m a.s.l.; 11 Oct. 2022; C. Haddad et al. leg.; sifting litter, Afromontane forest; NMBA 19552.



Figure 4. Distribution records of *Chumma bicolor* Jocqué & Alderweireldt, 2018 (circles), *C. foliata* Jocqué & Alderweireldt, 2018 (stars), *C. foordi* sp. n. (hexagon), *C. gastroperforata* Jocqué, 2001 (triangles) and an undetermined *Chumma* sp. (inverted triangle). Black icons are published records and white icons are new records presented here. Published records are sourced from Jocqué (2001), Jocqué and Alderweireldt (2018) and Dippenaar-Schoeman et al. (2022), with historical misidentifications corrected.

Distribution. Jocqué (2001) initially described *C. gastroperforata* based on material from four localities (Witelsbos [type locality], Van Huyssteenbos, Silverrivier and Saasveld), but later included the paratypes from the latter two localities under *C. striata* Jocqué & Alderweireldt, 2018, together with its holotype from Rosendal farm near Prince Albert. However, Dippenaar-Schoeman et al. (2022) incorrectly included all five localities under *C. gastroperforata*; only Witelsbos and Van Huyssteenbos are still valid. We report *C. gastroperforata* from five additional localities here (Fig. 4).

***Chumma* sp.**

Material examined. SOUTH AFRICA; Northern Cape Province • 1 subadult ♂; Ni-gramoep Slow Living Guest Farm; 29°31.460'S, 17°35.628'E; 840 m a.s.l.; 10 Jan. 2021; C. Haddad et al. leg.; leaf litter, west-facing slope; NCA 2021/652.

Distribution. Although this species is only known from a single subadult male, it is the first record from the Northern Cape Province, extending the range of the genus by more than 450 km northwards in the western extreme of its distribution (Fig. 4). This disjunct distribution of the genus suggests that it likely occurs in Fynbos and Succulent Karoo biotopes along the western interior of South Africa too. Its apparent absence here could be attributed to the historically poor sampling effort in this part of the country, whereas the southern and central parts of the country where most *Chumma* have been recorded (Figs 4, 5) are comparatively well-sampled (Dippenaar-Schoeman et al. 2023).



Figure 5. Distribution records of *Chumma inquieta* Jocqué, 2001 (squares), *C. interfluvialis* Jocqué & Alderweireldt, 2018 (circle), *C. lesotho* Jocqué & Alderweireldt, 2018 (triangle), *C. striata* Jocqué & Alderweireldt, 2018 (inverted triangles), *C. subridens* Jocqué & Alderweireldt, 2018 (hexagons) and *C. tsitsikamma* Jocqué & Alderweireldt, 2018 (star). Records are sourced from Jocqué (2001), Jocqué and Alderweireldt (2018) and Dippenaar-Schoeman et al. (2022), with historical misidentifications corrected.

Acknowledgments

We are grateful to the various collectors that assisted with the field work resulting in most of the new records presented in this paper, which was made possible through grants from the National Research Foundation of South Africa to C.H. (#129108 and FBIS230515106311). Trudie Peyper (National Museum, Bloemfontein) and Robin Lyle (National Collection of Arachnida, Pretoria) are thanked for accessioning the collected material. YM thanks Seppo Koponen and Ilari E. Sääksjärvi (Turku, Finland) for arranging a research visit to the Zoological Museum of the University of Turku and for the use of its facilities.

Additional information

Conflict of interest

The authors have declared that no competing interests exist.

Ethical statement

No ethical statement was reported.

Funding

This work was supported by National Research Foundation.

Author contributions

Y.M. prepared the species description and microscope images and contributed to writing the text. C.H. provided new distribution records, prepared the distribution map and contributed to writing the text.

Author ORCIDs

Yuri M. Marusik  <https://orcid.org/0000-0002-4499-5148>

Charles R. Haddad  <https://orcid.org/0000-0002-2317-7760>

Data availability

All of the data that support the findings of this study are available in the main text or Supplementary Information.

References

- Almeida-Silva LM (2013) Cladistic analysis of Macroibunidae Petrunkevitch, 1928 and revision of Macroibuninae (Araneae). Unpublished Ph.D thesis, University of São Paulo, São Paulo, [ix +] 322 pp.
- Crews SC, Garcia EL, Spagna JC, Van Dam MH, Esposito LA (2020) The life aquatic with spiders (Araneae): repeated evolution of aquatic habitat association in Dictynidae and allied taxa. *Zoological Journal of the Linnean Society* 189(3): 862–920 [+ Suppl]. <https://doi.org/10.1093/zoolinnean/zlz139>
- Dippenaar-Schoeman AS, Haddad CR, Foord SH, Lotz LN, Jocqué R (2022) The Amaurobiidae of South Africa. Version 2. South African National Survey of Arachnida Photo Identification Guide, Irene, 26 pp. <https://doi.org/10.5281/zenodo.5981342>
- Dippenaar-Schoeman AS, Haddad CR, Lotz LN, Booysen R, Steenkamp RC, Foord S (2023) Checklist of the spiders (Araneae) of South Africa. *African Invertebrates* 64(3): 221–281. <https://doi.org/10.3897/AfrInvertebr.64.111047>
- Gorneau JA, Crews SC, Cala-Riquelme F, Montana KO, Spagna JC, Ballarin F, Almeida-Silva LM, Esposito LA (2023) Webs of intrigue: museum genomics elucidate relationships of the marronoid spider clade (Araneae). *Insect Systematics and Diversity* 7(5): 1–18. <https://doi.org/10.1093/isd/ixad021>
- Jocqué R (2001) Chummidae, a new spider family (Arachnida, Araneae) from South Africa. *Journal of Zoology* 254(4): 481–493. <https://doi.org/10.1017/S095283690100098X>
- Jocqué R, Alderweireldt M (2018) New Chummidae (Araneae): Quadrupling the size of the clade. *European Journal of Taxonomy* 412(412): 1–25. <https://doi.org/10.5852/ejt.2018.412>
- Kulkarni S, Wood HM, Hormiga G (2023) Advances in the reconstruction of the spider tree of life: A roadmap for spider systematics and comparative studies. *Cladistics* 39(6): 479–532. <https://doi.org/10.1111/cla.12557>
- Wheeler WC, Coddington JA, Crowley LM, Dimitrov D, Goloboff PA, Griswold CE, Hormiga G, Prendini L, Ramírez MJ, Sierwald P, Almeida-Silva LM, Álvarez-Padilla F, Arnedo MA, Benavides LR, Benjamin SP, Bond JE, Grismado CJ, Hasan E, Hedin M, Izquierdo MA, Labarque FM, Ledford J, Lopardo L, Maddison WP, Miller JA, Piacentini LN, Platnick NI, Polotow D, Silva-Dávila D, Scharff N, Szűts T, Ubick D, Vink C, Wood HM, Zhang JX (2017) The spider tree of life: Phylogeny of Araneae based on target-gene analyses from an extensive taxon sampling. *Cladistics* 33(6): 576–616. <https://doi.org/10.1111/cla.12182>
- WSC (2024) World Spider Catalog. Version 25.5. Natural History Museum Bern. <http://wsc.nmbe.ch> <https://doi.org/10.24436/2> [accessed on 27 August 2024]

Supplementary material 1

Details of collecting data of *Chumma* spiders from western South Africa

Authors: Yuri M. Marusik, Charles R. Haddad

Data type: xlsx

Explanation note: Summary of collecting data of *Chumma* species from South Africa (new species and new records).

Copyright notice: This dataset is made available under the Open Database License (<http://opendatacommons.org/licenses/odbl/1.0/>). The Open Database License (ODbL) is a license agreement intended to allow users to freely share, modify, and use this Dataset while maintaining this same freedom for others, provided that the original source and author(s) are credited.

Link: <https://doi.org/10.3897/AfrInvertebr.65.138735.suppl1>

Research Article

Small-scale variations in spider and springtail assemblages between termite mounds and the surrounding grassland matrix

Hannelene Badenhorst¹, Charles Richard Haddad¹, Charlene Janion-Scheepers²

¹ Department of Zoology & Entomology, University of the Free State, P.O. Box 339, Bloemfontein, 9300, South Africa

² Department of Biological Sciences, University of Cape Town, Private Bag X3, Rondebosch, Cape Town, 7701, South Africa

Corresponding author: Charles Richard Haddad (HaddadCR@ufs.ac.za)



This article is part of:

Gedenkschrift for Prof. Stefan H. Foord

Edited by Galina Azarkina, Ansie Dippenaar-Schoeman, Charles Haddad, Robin Lyle, John Mldgley, Caswell Munyai

Academic editor: Robin Lyle

Received: 16 October 2024

Accepted: 3 December 2024

Published: 30 December 2024

ZooBank: <https://zoobank.org/65D770A1-DECE-4D76-A24C-7E49105CB86D>

Citation: Badenhorst H, Haddad CR, Janion-Scheepers C (2024) Small-scale variations in spider and springtail assemblages between termite mounds and the surrounding grassland matrix.

African Invertebrates 65(2): 339–367. <https://doi.org/10.3897/AfrInvertebr.65.139404>

Copyright: © Hannelene Badenhorst et al. This is an open access article distributed under terms of the Creative Commons Attribution License (Attribution 4.0 International – CC BY 4.0).

Abstract

The snouted harvester termite (*Trinervitermes trinervoides* (Sjöstedt, 1911)) is a widespread grass-eating termite species that constructs thermoregulated dome-shaped mounds. However, little is known about the influence of these mounds on the arthropod assemblage structure in the surrounding grassland matrix, and whether the mounds represent ecological islands. Spiders and springtails are two ecologically important arthropod groups often associated with termites or their mounds. We investigated their assemblage composition inside and around active and abandoned *T. trinervoides* mounds in a central South African grassland. In total, 838 spiders (59 spp., 22 families) and 217 857 springtails (24 spp., 9 families) were collected from 96 pitfall traps, placed at four microhabitats in and around each of 12 active and 12 abandoned mounds during March 2019. The most abundant and species-rich spider families include the Gnaphosidae (n = 270, 10 spp.), Zodariidae (n = 86, 7 spp.), Lycosidae (n = 86, 6 spp.) and Salticidae (n = 77, 5 spp.), whereas the springtail fauna was dominated by Brachystomellidae (n = 56 521, 1 species), Bourletiellidae (n = 49 573, 7 species), Sminthuridae (n = 44 491, 3 species), Isotomidae (n = 32 288, 1 species) and Entomobryidae (n = 26 216, 7 species). Indicator analysis showed that the spiders *Zelotes sclateri* Tucker, 1923, *Heliocapensis termitophagus* (Wesołowska & Haddad, 2002) and *Scytodes elizabethae* Purcell, 1904 are associated with abandoned mounds, but no springtails showed an association based on the IndVal analysis of the eight microhabitats (lumped data), even though the undescribed *Cyphoderus* sp. were mostly collected inside active mounds. The mounds thus had a negligible influence on the spatial distribution of springtails in the surrounding grassland. The different spider and springtail assemblages sampled indicate that both active and abandoned mounds function as ecological islands in grasslands, but that mound size does not affect their abundance or species richness in the different microhabitats sampled.

Key words: Araneae, Collembola, diversity, pitfall trap, termitophile, *Trinervitermes trinervoides*

Introduction

Termitaria are a common sight throughout the savannas and grasslands of Africa (Uys 2002). Aside from serving as the nests for the organisms constructing them, they play a significant role in these ecosystems by creating nutrient

islands (Dangerfield 1991) and providing refuge, food and spatial resources to a range of animals, including a variety of termitophilous arthropods (Warren 1919), mammals (Fleming and Loveridge 2003) and predacious ants (Tuma et al. 2020), amongst others. Furthermore, termite mounds constructed in savannas can often have very strong effects on the soil nutrients and vegetation on and surrounding them (e.g. Dangerfield 1991; Joseph et al. 2013; Davies et al. 2014).

Trinervitermes trinervoides (Sjöstedt, 1911) is a widespread termite species within the semi-arid grasslands and savannas of South Africa, where it predominantly feeds on grass litter (Adam et al. 2018) and constructs characteristic dome-shaped mounds (Coaton 1948; Uys 2002; Field and Duncan 2013). The mounds are used to store grass fragments that not only act as a constant food supply, but aid in thermoregulation, helping maintain a narrow range in core nest temperature (Field and Duncan 2013). Even though many studies have focused on *T. trinervoides* ecology (Potts and Hewitt 1973, 1974; Adam et al. 2005, 2008, 2012, 2018; Adam and Mitchell 2009; Field and Duncan 2013; Conlon et al. 2016; Mills and Sirami 2018; Nampa and Ndlovu 2019; Ndlovu et al. 2021), as well as mound degradation and opportunistic occupation/invasion of the abandoned *T. trinervoides* mounds by many vertebrates and some invertebrates (Smith and Yeaton 1998; Haddad and Dippenaar-Schoeman 2002, 2006; Wesolowska and Haddad 2002; Gosling et al. 2012), there is relatively little known of the arthropods that cohabit the active nests and their dynamics in the surrounding grasslands.

As in savanna landscapes, *T. trinervoides* mounds in central South African grasslands have a direct influence on the grassy and shrubby vegetation around them, with clear compositional differences between active and abandoned mounds (Smith and Yeaton 1998). These vegetation changes inevitably provide different resources to the arthropods dependent on them, which will likely cause changes in the composition of phytophagous and detritivorous arthropods feeding on the plant material (as found by Leitner et al. 2020 in savanna), as well as predators of those arthropods, such as spiders, which are affected by vegetation structure on and around mounds (Nduwarugira et al. 2016). Furthermore, active and abandoned mounds' internal temperatures are independent of (more stable) and dependent (fluctuating) on ambient temperatures, respectively (Ndlovu et al. 2021), which would directly impact the organisms occupying each mound. We were therefore interested in assessing whether *T. trinervoides* mounds fulfil the role of ecological islands within a grassland matrix, similar to other termitaria elsewhere (Fleming and Loveridge 2003; Joseph et al. 2013; Chen et al. 2021), and how different mound types affect the organisms occupying them and their surroundings.

Spiders (Araneae) and springtails (Collembola) are two very ecologically significant arthropod groups that function as predators and detritivores in terrestrial ecosystems, respectively (Janion-Scheepers et al. 2016). Spiders are the most diverse group of terrestrial predators, with more than 52 300 species described globally (World Spider Catalog 2024), of which around 2 265 species are known from South Africa (Dippenaar-Schoeman et al. 2023). They contribute significantly to the natural limitation of terrestrial arthropod populations, particularly insects (Nyffeler and Birkhofer 2017), with springtails often forming a considerable portion of the diet of generalist spiders (e.g. Birkhofer et al. 2008, 2011), or even being exclusively fed on by specialists (Korenko et

al. 2014). Some South African spider species have adapted their behaviour and activity patterns to specialise and mainly feed on termites (e.g. Wesołowska and Haddad 2002; Pekár et al. 2020), with *Ammoxenus amphalodes* Dippenaar & Meyer, 1980 being a true predator specialist of *Hodotermes mossambicus* (Hagen, 1853) (Dippenaar-Schoeman et al. 1996; Petráková et al. 2015; Haddad et al. 2016; Pekár et al. 2018; Henschel et al. 2023).

In contrast, springtails are a small hexapod order with about 9500 described species worldwide (Bellinger et al. 2023), and only 133 species have been recorded from South Africa (Janion-Scheepers 2021). Despite their comparatively low species richness, they are widely recognised as being one of the most important groups of terrestrial detritivores in soil mesofaunal assemblages, playing a key role in the breakdown of decomposing organic material, while also serving as food to many predators, including spiders (Rusek 1998). Springtails from the tribe Cyphoderini are commonly collected in association with ants and termites. They move freely in termite mounds and are presumed to be scavengers, and their abundance could be attributed to the narrow ranges in humidity and temperatures maintained in the host species' nests (Kistner 1982).

The aim of this study was to characterise the springtail and spider assemblages that occur inside and around the mounds of the snouted harvester termite *T. trinervoides* in central South African grasslands. As living mounds are closed off from the surrounding environment by their continuous exterior crust (Field and Duncan 2013) that is inaccessible to most macroarthropods, we hypothesised 1) that both spider and springtail abundance, species richness and diversity would increase from inside the mounds to 3 m away from the mounds, and 2) that the assemblages in the grassland matrix and around the edges of mounds would be the most similar, indicating that mounds have a limited influence on assemblages in the surrounding grassland habitat. Consequently, 3) that the assemblages inside or on the outer crust of mounds would support the concept of *T. trinervoides* termitaria as islands, as has been proposed for *Macrotermes* and *Odontotermes* termites in savanna and forests (e.g. Fleming and Loveridge 2003; Joseph et al. 2013; Chen et al. 2021). Lastly, considering the frequently obligate association of Cyphoderini springtails with colonies of social insects (e.g. Paclt 1967; Kistner 1982; Janion-Scheepers et al. 2015; Parmentier and Braem 2024), we hypothesised 4) that *Cyphoderus* springtails would be collected exclusively from the inside of living *T. trinervoides* mounds.

Material and methods

Study area

This study was conducted in the grassland areas on the western side of the main campus of the University of the Free State in Bloemfontein, South Africa (29°06'43.7"S, 26°10'43.9"E). The study area had a dense grass litter cover on the soil surface due to annual mowing. The vegetation mostly consists of a mixture of grass species (mainly *Themeda triandra*, *Eragrostis lehmanniana*, *Eragrostis curvula*, *Digitaria eriantha* and *Aristida congesta*), a variety of herbaceous plant species (including *Nidorella resedifolia*, *Hibiscus pusillus*, *Pentzia globosa* and *Selago densiflora*), dwarf-shrubs (including *Felicia muricata*) and trees (Dingaen and Du Preez 2013). The tree species consist of mostly

indigenous species, such as *Searsia lancea* and *Olea europaea* subsp. *africana*, as well as a few alien species such as *Quercus stellata*, *Fraxinus angustifolia* and *Pinus taeda*. Bloemfontein is a summer rainfall area with an annual average of 550 mm of rain, mainly in the form of thunderstorms (Dingaen and Du Preez 2017). Bloemfontein experienced above average rainfall (± 602 mm) during 2019 (Moeletsi et al. 2022), of which 46 mm fell during the 21-day study period, indicated below.

Sampling Araneae and Collembola

A total of 96 pitfall traps (volume 350 ml, mouth diameter 60 mm) were placed in and around 12 active and 12 abandoned *T. trinervoides* mounds from 5–26 March 2019 (21 days). A KML (Keyhole Markup Language) file for viewing the locations of each of the 24 mounds interactively in Google Earth (<http://earth.google.com/>) is available as a Suppl. material 1. At each of the studied termite mounds, four pitfall traps were placed in specific microhabitats: the first was placed inside, the second trap on the top of the mound outside, the third at the base of the mound in the soil (0 m away), and the final pitfall trap at 3 m from the mound in the natural grassland matrix (Fig. 1). We considered active and abandoned mounds to represent different abiotic conditions, as they have contrasting internal thermal and structural conditions and effects on the surrounding vegetation, so considered the four trap positions of each mound type to represent a different microhabitat, i.e. eight in total. For abandoned mounds, we scored the degree of perforation of the external crust following the scale proposed by Haddad and Dippenaar-Schoeman (2002).

To avoid spatial pseudoreplication and account for any potential movement of arthropods, mounds were separated by a minimum of 25 m; most inter-mound distances, however, exceeded 50 m. As termite mound size can affect the number of organisms sampled (e.g. Haddad and Dippenaar-Schoeman 2002; Leitner et al. 2020), we improved the comparability of the mounds sampled by only selecting well-established mounds with a height of >25 cm and basal diameter >50 cm (Suppl. material 2).

We used a spade to dig a $\sim 25 \times 25$ cm square into the outer crust of the mound on the top of the northern side in order to plant pitfalls inside the mound structure, and gently removed the excavated material before using an augur to dig a hole into the tunnel structure before placing the bottle flush with the bottom of the cavity. After filling the bottle with preservative, the square crust was returned to its position, the cracks filled with loose sand from the base of the mound on the southern side, and water dripped onto the crack to seal it and (in the case of active mounds) facilitate repair by the workers. For traps placed on the outer surface, we used the augur to excavate the required cavity on the top of the southern side (about 30–50 cm from the northern excavation), placed the bottle, and filled any cracks as described above. Traps at 0 m were planted at the base of the mound and those at 3 m were planted in natural *Themeda triandra*-dominated grassland, both on the northern side of each mound and flush with the soil surface (Fig. 1).

Each pitfall trap was filled with 50 ml ethylene glycol as a preservative. The traps were inspected daily and those that were filled more than halfway by heavy rainfall during the sampling period were emptied and the preservative replaced.

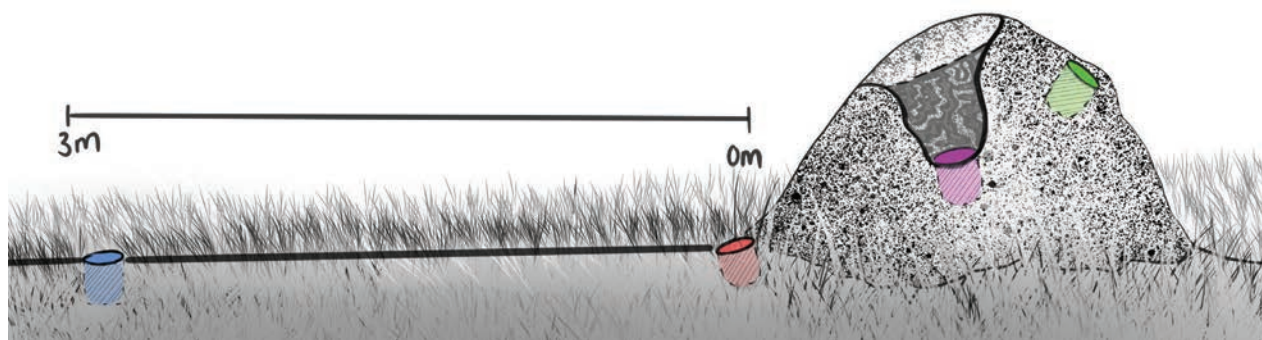


Figure 1. Study arrangement, showing the placement of the four pitfall traps in the microhabitats associated with an active *Trinervitermes trinervoides* mound: inside (purple), on top (green), at 0 m (red) and 3 m away (blue) from a mound. Illustration: M. Peach.

All the replaced samples were merged with their replacement traps after the sampling was concluded. The contents of the traps were washed from the ethylene glycol into a 70% ethanol solution. Springtails were quantified and sorted to morphospecies by the first author and identified to genus level by the first and third authors using a provisional key (Janion-Scheepers 2021). Spiders were sorted and identified to species level by the second author using literature available on the World Spider Catalog (2024).

Statistical analysis

For some of the statistical analyses, the 96 replicates were lumped to represent the four microhabitats sampled in and around the active or abandoned mounds. The spider and springtail data were analysed using Microsoft® Excel® v.2311 (Microsoft Corporation 2021), PRIMER v7 statistical software (PRIMER-e 2017) and RStudio (RStudio Team 2020). Data processing and visualisation in RStudio required additional installation of multiple software packages, including *vegan* (Oksanen et al. 2019), *indicspecies* (De Caceres and Legendre 2009) and *ggVennDiagram* (Gao et al. 2021). Rarefaction curves were prepared in RStudio, based on the eight microhabitats for each of the focus arthropod groups. Sample completeness was calculated as the ratio between observed species richness (S_{obs}) and Chao1 estimated species richness (S_{Chao1}) with the below formula, as described by Chao et al. (2009):

$$\text{Sample completeness} = \frac{S_{obs}}{S_{Chao1}}$$

and S_{Chao1} (estimated species richness) was calculated with the following formula:

$$S_{Chao1} = S_{obs} + \frac{f_1^2}{2f_2}$$

where f_1 is the number of species only represented by one individual (singletons) and f_2 the number of species only represented by two individuals (doubletons). Chao et al. (2009) further stipulated that when $f_1 = 0$ or the undetected number of species is less than 0.5, sampling is deemed complete. However, if $f_2 = 0$, S_{Chao1} is calculated with the following modified formula:

$$S_{Chao1} = S_{obs} + \frac{f_1(f_1 - 1)}{2(f_2 + 1)}$$

Sample coverage (C_n) was determined for both the spider and springtail assemblages of each microhabitat by means of the formula below:

$$C_n = 1 - \frac{f_1}{n} \left[\frac{(n-1)f_1}{((n-1)f_1) + 2f_2} \right]$$

where n is the abundance, f_1 is the number of singletons, and f_2 is the number of doubletons (Chao and Jost 2012).

Alpha diversity (species abundance, species richness, Shannon's diversity index and Pielou's evenness) was calculated for each of the microhabitats, with differences between the groups tested by means of the Kruskal-Wallis rank sum test and post hoc testing done using the pairwise Wilcoxon rank sum test. To assess whether mound size (volume and circumference) affected abundance and species richness of the two orders, we used linear regression for each of the microhabitats for active and abandoned mounds separately. Mound circumference was measured in the field (Suppl. material 2), with the estimated volume of each mound being calculated using the equation for the volume an ellipsoid, divided by two, following Ndlovu et al. (2021). Beta diversity analyses were conducted by performing non-metric multi-dimensional scaling (NMDS) analyses based on the Bray-Curtis distance using PAST version 2.07 (Hammer et al. 2001).

An analysis of similarities (ANOSIM) was performed with RStudio on the NMDS datasets (Bray-Curtis dissimilarity measure, permutations = 9999) to test whether there were statistical differences between the assemblages in the eight microhabitats. Indicator species analyses were performed to identify species that were statistically more abundant in specific microhabitats. Similarity percentage (SIMPER) analyses were done in PRIMER to determine the contribution of individual species towards the dissimilarities observed between the four microhabitat types, as well as between the colony activity status. Venn diagrams were constructed in RStudio to illustrate the sharing of species and hierarchical cluster dendrograms based on Bray-Curtis similarity distances were constructed in PRIMER to illustrate the clustering of microhabitats with similar assemblage structures. Only clusters with a similarity percentage of higher than 60% are considered ecologically important. Microsoft Excel was used to calculate Sørensen's quotient of similarity (C_s , range between 0 and 1) with the below formula:

$$C_s = \frac{2ab}{a+b}$$

where ab is the number of shared species between two samples, a is the species richness of Sample 1 and b is the species richness of Sample 2. In the current study, Sørensen's quotient of similarity was used to compare the springtail and spider assemblages, respectively, between the eight different microhabitats. Values closer to 1 indicate higher similarity in faunal assemblages between the compared microhabitats and values closer to 0 indicate a more unique faunistic composition.

Results

The rarefaction curves for both Araneae (Suppl. material 3: fig. S3A) and Collembola (Suppl. material 3: fig. S3B) collected from eight microhabitats tapered off, indicating that sampling was sufficient for evaluating the species richness of the spider and springtail assemblages from these microhabitats. Coverage values for both spiders and springtails from the eight microhabitats were all above 0.7 (Suppl. materials 4, 5).

Assemblage composition and structure

Araneae

A total of 838 spider individuals, representing 59 species from 22 families, were collected from eight microhabitats situated in and around the 24 *Trinervitermes trinervoides* mounds (Suppl. material 4). The most abundant and species-rich spider families include the Gnaphosidae (n = 270, 10 spp.), Zodariidae (n = 86, 7 spp.), Lycosidae (n = 86, 6 spp.) and Salticidae (n = 77, 5 spp.). Spider abundance, species richness and diversity were higher in the traps situated at 0 m and 3 m away from both the active and abandoned mounds, than inside or on top of mounds.

The Kruskal-Wallis rank sum test showed significant differences for the spider abundance, species richness and Shannon's diversity (all $P < 0.001$). Pairwise comparisons using Wilcoxon rank sum test revealed that the spider abundance inside the active mounds was significantly lower than that of the other microhabitats. The spider abundance was also significantly lower on the outside of the active termite mounds than in most of the other microhabitats (Fig. 2, Suppl. material 6). The spider abundance at the foot of the abandoned mounds, at 0 m away, was significantly higher than that of most of the other microhabitats (Fig. 2, Suppl. material 6).

Spider species richness of the pitfalls inside and outside (on top of) mounds was lower than those at 0 m and 3 m away from mounds for both active and abandoned mounds (Suppl. material 7). Similarly, the Shannon's diversity values of the inside and outside microhabitats was significantly lower than that of the pitfalls 0 m and 3 m away from mounds, whether active or abandoned (Fig. 2, Suppl. material 8). Pielou's evenness was consistent in seven of the eight microhabitats and showed that no one species dominated any of these microhabitats. The linear regression showed that mound size (circumference and volume) did not have a strong effect on either abundance or species richness, irrespective of microhabitat, with the exception of species richness at the base of abandoned mounds, which decreased slightly with mound size; most R^2 values were <0.1 (Suppl. material 9).

Collembola

In total, 217 857 springtail individuals representing 24 species in nine families were collected from the eight microhabitats (Suppl. material 5). Brachystomellidae (n = 56 521, 1 species), Bourletiellidae (n = 49 573, 7 species), Sminthurididae (n = 44 491, 3 species), Isotomidae (n = 32 288, 1 species) and Entomobryidae (n = 26 216, 7 species) were the most abundant families. *Cyphoderus* sp. (n = 18 065)

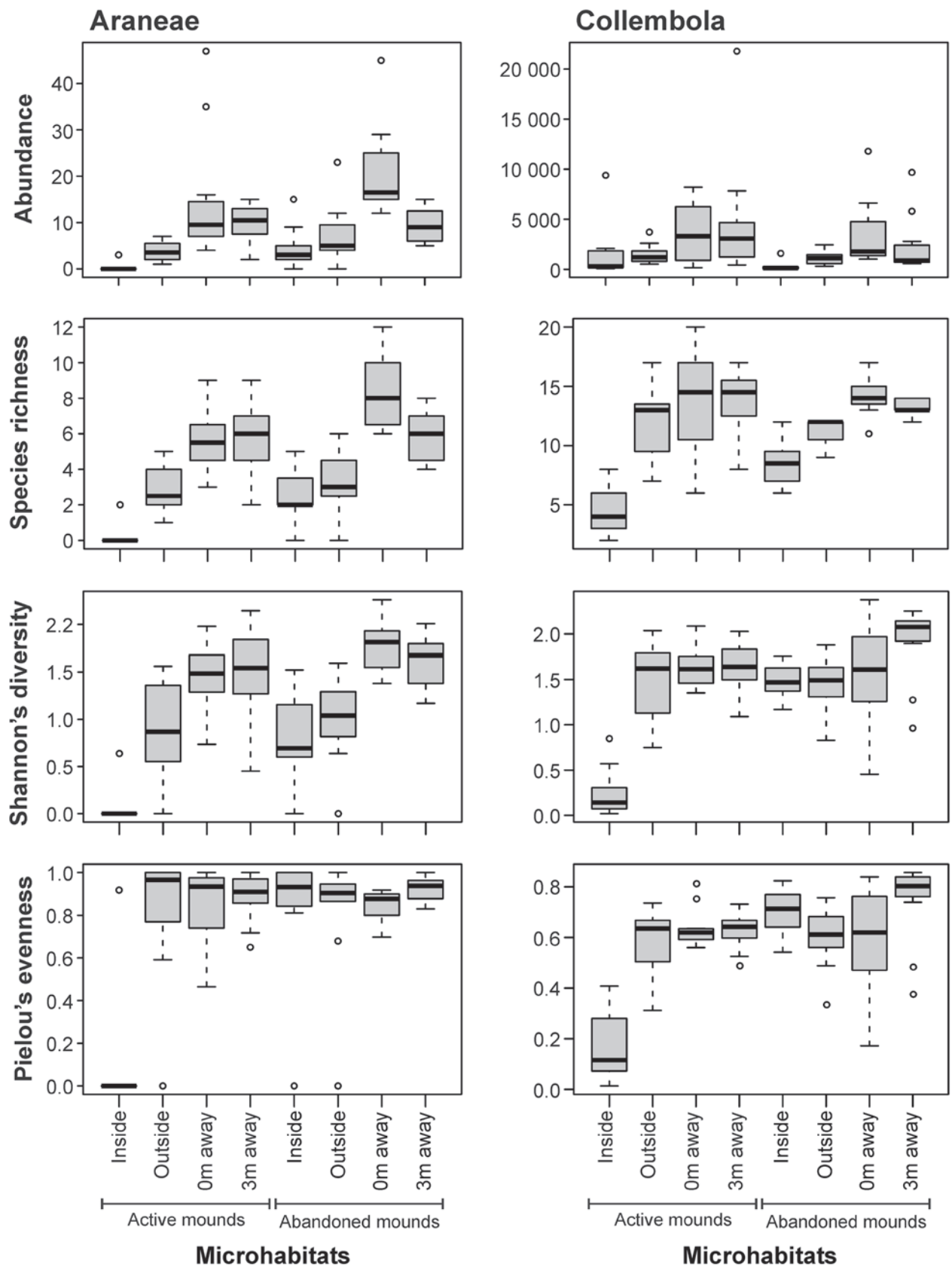


Figure 2. Abundance and alpha diversity of the spider (Araneae) and springtail (Collembola) assemblages sampled at each of the eight microhabitats (12 replicates), illustrated by means of box-and-whisker plots.

was a major contributor to the Entomobryidae abundance and 96.5% of these individuals were collected from inside the active mounds. The families Orchesellidae (n = 5 887, 2 species), Neanuridae (n = 2 537, 1 species), Mackenziellidae (n = 336, 1 species) and Katiannidae (n = 8, 1 species) were less abundant.

Springtail abundance was higher in traps that were situated at 0 m and 3 m away from both the active and abandoned mounds, than on the inside or on top of the active and abandoned mounds, respectively (Fig. 2). The Kruskal-Wallis rank sum test showed significant differences in springtail abundance, species richness and Shannon's diversity between microhabitats (all $P < 0.001$). Pairwise comparisons using the Wilcoxon rank sum test revealed that springtail abundances inside the abandoned mounds were significantly lower ($P < 0.001$) than in six of the other seven microhabitats (Fig. 2, Suppl. material 10). As in the case of the spiders, the linear regression found no association between mound size (circumference and volume) and springtail abundance and species richness, with all the R^2 values below 0.2 (Suppl. material 9).

The differences in springtail species richness were due to the lower species richness inside the active mounds, as well as inside and on the outside of the abandoned mounds (Suppl. material 11). Springtail diversity was the lowest inside the active mounds, which was the main cause of the significant difference observed in Shannon's diversity values between the microhabitats (Suppl. material 12). Overall, Pielou's evenness showed moderate to high evenness values, except for the inside of the active mounds, which were dominated by an undescribed *Cyphoderus* sp. (Fig. 2).

Assemblage comparisons

The abundance-based NMDS analyses of both the spider (stress: 0.116, good representation) and springtail (stress: 0.046, strong representation) assemblages showed that assemblages from the inside of the active mounds were different from those occupying the other microhabitats (Fig. 3A, B). The ANOSIM results comparing the spider assemblages between active and abandoned mounds ($R = 0.1979$, $P = 0.1151$), as well as the different microhabitats ($R = 0.3542$, $P = 0.0863$) showed that there were no statistically significant differences in the spider assemblages based on these factors when tested independently. The ANOSIM results for springtail assemblage comparisons also found no statistical differences between assemblages associated with active or abandoned mounds ($R = 0.04167$, $P = 0.3943$), nor between the four different types of microhabitats ($R = 0.1667$, $P = 0.1945$), irrespective of mound status.

Indicator species analysis of the spider abundance data (lumped according to eight microhabitats) showed that *Zelotes sclateri* Tucker, 1923 (Gnaphosidae), *Heliocapensis termitophagus* (Wesołowska & Haddad, 2002) (Salticidae) and *Scytodes elizabethae* Purcell, 1904 (Scytodidae) are associated with abandoned mounds and their surroundings. These findings were supported by the SIMPER analysis (Suppl. material 13). The springtail abundance data (lumped according to eight microhabitats) did not show any statistically significant species as indicators of a specific microhabitat or the status of the mounds. However, SIMPER analyses showed that the unidentified *Cyphoderus* sp. contrib-

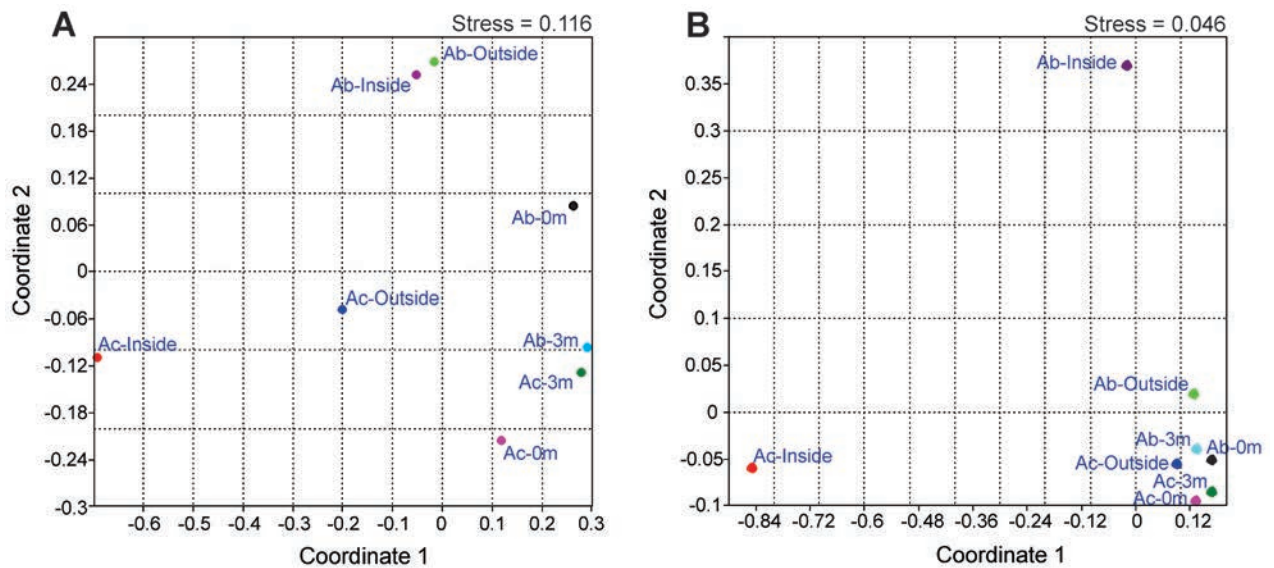


Figure 3. Non-metric multidimensional scaling (NMDS) analyses on the abundance-based datasets of spider (A) and springtail (B) assemblages collected from eight microhabitats associated with active (Ac) and abandoned (Ab) *Trinervitermes trinervoides* mounds and the surrounding grassland, based on the Bray-Curtis similarity index.

uted to the differences observed between the active and abandoned mounds, as well as between the inside of active mounds and the other microhabitats (Suppl. material 14).

Venn diagrams only consider the presence and absence of species in the specific microhabitats and exclude their abundance, which could provide valuable insights into the success and level of specialisation of a species in a specific microhabitat. All the microhabitats showed the presence of unique spider species, except the inside of active mounds (Fig. 4A). Only two spider species were collected from inside a single active mound, viz. *Theuma fusca* Purcell, 1907 (Prodidomidae; n = 1) and *Enoplognatha molesta* O.P.-Cambridge, 1904 (Theridiidae; n = 2), which were commonly recorded from all the other microhabitats. It was noted that nearly half of the total springtail species richness was shared between all eight microhabitats (Fig. 4B). None of the springtail species were exclusively collected from the inside or outside of either active or abandoned mounds. Only three microhabitats showed the presence of unique springtail species with respect to the mound status-specific analysis and include the 0 m away (4 species) and 3 m away (1 species) from abandoned mounds, as well as 0 m away (2 species) from active mounds.

The hierarchical cluster dendrograms based on the Bray-Curtis similarity of the springtail and spider assemblages showed that the similarities between spider assemblages of the eight microhabitats were mostly less than 60% similar (Fig. 4C). The habitats that were away from the mounds, both active and abandoned, showed the highest similarity (Fig. 4C, Suppl. material 15). The springtail assemblage showed high levels of similarity (> 60%) between most assemblages, with only the assemblage inhabiting the inside of active mounds showing a moderate level of uniqueness (Fig. 4D, Suppl. material 16).

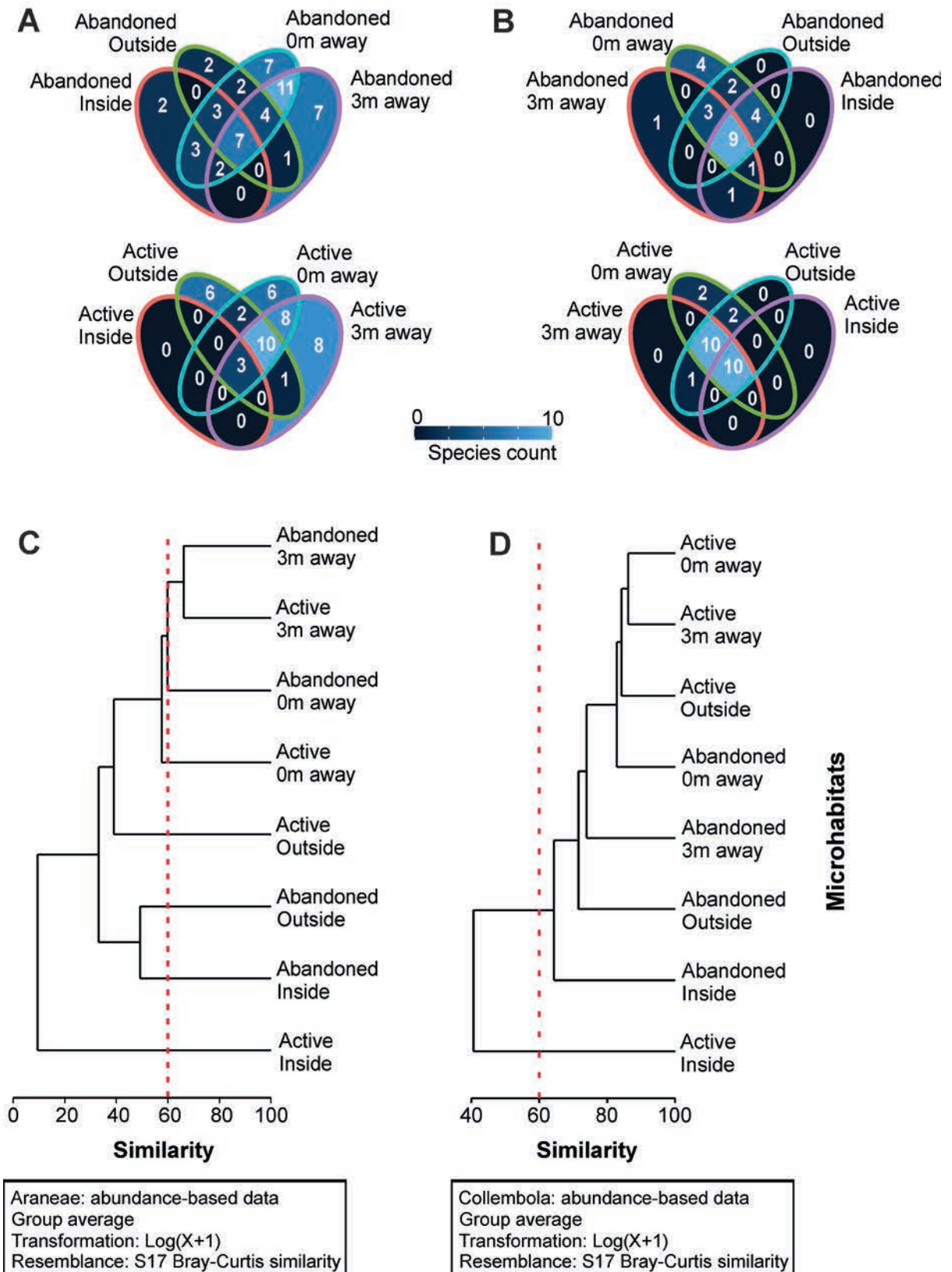


Figure 4. Venn diagrams (**A, B**) and hierarchical cluster dendrograms (**C, D**) illustrating the similarities between the spider (**A, C**) and springtail (**B, D**) assemblages from the different microhabitats. Cophenetic correlation values close to 1 indicate that the cluster dendrograms represent the data very well; these values are 0.948 and 0.960 for the spiders and springtails, respectively.

Discussion

This is the first study in South Africa to investigate the spider and springtail assemblages both inside and around the mounds of the snouted harvester termite, *T. trinervoides*, and how their composition differs. The sampling coverage values per mound for spiders were very high for both the active (0.733–0.931) and abandoned mounds (0.896–0.952). These values suggest that most of the expected species for this site and the specific sampling period were collected, but that additional sampling could provide a few additional species, especially at 0 m away from the active mounds. The sample coverage for the springtails of all eight microhabitats was all equal to 1, indicating that the sampling effort was sufficient and all the epedaphic springtail species that were present in these microhabitats during the sampling period were collected. The addition of other sampling methods and seasonal surveys could, however, contribute more species for both taxa.

Spider assemblages

Spiders play an important role in arthropod population dynamics in terrestrial environments (Nyffeler and Birkhofer 2017) and are abundant terrestrial predators in the Free State Province's grassland ecosystems (Haddad et al. 2013). The present study found the Gnaphosidae, Zodariidae, Lycosidae and Salticidae to be the most abundant and species-rich families sampled, which according to Dippenaar-Schoeman et al. (2023), represents four of the six most species-rich spider families in South Africa (Table 1). These four families primarily consist of ground-dwelling spiders. The absence of Araneidae and scarcity of Thomisidae was expected, as both families primarily live on plants (Dippenaar-Schoeman 2023). Sampled spider assemblages are greatly influenced by sampling methods and this study only made use of pitfall trapping, which mainly collects active ground-dwelling spiders (Haddad et al. 2013). Many of the spider species sampled during this study are ground-dwellers that are commonly collected in pitfall traps in the Grassland Biome, as well as in association with different termite species (e.g. Haddad and Dippenaar-Schoeman 2006; Haddad et al. 2015; Haddad and Butler 2018).

Alpha diversity (abundance, species richness and Shannon's diversity) showed a significant decrease in the spider assemblages that were inside or

Table 1. The six most species-rich spider families from South Africa (Dippenaar-Schoeman et al. 2023), with four of them also being the most abundant and species-rich in the present study (indicated by *).

| Six most species-rich families in RSA | South Africa (RSA) | | Present study | |
|---------------------------------------|--------------------|---------|---------------|---------|
| | Genera | Species | Genera | Species |
| Salticidae* | 80 | 354 | 4 | 5 |
| Gnaphosidae* | 28 | 195 | 7 | 9 |
| Thomisidae | 38 | 143 | 3 | 3 |
| Lycosidae* | 24 | 113 | 6 | 6 |
| Araneidae | 40 | 100 | 0 | 0 |
| Zodariidae* | 21 | 97 | 7 | 7 |

on top of both the active and abandoned termite mounds compared to those occurring at 0 m and 3 m away from the mounds, only partly supporting hypothesis 1. Spider abundance, species richness and diversity were, in fact, the highest at 0 m away, suggesting that the mounds may serve as a structural barrier that disrupts the running activity of spiders while foraging, increasing their pitfall capture rates in this microhabitat. This microhabitat had similar spider assemblages to the pitfalls 3 m away from mounds, as it is situated in the edge area between the mounds and the grassland.

However, none of the microhabitats supported statistically different spider assemblages, as the grassland assemblages (3 m away from active and abandoned mounds) and those at the mound periphery (0 m away) shared many species (Fig. 4), supporting hypothesis 2. This would indicate that the considerable effects that the mounds have on soil characteristics and vegetation composition and productivity between active and abandoned mounds of different ages (Smith and Yeaton 1998) have little effect on higher trophic levels, such as active ground-dwelling predators. The assemblages in the surrounding grassland also did not differ significantly from those on top of or inside the mounds, contrary to hypothesis 3. This seems somewhat contradictory to expectations, as the only three indicator species were specifically associated with the abandoned mound structures. Additionally, the nMDS analysis clearly indicated that the assemblages of the inside and outside of abandoned mounds were very similar, but different from those of the surrounding grassland and of active mounds; this was likely biased by the low spider numbers inside active mounds ($n = 3$). So, although the ANOSIM results do not support hypothesis 4, i.e. that *T. trinervoides* termitaria function as ecological islands, the nMDS results do support this hypothesis, at least in the case of spiders.

This is further supported by the very low spider abundance and species richness on and inside active mounds. This is most likely related to the chemical defence exhibited by *Trinervitermes* species, whose soldiers have a nasutiform head and release repellent terpene compounds when disturbed (Nel 1968; Prestwich et al. 1976a, b; Prestwich 1977). These chemicals evidently have no effect on particular nest associates such as *Cyphoderus* sp. and specialist mammalian predators such as the aardwolf and armadillo (Richardson 1987; Richardson and Levitan 1994; Taylor and Skinner 2000; De Vries et al. 2011), but our results suggest that they may effectively deter spiders inside active mounds. This may also explain why the mound specialist jumping spider, *H. termitophagus*, is only found associated with abandoned and not active mounds (Wesołowska and Haddad 2002) and likely displays euryphagous specialist habits rather than stenophagy on the host termites (Michálek et al. 2021). This suggests that the mounds are generally unsuitable as foraging grounds for ground-dwelling spiders, despite the obviously plentiful food source, and that they represent bare islands that are not suitable for occupation by predominantly generalist predators.

Abandoned mounds play an important role as refuge for many arthropods, including spiders, which also makes these mounds prey-rich areas for many opportunistic spiders (Haddad and Dippenaar-Schoeman 2006). According to Theron (2013), these abandoned mounds are also inhabited by ants, which form part of the diet of predators that visit the mounds, such as ant-eating spiders (all of the Zodariidae sampled except *Cydrela* sp.), or serve as models

of ant-mimicking spiders (Gnaphosidae: *Micaria* spp.), which were collected inside and around the studied mounds. However, only three species (*Z. sclateri*, *H. termitophagus* and *S. elizabethae*) were statistically linked with abandoned *T. trinervoides* mounds and their nearby surrounding grassland. Of these, *H. termitophagus* is the only one that has previously been found specifically associated with abandoned *T. trinervoides* mounds (Wesołowska and Haddad 2002); the other two are widespread in South Africa and have no specific habitat associations (Haddad and Dippenaar-Schoeman 2006; Butler and Haddad 2011; Haddad et al. 2015; Dippenaar-Schoeman et al. 2021a, b).

Springtail assemblages

Springtails are abundant terrestrial arthropods with a global distribution, inhabiting a wide range of terrestrial environments that include the nests of ants and termites (Bellini et al. 2023; Oliveira et al. 2023). Springtails are important prey items for many ants and spiders (Basset et al. 2020). Studies by Wesołowska and Haddad (2002) and Michálek et al. (2021) showed that *H. termitophagus* does not only feed on termites, but on a broader spectrum of arthropods, including springtails.

Alpha diversity (abundance and species richness) showed a significant decrease in the springtail assemblages that were inside or on top of both active and abandoned termite mounds with respect to those inhabiting the 0 m and 3 m microhabitats. However, similar to spiders, abundance and species richness were highest at 0 m, thus only partly supporting hypothesis 1. Most of the springtail species were present in the majority of the microhabitats, indicating little to no habitat selection taking place. This was evident in the high collembolan diversity values observed in most microhabitats, excluding the inside of the active mounds that were mainly inhabited by *Cyphoderus* individuals (Fig. 4); thus, hypothesis 2 was not supported. As in the case of spiders, there is evidence that supports *T. trinervoides* mounds being ecological islands (nMDS analysis), although this is contradicted by the ANOSIM results. There is thus partial support for hypothesis 3.

The high number of *Cyphoderus* individuals showed that it was influenced by the mound activity, as their abundance ratio between the active and abandoned mounds are 147.7:1 individual. Although *Cyphoderus* was collected from the other microhabitats, their abundance on the inside of the active mounds was far higher than that of any of the other microhabitats, including the inside of abandoned mounds. This indicates that these springtails either have a relationship with the termites or exploit the living conditions created inside the mounds by active harvester termite colonies, which supports hypothesis 4. According to Kistner (1982), members of the tribe Cyphoderini, including *Cyphoderus* spp., are associated with ants and termites, and can occasionally be observed in sampling data away from ant and termite nests, as it is suggested that they can follow chemical trails of their host species.

This study also contributed important new springtail genus records for the Free State Province and South Africa (species absent from the species lists available in Thibaud (2013), Janion-Scheepers et al. 2015 and Janion-Scheepers 2021)), from which undescribed species will be described by the respective taxonomists. Interesting new springtail family records for the Free State Province

include the families Orchesellidae (genera *Capbrya* Barra, 1999 and *Nothobrya* Arlé, 1961) and Mackenziellidae (genus *Mackenziella* Hammer, 1953). This is the first record of *Nothobrya* for South Africa, and although *Capbrya* was thought to be a genus endemic to South Africa, a new species from this genus was recently described from Brazil (Nunes et al. 2020). The family Mackenziellidae currently only has one described species worldwide, *M. psocoides* Hammer, 1953 (Bellinger et al. 2023), and was redescribed by Fjellberg (1989). Fjellberg extracted this species from moss in an area that experiences periods of drought during the summer and suggested that it has a well-adapted life strategy to overcome these conditions. The addition of these new records to the Free State play an important role in understanding the distribution and ecology of springtails.

Suggestions for sampling termitophiles in *T. trinervoides* mounds

Although Collembola (especially Cyphoderini) were very effectively sampled from the interior of active mounds, the scarcity of spiders therein was somewhat surprising. Costa et al. (2009) reported 34 species of spiders from the mounds of *Cornitermes cumulans* (Kollar, 1832) in Brazil, whereas Lawrence (1952) and Benoit (1964, 1976) described numerous species of spiders from termite nest interiors in tropical Africa. One would thus expect *T. trinervoides* mound interiors to be ideal environments in which termitophilous spiders could survive, particularly as the internal environment of these termitaria is generally stable compared to ambient temperature fluctuations (Field and Duncan 2013; Ndlovu et al. 2021) and provides an effective barrier against other external factors such as rainfall and extreme heat.

As such, two factors may potentially be of importance in explaining the results of our study. Cristaldo et al. (2012) found that nest size was a crucial factor shaping the occupation of *Constrictotermes cyphergaster* (Silvestri, 1901), with particular critical lower limits in nest volume affecting the establishment of termitophiles and inquilines. Similarly, Marins et al. (2016) found an increase in the abundance and richness of co-inhabitants with increasing *Cornitermes cumulans* mound size. The nests sampled in our study (Suppl. material 2; 27–76 cm high) could be considered as moderately large for *T. trinervoides* when compared to other studies in the literature (heights of 20–80 cm in the central Free State in Smith and Yeaton 1998; 12–64 cm in the central Free State in Adam et al. 2018; approximately 1 m in KwaZulu-Natal Province in Ndlovu et al. 2021). Nest size thus seems unlikely to explain the lack of termitophilous spiders.

More likely, therefore, is the inadequacy of the sampling approach. Most of the pitfalls inside the active mounds were filled with termites by the time the sampling period of 21 days was completed, which may have reduced the capture of both springtails and spiders. As this was the first time such trapping had been attempted in *T. trinervoides* mounds, its efficacy in capturing termites could not have been foreseen. Replacing the pitfalls intermittently was not an option, as this would disturb the interior conditions of the mound and undo the repairs to the mound crust effected by the worker termites. A more plausible solution to effectively sampling termitophiles in active mounds in future would be the excavation of the mounds, as done by Haddad and Dippenaar-Schoeman (2002, 2006) for abandoned mounds. This would enable sampling arthropods from the deepest parts of the nest that are inaccessible to pitfall trapping.

Conclusion

This study provided insights into the biodiversity patterns of springtail and spider assemblages that co-inhabit active and abandoned *T. trinervoides* mounds, as well as the surrounding grassland. It showed that the spider assemblages inside and on top of the mounds were different from those at the foot of the mounds and 3 m away from the mounds in the grassland, although ANOSIM analysis found no significant differences in assemblage composition. Springtail species were more generally distributed outside mounds and in grasslands, with only the inside of the active and abandoned mounds showing signs of selection for these specific microhabitats, as indicated by their lower species richness. This study shows that both active and abandoned mounds should be treated as islands in the grassland matrix, as their spider and springtail assemblages differed from that of the surrounding area. This study further provides a baseline dataset for future research to focus on the diversity of termitophilous springtails in southern Africa, which remain very understudied.

Acknowledgments

Jehane Saaiman, Anke de Smidt, Sylvia van der Merwe and Jason Botham are thanked for assistance with the initial sorting of the pitfall trap material.

Additional information

Conflict of interest

The authors have declared that no competing interests exist.

Ethical statement

Ethical clearance was obtained from the University of the Free State Animal Ethics Committee (UFS-AED2017-006101).

Funding

This study was funded by a grant from the University of the Free State Research Directorate to the Department of Zoology and Entomology for the Grassland Biodiversity Programme.

Author contributions

H.B. conducted field work, did initial sorting of samples, did morphospecies sorting and identification of Collembola, conducted analyses, and wrote the first draft of the manuscript; C.R.H. conceptualized the study, conducted field work, identified the Araneae, and prepared the publication draft of the manuscript; C.J.-S. identified some of the Collembola and helped with analyses. All authors contributed to the writing of the publication draft of the manuscript. This work forms part of the Ph.D study of H.B. under the supervision of C.R.H. and C.J.-S.

Author ORCIDs

Hannelene Badenhorst  <https://orcid.org/0000-0001-6012-3043>

Charles Richard Haddad  <https://orcid.org/0000-0002-2317-7760>

Charlene Janion-Scheepers  <https://orcid.org/0000-0001-5942-7912>

Data availability

All of the data that support the findings of this study are available in the main text or Supplementary Information.

References

- Adam RA, Mitchell JD (2009) Energetics and development of incipient colonies of the harvester termite, *Trinervitermes trinervoides* (Sjöstedt) (Termitidae, Nasutitermitinae). *Insectes Sociaux* 56(1): 21–27. <https://doi.org/10.1007/s00040-008-1032-3>
- Adam RA, Mitchell JD, Van der Westhuizen MC (2005) Food preferences in laboratory colonies of the harvester termite, *Trinervitermes trinervoides* (Sjöstedt) (Termitidae: Nasutitermitinae). *African Entomology* 13: 193–200.
- Adam RA, Mitchell JD, Van der Westhuizen MC (2008) Aspects of foraging in the harvester termite, *Trinervitermes trinervoides* (Sjöstedt) (Termitidae: Nasutitermitinae). *African Entomology* 16(2): 153–161. <https://doi.org/10.4001/1021-3589-16.2.153>
- Adam RA, Mitchell JD, Van der Westhuizen MC (2012) The role of the harvester termite, *Trinervitermes trinervoides* (Termitidae: Nasutitermitinae), in a semi-arid grassland ecosystem in South Africa: nest populations and caste composition. *African Entomology* 20(2): 239–251. <https://doi.org/10.4001/003.020.0202>
- Adam RA, Mitchell JD, Van der Westhuizen MC (2018) The role of the harvester termite, *Trinervitermes trinervoides* (Termitidae: Nasutitermitinae), in a semi-arid grassland ecosystem in South Africa: abundance, biomass and grass consumption. *African Entomology* 26(1): 36–44. <https://doi.org/10.4001/003.026.0036>
- Basset Y, Palacios-Vargas JG, Donoso DA, Castaño-Meneses G, Decaëns T, Lamarre GP, De León LF, Rivera M, García-Gómez A, Perez F, Bobadilla R, Lopez Y, Ramirez JA, Cruz MM, Galván AA, Mejía-Recamier BE, Barrios H (2020) Enemy-free space and the distribution of ants, springtails and termites in the soil of one tropical rainforest. *European Journal of Soil Biology* 99: 103193. <https://doi.org/10.1016/j.ejsobi.2020.103193>
- Bellinger PF, Christiansen KA, Janssens F (2023) Checklist of the Collembola of the World. <http://www.collembola.org> [accessed on 23/12/2023]
- Bellini BC, Weiner WM, Winck BR (2023) Systematics, ecology and taxonomy of Collembola: Introduction to the special issue. *Diversity* 15(2): 221. <https://doi.org/10.3390/d15020221>
- Benoit PLG (1964) La découverte d'Oonopidae anophtalmes dans des termitières africaines (Araneae). *Revue de Zoologie et de Botanique Africaines* 70: 174–187.
- Benoit PLG (1976) Un nouveau genre d'Oonopidae, termitobie et aveugle, en Afrique Centrale. *Revue Zoologique Africaine* 90: 177–180.
- Birkhofer K, Wise DH, Scheu S (2008) Subsidy from the detrital food web, but not microhabitat complexity, affects the role of generalist predators in an aboveground herbivore food web. *Oikos* 117(4): 494–500. <https://doi.org/10.1111/j.0030-1299.2008.16361.x>
- Birkhofer K, Wolters V, Diekötter T (2011) Density-dependent and -independent effects on the joint use of space by predators and prey in terrestrial arthropod food-webs. *Oikos* 120(11): 1705–1711. <https://doi.org/10.1111/j.1600-0706.2011.19546.x>
- Butler VP, Haddad CR (2011) Spider assemblages associated with leaf litter of three tree species in central South Africa (Arachnida: Araneae). *African Journal of Ecology* 49(3): 301–310. <https://doi.org/10.1111/j.1365-2028.2011.01265.x>
- Chao A, Jost L (2012) Coverage-based rarefaction and extrapolation: Standardizing samples by completeness rather than size. *Ecology* 93(12): 2533–2547. <https://doi.org/10.1890/11-1952.1>

- Chao A, Colwell RK, Lin C-W, Gotelli NJ (2009) Sufficient sampling for asymptotic minimum species richness estimators. *Ecology* 90(4): 1125–1133. <https://doi.org/10.1890/07-2147.1>
- Chen C, Zou X, Wu J, Zhu X, Jiang X, Zhang W, Zeng H, Liu W (2021) Accumulation and spatial homogeneity of nutrients within termite (*Odontotermes yunnanensis*) mounds in the Xishuangbanna region, SW China. *Catena* 198: 105057. <https://doi.org/10.1016/j.catena.2020.105057>
- Coaton WGH (1948) *Trinervitermes* species – the snouted harvester termites. Department of agriculture, entomology series no. 23. Government Printer. Pretoria, RSA.
- Conlon BH, De Beer ZW, De Fine Licht H, Aanen DK, Poulsen M (2016) Phylogenetic analyses of *Podaxis* specimens from Southern Africa reveal hidden diversity and new insights into associations with termites. *Fungal Biology* 120(9): 1065–1076. <https://doi.org/10.1016/j.funbio.2016.05.011>
- Costa D, Carvalho RA, de Lima Filho GF, Brandao D (2009) Inquilines and invertebrate fauna associated with termite nests of *Cornitermes cumulans* (Isoptera, Termitidae) in the Emas National Park, Mineiros, Goiás, Brazil. *Sociobiology* 53: 443–453.
- Cristaldo P, Rosa CS, Florencio DF, Marins A, De Souza O (2012) Termitarium volume as a determinant of invasion by obligatory termitophiles and inquilines in the nests of *Constrictotermes cyphergaster* (Termitidae, Nasutitermitinae). *Insectes Sociaux* 59(4): 541–548. <https://doi.org/10.1007/s00040-012-0249-3>
- Dangerfield JM (1991) Soil modification by *Cubitermes sankurensis* (Wassmann) (Isoptera: Termitidae) within miombo woodland site in Zimbabwe. *African Journal of Ecology* 29: 267–269. <https://doi.org/10.1111/j.1365-2028.1991.tb01009.x>
- Davies AB, Levick SR, Asner GP, Robertson MP, Van Rensburg BJ, Parr CL (2014) Spatial variability and abiotic determinants of termite mounds throughout a savanna catchment. *Ecography* 37(9): 852–862. <https://doi.org/10.1111/ecog.00532>
- De Cáceres M, Legendre P (2009) Associations between species and groups of sites: indices and statistical inference. *Ecology* 90(12): 3566–3574. <https://doi.org/10.1890/08-1823.1>
- De Vries JL, Pirk CWW, Bateman PW, Cameron EZ, Dalerum F (2011) Extension of the diet of an extreme foraging specialist, the aardwolf (*Proteles cristata*). *African Zoology* 46(1): 194–196. <https://doi.org/10.1080/15627020.2011.11407494>
- Dingaan MNV, Du Preez PJ (2013) Grassland communities of urban open spaces in Bloemfontein, Free State, South Africa. *Koedoe* 55(1): 1075. <https://doi.org/10.4102/koedoe.v55i1.1075>
- Dingaan MNV, Du Preez PJ (2017) Floristic composition and species diversity of urban vegetation in Bloemfontein, Free State, South Africa. *Bothalia* 47(2): a2244. <https://doi.org/10.4102/abc.v47i1.2244>
- Dippenaar-Schoeman AS (2023) Field guide to the spiders of South Africa. Struik Nature, Cape Town, R.S.A.
- Dippenaar-Schoeman AS, Haddad CR, Booyesen R, Foord SH, Lotz LN (2021a) The Scytodidae of South Africa. Version 1. South African National Survey of Arachnida Photo Identification Guide, Irene, 41 pp. <https://doi.org/10.5281/zenodo.7157802>
- Dippenaar-Schoeman AS, Haddad CR, Booyesen R, Foord SH, Lotz LN (2021b) The Gnaphosidae of South Africa. Part 4 (Z). Version 1. South African National Survey of Arachnida Photo Identification Guide, Irene, 53 pp. <https://doi.org/10.5281/zenodo.7197783>
- Dippenaar-Schoeman AS, Haddad CR, Lotz LN, Booyesen R, Steenkamp RC, Foord SH (2023) Checklist of the spiders (Araneae) of South Africa. *African Invertebrates* 64(3): 221–289. <https://doi.org/10.3897/AfrInvertebr.64.111047>

- Field MA, Duncan FD (2013) Does thermoregulation occur in the mounds of the harvester termite, *Trinervitermes trinervoides* (Sjöstedt) (Isoptera: Termitidae)? *African Entomology* 21(1): 45–57. <https://doi.org/10.4001/003.021.0110>
- Fjellberg A (1989) Redescription of *Mackenziella psocoides* Hammer, 1953 and discussion of its systematic position (Collembola, Mackenziellidae). *Proceedings of the Third International Seminar on Apterygota, Siena*, 93–105.
- Fleming PA, Loveridge JP (2003) Miombo woodland termite mounds: Resource islands for small vertebrates? *Journal of Zoology (London, England)* 259(2): 161–168. <https://doi.org/10.1017/S0952836902003084>
- Gao C-H, Yu G, Cai P (2021) ggVennDiagram: An intuitive, easy-to-use, and highly customizable R package to generate Venn diagram. *Frontiers in Genetics* 12: 706907. <https://doi.org/10.3389/fgene.2021.706907>
- Gosling CM, Cromsigt JPGM, Mpanza N, Oloff H (2012) Effects of erosion from mounds of different termite genera on distinct functional grassland types in an African savannah. *Ecosystems* 15(1): 128–139. <https://doi.org/10.1007/s10021-011-9497-8>
- Haddad CR, Butler VP (2018) Ground-dwelling spider assemblages in contrasting habitats in the central South African Grassland Biome. *Koedoe* 60(1): a1482. <https://doi.org/10.4102/koedoe.v60i1.1482>
- Haddad CR, Dippenaar-Schoeman AS (2002) The influence of mound structure on the diversity of spiders (Araneae) inhabiting the abandoned mounds of the snouted harvester termite *Trinervitermes trinervoides*. *The Journal of Arachnology* 30(2): 403–408. [https://doi.org/10.1636/0161-8202\(2002\)030\[0403:TIOMSO\]2.0.CO;2](https://doi.org/10.1636/0161-8202(2002)030[0403:TIOMSO]2.0.CO;2)
- Haddad CR, Dippenaar-Schoeman AS (2006) Spiders (Araneae) inhabiting abandoned mounds of the snouted harvester termite *Trinervitermes trinervoides* (Sjöstedt) (Isoptera: Termitidae: Nasutitermitinae) in the Free State, South Africa, with notes on their biology. *Navorsinge van die Nasionale Museum Bloemfontein* 22: 2–15.
- Haddad CR, Dippenaar-Schoeman AS, Foord SH, Lotz LN, Lyle R (2013) The faunistic diversity of spiders (Arachnida: Araneae) of the South African Grassland Biome. *Transactions of the Royal Society of South Africa* 68(2): 97–122. <https://doi.org/10.1080/0035919X.2013.773267>
- Haddad CR, Foord SH, Fourie R, Dippenaar-Schoeman AS (2015) Effects of a fast-burning spring fire on the ground-dwelling spider assemblages (Arachnida: Araneae) in a central South African grassland habitat. *African Zoology* 50(4): 281–292. <https://doi.org/10.1080/15627020.2015.1088400>
- Haddad CR, Brabec M, Pekár S, Fourie R (2016) Seasonal population dynamics of a specialised termite-eating spider (Araneae: Ammoxenidae) and its prey (Isoptera: Hodotermitidae). *Pedobiologia* 59(3): 105–110. <https://doi.org/10.1016/j.pedobi.2016.03.003>
- Hammer Ø, Harper DAT, Ryan PD (2001) Past: Paleontological statistics software package for education and data analysis. *Palaeontologia Electronica* 4: 1–9.
- Henschel JR, Dean WRJ, Milton SJ, Dippenaar-Schoeman AS (2023) Coexistence of *Ammoxenus* (Gnaphosidae) spider species on and between termitaria of *Microhodotermes viator* (Hodotermitidae) at a Karoo site. *African Entomology* 31: e16110. <https://doi.org/10.17159/2254-8854/2023/a16110>
- Janion-Scheepers C (2021) Collembola of South Africa. www.collembola.co.za [accessed on 23 December 2023]
- Janion-Scheepers C, DeHarveng L, Bedos A, Chown SL (2015) Updated list of Collembola species currently recorded from South Africa. *ZooKeys* 503: 55–88. <https://doi.org/10.3897/zookeys.503.8966>

- Janion-Scheepers C, Measey J, Braschler B, Chown SL, Coetzee L, Colville J, Dames J, Davies AB, Davies S, Davis A, Dippenaar-Schoeman AS, Duffy G, Fourie D, Griffiths C, Haddad CR, Hamer M, Herbert D, Hugo-Coetzee LEA, Jacobs A, Jansen van Rensburg C, Lamani S, Lotz LN, Louw Svd M, Lyle R, Malan A, Marais M, Neethling JA, Nxele T, Plisko D, Prendini L, Rink AN, Swart A, Theron P, Truter M, Ueckermann E, Uys VM, Villet MH, Willows-Munrow S, Wilson JRU (2016) Soil biota in a megadiverse country: Current knowledge and future research directions in South Africa. *Pedobiologia* 59(3): 129–174. <https://doi.org/10.1016/j.pedobi.2016.03.004>
- Joseph GS, Seymour CL, Cumming GS, Cumming DHM, Mahlangu Z (2013) Termite mounds as islands: Woody plant assemblages relative to termitarium size and soil properties. *Journal of Vegetation Science* 24(4): 702–711. <https://doi.org/10.1111/j.1654-1103.2012.01489.x>
- Kistner DH (1982) Chapter 1: The Social Insects' Bestiary. Section 3A: Collembola or Springtails. In: Hermann HR (Ed.) *Social insects*, volume III. Academic Press Inc., New York, 19–22. <https://doi.org/10.1016/B978-0-12-342203-3.50008-4>
- Korenko S, Hamouzavá K, Pekár S (2014) Trophic niche and predatory behavior of the goblin spider *Triaeris stenaspis* (Oonopidae): A springtail specialist? *The Journal of Arachnology* 42(1): 74–78. <https://doi.org/10.1636/Hi12-90.1>
- Lawrence RF (1952) A collection of cavernicolous and termitophilous Arachnida from the Belgian Congo. *Revue de Zoologie et de Botanique Africaines* 46: 1–17.
- Leitner M, Davies AB, Robertson MP, Parr CL, Van Rensburg BJ (2020) Termite mounds create heterogeneity in invertebrate communities across a savanna rainfall gradient. *Biodiversity and Conservation* 29(4): 1427–1441. <https://doi.org/10.1007/s10531-020-01943-5>
- Marins A, Costa D, Russo L, Campbell C, DeSouza O, Bjornstad O, Shea K (2016) Termite cohabitation: The relative effect of biotic and abiotic factors on mound biodiversity. *Ecological Entomology* 41(5): 532–541. <https://doi.org/10.1111/een.12323>
- Michálek O, Pekár S, Haddad CR (2021) Fundamental trophic niche of two prey-specialized jumping spiders, *Cyrrba algerina* and *Heliophanus termitophagus* (Araneae: Salticidae). *The Journal of Arachnology* 49(2): 268–271. <https://doi.org/10.1636/JoA-S-20-060>
- Microsoft Corporation (2021) Microsoft Excel software. Redmond, U.S.A. <https://office.microsoft.com/excel>
- Mills AJ, Sirami C (2018) Nutrient enrichment of ecosystems by fungus-growing versus non-fungus-growing termites. *Journal of Tropical Ecology* 34(6): 385–389. <https://doi.org/10.1017/S0266467418000330>
- Moeletsi ME, Myeni L, Kaempffer LC, Vermaak D, De Nysschen G, Henningse C, Nel I, Rowswell D (2022) Climate dataset for South Africa by the Agricultural Research Council. *Data* 7(8): 117. <https://doi.org/10.3390/data7080117>
- Nampa G, Ndlovu M (2019) Association benefits between harvester termites (*Trinervitermes trinervoides*) and num-num plants (*Carissa bispinosa*) in a semi-arid savanna setting. *Journal of Arid Environments* 171: 104005. <https://doi.org/10.1016/j.jaridenv.2019.104005>
- Ndlovu M, Nampa G, Joseph GS, Seymour CL (2021) Plant shade enhances thermoregulation of internal environments in *Trinervitermes trinervoides* mounds. *Journal of Thermal Biology* 100: 103068. <https://doi.org/10.1016/j.jtherbio.2021.103068>
- Nduwarugira D, Jocqué R, Havyarimana F, Mpawenayo B, Roisin Y (2016) Role of termite mounds on the distribution of spiders in miombo woodland of south-western Burundi. *Arachnology* 17(1): 28–38. <https://doi.org/10.13156/arac.2006.17.1.28>

- Nel JJC (1968) Aggressive behaviour of the harvester termites *Hodotermes mossambicus* and *Trinervitermes trinervoides* (Sjöstedt). *Insectes Sociaux* 15(2): 145–156. <https://doi.org/10.1007/BF02223463>
- Nunes RC, Santos-Costa RC, Bellini BC (2020) The first Neotropical *Capbrya* Barra, 1999 (Collembola: Orchesellidae: Nothobryinae) and the reinterpretation of Nothobryinae systematics. *Zoologischer Anzeiger* 288: 24–42. <https://doi.org/10.1016/j.jcz.2020.06.009>
- Nyffeler M, Birkhofer K (2017) An estimated 400–800 million tons of prey are annually killed by the global spider community. *Naturwissenschaften* 104(3–4): 30. <https://doi.org/10.1007/s00114-017-1440-1>
- Oksanen J, Blanchet FG, Kindt R, Legendre P, Minchin PR, O’Hara RB, Simpson GL, Solyomos P, Stevens MHH, Wagner H (2019) *vegan*: Community Ecology Package. R Package Version 2.5-6. <https://CRAN.R-project.org/package=vegan>
- Oliveira JVL, Zeppelini D, Castaño-Meneses G, Palacios-Vargas JG (2023) Neotropical *Cyphoderus* (Collembola: Paronellidae), with comments about myrmecophily and the description of new species. *Neotropical Entomology* 52(4): 652–696. <https://doi.org/10.1007/s13744-022-01015-z>
- Paclt J (1967) On South and Central African Collembola. *Journal of the Entomological Society of Southern Africa* 29: 135–147.
- Parmentier T, Braem S (2024) Structural variation of ant nests mediates the local distribution and abundance of an associate. *Entomologia Experimentalis et Applicata* 172(7): 626–635. <https://doi.org/10.1111/eea.13429>
- Pekár S, Bočánek O, Michálek O, Petráková L, Haddad CR, Šedo O, Zdráhal Z (2018) Venom gland size and venom composition – essential trophic adaptations of venomous predators: The case study using spiders. *Molecular Ecology* 27(21): 4257–4269. <https://doi.org/10.1111/mec.14859>
- Pekár S, Petráková Dušátková L, Michálek O, Haddad CR (2020) Coexistence of two termite-eating specialists (Araneae). *Ecological Entomology* 45(6): 1307–1317. <https://doi.org/10.1111/een.12914>
- Petráková L, Líznarová E, Pekár S, Haddad CR, Sentenská L, Symondson WOC (2015) Discovery of a monophagous true predator, a specialist termite-eating spider (Araneae: Ammoxenidae). *Scientific Reports* 5(1): 14013. <https://doi.org/10.1038/srep14013>
- Potts RC, Hewitt PH (1973) The distribution of intestinal bacteria and cellulase activity in the harvester termite *Trinervitermes trinervoides* (Nasutitermitinae). *Insectes Sociaux* 20(3): 215–220. <https://doi.org/10.1007/BF02223191>
- Potts RC, Hewitt PH (1974) Some properties and reaction characteristics of the partially purified cellulase from the termite *Trinervitermes trinervoides* (Nasutitermitinae). *Comparative Biochemistry and Physiology* 47: 327–337. [https://doi.org/10.1016/0305-0491\(74\)90062-5](https://doi.org/10.1016/0305-0491(74)90062-5)
- Prestwich GD (1977) Chemical composition of the soldier secretions of the termite – *Trinervitermes graciosus*. *Insect Biochemistry* 7(1): 91–94. [https://doi.org/10.1016/0020-1790\(77\)90062-2](https://doi.org/10.1016/0020-1790(77)90062-2)
- Prestwich GD, Tanis SP, Pilkiewicz FG, Miura I, Nakanishi K (1976a) Nasute termite soldier frontal gland secretions. 2. structures of trinervitene congeners from *Trinervitermes* soldiers. *Journal of the American Chemical Society* 98(19): 6062–6064. <https://doi.org/10.1021/ja00435a061>
- Prestwich GD, Tanis SP, Springer JP, Clardy J (1976b) Nasute termite soldier frontal gland secretions. 1. Structure of trinervi-2 β ,3 α ,9 χ -triol-9-O-acetate, a novel diterpene from *Trinervitermes* soldiers. *Journal of the American Chemical Society* 98(19): 6061–6062. <https://doi.org/10.1021/ja00435a060>

- PRIMER-e (2017) PRIMER v7 and PERMANOVA+ statistical software. Auckland, New Zealand. <https://www.primer-e.com/>
- R Studio Team (2020) RStudio: Integrated Development for R. RStudio, Inc. Boston, U.S.A. <http://www.rstudio.com/>
- Richardson PRK (1987) Food consumption and seasonal variation in the diet of the aardwolf *Proteles cristatus* in southern Africa. *Zeitschrift für Säugetierkunde* 52(5): 307–325.
- Richardson PKR, Levitan CD (1994) Tolerance of aardwolves to defence secretions of *Trinervitermes trinervoides*. *Journal of Mammalogy* 75(1): 84–91. <https://doi.org/10.2307/1382238>
- Rusek J (1998) Biodiversity of Collembola and their functional role in the ecosystem. *Biodiversity and Conservation* 7(9): 1207–1219. <https://doi.org/10.1023/A:1008887817883>
- Smith FR, Yeaton RI (1998) Disturbance by the mound-building termite, *Trinervitermes trinervoides*, and vegetation patch dynamics in a semi-arid, southern African grassland. *Plant Ecology* 137(1): 41–53. <https://doi.org/10.1023/A:1008004431093>
- Taylor WA, Skinner JD (2000) Associative feeding between Aardwolves (*Proteles cristatus*) and Aardvarks (*Orycteropus afer*). *Mammal Review* 30(2): 141–143. <https://doi.org/10.1046/j.1365-2907.2000.00062.x>
- Theron CD (2013) Population structure and predation in the harvester termite, *Trinervitermes trinervoides* (Sjöstedt). M.Sc. Thesis, University of Pretoria, 66 pp.
- Thibaud J-M (2013) Essai sur l'état des connaissances de la diversité des Collemboles de l'Empire Africano–Malgache. *Russian Entomological Journal* 22: 233–248. <https://doi.org/10.15298/rusentj.23.4.01>
- Tuma J, Eggleton P, Fayle TM (2020) Ant-termite interactions: An important but under-explored ecological linkage. *Biological Reviews of the Cambridge Philosophical Society* 95(3): 555–572. <https://doi.org/10.1111/brv.12577>
- Uys V (2002) A guide to the termite genera of southern Africa. ARC-Plant Protection Research Institute. Pretoria, R.S.A.
- Warren E (1919) Termites and Termitophiles. *South African Journal of Science* 16: 93–112.
- Wesołowska W, Haddad CR (2002) A new termitivorous jumping spider from South Africa (Araneae Salticidae). *Tropical Zoology* 15(2): 197–207. <https://doi.org/10.1080/03946975.2002.10531174>
- World Spider Catalog (2024) World Spider Catalog. Version 25.5. Natural History Museum Bern. <https://doi.org/10.24436/2> [accessed on 14 October 2024]

Supplementary material 1

KML (Keyhole Markup Language) file for viewing the locations of each of the 24 mounds interactively in Google Earth

Authors: Hannelene Badenhorst, Charles Richard Haddad, Charlene Janion-Scheepers

Data type: kml

Copyright notice: This dataset is made available under the Open Database License (<http://opendatacommons.org/licenses/odbl/1.0/>). The Open Database License (ODbL) is a license agreement intended to allow users to freely share, modify, and use this Dataset while maintaining this same freedom for others, provided that the original source and author(s) are credited.

Link: <https://doi.org/10.3897/AfrInvertebr.65.139404.suppl1>

Supplementary material 2

Summary of the structural characteristics of the 12 active (Ac) and 12 abandoned (Ab) *Trinervitermes trinervoides* mounds sampled

Authors: Hannelene Badenhorst, Charles Richard Haddad, Charlene Janion-Scheepers

Data type: pdf

Explanation note: Degree of perforation follows the scale proposed by Haddad and Dippenaar-Schoeman (2002).

Copyright notice: This dataset is made available under the Open Database License (<http://opendatacommons.org/licenses/odbl/1.0/>). The Open Database License (ODbL) is a license agreement intended to allow users to freely share, modify, and use this Dataset while maintaining this same freedom for others, provided that the original source and author(s) are credited.

Link: <https://doi.org/10.3897/AfrInvertebr.65.139404.suppl2>

Supplementary material 3

Rarefaction curves of the spider (A) and springtail (B) species richness for each of the eight microhabitats.

Authors: Hannelene Badenhorst, Charles Richard Haddad, Charlene Janion-Scheepers

Data type: pdf

Copyright notice: This dataset is made available under the Open Database License (<http://opendatacommons.org/licenses/odbl/1.0/>). The Open Database License (ODbL) is a license agreement intended to allow users to freely share, modify, and use this Dataset while maintaining this same freedom for others, provided that the original source and author(s) are credited.

Link: <https://doi.org/10.3897/AfrInvertebr.65.139404.suppl3>

Supplementary material 4

Spider species collected from four microhabitats associated with the active (Ac) and abandoned (Ab) mounds of the snouted harvester termite, *Trinervitermes trinervoides*, and the surrounding grassland.

Authors: Hannelene Badenhorst, Charles Richard Haddad, Charlene Janion-Scheepers

Data type: pdf

Copyright notice: This dataset is made available under the Open Database License (<http://opendatacommons.org/licenses/odbl/1.0/>). The Open Database License (ODbL) is a license agreement intended to allow users to freely share, modify, and use this Dataset while maintaining this same freedom for others, provided that the original source and author(s) are credited.

Link: <https://doi.org/10.3897/AfrInvertebr.65.139404.suppl4>

Supplementary material 5

Springtail species collected from four microhabitats associated with the active (Ac) and abandoned (Ab) mounds of the snouted harvester termite, *Trinervitermes trinervoides*, and the surrounding grassland.

Authors: Hannelene Badenhorst, Charles Richard Haddad, Charlene Janion-Scheepers
Data type: pdf

Copyright notice: This dataset is made available under the Open Database License (<http://opendatacommons.org/licenses/odbl/1.0/>). The Open Database License (ODbL) is a license agreement intended to allow users to freely share, modify, and use this Dataset while maintaining this same freedom for others, provided that the original source and author(s) are credited.

Link: <https://doi.org/10.3897/AfrInvertebr.65.139404.suppl5>

Supplementary material 6

Results from the Wilcoxon rank sum test analysis performed for spider abundance collected from eight microhabitats inside and around active (Ac) and abandoned (Ab) *Trinervitermes trinervoides* mounds, with significant differences ($P < 0.05$) indicated by an asterisk

Authors: Hannelene Badenhorst, Charles Richard Haddad, Charlene Janion-Scheepers
Data type: pdf

Explanation note: Microhabitats: In = inside mounds; Out = outside, on top of mound;
0m = 0 m away from mound; 3m = 3 m away from mound.

Copyright notice: This dataset is made available under the Open Database License (<http://opendatacommons.org/licenses/odbl/1.0/>). The Open Database License (ODbL) is a license agreement intended to allow users to freely share, modify, and use this Dataset while maintaining this same freedom for others, provided that the original source and author(s) are credited.

Link: <https://doi.org/10.3897/AfrInvertebr.65.139404.suppl6>

Supplementary material 7

Results from the Wilcoxon rank sum test analysis performed for spider species richness collected from eight microhabitats inside and around active (Ac) and abandoned (Ab) *Trinervitermes trinervoides* mounds, with significant differences ($P < 0.05$) indicated by an asterisk

Authors: Hannelene Badenhorst, Charles Richard Haddad, Charlene Janion-Scheepers
Data type: pdf

Explanation note: Microhabitats: In = inside mounds; Out = outside, on top of mound;
0m = 0 m away from mound; 3m = 3 m away from mound.

Copyright notice: This dataset is made available under the Open Database License (<http://opendatacommons.org/licenses/odbl/1.0/>). The Open Database License (ODbL) is a license agreement intended to allow users to freely share, modify, and use this Dataset while maintaining this same freedom for others, provided that the original source and author(s) are credited.

Link: <https://doi.org/10.3897/AfrInvertebr.65.139404.suppl7>

Supplementary material 8

Results from the Wilcoxon rank sum test analysis performed for the Shannon's diversity index values of the spider assemblages collected from eight microhabitats inside and around active (Ac) and abandoned (Ab) *Trinervitermes trinervoides* mounds, with significant differences ($P < 0.05$) indicated by an asterisk

Authors: Hannelene Badenhorst, Charles Richard Haddad, Charlene Janion-Scheepers

Data type: pdf

Explanation note: Microhabitats: In = inside mounds; Out = outside, on top of mound; 0m = 0 m away from mound; 3m = 3 m away from mound.

Copyright notice: This dataset is made available under the Open Database License (<http://opendatacommons.org/licenses/odbl/1.0/>). The Open Database License (ODbL) is a license agreement intended to allow users to freely share, modify, and use this Dataset while maintaining this same freedom for others, provided that the original source and author(s) are credited.

Link: <https://doi.org/10.3897/AfrInvertebr.65.139404.suppl8>

Supplementary material 9

Results of simple linear regression of spider and springtail abundance and species richness collected from eight microhabitats inside and around active (Ac) and abandoned (Ab) *Trinervitermes trinervoides* mounds relative to mound volume and circumference

Authors: Hannelene Badenhorst, Charles Richard Haddad, Charlene Janion-Scheepers

Data type: pdf

Explanation note: Only R^2 values above 0.25 are indicated in bold. Microhabitats: In = inside mounds; Out = outside, on top of mound; 0m = 0 m away from mound; 3m = 3 m away from mound.

Copyright notice: This dataset is made available under the Open Database License (<http://opendatacommons.org/licenses/odbl/1.0/>). The Open Database License (ODbL) is a license agreement intended to allow users to freely share, modify, and use this Dataset while maintaining this same freedom for others, provided that the original source and author(s) are credited.

Link: <https://doi.org/10.3897/AfrInvertebr.65.139404.suppl9>

Supplementary material 10

Results from the Wilcoxon rank sum test analysis performed for springtail abundance collected from eight microhabitats inside and around active (Ac) and abandoned (Ab) *Trinervitermes trinervoides* mounds, with significant differences ($P < 0.05$) indicated by an asterisk

Authors: Hannelene Badenhorst, Charles Richard Haddad, Charlene Janion-Scheepers

Data type: pdf

Explanation note: Microhabitats: In = inside mounds; Out = outside, on top of mound; 0m = 0 m away from mound; 3m = 3 m away from mound.

Copyright notice: This dataset is made available under the Open Database License (<http://opendatacommons.org/licenses/odbl/1.0/>). The Open Database License (ODbL) is a license agreement intended to allow users to freely share, modify, and use this Dataset while maintaining this same freedom for others, provided that the original source and author(s) are credited.

Link: <https://doi.org/10.3897/AfrInvertebr.65.139404.suppl10>

Supplementary material 11

Results from the Wilcoxon rank sum test analysis performed for springtail species richness collected from eight microhabitats inside and around active (Ac) and abandoned (Ab) *Trinervitermes trinervoides* mounds, with significant differences ($P < 0.05$) indicated by an asterisk

Authors: Hannelene Badenhorst, Charles Richard Haddad, Charlene Janion-Scheepers

Data type: pdf

Explanation note: Microhabitats: In = inside mounds; Out = outside, on top of mound; 0m = 0 m away from mound; 3m = 3 m away from mound.

Copyright notice: This dataset is made available under the Open Database License (<http://opendatacommons.org/licenses/odbl/1.0/>). The Open Database License (ODbL) is a license agreement intended to allow users to freely share, modify, and use this Dataset while maintaining this same freedom for others, provided that the original source and author(s) are credited.

Link: <https://doi.org/10.3897/AfrInvertebr.65.139404.suppl11>

Supplementary material 12

Results from the Wilcoxon rank sum test analysis performed for the Shannon's diversity index values of the springtails assemblages collected from eight microhabitats inside and around active (Ac) and abandoned (Ab) *Trinervitermes trinervoides* mounds, with significant differences ($P < 0.05$) indicated by an asterisk

Authors: Hannelene Badenhorst, Charles Richard Haddad, Charlene Janion-Scheepers

Data type: pdf

Explanation note: Microhabitats: In = inside mounds; Out = outside, on top of mound; 0m = 0 m away from mound; 3m = 3 m away from mound.

Copyright notice: This dataset is made available under the Open Database License (<http://opendatacommons.org/licenses/odbl/1.0/>). The Open Database License (ODbL) is a license agreement intended to allow users to freely share, modify, and use this Dataset while maintaining this same freedom for others, provided that the original source and author(s) are credited.

Link: <https://doi.org/10.3897/AfrInvertebr.65.139404.suppl12>

Supplementary material 13

Results obtained from the similarity percentage (SIMPER) analyses showing the percentage dissimilarity between spider assemblages of different microhabitats in and around active and abandoned *Trinervitermes trinervoides* termite mounds, presented as average abundance (Av. Abun) per group, average dissimilarity (Av. Diss), contribution percentage (Contrib %) and cumulative percentage (Cum. %) of spider species towards these dissimilarities

Authors: Hannelene Badenhorst, Charles Richard Haddad, Charlene Janion-Scheepers

Data type: pdf

Explanation note: The list only includes the species contributing up to a cumulative percentage (Cum. %) of 70% of the observed dissimilarity.

Copyright notice: This dataset is made available under the Open Database License (<http://opendatacommons.org/licenses/odbl/1.0/>). The Open Database License (ODbL) is a license agreement intended to allow users to freely share, modify, and use this Dataset while maintaining this same freedom for others, provided that the original source and author(s) are credited.

Link: <https://doi.org/10.3897/AfrInvertebr.65.139404.suppl13>

Supplementary material 14

Results obtained from the similarity percentage (SIMPER) analyses showing the percentage dissimilarity between springtail assemblages of different microhabitats in and around active and abandoned *Trinervitermes trinervoides* termite mounds, presented as average abundance (Av. Abun) per group, average dissimilarity (Av. Diss), contribution percentage (Contrib %) and cumulative percentage (Cum. %) of spider species towards these dissimilarities

Authors: Hannelene Badenhorst, Charles Richard Haddad, Charlene Janion-Scheepers

Data type: pdf

Explanation note: The list below only includes the species contributing up to a cumulative percentage (Cum. %) of 70% of the observed dissimilarity.

Copyright notice: This dataset is made available under the Open Database License (<http://opendatacommons.org/licenses/odbl/1.0/>). The Open Database License (ODbL) is a license agreement intended to allow users to freely share, modify, and use this Dataset while maintaining this same freedom for others, provided that the original source and author(s) are credited.

Link: <https://doi.org/10.3897/AfrInvertebr.65.139404.suppl14>

Supplementary material 15

Sørensen's quotient of similarity of the spider assemblages collected from eight microhabitats inside and around active (Ac) and abandoned (Ab) *Trinervitermes trinervoides* mounds

Authors: Hannelene Badenhorst, Charles Richard Haddad, Charlene Janion-Scheepers

Data type: pdf

Explanation note: Microhabitats: In = inside mounds; Out = outside, on top of mound; 0m = 0 m away from mound; 3m = 3 m away from mound.

Copyright notice: This dataset is made available under the Open Database License (<http://opendatacommons.org/licenses/odbl/1.0/>). The Open Database License (ODbL) is a license agreement intended to allow users to freely share, modify, and use this Dataset while maintaining this same freedom for others, provided that the original source and author(s) are credited.

Link: <https://doi.org/10.3897/AfrInvertebr.65.139404.suppl15>

Supplementary material 16

Sørensen's quotient of similarity of the springtail assemblages collected from eight microhabitats inside and around active (Ac) and abandoned (Ab) *Trinervitermes trinervoides* mounds

Authors: Hannelene Badenhorst, Charles Richard Haddad, Charlene Janion-Scheepers

Data type: pdf

Explanation note: Microhabitats: In = inside mounds; Out = outside, on top of mound; 0m = 0 m away from mound; 3m = 3 m away from mound.

Copyright notice: This dataset is made available under the Open Database License (<http://opendatacommons.org/licenses/odbl/1.0/>). The Open Database License (ODbL) is a license agreement intended to allow users to freely share, modify, and use this Dataset while maintaining this same freedom for others, provided that the original source and author(s) are credited.

Link: <https://doi.org/10.3897/AfrInvertebr.65.139404.suppl16>

